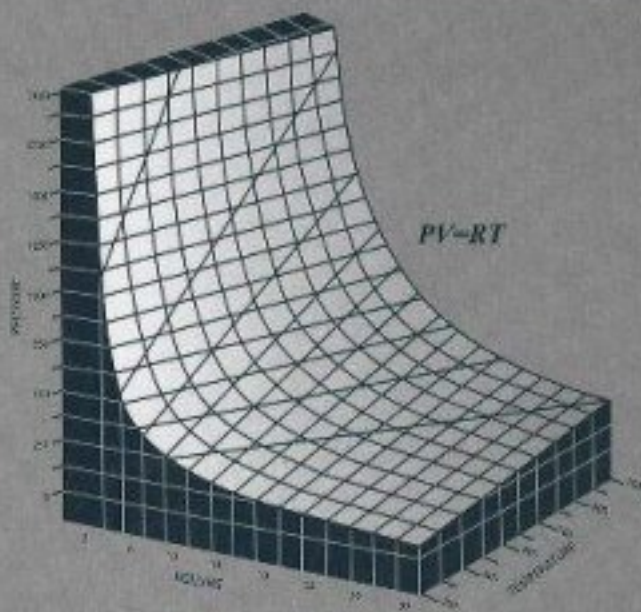




Gulf Publishing Company

Equations of State and PVT Analysis

Applications for Improved Reservoir Modeling



Tarek Ahmed

Equations of State and PVT Analysis

*Applications for Improved
Reservoir Modeling*

Tarek Ahmed, Ph.D., P.E.



Gulf Publishing Company
Houston, Texas

**Equations of State and PVT Analysis:
Applications for Improved Reservoir Modeling**

Copyright © 2007 by Gulf Publishing Company, Houston, Texas. All rights reserved. No part of this publication may be reproduced or transmitted in any form without the prior written permission of the publisher.

HOUSTON, TX:
Gulf Publishing Company
2 Greenway Plaza, Suite 1020
Houston, TX 77046

AUSTIN, TX:
427 Sterzing Street, Suite 104
Austin, TX 78704

10 9 8 7 6 5 4 3 2 1

Library of Congress Cataloging-in-Publication Data

Ahmed, Tarek H.

Equations of state and PVT analysis : applications for improved reservoir modeling / Tarek Ahmed.
p. cm.

Includes bibliographical references and index.

ISBN 1-933762-03-9 (alk. paper)

1. Reservoir oil pressure—Mathematical models. 2. Phase rule and equilibrium—Mathematical models. 3. Petroleum—Underground storage. I. Title.

TN871.18.A34 2007

622'.3382—dc22

2006033818

Printed in the United States of America

Printed on acid-free paper. ∞

Text design and composition by Ruth Maassen.

*This book is dedicated to my children
Carsen, Justin, Jennifer, and Brittany Ahmed*

Acknowledgments

It is my hope that the information presented in this textbook will improve the understanding of the subject of *equations of state* and *phase behavior*. Much of the material on which this book is based was drawn from the publications of the Society of Petroleum Engineers. Tribute is paid to the educators, engineers, and authors who have made numerous and significant contributions to the field of phase equilibria. I would like to specially acknowledge the significant contributions that have been made to this fascinating field of phase behavior and equations of state by Dr. Curtis Whitson, Dr. Abbas Firoozabadi, and Dr. Bill McCain.

I would like to express appreciation to Anadarko Petroleum Corporation for granting me the permission to publish this book. Special thanks to Mark Pease, Bob Daniels, and Jim Ashton.

I would like express my sincere appreciation to a group of engineers with Anadarko Petroleum Corporation for working with me and also for sharing their knowledge with me; in particular, Brian Roux, Eulalia Munoz-Cortijo, Jason Gaines, Aydin Centilmen, Kevin Corrigan, Dan Victor, John Allison, P. K. Pande, Scott Albertson, Chad McAllaster, Craig Walters, Dane Cantwell, and Julie Struble.

This book could not have been completed without the editorial staff of Gulf Publishing Company; in particular, Jodie Allen and Ruth Maassen. Special thanks to my friend Wendy for typing the manuscript; I do very much appreciate it, Wendy.

Preface

The primary focus of this book is to present the basic fundamentals of equations of state and PVT laboratory analysis and their practical applications in solving reservoir engineering problems. The book is arranged so it can be used as a textbook for senior and graduate students or as a reference book for practicing petroleum engineers.

Chapter 1 reviews the principles of hydrocarbon phase behavior and illustrates the use of phase diagrams in characterizing reservoirs and hydrocarbon systems. Chapter 2 presents numerous mathematical expressions and graphical relationships that are suitable for characterizing the undefined hydrocarbon-plus fractions. Chapter 3 provides a comprehensive and updated review of natural gas properties and the associated well-established correlations that can be used to describe the volumetric behavior of gas reservoirs. Chapter 4 discusses the PVT properties of crude oil systems and illustrates the use of laboratory data to generate the properties of crude oil for suitable use or conducting reservoir engineering studies. Chapter 5 reviews developments and advances in the field of empirical cubic equations of state and demonstrates their practical applications in solving phase equilibria problems. Chapter 6 discusses issues related to flow assurance that include asphaltene deposition, wax precipitation, and formation of hydrates.

About the Author

Tarek Ahmed, Ph.D., P.E., is a Reservoir Engineering Advisor with Anadarko Petroleum Corporation. Before joining the corporation, Dr. Ahmed was a professor and the head of the Petroleum Engineering Department at Montana Tech of the University of Montana. He has a Ph.D. from the University of Oklahoma, an M.S. from the University of Missouri–Rolla, and a B.S. from the Faculty of Petroleum (Egypt)—all degrees in petroleum engineering. Dr. Ahmed is also the author of other textbooks, including *Hydrocarbon Phase Behavior* (Gulf Publishing Company, 1989), *Advanced Reservoir Engineering* (Elsevier, 2005), and *Reservoir Engineering Handbook* (Elsevier, 2000; 2nd edition, 2002; 3rd edition, 2006).

Contents

Preface ix

Acknowledgments xi

<u>1</u>	Fundamentals of Hydrocarbon Phase Behavior	1
	Single-Component Systems	1
	Two-Component Systems	19
	Three-Component Systems	28
	Multicomponent Systems	29
	Classification of Reservoirs and Reservoir Fluids	32
	Phase Rule	54
	Problems	55
	References	57
<u>2</u>	Characterizing Hydrocarbon-Plus Fractions	59
	Generalized Correlations	62
	PNA Determination	82
	Graphical Correlations	92
	Splitting and Lumping Schemes	99
	Problems	130
	References	132
<u>3</u>	Natural Gas Properties	135
	Behavior of Ideal Gases	136
	Behavior of Real Gases	141
	Problems	176
	References	178
<u>4</u>	PVT Properties of Crude Oils	181
	Crude Oil Gravity	182
	Specific Gravity of the Solution Gas	183
	Crude Oil Density	184
	Gas Solubility	200

Bubble-Point Pressure	207
Oil Formation Volume Factor	213
Isothermal Compressibility Coefficient of Crude Oil	218
Undersaturated Oil Properties	228
Total-Formation Volume Factor	231
Crude Oil Viscosity	237
Surface/Interfacial Tension	246
PVT Correlations for Gulf of Mexico Oil	249
Properties of Reservoir Water	253
Laboratory Analysis of Reservoir Fluids	256
Problems	321
References	327

5 Equations of State and Phase Equilibria 331

Equilibrium Ratios	331
Flash Calculations	335
Equilibrium Ratios for Real Solutions	339
Equilibrium Ratios for the Plus Fractions	349
Vapor-Liquid Equilibrium Calculations	352
Equations of State	365
Equation-of-State Applications	398
Simulation of Laboratory PVT Data by Equations of State	409
Tuning EOS Parameters	440
Original Fluid Composition from a Sample Contaminated with Oil-Based Mud	448
Problems	450
References	453

6 Flow Assurance 457

Hydrocarbon Solids: Assessment of Risk	458
Phase Behavior of Asphaltenes	470
Asphaltene Deposit Envelope	480
Modeling the Asphaltene Deposit	482
Phase Behavior of Waxes	495
Modeling Wax Deposit	502
Prediction of Wax Appearance Temperature	505
Gas Hydrates	506
Problems	530
References	531

Appendix 535

Index 551

1

Fundamentals of Hydrocarbon Phase Behavior

A *PHASE* IS DEFINED AS ANY homogeneous part of a system that is physically distinct and separated from other parts of the system by definite boundaries. For example, ice, liquid water, and water vapor constitute three separate phases of the pure substance H_2O , because each is homogeneous and physically distinct from the others; moreover, each is clearly defined by the boundaries existing between them. Whether a substance exists in a solid, liquid, or gas phase is determined by the temperature and pressure acting on the substance. It is known that ice (solid phase) can be changed to water (liquid phase) by increasing its temperature and, by further increasing the temperature, water changes to steam (vapor phase). This change in phases is termed *phase behavior*.

Hydrocarbon systems found in petroleum reservoirs are known to display multiphase behavior over wide ranges of pressures and temperatures. The most important phases that occur in petroleum reservoirs are a liquid phase, such as crude oils or condensates, and a gas phase, such as natural gases.

The conditions under which these phases exist are a matter of considerable practical importance. The experimental or the mathematical determinations of these conditions are conveniently expressed in different types of diagrams, commonly called *phase diagrams*.

The objective of this chapter is to review the basic principles of hydrocarbon phase behavior and illustrate the use of phase diagrams in describing and characterizing the volumetric behavior of single-component, two-component, and multicomponent systems.

Single-Component Systems

The simplest type of hydrocarbon system to consider is that containing one component. The word *component* refers to the number of molecular or atomic species present in the substance.

A single-component system is composed entirely of one kind of atom or molecule. We often use the word *pure* to describe a single-component system.

The qualitative understanding of the relationship between temperature T , pressure p , and volume V of pure components can provide an excellent basis for understanding the phase behavior of complex petroleum mixtures. This relationship is conveniently introduced in terms of experimental measurements conducted on a pure component as the component is subjected to changes in pressure and volume at a constant temperature. The effects of making these changes on the behavior of pure components are discussed next.

Suppose a fixed quantity of a pure component is placed in a cylinder fitted with a frictionless piston at a fixed temperature T_1 . Furthermore, consider the initial pressure exerted on the system to be low enough that the entire system is in the vapor state. This initial condition is represented by point E on the pressure/volume phase diagram (p - V diagram) as shown in Figure 1-1. Consider the following sequential experimental steps taking place on the pure component:

1. The pressure is increased isothermally by forcing the piston into the cylinder. Consequently, the gas volume decreases until it reaches point F on the diagram, where the liquid begins to condense. The corresponding pressure is known as the *dew-point pressure*, p_d , and defined as the pressure at which the first droplet of liquid is formed.
2. The piston is moved further into the cylinder as more liquid condenses. This condensation process is characterized by a constant pressure and represented by the horizontal line FG . At point G , traces of gas remain and the corresponding pressure is called the *bubble-point pressure*, p_b , and defined as the pressure at which the first sign of

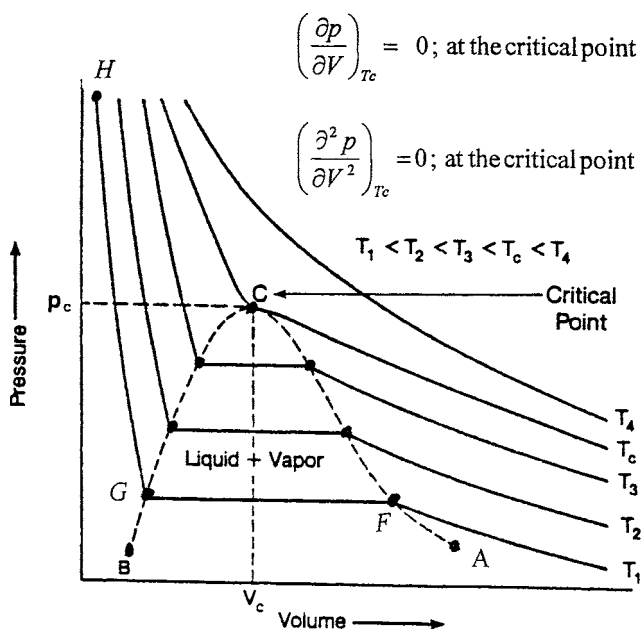


FIGURE 1-1 Typical pressure/volume diagram for a pure component.

gas formation is detected. A characteristic of a single-component system is that, at a given temperature, the dew-point pressure and the bubble-point pressure are equal.

3. As the piston is forced slightly into the cylinder, a sharp increase in the pressure (point H) is noted without an appreciable decrease in the liquid volume. That behavior evidently reflects the low compressibility of the liquid phase.

By repeating these steps at progressively increasing temperatures, a family of curves of equal temperatures (isotherms) is constructed as shown in Figure 1–1. The dashed curve connecting the dew points, called the *dew-point curve* (line FC), represents the states of the “saturated gas.” The dashed curve connecting the bubble points, called the *bubble-point curve* (line GC), similarly represents the “saturated liquid.” These two curves meet at a point C , which is known as the *critical point*. The corresponding pressure and volume are called the *critical pressure*, p_c , and *critical volume*, V_c , respectively. Note that, as the temperature increases, the length of the straight line portion of the isotherm decreases until it eventually vanishes and the isotherm merely has a horizontal tangent and inflection point at the critical point. This isotherm temperature is called the *critical temperature*, T_c , of that single component. This observation can be expressed mathematically by the following relationship:

$$\left(\frac{\partial p}{\partial V} \right)_{T_c} = 0, \text{ at the critical point} \quad (1-1)$$

$$\left(\frac{\partial^2 p}{\partial V^2} \right)_{T_c} = 0, \text{ at the critical point} \quad (1-2)$$

Referring to Figure 1–1, the area enclosed by the area $AFCGB$ is called the *two-phase region* or the *phase envelope*. Within this defined region, vapor and liquid can coexist in equilibrium. Outside the phase envelope, only one phase can exist.

The critical point (point C) describes the critical state of the pure component and represents the limiting state for the existence of two phases, that is, liquid and gas. In other words, for a single-component system, the critical point is defined as the highest value of pressure and temperature at which two phases can coexist. A more generalized definition of the critical point, which is applicable to a single- or multicomponent system, is this: The critical point is the point at which all intensive properties of the gas and liquid phases are equal.

An intensive property is one that has the same value for any part of a homogeneous system as it does for the whole system, that is, a property independent of the quantity of the system. Pressure, temperature, density, composition, and viscosity are examples of intensive properties.

Many characteristic properties of pure substances have been measured and compiled over the years. These properties provide vital information for calculating the thermodynamic properties of pure components as well as their mixtures. The most important of these properties include

- Critical pressure, p_c .
- Critical temperature, T_c .
- Critical volume, V_c .

- Critical compressibility factor, Z_c .
- Boiling point temperature, T_b .
- Acentric factor, ω .
- Molecular weight, M .
- Specific gravity, γ .

Those physical properties needed for hydrocarbon phase behavior calculations are presented in Table 1-1 for a number of hydrocarbon and nonhydrocarbon components.

Another means of presenting the results of this experiment is shown in Figure 1-2, in which the pressure and temperature of the system are the independent parameters. Figure 1-2 shows a typical pressure/temperature diagram (p/T diagram) of a single-component system with solid lines that clearly represent three different phase boundaries: vapor-liquid, vapor-solid, and liquid-solid phase separation boundaries. As shown in the illustration, line AC terminates at the critical point (point C) and can be thought of as the dividing line between the areas where liquid and vapor exist. The curve is commonly called the *vapor-pressure curve* or the *boiling-point curve*. The corresponding pressure at any point on the curve is called the *vapor pressure*, p_v , with a corresponding temperature termed the *boiling-point temperature*.

The vapor-pressure curve represents the conditions of pressure and temperature at which two phases, vapor and liquid, can coexist in equilibrium. Systems represented by a point located below the vapor-pressure curve are composed only of the vapor phase. Similarly, points above the curve represent systems that exist in the liquid phase. These remarks can be conveniently summarized by the following expressions:

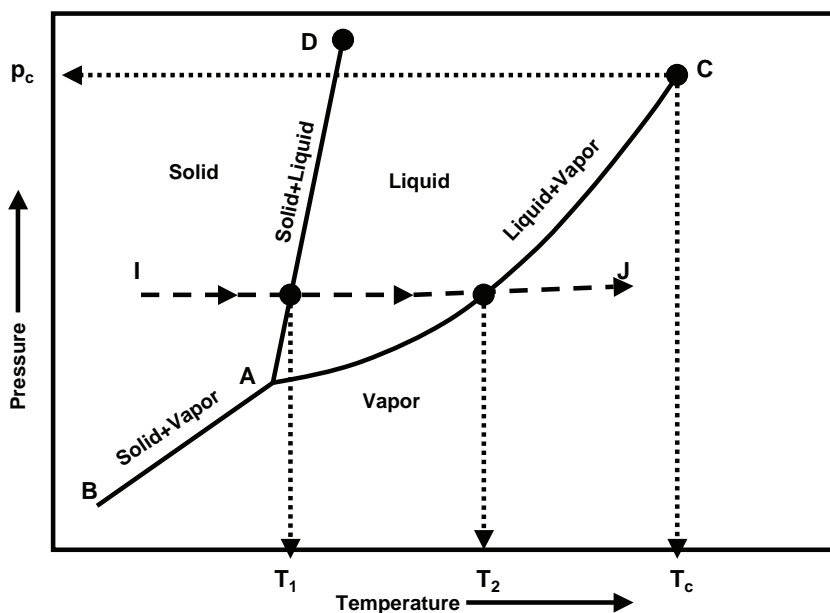


FIGURE 1-2 Typical pressure/temperature diagram for a single-component system.

If $p < p_v \rightarrow$ the system is entirely in the vapor phase;

If $p > p_v \rightarrow$ the system is entirely in the liquid phase;

If $p = p_v \rightarrow$ the vapor and liquid coexist in equilibrium;

where p is the pressure exerted on the pure substance. It should be pointed out that these expressions are valid only if the system temperature is below the critical temperature T_c of the substance.

The lower end of the vapor-pressure line is limited by the triple point A . This point represents the pressure and temperature at which solid, liquid, and vapor coexist under equilibrium conditions. The line AB is called the *sublimation pressure curve* of the solid phase, and it divides the area where solid exists from the area where vapor exists. Points above AB represent solid systems, and those below AB represent vapor systems. The line AD is called the *melting curve* or *fusion curve* and represents the change of melting point temperature with pressure. The fusion (melting) curve divides the solid phase area from the liquid phase area, with a corresponding temperature at any point on the curve termed the *fusion* or *melting-point temperature*. Note that the solid-liquid curve (fusion curve) has a steep slope, which indicates that the triple-point for most fluids is close to their normal melting-point temperatures. For pure hydrocarbons, the melting point generally increases with pressure so the slope of the line AD is positive. Water is the exception in that its melting point decreases with pressure, so in this case, the slope of the line AD is negative.

Each pure hydrocarbon has a p/T diagram similar to the one shown in Figure 1-2. Each pure component is characterized by its own vapor pressures, sublimation pressures, and critical values, which are different for each substance, but the general characteristics are similar. If such a diagram is available for a given substance, it is obvious that it could be used to predict the behavior of the substance as the temperature and pressure are changed. For example, in Figure 1-2, a pure component system is initially at a pressure and temperature represented by the point I , which indicates that the system exists in the solid phase state. As the system is heated at a constant pressure until point J is reached, no phase changes occur under this isobaric temperature increase and the phase remains in the solid state until the temperature reaches T_1 . At this temperature, which is identified as the melting point at this constant pressure, liquid begins to form and the temperature remains constant until all the solid has disappeared. As the temperature is further increased, the system remains in the liquid state until the temperature T_2 is reached. At T_2 (which is the boiling point at this pressure), vapor forms and again the temperature remains constant until all the liquid has vaporized. The temperature of this vapor system now can be increased until the point J is reached. It should be emphasized that, in the process just described, only the phase changes were considered. For example, in going from just above T_1 to just below T_2 , it was stated that only liquid was present and no phase change occurred. Obviously, the intensive properties of the liquid are changed as the temperature is increased. For example, the increase in temperature causes an increase in volume with a resulting decrease in the density. Similarly, other physical properties of the liquid are altered, but the properties of the system are those of a liquid and no other phases appear during this part of the isobaric temperature increase.

TABLE 1-1 *Physical Properties for Pure Components, Physical Constants*

Physical Constants											
	See Note No. →		A.	B.		C.	D.	Critical constants			
Number	Compound	Formula	Molar mass (molecular weight)	Boiling point, °F 14.696 psia	Vapor pressure, psia 100 °F	Freezing point, °F 14.696 psia	Refractive index, n_D 60 °F	Pressure, psia	Temperature, °F	Volume, ft ³ /lbm	Number
1	Methane	CH ₄	16.043	-258.73	(5000)*	-296.44*	1.00042*	666.4	-116.67	0.0988	1
2	Ethane	C ₂ H ₆	30.070	-127.49	(800)*	-297.04*	1.20971*	706.5	89.92	0.0783	2
3	Propane	C ₃ H ₈	44.097	-43.75	188.64	-305.73*	1.29480*	616.0	206.06	0.0727	3
4	Isobutane	C ₄ H ₁₀	58.123	10.78	72.581	-255.28	1.3245*	527.9	274.46	0.0714	4
5	n-Butane	C ₄ H ₁₀	58.123	31.08	51.706	-217.05	1.33588*	550.6	305.62	0.0703	5
6	Isopentane	C ₅ H ₁₂	72.150	82.12	20.445	-255.82	1.35631	490.4	369.10	0.0679	6
7	n-Pentane	C ₅ H ₁₂	72.150	96.92	15.574	-201.51	1.35992	488.6	385.8	0.0675	7
8	Neopentane	C ₅ H ₁₂	72.150	49.10	36.69	2.17	1.342*	464.0	321.13	0.0673	8
9	n-Hexane	C ₆ H ₁₄	86.177	155.72	4.9597	-139.58	1.37708	436.9	453.6	0.0688	9
10	2-Methylpentane	C ₆ H ₁₄	86.177	140.47	6.769	-244.62	1.37387	436.6	435.83	0.0682	10
11	3-Methylpentane	C ₆ H ₁₄	86.177	145.89	6.103	—	1.37888	453.1	448.4	0.0682	11
12	Neohexane	C ₆ H ₁₄	86.177	121.52	9.859	-147.72	1.37126	446.8	420.13	0.0667	12
13	2,3-Dimethylbutane	C ₆ H ₁₄	86.177	136.36	7.406	-199.38	1.37730	453.5	440.29	0.0665	13
14	n-Heptane	C ₇ H ₁₆	100.204	209.16	1.620	-131.05	1.38989	396.8	512.7	0.0691	14
15	2-Methylhexane	C ₇ H ₁₆	100.204	194.09	2.272	-180.89	1.38714	396.5	495.00	0.0673	15
16	3-Methylhexane	C ₇ H ₁₆	100.204	197.33	2.131	—	1.39091	408.1	503.80	0.0646	16
17	3-Ethylpentane	C ₇ H ₁₆	100.204	200.25	2.013	-181.48	1.39566	419.3	513.39	0.0665	17
18	2,2-Dimethylpentane	C ₇ H ₁₆	100.204	174.54	3.494	-190.86	1.38446	402.2	477.23	0.0665	18
19	2,4-Dimethylpentane	C ₇ H ₁₆	100.204	176.89	3.293	-182.63	1.38379	396.9	475.95	0.0668	19
20	3,3-Dimethylpentane	C ₇ H ₁₆	100.204	186.91	2.774	-210.01	1.38564	427.2	505.87	0.0662	20
21	Triptane	C ₇ H ₁₆	100.204	177.58	3.375	-12.81	1.39168	428.4	496.44	0.0636	21
22	n-Octane	C ₈ H ₁₈	114.231	258.21	0.53694	-70.18	1.39956	360.7	564.22	0.0690	22
23	Diisobutyl	C ₈ H ₁₈	114.231	228.39	1.102	-132.11	1.39461	360.6	530.44	0.0676	23
24	Isooctane	C ₈ H ₁₈	114.231	210.63	1.709	-161.27	1.38624	372.4	519.46	0.0656	24
25	n-Nonane	C ₉ H ₂₀	128.258	303.47	0.17953	-64.28	1.40746	331.8	610.68	0.0684	25
26	n-Decane	C ₁₀ H ₂₂	142.285	345.48	0.06088	-21.36	1.41385	305.2	652.0	0.0679	26
27	Cyclopentane	C ₅ H ₁₀	70.134	120.65	9.915	-136.91	1.40896	653.8	461.2	0.0594	27
28	Methylcyclopentane	C ₆ H ₁₂	84.161	161.25	4.503	-224.40	1.41210	548.9	499.35	0.0607	28
29	Cyclohexane	C ₆ H ₁₂	84.161	177.29	3.266	43.77	1.42862	590.8	536.6	0.0586	29
30	Methylcyclohexane	C ₇ H ₁₄	98.188	213.68	1.609	-195.87	1.42538	503.5	570.27	0.0600	30

31	Ethene(Ethylene)	C ₂ H ₄	28.054	-154.73	(1400)*	-272.47*	(1.228)*	731.0	48.54	0.0746	31
32	Propene(Propylene)	C ₃ H ₆	42.081	-53.84	227.7	-301.45*	1.3130*	668.6	197.17	0.0689	32
33	1-Butene(Butylene)	C ₄ H ₈	56.108	20.79	62.10	-301.63*	1.3494*	583.5	295.48	0.0685	33
34	cis-2-Butene	C ₄ H ₈	56.108	38.69	45.95	-218.06	1.3665*	612.1	324.37	0.0668	34
35	trans-2-Butene	C ₄ H ₈	56.108	33.58	49.87	-157.96	1.3563*	587.4	311.86	0.0679	35
36	Isobutene	C ₄ H ₈	56.108	19.59	63.02	-220.65	1.3512*	580.2	292.55	0.0682	36
37	1-Pentene	C ₅ H ₁₀	70.134	85.93	19.12	-265.39	1.37426	511.8	376.93	0.0676	37
38	1,2-Butadiene	C ₄ H ₆	54.092	51.53	36.53	-213.16	—	(653.)*	(340.)*	(0.065)*	38
39	1,3-Butadiene	C ₄ H ₆	54.092	24.06	59.46	-164.02	1.3975*	627.5	305.	0.0654	39
40	Isoprene	C ₅ H ₈	68.119	93.31	16.68	-230.73	1.42498	(558.)*	(412.)*	(0.065)*	40
41	Acetylene	C ₂ H ₂	26.038	-120.49*	—	-114.5*	—	890.4	95.34	0.0695	41
42	Benzene	C ₆ H ₆	78.114	176.18	3.225	41.95	1.50396	710.4	552.22	0.0531	42
43	Toluene	C ₇ H ₈	92.141	231.13	1.033	-139.00	1.49942	595.5	605.57	0.0550	43
44	Ethylbenzene	C ₈ H ₁₀	106.167	277.16	0.3716	-138.966	1.49826	523.0	651.29	0.0565	44
45	o-Xylene	C ₈ H ₁₀	106.167	291.97	0.2643	-13.59	1.50767	541.6	674.92	0.0557	45
46	m-Xylene	C ₈ H ₁₀	106.167	282.41	0.3265	-54.18	1.49951	512.9	651.02	0.0567	46
47	p-Xylene	C ₈ H ₁₀	106.167	281.07	0.3424	55.83	1.49810	509.2	649.54	0.0570	47
48	Styrene	C ₈ H ₈	104.152	293.25	0.2582	-23.10	1.54937	587.8	(703.)*	0.0534	48
49	Isopropylbenzene	C ₉ H ₁₂	120.194	306.34	0.1884	-140.814	1.49372	465.4	676.3	0.0572	49
50	Methyl alcohol	CH ₄ O	32.042	148.44	4.629	-143.79	1.33034	1174.	463.08	0.0590	50
51	Ethyl alcohol	C ₂ H ₆ O	46.069	172.90	2.312	-173.4	1.36346	890.1	465.39	0.0581	51
52	Carbon monoxide	CO	28.010	-312.68	—	-337.00*	1.00036*	507.5	-220.43	0.0532	52
53	Carbon dioxide	CO ₂	44.010	-109.257*	—	-69.83*	1.00048*	1071.	87.91	0.0344	53
54	Hydrogen sulfide	H ₂ S	34.08	-76.497	394.59	-121.88*	1.00060*	1300.	212.45	0.0461	54
55	Sulfur dioxide	SO ₂	64.06	14.11	85.46	-103.86*	1.00062*	1143.	315.8	0.0305	55
56	Ammonia	NH ₃	17.0305	-27.99	211.9	-107.88*	1.00036*	1646.	270.2	0.0681	56
57	Air	N ₂ +O ₂	28.9625	-317.8	—	—	1.00028*	546.9	-221.31	0.0517	57
58	Hydrogen	H ₂	2.0159	-422.955*	—	-435.26*	1.00013*	188.1	-399.9	0.0165	58
59	Oxygen	O ₂	31.9988	-297.332*	—	-361.820*	1.00027*	731.4	-181.43	0.0367	59
60	Nitrogen	N ₂	28.0134	-320.451	—	-346.00*	1.00028*	493.1	-232.51	0.0510	60
61	Chlorine	Cl ₂	70.906	-29.13	157.3	-149.73*	1.3878*	1157.	290.75	0.0280	61
62	Water	H ₂ O	18.0153	212.000*	0.9501	32.00	1.33335	3198.8	705.16	0.04975	62
63	Helium	He	4.0026	-452.09	—	—	1.00003*	32.99	-450.31	0.2300	63
64	Hydrogen chloride	HCl	36.461	-121.27	906.71	-173.52*	1.00042*	1205.	124.77	0.0356	64

TABLE 1-1 *continued*

Physical Constants

Number	See Note No. -> Compound	K.					L. Heat of vaporization 14,696 psia at boiling point, Btu/lbm	M. Air required for combustion ideal gas ft ³ (air)/ft ³ (gas)	Flammability		ASTM		Number
		Heating value, 60°F							limits, vol %		octane		
		Net		Gross					in		number		
		Btu/ft ³ Ideal gas, 14,696 psia	Btu/lbm Liquid	Btu/ft ³ Ideal gas, 14,696 psia	Btu/lbm Liquid	Btu/gal. Liquid			Lower	Higher	Motor method D-357	Research method D-908	
1	Methane	909.4	—	1010.0	—	—	219.45	9.548	5.0	15.0	—	—	1
2	Ethane	1618.7	20277.*	1769.6	22181.*	65869.*	211.14	16.710	2.9	13.0	+0.05	+1.6*	2
3	Propane	2314.9	19757.*	2516.1	21489.*	90830.*	183.01	23.871	2.0	9.5	97.1	+1.6*	3
4	Isobutane	3000.4	19437.*	3251.9	21079.*	98917.*	157.23	31.032	1.8	8.5	97.6	+0.1*	4
5	n-Butane	3010.8	19494.*	3262.3	21136.*	102911.*	165.93	31.032	1.5	9.0	89.6*	93.8*	5
6	Isopentane	3699.0	19303.	4000.9	20891.	108805.	147.12	38.193	1.3	8.0	90.3	92.3	6
7	n-Pentane	3706.9	19335.	4008.9	20923.	110091.	153.57	38.193	1.4	8.3	82.6*	81.7*	7
8	Neopentane	3682.9	19235.*	3984.7	20822.*	103577.*	135.58	38.193	1.3	7.5	80.2	85.5	8
9	n-Hexane	4403.8	19232.	4755.9	20783.	115021.	143.94	45.355	1.1	7.7	26.0	24.8	9
10	2-Methylpentane	4395.2	19202.	4747.3	20753.	113822.	138.45	45.355	1.18	7.0	73.5	73.4	10
11	3-Methylpentane	4398.2	19213.	4750.3	20764.	115813.	140.05	45.355	1.2	7.7	74.3	74.5	11
12	Neohexane	4384.0	19163.	4736.2	20714.	112916.	131.23	45.355	1.2	7.0	93.4	91.8	12
13	2,3-Dimethylbutane	4392.9	19195.	4745.0	20746.	115246.	136.07	45.355	1.2	7.0	94.3	+0.3	13
14	n-Heptane	5100.0	19155.	5502.5	20679.	118648.	136.00	52.516	1.0	7.0	0.0	0.0	14
15	2-Methylhexane	5092.2	19133.	5494.6	20657.	117644.	131.58	52.516	1.0	7.0	46.4	42.4	15
16	3-Methylhexane	5096.0	19146.	5498.6	20671.	119197.	132.10	52.516	(1.01)	(6.6)	55.8	52.0	16
17	3-Ethylpentane	5098.3	19154.	5500.7	20679.	121158.	132.82	52.516	(1.00)	(6.5)	69.3	65.0	17
18	2,2-Dimethylpentane	5079.6	19095.	5481.9	20620.	116606.	125.12	52.516	(1.09)	(6.8)	95.6	92.8	18
19	2,4-Dimethylpentane	5084.2	19111.	5486.7	20635.	116526.	126.57	52.516	(1.08)	(6.8)	83.8	83.1	19
20	3,3-Dimethylpentane	5086.4	19119.	5488.8	20643.	120080.	127.20	52.516	(1.04)	(7.0)	86.6	80.8	20
21	Triptane	5081.2	19103.	5483.5	20628.	119451.	124.21	52.516	(1.08)	(6.8)	+0.1	+1.8	21
22	n-Octane	5796.1	19096.	6248.9	20601.	121422.	129.52	59.677	0.8	6.5	—	—	22
23	Diisobutyl	5780.5	19047.	6233.5	20552.	119586.	122.83	59.677	(0.92)	(6.3)	55.7	55.2	23
24	Isooctane	5778.8	19063.	6231.7	20568.	119389.	112.94	59.677	0.95	6.0	100.0	100.0	24
25	n-Nonane	6493.2	19054.	6996.5	20543.	123634.	124.36	66.839	0.7	5.6	—	—	25
26	n-Decane	7189.6	19018.	7742.9	20494.	125448.	119.65	74.000	0.7	5.4	—	—	26
27	Cyclopentane	3512.1	18825.	3763.7	20186.	126304.	167.33	35.806	(1.48)	(8.3)	84.9*	+0.1	27
28	Methylcyclopentane	4199.4	18771.	4501.2	20132.	126467.	148.54	42.968	1.0	8.35	80.0	91.3	28
29	Cyclohexane	4179.7	18675.	4481.7	20036.	130873.	153.03	42.968	1.2	8.35	77.2	83.0	29
30	Methylcyclohexane	4863.6	18640.	5215.9	20002.	129071.	136.30	50.129	1.1	6.7	71.1	74.8	30

31	Ethene(Ethylene)	1499.1	—	1599.8	—	—	207.41	14.323	2.7	36.0	75.6	+0.03	31
32	Propene(Propylene)	2181.8	(19858.)	2332.7	(21208.)	(92113.)	188.19	21.484	2.0	11.7	84.9	+0.2	32
33	1-Butene(Butylene)	2878.7	19309.*	3079.9	20670.*	103582.*	167.96	28.645	1.6	10.	80.8*	97.4	33
34	cis-2-Butene	2871.0	19241.*	3072.2	20602.*	107724.*	178.89	28.645	1.6	10.	83.5	100.0	34
35	trans-2-Butene	2866.8	19221.*	3068.0	20582.*	104666.*	174.37	28.645	1.6	10.	—	—	35
36	Isobutene	2859.9	19182.*	3061.1	20543.*	102830.*	169.47	28.645	1.6	10.	—	—	36
37	1-Pentene	3575.0	19184.	3826.5	20545.	110602.	154.48	35.806	1.3	10.	77.1	90.9	37
38	1,2-Butadiene	2789.0	19378.*	2939.9	20437.*	112111.*	191.88	26.258	(1.62)	(10.3)	—	—	38
39	1,3-Butadiene	2729.0	18967.*	2879.9	20025.*	104717.*	185.29	26.258	2.0	12.5	—	—	39
40	Isoprene	3410.8	18832.	3612.1	19953.	114141.	163.48	33.419	(1.12)	(8.5)	81.0	99.1	40
41	Acetylene	1423.2	(20887.)	1473.5	(21613.)	(75204.)	151.90	11.935	1.5	100.	—	—	41
42	Benzene	3590.9	17256.	3741.8	17989.	132651.	169.24	35.806	1.2	8.0	+2.8	—	42
43	Toluene	4273.6	17421.	4475.0	18250.	132661.	154.83	42.968	1.2	7.1	+0.3	+5.8	43
44	Ethylbenzene	4970.5	17593.	5222.2	18492.	134387.	144.02	50.129	1.0	8.0	97.9	+0.8	44
45	o-Xylene	4958.2	17544.	5209.9	18444.	136036.	149.10	50.129	1.0	7.6	100.0	—	45
46	m-Xylene	4956.3	17541.	5207.9	18440.	133559.	147.24	50.129	1.0	7.0	+2.8	+4.0	46
47	p-Xylene	4957.1	17545.	5208.8	18444.	133131.	145.71	50.129	1.0	7.0	+1.2	+3.4	47
48	Styrene	4829.8	17414.	5031.1	18147.	137841.	152.85	47.742	1.1	8.0	+0.2	+3.5*	48
49	Isopropylbenzene	5660.9	17709.	5962.8	18662.	134792.	134.24	57.290	0.8	6.5	99.3	+2.1	49
50	Methyl alcohol	766.1	8559.	866.7	9751.	64731.	462.58	7.161	5.5	44.0	—	—	50
51	Ethyl alcohol	1448.1	11530.	1599.1	12770.	84539.	359.07	14.323	3.28	19.0	—	—	51
52	Carbon monoxide	320.5	—	320.5	—	—	92.77	2.387	12.50	74.20	—	—	52
53	Carbon dioxide	0.0	—	0.0	—	—	246.47*	—	—	—	—	—	53
54	Hydrogen sulfide	586.8	6337.*	637.1	6897.*	46086.*	235.63	7.161	4.30	45.50	—	—	54
55	Sulfur dioxide	0.0	—	0.0	—	—	167.22	—	—	—	—	—	55
56	Ammonia	359.0	—	434.4	—	—	589.48	3.581	15.50	27.00	—	—	56
57	Air	0.0	—	0.0	—	—	88.20	—	—	—	—	—	57
58	Hydrogen	273.8	—	324.2	—	—	192.74	2.387	4.00	74.20	—	—	58
59	Oxygen	0.0	—	0.0	—	—	91.59	—	—	—	—	—	59
60	Nitrogen	0.0	—	0.0	—	—	85.59	—	—	—	—	—	60
61	Chlorine	—	—	—	—	—	123.75	—	—	—	—	—	61
62	Water	0.0	*	*	0.0	0.0	970.18	—	—	—	—	—	62
63	Helium	0.0	—	0.0	—	—	—	—	—	—	—	—	63
64	Hydrogen chloride	—	—	—	—	—	190.43	—	—	—	—	—	64

Note: Numbers in this table do not have accuracies greater than 1 part in 1000; in some cases extra digits have been added to calculated values to achieve consistency or to permit recalculation of experimental values.

Source: GSPA Engineers Data Book, 10th ed. Tulsa, OK: Gas Processors Suppliers Association, 1987. Courtesy of the Gas Processors Suppliers Association.

A method that is particularly convenient for plotting the vapor pressure as a function of temperature for pure substances is shown in Figure 1–3. The chart is known as a Cox chart. Note that the vapor pressure scale is logarithmic, while the temperature scale is entirely arbitrary.

EXAMPLE 1–1

A pure propane is held in a laboratory cell at 80°F and 200 psia. Determine the “existence state” (i.e., as a gas or liquid) of the substance.

SOLUTION

From a Cox chart, the vapor pressure of propane is read as $p_v = 150$ psi, and because the laboratory cell pressure is 200 psi (i.e., $p > p_v$), this means that the laboratory cell contains a liquefied propane.

The vapor pressure chart as presented in Figure 1–3 allows a quick estimation of the vapor pressure p_v of a pure substance at a specific temperature. For computer applications, however, an equation is more convenient. Lee and Kesler (1975) proposed the following generalized vapor pressure equation:

$$p_v = p_c \exp(A + \omega B) \quad (1-3)$$

with

$$A = 5.92714 - \frac{6.09648}{T_r} - 1.2886 \ln(T_r) + 0.16934(T_r)^6 \quad (1-4)$$

$$B = 15.2518 - \frac{15.6875}{T_r} - 13.4721 \ln(T_r) + 0.4357(T_r)^6 \quad (1-5)$$

The term T_r , called the *reduced temperature*, is defined as the ratio of the absolute system temperature to the critical temperature of the fraction, or

$$T_r = \frac{T}{T_c}$$

where

T_r = reduced temperature

T = substance temperature, °R

T_c = critical temperature of the substance, °R

p_c = critical pressure of the substance, psia

ω = acentric factor of the substance

The acentric factor ω was introduced by Pitzer (1955) as a correlating parameter to characterize the centricity or nonsphericity of a molecule, defined by the following expression:

$$\omega = -\log \left(\frac{p_v}{p_c} \right)_{T=0.7T_c} - 1 \quad (1-6)$$

where

p_c = critical pressure of the substance, psia

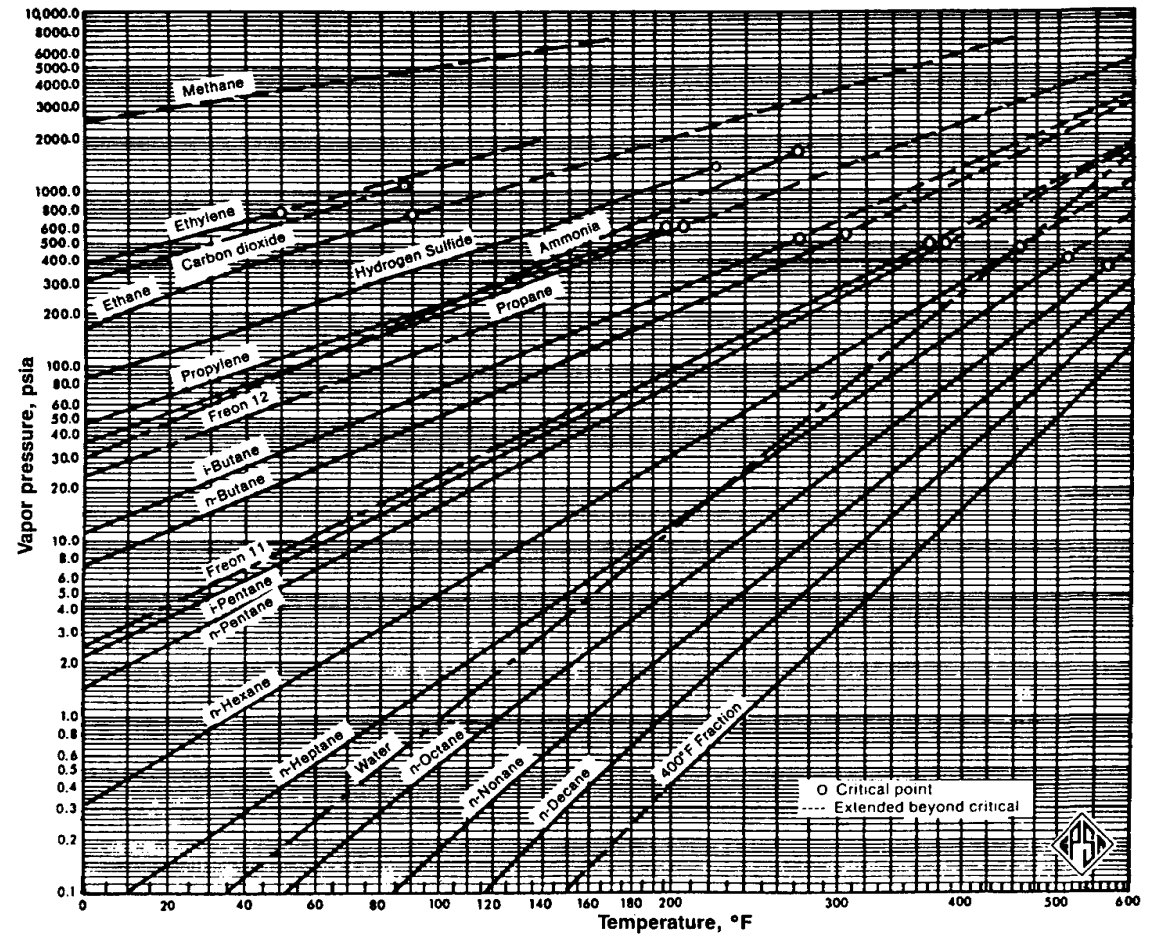


FIGURE 1-3 Vapor pressure chart for hydrocarbon components.

Source: GPSA Engineering Data Book, 10th ed. Tulsa, OK: Gas Processors Suppliers Association, 1987. Courtesy of the Gas Processors Suppliers Association.

p_v = vapor pressure of the substance at a temperature equal to 70% of the substance critical temperature (i.e., $T = 0.7T_c$), psia

The acentric factor frequently is used as a third parameter in corresponding states and equation-of-state correlations. Values of the acentric factor for pure substances are tabulated in Table 1-1.

EXAMPLE 1-2

Calculate the vapor pressure of propane at 80°F by using the Lee and Kesler correlation.

SOLUTION

Obtain the critical properties and the acentric factor of propane from Table 1-1:

$$T_c = 666.01^\circ\text{R}$$

$$p_c = 616.3 \text{ psia}$$

$$\omega = 0.1522$$

Calculate the reduced temperature:

$$T_r = \frac{T}{T_c} = \frac{540}{666.01} = 0.81108$$

Solve for the parameters A and B by applying equations (1-4) and (1-5), respectively, to give

$$A = 5.92714 - \frac{6.09648}{T_r} - 1.2886 \ln(T_r) + 0.16934(T_r)^6$$

$$A = 5.92714 - \frac{6.09648}{0.81108} - 1.2886 \ln(0.81108) + 0.16934(0.81108)^6 = -1.273590$$

$$B = 15.2518 - \frac{15.6875}{T_r} - 13.4721 \ln(T_r) + 0.4357(T_r)^6$$

$$B = 15.2518 - \frac{15.6875}{0.81108} - 13.4721 \ln(0.81108) + 0.4357(0.81108)^6 = -1.147045$$

Solve for p_v by applying equation (1-3):

$$p_v = p_c \exp(A + \omega B)$$

$$p_v = (616.3) \exp[-1.27359 + 0.1572(-1.147045)] = 145 \text{ psia}$$

The densities of the saturated phases of a pure component (i.e., densities of the coexisting liquid and vapor) may be plotted as a function of temperature, as shown in Figure 1-4. Note that, for increasing temperature, the density of the saturated liquid is decreasing, while the density of the saturated vapor increases. At the critical point C , the densities of vapor and liquid converge at the *critical density* of the pure substance, that is, ρ_c . At this critical point C , all other properties of the phases become identical, such as viscosity, weight, and density.

Figure 1-4 illustrates a useful observation, the law of the rectilinear diameter, which states that the arithmetic average of the densities of the liquid and vapor phases is a linear function of the temperature. The straight line of average density versus temperature makes an easily defined intersection with the curved line of densities. This intersection

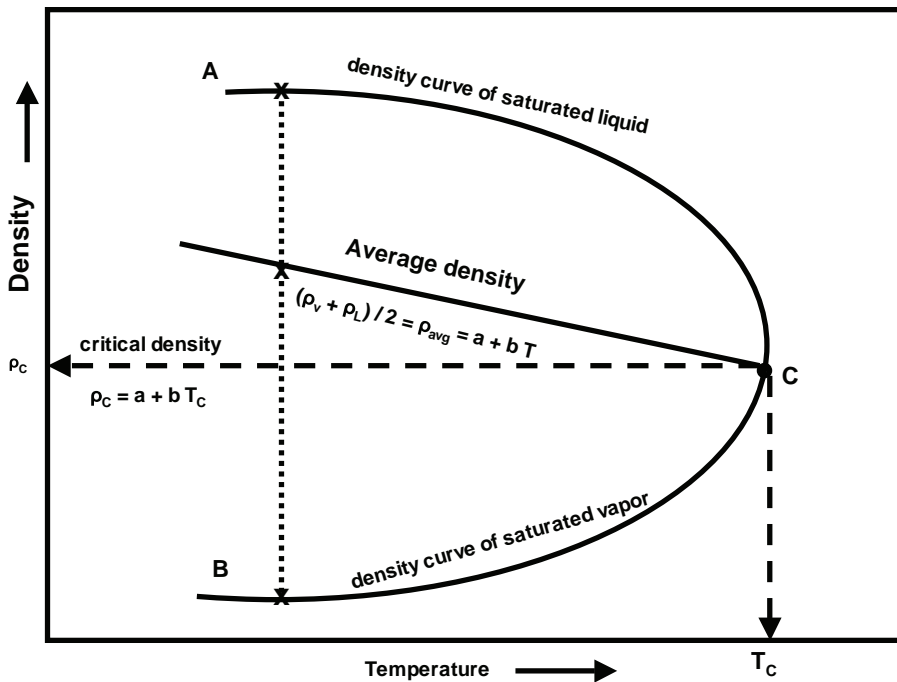


FIGURE 1-4 Typical temperature/density diagram.

then gives the critical temperature and density. Mathematically, this relationship is expressed as follows:

$$\frac{\rho_v + \rho_L}{2} = \rho_{\text{avg}} = a + bT \quad (1-7)$$

where

ρ_v = density of the saturated vapor, lb/ft³

ρ_L = density of the saturated liquid, lb/ft³

ρ_{avg} = arithmetic average density, lb/ft³

T = temperature, °R

a, b = intercept and slope of the straight line

Since, at the critical point, ρ_v and ρ_L are identical, equation (1-7) can be expressed in terms of the critical density as follows:

$$\rho_c = a + bT_c \quad (1-8)$$

where ρ_c = critical density of the substance, lb/ft³. Combining equation (1-7) with (1-8) and solving for the critical density gives

$$\rho_c = \left[\frac{a + bT}{a + bT_c} \right] \rho_{\text{avg}}$$

This density-temperature diagram is useful in calculating the critical volume from density data. The experimental determination of the critical volume sometimes is difficult, since it requires the precise measurement of a volume at a high temperature and pressure.

However, it is apparent that the straight line obtained by plotting the average density versus temperature intersects the critical temperature at the critical density. The molal critical volume is obtained by dividing the molecular weight by the critical density:

$$V_c = \frac{M}{\rho_c}$$

where

V_c = critical volume of pure component, $\text{ft}^3/\text{lb}_m - \text{mol}$

M = molecular weight, $\text{lb}_m/\text{lb}_m - \text{mol}$

ρ_c = critical density, lb_m/ft^3

Figure 1-5 shows the saturated densities for a number of fluids of interest to the petroleum engineer. Note that, for each pure substance, the upper curve is termed the *saturated liquid density curve*, while the lower curve is labeled the *saturated vapor density curve*. Both curves meet and terminate at the critical point represented by a “dot” in the diagram.

EXAMPLE 1-3

Calculate the saturated liquid and gas densities of n-butane at 200°F.

SOLUTION

From Figure 1-5, read both values of liquid and vapor densities at 200°F to give

Liquid density $\rho_L = 0.475 \text{ gm/cm}^3$

Vapor density $\rho_v = 0.035 \text{ gm/cm}^3$

The density-temperature diagram also can be used to determine the state of a single-component system. Suppose the *overall* density of the system, ρ_o , is known at a given temperature. If this overall density is less than or equal to ρ_v , it is obvious that the system is composed entirely of vapor. Similarly, if the overall density ρ_o is greater than or equal to ρ_L , the system is composed entirely of liquid. If, however, the overall density is between ρ_L and ρ_v , it is apparent that both liquid and vapor are present. To calculate the weights of liquid and vapor present, the following volume and weight balances are imposed:

$$m_L + m_v = m_t$$

$$V_L + V_v = V_t$$

where

m_L , m_v , and m_t = the mass of the liquid, vapor, and total system, respectively

V_L , V_v , and V_t = the volume of the liquid, vapor, and total system, respectively

Combining the two equations and introducing the density into the resulting equation gives

$$\frac{m_t - m_v}{\rho_L} + \frac{m_v}{\rho_v} = V_t \quad (1-9)$$

EXAMPLE 1-4

Ten pounds of a hydrocarbon are placed in a 1 ft^3 vessel at 60°F. The densities of the coexisting liquid and vapor are known to be 25 lb/ft^3 and 0.05/ ft^3 , respectively, at this temperature. Calculate the weights and volumes of the liquid and vapor phases.

SOLUTION

Step 1 Calculate the density of the overall system:

$$\rho_t = \frac{m_t}{V_t} = \frac{10}{1.0} = 10 \text{ lb/ft}^3$$

Step 2 Since the overall density of the system is between the density of the liquid and the density of the gas, the system must be made up of both liquid and vapor.

Step 3 Calculate the weight of the vapor from equation (1-9):

$$\frac{10 - m_v}{25} + \frac{m_v}{0.05} = 1$$

Solving the above equation for m_v , gives

$$m_v = 0.030 \text{ lb}$$

$$m_L = 10 - m_v = 10 - 0.03 = 9.97 \text{ lb}$$

Step 4 Calculate the volume of the vapor and liquid phases:

$$V_v = \frac{m_v}{\rho_v} = \frac{0.03}{0.05} = 0.6 \text{ ft}^3$$

$$V_L = V_t - V_v = 1 - 0.6 = 0.4 \text{ ft}^3$$

EXAMPLE 1-5

A utility company stored 58 million lbs, that is $m_t = 58,000,000 \text{ lb}$, of propane in a washed-out underground salt cavern of volume 480,000 bbl ($V_t = 480,000 \text{ bbl}$) at a temperature of 110°F. Estimate the weight and volume of liquid propane in storage in the cavern.

SOLUTION

Step 1 Calculate the volume of the cavern in ft^3 :

$$V_t = (480,000)(5.615) = 2,695,200 \text{ ft}^3$$

Step 2 Calculate the total density of the system:

$$\rho_t = \frac{m_t}{V_t} = \frac{58,000,000}{2,695,200} = 21.52 \text{ lb/ft}^3$$

Step 3 Determine the saturated densities of propane from the density chart of Figure 1-5 at 110°F:

$$\rho_L = 0.468 \text{ gm/cm}^3 = (0.468)(62.4) = 29.20 \text{ lb/ft}^3$$

$$\rho_v = 0.03 \text{ gm/cm}^3 = (0.03)(62.4) = 1.87 \text{ lb/ft}^3$$

Step 4 Test for the existing phases. Since

$$\rho_v < \rho_t < \rho_L$$

$$1.87 < 21.52 < 29.20$$

both liquid and vapor are present.

Step 5 Solve for the weight of the vapor phase by applying equation (1-9)

$$\frac{58,000,000 - m_v}{29.20} + \frac{m_v}{1.87} = 2,695,200$$

$$m_v = 1,416,345 \text{ lb}$$

$$V_v = \frac{m_v}{\rho} = \frac{1,416,345}{1.87} = 757,404 \text{ ft}^3$$

Step 6 Solve for the volume and weight of propane:

$$V_L = V_t - V_v = 2,695,200 - 757,404 = 1,937,796 \text{ ft}^3 \text{ (72\% of total volume);}$$

$$m_L = m_t - m_v = 58,000,000 - 1,416,345 = 56,583,655 \text{ lb (98\% of total weight).}$$

The example demonstrates the simplest case of phase separation, that of a pure component. In general, petroleum engineers are concerned with calculating phase separations of complex mixtures representing crude oil, natural gas, and condensates.

Rackett (1970) proposed a simple generalized equation for predicting the saturated liquid density, ρ_L , of pure compounds. Rackett expressed the relation in the following form:

$$\rho_L = \frac{Mp_c}{RT_c Z_c^a} \quad (1-10)$$

with the exponent a given as

$$a = 1 + (1 - T_r)^{2/7}$$

where

M = molecular weight of the pure substance

p_c = critical pressure of the substance, psia

T_c = critical temperature of the substance, °R

Z_c = critical gas compressibility factor;

R = gas constant, $10.73 \text{ ft}^3 \text{ psia/lb-mole, } ^\circ\text{R}$

$T_r = \frac{T}{T_c}$, reduced temperature

T = temperature, °R

Spencer and Danner (1973) modified Rackett's correlation by replacing the critical compressibility factor Z_c in equation (1-9) with a parameter called *Rackett's compressibility factor*, Z_{RA} , that is a unique constant for each compound. The authors proposed the following modification of the Rackett equation:

$$\rho_L = \frac{Mp_c}{RT_c (Z_{RA})^a} \quad (1-11)$$

with the exponent a as defined previously by

$$a = 1 + (1 + T_r)^{2/7}$$

The values of Z_{RA} are given in Table 1-2 for selected components.

If a value of Z_{RA} is not available, it can be estimated from a correlation proposed by Yamada and Gunn (1973) as

$$Z_{RA} = 0.29056 - 0.08775\omega \quad (1-12)$$

where ω is the acentric factor of the compound.

TABLE 1-2 Values of Z_{RA} for Selected Pure Components

Carbon dioxide	0.2722	n-pentane	0.2684
Nitrogen	0.2900	n-hexane	0.2635
Hydrogen sulfide	0.2855	n-heptanes	0.2604
Methane	0.2892	i-octane	0.2684
Ethane	0.2808	n-octane	0.2571
Propane	0.2766	n-nonane	0.2543
i-butane	0.2754	n-decane	0.2507
n-butane	0.2730	n-undecane	0.2499
i-Pentane	0.2717		

EXAMPLE 1-6

Calculate the saturated liquid density of propane at 160°F by using (1) the Rackett correlation and (2) the modified Rackett equation.

SOLUTION

Find the critical properties of propane from Table 1-1, to give

$T_c = 666.06^\circ\text{R}$
 $p_c = 616.0 \text{ psia}$
 $M = 44.097$
 $V_c = 0.0727 \text{ ft}^3/\text{lb}$

Calculate Z_c by applying the real gas equation of state:

$$Z = \frac{pv}{nRT} = \frac{pv}{(m / M)RT}$$

or

$$Z = \frac{pVM}{RT}$$

where v = substance volume, ft^3 , and V = substance volume, ft^3/lb , at the critical point:

$$Z_c = \frac{p_c V_c M}{RT_c}$$
$$Z_c = \frac{(616.0)(0.0727)(44.097)}{(10.73)(666.06)} = 0.2763$$
$$T_r = \frac{T}{T_c} = \frac{160 + 460}{666.06} = 0.93085$$

For the Rackett correlation, solve for the saturated liquid density by applying the Rackett equation, equation (1-10):

$$a = 1 + (1 - T_r)^{2/7} = 1 + (1 - 0.93085)^{2/7} = 1.4661$$
$$\rho_L = \frac{Mp_c}{RT_c Z_c^a}$$

$$\rho_L = \frac{(44.097)(616.0)}{(10.73)(666.06)(0.2763)^{1.4661}}$$

For the modified Rackett equation, from Table 1–2, find the Rackett compressibility factor $Z_{RA} = 0.2766$; then, the modified Rackett equation, equation (1–11); gives

$$\rho_L = \frac{(44.097)(616.0)}{(10.73)(666.06)(0.2766)^{1.4661}} = 25.01 \text{ lb/ft}^3$$

Two-Component Systems

A distinguishing feature of the single-component system is that, at a fixed temperature, two phases (vapor and liquid) can exist in equilibrium at only one pressure; this is the vapor pressure. For a binary system, two phases can exist in equilibrium at various pressures at the same temperature. The following discussion concerning the description of the phase behavior of a two-component system involves many concepts that apply to the more complex multicomponent mixtures of oils and gases.

An important characteristic of binary systems is the variation of their thermodynamic and physical properties with the composition. Therefore, it is necessary to specify the composition of the mixture in terms of mole or weight fractions. It is customary to designate one of the components as the more volatile component and the other the less volatile component, depending on their relative vapor pressure at a given temperature.

Suppose that the examples previously described for a pure component are repeated, but this time we introduce into the cylinder a binary mixture of a known overall composition. Consider that the initial pressure p_1 exerted on the system, at a fixed temperature of T_1 , is low enough that the entire system exists in the vapor state. This initial condition of pressure and temperature acting on the mixture is represented by point 1 on the p/V diagram of Figure 1–6. As the pressure is increased isothermally, it reaches point 2, at which an infinitesimal amount of liquid is condensed. The pressure at this point is called the *dew-point pressure*, p_d , of the mixture. It should be noted that, at the dew-point pressure, the composition of the vapor phase is equal to the overall composition of the binary mixture. As the total volume is decreased by forcing the piston inside the cylinder, a noticeable increase in the pressure is observed as more and more liquid is condensed. This condensation process is continued until the pressure reaches point 3, at which traces of gas remain. At point 3, the corresponding pressure is called the *bubble-point pressure*, p_b . Because, at the bubble point, the gas phase is only of infinitesimal volume, the composition of the liquid phase therefore is identical with that of the whole system. As the piston is forced further into the cylinder, the pressure rises steeply to point 4 with a corresponding decreasing volume.

Repeating the previous examples at progressively increasing temperatures, a complete set of isotherms is obtained on the p/V diagram of Figure 1–7 for a binary system consisting of n-pentane and n-heptane. The bubble-point curve, as represented by line AC , represents the locus of the points of pressure and volume at which the first bubble of gas is formed. The dew-point curve (line BC) describes the locus of the points of pressure and volume at which the first droplet of liquid is formed. The two curves meet at the critical

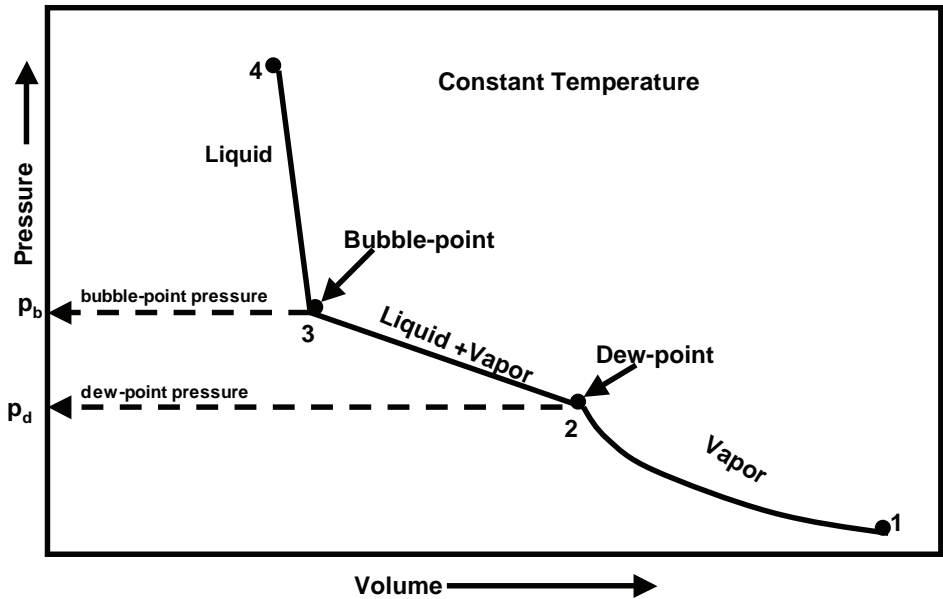


FIGURE 1-6 Pressure/volume isotherm for a two-component system.

point (point C). The critical pressure, temperature, and volume are given by p_c , T_c , and V_c respectively. Any point within the phase envelope (line ACB) represents a system consisting of two phases. Outside the phase envelope, only one phase can exist.

If the bubble-point pressure and dew-point pressure for the various isotherms on a p/V diagram are plotted as a function of temperature, a p/T diagram similar to that shown in Figure 1-8 is obtained. Figure 1-8 indicates that the pressure/temperature relationships no longer can be represented by a simple vapor pressure curve, as in the case of a single-component system, but take on the form illustrated in the figure by the phase envelope ACB. The dashed lines within the phase envelope are called *quality lines*; they describe the pressure and temperature conditions of equal volumes of liquid. Obviously, the bubble-point curve and the dew-point curve represent 100% and 0% liquid, respectively.

Figure 1-9 demonstrates the effect of changing the composition of the binary system on the shape and location of the phase envelope. Two of the lines shown in the figure represent the vapor-pressure curves for methane and ethane, which terminate at the critical point. Ten phase boundary curves (phase envelopes) for various mixtures of methane and ethane also are shown. These curves pass continuously from the vapor-pressure curve of the one pure component to that of the other as the composition is varied. The points labeled 1-10 represent the critical points of the mixtures as defined in the legend of Figure 1-9. The dashed curve illustrates the locus of critical points for the binary system.

It should be noted by examining Figure 1-9 that, when one of the constituents becomes predominant, the binary mixture tends to exhibit a relatively narrow phase envelope and displays critical properties close to the predominant component. The size of the phase envelope enlarges noticeably as the composition of the mixture becomes evenly distributed between the two components.

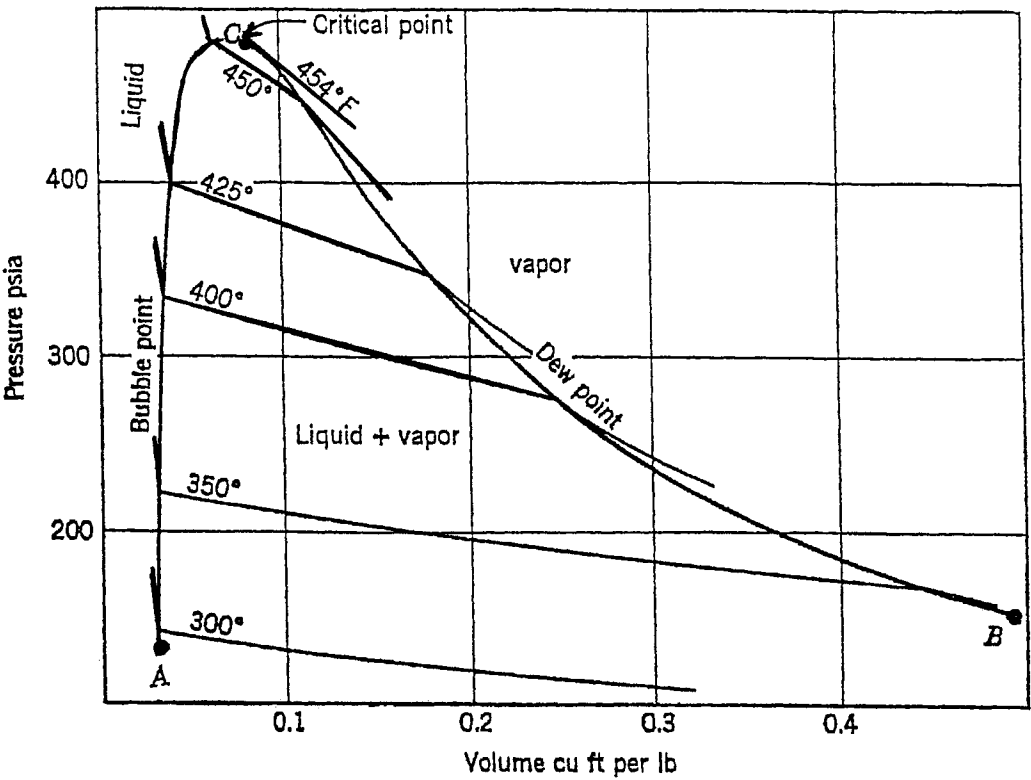


FIGURE 1-7 Pressure/volume diagram for the *n*-pentane and *n*-heptane system containing 52.4 wt % *n*-heptane.

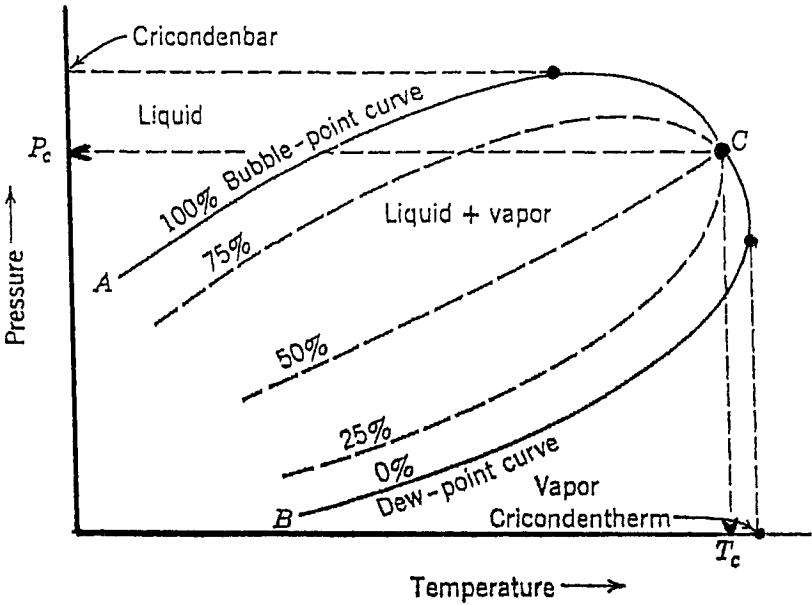


FIGURE 1-8 Typical temperature/pressure diagram for a two-component system.

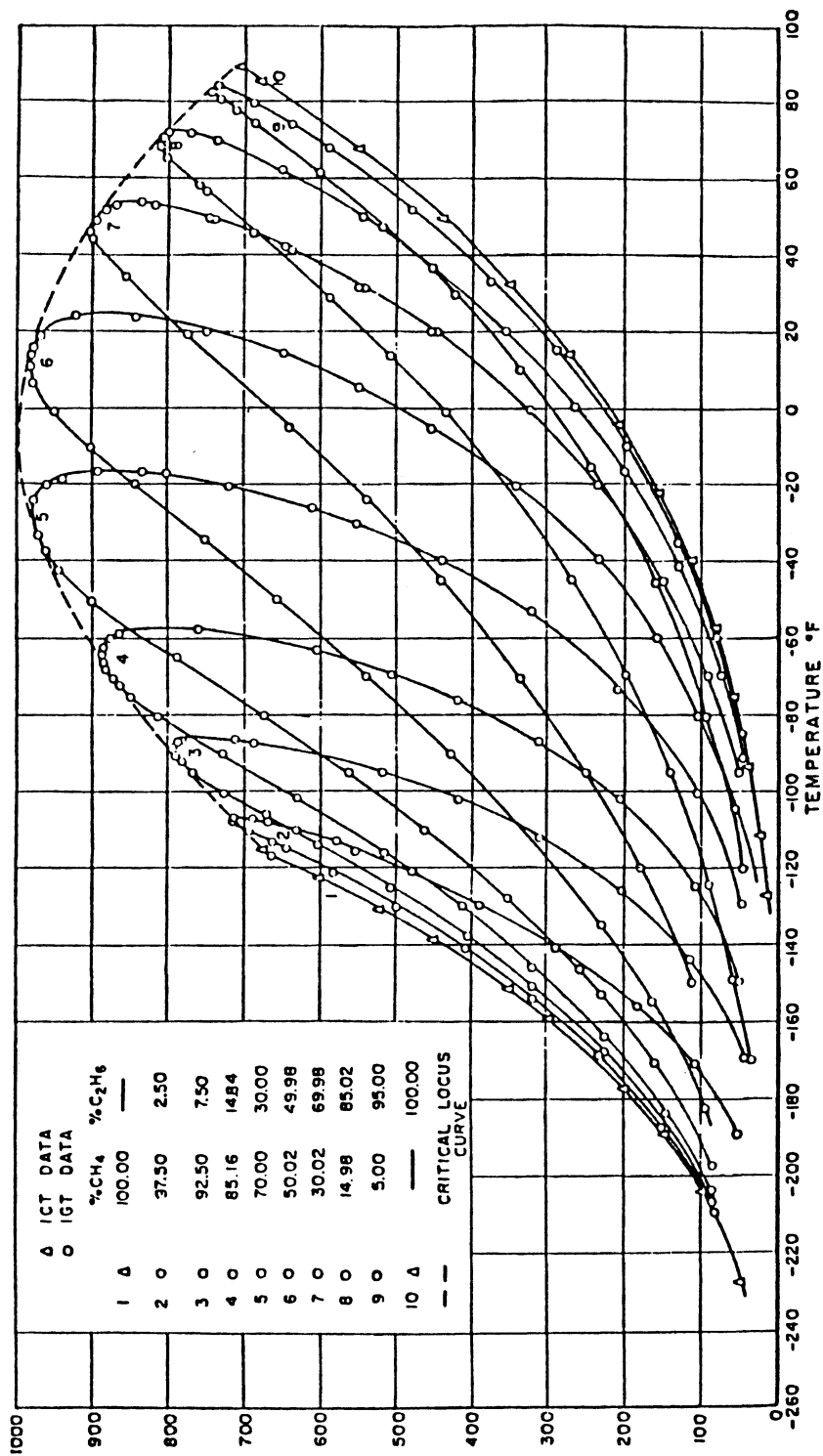


FIGURE 1-9 Phase diagram of a methane/ethane mixture.
Courtesy of the Institute of Gas Technology.

Figure 1–10 shows the critical loci for a number of common binary systems. Obviously, the critical pressure of mixtures is considerably higher than the critical pressure of the components in the mixtures. The greater the difference in the boiling point of the two substances, the higher the critical pressure of the mixture.

Pressure/Composition Diagram for Binary Systems

As pointed out by Burcik (1957), the pressure/composition diagram, commonly called the *p/x diagram*, is another means of describing the phase behavior of a binary system, as its overall composition changes at a constant temperature. It is constructed by plotting the dew-point and bubble-point pressures as a function of composition.

The bubble-point and dew-point lines of a binary system are drawn through the points that represent these pressures as the composition of the system is changed at a constant temperature. As illustrated by Burcik (1957), Figure 1–11 represents a typical pressure/composition diagram for a two-component system. Component 1 is described as the more volatile fraction and component 2 as the less volatile fraction. Point *A* in the figure represents the vapor pressure (dew point, bubble point) of the more volatile component, while point *B* represent that of the less volatile component. Assuming a composition of 75% by weight of component 1 (i.e., the more volatile component) and 25% of component 2, this mixture is characterized by a dew-point pressure represented as point *C* and a bubble-point pressure of point *D*. Different combinations of the two components produce different values for the bubble-point and dew-point pressures. The curve *ADYB* represents the bubble-point pressure curve for the binary system as a function of composition, while the line *ACXB* describes the changes in the dew-point pressure as the composition of the system changes at a constant temperature. The area below the dew-point line represents vapor, the area above the bubble-point line represents liquid, and the area between these two curves represents the two-phase region, where liquid and vapor coexist.

In the diagram in Figure 1–11, the composition is expressed in weight percent of the less volatile component. It is to be understood that the composition may be expressed equally well in terms of weight percent of the more volatile component, in which case the bubble-point and dew-point lines have the opposite slope. Furthermore, the composition may be expressed in terms of mole percent or mole fraction as well.

The points *X* and *Y* at the extremities of the horizontal line *XY* represent the composition of the coexisting of the vapor phase (point *X*) and the liquid phase (point *Y*) that exist in equilibrium at the same pressure. In other words, at the pressure represented by the horizontal line *XY*, the compositions of the vapor and liquid that coexist in the two-phase region are given by w_v and w_L , and they represent the weight percentages of the less volatile component in the vapor and liquid, respectively.

In the *p/x* diagram shown in Figure 1–12, the composition is expressed in terms of the mole fraction of the *more* volatile component. Assume that a binary system with an overall composition of z exists in the vapor phase state as represented by point *A*. If the pressure on the system is increased, no phase change occurs until the dew point, *B*, is reached at pressure P_1 . At this dew-point pressure, an infinitesimal amount of liquid forms whose composition is given by x_1 . The composition of the vapor still is equal to the original composition z . As the

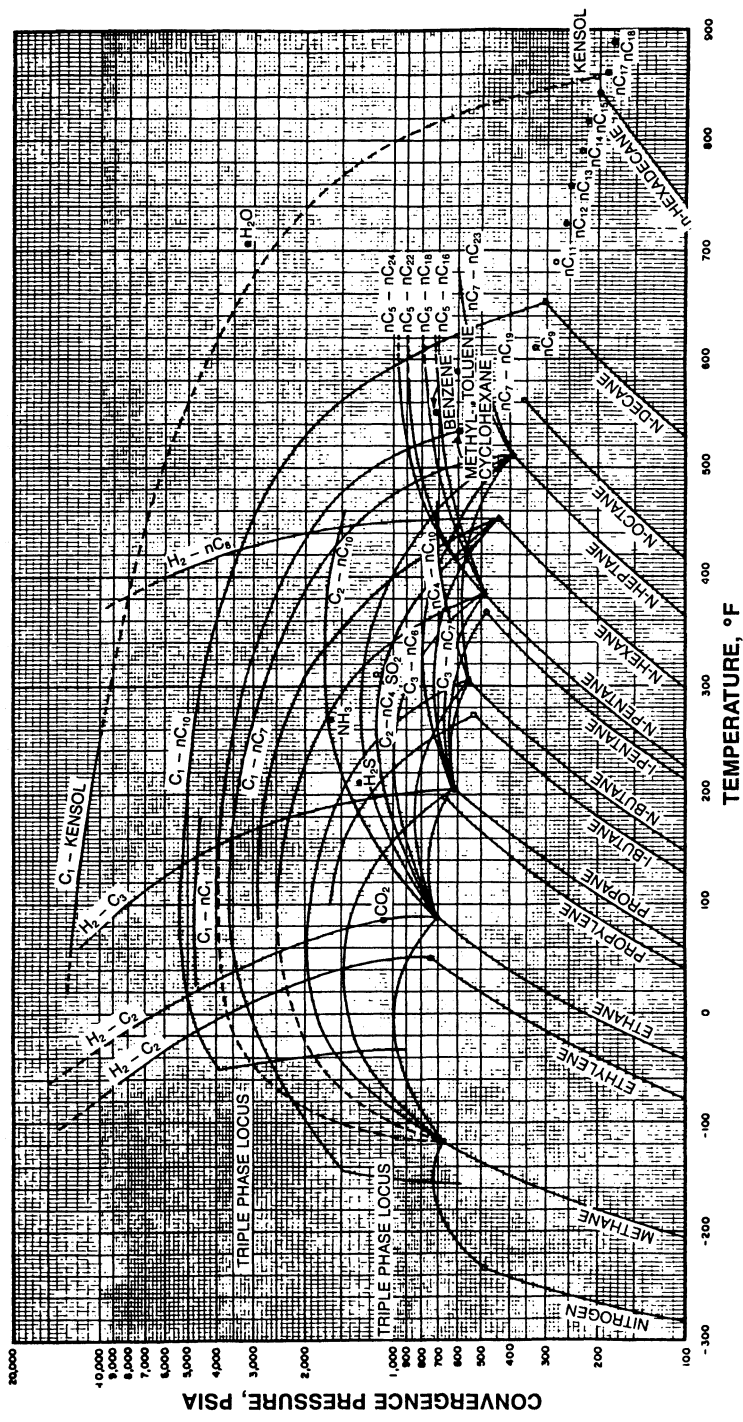


FIGURE 1-10 Convergence pressures for binary systems.
Source: GPSA Engineering Data Book, 10th ed. Tulsa, OK: Gas Processors Suppliers Association.

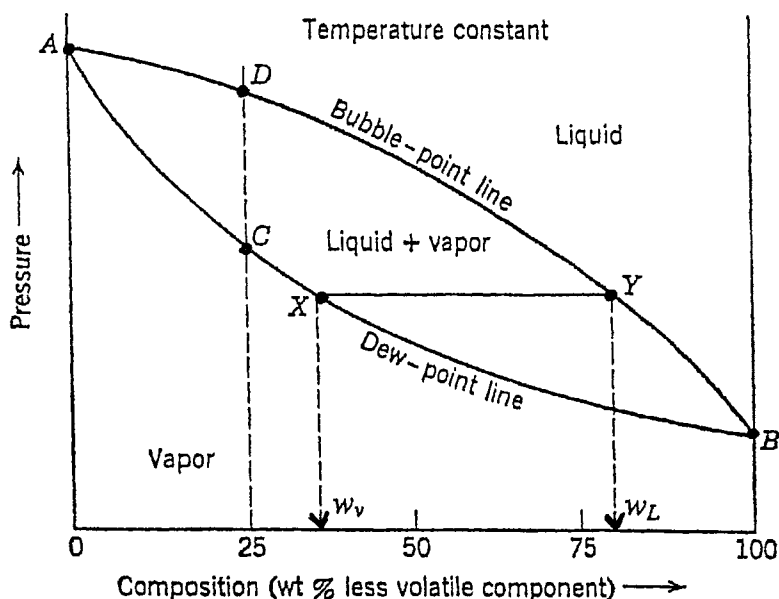


FIGURE 1-11 Typical pressure/composition diagram for a two-component system. Composition expressed in terms of weight percent of the less volatile component.

pressure is increased, more liquid forms and the compositions of the coexisting liquid and vapor are given by projecting the ends of the straight, horizontal line through the two-phase region of the composition axis. For example, at p_2 , both liquid and vapor are present and the compositions are given by x_2 and y_2 . At pressure p_3 , the bubble point, C , is reached. The composition of the liquid is equal to the original composition z with an infinitesimal amount of vapor still present at the bubble point with a composition given by y_3 .

As indicated already, the extremities of a horizontal line through the two-phase region represent the compositions of coexisting phases. Burcik (1957) points out that the *composition* and the *amount* of a each phase present in a two-phase system are of practical interest and use in reservoir engineering calculations. At the dew point, for example, only an infinitesimal amount of liquid is present, but it consists of finite mole fractions of the two components. An equation for the relative *amounts* of liquid and vapor in a two-phase system may be derived as follows:

Let

n = total number of moles in the binary system

n_L = number of moles of liquid

n_v = number of moles of vapor

z = mole fraction of the more volatile component in the system

x = mole fraction of the more volatile component in the liquid phase

y = mole fraction of the more volatile component in the vapor phase

By definition,

$$n = n_L + n_v$$

$$nz = \text{moles of the more volatile component in the system}$$

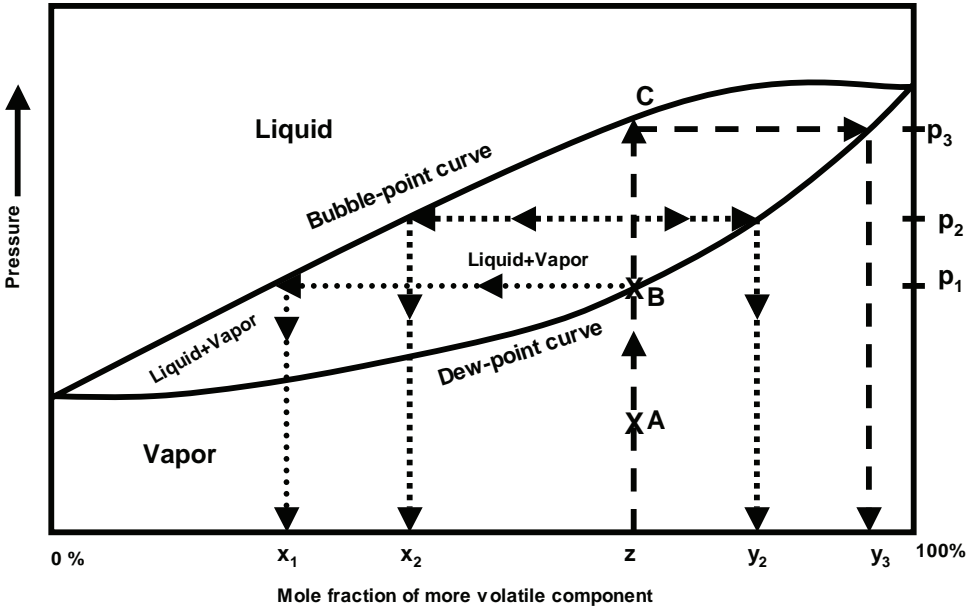


FIGURE 1-12 Pressure/composition diagram illustrating isothermal compression through the two-phase region.

$n_L x$ = moles of the more volatile component in the liquid

$n_v y$ = moles of the more volatile component in the vapor

A material balance on the more volatile component gives

$$nz = n_L x + n_v y \quad (1-13)$$

and

$$n_L = n - n_v$$

Combining these two expressions gives

$$nz = (n - n_v)x + n_v y$$

and rearranging one obtains

$$\frac{n_v}{n} = \frac{z - x}{y - x} \quad (1-14)$$

Similarly, if n_v is eliminated in equation (1-13) instead of n_L , we obtain

$$\frac{n_L}{n} = \frac{z - y}{x - y} \quad (1-15)$$

The geometrical interpretation of equations (1-14) and (1-15) is shown in Figure 1-13, which indicates that these equations can be written in terms of the two segments of the horizontal line AC . Since $z - x$ = the length of segment AB , and $y - x$ = the total length of horizontal line AC , equation (1-14) becomes

$$\frac{n_v}{n} = \frac{z - x}{y - x} = \frac{AB}{AC} \quad (1-16)$$

Similarly, equation (1-15) becomes

$$\frac{n_L}{n} = \frac{BC}{AC} \quad (1-17)$$

Equation (1-16) suggests that the ratio of the number of moles of vapor to the total number of moles in the system is equivalent to the length of the line segment AB that connects the overall composition to the liquid composition divided by the total length $psia$. This rule is known as the *inverse lever rule*. Similarly, the ratio of number of moles of liquid to the total number of moles in the system is proportional to the distance from the overall composition to the vapor composition BC divided by the total length AC . It should be pointed out that the straight line that connects the liquid composition with the vapor composition, that is, line AC , is called the *tie line*. Note that results would have been the same if the mole fraction of the less volatile component had been plotted on the phase diagram instead of the mole fraction of the more volatile component.

EXAMPLE 1-7

A system is composed of 3 moles of isobutene and 1 mole of n-heptanes. The system is separated at a fixed temperature and pressure and the liquid and vapor phases recovered. The mole fraction of isobutene in the recovered liquid and vapor are 0.370 and 0.965, respectively. Calculate the number of moles of liquid n_L and vapor n_V recovered.

SOLUTION

Step 1 Given $x = 0.370$, $y = 0.965$, and $n = 4$, calculate the overall mole fraction of isobutane in the system:

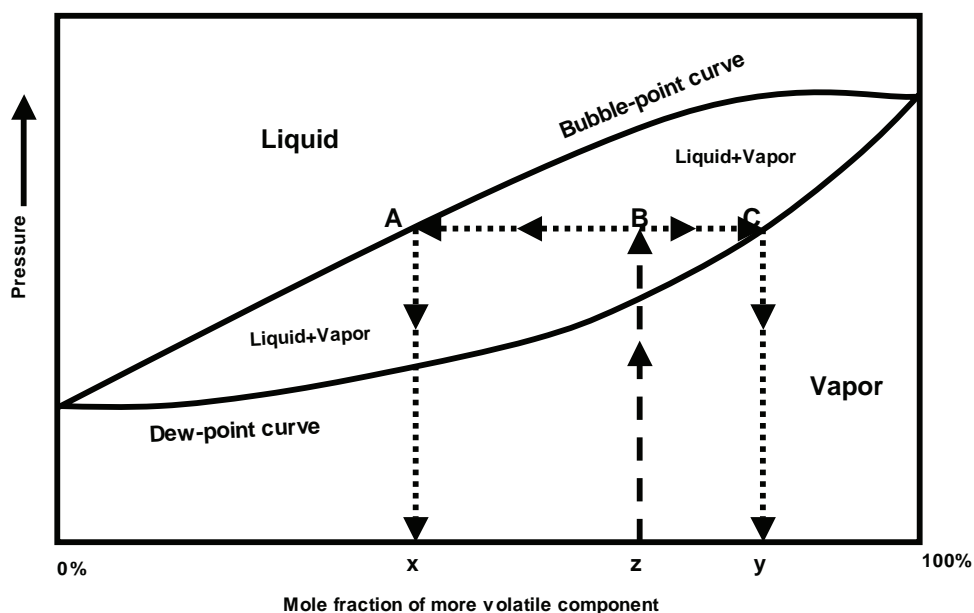


FIGURE 1-13 Geometrical interpretation of equations for the amount of liquid and vapor in the two-phase region.

$$z = \frac{3}{4} = 0.750$$

Step 2 Solve for the number of moles of the vapor phase by applying equation (1-14):

$$n_v = n \left(\frac{z - x}{y - x} \right) = 4 \left(\frac{0.750 - 0.370}{0.965 - 0.375} \right) = 2.56 \text{ moles of vapor}$$

Step 3 Determine the quantity of liquid:

$$n_L = n - n_v = 4 - 2.56 = 1.44 \text{ moles of liquid}$$

The quantity of n_L also could be obtained by substitution in equation (1-15):

$$n_L = n \left(\frac{z - y}{x - y} \right) = 4 \left(\frac{0.750 - 0.965}{0.375 - 0.965} \right) = 1.44$$

If the composition is expressed in weight fraction instead of mole fraction, similar expressions to those expressed by equations (1-14) and (1-15) can be derived in terms of weights of liquid and vapor. Let

m_t = total mass (weight) of the system

m_L = total mass (weight) of the liquid

m_v = total mass (weight) of the vapor

w_o = *weight fraction* of the more volatile component in the original system

w_L = weight fraction of the more volatile component in the liquid

w_v = weight fraction of the more volatile component in the vapor

A material balance on the more volatile component leads to the following equations:

$$\begin{aligned} \frac{m_v}{m_t} &= \frac{w_o - w_L}{w_v - w_L} \\ \frac{m_L}{m_t} &= \frac{w_o - w_v}{w_L - w_v} \end{aligned}$$

Three-Component Systems

The phase behavior of mixtures containing three components (ternary systems) is conveniently represented in a triangular diagram, such as that shown in Figure 1-14. Such diagrams are based on the property of equilateral triangles that the sum of the perpendicular distances from any point to each side of the diagram is a constant and equal to the length on any of the sides. Thus, the composition x_i of the ternary system as represented by point A in the interior of the triangle of Figure 1-14 is

$$\text{Component 1} \quad x_1 = \frac{L_1}{L_T}$$

$$\text{Component 2} \quad x_2 = \frac{L_2}{L_T}$$

$$\text{Component 3} \quad x_3 = \frac{L_3}{L_T}$$

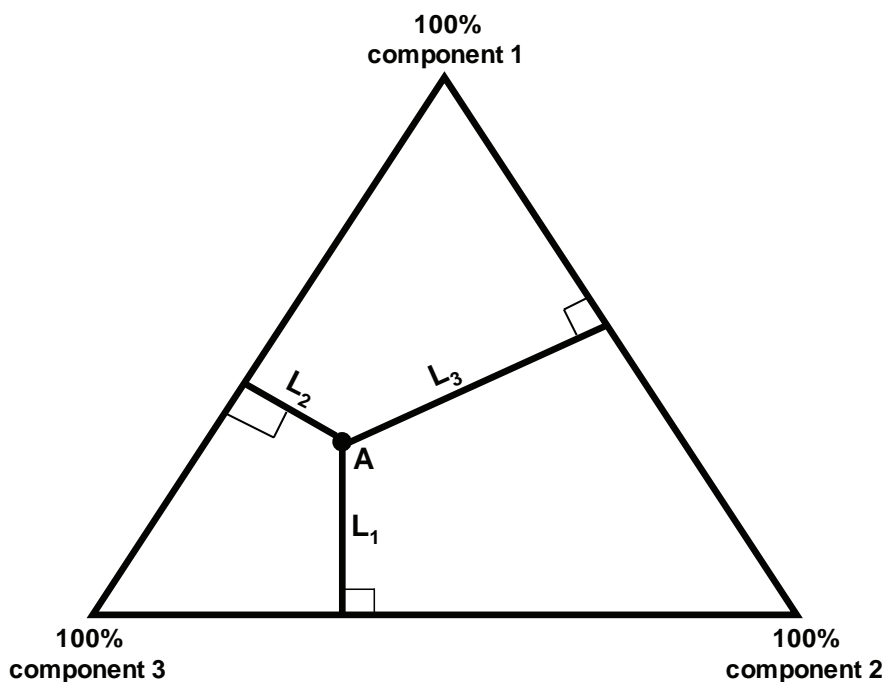


FIGURE 1-14 *Properties of the three-component diagram.*

where

$$L_T = L_1 + L_2 + L_3$$

Typical features of a ternary phase diagram for a system that exists in the two-phase region at fixed pressure and temperature are shown in Figure 1-15. Any mixture with an overall composition that lies inside the binodal curve (phase envelope) will split into liquid and vapor phases. The line that connects the composition of liquid and vapor phases that are in equilibrium is called the *tie line*. Any other mixture with an overall composition that lies on that tie line will split into the same liquid and vapor compositions. Only the amounts of liquid and gas change as the overall mixture composition changes from the liquid side (bubble-point curve) on the binodal curve to the vapor side (dew-point curve). If the mole fractions of component i in the liquid, vapor, and overall mixture are x_i , y_i , and z_i , the fraction of the total number of moles in the liquid phase n_l is given by

$$n_l = \frac{y_i - z_i}{y_i - x_i}$$

This expression is another *lever rule*, similar to that described for binary diagrams. The liquid and vapor portions of the binodal curve (phase envelope) meet at the plait point (critical point), where the liquid and vapor phases are identical.

Multicomponent Systems

The phase behavior of multicomponent hydrocarbon systems in the two-phase region, that is, the liquid-vapor region, is very similar to that of binary systems. However, as the

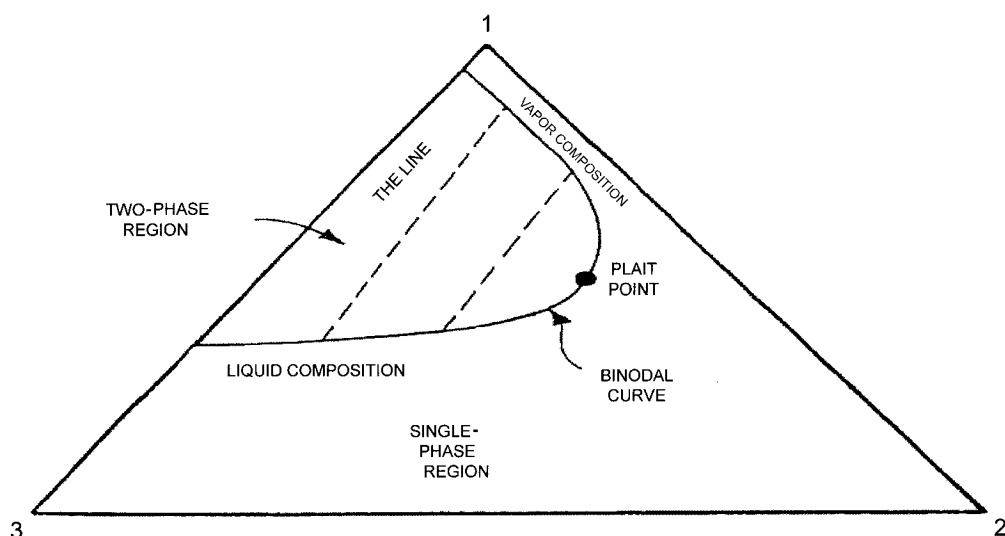


FIGURE 1-15 Three-component phase diagram at a constant temperature and pressure for a system that forms a liquid and a vapor.

system becomes more complex with a greater number of different components, the pressure and temperature ranges in which two phases lie increase significantly.

The conditions under which these phases exist are a matter of considerable practical importance. The experimental or the mathematical determinations of these conditions are conveniently expressed in different types of diagrams, commonly called *phase diagrams*. One such diagram is called the *pressure-temperature diagram*.

Figure 1-16 shows a typical pressure/temperature diagram (p/T diagram) of a multicomponent system with a specific overall composition. Although a different hydrocarbon system would have a different phase diagram, the general configuration is similar.

These multicomponent p/T diagrams are essentially used to classify reservoirs, specify the naturally occurring hydrocarbon systems, and describe the phase behavior of the reservoir fluid.

To fully understand the significance of the p/T diagrams, it is necessary to identify and define the following key points on the p/T diagram:

- **Cricondentherm (T_{ct})** The cricondentherm is the maximum temperature above which liquid cannot be formed regardless of pressure (point E). The corresponding pressure is termed the *cricondentherm pressure*, p_{ct} .
- **Cricondenbar (p_{cb})** The cricondenbar is the maximum pressure above which no gas can be formed regardless of temperature (point D). The corresponding temperature is called the *cricondenbar temperature*, T_{cb} .
- **Critical point** The critical point for a multicomponent mixture is referred to as the state of pressure and temperature at which all intensive properties of the gas and liquid phases are equal (point C). At the critical point, the corresponding pressure and temperature are called the *critical pressure*, p_c , and *critical temperature*, T_c , of the mixture.

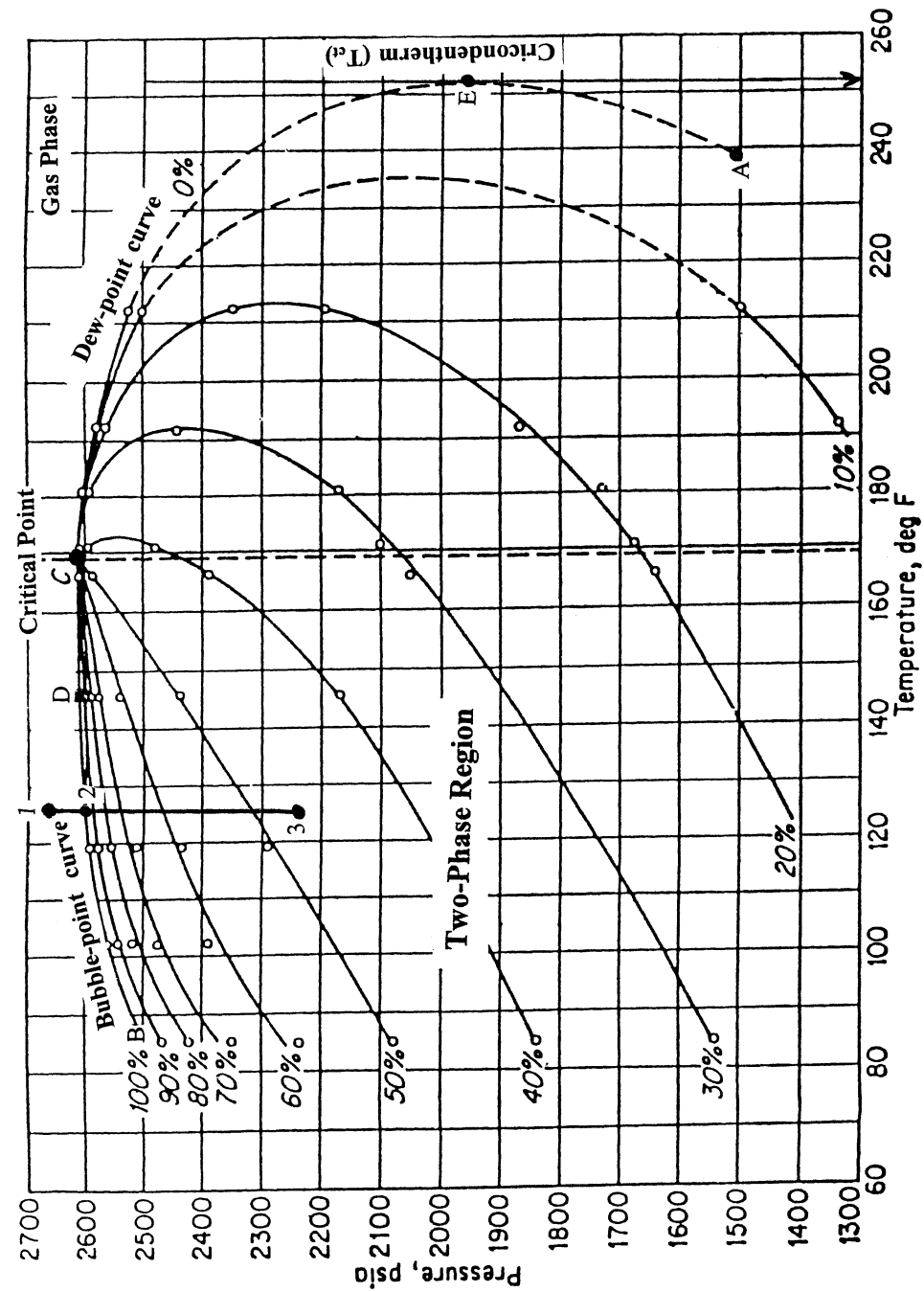


FIGURE 1-16 Typical p/T diagram for a multicomponent system.

- *Phase envelope (two-phase region)* The region enclosed by the bubble-point curve and the dew-point curve (line BCA), where gas and liquid coexist in equilibrium, is identified as the phase envelope of the hydrocarbon system.
- *Quality lines* The dashed lines within the phase diagram are called *quality lines*. They describe the pressure and temperature conditions for equal volumes of liquids. Note that the quality lines converge at the critical point (point C).
- *Bubble-point curve* The bubble-point curve (line BC) is defined as the line separating the liquid phase region from the two-phase region.
- *Dew-point curve* The dew-point curve (line AC) is defined as the line separating the vapor phase region from the two-phase region.

Classification of Reservoirs and Reservoir Fluids

Petroleum reservoirs are broadly classified as oil or gas reservoirs. These broad classifications are further subdivided depending on

1. The composition of the reservoir hydrocarbon mixture.
2. Initial reservoir pressure and temperature.
3. Pressure and temperature of the surface production.
4. Location of the reservoir temperature with respect to the critical temperature and the cricondentherm.

In general, reservoirs are conveniently classified on the basis of the location of the point representing the initial reservoir pressure p_i and temperature T with respect to the p/T diagram of the reservoir fluid. Accordingly, reservoirs can be classified into basically two types:

- *Oil reservoirs* If the reservoir temperature, T , is less than the critical temperature, T_c , of the reservoir fluid, the reservoir is classified as an oil reservoir.
- *Gas reservoirs* If the reservoir temperature is greater than the critical temperature of the hydrocarbon fluid, the reservoir is considered a gas reservoir.

Oil Reservoirs

Depending on initial reservoir pressure, p_i , oil reservoirs can be subclassified into the following categories:

1. *Undersaturated oil reservoir* If the initial reservoir pressure, p_i (as represented by point 1 on Figure 1–16), is greater than the bubble-point pressure, p_b , of the reservoir fluid, the reservoir is an undersaturated oil reservoir.
2. *Saturated oil reservoir* When the initial reservoir pressure is equal to the bubble-point pressure of the reservoir fluid, as shown on Figure 1–16 by point 2, the reservoir is a saturated oil reservoir.

3. *Gas-cap reservoir* If the initial reservoir pressure is below the bubble-point pressure of the reservoir fluid, as indicated by point 3 on Figure 1–16, the reservoir is a gas-cap or two-phase reservoir, in which an oil phase underlies the gas or vapor phase.

Crude oils cover a wide range in physical properties and chemical compositions, and it is often important to be able to group them into broad categories of related oils. In general, crude oils are commonly classified into the following types:

- Ordinary black oil.
- Low-shrinkage crude oil.
- High-shrinkage (volatile) crude oil.
- Near-critical crude oil.

This classification essentially is based on the properties exhibited by the crude oil, including:

- Physical properties, such as API gravity of the stock-tank liquid.
- Composition.
- Initial producing gas/oil ratio (GOR).
- Appearance, such as color of the stock-tank liquid.
- Pressure-temperature phase diagram.

Three of the above properties generally are available: initial GOR, API gravity, and color of the separated liquid.

The initial producing GOR perhaps is the most important indicator of fluid type. Color has not been a reliable means of differentiating clearly between gas condensates and volatile oils, but in general, dark colors indicate the presence of heavy hydrocarbons. No sharp dividing lines separate these categories of hydrocarbon systems, only laboratory studies could provide the proper classification. In general, reservoir temperature and composition of the hydrocarbon system greatly influence the behavior of the system.

1. *Ordinary black oil* A typical p/T phase diagram for ordinary black oil is shown in Figure 1–17. Note that quality lines that are approximately equally spaced characterize this black oil phase diagram. Following the pressure reduction path, as indicated by the vertical line EF in Figure 1–17, the liquid shrinkage curve, shown in Figure 1–18, is prepared by plotting the liquid volume percent as a function of pressure. The liquid shrinkage curve approximates a straight line except at very low pressures. When produced, ordinary black oils usually yield gas/oil ratios between 200 and 700 scf/STB and oil gravities of 15 to 40 API. The stock-tank oil usually is brown to dark green in color.
2. *Low-shrinkage oil* A typical p/T phase diagram for low-shrinkage oil is shown in Figure 1–19. The diagram is characterized by quality lines that are closely spaced near the dew-point curve. The liquid shrinkage curve, given in Figure 1–20, shows the

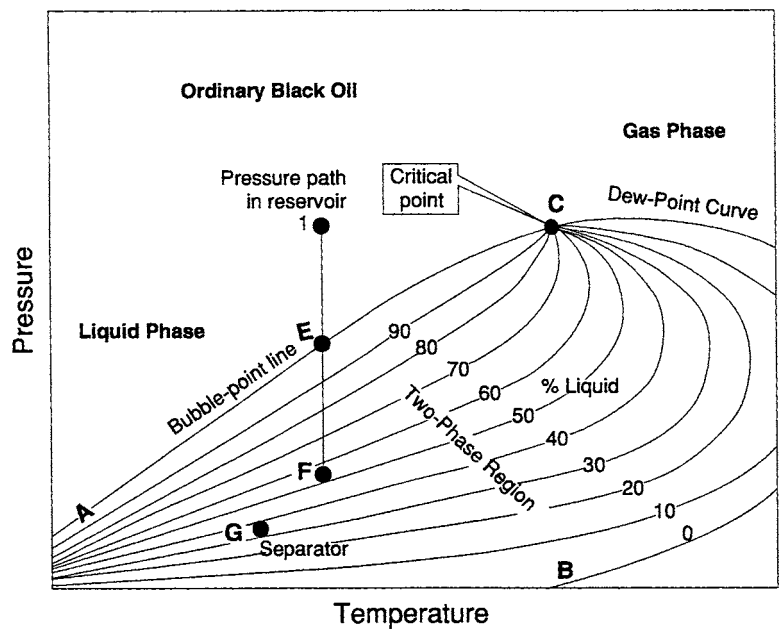


FIGURE 1-17 Typical p/T diagram for ordinary black oil.

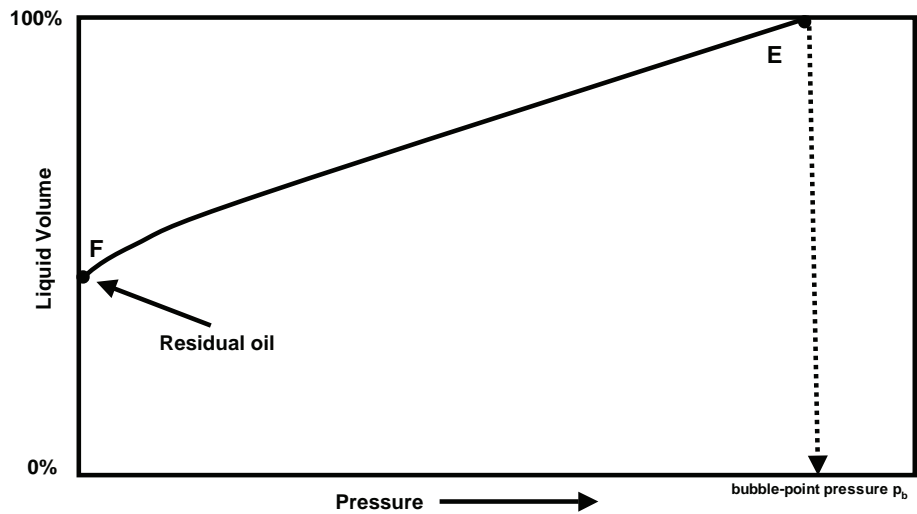


FIGURE 1-18 Liquid shrinkage curve for black oil.

shrinkage characteristics of this category of crude oils. The other associated properties of this type of crude oil are

- Oil formation volume factor less than 1.2 bbl/STB.
- Gas-oil ratio less than 200 scf/STB.
- Oil gravity less than 35° API.
- Black or deeply colored.

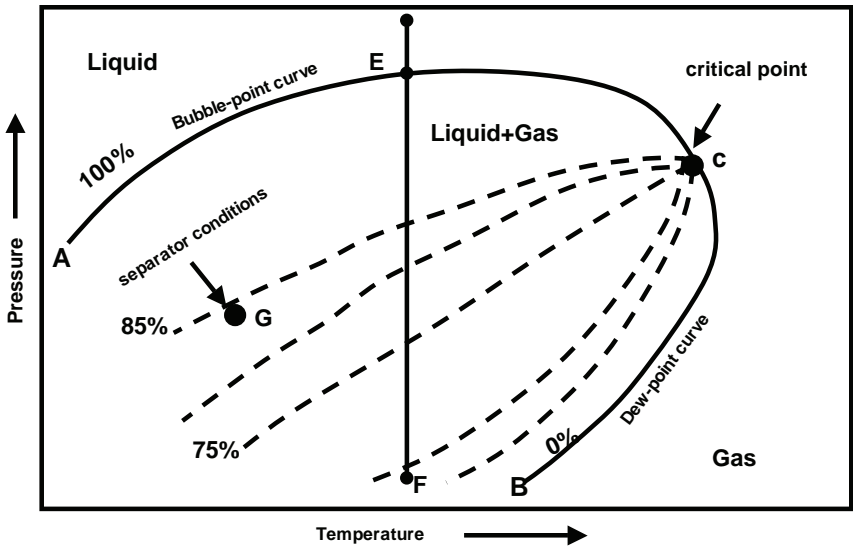


FIGURE 1-19 Typical phase diagram for low-shrinkage oil.

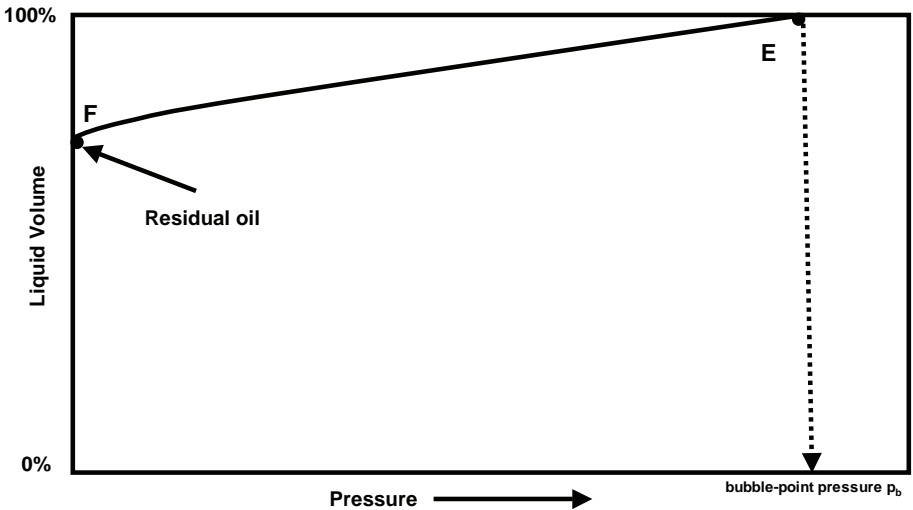


FIGURE 1-20 Oil shrinkage curve for low-shrinkage oil.

- Substantial liquid recovery at separator conditions as indicated by point G on the 85% quality line of Figure 1-19.
3. *Volatile crude oil* The phase diagram for a volatile (high-shrinkage) crude oil is given in Figure 1-21. Note that the quality lines are close together near the bubble point, and at lower pressures, they are more widely spaced. This type of crude oil is commonly characterized by a high liquid shrinkage immediately below the bubble point, shown in Figure 1-22. The other characteristic properties of this oil include:
- Oil formation volume factor greater than 1.5 bbl/STB.

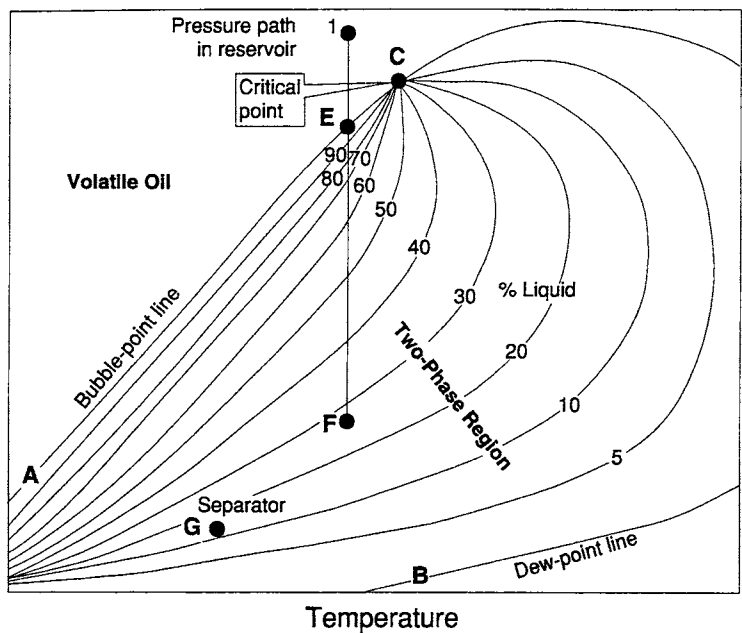


FIGURE 1-21 Typical p/T diagram for a volatile crude oil.

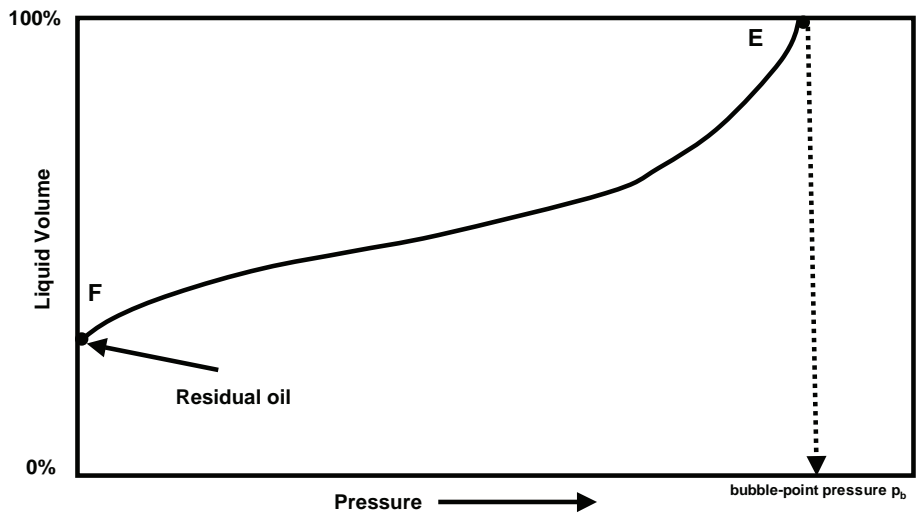


FIGURE 1-22 Typical liquid shrinkage curve for a volatile crude oil.

- Gas-oil ratios between 2000 and 3000 scf/STB.
- Oil gravities between 45° and 55° API.
- Lower liquid recovery of separator conditions, as indicated by point G on Figure 1-19.
- Greenish to orange in color.

Solution gas released from a volatile oil contains significant quantities of stock-tank liquid (condensate) when the solution gas is produced at the surface. Solution gas from black oils usually is considered “dry,” yielding insignificant stock-tank liquid when

produced to surface conditions. For engineering calculations, the liquid content of released solution gas perhaps is the most important distinction between volatile oils and black oils. Another characteristic of volatile oil reservoirs is that the API gravity of the stock tank liquid increases in the later life of the reservoirs.

4. *Near-critical crude oil* If the reservoir temperature, T , is near the critical temperature, T_c , of the hydrocarbon system, as shown in Figure 1–21, the hydrocarbon mixture is identified as a near-critical crude oil. Because all the quality lines converge at the critical point, an isothermal pressure drop (as shown by the vertical line EF in Figure 1–23) may shrink the crude oil from 100% of the hydrocarbon pore volume at the bubble point to 55% or less at a pressure 10 to 50 psi below the bubble point. The shrinkage characteristic behavior of the near-critical crude oil is shown in Figure 1–24. This high shrinkage creates high gas saturation in the pore space and because of the gas-oil relative permeability characteristics of most reservoir rocks; free gas achieves high mobility almost immediately below the bubble-point pressure.

The near-critical crude oil is characterized by a high GOR, in excess of 3000 scf/STB, with an oil formation volume factor of 2.0 bbl/STB or higher. The compositions of near-critical oils usually are characterized by 12.5 to 20 mol% heptanes-plus, 35% or more of ethane through hexanes, and the remainder methane. It should be pointed out that near-critical oil systems essentially are considered the borderline to very rich gas condensates on the phase diagram.

Figure 1–25 compares the characteristic shape of the liquid shrinkage curve for each crude oil type.

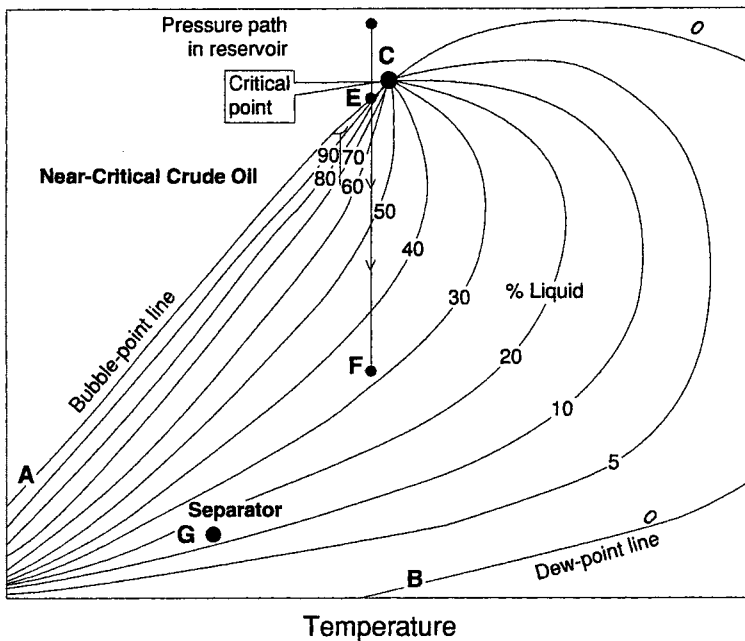


FIGURE 1–23 Phase diagram for a near-critical crude oil.

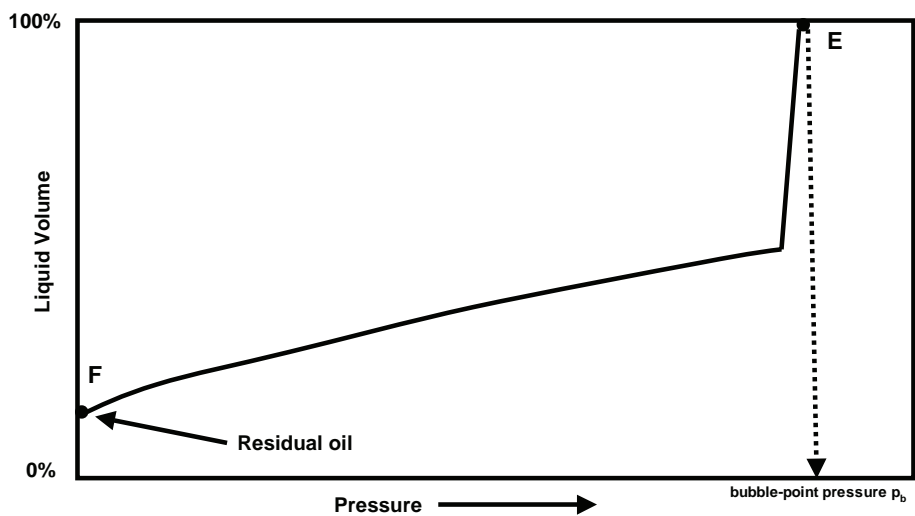


FIGURE 1-24 Typical liquid shrinkage curve for a near-critical crude oil.

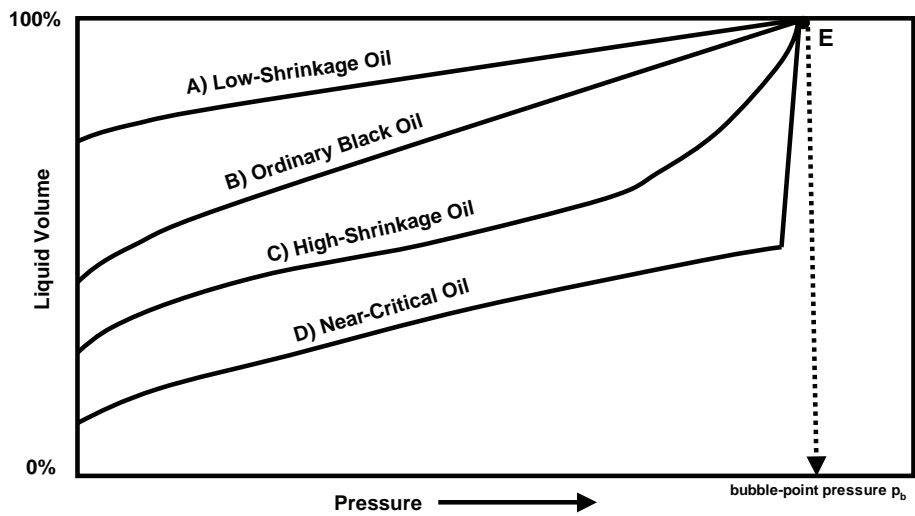


FIGURE 1-25 Liquid shrinkage curves for crude oil systems.

Gas Reservoirs

In general, if the reservoir temperature is above the critical temperature of the hydrocarbon system, the reservoir is classified as a natural gas reservoir. Natural gases can be categorized on the basis of their phase diagram and the prevailing reservoir condition into four categories:

- 1. Retrograde gas reservoirs.
- 2. Near-critical gas-condensate reservoirs.
- 3. Wet gas reservoirs.
- 4. Dry gas reservoirs.

In some cases, when condensate (stock-tank liquid) is recovered from a surface process facility, the reservoir is mistakenly classified as a retrograde gas reservoir. Strictly speaking, the definition of a retrograde gas reservoir depends only on reservoir temperature.

Retrograde Gas Reservoirs

If the reservoir temperature, T , lies between the critical temperature, T_c , and criconden-therm, T_{ct} , of the reservoir fluid, the reservoir is classified as a retrograde gas-condensate reservoir. This category of gas reservoir has a unique type of hydrocarbon accumulation, in that the special thermodynamic behavior of the reservoir fluid is the controlling factor in the development and the depletion process of the reservoir. When the pressure is decreased on these mixtures, instead of expanding (if a gas) or vaporizing (if a liquid) as might be expected, they vaporize instead of condensing.

Consider that the initial condition of a retrograde gas reservoir is represented by point 1 on the pressure-temperature phase diagram of Figure 1–26. Because the reservoir pressure is above the upper dew-point pressure, the hydrocarbon system exists as a single phase (i.e., vapor phase) in the reservoir. As the reservoir pressure declines isothermally during production from the initial pressure (point 1) to the upper dew-point pressure (point 2), the attraction between the molecules of the light and heavy components move further apart. As this occurs, attraction between the heavy component molecules becomes more effective, therefore, liquid begins to condense. This retrograde condensation process continues with decreasing pressure until the liquid dropout reaches its maximum at point 3. Further reduction in pressure permits the heavy molecules to commence the normal vaporization process. This is the process whereby fewer gas molecules strike the liquid

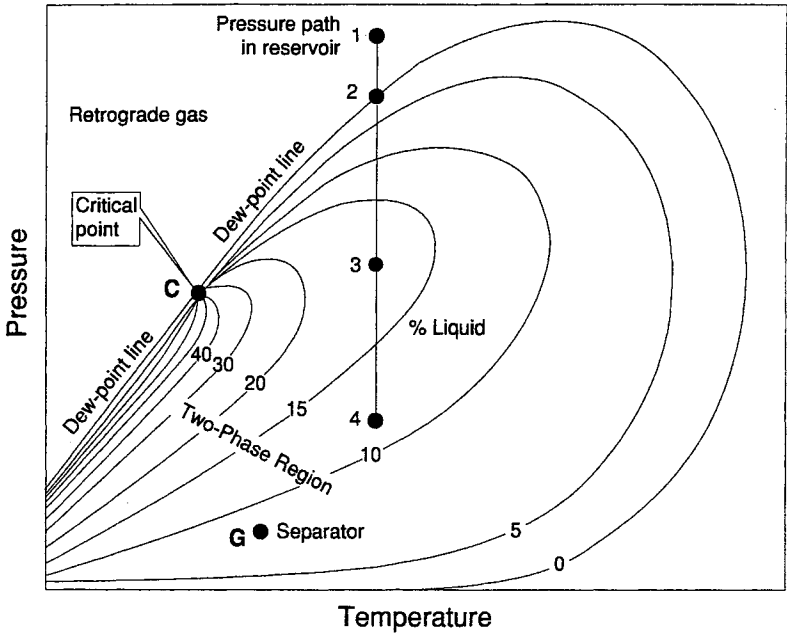


FIGURE 1–26 Typical phase diagram of a retrograde system.

surface and more molecules leave than enter the liquid phase. The vaporization process continues until the reservoir pressure reaches the lower dew-point pressure. This means that all the liquid that formed must vaporize because the system essentially is all vapor at the lower dew point.

Figure 1–27 shows a typical liquid shrinkage volume curve for a relatively rich condensate system. The curve is commonly called the *liquid dropout curve*. The maximum liquid dropout (LDO) is 26.5%, which occurs when the reservoir pressure drops from a dew-point pressure of 5900 psi to 2800 psi. In most gas-condensate reservoirs, the condensed liquid volume seldom exceeds more than 15–19% of the pore volume. This liquid saturation is not large enough to allow any liquid flow. It should be recognized, however,

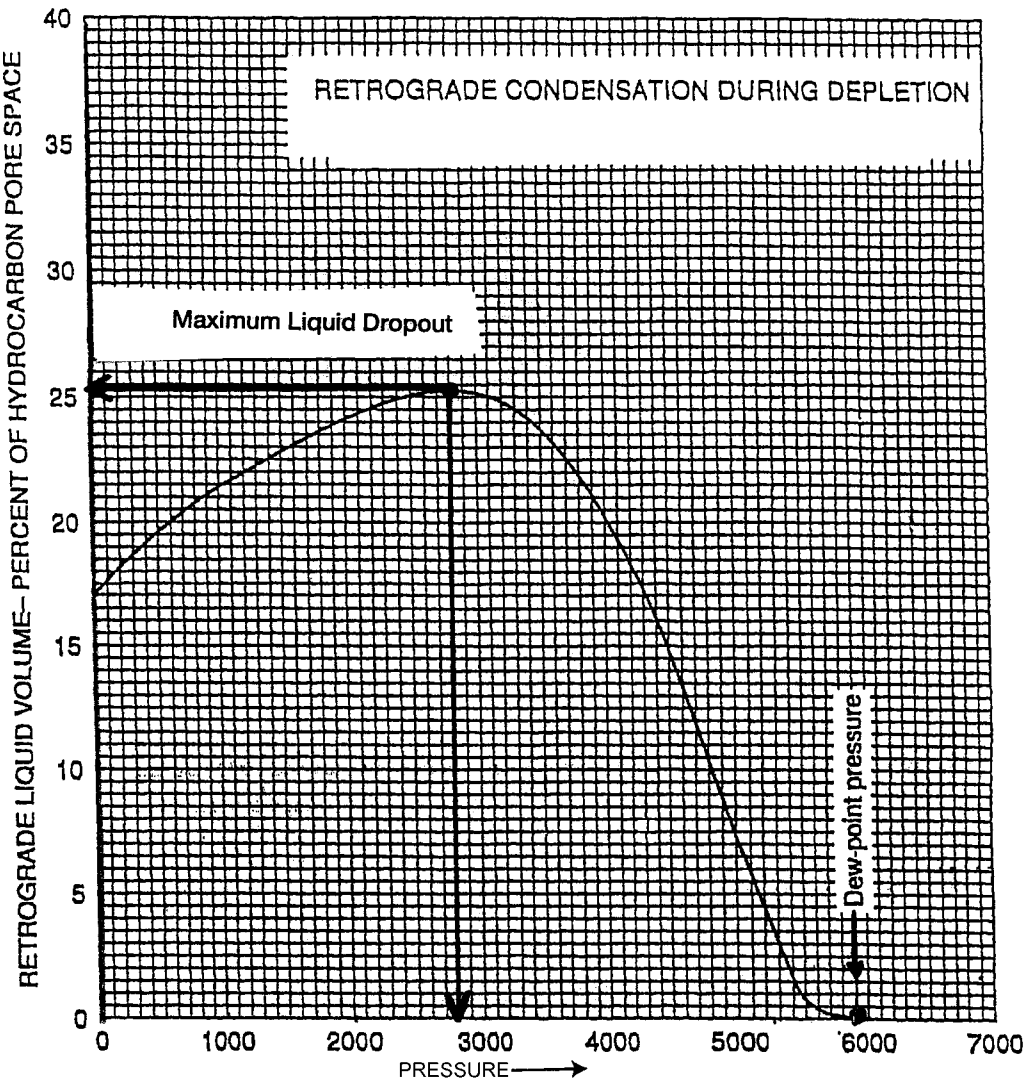


FIGURE 1–27 Typical liquid dropout curve.

that around the well bore, where the pressure drop is high, enough liquid dropout might accumulate to give two-phase flow of gas and retrograde liquid.

The associated physical characteristics of this category are

- Gas-oil ratios between 8000 and 70,000 scf/STB. Generally, the gas-oil ratio for a condensate system increases with time due to the liquid dropout and the loss of heavy components in the liquid.
- Condensate gravity above 50° API.
- Stock-tank liquid is usually water-white or slightly colored.

It should be pointed out that the gas that comes out of the solution from a volatile oil and remains in the reservoir typically is classified a retrograde gas and exhibits the retrograde condensate with pressure declines.

There is a fairly sharp dividing line between oils and condensates from a compositional standpoint. Reservoir fluids that contain heptanes and are in concentration of more than 12.5 mol% almost always are in the liquid phase in the reservoir. Oils have been observed with heptanes and heavier concentrations as low as 10% and condensates as high as 15.5%. These cases are rare, however, and usually have very high tank liquid gravities.

Near-Critical Gas-Condensate Reservoirs

If the reservoir temperature is near the critical temperature, as shown in Figure 1–28, the hydrocarbon mixture is classified as a near-critical gas condensate. The volumetric behavior of this category of natural gas is described through the isothermal pressure declines, as shown by the vertical line 1–3 in Figure 1–28 and the corresponding liquid dropout curve of Figure 1–29. Because all the quality lines converge at the critical point, a rapid liquid buildup immediately occurs below the dew point (Figure 1–29) as the pressure is reduced to point 2.

This behavior can be justified by the fact that several quality lines are crossed very rapidly by the isothermal reduction in pressure. At the point where the liquid ceases to build up and begins to shrink again, the reservoir goes from the retrograde region to a normal vaporization region.

Wet Gas Reservoirs

A typical phase diagram of a wet gas is shown in Figure 1–30, where the reservoir temperature is above the cricondentherm of the hydrocarbon mixture. Because the reservoir temperature exceeds the cricondentherm of the hydrocarbon system, the reservoir fluid always remains in the vapor phase region as the reservoir is depleted isothermally, along the vertical line *AB*. However, as the produced gas flows to the surface, the pressure and temperature of the gas decline. If the gas enters the two-phase region, a liquid phase condenses out of the gas and is produced from the surface separators. This is caused by a sufficient decrease in the kinetic energy of heavy molecules with temperature drop and their subsequent change to liquid through the attractive forces between molecules.

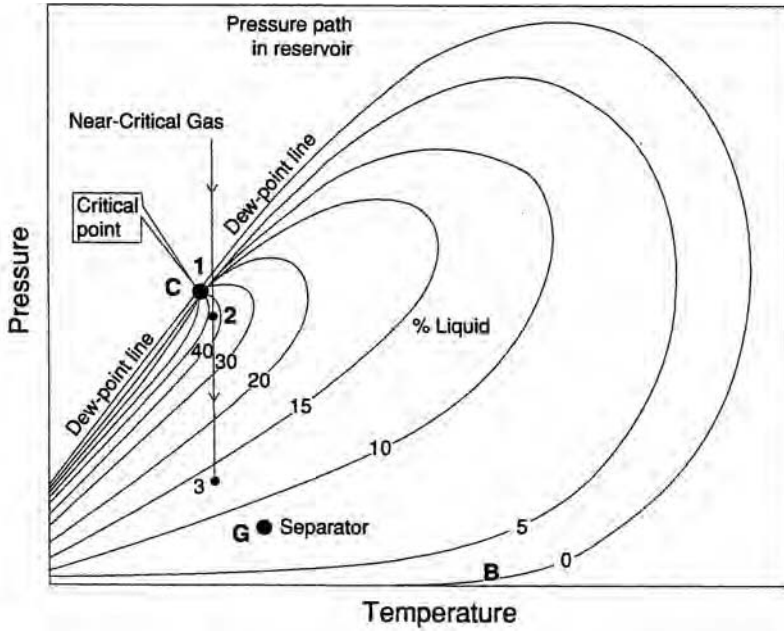


FIGURE 1-28 Typical phase diagram for a near-critical gas condensate reservoir.

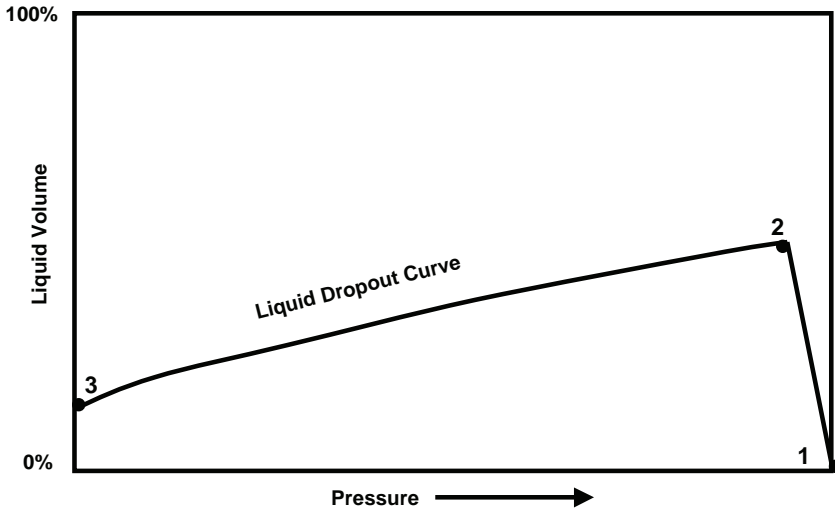


FIGURE 1-29 Liquid shrinkage curve for a near-critical gas condensate system.

Wet gas reservoirs are characterized by the following properties:

- Gas oil ratios between 60,000 and 100,000 scf/STB.
- Stock-tank oil gravity above 60° API.
- Liquid is water-white in color.
- Separator conditions (i.e., separator pressure and temperature) lie within the two-phase region.

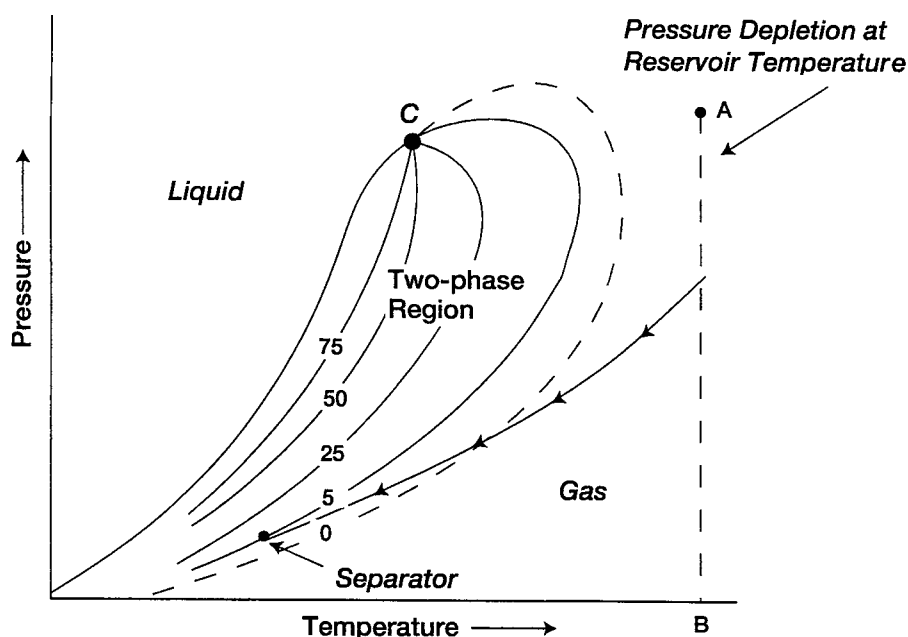


FIGURE 1-30 Phase diagram for a wet gas.

Source: After N. J. Clark, *Elements of Petroleum Reservoirs*, 2nd ed. Tulsa, OK: Society of Petroleum Engineers, 1969.

Dry Gas Reservoirs

The hydrocarbon mixture exists as a gas both in the reservoir and the surface facilities. The only liquid associated with the gas from a dry gas reservoir is water. Figure 1-31 is a phase diagram of a dry gas reservoir. Usually, a system that has a gas/oil ratio greater than 100,000 scf/STB is considered to be a dry gas. The kinetic energy of the mixture is so high and attraction between molecules so small that none of them coalesce to a liquid at stock-tank conditions of temperature and pressure.

It should be pointed out that the listed classifications of hydrocarbon fluids might be also characterized by the initial composition of the system. McCain (1994) suggests that the heavy components in the hydrocarbon mixtures have the strongest effect on fluid characteristics. The ternary diagram shown in Figure 1-32 with equilateral triangles can be conveniently used to roughly define the compositional boundaries that separate different types of hydrocarbon systems.

Fluid samples obtained from a new field discovery may be instrumental in defining the existence of a two-phase, that is, gas-cap, system with an overlying gas cap or underlying oil rim. As the compositions of the gas and oil zones are completely different from each other, both systems may be represented separately by individual phase diagrams, which bear little relation to each other or to the composite. The oil zone will be at its bubble point and produced as a saturated oil reservoir but modified by the presence of the gas cap. Depending on the composition and phase diagram of the gas, the gas-cap gas may be a retrograde gas cap, as shown in Figure 1-33, or dry or wet, as shown in Figure 1-34. Therefore, a discovery well drilled through a saturated reservoir fluid usually requires further field delineation

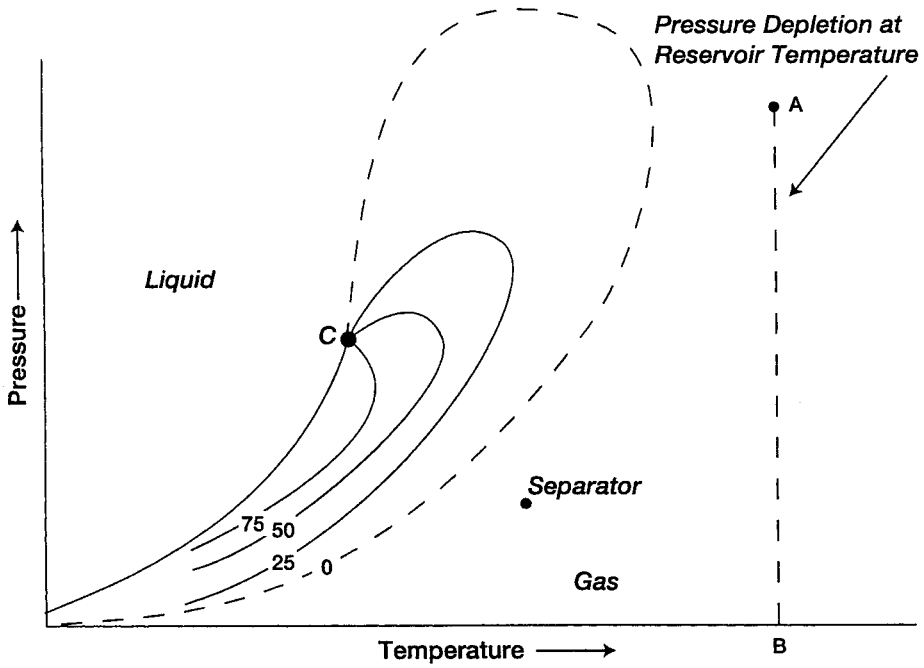


FIGURE 1-31 Phase diagram for a dry gas.

Source: After N. J. Clark, *Elements of Petroleum Reservoirs*, 2nd ed. Tulsa, OK: Society of Petroleum Engineers, 1969.

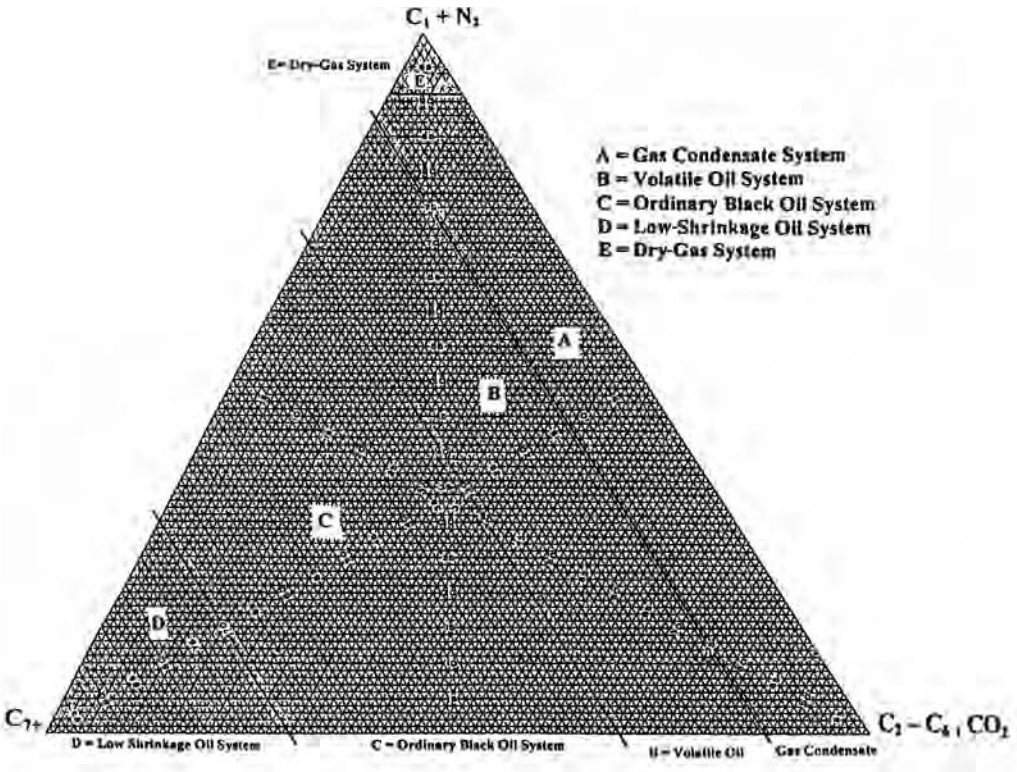


FIGURE 1-32 Composition of various reservoir fluid systems.

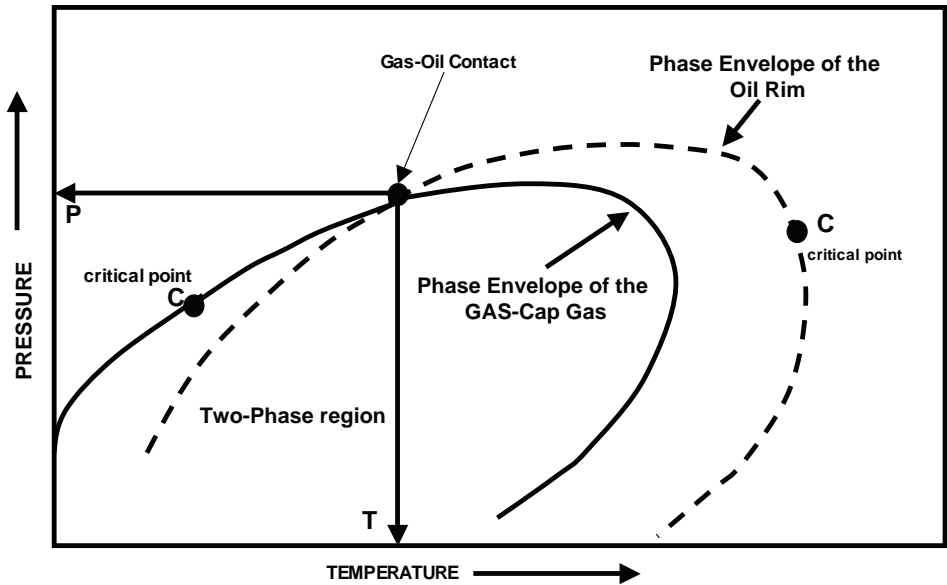


FIGURE 1-33 *Retrograde gas-cap reservoir.*

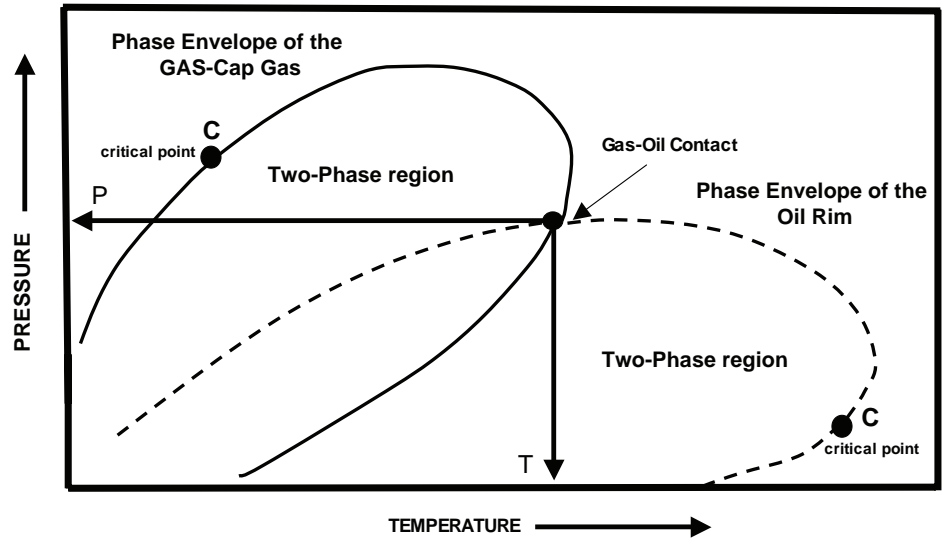


FIGURE 1-34 *Dry gas-cap reservoir.*

to substantiate the presence of a second equilibrium phase above (i.e., gas cap) or below (i.e., oil rim) the tested well. This may entail running a repeat-formation-tester tool to determine fluid-pressure gradient as a function of depth; or a new well may be required up dip or down dip to that of the discovery well.

When several samples are collected at various depths, they exhibit PVT properties as a function of the depth expressed graphically to locate the gas-oil contact (GOC). The variations of PVT properties can be expressed graphically in terms of the compositional

changes of C_1 and C_{7+} with depth and in terms of well-bore and stock-tank densities with depth, as shown in Figures 1–35 through 1–37.

Defining the fluid contacts, that is, GOC and water-oil contact (WOC), are extremely important when determining the hydrocarbon initially in place and planning field development. The uncertainty in the location of the fluid contacts can have a significant impact on the reserves estimate. Contacts can be determined by

1. Electrical logs, such as resistivity tools.
2. Pressure measurements, such as a repeat formation tester (RFT) or a modular formation dynamic tester (MDT).
3. Possibly by interpreting seismic data.

Normally, unless a well penetrates a fluid contact directly, there remains doubt as to its locations. The RFT is a proprietary name used by Schlumberger for an open-hole logging tool used to establish vertical pressure distribution in the reservoir (i.e., it provides a pressure-depth profile in the reservoir) and to obtain fluid samples. At the appraisal stage of a new field, the RFT survey provides the best-quality pressure data and routinely is run to establish fluid contacts. The surveys are usually straightforward to interpret compared to the drill-stem tests (DSTs), because no complex buildup analysis is required to determine the reservoir pressure nor are any extensive depth corrections to be applied, since the gauge depth is practically coincidental with that of the RFT probe.

The RFT tool is fitted with a pressure transducer and positioned across the target zone. The device is placed against the side of the bore hole by a packer. A probe that consists of two pretest chambers, each fitted with a piston, is pushed against the formation and

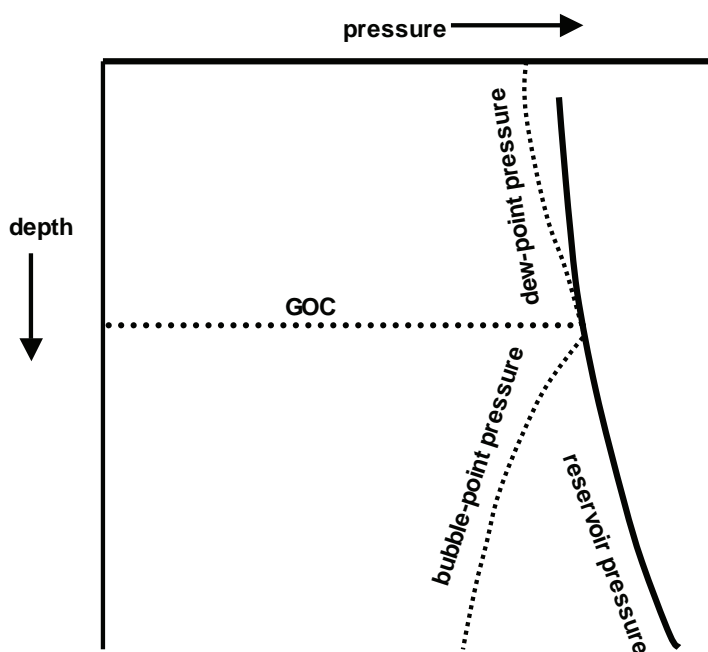


FIGURE 1–35 Determination of GOC from pressure gradients.

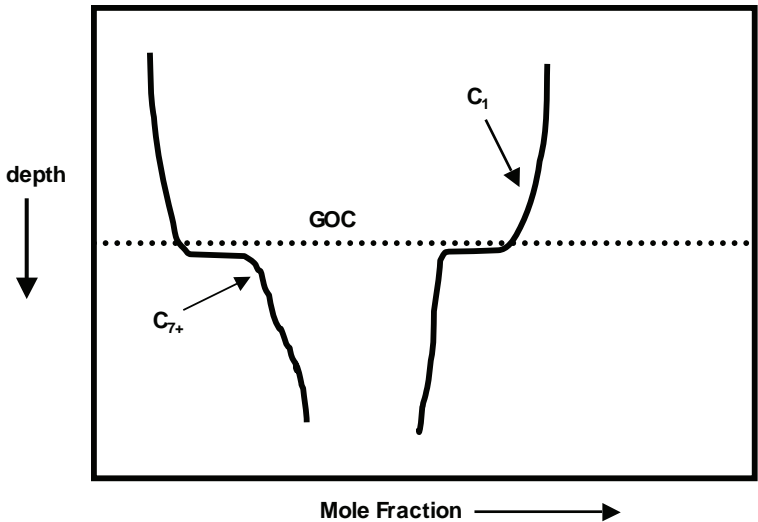


FIGURE 1-36 Compositional changes of C_1 and C_{7+} with depth.

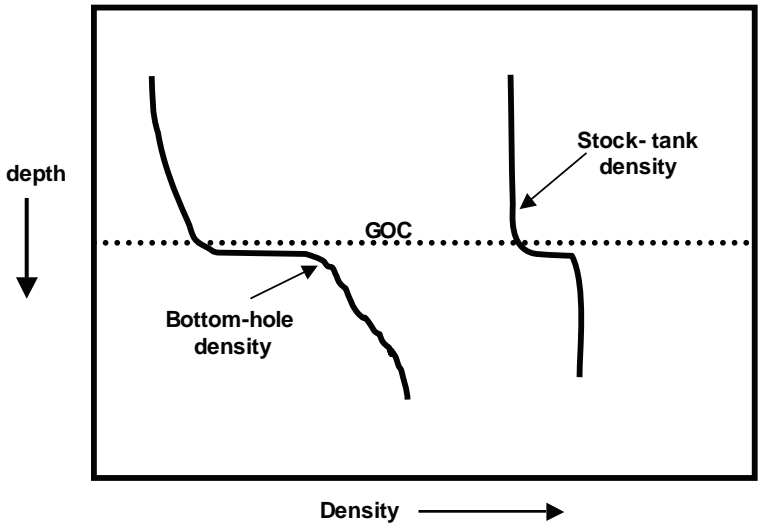


FIGURE 1-37 Variation of well-bore and stock-tank density with depth.

through the mud cake. A pressure drawdown is created at the probe by withdrawing the pistons in the pretest chambers. These two chambers operate in series: The first piston is withdrawn slowly (taking about 4 seconds to withdraw 10 cm³ of fluid); the second piston is withdrawn at a faster rate, 5 seconds for 10 cm³. Before the tool is set against the formation, the pressure transducer records the mud pressure at the target depth.

As the first pretest chamber is filled (slowly) with fluid; the first main pressure drop Δp_1 is observed, followed by Δp_2 as the second pretest chamber is filled. The tighter the formation, the larger Δp_1 and Δp_2 are. The recording, therefore, gives a qualitative indication of the permeability of the reservoir. Because the flow rate and pressure drop are

known, the actual formation permeability can be calculated, and this is done by the CSU (the computer in the logging unit). Caution should be attached to the permeability values, since a very small part of the reservoir is being tested and the analysis assumes a particular flow regime, which may not be representative in some cases. The reliability of the values should be regarded as indicating the order of magnitude of the permeability.

Once both drawdowns have occurred, fluid withdrawal stops and the formation pressure is allowed to recover. This recovery is recorded as the pressure buildup, which should stabilize at the true formation fluid pressure at the depth. Note that the drawdown pressure drops, Δp_1 and Δp_2 , are relative to the final pressure buildup and not to the initial pressure, which was the mud pressure. The rate of pressure buildup can be used to estimate permeability; the test therefore gives three permeability estimates at the same sample point.

A tight formation leads to very large pressure drawdowns and a slow buildup. If the pressure has not built up within 4–5 minutes, the pressure test usually is abandoned for fear of the tool becoming stuck. The tool is retracted and the process repeated at a new depth. Once the tool is unset, the pressure reading should return to the same mud pressure as prior to setting. This is used as a quality control check on gauge drift. There is no limit as to the number of depths at which pressure samples may be taken.

If a fluid sample is required, this can be done by diverting the fluid flow during sampling to sample chambers in the tool.

It should be pointed out that, when plotting the pressure against depth, the unit of pressures must be kept consistent, that is, either in absolute pressure (psia) or gauge pressure (psig). The depth must be the true vertical depth, preferably below the subsurface datum depth.

The basic principle of pressure versus depth plotting is illustrated in Figure 1–38. This illustration shows two wells:

- Well 1 penetrates the gas cap with a recorded gas pressure of p_g and a measured gas density of ρ_g .
- Well 2 penetrates the oil zone with a recorded oil pressure of p_o and oil density of ρ_o .

The gas, oil, and water gradients can be calculated from:

$$\frac{dp_g}{db} = \frac{\rho_g}{144} = \gamma_g$$

$$\frac{dp_o}{db} = \frac{\rho_o}{144} = \gamma_o$$

$$\frac{dp_w}{db} = \frac{\rho_w}{144} = \gamma_w$$

where

dp/db = fluid gradient, psi/ft

γ_g = gas gradient, psi/ft

γ_o = oil gradient, psi/ft

γ_w = water gradient, psi/ft

ρ_g = gas density, lb/ft³

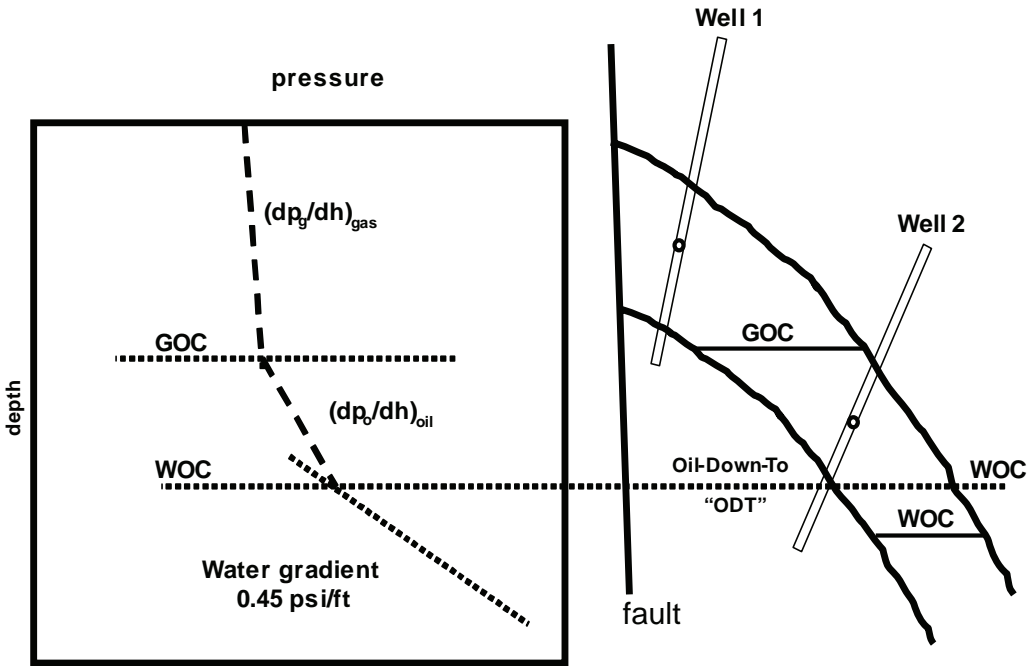


FIGURE 1-38 Pressure gradient versus depth.

ρ_o = oil density, lb/ft³

ρ_w = water density, lb/ft³

As shown in Figure 1-38, the intersection of the gas and oil gradient lines locates the position of the gas-oil contact. Note that the oil can be seen only down to a level termed the oil-down-to (ODT) level. The level is assigned to the oil-water contact unless a well is drilled further downdip to locate the WOC.

Figure 1-39 shows another case where a well penetrated an oil column. Oil can be seen down to the ODT level. However, a gas cap may exist. If the pressure of the oil is recorded as p_o and the bubble-point pressure is measured as p_b at this specific depth, the gas-oil contact can be determined from

$$\Delta D = \frac{p_o - p_b}{\left(\frac{dp}{dh}\right)_{oil}} = \frac{p_o - p_b}{\gamma_o} \quad (1-18)$$

If the calculated value of ΔD locates the GOC within the reservoir, then there is a possibility that a gas cap exists, but this is not certain. Equation (1-18) assumes that the PVT properties, including the bubble-point pressure, do not vary with depth. The only way to be certain that a gas cap exists is to drill a crestal well.

A similar scenario that can be encountered is illustrated Figure 1-40. Here, a discovery well penetrates a gas column with gas as seen down to the gas-down-to (GDT) level, which allows the possibility of a downdip oil rim. If the field operator feels that an oil rim

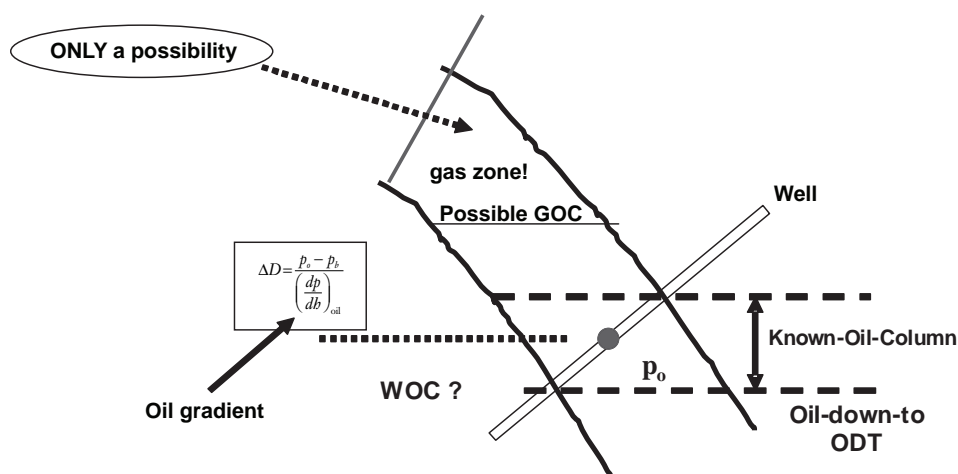


FIGURE 1-39 A well in the oil rim. A discovery well penetrates an oil column. What is the possibility of a gas cap updip?

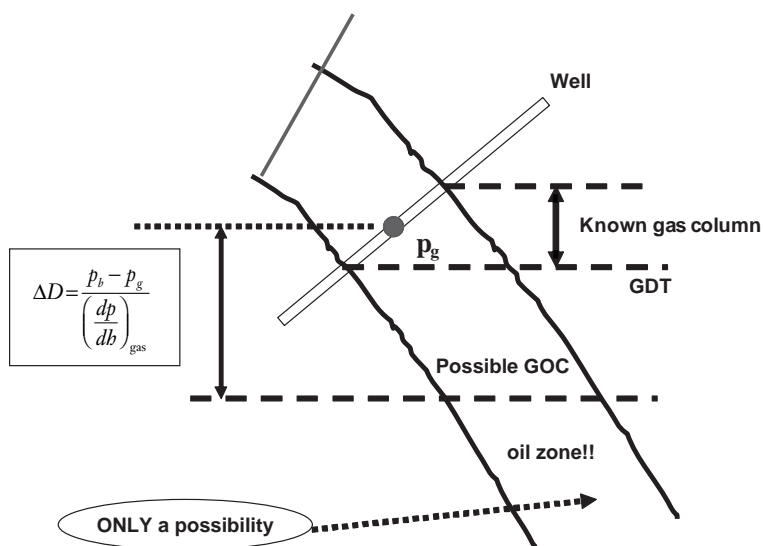


FIGURE 1-40 A discovery well penetrates a gas column. What is the possibility of an oil rim?

exists, based on similarity with other fields in the area, the distance to GOC can be estimated from

$$\Delta D = \frac{p_b - p_g}{\left(\frac{dp}{db}\right)_{gas}} = \frac{p_b - p_g}{\gamma_g}$$

Figure 1-41 shows a case where two wells are drilled: The first well is in the gas column and the second penetrates the water zone. Of course, only two possibilities could exist:

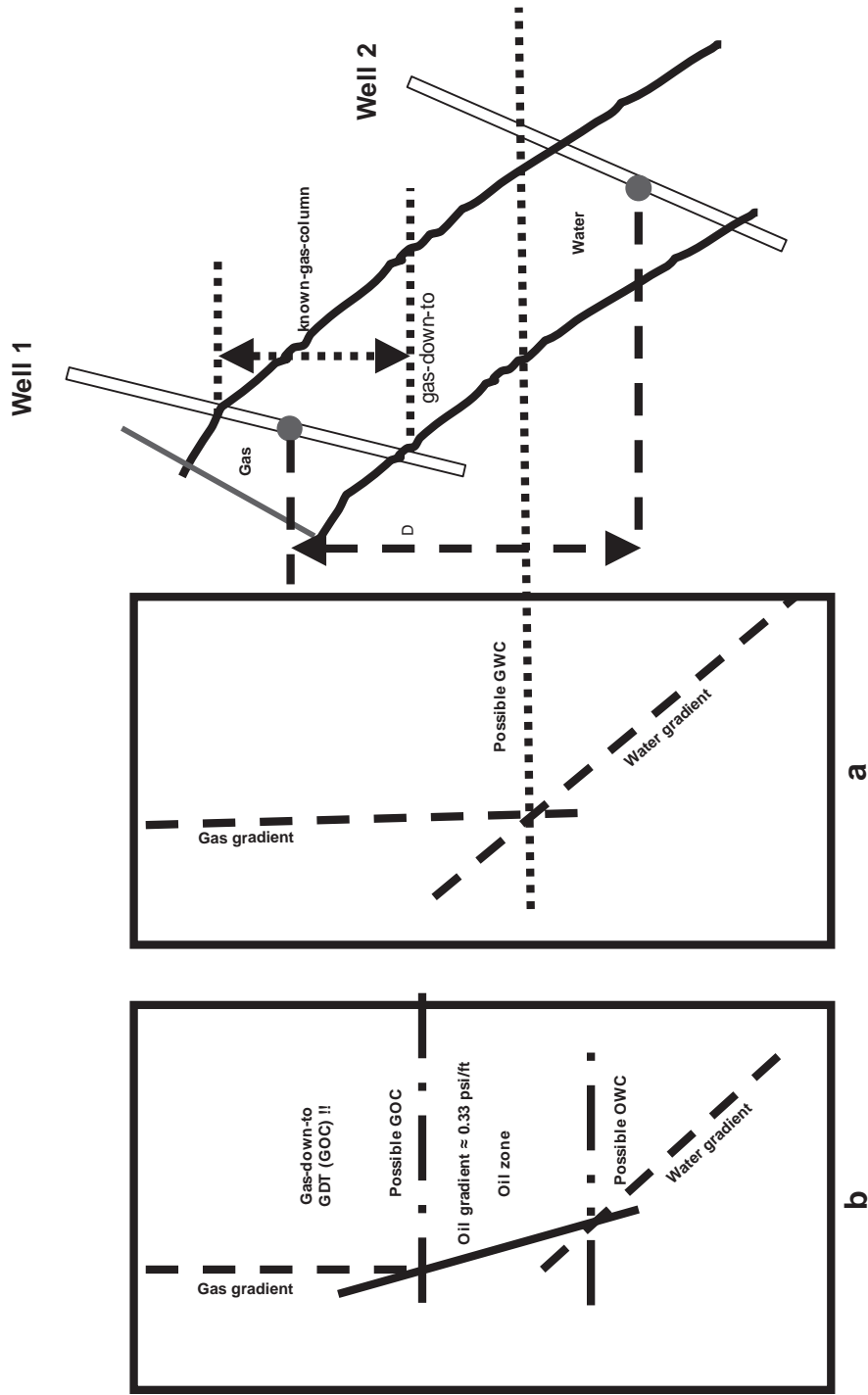


FIGURE 1-41 Two discovery wells.

1. The first possibility is shown in Figure 1–41(a), which suggests a known gas column with an underlying water zone. Also, the gas-water contact (GWC) has not been established. A “possible” GWC can be calculated from the following relationship:

$$D_1 = \frac{p_g - \left[p_w - D \left(\frac{dp}{db} \right)_{\text{water}} \right]}{\left(\frac{dp}{db} \right)_{\text{water}} - \left(\frac{dp}{db} \right)_{\text{gas}}} = \frac{p_g - [p_w - D\gamma_{\text{water}}]}{\gamma_{\text{water}} - \gamma_{\text{gas}}}$$

where

γ = fluid gradient, psi/ft that is, $\rho/144$

ρ = fluid density, lb/ft³

D_1 = vertical distance between gas well and GWC, ft

D = vertical distance between the two wells

$dp/db = \gamma$ = fluid gradient, psi/ft

2. The second possibility is shown in Figure 1–41(a), where a possible oil zone exists between the two wells. Assuming a range of oil gradients, such as 0.28–0.38 psi/ft, the maximum possible oil thickness can be estimated graphically as shown in Figure 1–41(b), by drawing a line originating at the GDT level with a slope in the range of 0.28–0.38 psi/ft to intersect with the water gradient line.

If the bubble point pressure can be assumed, the maximum oil column thickness can be estimated, as shown in Figure 1–42, from the following expression:

$$\Delta D_2 = \frac{\Delta D \left(\frac{dp_w}{db} \right) - (p_w - p_b) - (p_b - p_g) \frac{dp_w / db}{dp_g / db}}{\frac{dp_w}{db} - \frac{dp_o}{db}} = \frac{\Delta D \gamma_w - (p_w - p_b) - (p_b - p_g) \frac{\gamma_w}{\gamma_g}}{\gamma_w - \gamma_o}$$

where

ΔD_2 = maximum possible oil column thickness, ft

ΔD = vertical distance between the two wells, ft

dp/db = fluid pressure gradient, psi/ft

EXAMPLE 1–8

Figure 1–43 shows two wells. One penetrated the gas zone at 4950 ft true vertical depth (TVD) and the other in the water zone at 5150 ft. Pressures and PVT data follow:

$$p_g = 1745 \text{ psi}$$

$$\rho_g = 14.4 \text{ lb/ft}^3$$

$$p_w = 1808 \text{ psi}$$

$$\rho_w = 57.6 \text{ lb/ft}^3$$

A nearby field has a bubble-point pressure of 1750 psi and an oil density of 50.4 lb/ft³ ($\rho_o = 50.4 \text{ lb/ft}^3$). Calculate

1. Possible depth to GOC.

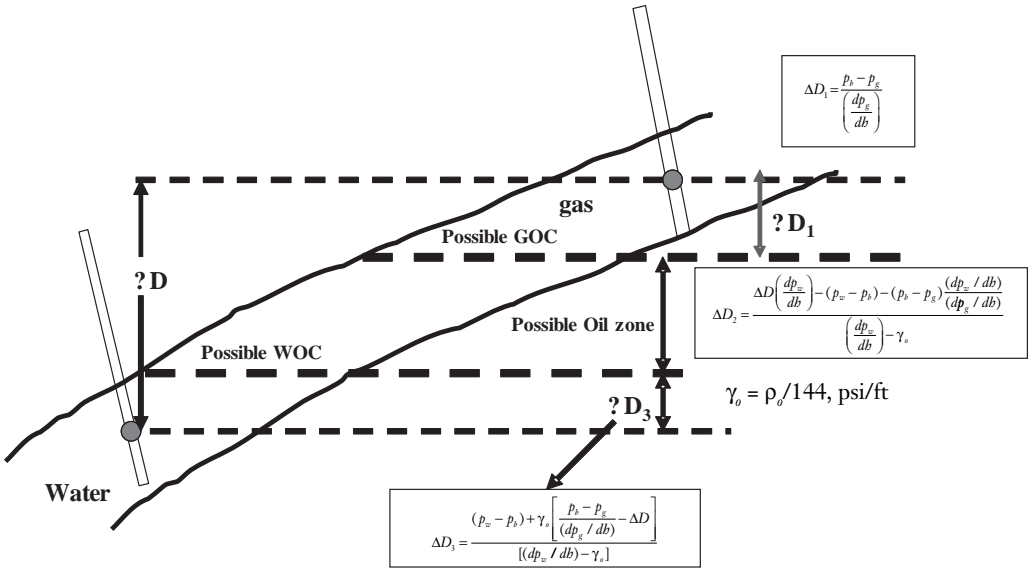


FIGURE 1-42 Two discovery wells, maximum possible oil thickness.

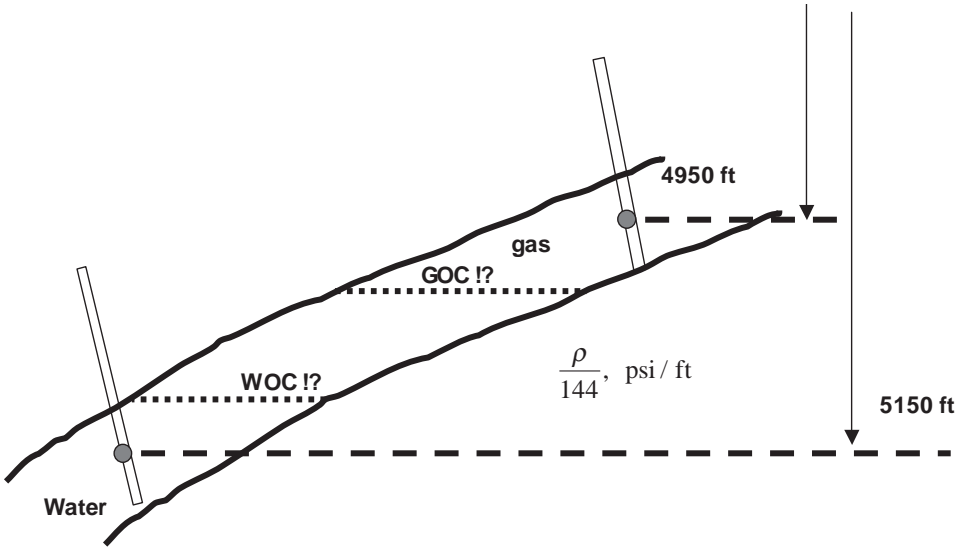


FIGURE 1-43 Example 1-8.

2. Maximum possible oil column thickness.
3. Possible depth to WOC.

SOLUTION

Step 1 Calculate the pressure gradient of each phase:

$$\text{Gas phase} \quad \left(\frac{dp}{db}\right)_{\text{gas}} = \frac{\rho_g}{144} = \frac{14.4}{144} = 0.1 \text{ psi/ft}$$

$$\text{Oil phase} \quad \left(\frac{dp}{db} \right)_{\text{oil}} = \frac{\rho_o}{144} = \frac{50.4}{144} = 0.35 \text{ psi/ft}$$

$$\text{Water phase} \quad \left(\frac{dp}{db} \right)_{\text{water}} = \frac{\rho_w}{144} = \frac{57.6}{144} = 0.4 \text{ psi/ft}$$

Step 2 Calculate the distance to the possible GOC:

$$\text{GOC} = 4950 + \frac{p_b - p_g}{dp_g / db} = 4950 + \frac{1750 - 1745}{0.10} = 5000 \text{ ft}$$

Step 3 Calculate maximum oil rim thickness:

$$\Delta D_2 = \frac{\Delta D \gamma_w - (p_w - p_b) - (p_b - p_g) \frac{\gamma_w}{\gamma_g}}{\gamma_w - \gamma_o}$$

$$\Delta D_2 = \text{maximum oil thickness} = \frac{200(0.4) - (1808 - 1750) - (1750 - 1745) \frac{(0.4)}{(0.1)}}{(0.4) - (0.35)} = 40 \text{ ft}$$

Step 4 Possible depth to WOC:

$$\text{WOC} = 5000 + 40 = 5040 \text{ ft}$$

Phase Rule

It is appropriate at this stage to introduce and define the concept of the phase rule. Gibbs (1948 [1876]) derived a simple relationship between the number of phases, P , in equilibrium, the number of components, C , and the number of independent variables, F , that must be specified to describe the state of the system completely.

Gibbs proposed the following fundamental statement of the phase rule:

$$F = C - P + 2 \quad (1-19)$$

where

F = number of variables required to determine the state of the system at equilibrium or number of degrees of freedom (such as pressure, temperature, density)

C = number of independent components

P = number of phases

A phase was defined as a homogeneous system of uniform physical and chemical compositions. The degrees of freedom, F , for a system include the intensive properties such as temperature, pressure, density, and composition (concentration) of phases. These independent variables must be specified to define the system completely. In a single component ($C = 1$), two-phase system ($P = 2$), there is *only* 1 degree of freedom ($F = 1 - 2 + 2 = 1$); therefore, only pressure or temperature needs to be specified to determine the thermodynamic state of the system.

The phase rule as described by equation (1-19) is useful in several ways. It indicates the maximum number of equilibrium phases that can coexist and the number of compo-

nents present. It should be pointed out that the phase rule does not determine the nature, exact composition, or total quantity of the phases. Furthermore, it applies only to a system in stable equilibrium and does not determine the rate at which this equilibrium is attained.

The importance and the practical application of the phase rule are illustrated through the following examples.

EXAMPLE 1-9

For a single-component system, determine the number of degrees of freedom required for the system to exist in the single-phase region.

SOLUTION

Applying equation (1-19) gives $F = 1 - 1 + 2 = 2$. Two degrees of freedom must be specified for the system to exist in the single-phase region. These must be the pressure p and the temperature T .

EXAMPLE 1-10

What degrees of freedom are allowed for a two-component system in two phases?

SOLUTION

Since $C = 2$ and $P = 2$, applying equation (1-19) yields $F = 2 - 2 + 2 = 2$. The two degrees of freedom could be the system pressure p and the system temperature T , and the concentration (mole fraction), or some other combination of T , p , and composition.

EXAMPLE 1-11

For a three-component system, determine the number of degrees of freedom that must be specified for the system to exist in the one-phase region.

SOLUTION

Using the phase rule expression gives $F = 3 - 1 + 2 = 4$, four independent variables must be specified to fix the system. The variables could be the pressure, temperature, and mole fractions of two of the three components.

From the foregoing discussion it can be observed that hydrocarbon mixtures may exist in either the gas or liquid state, depending on the reservoir and operating conditions to which they are subjected. The qualitative concepts presented may be of aid in developing quantitative analyses. Empirical equations of state are commonly used as a quantitative tool in describing and classifying the hydrocarbon system. These equations of state require

- Detailed compositional analysis of the hydrocarbon system.
- Complete description of the physical and critical properties of the mixture of the individual components.

Problems

1. The following is a list of the compositional analysis of different hydrocarbon systems, with the compositions as expressed in terms of mol%. Classify each of these systems.

Component	System 1	System 2	System 3	System 4
C_1	68.00	25.07	60.00	12.15
C_2	9.68	11.67	8.15	3.10
C_3	5.34	9.36	4.85	2.51
C_4	3.48	6.00	3.12	2.61
C_5	1.78	3.98	1.41	2.78
C_6	1.73	3.26	2.47	4.85
C_{7+}	9.99	40.66	20.00	72.00

2. A pure component has the following vapor pressure:
- | | | | | |
|---------------------|-------|--------|--------|--------|
| $T, ^\circ\text{F}$ | 104 | 140 | 176 | 212 |
| p_v, psi | 46.09 | 135.04 | 345.19 | 773.75 |
- a. Plot these data to obtain a nearly straight line.
 - b. Determine the boiling point at 200 psi.
 - c. Determine the vapor pressure at 250°F.
3. The critical temperature of a pure component is 260°F. The densities of the liquid and vapor phase at different temperatures are
- | | | | | |
|--------------------------|--------|--------|--------|--------|
| $T, ^\circ\text{F}$ | 86 | 122 | 158 | 212 |
| $\rho_L, \text{lb/ft}^3$ | 40.280 | 38.160 | 35.790 | 30.890 |
| $\rho_v, \text{lb/ft}^3$ | 0.886 | 1.691 | 2.402 | 5.054 |
- Determine the critical density of the substance.
4. Using the Lee and Kesler vapor correlation, calculate the vapor pressure of i-butane at 100°F. Compare the calculated vapor pressure with that obtained from the Cox charts.
5. Calculate the saturated liquid density of n-butane at 200°F using
- a. The Rackett correlation.
 - b. The modified Rackett correlation.
- Compare the calculated two values with the experimental value determined from Figure 1–5.
6. What is the maximum number of phases that can be in equilibrium at constant temperature and pressure in one-, two-, and three-component systems?
7. For a seven-component system, determine the number of degrees of freedom that must be specified for the system to exist in the following regions:
- a. One-phase region.
 - b. Two-phase region.
8. Figure 1–9 shows the phase diagrams of eight mixtures of methane and ethane along with the vapor pressure curves of the two components. Determine
- a. Vapor pressure of methane at –160°F.
 - b. Vapor pressure of ethane at 60°F.
 - c. Critical pressure and temperature of mixture 7.
 - d. Cricondenbar and cricondentherm of mixture 7.

- e. Upper and lower dew-point pressures of mixture 6 at 20°F.
- f. The bubble-point and dew-point pressures of mixture 8 at 60°F.
9. Using Figure 1–9, prepare and identify the different phase regions of the pressure/composition diagram for the following temperatures:
 - a. –120°F.
 - b. 20°F.
10. Using Figure 1–9, prepare the temperature-composition diagram (commonly called the *T/X diagram*) at the following pressures:
 - a. 300 psia.
 - b. 700 psia.
 - c. 800 psia.
11. Derive equations for the amounts of liquid and vapor present in the two-phase region when the composition is expressed in terms of
 - a. Weight fraction of the more volatile component.
 - b. Weight fraction of the less volatile component.
12. A 20 ft³ capacity tank is evacuated and thermostated at 60°F. Five pounds of liquid propane is injected. What is the pressure in the tank and the proportions of liquid and vapor present? Repeat calculations for 100 lbs of propane injected.

References

- Ahmed, T. "Composition Modeling of Tyler and Mission Canyon Formation Oils with CO₂ and Lean Gasses." Final report submitted to Montana's on a New Track for Science (MONTs), Montana National Science Foundation Grant Program, 1985.
- Burcik, E. *Properties of Petroleum Reservoir Fluids*. Boston: International Human Resources Development Corporation (IHRDC), 1957.
- Clark, N. "It Pays to Know Your Petroleum." *World Oil* 136 (March 1953): 165–172.
- Clark, N. *Elements of Petroleum Reservoirs*, 2nd ed. Dallas: Society of Petroleum Engineers, 1969.
- Edmister, W. C. "Applied Hydrocarbon Thermodynamic, Part 4, Compressibility Factors and Equations of State," *Petroleum Refinery* 37 (April 1958): 173–179.
- Gibbs, J. W. *The Collected Works of J. Willard Gibbs*, trans. Connecticut Academy of Arts and Sciences, vol. 1. New Haven: Yale University Press, 1948, original text published 1876.
- Katz, D. L., and A. Firoozabadi. "Predicting Phase Behavior of Condensate/Crude-Oil Systems Using Methane Interaction Coefficients." *Journal of Petroleum Technology* (November 1978): 1649–1655.
- Lee, B. I., and M. G. Kesler. "A Generalized Thermodynamics Correlation Based on Three-Parameter Corresponding States." *AICHE Journal* 21, no. 3 (May 1975): 510–527.
- McCain, W. D. "Heavy Components Control Reservoir Fluid Behavior." *Journal of Petroleum Technology* (September 1994): 746–750.
- Nath, J. "Acentric Factor and Critical Volumes for Normal Fluids." *Ind. Eng. Chem. Fundam.* 21, no. 3 (1985): 325–326.
- Pitzer, K. S. "The Volumetric and Thermodynamics Properties of Fluids." *Journal of the American Chemical Society* 77, no. 13 (July 1955): 3427–3433.

- Rackett, H. G. "Equation of State for Saturated Liquids." *Journal of Chemical Engineering Data* 15, no. 4 (1970): 514–517.
- Riazi, M. R., and T. E. Daubert. "Characterization Parameters for Petroleum Fractions." *Ind. Eng. Chem. Res.* 26, no. 24 (1987): 755–759.
- Salerno, S., et al. "Prediction of Vapor Pressures and Saturated Vol." *Fluid Phase Equilibria* 27 (June 10, 1985): 15–34.
- Spencer, F. F., and R. P. Danner. "Prediction of Bubble-Point Density of Mixtures," *Journal of Chemical Engineering Data* 18, no. 2 (1973): 230–234.
- Yamada, T., and R. Gunn. "Saturated Liquid Molar Volumes: The Rackett Equation," *Journal of Chemical Engineering Data* 18, no. 2 (1973): 234–236.

2

Characterizing Hydrocarbon-Plus Fractions

THERE ARE DIFFERENT WAYS to classify the components of the reservoir fluids. Normally, the constituents of a hydrocarbon system are classified into the following two categories: well-defined petroleum fractions and undefined petroleum fractions. The *well-defined* components include

- Nonhydrocarbon fractions, that is, CO₂, N₂, H₂S.
- Methane C₁ through normal pentane n-C₅. Methane through propane exhibit unique molecular structures, while butane C₄ can exist as two isomers and pentane C₅ as three isomers.
- Hexane C₆ and heavier, where the number of isomers rises exponentially.

Katz and Firoozabadi (1978) presented a generalized set of physical properties for the petroleum fractions C₆ through C₄₅ that are expressed as a single carbon number (SCN), such as the C₆ group, C₇ group, or C₈ group. The tabulated properties of these groups include the average boiling point, specific gravity, and molecular weight. The authors proposed a set of tabulated properties generated by analyzing the physical properties of 26 condensates and crude oil systems. These generalized properties are given in Table 2–1.

Ahmed (1985) correlated Katz and Firoozabadi's (1978) tabulated physical properties with the number of carbon atoms of the fraction by using a regression model. The generalized equation has the following form:

$$\theta = a_1 + a_2n + a_3n^2 + a_4n^3 + \frac{a_5}{n}$$

where

θ = any physical property, such as T_c , p_c , or V_c

TABLE 2-1 Generalized Physical Properties

Group	T _b (°R)	γ	K	M	T _c (°R)	P _c (psia)	ω	V _c (ft ³ /lb)
C ₆	607	0.690	12.27	84	923	483	0.250	0.06395
C ₇	658	0.727	11.96	96	985	453	0.280	0.06289
C ₈	702	0.749	11.87	107	1,036	419	0.312	0.06264
C ₉	748	0.768	11.82	121	1,085	383	0.348	0.06258
C ₁₀	791	0.782	11.83	134	1,128	351	0.385	0.06273
C ₁₁	829	0.793	11.85	147	1,166	325	0.419	0.06291
C ₁₂	867	0.804	11.86	161	1,203	302	0.454	0.06306
C ₁₃	901	0.815	11.85	175	1,236	286	0.484	0.06311
C ₁₄	936	0.826	11.84	190	1,270	270	0.516	0.06316
C ₁₅	971	0.836	11.84	206	1,304	255	0.550	0.06325
C ₁₆	1,002	0.843	11.87	222	1,332	241	0.582	0.06342
C ₁₇	1,032	0.851	11.87	237	1,360	230	0.613	0.06350
C ₁₈	1,055	0.856	11.89	251	1,380	222	0.638	0.06362
C ₁₉	1,077	0.861	11.91	263	1,400	214	0.662	0.06372
C ₂₀	1,101	0.866	11.92	275	1,421	207	0.690	0.06384
C ₂₁	1,124	0.871	11.94	291	1,442	200	0.717	0.06394
C ₂₂	1,146	0.876	11.95	300	1,461	193	0.743	0.06402
C ₂₃	1,167	0.881	11.95	312	1,480	188	0.768	0.06408
C ₂₄	1,187	0.885	11.96	324	1,497	182	0.793	0.06417
C ₂₅	1,207	0.888	11.99	337	1,515	177	0.819	0.06431
C ₂₆	1,226	0.892	12.00	349	1,531	173	0.844	0.06438
C ₂₇	1,244	0.896	12.00	360	1,547	169	0.868	0.06443
C ₂₈	1,262	0.899	12.02	372	1,562	165	0.894	0.06454
C ₂₉	1,277	0.902	12.03	382	1,574	161	0.915	0.06459
C ₃₀	1,294	0.905	12.04	394	1,589	158	0.941	0.06468
C ₃₁	1,310	0.909	12.04	404	1,603	143	0.897	0.06469
C ₃₂	1,326	0.912	12.05	415	1,616	138	0.909	0.06475
C ₃₃	1,341	0.915	12.05	426	1,629	134	0.921	0.06480
C ₃₄	1,355	0.917	12.07	437	1,640	130	0.932	0.06489
C ₃₅	1,368	0.920	12.07	445	1,651	127	0.942	0.06490
C ₃₆	1,382	0.922	12.08	456	1,662	124	0.954	0.06499
C ₃₇	1,394	0.925	12.08	464	1,673	121	0.964	0.06499
C ₃₈	1,407	0.927	12.09	475	1,683	118	0.975	0.06506
C ₃₉	1,419	0.929	12.10	484	1,693	115	0.985	0.06511
C ₄₀	1,432	0.931	12.11	495	1,703	112	0.997	0.06517
C ₄₁	1,442	0.933	12.11	502	1,712	110	1.006	0.06520
C ₄₂	1,453	0.934	12.13	512	1,720	108	1.016	0.06529
C ₄₃	1,464	0.936	12.13	521	1,729	105	1.026	0.06532
C ₄₄	1,477	0.938	12.14	531	1,739	103	1.038	0.06538
C ₄₅	1,487	0.940	12.14	539	1,747	101	1.048	0.06540

Source: Permission to publish from the Society of Petroleum Engineers of the AIME. © SPE-AIME.

n = number of carbon atoms, that is, 6, 7, . . . , 45

$a_1 - a_5$ = coefficients of the equation as tabulated in Table 2-2

The *undefined* petroleum fractions are those heavy components lumped together and identified as the plus-fraction; for example, C₇₊ fraction. Nearly all naturally occurring hydrocarbon systems contain a quantity of heavy fractions that are not well defined and

TABLE 2-2 *Coefficients of the Equation*

θ	a_1	a_2	a_3	a_4	a_5
M	-131.11375000	24.96156000	-0.34079022	2.4941184×10^{-3}	468.3257500
$T_c, ^\circ R$	915.53747000	41.42 133700	-0.75868590	5.8675351×10^{-3}	-1.3028779×10^3
p_c , psia	275.56275000	-12.52226900	0.29926384	$-2.8452129 \times 10^{-3}$	1.7117226×10^3
$T_b, ^\circ R$	434.38878000	50.12527900	-0.9097293	7.0280657×10^{-3}	-601.856510
ω	-0.50862704	$8.70021100 \times 10^{-2}$	$-1.84848140 \times 10^{-3}$	1.4663890×10^{-5}	1.8518106
γ	0.86714949	$3.41434080 \times 10^{-3}$	$-2.83962700 \times 10^{-5}$	2.4943308×10^{-8}	-1.1627984
V_c , ft ³ /lb	5.223458×10^{-2}	$7.87091369 \times 10^{-4}$	$-1.93244320 \times 10^{-5}$	1.7547264×10^{-7}	4.4017952×10^{-2}

not mixtures of discretely identified components. Methods of characterizing the undefined petroleum fractions are the main subject of this chapter.

A proper description of the physical properties of the plus fractions and other undefined petroleum fractions in hydrocarbon mixtures is essential in performing reliable phase behavior calculations and compositional modeling studies. Frequently, a distillation analysis or a chromatographic analysis is available for this undefined fraction. Other physical properties, such as molecular weight and specific gravity, also may be measured for the entire fraction or various cuts of it.

To use any of the thermodynamic property-prediction models, such as an equation of state, to predict the phase and volumetric behavior of complex hydrocarbon mixtures, one must be able to provide the acentric factor, critical temperature, and critical pressure for both the defined and undefined (heavy) fractions in the mixture. The problem of how to adequately characterize these undefined plus fractions in terms of their critical properties and acentric factors has been long recognized in the petroleum industry. Whitson (1984) presented an excellent documentation on the influence of various heptanes-plus (C_{7+}) characterization schemes on predicting the volumetric behavior of hydrocarbon mixtures by equations of state.

Usually the data available on hydrocarbon-plus fractions can be divided into the following three groups:

- Group 1* A complete true boiling point (TBP) analysis in which the C_{7+} fraction is divided into fractions or "cuts," characterized by boiling-point range. The distillation provides the key data for C_{7+} characterization, including molecular weight, specific gravity, and boiling point of each distillation cut. Each TBP cut often is treated as a component with a unique boiling point, T_c , p_c , and other properties associated with pure components.
- Group 2* A chromatographic analysis, by liquid or gas chromatograph (GC) of the plus fraction is designed to provide the relative amount of fractions that make up the C_{7+} . This simulated distillation process requires smaller samples and is less expensive than the TBP distillation. However, simulated distillation results can be calibrated against TBP data to provide with the physical properties of individual fractions.
- Group 3* No distillation data is reported, rather the specific gravity and molecular weight of heavy fractions are the only available information on the fraction.

Based on the available data on the plus fraction, three approaches commonly are used to generate properties of the plus fractions: generalized correlations, correlations based on the *PNA* determination, and graphical correlations. These three techniques of characterizing the undefined petroleum fractions are detailed here.

Generalized Correlations

The molecular weight, M , specific gravity, γ , and boiling point temperature, T_b , are considered the key properties that reflect the chemical makeup of petroleum fractions. Watson, Nelson, and Murphy (1935) introduced a widely used characterization factor, commonly known as the *Watson* or *universal oil products* (UOP) *characterization factor*, based on the normal boiling point and specific gravity. This characterization parameter is given by the following expression:

$$K_w = \frac{T_b^{1/3}}{\gamma} \quad (2-1)$$

where

K_w = Watson characterization factor

T_b = normal boiling point temperature, °R

γ = specific gravity

The characterization parameter K_w varies roughly from 8.5 to 13.5 as follows:

- For paraffinic, P , compounds, K_w ranges from 12.5 to 13.5.
- For naphthenic, N , compounds, K_w ranges from 11.0 to 12.5.
- For aromatic, A , compounds, K_w ranges from 8.5 to 11.0.

It should be pointed out that some overlap in K_w exists among these three families of hydrocarbons, and a combination of paraffins and aromatics compounds obviously “appear” as a naphthenic compounds. However, these characterization factors are essentially used to provide a qualitative measure of the composition of a petroleum fraction. The Watson characterization factor is widely used as a parameter for correlating petroleum-fraction properties, such as molecular weight, viscosity, vapor pressure, and critical properties.

Whitson (1980) suggests that the Watson factor can be correlated with the molecular weight M and specific gravity γ by the following expression:

$$K_w \approx 4.5579 \left[\frac{M^{0.15178}}{\gamma^{0.84573}} \right] \quad (2-2)$$

Whitson and Brule (2000) observed that K_w , as correlated with $M_{C_{7+}}$ and $\gamma_{C_{7+}}$ in the expression, often is a constant for a given field. The authors suggest that a plot of molecular weight versus specific gravity of the plus fractions is useful for checking the consistency of C_{7+} molecular weight and specific gravity measurements. Austad (1983) and Whitson and Brule (2000) illustrated this observation by plotting M versus γ for C_{7+} fractions from

data on two North Sea fields, as shown in Figures 2-1 and 2-2. Data for the gas condensate in Figure 2-1 indicate an average $(K_w)_{C_{7+}} = 11.99 \pm 0.01$ for a range of molecular weights from 135 to 150. The volatile oil shown in Figure 2-2 has an average $(K_w)_{C_{7+}} = 11.90 \pm 0.01$ for a range of molecular weights from 220 to 255. The high degree of correlation for these two fields suggests accurate molecular-weight measurements by the laboratory. In general, the spread in $(K_w)_{C_{7+}}$ values exceeds ± 0.01 when measurements are performed by a commercial laboratory.

Whitson and Brule state that, when the characterization factor for a field can be determined, equation (2-2) is useful for checking the consistency of C_{7+} molecular-weight and specific-gravity measurements. Significant deviation in $(K_w)_{C_{7+}}$, such as ± 0.03 for the North Sea fields just mentioned, indicates possible error in the measured data. Because molecular weight is more prone to error than determination of specific gravity, an anomalous $(K_w)_{C_{7+}}$ usually indicates an erroneous molecular-weight measurement. For the gas condensate in Figure 2-1, a C_{7+} sample with a specific gravity of 0.775 would be expected to have a molecular weight ≈ 141 for $(K_w)_{C_{7+}} = 11.99$. If the measured value is 135, the Watson characterization factor would be 11.90. In this case, the C_{7+} molecular weight should be redetermined.

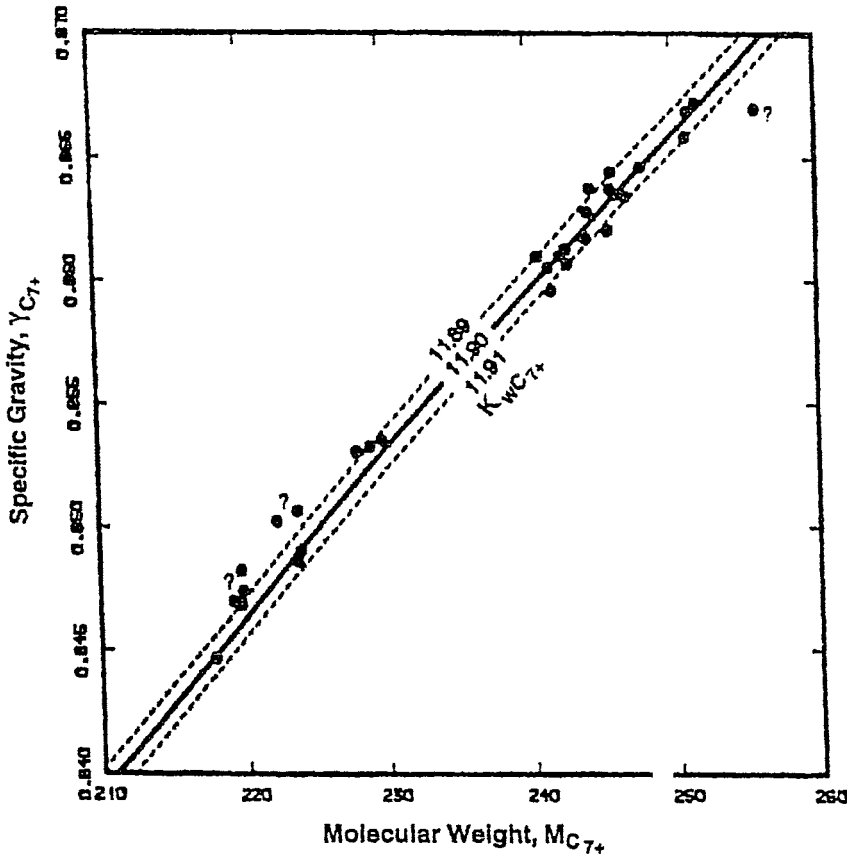


FIGURE 2-1 Specific gravity versus molecular weight of C_{7+} fraction for a North Sea volatile oil.
Source: After Austad (1983) and Whitson and Brule (2000).

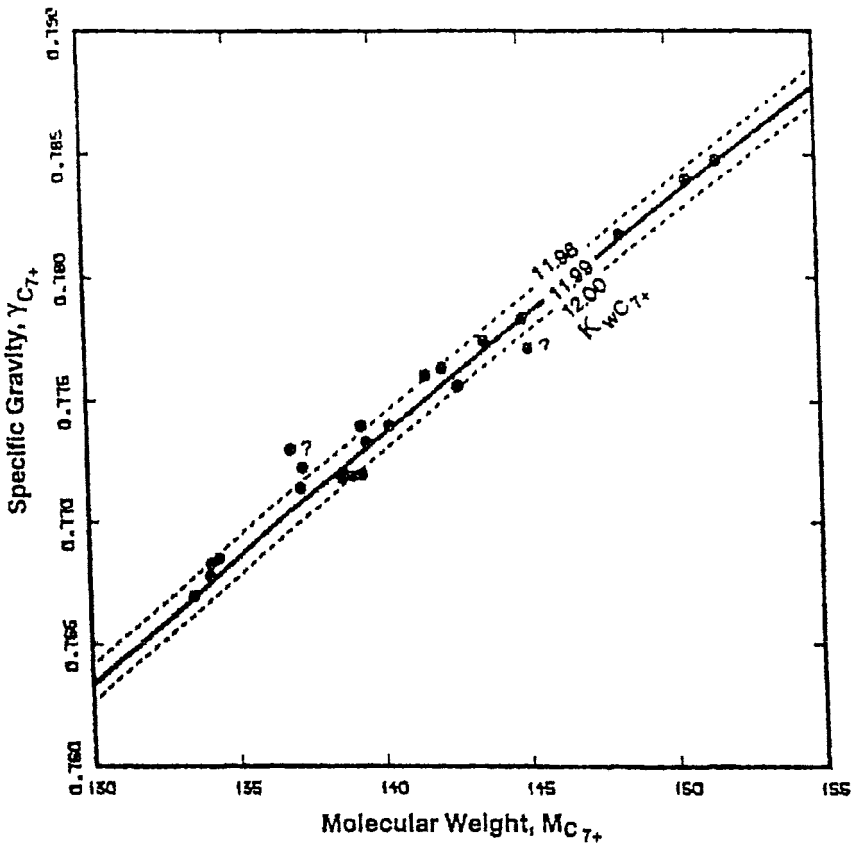


FIGURE 2-2 Specific gravity versus molecular weight of C_{7+} fraction for a North Sea gas condensate field.

Source: After Austad (1983) and Whitson and Brule (2000).

Equation (2-2) can also be used to calculate specific gravity of C_{7+} fractions determined by simulated distillation or a synthetic split (i.e., when only mole fractions and molecular weights or specific gravity are known). Assuming a constant K_w for each fraction, specific gravity γ_i or the molecular weight can be calculated from

$$\gamma_i = 6.0108 \left[\frac{M_i^{0.17947}}{K_w^{1.18241}} \right] \quad (2-3)$$

or

$$M_i = \left[0.16637 \gamma_i K_w^{1.18241} \right]^{5.5720}$$

To use any of the thermodynamic property-prediction models, such as an equation of state, to predict the phase and volumetric behavior of complex hydrocarbon mixtures, one must be able to provide the acentric factor, ω , critical temperature, T_c , and critical pressure, p_c , for both the defined and undefined (heavy) fractions in the mixture. The problem of how to adequately characterize these undefined plus fractions in terms of their critical properties and acentric factors has been long recognized in the petroleum industry. Whit-

son (1984) presented excellent documentation on the influence of various heptanes-plus (C_{7+}) characterization schemes on predicting the volumetric behavior of hydrocarbon mixtures by equations of state.

Numerous correlations are available for estimating the physical properties of petroleum fractions. Most of these correlations use the specific gravity, γ , and the boiling point, T_b , correlation parameters. Selecting proper values for these parameters is very important, because slight changes in these parameters can cause significant variations in the predicted results. Several of these correlations follow.

Riazi and Daubert's Generalized Correlations

Riazi and Daubert (1980) developed a simple two-parameter equation for predicting the physical properties of pure compounds and undefined hydrocarbon mixtures. The proposed generalized empirical equation is based on the use of the normal boiling point and specific gravity as correlating parameters. The basic equation is

$$\theta = a T_b^b \gamma^c \tag{2-4}$$

where

- θ = any physical property (T_c , p_c , V_c , or M)
- T_b = normal boiling point, °R
- γ = specific gravity
- M = molecular weight
- T_c = critical temperature, °R
- p_c = critical pressure, psia
- V_c = critical volume, ft³/lb
- a , b , c = correlation constants are given in Table 2-3 for each property

The expected average errors for estimating each property are included in the table. Note that the prediction accuracy is reasonable over the boiling-point range of 100–850°F. Riazi and Daubert (1987) proposed improved correlations for predicting the physical properties of petroleum fractions by taking into consideration the following factors: accuracy, simplicity, generality, availability of input parameters, ability to extrapolate, and finally, comparability with similar correlations developed in recent years.

The authors proposed the following modification of equation (2-4), which maintains the simplicity of the previous correlation while significantly improving its accuracy:

$$\theta = a \theta_1^b \theta_2^c \exp [d \theta_1 + e \theta_2 + f \theta_1 \theta_2]$$

TABLE 2-3 Correlation Constants for Equation (2-4)

θ	a	b	c	Deviation %	
				Average	Maximum
M	-4.56730×10^{-5}	2.19620	-1.0164	2.6	11.8
T_c , °R	24.27870	0.58848	0.3596	1.3	10.6
p_c , psia	-3.12281×10^9	-2.31250	2.3201	3.1	-9.3
V_c , ft ³ /lb	-7.52140×10^{-3}	0.28960	-0.7666	2.3	-9.1

where θ = any physical property and a – f = constants for each property.

Riazi and Daubert stated that θ_1 and θ_2 can be any two parameters capable of characterizing the molecular forces and molecular size of a compound. They identified (T_b, γ) and (M, γ) as appropriate pairs of input parameters in the equation. The authors finally proposed the following two forms of the generalized correlation.

In the first form, the boiling point, T_b , and the specific gravity, γ , of the petroleum fraction are used as correlating parameters:

$$\theta = aT_b^b \gamma^c \exp \left[dT_b + e\gamma + fT_b \gamma \right] \tag{2-5}$$

The constants a – f for each property θ are given in Table 2–4.

In the second form, the molecular weight, M , and specific gravity, γ , of the component are used as correlating parameters. Their mathematical expression has the following form:

$$\theta = a(M)^b \gamma^c \exp \left[d(M) + e\gamma + f(M)\gamma \right] \tag{2-6}$$

In developing and obtaining the coefficients a – f , as given in Table 2–5, the authors used data on the properties of 38 pure hydrocarbons in the carbon number range 1–20, including paraffins, olefins, naphthenes, and aromatics in the molecular weight range 70–300 and the boiling point range 80–650°F.

Cavett’s Correlations

Cavett (1962) proposed correlations for estimating the critical pressure and temperature of hydrocarbon fractions. The correlations received wide acceptance in the petroleum industry due to their reliability in extrapolating conditions beyond those of the data used in developing the correlations. The proposed correlations were expressed analytically as functions of the normal boiling point, T_b , in °F and API gravity. Cavett proposed the following expressions for estimating the critical temperature and pressure of petroleum fractions:

Critical temperature

$$T_c = a_o + a_1(T_b) + a_2(T_b)^2 + a_3(\text{API})(T_b) + a_4(T_b)^3 + a_5(\text{API})(T_b)^2 + a_6(\text{API})^2(T_b)^2 \tag{2-7}$$

TABLE 2-4 Correlation Constants for Equation (2-5)

θ	a	b	c	d	e	f
M	581.96000	−0.97476	6.51274	5.43076×10^{-4}	9.53384	1.11056×10^{-3}
$T_c, ^\circ\text{R}$	10.6443	0.81067	0.53691	-5.17470×10^{-4}	−0.54444	3.59950×10^{-4}
p_c, psia	6.16200×10^6	−0.48440	4.08460	-4.72500×10^{-3}	−4.80140	3.19390×10^{-3}
$V_c, \text{ft}^3/\text{lb}$	6.23300×10^{-4}	0.75060	−1.20280	-1.46790×10^{-3}	−0.26404	1.09500×10^{-3}

TABLE 2-5 Correlation Constants for Equation (2-6)

θ	a	b	c	d	e	f
$T_c, ^\circ\text{R}$	544.40000	0.299800	1.05550	-1.34780×10^{-4}	−0.616410	0.00000
P_c, psia	4.52030×10^4	−0.806300	1.60150	-1.80780×10^{-3}	−0.308400	0.00000
$V_c, \text{ft}^3/\text{lb}$	1.20600×10^{-2}	0.203780	−1.30360	-2.65700×10^{-3}	0.528700	2.60120×10^{-3}
$T_b, ^\circ\text{R}$	6.77857	0.401673	−1.58262	3.77409×10^{-3}	2.984036	-4.25288×10^{-3}

Critical pressure

$$\log(p_c) = b_0 + b_1(T_b) + b_2(T_b)^2 + b_3(\text{API})(T_b) + b_4(T_b)^3 + b_5(\text{API})(T_b)^2 + b_6(\text{API})^2(T_b) + b_7(\text{API})^2(T_b)^2 \quad (2-8)$$

where

T_c = critical temperature, °R

p_c = critical pressure, psia

T_b = normal boiling point, °F

API = API gravity of the fraction

Note that the normal boiling point in the above relationships is expressed in °F.

The coefficients of equations (2-7) and (2-8) are tabulated in the table below. Cavett presented these correlations without reference to the type and source of data used for their development.

i	a_i	b_i
0	768.0712100000	2.82904060
1	1.7133693000	$0.94120109 \times 10^{-3}$
2	-0.0010834003	$-0.30474749 \times 10^{-5}$
3	-0.0089212579	$-0.20876110 \times 10^{-4}$
4	$0.3889058400 \times 10^{-6}$	$0.15184103 \times 10^{-8}$
5	$0.5309492000 \times 10^{-5}$	$0.11047899 \times 10^{-7}$
6	$0.3271160000 \times 10^{-7}$	$-0.48271599 \times 10^{-7}$
7		$0.13949619 \times 10^{-9}$

Kesler-Lee's Correlations

Kesler and Lee (1976) proposed a set of equations to estimate the critical temperature, critical pressure, acentric factor, and molecular weight of petroleum fractions. The equations, as follow, use specific gravity, γ , and boiling point, T_b , in °R as input parameters for their proposed relationships:

Critical pressure

$$\ln(p_c) = 8.3634 - \frac{0.0566}{\gamma} - \left[0.24244 + \frac{2.2898}{\gamma} + \frac{0.11857}{\gamma^2} \right] 10^{-3} T_b + \left[1.4685 + \frac{3.648}{\gamma} + \frac{0.47227}{\gamma^2} \right] 10^{-7} T_b^2 - \left[0.42019 + \frac{1.6977}{\gamma^2} \right] 10^{-10} T_b^3 \quad (2-9)$$

Critical temperature

$$T_c = 341.7 + 811.1\gamma + [0.4244 + 0.1174\gamma]T_b + \frac{[0.4669 - 3.26238\gamma]10^5}{T_b} \quad (2-10)$$

Molecular weight

$$M = -12,272.6 + 9,486.4\gamma + [4.6523 - 3.3287\gamma]T_b + [1 - 0.77084\gamma - 0.02058\gamma^2] \left[1.3437 - \frac{720.79}{T_b} \right] \frac{10^7}{T_b} + [1 - 0.80882\gamma - 0.02226\gamma^2] \left[1.8828 - \frac{181.98}{T_b} \right] \frac{10^{12}}{T_b^3} \quad (2-11)$$

This equation was obtained by regression analysis using the available data on molecular weights ranging from 60 to 650.

The acentric factor is found by defining the Watson characterization factor, K , and the reduced boiling point, θ , by the following relationships:

$$K = \frac{[T_b]^{1/3}}{\gamma}$$

$$\theta = \frac{T_b}{T_c}$$

where T_b = boiling point, °R.

Kessler and Lee proposed the following two expressions for calculating the acentric factor:

For $\theta > 0.8$:

$$\omega = -7.904 + 0.1352K - 0.007465K^2 + 8.359\theta + ([1.408 - 0.01063K]/\theta) \quad (2-12)$$

For $\theta < 0.8$:

$$\omega = \frac{-\ln\left[\frac{p_c}{14.7}\right] - 5.92714 + \frac{6.09648}{\theta} + 1.28862 \ln[\theta] - 0.169347\theta^6}{15.2518 - \frac{15.6875}{\theta} - 13.4721 \ln[\theta] + 0.43577\theta^6} \quad (2-13)$$

where

p_c = critical pressure, psia

T_c = critical temperature, °R

T_b = boiling point, °R

ω = acentric factor

M = molecular weight

γ = specific gravity

Kesler and Lee stated that equations (2-9) and (2-10) give values for p_c and T_c that are nearly identical with those from the API data book up to a boiling point of 1200°F. Modifications were introduced to extend the correlations beyond the boiling point limit of 1200°F. These extensions (extrapolations) were achieved by ensuring that the critical pressure approaches the atmospheric pressure as the boiling point approaches critical temperature.

Winn and Sim-Daubert's Correlations

Sim and Daubert (1980) concluded that the Winn (1957) monograph is the most accurate method for characterizing petroleum fractions. For this reason, Sim and Daubert represented the critical pressure, critical temperature, and molecular weight of the Winn monograph analytically by the following equations:

$$p_c = 3.48242 \times 10^9 T_b^{-2.3177} \gamma^{2.4853} \quad (2-14)$$

$$T_c = \exp\left[3.9934718 T_b^{0.08615} \gamma^{0.04614}\right] \quad (2-15)$$

$$M = 1.4350476 \times 10^{-5} T_b^{2.3776} \gamma^{-0.9371} \quad (2-16)$$

where

p_c = critical pressure, psia

T_c = critical temperature, °R

T_b = boiling point, °R

Watansiri-Owens-Starling's Correlations

Watansiri, Owens, and Starling (1985) developed a set of correlations to estimate the critical properties and acentric factor of coal compounds and other hydrocarbons and their derivatives. The proposed correlations express the characterization parameters as functions of the normal boiling point, specific gravity, and molecular weight. These relationships have the following forms:

Critical temperature

$$\ln(T_c) = -0.0650504 - 0.0005217T_b + 0.03095 \ln[M] + 1.11067 \ln(T_b) \quad (2-17)$$

$$+ M[0.078154\gamma^{1/2} - 0.061061\gamma^{1/3} - 0.016943\gamma]$$

where T_c = critical temperature, °R.

Critical volume

$$\ln(V_c) = 76.313887 - 129.8038\gamma + 63.1750\gamma^2 - 13.175\gamma^3 + 1.10108 \ln[M] \quad (2-18)$$

$$+ 42.1958 \ln[\gamma]$$

where V_c = critical volume, ft³/lb-mole.

Critical pressure

$$\ln(p_c) = 6.6418853 + 0.01617283 \left[\frac{T_c}{V_c} \right]^{0.8} - 8.712 \left[\frac{M}{T_c} \right] - 0.08843889 \left[\frac{T_b}{M} \right] \quad (2-19)$$

where p_c = critical pressure, psia.

Acentric factor

$$\omega = \left\{ \begin{array}{l} 5.12316667 \times 10^{-4} T_b + 0.281826667(T_b/M) + 382.904/M \\ + 0.074691 \times 10^{-5} (T_b/\gamma)^2 - 0.12027778 \times 10^{-4} (T_b)(M) \\ + 0.001261(\gamma)(M) + 0.1265 \times 10^{-4} (M)^2 \\ + 0.2016 \times 10^{-4} (\gamma)(M)^2 - 66.29959 \frac{(T_b)^{1/3}}{M} \\ - 0.00255452 \frac{T_b^{2/3}}{\gamma^2} \end{array} \right\} \left[\frac{5T_b}{9M} \right] \quad (2-20)$$

The proposed correlations produce an average absolute relative deviation of 1.2% for T_c , 3.8% for V_c , 5.2% for p_c , and 11.8% for ω .

Edmister's Correlations

Edmister (1958) proposed a correlation for estimating the acentric factor, ω , of pure fluids and petroleum fractions. The equation, widely used in the petroleum industry, requires boiling point, critical temperature, and critical pressure. The proposed expression is given by the following relationship:

$$\omega = \frac{3[\log(p_c/14.70)]}{7[(T_c/T_b - 1)]} - 1 \quad (2-21)$$

where

ω = acentric factor

p_c = critical pressure, psia

T_c = critical temperature, °R

T_b = normal boiling point, °R

If the acentric factor is available from another correlation, the Edmister equation can be rearranged to solve for any of the three other properties (providing the other two are known).

Critical Compressibility Factor Correlations

The critical compressibility factor is defined as the component compressibility factor calculated at its critical point. This property can be conveniently computed by the real gas equation of state at the critical point, or

$$Z_c = \frac{p_c V_c}{RT_c} \quad (2-22)$$

where R = universal gas constant, 10.73 psia ft³/lb-mole, °R, and V_c = critical volume, ft³/lb-mole.

If the critical volume, V_c , is given in ft³/lb, equation (2-22) is written as

$$Z_c = \frac{p_c V_c M}{RT_c}$$

where M = molecule weight and V_c = critical volume, ft³/lb.

The accuracy of equation (2-22) depends on the accuracy of the values of p_c , T_c , and V_c . The following table presents a summary of the critical compressibility estimation methods.

Method	Year	Z_c	Equation No.
Haugen	1959	$Z_c = 1/(1.28\omega + 3.41)$	(2-23)
Reid, Prausnitz, and Sherwood	1977	$Z_c = 0.291 - 0.080\omega$	(2-24)
Salerno et al.	1985	$Z_c = 0.291 - 0.080\omega - 0.016\omega^2$	(2-25)
Nath	1985	$Z_c = 0.2918 - 0.0928\omega$	(2-26)

Rowe's Characterization Method

Rowe (1978) proposed a set of correlations for estimating the normal boiling point, the critical temperature, and the critical pressure of the heptanes-plus fraction C_{7+} . The prediction of the C_{7+} properties is based on the assumption that the "lumped" fraction behaves as a normal paraffin hydrocarbon. Rowe used the number of carbon atoms, n , as the only correlating parameter. He proposed the following set of formulas for characterizing the C_{7+} fraction in terms of the critical temperature, critical pressure, and boiling point temperature:

$$\text{Critical temperature } (T_c)_{C_{7+}} = 1.8[961 - 10^n] \quad (2-27)$$

with the coefficient a as defined by

$$a = 2.95597 - 0.090597n^{2/3}$$

The parameter n is the number of carbon atoms, calculated from the molecular weight of the C_{7+} fraction by the following relationship:

$$n = \frac{M_{C_{7+}} - 2.0}{14} \quad (2-28)$$

where $(T_c)_{C_{7+}}$ = critical temperature of C_{7+} , °R, and $M_{C_{7+}}$ = molecular weight of the heptanes-plus fraction.

$$\text{Critical pressure } (p_c)_{C_{7+}} = \frac{10^{(4.89165+Y)}}{(T_c)_{C_{7+}}} \quad (2-29)$$

with the parameter Y as given by

$$Y = -0.0137726826n + 0.6801481651$$

and where $(p_c)_{C_{7+}}$ is the critical pressure of the C_{7+} in psia.

$$\text{Boiling point temperature } (T_b)_{C_{7+}} = 0.0004347(T_c)_{C_{7+}}^2 + 265 \quad (2-30)$$

Based on the analysis of 843 true-boiling-point fractions from 68 reservoir C_{7+} samples, Soreide (1989) proposed the following relationship for estimating the boiling point temperature as a function of molecular weight and specific gravity of the fraction:

$$T_b = 1928.3 - \left[\frac{1.695 \times 10^5 \gamma^{3.266}}{M^{0.03522}} \right] \exp \left[-4.922 \times 10^{-3} M - 4.7685\gamma + 3.462 \times 10^{-3} M\gamma \right]$$

where T_b is expressed in °R.

Standing's Correlations

Matthews, Roland, and Katz (1942) presented graphical correlations for determining the critical temperature and pressure of the heptanes-plus fraction. Standing (1977) expressed these graphical correlations more conveniently in mathematical forms as follows:

$$(T_c)_{C_{7+}} = 608 + 364 \log[(M)_{C_{7+}} - 71.2] + [2450 \log(M)_{C_{7+}} - 3800] \log(\gamma)_{C_{7+}} \quad (2-31)$$

$$(p_c)_{C_{7+}} = 1188 - 431 \log[(M)_{C_{7+}} - 61.1] + \{2319 - 852 \log[(M)_{C_{7+}} - 53.7][(\gamma)_{C_{7+}} - 0.8]\} \quad (2-32)$$

where $(M)_{C_{7+}}$ and $(\gamma)_{C_{7+}}$ are the molecular weight and specific gravity of the C_{7+} .

Willman-Teja's Correlations

Willman and Teja (1987) proposed correlations for determining the critical pressure and critical temperature of the n-alkane homologous series. The authors used the normal boiling point and the number of carbon atoms of the n-alkane as a correlating parameter. The applicability of the Willman and Teja proposed correlations can be extended to predict the critical temperature and pressure of the undefined petroleum fraction by recalculating the exponents of the original expressions. These exponents were recalculated by using a non-linear regression model to best match the critical properties data of Bergman, Tek, and Katz (1977) and Whitson (1980). The empirical formulas are given by

$$T_c = T_b [1 + (1.25127 + 0.137242n)^{-0.884540633}] \quad (2-33)$$

$$P_c = \frac{339.0416805 + 1184.157759n}{[0.873159 + 0.54285n]^{1.9265669}} \quad (2-34)$$

where n = number of carbon atoms, and T_b = the average boiling point of the undefined fraction, °R.

Hall-Yarborough's Correlations

Hall and Yarborough (1971) proposed a simple expression to determine the critical volume of a fraction from its molecular weight and specific gravity:

$$v_c = \frac{0.025M^{1.15}}{\gamma^{0.7935}} \quad (2-35)$$

where v_c is the critical volume as expressed in ft³/lb-mole. Note that, to express the critical volume in ft³/lb, the relationship is given by

$$v_c = MV_c$$

where

M = molecular weight

V_c = critical volume in ft³/lb

v_c = critical volume in ft³/lb-mol

Obviously, the critical volume also can be calculated by applying the real gas equation of state at the critical point of the component as

$$pV = Z \left(\frac{m}{M} \right) RT$$

and, at the critical point,

$$V_c = \frac{Z_c RT_c}{p_c M}$$

Magoulas-Tassios's Correlations

Magoulas and Tassios (1990) correlated the critical temperature, critical pressure, and acentric factor with the specific gravity, γ , and molecular weight, M , of the fraction as expressed by the following relationships:

$$T_c = -1247.4 + 0.792M + 1971\gamma - \frac{27,000}{M} + \frac{707.4}{\gamma}$$

$$\ln(p_c) = 0.01901 - 0.0048442M + 0.13239\gamma + \frac{227}{M} - \frac{1.1663}{\gamma} + 1.2702 \ln(M)$$

$$\omega = -0.64235 + 0.00014667M + 0.021876\gamma - \frac{4.559}{M} + 0.21699 \ln(M)$$

where T_c = critical temperature, °R, and p_c = critical pressure, psia.

Twu's Correlations

Twu (1984) developed a suite of critical properties, based on perturbation-expansion theory with normal paraffins as the reference states, that can be used for determining the critical and physical properties of undefined hydrocarbon fractions, such as C_{7+} . The methodology is based on selecting (finding) a normal paraffin fraction with a boiling temperature T_{bC+} identical to that of the hydrocarbon plus fraction, such as C_{7+} . Having selected the proper normal paraffin fraction, we perform the following two steps:

Step 1 Calculate the properties of the normal paraffins from

- Critical temperature of normal paraffins, T_{cPi} , in °R:

$$T_{cPi} = T_{bC+} \left[A_1 + A_2 T_{bC+} + A_3 T_{bC+}^2 + A_4 T_{bC+}^3 + \frac{A_5}{(A_6 T_{bC+})^{13}} \right]$$

where

$$A_1 = 0.533272$$

$$A_2 = 0.191017(10^{-3})$$

$$A_3 = 0.779681(10^{-7})$$

$$A_4 = -0.284376(10^{-10})$$

$$A_5 = 0.959468(10^2)$$

$$A_6 = 0.01$$

- Critical pressure of normal paraffins, p_{cPi} , in psia:

$$p_{cPi} = \left[A_1 + A_2 \alpha_i^{0.5} + A_3 \alpha_i + A_4 \alpha_i^2 + A_5 \alpha_i^4 \right]^2$$

with

$$\alpha_i = 1 - \frac{T_{bC+}}{T_{cPi}}$$

where

$$A_1 = 3.83354$$

$$A_2 = 1.19629$$

$$A_3 = 34.8888$$

$$A_4 = 36.1952$$

$$A_5 = 104.193$$

- Specific gravity of normal paraffins, γ_{Pi} :

$$\gamma_{Pi} = A_1 + A_2 \alpha_i + A_3 \alpha_i^3 + A_4 \alpha_i^{12}$$

with

$$\alpha_i = 1 - \frac{T_{bC+}}{T_{cPi}}$$

where

$$A_1 = 0.843593$$

$$A_2 = -0.128624$$

$$A_3 = -3.36159$$

$$A_4 = -13749.5$$

- Critical volume of normal paraffins, v_{cP} , in $\text{ft}^3/\text{lb}_m \text{ mol}$:

$$v_{cP} = [1 - A_1 + A_2 \alpha_i + A_3 \alpha_i^3 + A_4 \alpha_i^{14}]^{-8}$$

with

$$\alpha_i = 1 - \frac{T_{bC+}}{T_{cPi}}$$

where

$$A_1 = -0.419869$$

$$A_2 = 0.505839$$

$$A_3 = 1.56436$$

$$A_4 = 9481.7$$

Step 2 Calculate the properties of the *plus fraction* from

- Critical temperature of the plus fraction, T_{C+} , in $^{\circ}\text{R}$:

$$T_{C+} = T_{cPi} \left[\frac{1 + 2f_{Ti}}{1 - 2f_{Ti}} \right]^2$$

with

$$f_{Ti} = \{\exp[5(\gamma_{pi} - \gamma_{C+})] - 1\} \left[\frac{A_1}{T_{bC+}^{0.5}} + \left(A_2 + \frac{A_3}{T_{bC+}^{0.5}} \right) \{\exp[5(\gamma_{pi} - \gamma_{C+})] - 1\} \right]$$

where

$$A_1 = -0.362456$$

$$A_2 = 0.0398285$$

$$A_3 = -0.948125$$

- Critical volume of the plus fraction, v_{c+} , in $\text{ft}^3/\text{lb}_m \text{ mol}$:

$$v_{C+} = v_{cPi} \left[\frac{1 + 2f_v}{1 - 2f_v} \right]^2$$

with

$$f_v = \{\exp[4(\gamma_{pi}^2 - \gamma_{C+}^2)] - 1\} \left[\frac{A_1}{T_{bC+}^{0.5}} + \left(A_2 + \frac{A_3}{T_{bC+}^{0.5}} \right) \{\exp[4(\gamma_{pi}^2 - \gamma_{C+}^2)] - 1\} \right]$$

where

$$A_1 = 0.466590$$

$$A_2 = -0.182421$$

$$A_3 = 3.01721$$

- Critical pressure of the plus fraction, p_{c+} , in psia:

$$p_{C+} = p_{cPi} \left(\frac{T_{C+}}{T_{cPi}} \right) \left(\frac{v_{cPi}}{v_{C+}} \right) \left[\frac{1 + 2f_{pi}}{1 - 2f_{pi}} \right]^2$$

with

$$f_{pi} = \{\exp[0.5(\gamma_{pi} - \gamma_{C+})] - 1\} \left(\left(A_1 + \frac{A_2}{T_{bC+}^{0.5}} + A_3 T_{bC+} \right) + \left(A_4 + \frac{A_5}{T_{bC+}^{0.5}} + A_6 T_{bC+} \right) \{\exp[0.5(\gamma_{pi} - \gamma_{C+})] - 1\} \right)$$

where

$$A_1 = 2.53262$$

$$A_2 = -46.19553$$

$$A_3 = -0.00127885$$

$$A_4 = -11.4277$$

$$A_5 = 252.14$$

$$A_6 = 0.00230535$$

EXAMPLE 2-1

Estimate the critical properties and the acentric factor of the heptanes-plus fraction, that is, C_{7+} , with a measured molecular weight of 150 and specific gravity of 0.78 by using the Riazi-Daubert equation (2-5) and Edmister's equation.

SOLUTION

For the Riazi-Daubert equation, use equation (2-5) with the proper coefficients a - f to estimate T_c , P_c , V_c , and T_b :

$$\theta = aT_b^b \gamma^c \exp[dT_b + e\gamma + fT_b\gamma]$$

$$T_c = 544.2(150)^{0.2998}(0.78)^{1.0555} \exp[-1.3478 \times 10^{-4}(150) - 0.61641(0.78) + 0] \\ = 1139.4^\circ\text{R}$$

$$p_c = 4.5203 \times 10^4(150)^{-0.8063}(0.78)^{1.6015} \exp[-1.8078 \times 10^{-3}(150) - 0.3084(0.78) + 0] \\ = 320.3 \text{ psia}$$

$$V_c = 1.206 \times 10^{-2}(150)^{0.20378}(0.78)^{-1.3036} \exp[-2.657 \times 10^{-3}(150) + 0.5287(0.78) \\ = 2.6012 \times 10^{-3}(150)(0.78)] = 0.06035 \text{ ft}^3/\text{lb}$$

$$T_b = 6.77857(150)^{0.401673}(0.78)^{-1.58262} \exp[3.77409 \times 10^{-3}(150) + 2.984036(0.78) \\ - 4.25288 \times 10^{-3}(150)(0.78)] = 825.26^\circ\text{R}$$

Use Edmister's equation (2-21) to estimate the acentric factor:

$$\omega = \frac{3[\log(p_c/14.70)]}{7[(T_c/T_b) - 1]} - 1$$

$$\omega = \frac{3[\log(320.3/14.7)]}{7[1139.4/825.26 - 1]} - 1 = 0.5067$$

EXAMPLE 2-2

Estimate the critical properties, molecular weight, and acentric factor of a petroleum fraction with a boiling point of 198°F and specific gravity of 0.7365 by using the following methods:

- Riazi-Daubert (equation 2-4).
- Riazi-Daubert (equation 2-5).

- Cavett.
- Kesler-Lee.
- Winn and Sim-Daubert.
- Watansiri-Owens-Starling.

SOLUTION USING RIAZI-DAUBERT (EQUATION 2-4)

$$\begin{aligned}
 M &= 4.5673 \times 10^{-5} (658)^{2.1962} (0.7365)^{-1.0164} = 96.4 \\
 T_c &= 24.2787 (658)^{0.58848} (0.7365)^{0.3596} = 990.67^\circ\text{R} \\
 p_c &= 3.12281 \times 10^9 (658)^{-2.3125} (0.7365)^{2.3201} = 466.9 \text{ psia} \\
 V_c &= 7.5214 \times 10^{-3} (658)^{0.2896} (0.7365)^{-0.7666} = 0.06227 \text{ ft}^3/\text{lb}
 \end{aligned}$$

Step 1 Solve for Z_c by applying the preceding calculated properties in equation (2-22):

$$Z_c = \frac{p_c V_c M}{RT_c} = \frac{(466.9)(0.06227)(96.4)}{(10.73)(990.67)} = 0.26365$$

Solve for ω by applying equation (2-21):

$$\begin{aligned}
 \omega &= \frac{3[\log(p_c/14.70)]}{7[(T_c/T_b - 1)]} - 1 \\
 \omega &= \frac{3[\log(466.9/14.7)]}{7[(990.67/658) - 1]} - 1 = 0.2731
 \end{aligned}$$

SOLUTION USING RIAZI-DAUBERT (EQUATION 2-5).

Applying equation (2-5) and using the appropriate constants yields

$$\begin{aligned}
 M &= 96.911 \\
 T_c &= 986.7^\circ\text{R} \\
 p_c &= 465.83 \text{ psia} \\
 V_c &= 0.06257 \text{ ft}^3/\text{lb}
 \end{aligned}$$

Step 1 Solve for the acentric factor and critical compressibility factor by applying equations (2-21) and (2-22), respectively.

Step 2

$$\omega = \frac{3[\log(p_c/14.70)]}{7[(T_c/T_b - 1)]} - 1 = 0.2877$$

Step 3

$$Z_c = \frac{p_c V_c M}{RT_c} = \frac{(465.83)(0.06257)(96.911)}{10.73(986.7)} = 0.2668$$

SOLUTION USING CAVETT'S CORRELATIONS

Step 1 Solve for T_c by applying equation (2-7) with the coefficients as provided by Cavett (see table on p. 67):

$$T_c = a_0 + a_1(T_b) + a_2(T_b)^2 + a_3(\text{API})(T_b) + a_4(T_b)^3 + a_5(\text{API})(T_b)^2 + a_6(E)^2(T_b)^2$$

to give $T_c = 978.1^\circ\text{R}$.

Step 2 Calculate p_c with equation (2-8):

$$\log(p_c) = b_0 + b_1(T_b) + b_2(T_b)^2 + b_3(\text{API})(T_b) + b_4(T_b)^3 + b_5(\text{API})(T_b)^2 + b_6(\text{API})^2(T_b) + b_7(\text{API})^2(T_b)^2$$

to give $p_c = 466.1$ psia.

Step 3 Solve for the acentric factor by applying the Edmister correlation (equation 2-21):

$$\omega = \frac{3[\log(466.1/14.7)]}{7[(980/658) - 1]} - 1 = 0.3147$$

Step 4 Compute the critical compressibility by using equation (2-25):

$$Z_c = 0.291 - 0.080\omega - 0.016\omega^2$$

$$Z_c = 0.291 - (0.08)(0.3147) - 0.016(0.3147)^2 = 0.2642$$

Step 5 Estimate V_c from equation (2-22):

$$v_c = \frac{Z_c RT_c}{p_c} = \frac{(0.2642)(10.731)(980)}{466.1} = 5.9495 \text{ ft}^3/\text{lb-mole}$$

Assume

$$M = 96$$

$$V_c = \frac{5.9495}{96} = 0.06197 \text{ ft}^3/\text{lb}$$

SOLUTION BY USING KESLER-LEE'S CORRELATIONS

Step 1 Calculate p_c from equation (2-9) or

$$\ln(p_c) = 8.3634 - 0.0566/\gamma - [0.24244 + 2.2898/\gamma + 0.11857/\gamma^2]10^{-3}T_b$$

$$+ [1.4685 + 3.648/\gamma + 0.47227/\gamma^2]10^{-7}T_b^2$$

$$- [0.42019 + 1.6977/\gamma^2]10^{-10}T_b^3$$

to give $p_c = 470$ psia.

Step 2 Solve for T_c by using equation (2-10); that is,

$$T_c = 341.7 + 811.1\gamma + [0.4244 + 0.1174\gamma]T_b + \frac{[0.4669 - 3.26238\gamma]10^5}{T_b}$$

to give $T_c = 980^\circ\text{R}$.

Step 3 Calculate the molecular weight, M , by using equation (2-11):

$$M = -12,272.6 + 9,486.4\gamma + [4.6523 - 3.3287\gamma]T_b + [1 - 0.77084\gamma - 0.02058\gamma^2]$$

$$\left[1.3437 - \frac{720.79}{T_b}\right]\frac{10^7}{T_b} + [1 - 0.80882\gamma - 0.02226\gamma^2]\left[1.8828 - \frac{181.98}{T_b}\right]\frac{10^{12}}{T_b^3}$$

to give $M = 98.7$.

Step 4 Compute the Watson characterization factor K and the parameter θ :

$$K = \frac{(658)^{1/3}}{0.7365} = 11.8$$

$$\theta = \frac{658}{980} = 0.671$$

Step 5 Solve for acentric factor by applying equation (2-13):

$$\omega = \frac{-\ln\left[\frac{p_c}{14.7}\right] - 5.92714 + \frac{6.09648}{\theta} + 1.28862 \ln[\theta] - 0.169347\theta^6}{15.2518 - \frac{15.6875}{\theta} - 13.4721 \ln[\theta] + 0.43577\theta^6}$$

Substituting gives $\omega = 0.306$.

Step 6 Estimate for the critical gas compressibility, Z_c , by using equation (2-26):

$$Z_c = 0.2918 - 0.0928\omega$$

$$Z_c = 0.2918 - (0.0928)(0.306) = 0.2634$$

Step 7 Solve for V_c by applying equation (2-22):

$$V_c = \frac{Z_c RT_c}{p_c M} = \frac{(0.2634)(10.73)(980)}{(470)(98.7)} = 0.0597 \text{ ft}^3/\text{lb}$$

SOLUTION USING WINN-SIM-DAUBERT APPROACH

Step 1 Estimate p_c from equation (2-16):

$$p_c = (3.48242 \times 10^9) \frac{\gamma^{2.4853}}{T_b^{2.3177}}$$

$$p_c = 478.6 \text{ psia}$$

Step 2 Solve for T_c by applying equation (2-15):

$$T_c = \exp\left[3.9934718 T_b^{0.08615} \gamma^{0.04614}\right]$$

$$T_c = 979.2^\circ\text{R}$$

Step 3 Calculate M from equation (2-16):

$$M = (1.4350476 \times 10^{-5}) \frac{T_b^{2.3776}}{\gamma^{0.9371}}$$

$$M = 95.93$$

Step 4 Solve for the acentric factor from equation (2-21):

$$\omega = 0.3280$$

Solve for Z_c by applying equation (2-24):

$$Z_c = 0.291 - (0.08)(0.3280) = 0.2648$$

Step 5 Calculate the critical volume V_c from equation (2-22):

$$V_c = \frac{(0.2648)(10.731)(979.2)}{(478.6)(95.93)} = 0.06059 \text{ ft}^3/\text{lb}$$

SOLUTION USING THE WATANSIRI-OWENS-STARLING CORRELATIONS

Step 1 Because equations (2–17) through (2–19) require the molecular weight, assume $M=96$.

Step 2 Calculate T_c from equation (2–17):

$$\ln(T_c) = -0.0650504 - 0.0005217T_b + 0.03095 \ln[M] + 1.11067 \ln(T_b) \\ + M[0.078154\gamma^{1/2} - 0.061061\gamma^{1/3} - 0.016943\gamma] \\ T_c = 980.0^\circ\text{R}$$

Step 3 Determine the critical volume from equation (2–18) to give

$$\ln(V_c) = 76.313887 - 129.8038\gamma + 63.1750\gamma^2 - 13.175\gamma^3 + 1.10108 \ln[M] \\ + 42.1958 \ln[\gamma] \\ V_c = 0.06548 \text{ ft}^3/\text{lb}$$

Step 4 Solve for the critical pressure of the fraction by applying equation (2–19) to produce

$$\ln(p_c) = 6.6418853 + 0.01617283 \left[\frac{T_c}{V_c} \right]^{0.8} - 8.712 \left[\frac{M}{T_c} \right] - 0.08843889 \left[\frac{T_b}{M} \right] \\ p_c = 426.5 \text{ psia}$$

Step 5 Calculate the acentric factor from equation (2–20) to give $\omega = 0.2222$.

Step 6 Compute the critical compressibility factor by applying equation (2–26) to give $Z_c = 0.27112$.

The following table summarizes the results for this example.

Method	T_c , °R	p_c , psia	V_c , ft ³ /lb-mole	M	ω	Z_c
Riazi-Daubert no. 1	990.67	466.90	0.06227	96.400	0.2731	0.26365
Riazi-Daubert no. 2	986.70	465.83	0.06257	96.911	0.2877	0.66800
Cavett	978.10	466.10	0.06197	—	0.3147	0.26420
Kesler-Lee	980.00	469.00	0.05970	98.700	0.3060	0.26340
Winn	979.20	478.60	0.06059	95.930	0.3280	0.26480
Watansiri	980.00	426.50	0.06548	—	0.2222	0.27112

EXAMPLE 2-3

If the molecular weight and specific gravity of the heptanes-plus fraction are 216 and 0.8605, respectively, calculate the critical temperature and pressure by using

- Rowe's correlations.
- Standing's correlations.
- Magoulas-Tassios's correlations.

SOLUTION USING ROWE'S CORRELATIONS

Step 1 Calculate the number of carbon atoms of C_{7+} from equation (2–28) to give

$$n = \frac{M_{C_{7+}} - 2.0}{14} = \frac{216 - 2.0}{14} = 15.29$$

Step 2 Calculate the coefficient a :

$$a = 2.95597 - 0.090597 (15.29)^{2/3} = 2.39786$$

Step 3 Solve for the critical temperature from equation (2–27) to yield

$$(T_c)_{C_{7+}} = 1.8[961 - 10^{2.39786}] = 1279.8^\circ\text{R}$$

Step 4 Calculate the coefficient Y :

$$Y = -0.0137726826(2.39786) + 0.6801481651 = 0.647123$$

Step 5 Solve for the critical pressure from equation (2–29) to give

$$(p_c)_{C_{7+}} = \frac{10^{(4.89165+Y)}}{(T_c)_{C_{7+}}} = \frac{10^{(4.89165+0.647123)}}{1279.8} = 270 \text{ psi}$$

SOLUTION USING STANDING'S CORRELATIONS

Step 1 Solve for the critical temperature by using equation (2–31) to give

$$(T_c)_{C_{7+}} = 608 + 364 \log[(M)_{C_{7+}} - 71.2] + [2450 \log(M)_{C_{7+}} - 3800] \log(\gamma)_{C_{7+}}$$

$$(T_c)_{C_{7+}} = 1269.3^\circ\text{R}$$

Step 2 Calculate the critical pressure from equation (2–32) to yield

$$(p_c)_{C_{7+}} = 1188 - 431 \log[(M)_{C_{7+}} - 61.1] + [2319 - 852 \log[(M)_{C_{7+}} - 53.7]](\gamma)_{C_{7+}} - 0.8]$$

$$(p_c)_{C_{7+}} = 270 \text{ psia}$$

SOLUTION USING THE MAGOULAS-TASSIOS CORRELATIONS

$$T_c = -1247.4 + 0.792M + 1971\gamma - \frac{27,000}{M} + \frac{707.4}{\gamma}$$

$$T_c = -1247.4 + 0.792(216) + 1971(0.8605) - \frac{27,000}{216} + \frac{707.4}{0.8605} = 1317^\circ\text{R}$$

$$\ln(p_c) = 0.01901 - 0.0048442M + 0.13239\gamma + \frac{227}{M} - \frac{1.1663}{\gamma} + 1.2702 \ln(M)$$

$$\ln(p_c) = 0.01901 - 0.0048442(216) + 0.13239(0.8605) + \frac{227}{216} - \frac{1.1663}{0.8605}$$

$$+ 1.2702 \ln(216) = 5.6098$$

$$p_c = \exp(5.6098) = 273 \text{ psi}$$

EXAMPLE 2-4

Calculate the critical properties and the acentric factor of C_{7+} with a measured molecular weight of 198.71 and specific gravity of 0.8527. Employ the following methods:

- Rowe's correlations.
- Standing's correlations.
- Riazi-Daubert's correlations.
- Magoulas-Tassios's correlations.

SOLUTION BY USING ROWE'S CORRELATIONS

Step 1 Calculate the number of carbon atoms, n , and the coefficient a of the fraction to give

$$n = \frac{198.71 - 2}{14} = 14.0507$$

$$a = 2.95597 - 0.090597n^{2/3}$$

$$a = 2.95597 - 0.090597(14.0507)^{2/3} = 2.42844$$

Step 2 Determine T_c from equation (2-27) to give

$$(T_c)_{C_{7+}} = 1.8[961 - 10^a]$$

$$(T_c)_{C_{7+}} = 1.8[961 - 10^{2.42844}] = 1247^\circ\text{R}$$

Step 3 Calculate the coefficient Y :

$$Y = -0.0137726826n + 0.6801481651$$

$$Y = -0.0137726826(2.42844) + 0.6801481651 = 0.6467$$

Step 4 Compute p_c from equation (2-29) to yield

$$(p_c)_{C_{7+}} = \frac{10^{(4.89165 + 0.6467)}}{1247} = 277 \text{ psi}$$

Step 5 Determine T_b by applying equation (2-30) to give

$$(T_b)_{C_{7+}} = 0.0004347(T_c)_{C_{7+}}^2 + 265 = 0.0004347(1247)^2 + 265 = 941^\circ\text{R}$$

Step 6 Solve for the acentric factor by applying equation (2-21) to give

$$\omega = \frac{3[\log(p_c/14.70)]}{7[(T_c/T_b) - 1]} - 1$$

$$\omega = 0.6123$$

SOLUTION USING STANDING'S CORRELATIONS

Step 1 Solve for the critical temperature of C_{7+} by using equation (2-31) to give

$$(T_c)_{C_{7+}} = 608 + 364 \log[(M)_{C_{7+}} - 71.2] + [2450 \log(M)_{C_{7+}} - 3800] \log(\gamma)_{C_{7+}}$$

$$(T_c)_{C_{7+}} = 1247.73^\circ\text{R}$$

Step 2 Calculate the critical pressure from equation (2-32) to give

$$(p_c)_{C_{7+}} = 1188 - 431 \log[(M)_{C_{7+}} - 61.1] + [2319 - 852 \log[(M)_{C_{7+}} - 53.7]][(\gamma)_{C_{7+}} - 0.8]$$

$$(p_c)_{C_{7+}} = 291.41 \text{ psia}$$

SOLUTION USING RIAZI-DAUBERT'S CORRELATIONS

Step 1 Solve equation (2-6) for T_c to give $T_c = 1294.1^\circ\text{R}$.

Step 2 Calculate p_c from equation (2-6) to give $p_c = 263.67$.

Step 3 Determine T_b by applying equation (2-6) to give $T_b = 958.5^\circ\text{R}$.

Step 4 Solve for the acentric factor from equation (2-21) to give

$$\omega = \frac{3[\log(p_c/14.70)]}{7[(T_c/T_b) - 1]} - 1$$

$$\omega = 0.5346$$

SOLUTION USING MAGOULAS-TASSIOS'S CORRELATIONS

$$T_c = -1247.4 + 0.792M + 1971\gamma - \frac{27,000}{M} + \frac{707.4}{\gamma}$$

$$T_c = -1247.4 + 0.792(198.71) + 1971(0.8527) - \frac{27,000}{198.71} + \frac{707.4}{0.8527} = 1284^\circ\text{R}$$

$$\ln(p_c) = 0.01901 - 0.0048442M + 0.13239\gamma + \frac{227}{M} - \frac{1.1663}{\gamma} + 1.2702 \ln(M)$$

$$\ln(p_c) = 0.01901 - 0.0048442(198.71) + 0.13239(0.8527) + \frac{227}{198.71} - \frac{1.1663}{0.8527} + 1.2702 \ln(198.71) = 5.6656$$

$$p_c = \exp(5.6656) = 289 \text{ psi}$$

$$\omega = -0.64235 + 0.0014667M + 0.21876\gamma \frac{4.559}{M} + 0.21699 \ln(M)$$

$$\omega = -0.64235 + 0.0014667(198.71) + 0.021876(0.8527) - \frac{4.559}{198.71} + 0.21699 \ln(198.71) = 0.531$$

PNA Determination

The vast number of hydrocarbon compounds making up naturally occurring crude oil has been grouped chemically into several series of compounds. Each series consists of those compounds similar in their molecular makeup and characteristics. Within a given series, the compounds range from extremely light, or chemically simple, to heavy, or chemically complex. In general, it is assumed that the heavy (undefined) hydrocarbon fractions are composed of three hydrocarbon groups: paraffins (*P*), naphthenes (*N*), and aromatics (*A*).

The PNA content of the plus fraction of the undefined hydrocarbon fraction can be estimated experimentally from distillation or a chromatographic analysis. Both types of analysis provide information valuable for use in characterizing the plus fractions.

In the distillation process, the hydrocarbon-plus fraction is subjected to a standardized analytical distillation, first at atmospheric pressure, then in a vacuum at a pressure of 40 mm Hg. Usually the temperature is taken when the first droplet distills over. Ten fractions (cuts) are then distilled off, the first one at 50°C and each successive one with a boiling range of 25°C. For each distillation cut, the volume, specific gravity, and molecular weight, among other measurements, are determined. Cuts obtained in this manner are identified by the boiling-point ranges in which they were collected.

Figure 2-3 shows a typical graphical presentation of the molecular weight, specific gravity, and the true boiling point as a function of the volume fraction of liquid vaporized. Note that, when a single boiling point is given for a plus fraction, it is given as its volume-average boiling point (VABP).

Bergman et al. (1977) outlined the chromatographic analysis procedure by which distillation cuts are characterized by the density and molecular weight as well as by weight-average boiling point (WABP).

Based on the data from the TBP distillation, the plus fraction is divided into pseudo or hypothetical components suitable for calculating equations of state. Average boiling point,

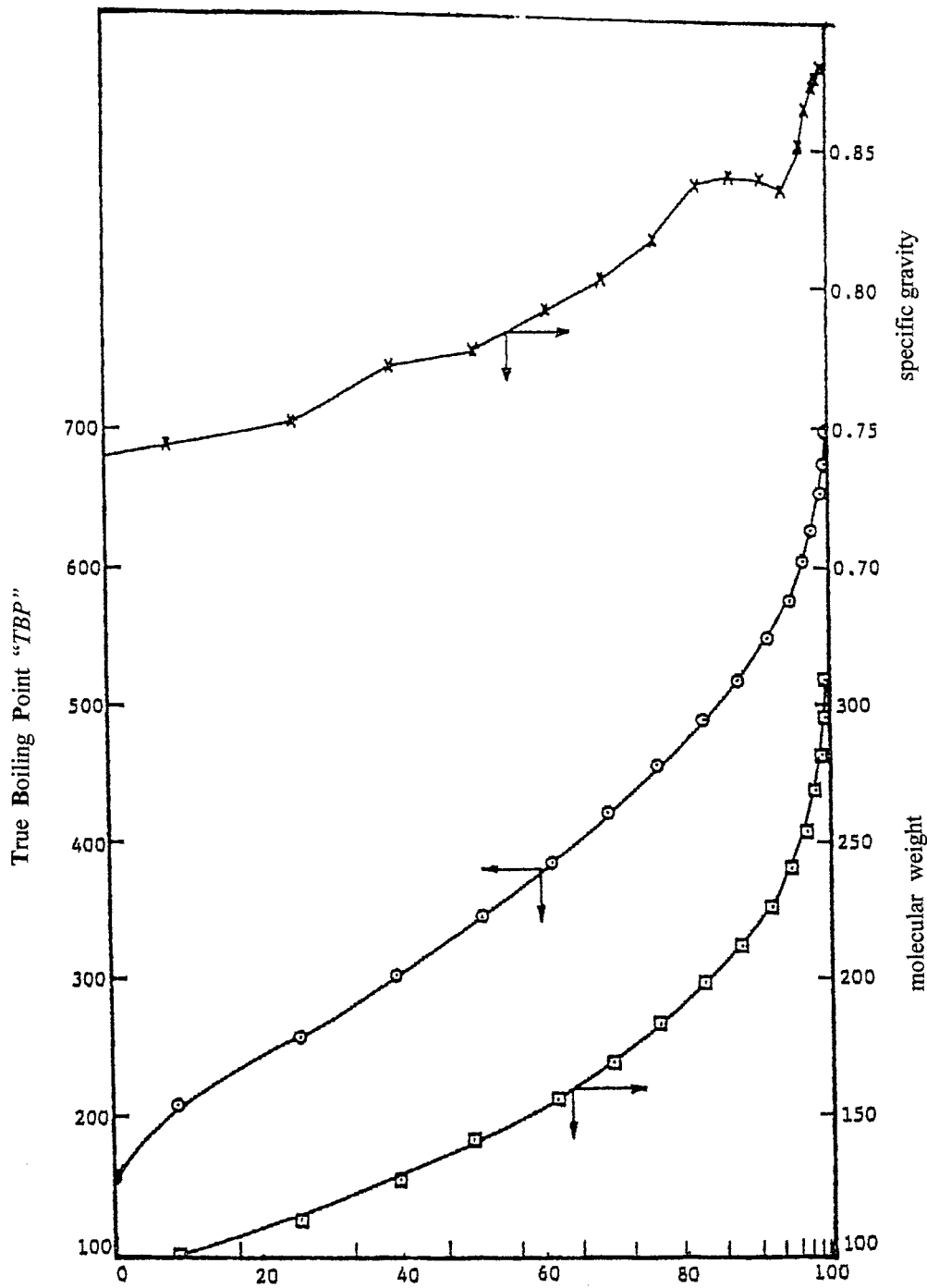


FIGURE 2-3 TBP, specific gravity, and molecular weight of a C_{7+} fraction.

molecular weight, and specific gravity of each pseudo component usually are taken at the mid-volume percent of the cut, that is, between V_i and V_{i-1} . The TBP associated with that specific pseudo component i , that is, T_{bi} , is given by

$$T_{bi} = \frac{1}{V_i - V_{i-1}} \int_{V_{i-1}}^{V_i} T_{bt}(V) dV$$

where $V_i - V_{i-1}$ = volumetric cut of the TBP curve associated with pseudo component i $T_{bt}(V)$ = true boiling-point temperature versus liquid volume percent distilled.

The mass (m_i) of each distillation cut is measured directly during the TBP analysis. The cut is quantified in moles n_i with molecular weight (M_i) and the measured mass (m_i), by definition, as

$$n_i = m_i / M_i$$

Volume of the fraction is calculated from the mass and the density (ρ_i) or specific gravity (γ_i) as

$$V_i = m_i / \rho_i$$

The term M_i is measured by a cryoscopic method, based on freezing-point depression, and γ_i is measured by a pycnometer or electronic densitometer. Note that, when the specific gravity and molecular weight of the plus fraction are the *only* data available, the physical properties of each cut with a specified T_{bi} can be approximated by assuming a constant K_w (Watson factor) for each fraction. The specific steps of the procedure follow.

Step 1 Calculate the characterization parameter K_w for the plus fraction from equation (2-1); that is,

$$K_w = \left[\frac{T_b^{1/3}}{\gamma} \right]_{C_{7+}}$$

or approximated by Whitson's equation; that is, equation (2-2), as

$$K_w \approx 4.5579 \frac{M_{C_{7+}}^{0.15178}}{\gamma_{C_{7+}}^{0.84573}}$$

where T_b is the normal boiling point of the C_{7+} in °R.

Step 2 Assuming a constant K_w for each selected pseudo fraction, calculate the specific gravity of each cut by rearranging equation (2-2):

$$\gamma_i = \frac{T_{bi}^{1/3}}{K_w}$$

where T_{bi} = pseudo compound boiling point as determined from the distillation curve, °R, and K_w = Watson characterization parameter for the plus fraction.

Step 3 Estimate the molecular weight of each pseudo component. M_i , from equation (2-2):

$$M_i = 45.69 \times 10^{-6} \gamma_i^{5.57196} K_w^{6.58834}$$

Miquel, Hernandez, and Castells (1992) proposed the following guidelines when selecting the proper number of pseudo components from the TBP distillation curve:

1. The pseudo-component breakdown can be made from either equal volumetric fractions or regular temperature intervals in the TBP curve. To reproduce the shape of the TBP curve better and reflect the relative distribution of light, middle, and heavy components in the fraction, a breakdown with equal TBP temperature intervals is recommended. When equal volumetric fractions are taken, information about light initial and heavy end components can be lost.
2. Use between 5 and 15 fractions to describe the plus fraction.
3. If the TBP curve is relatively “steep,” use between 10 and 15 fractions.
4. If the curve is relatively “flat,” use 5 to 8 fractions.
5. If the TBP curve contains sections that are relatively “steep” and other sections that are relatively “flat,” use several fractions to describe the “steep” portion of the curve and 1 to 3 to describe the “flat” portion of the curve.
6. Use the specific gravity, molecular weight, and PNA curves to locate the “best break point” for the various fractions. Best break points are qualitatively defined as those that yield component properties that require minimum averaging across a wildly oscillating curve.
7. The number of pseudo components selected has to be enough to reproduce the volatility properties of the fraction properly, especially in fractions with wide boiling-temperature ranges. On the other hand, too many pseudo components require excessively long computer time for further calculations (i.e., vapor/liquid equilibria and process simulation calculations).
8. The mean average boiling point (T_b) is recommended as the most representative mixture boiling point because it allows better reproduction of the properties of the entire mixture.

Generally, five methods are used to define the normal boiling point for petroleum fractions:

1. Volume-average boiling point, defined mathematically by the following expression:

$$\text{VABP} = \sum_i V_i T_{bi} \quad (2-36)$$

where T_{bi} = boiling point of the distillation cut i , °R, and V_i = volume fraction of the distillation cut i .

2. Weight-average boiling point, defined by the following expression:

$$\text{WABP} = \sum_i w_i T_{bi} \quad (2-37)$$

where w_i = weight fraction of the distillation cut i .

3. Molar-average boiling point (MABP), given by the following relationship:

$$\text{MABP} = \sum_i x_i T_{bi} \quad (2-38)$$

where x_i = mole fraction of the distillation cut i .

4. Cubic-average boiling point (CABP), which is defined as:

$$\text{CABP} = \left[\sum_i x_i T_{bi}^{1/3} \right]^3 \quad (2-39)$$

5. Mean-average boiling point (MeABP):

$$\text{MeABP} = \frac{\text{MABP} + \text{CABP}}{2} \quad (2-40)$$

As indicated by Edmister and Lee (1984), these five expressions for calculating normal boiling points result in values that do not differ significantly from one another for narrow boiling petroleum fractions.

All three parameters (i.e., molecular weight, specific gravity, and VABP/WABP) are employed, as discussed later, to estimate the PNA content of the heavy hydrocarbon fraction, which in turn is used to predict the critical properties and acentric factor of the fraction. Hopke and Lin (1974), Erbar (1977), Bergman et al. (1977), and Robinson and Peng (1978) used the PNA concept to characterize the undefined hydrocarbon fractions. As a representative of this characterization approach, the Robinson-Peng method and the Bergman method are discussed next.

Peng-Robinson's Method

Robinson and Peng (1978) proposed a detailed procedure for characterizing heavy hydrocarbon fractions. The procedure is summarized in the following steps.

Step 1 Calculate the PNA content (X_p , X_N , X_A) of the undefined fraction by solving the following three rigorously defined equations:

$$\sum_{i=PNA} X_i = 1 \quad (2-41)$$

$$\sum_{i=PNA} [M_i T_{bi} X_i] = (M)(\text{WABP}) \quad (2-42)$$

$$\sum_{i=PNA} [M_i X_i] = M \quad (2-43)$$

where

X_p = mole fraction of the paraffinic group in the undefined fraction

X_N = mole fraction of the naphthenic group in the undefined fraction

X_A = mole fraction of the aromatic group in the undefined fraction

WABP = weight average boiling point of the undefined fraction, °R

M = molecular weight of the undefined fraction

(M_i) = average molecular weight of each cut (i.e., PNA)

(T_{bi}) = boiling point of each cut, °R

Equations 2-41 through 2-43 can be written in a matrix form as follows:

$$\begin{bmatrix} 1 & 1 & 1 \\ [M \cdot T_b]_p & [M \cdot T_b]_N & [M \cdot T_b]_A \\ [M]_p & [M]_N & [M]_A \end{bmatrix} \begin{bmatrix} X_p \\ X_N \\ X_A \end{bmatrix} = \begin{bmatrix} 1 \\ M \cdot \text{WABP} \\ M \end{bmatrix} \quad (2-44)$$

Robinson and Peng pointed out that it is possible to obtain negative values for the *PNA* contents. To prevent these negative values, the authors imposed the following constraints:

$$0 \leq X_P \leq 0.90$$

$$X_N \geq 0.00$$

$$X_A \geq 0.00$$

Solving equation (2-44) for the PNA content requires the weight-average boiling point and molecular weight of the cut of the undefined hydrocarbon fraction. If the experimental values of these cuts are not available, the following correlations proposed by Robinson and Peng can be used.

For determination of $(T_b)_P$, $(T_b)_N$, and $(T_b)_A$,

$$\text{Paraffinic group } \ln(T_b)_P = \ln(1.8) + \sum_{i=1}^6 [a_i(n-6)^{i-1}] \quad (2-45)$$

$$\text{Naphthenic group } \ln(T_b)_N = \ln(1.8) + \sum_{i=1}^6 [a_i(n-6)^{i-1}] \quad (2-46)$$

$$\text{Aromatic group } \ln(T_b)_A = \ln(1.8) + \sum_{i=1}^6 [a_i(n-6)^{i-1}] \quad (2-47)$$

where n = number of carbon atoms in the undefined hydrocarbon fraction, and a_i = coefficients of the equations, which are given below.

Coefficient	Paraffin, <i>P</i>	Napthene, <i>N</i>	Aromatic, <i>A</i>
a_1	5.83451830	5.85793320	5.86717600
a_2	$0.84909035 \times 10^{-1}$	$0.79805995 \times 10^{-1}$	$0.80436947 \times 10^{-1}$
a_3	$-0.52635428 \times 10^{-2}$	$-0.43098101 \times 10^{-2}$	$-0.47136506 \times 10^{-2}$
a_4	$0.21252908 \times 10^{-3}$	$0.14783123 \times 10^{-3}$	$0.18233365 \times 10^{-3}$
a_5	$-0.44933363 \times 10^{-5}$	$-0.27095216 \times 10^{-5}$	$-0.38327239 \times 10^{-5}$
a_6	$0.37285365 \times 10^{-7}$	$0.19907794 \times 10^{-7}$	$0.32550576 \times 10^{-7}$

For the determination of $(M)_P$, $(M)_N$, and $(M)_A$,

$$\text{Paraffinic group } (M)_P = 14.026n + 2.016 \quad (2-48)$$

$$\text{Naphthenic group } (M)_N = 14.026n - 14.026 \quad (2-49)$$

$$\text{Aromatic group } (M)_A = 14.026n - 20.074 \quad (2-50)$$

Step 2 Having obtained the PNA content of the undefined hydrocarbon fraction, as outlined in step 1, calculate the critical pressure of the fraction by applying the following expression:

$$p_c = X_P(p_c)_P + X_N(p_c)_N + X_A(p_c)_A \quad (2-51)$$

where p_c = critical pressure of the heavy hydrocarbon fraction, psia.

The critical pressure for each cut of the heavy fraction is calculated according to the following equations:

$$\text{Paraffinic group } (p_c)_P = \frac{206.126096n + 29.67136}{(0.227n + 0.340)^2} \quad (2-52)$$

$$\text{Naphthenic group } (p_c)_N = \frac{206.126096n - 206.126096}{(0.227n - 0.137)^2} \quad (2-53)$$

$$\text{Aromatic group } (p_c)_A = \frac{206.126096n - 295.007504}{(0.227n - 0.325)^2} \quad (2-54)$$

Step 3 Calculate the acentric factor of each cut of the undefined fraction by using the following expressions:

$$\text{Paraffinic group } (\omega)_P = 0.432n + 0.0457 \quad (2-55)$$

$$\text{Naphthenic group } (\omega)_N = 0.0432n - 0.0880 \quad (2-56)$$

$$\text{Aromatic group } (\omega)_A = 0.0445n - 0.0995 \quad (2-57)$$

Step 4 Calculate the critical temperature of the fraction under consideration by using the following relationship:

$$T_c = X_P(T_c)_P + X_N(T_c)_N + X_A(T_c)_A \quad (2-58)$$

where T_c = critical temperature of the fraction, °R.

The critical temperatures of the various cuts of the undefined fractions are calculated from the following expressions:

$$\text{Paraffinic group } (T_c)_P = S \left\{ 1 + \frac{3 \log[(P_c)_P] - 3.501952}{7[1 + (\omega)_P]} \right\} (T_b)_P \quad (2-59)$$

$$\text{Naphthenic group } (T_c)_N = S_1 \left\{ 1 + \frac{3 \log[(P_c)_N] - 3.501952}{7[1 + (\omega)_P]} \right\} (T_b)_N \quad (2-60)$$

$$\text{Aromatic group } (T_c)_A = S_1 \left\{ 1 + \frac{3 \log[(P_c)_A] - 3.501952}{7[1 + (\omega)_A]} \right\} (T_b)_A \quad (2-61)$$

where the correction factors S and S_1 are defined by the following expressions:

$$S = 0.99670400 + 0.00043155n$$

$$S_1 = 0.99627245 + 0.00043155n$$

Step 5 Calculate the acentric factor of the heavy hydrocarbon fraction by using the Edmister correlation (equation 2-21) to give

$$\omega = \frac{3[\log(P_c/14.7)]}{7[(T_c/T_b) - 1]} - 1 \quad (2-62)$$

where

ω = acentric factor of the heavy fraction

P_c = critical pressure of the heavy fraction, psia

T_c = critical temperature of the heavy fraction, °R

T_b = average-weight boiling point, °R

EXAMPLE 2-5

Calculate the critical pressure, critical temperature, and acentric factor of an undefined hydrocarbon fraction with a measured molecular weight of 94 and a weight-average boiling point of 655°R. The number of carbon atoms of the component is 7; that is, $n = 7$.

SOLUTION

Step 1 Calculate the boiling point of each cut by applying equations (2-45) through (2-47) to give

$$(T_b)_P = \exp \left\{ \ln(1.8) + \sum_{i=1}^6 [a_i(n-6)^{i-1}] \right\} = 666.58^\circ\text{R}$$

$$(T_b)_N = \exp \left\{ \ln(1.8) + \sum_{i=1}^6 [a_i(n-6)^{i-1}] \right\} = 630^\circ\text{R}$$

$$(T_b)_A = \exp \left\{ \ln(1.8) + \sum_{i=1}^6 [a_i(n-6)^{i-1}] \right\} = 635.85^\circ\text{R}$$

Step 2 Compute the molecular weight of various cuts by using equations (2-48) through (2-50) to yield

$$(M)_P = 14.026 \times 7 + 2.016 = 100.198$$

$$(M)_N = 14.0129 \times 7 - 14.026 = 84.156$$

$$(M)_A = 14.026 \times 7 - 20.074 = 78.180$$

Step 3 Solve equation (2-44) for X_P , X_N , and X_A :

$$\begin{bmatrix} 1 & 1 & 1 \\ 66689.78 & 53018.28 & 49710.753 \\ 199.198 & 84.156 & 78.180 \end{bmatrix} \begin{bmatrix} X_P \\ X_N \\ X_A \end{bmatrix} = \begin{bmatrix} 1 \\ 61570 \\ 94 \end{bmatrix}$$

to give:

$$X_P = 0.6313$$

$$X_N = 0.3262$$

$$X_A = 0.04250$$

Step 4 Calculate the critical pressure of each cut in the undefined fraction by applying equations (2-52) and (2-54).

$$(p_c)_P = \frac{206.126096 \times 7 + 29.67136}{(0.227 \times 7 + 0.340)^2} = 395.70 \text{ psia}$$

$$(p_c)_N = \frac{206.126096 \times 7 - 206.126096}{(0.227 \times 7 - 0.137)^2} = 586.61$$

$$(p_c)_A = \frac{206.126096 \times 7 - 295.007504}{(0.227 \times 7 - 0.325)^2} = 718.46$$

Step 5 Calculate the critical pressure of the heavy fraction from equation (2-51) to give

$$p_c = X_P(p_c)_P + X_N(p_c)_N + X_A(p_c)_A$$

$$p_c = 0.6313(395.70) + 0.3262(586.61) + 0.0425(718.46) = 471 \text{ psia}$$

Step 6 Compute the acentric factor for each cut in the fraction by using equations (2-55) through (2-57) to yield

$$(\omega)_P = 0.432 \times 7 + 0.0457 = 0.3481$$

$$(\omega)_N = 0.0432 \times 7 - 0.0880 = 0.2144$$

$$(\omega)_A = 0.0445 \times 7 - 0.0995 = 0.2120$$

Step 7 Solve for $(T_c)_P$, $(T_c)_N$, and $(T_c)_A$ by using equations (2-59) through (2-61) to give

$$S = 0.99670400 + 0.00043155 \times 7 = 0.99972$$

$$S_1 = 0.99627245 + 0.00043155 \times 7 = 0.99929$$

$$(T_c)_P = 0.99972 \left\{ 1 + \frac{3 \log[395.7] - 3.501952}{7[1+0.3481]} \right\} 666.58 = 969.4^\circ\text{R}$$

$$(T_c)_N = 0.99929 \left\{ 1 + \frac{3 \log[586.61] - 3.501952}{7[1+0.2144]} \right\} 630 = 947.3^\circ\text{R}$$

$$(T_c)_A = 0.99929 \left\{ 1 + \frac{3 \log[718.46] - 3.501952}{7[1+0.212]} \right\} 635.85 = 1014.9^\circ\text{R}$$

Step 8 Solve for (T_c) of the undefined fraction from equation (2-58):

$$T_c = X_P (T_c)_P + X_N (T_c)_N + X_A (T_c)_A = 964.1^\circ\text{R}$$

Step 9 Calculate the acentric factor from equation (2-62) to give

$$\omega = \frac{3[\log(471.7/14.7)]}{7[(964.1/655) - 1]} - 1 = 0.3680$$

Bergman's Method

Bergman et al. (1977) proposed a detailed procedure for characterizing the undefined hydrocarbon fractions based on calculating the PNA content of the fraction under consideration. The proposed procedure was originated from analyzing extensive experimental data on lean gases and condensate systems. The authors, in developing the correlation, assumed that the paraffinic, naphthenic, and aromatic groups have the same boiling point. The computational procedure is summarized in the following steps.

Step 1 Estimate the weight fraction of the aromatic content in the undefined fraction by applying the following expression:

$$w_A = 8.47 - K_w \quad (2-63)$$

where

w_A = weight fraction of aromatics

K_w = Watson characterization factor, defined mathematically by the following expression

$$K_w = (T_b)^{1/3} / \gamma \quad (2-64)$$

γ = specific gravity of the undefined fraction

T_b = weight average boiling point, $^\circ\text{R}$

Bergman et al. imposed the following constraint on the aromatic content:

$$0.03 \leq w_A \leq 0.35$$

Step 2 With the estimate of the aromatic content, the weight fractions of the paraffinic and naphthenic cuts are calculated by solving the following system of linear equations:

$$w_P + w_N = 1 - w_A \quad (2-65)$$

$$\frac{w_P}{\gamma_P} + \frac{w_N}{\gamma_N} = \frac{1}{\gamma} - \frac{w_A}{\gamma_A} \quad (2-66)$$

where

w_p = weight fraction of the paraffin cut

w_N = weight fraction of the naphthene cut

γ = specific gravity of the undefined fraction

$\gamma_p, \gamma_N, \gamma_A$ = specific gravity of the three groups at the weight average boiling point of the undefined fraction. These gravities are calculated from the following relationships:

$$\gamma_p = 0.582486 + 0.00069481(T_b - 460) - 0.7572818(10^{-6})(T_b - 460)^2 + 0.3207736(10^{-9})(T_b - 460)^3 \quad (2-67)$$

$$\gamma_N = 0.694208 + 0.0004909267(T_b - 460) - 0.659746(10^{-6})(T_b - 460)^2 + 0.330966(10^{-9})(T_b - 460)^3 \quad (2-68)$$

$$\gamma_A = 0.916103 - 0.000250418(T_b - 460) + 0.357967(10^{-6})(T_b - 460)^2 - 0.166318(10^{-9})(T_b - 460)^3 \quad (2-69)$$

A minimum paraffin content of 0.20 was set by Bergman et al. To ensure that this minimum value is met, the estimated aromatic content that results in negative values of w_p is increased in increments of 0.03 up to a maximum of 15 times until the paraffin content exceeds 0.20. They pointed out that this procedure gives reasonable results for fractions up to C_{15} .

Step 3 Calculate the critical temperature, the critical pressure, and acentric factor of each cut from the following expressions.

For paraffins,

$$(T_c)_p = 275.23 + 1.2061(T_b - 460) - 0.00032984(T_b - 460)^2 \quad (2-70)$$

$$(p_c)_p = 573.011 - 1.13707(T_b - 460) + 0.00131625(T_b - 460)^2 - 0.85103(10^{-6})(T_b - 460)^3 \quad (2-71)$$

$$(\omega)_p = 0.14 + 0.0009(T_b - 460) + 0.233(10^{-6})(T_b - 460)^2 \quad (2-72)$$

For naphthenes,

$$(T_c)_N = 156.8906 + 2.6077(T_b - 460) - 0.003801(T_b - 460)^2 + 0.2544(10^{-5})(T_b - 460)^3 \quad (2-73)$$

$$(p_c)_N = 726.414 - 1.3275(T_b - 460) + 0.9846(10^{-3})(T_b - 460)^2 - 0.45169(10^{-6})(T_b - 460)^3 \quad (2-74)$$

$$(\omega)_N = (\omega)_p - 0.075 \quad (2-75)$$

Bergman et al. assigned the following special values of the acentric factor to the C_8 , C_9 , and C_{10} naphthenes:

$$C_8 \quad (\omega)_N = 0.26$$

$$C_9 \quad (\omega)_N = 0.27$$

$$C_{10} \quad (\omega)_N = 0.35$$

For the aromatics,

$$(T_c)_A = 289.535 + 1.7017(T_b - 460) - 0.0015843(T_b - 460)^2 + 0.82358(10^{-6})(T_b - 460)^3 \quad (2-76)$$

$$(p_c)_A = 1184.514 - 3.44681(T_b - 460) + 0.0045312(T_b - 460)^2 - 0.23416(10^{-5})(T_b - 460)^3 \quad (2-77)$$

$$(\omega)_A = (\omega)_p - 0.1 \quad (2-78)$$

Step 4 Calculate the critical pressure, the critical temperature, and acentric factor of the undefined fraction from the following relationships:

$$p_c = X_p(p_c)_p + X_N(p_c)_N + X_A(p_c)_A \quad (2-79)$$

$$T_c = X_p(T_c)_p + X_N(T_c)_N + X_A(T_c)_A \quad (2-80)$$

$$\omega = X_p(\omega)_p + X_N(\omega)_N + X_A(\omega)_A \quad (2-81)$$

Whitson (1984) suggested that the Peng-Robinson and Bergman PNA methods are not recommended for characterizing reservoir fluids containing fractions heavier than C_{20} .

Based on Bergman et al.'s work, Silva and Rodriguez (1992) suggested the use of the following two expressions when the boiling point temperature and specific gravity of the cut are not available:

$$T_b = 447.08723 \ln\left(\frac{M}{64.2576}\right) + 460$$

Use the preceding calculated value of T_b to calculate the specific gravity of the fraction from the following expression:

$$\gamma = 0.132467 \ln(T_b - 460) + 0.0116483$$

where the boiling point temperature T_b is expressed in °R.

Graphical Correlations

Several mathematical correlations for determining the physical and critical properties of petroleum fractions have been presented. These correlations are readily adapted to computer applications. However, it is important to present the properties in graphical forms for a better understanding of the behaviors and interrelationships of the properties.

Boiling Points

Numerous graphical correlations have been proposed over the years for determining the physical and critical properties of petroleum fractions. Most of these correlations use the normal boiling point as one of the correlation parameters. As stated previously, five methods are used to define the normal boiling point:

1. Volume-average boiling point (VABP).
2. Weight-average boiling point (WABP).
3. Molal-average boiling point (MABP).
4. Cubic-average boiling point (CABP).
5. Mean-average boiling point (MeABP).

Figure 2-4 shows the conversions between the VABP and the other four averaging types of boiling-point temperatures.

The following steps summarize the procedure of using Figure 2–4 in determining the desired average boiling point temperature.

Step 1 On the basis of ASTM D-86 distillation data, calculate the volumetric average boiling point from the following expressions:

$$\text{VABP} = (t_{10} + t_{30} + t_{50} + t_{70} + t_{90})/5 \quad (2-82)$$

where t is the temperature in °F and the subscripts 10, 30, 50, 70, and 90 refer to the volume percent recovered during the distillation.

Step 2 Calculate the 10% to 90% “slope” of the ASTM distillation curve from the following expression:

$$\text{Slope} = (t_{90} - t_{10})/80 \quad (2-83)$$

Enter the value of the slope in the graph and travel vertically to the appropriate set for the type of boiling point desired.

Step 4 Read from the ordinate a correction factor for the VABP and apply the relationship:

$$\text{Desired boiling point} = \text{VABP} + \text{correction factor} \quad (2-84)$$

The use of the graph can best be illustrated by the following examples.

EXAMPLE 2–6

The ASTM distillation data for a 55°API gravity petroleum fraction is given below. Calculate WAPB, MABP, CABP, and MeABP.

Cut	Distillation % Over	Temperature, °F
1	IBP*	159
2	10	178
3	20	193
4	30	209
5	40	227
6	50	253
7	60	282
8	70	318
9	80	364
10	90	410
Residue	EP**	475

*Initial boiling point.

** End point.

SOLUTION

Step 1 Calculate VABP from equation (2–82):

$$\text{VABP} = (178 + 209 + 253 + 318 + 410)/5 = 273^\circ\text{F}$$

Step 2 Calculate the distillation curve slope from equation (2–83):

$$\text{Slope} = (410 - 178)/80 = 2.9$$

Step 3 Enter the slope value of 2.9 in Figure 2–4 and move down to the appropriate set of boiling point curves. Read the corresponding correction factors from the ordinate to give

Correction factors for WABP = 6°F

Correction factors for CABP = –7°F

Correction factors for MeABP = –18°F

Correction factors for MABP = –33°F

Step 4 Calculate the desired boiling point by applying equation (2–84):

$$\text{WABP} = 273 + 6 = 279^{\circ}\text{F}$$

$$\text{CABP} = 273 - 7 = 266^{\circ}\text{F}$$

$$\text{MeABP} = 273 - 18 = 255^{\circ}\text{F}$$

$$\text{MABP} = 273 - 33 = 240^{\circ}\text{F}$$

Molecular Weight

Figure 2–5 shows a convenient graphical correlation for determining the molecular weight of petroleum fractions from their MeABP and API gravities. The following example illustrates the practical application of the graphical method.

EXAMPLE 2–7

Calculate the molecular weight of the petroleum fraction with an API gravity and MeABP as given in Example 2–6.

SOLUTION

From Example 2–6,

$$\text{API} = 55^{\circ}$$

$$\text{MeABP} = 255^{\circ}\text{F}$$

Enter these values in Figure 2–5 to give

$$\text{MW} = 118$$

Critical Temperature

The critical temperature of a petroleum fraction can be determined by using the graphical correlation shown in Figure 2–6. The required correlation parameters are the API gravity and the molal-average boiling point of the undefined fraction.

EXAMPLE 2–8

Calculate the critical temperature of the petroleum fraction with physical properties as given in Example 2–6.

SOLUTION

From Example 2–6,

$$\text{API} = 55^{\circ}$$

$$\text{MABP} = 240^{\circ}\text{F}$$

Enter the above values in Figure 2–6 to give $T_c = 600^{\circ}\text{F}$.

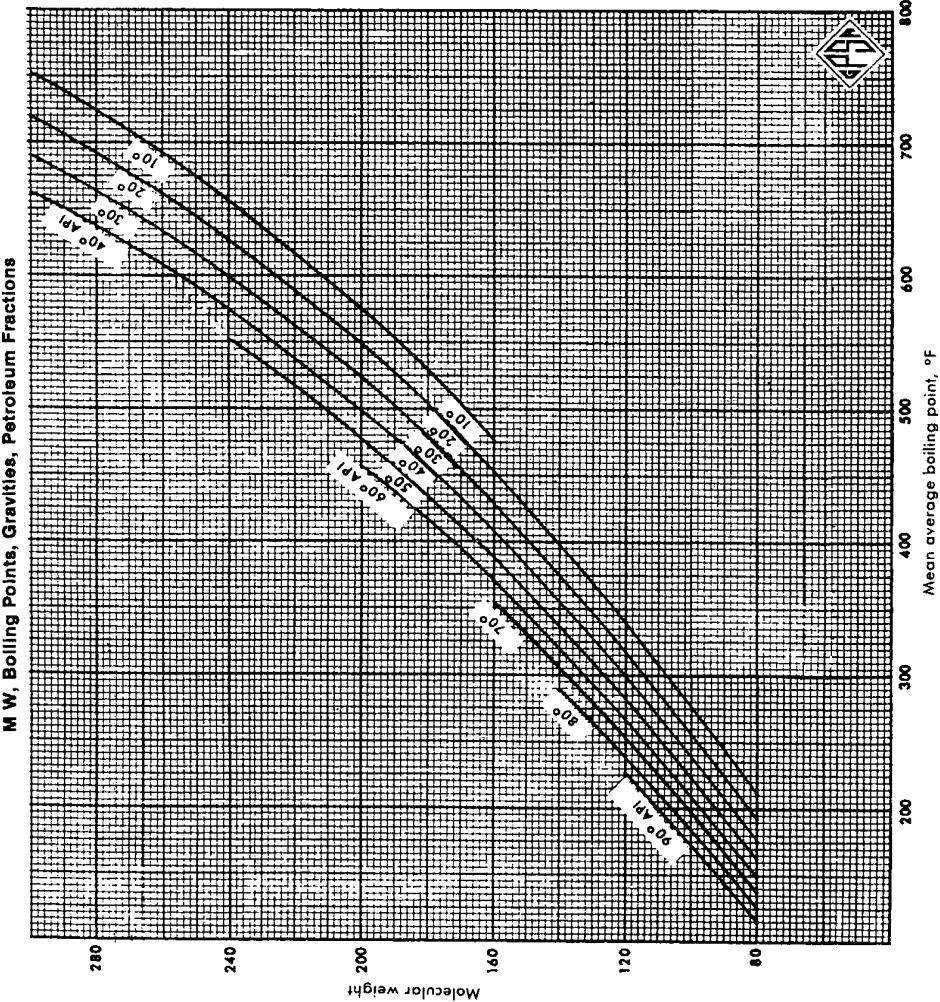


FIGURE 2-5 Relationship among molecular weight, API gravity, and mean average boiling points.
Source: GPSA Engineering Data Book, 10th ed. Tulsa, OK: Gas Processors Suppliers Association, 1987. Courtesy of the Gas Processors Suppliers Association.

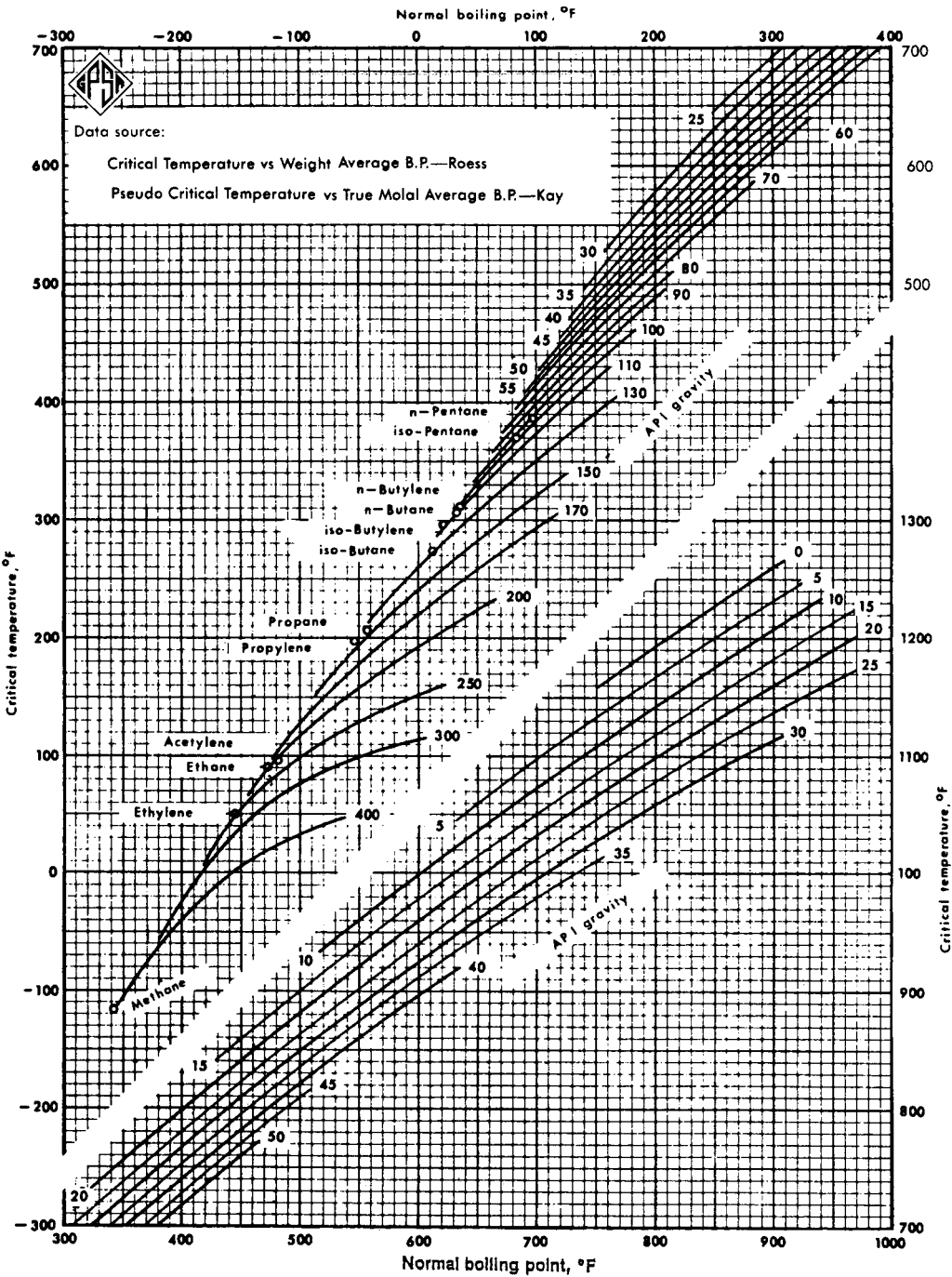


FIGURE 2-6 Critical temperature as a function of API gravity and boiling points.

Source: GPSA Engineering Data Book, 10th ed. Tulsa, OK: Gas Processors Suppliers Association, 1987. Courtesy of the Gas Processors Suppliers Association.

Critical Pressure

Figure 2-7 is a graphical correlation of the critical pressure of the undefined petroleum fractions as a function of the mean-average boiling point and the API gravity. The following example shows the practical use of the graphical correlation.

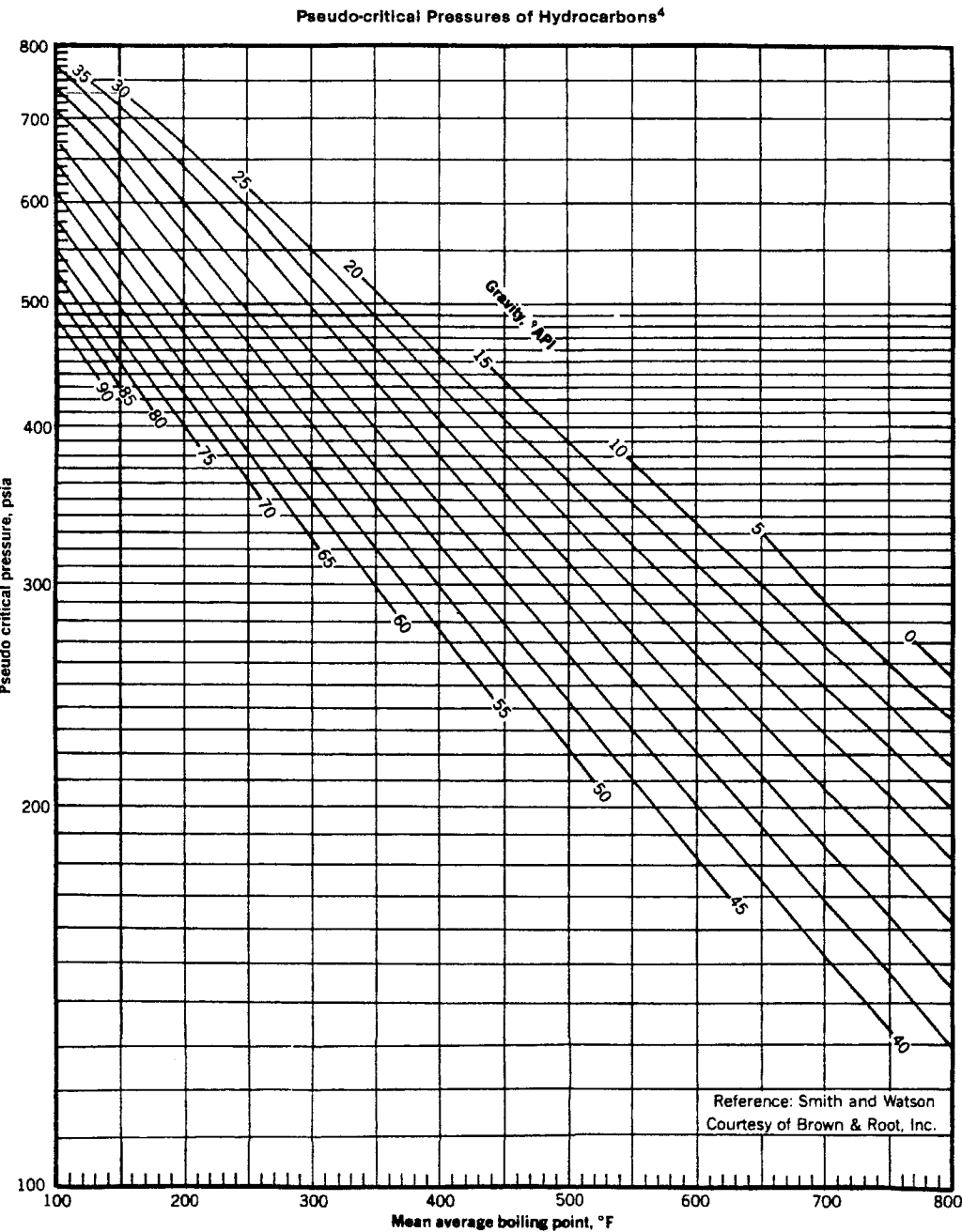


FIGURE 2-7 Relationship among critical pressure, API gravity, and mean-average boiling points.
Source: GPSA Engineering Data Book, 10th ed. Tulsa, OK: Gas Processors Suppliers Association, 1987. Courtesy of the Gas Processors Suppliers Association.

EXAMPLE 2-9

Calculate the critical pressure of the petroleum fraction from Example 2-6.

SOLUTION

From Example 2-6,

$$\text{API} = 55^\circ$$

$$\text{MeABP} = 255^\circ\text{F}$$

Determine the critical pressure of the fraction from Figure 2-7, to give $p_c = 428$ psia.

Splitting and Lumping Schemes

The hydrocarbon-plus fractions that constitute a significant portion of naturally-occurring hydrocarbon fluids create major problems when predicting the thermodynamic properties and the volumetric behavior of these fluids by equations of state. These problems arise due to the difficulty of properly characterizing the plus fractions (heavy ends) in terms of their critical properties and acentric factors.

Whitson (1980) and Maddox and Erbar (1982, 1983), among others, show the distinct effect of the heavy fractions characterization procedure on PVT relationships prediction by equations of state. Usually, these undefined plus fractions, commonly known as the C_{7+} fractions, contain an undefined number of components with a carbon number higher than 6. Molecular weight and specific gravity of the C_{7+} fraction may be the only measured data available.

In the absence of detailed analytical TBP distillation or chromatographic analysis data for the plus fraction in a hydrocarbon mixture, erroneous predictions and conclusions can result if the plus fraction is used directly as a single component in the mixture phase behavior calculations. Numerous authors have indicated that these errors can be substantially reduced by “splitting” or “breaking down” the plus fraction into a manageable number of fractions (pseudo components) for equation-of-state calculations.

The problem, then, is how to adequately split a C_{7+} fraction into a number of pseudo components characterized by mole fraction, molecular weight, and specific gravity. These characterization properties, when properly combined, should match the measured plus fraction properties, that is, $(M)_{7+}$ and $(\gamma)_{7+}$.

Splitting Schemes

Splitting schemes refer to the procedures of dividing the heptanes-plus fractions into hydrocarbon groups with a single carbon number (C_7 , C_8 , C_9 , etc.), described by the same physical properties used for pure components.

Several authors have proposed different schemes for extending the molar distribution behavior of C_{7+} in terms of mole fraction as a function of molecular weight or number of carbon atoms. In general, the proposed schemes are based on the observation that lighter systems, such as condensates, usually exhibit exponential molar distribution, while heavier systems often show left-skewed distributions. This behavior is shown schematically in Figure 2-8.

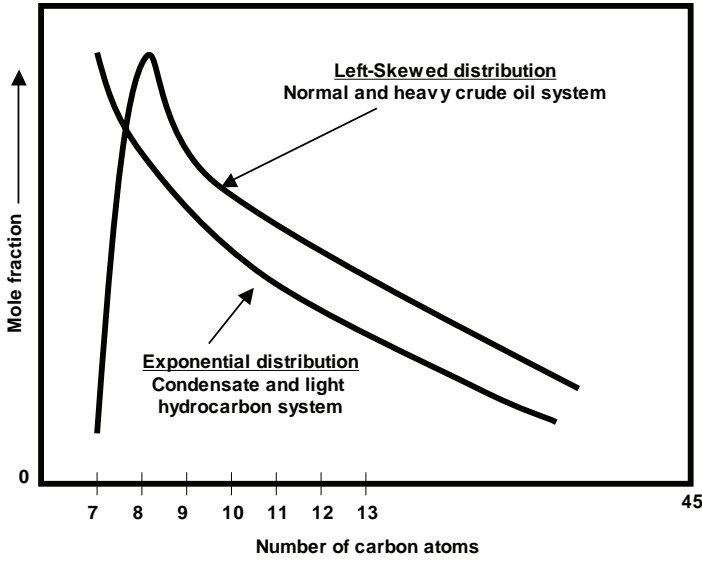


FIGURE 2-8 The exponential and left-skewed distribution functions.

Three important requirements should be satisfied when applying any of the proposed splitting models:

1. The sum of the mole fractions of the individual pseudo components is equal to the mole fraction of C_{7+} .
2. The sum of the products of the mole fraction and the molecular weight of the individual pseudo components is equal to the product of the mole fraction and molecular weight of C_{7+} .
3. The sum of the product of the mole fraction and molecular weight divided by the specific gravity of each individual component is equal to that of C_{7+} .

These requirements can be expressed mathematically by the following relationship:

$$\sum_{n=7}^{n+} z_n = z_{7+} \quad (2-85)$$

$$\sum_{n=7}^{n+} [z_n M_n] = z_{7+} M_{7+} \quad (2-86)$$

$$\sum_{n=7}^{n+} \frac{z_n M_n}{\gamma_n} = \frac{z_{7+} M_{7+}}{\gamma_{7+}} \quad (2-87)$$

Equations (2-86) and (2-87) can be solved for the molecular weight and specific gravity of the last fraction after splitting; as

$$M_{n+} = \frac{z_{7+} M_{7+} - \sum_{n=7}^{(n+)-1} [z_n M_n]}{z_{n+}}$$

$$\gamma_{n+} = \frac{z_{n+} M_{n+}}{\frac{z_{7+} M_{7+}}{\gamma_{7+}} - \sum_{n=7}^{(n+)-1} \frac{z_n M_n}{\gamma_n}}$$

where

z_{7+} = mole fraction of C_{7+}

n = number of carbon atoms

n_+ = last hydrocarbon group in the C_{7+} with n carbon atoms, such as 20+

z_n = mole fraction of pseudo component with n carbon atoms

M_{7+}, γ_{7+} = measured molecular weight and specific gravity of C_{7+}

M_n, γ_n = molecular weight and specific gravity of the pseudo component with n carbon atoms

Several splitting schemes have been proposed. These schemes, as discussed next, are used to predict the compositional distribution of the heavy plus fraction.

Katz's Method

Katz (1983) presented an easy-to-use graphical correlation for breaking down into pseudo components the C_{7+} fraction present in condensate systems. The method was originated by studying the compositional behavior of six condensate systems, using detailed extended analysis. On a semilog scale, the mole percent of each constituent of the C_{7+} fraction versus the carbon number in the fraction was plotted. The resulting relationship can be conveniently expressed mathematically by the following expression:

$$z_n = 1.38205 z_{7+} e^{-0.25903n} \quad (2-88)$$

where

z_{7+} = mole fraction of C_{7+} in the condensate system

n = number of carbon atoms of the pseudo component

z_n = mole fraction of the pseudo component with number of carbon atoms of n

Equation (2-88) is applied repeatedly until equation (2-85) is satisfied. The molecular weight and specific gravity of the last pseudo component can be calculated from equations (2-86) and (2-87), respectively.

The computational procedure of Katz's method is best explained through the following example.

EXAMPLE 2-10

A naturally-occurring condensate gas system has the following composition:

COMPONENT	z_i
C_1	0.9135
C_2	0.0403
C_3	0.0153
i- C_4	0.0039
n- C_4	0.0043
i- C_5	0.0015

COMPONENT	z_i
n-C ₅	0.0019
C ₆	0.0039
C ₇₊	0.0154

Molecular weight and specific gravity of C₇₊ are 141.25 and 0.797, respectively.
Using Katz’s splitting scheme, extend the compositional distribution of C₇₊ to the pseudo fraction C₁₆₊. Then, calculate M , γ , T_b , p_c , T_c , and ω of C₁₆₊.

SOLUTION

For calculation of the molar distribution using Katz’s method, applying equation (2–94) with $z_{7+} = 0.0154$ gives the following results.

n	Experimental z_n	Equation (2-88) z_n
7	0.00361	0.00347
8	0.00285	0.00268
9	0.00222	0.00207
10	0.00158	0.001596
11	0.00121	0.00123
12	0.00097	0.00095
13	0.00083	0.00073
14	0.00069	0.000566
15	0.00050	0.000437
16+	0.00094	0.001671*

*This value is obtained by applying equation (2–85); that is, $0.0154 - \sum_{n=7}^{15} z_n = 1.001671$.

The characterization of C₁₆₊ takes the following steps.

Step 1 Calculate the molecular weight and specific gravity of C₁₆₊ by solving equations (2–86) and (2–87) for these properties. The calculations are performed below.

n	z_n	M_n (Table 2–1)	$z_n M_n$	γ_n (Table 2–1)	$z_n \cdot M/\gamma_n$
7	0.00347	96	0.33312	0.727	0.4582
8	0.00268	107	0.28676	0.749	0.3829
9	0.00207	121	0.25047	0.768	0.3261
10	0.001596	134	0.213864	0.782	0.27348
11	0.00123	147	0.18081	0.793	0.22801
12	0.00095	161	0.15295	0.804	0.19024
13	0.00073	175	0.12775	0.815	0.15675
14	0.000566	190	0.10754	0.826	0.13019
15	0.000437	206	0.09002	0.836	0.10768
16+	0.001671	—	—	—	—
Σ			1.743284		2.25355

Then,

$$M_{16+} = \frac{(0.0154)(141.25) - 1.743284}{0.001671} = 258.5$$

$$M_{16+} = \frac{z_{7+} M_{7+} - \sum_{n=7}^{15} [z_n M_n]}{z_{16+}}$$

and

$$\gamma_{16+} = \frac{z_{16+} M_{16+}}{\frac{z_{7+} M_{7+}}{\gamma_{7+}} - \sum_{n=7}^{15} \frac{z_n M_n}{\gamma_n}}$$

$$\gamma_{16+} = \frac{(0.001671)(258.5)}{2.7293 - 2.25355} = 0.908$$

Step 2 Calculate the boiling points, critical pressure, and critical temperature of C_{16+} , using the Riazi-Daubert correlation, to give

$$T_c = 544.4(258.5)^{0.2998}(0.908)^{1.0555} \exp[-1.3478 \times 10^{-4}(258.5) + (-0.61641)(0.908) + 0]$$

$$= 1473^\circ\text{R}$$

$$p_c = 4.5203 \times 10^3 (258.5)^{-0.8063} (0.908)^{1.6015} \exp[-1.8078 \times 10^{-3}(258.5) + (-0.3084)(0.908) \cdot$$

$$= 215 \text{ psi}$$

$$T_b = 6.77857(258.5)^{0.401673} (0.908)^{-1.58262} \exp[3.77409 \times 10^{-3}(258.5) + (-0.3084)(0.908)$$

$$+ (-4.25288 \times 10^{-3})(258.5)(0.908)] = 1136^\circ\text{R}$$

Step 3 Calculate the acentric factor of C_{16+} by applying the Edmister correlation, to give

$$\omega = \frac{3}{7} \frac{\log(215/14.7)}{(1473/1136) - 1} - 1 = 0.684$$

Lohrenz's Method

Lohrenz, Bra, and Clark (1964) proposed that the heptanes-plus fraction could be divided into pseudo components with carbon number ranges from 7 to 40. They mathematically stated that the mole fraction z_n is related to its number of carbon atoms n and the mole fraction of the hexane fraction z_6 by the expression:

$$z_n = z_6 e^{A(n-6)^2 + B(n-6)} \quad (2-89)$$

The constants A and B are determined such that the constraints given by equations (2-85) through (2-87) are satisfied.

The use of equation (2-89) assumes that they individual C_{7+} components are distributed through the hexane mole fraction and tail off to an extremely small quantity of heavy hydrocarbons.

EXAMPLE 2-11

Rework Example 2-10 using the Lohrenz splitting scheme and assuming that a partial molar distribution of C_{7+} is available. The composition follows:

COMPONENT	z_i
C_1	0.9135
C_2	0.0403
C_3	0.0153
i- C_4	0.0039
n- C_4	0.0043
i- C_5	0.0015

COMPONENT	z_i
n-C ₅	0.0019
C ₆	0.0039
C ₇	0.00361
C ₈	0.00285
C ₉	0.00222
C ₁₀	0.00158
C ₁₁₊	0.00514

SOLUTION

Step 1 Determine the coefficients A and B of equation (2–89) by the least-squares fit to the mole fractions C₆ through C₁₀, to give

$$A = 0.03453$$
$$B = 0.08777$$

Step 2 Solve for the mole fraction of C₁₀ through C₁₅ by applying equation (2–89) and setting $z_6 = 0.0039$. This is shown below.

Component	Experimental z_n	Equation (2–89) z_n
C ₇	0.00361	0.00361
C ₈	0.00285	0.00285
C ₉	0.00222	0.00222
C ₁₀	0.00158	0.00158
C ₁₁	0.00121	0.00106
C ₁₂	0.00097	0.00066
C ₁₃	0.00083	0.00039
C ₁₄	0.00069	0.00021
C ₁₅	0.00050	0.00011
C ₁₆₊	0.00094	0.00271*

*Obtained by applying equation (2–85).

Step 3 Calculate the molecular weight and specific gravity of C₁₆₊ by applying equations (2–86) and (2–87), to give $(M)_{16+} = 233.3$ and $(\gamma)_{16+} = 0.943$.

Step 4 Solve for T_b , p_c , T_c , and ω by applying the Riazi-Daubert and Edmister correlations, to give

$$T_b = 1103^\circ\text{R}$$
$$p_c = 251 \text{ psia}$$
$$T_c = 1467^\circ\text{R}$$
$$\omega = 0.600$$

Pedersen’s Method

Pedersen, Thomassen, and Fredenslund (1982) proposed that, for naturally-occurring hydrocarbon mixtures, an exponential relationship exists between the mole fraction of a component and the corresponding carbon number. They expressed this relationship mathematically in the following form:

$$z_n = e^{(n-A)/B} \quad (2-90)$$

where A and B are constants.

For condensates and volatile oils, Pedersen and coworkers suggested that A and B can be determined by at least-squares fit to the molar distribution of the lighter fractions. Equation (2-90) can then be used to calculate the molar content of each of the heavier fractions by extrapolation. The classical constraints as given by equations (2-85) through (2-87) also are imposed.

EXAMPLE 2-12

Rework Example 2-11 by using the Pedersen splitting correlation.

SOLUTION

Step 1 Calculate the coefficients A and B by the least-squares fit to the molar distribution of C_6 through C_{10} , to give $A = -14.404639$ and $B = -3.8125739$.

Step 2 Solve for the mole fraction of C_{10} through C_{15} by applying equation (2-90), as shown below.

Component	Experimental z_n	Calculated z_n
C_7	0.00361	0.00361
C_8	0.00285	0.00285
C_9	0.00222	0.00222
C_{10}	0.00158	0.00166
C_{11}	0.00121	0.00128
C_{12}	0.00097	0.00098
C_{13}	0.00083	0.00076
C_{14}	0.00069	0.00058
C_{15}	0.00050	0.00045
C_{16+}	0.00094	0.00101*

*From equation (2-85).

Ahmed's Method

Ahmed, Cady, and Story (1985) devised a simplified method for splitting the C_{7+} fraction into pseudo components. The method originated from studying the molar behavior of 34 condensate and crude oil systems through detailed laboratory compositional analysis of the heavy fractions. The only required data for the proposed method are the molecular weight and the total mole fraction of the heptanes-plus fraction.

The splitting scheme is based on calculating the mole fraction, z_n , at a progressively higher number of carbon atoms. The extraction process continues until the sum of the mole fraction of the pseudo components equals the total mole fraction of the heptanes plus (z_{7+}).

$$z_n = z_{n+} \left[\frac{M_{(n+1)+} - M_{n+}}{M_{(n+1)+} - M_n} \right] \quad (2-91)$$

where

z_n = mole fraction of the pseudo component with a number of carbon atoms of n (z_7 , z_8 , z_9 , etc.)

M_n = molecular weight of the hydrocarbon group with n carbon atoms as given in Table 1-1

M_{n+} = molecular weight of the $n+$ fraction as calculated by the following expression:

$$M_{(n+1)+} = M_{7+} + S(n - 6) \quad (2-92)$$

where n is the number of carbon atoms and S is the coefficient of equation (2-92) with the values given below.

No. of Carbon Atoms	Condensate Systems	Crude Oil Systems
$n \leq 8$	15.5	16.5
$n > 8$	17.0	20.1

The stepwise calculation sequences of the proposed correlation are summarized in the following steps.

Step 1 According to the type of hydrocarbon system under investigation (condensate or crude oil), select the appropriate values for the coefficients.

Step 2 Knowing the molecular weight of C_{7+} fraction (M_{7+}), calculate the molecular weight of the octanes-plus fraction (M_{8+}) by applying equation (2-92).

Step 3 Calculate the mole fraction of the heptane fraction (z_7) by using equation (2-91).

Step 4 Repeat steps 2 and 3 for each component in the system (C_8 , C_9 , etc.) until the sum of the calculated mole fractions is equal to the mole fraction of C_{7+} of the system. The splitting scheme is best explained through the following example.

EXAMPLE 2-13

Rework Example 2-12 using Ahmed's splitting method.

SOLUTION

Step 1 Calculate the molecular weight of C_{8+} by applying equation (2-92).

$$M_{8+} = 141.25 + 15.5(7 - 6) = 156.75$$

Step 2 Solve for the mole fraction of heptane (z_7) by applying equation (2-91).

$$z_7 = z_{7+} \left[\frac{M_{8+} - M_{7+}}{M_{8+} - M_7} \right] = 0.0154 \left[\frac{156.75 - 141.25}{156.75 - 96} \right] = 0.00393$$

Step 3 Calculate the molecular weight of C_{9+} from equation (2-92).

$$M_{9+} = 141.25 + 15.5(8 - 6) = 172.25$$

Step 4 Determine the mole fraction of C_8 from equation (2-91).

$$z_8 = z_{8+} [(M_{9+} - M_{8+}) / (M_{9+} - M_8)]$$

$$z_8 = (0.0154 - 0.00393) [(172.5 - 156.75) / (172.5 - 107)] = 0.00276$$

Step 5 Repeat this extracting method outlined in the preceding steps, to give the following results.

Component	<i>n</i>	<i>M_{n+}</i> (Equation 2-92)	<i>M_n</i> (Table 2-1)	<i>z_n</i> (Equation 2-91)
C ₇	7	141.25	96	0.000393
C ₈	8	156.25	107	0.00276
C ₉	9	175.25	121	0.00200
C ₁₀	10	192.25	134	0.00144
C ₁₁	11	209.25	147	0.00106
C ₁₂	12	226.25	161	0.0008
C ₁₃	13	243.25	175	0.00061
C ₁₄	14	260.25	190	0.00048
C ₁₅	15	277.25	206	0.00038
C ₁₆₊	16+	294.25	222	0.00159*

*Calculated from equation (2-85).

Step 6 The boiling point, critical properties, and the acentric factor of C₁₆₊ then are determined using the appropriate methods, to give

$$M = 294.25$$

$$\gamma = 0.856$$

$$T_b = 1174.6^\circ\text{R}$$

$$p_c = 175.9 \text{ psia}$$

$$T_c = 1449.3^\circ\text{R}$$

$$\omega = 0.742$$

Whitson's Method

Whitson (1983) proposed that the three-parameter gamma probability function can be used to describe the molar distribution of the C₇₊ fraction. Unlike all previous splitting methods, the gamma function has the flexibility to describe a wider range of distribution by adjusting its variance, which is left as an adjustable parameter. Whitson expressed the function in the following form:

$$p(M) = \frac{(M - \eta)^{\alpha-1} \exp\{-(M - \eta) / \beta\}}{\beta^\alpha \Gamma(\alpha)}$$

with

$$\beta = \frac{M_{C_{7+}} - \eta}{\alpha}$$

where Γ = gamma function.

Whitson points out that the three parameters in the gamma distribution are α , η , and $M_{C_{7+}}$. The key parameter α defines the form of the distribution, and its value usually ranges from 0.5 to 2.5 for reservoir fluids; $\alpha = 1$ gives an exponential distribution. Application of the gamma distribution to heavy oils, bitumen, and petroleum residues indicates

that the upper limit for α is 25 to 30, which statistically approaches a log-normal distribution. Figure 2-9 illustrates Whitson’s model for several values of the parameter α . For $\alpha = 1$, the distribution is exponential. For values less than 1, the model gives accelerated exponential distribution, while values greater than 1 yield left-skewed distributions.

Whitson indicates that the parameter η can be physically interpreted as the minimum molecular weight found in the C_{7+} fraction. An approximate relation between α and η is

$$\eta \approx \frac{110}{1 - (1 + 4/\alpha^{0.7})}$$

Whitson, Anderson, and Soreide (1989) devised a more useful application of the gamma model by utilizing the “Gaussian quadrature function” to describe the molar distribution of the C_{7+} fraction.

Their method allows multiple reservoir-fluid samples from a common reservoir to be treated simultaneously with a single fluid characterization. Each fluid sample can have different C_{7+} properties when the split is made, so that each split fraction has the same molecular weight (and other properties, such as γ , T_b , T_c , p_c , and ω), while the mole fractions are different for each fluid sample. Example applications include the characterization of a gas cap and underlying reservoir oil and a reservoir with compositional gradient.

Whitson and coauthors outline the following procedure for splitting the C_{7+} into fractions.

Step 1 Given the molecular weight and specific gravity of the C_{7+} , calculate Watson’s characterization parameter from equation (2-2); that is,

$$K_w \approx 4.5579 \left[\frac{M^{0.15178}}{\gamma^{0.84573}} \right]$$

Step 2 Select the number of C_{7+} fractions, N ; for example, $N = 5$ means splitting the C_{7+} into five components.

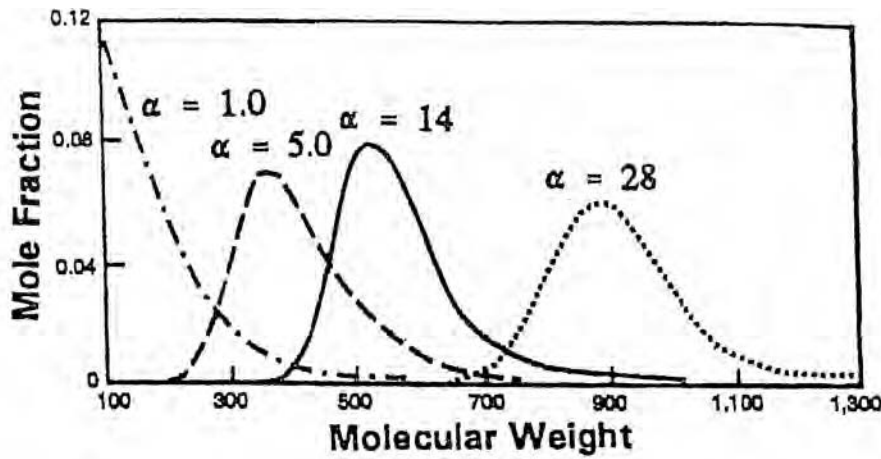


FIGURE 2-9 Gamma distributions for C_{7+} .

TABLE 2-6 Gaussian Quadrature Function Variables, X , and Weight Factors, W

	X	W
	Three Quadrature Points (plus fractions)	
1	0.415774556783	0.71109300992900
2	2.294280360279	0.27851773356900
3	6.289945082937	0.01038925650160
	Five Quadrature Points (plus fractions)	
1	0.263560319718	0.521755610583
2	1.413403059107	0.398666811083
3	3.596425771041	0.0759424496817
4	7.085810005859	0.00361175867992
5	12.640800844276	0.0000233699723858

Step 3 Based on the selected number of components, N , obtain N values for the Gaussian quadrature variables, X_i , and weight factors, W_i (i.e., X_1, \dots, X_N and W_1, \dots, W_N), from a mathematical handbook. Table 2-6 shows an example of Gaussian quadrature variables as given by Whitson.

Step 4 Specify the gamma function parameters η and α . When TBP data are not available to determine these two parameters, the authors recommend assigning the following values: $\eta = 90$ and $\alpha = 1$.

Step 5 Specify the molecular weight of the last fraction, N , that is, M_N . Whitson recommended the following value:

$$M_N = 2.5M_{C_{7+}} \quad (2-93)$$

Step 6 Calculate a modified β^* term from

$$\beta = \frac{M_N - \eta}{X_N} \quad (2-94)$$

Step 7 Calculate the parameter ∂ :

$$\partial = \exp\left(\frac{\alpha\beta^*}{M_{C_{7+}} - \eta} - 1\right) \quad (2-95)$$

Step 8 Calculate the C_{7+} mole fraction z_i and M_i for each fraction by applying the following relationships:

$$z_i = z_{C_{7+}} [W_i f(X_i)] \quad (2-96)$$

$$M_i = \eta + \beta^* X_i \quad (2-97)$$

with

$$f(X_i) = \frac{(X_i)^{\alpha-1}}{\Gamma(\alpha)} \frac{(1 + \ln \partial)^\alpha}{\partial^{X_i}} \quad (2-98)$$

where $i = 1, \dots, N$.

Abramowitz and Stegun (1970) approximated the gamma function $\Gamma(\alpha)$ by the following expression:

$$\Gamma(x+1) = 1 + \sum_{i=1}^8 A_i x^i \quad (2-99)$$

where $0 \leq x \leq 1$ and

$$\begin{aligned} A_1 &= -0.577191652 \\ A_2 &= 0.988205891 \\ A_3 &= -0.897056937 \\ A_4 &= 0.918206857 \\ A_5 &= -0.756704078 \\ A_6 &= 0.482199394 \\ A_7 &= -0.193527818 \\ A_8 &= 0.035868343 \end{aligned}$$

The recurrence formula $\Gamma(x+1) = x\Gamma(x)$ is used when x is greater or less than 1; that is, for $x > 1$ or $x < 1$. However, when $x = 1$, then $\Gamma(1) = 1$.

Step 9 Compare the *measured* molecular weight of the C_{7+} , that is, $M_{C_{7+}}$ with the molecular weight value $M_{C_{7+}}^*$ as calculated from

$$M_{C_{7+}}^* = \sum_{n=7}^N \left(\frac{z_n}{z_{C_{7+}}} \right) M_n \quad (2-100)$$

If $M_{C_{7+}}^*$ does not match the measured value, slightly modify the parameter ∂ and repeat steps 7 and 8 until a satisfactory match is achieved.

Step 10 Using the value of K_w as calculated in step 1, calculate the specific gravity of each of the fractions by applying equation (2-2):

$$\gamma_i = 6.0108 \left[\frac{M_i^{0.17947}}{K_w^{1.18241}} \right]$$

Whitson and Brule (2000) illustrated this procedure numerically through the following example.

EXAMPLE 2-14

Given that

$$\begin{aligned} z_{C_{7+}} &= 6.85\% \\ M_{C_{7+}} &= 143 \\ \gamma_{7+} &= 0.795 \end{aligned}$$

using Whitson's method, split the C_{7+} into five fractions; that is, $N = 5$.

SOLUTION

Step 1 Calculate K_w :

$$K_w \approx 4.5579 \left[\frac{M^{0.15178}}{\gamma^{0.84573}} \right] = 4.5579 \left[\frac{143^{0.15178}}{0.795^{0.84573}} \right] = 11.75$$

Step 2 Select the number of fractions, N ; for example, $N = 5$.

Step 3 Obtain Gaussian quadrature values X_i and W_i from Table 2–6, to give the following results.

Component	X_i	W_i
1	0.263560	0.52175561
2	1.413403	0.39866681
3	3.596426	0.07594245
4	7.085810	0.00361176
5	12.640801	0.00002337

Step 4 Assume $\alpha = 1$ and $\eta = 90$.

Step 5 Calculate M_N from equation (2–93):

$$M_N = 2.5$$

$$M_{C_{7+}} = (2.5)(143) = 358$$

To produce a better characterization, the authors used the higher value of $M_N = 500$.

Step 5 Calculate the parameter β^* from equation (2–94):

$$\beta = \frac{M_N - \eta}{X_N}$$

$$\beta^* = \frac{500 - 90}{12.640801} = 32.435$$

Step 6 Calculate the parameter ∂ from equation (2–95):

$$\partial = \exp\left(\frac{\alpha\beta^*}{M_{C_{7+}} - \eta} - 1\right)$$

$$\partial = \exp\left[\frac{(1)(32.435)}{143 - 90} - 1\right] = 0.6784$$

Step 7 Calculate the mole fraction of the first component, that is, z_1 , by applying equations (2–96) through (2–98) to produce

$$z_i = z_{C_{7+}} [W_i f(X_i)]$$

$$M_i = \eta + \beta^* X_i$$

$$f(X_i) = \frac{(X_i)^{\alpha-1}}{\Gamma(\alpha)} \frac{(1 + \ln \delta)^\alpha}{\delta^{X_i}}$$

$$f(X_1) = \frac{(0.26356)^{1-1}}{\Gamma(1)} \left[\frac{1 + \ln(0.6784)^1}{(0.6784)^{0.26356}} \right] = 0.677878$$

$$z_1 = 6.85(0.52175561)(0.677878) = 2.4228\%$$

$$M_1 = 90 + 32.435(0.26356) = 98.55$$

Repeat these calculations for $i = 2$ through 5 to give the following results, as given by Whitson and Brule.

<i>i</i>	<i>f</i> (<i>x_i</i>)	<i>z_i</i> %	<i>M_i</i>	<i>z_iM_i</i>
1	0.677878	2.4228	98.55	2.38767
2	1.059051	2.8921	135.84	3.92863
3	2.470516	1.2852	206.65	2.65586
4	9.567521	0.2367	319.83	0.75704
5	82.583950	0.0132	500.00	0.06600
				Σ = 9.7952

Step 8 Calculate the molecular weight of C₇₊ from equation (2–100), to give

$$M_{C_{7+}}^* = \sum_{n=7}^N \left(\frac{z_n}{z_{C_{7+}}} \right) M_n = \frac{9.7952}{0.0685} = 143$$

with identical match of the measured value.

Step 9 Calculate the specific gravity of first four fractions from

$$\gamma_i = 6.0108 \left[\frac{M_i^{0.17947}}{K_w^{1.18241}} \right] = 6.0108 \left[\frac{M_i^{0.17947}}{11.75^{1.18241}} \right]$$

which produces the following results.

<i>i</i>	<i>z_i</i> %	<i>M_i</i>	<i>γ_i</i>
1	2.4228	98.55	0.7439
2	2.8921	135.84	0.7880
3	1.2852	206.65	0.8496
4	0.2367	319.83	0.9189
5	0.0132	500.00	0.9377

Whitson and Brule indicated that, when characterizing multiple samples simultaneously, the values of *M_N*, *η*, and β* must be the same for all samples. Individual sample values of *M_{C₇₊}* and α, however, can be different. The result of this characterization is one set of molecular weights for the C₇₊ fractions, while each sample has different mole fractions *z_i* (so that their average molecular weights *M_{C₇₊}* are honored).

Lumping Schemes

Equations-of-state calculations frequently are burdened by the large number of components necessary to describe the hydrocarbon mixture for accurate phase-behavior modeling. Often, the problem is either lumping together the many experimental determined fractions or modeling the hydrocarbon system when the only experimental data available for the C₇₊ fraction are the molecular weight and specific gravity.

Generally, with a sufficiently large number of pseudo components used in characterizing the heavy fraction of a hydrocarbon mixture, a satisfactory prediction of the PVT behavior by the equation of state can be obtained. However, in compositional models, the cost and computing time can increase significantly with the increased number of components in the system. Therefore, strict limitations are set on the maximum number of components that can be used in compositional models and the original components have to be lumped into a smaller number of pseudo components.

The term *lumping* or *pseudoization* then denotes the reduction in the number of components used in equations-of-state calculations for reservoir fluids. This reduction is accomplished by employing the concept of the pseudo component. The pseudo component denotes a group of pure components lumped together and represented by a single component with a single carbon number (SCN).

Essentially, two main problems are associated with “regrouping” the original components into a smaller number without losing the predicting power of the equation of state:

1. How to select the groups of pure components to be represented by one pseudo component each.
2. What mixing rules should be used for determining the physical properties (e.g., p_c , T_c , M , γ , and ω) for the new lumped pseudo components.

Several unique published techniques can be used to address these lumping problems, notably the methods proposed by

- Lee et al. (1979).
- Whitson (1980).
- Mehra, Heidemann, and Aziz (1980).
- Montel and Gouel (1984).
- Schlijper (1984).
- Behrens and Sandler (1986).
- Gonzalez, Colonomos, and Rusinek (1986).

Several of these techniques are presented in the following discussion.

Whitson's Lumping Scheme

Whitson (1980) proposed a regrouping scheme whereby the compositional distribution of the C_{7+} fraction is reduced to only a few multiple carbon number (MCN) groups. Whitson suggested that the number of MCN groups necessary to describe the plus fraction is given by the following empirical rule:

$$N_g = \text{Int}[1 + 3.3 \log(N - n)] \quad (2-101)$$

where

N_g = number of MCN groups

Int = integer

N = number of carbon atoms of the last component in the hydrocarbon system

n = number of carbon atoms of the first component in the plus fraction, that is, $n = 7$ for C_{7+}

The integer function requires that the real expression evaluated inside the brackets be rounded to the nearest integer.

The molecular weights separating each MCN group are calculated from the following expression:

$$M_I = M_{C_7} \left(\frac{M_{N+}}{M_{C_7}} \right)^{I/N_g} \tag{2-102}$$

where

$(M)_{N+}$ = molecular weight of the last reported component in the extended analysis of the hydrocarbon system

M_{C_7} = molecular weight of C_7

$I = 1, 2, \dots, N_g$

For example, components with molecular weight of hydrocarbon groups M_{I-1} to M_I falling within the boundaries of these molecular weight values are included in the I th MCN group. Example 2-15 illustrates the use of equations (2-101) and (2-102).

EXAMPLE 2-15

Given the following compositional analysis of the C_{7+} fraction in a condensate system, determine the appropriate number of pseudo components forming in the C_{7+} :

COMPONENT	z_i
C_7	0.00347
C_8	0.00268
C_9	0.00207
C_{10}	0.001596
C_{11}	0.00123
C_{12}	0.00095
C_{13}	0.00073
C_{14}	0.000566
C_{15}	0.000437
C_{16+}	0.001671
M_{16+}	259

SOLUTION

Step 1 Determine the molecular weight of each component in the system:

COMPONENT	z_i	M_i
C_7	0.00347	96
C_8	0.00268	107
C_9	0.00207	121
C_{10}	0.001596	134
C_{11}	0.00123	147
C_{12}	0.00095	161
C_{13}	0.00073	175
C_{14}	0.000566	190
C_{15}	0.000437	206
C_{16+}	0.001671	259

Step 2 Calculate the number of pseudo components from equation (2–102).

$$N_g = \text{Int}[1 + 3.3 \log(16 - 7)]$$

$$N_g = \text{Int}[4.15]$$

$$N_g = 4$$

Step 3 Determine the molecular weights separating the hydrocarbon groups by applying equation (2–109).

$$M_I = 96 \left[\frac{259}{96} \right]^{1/4}$$

$$M_I = 96[2.698]^{1/4}$$

where the values for each pseudo component, when $M_I = 96[2.698]^{1/4}$, are

Pseudo component 1 = 123

Pseudo component 2 = 158

Pseudo component 3 = 202

Pseudo component 4 = 259

These are defined as:

Pseudo component 1 The first pseudo component includes all components with molecular weight in the range of 96 to 123. This group then includes C₇, C₈, and C₉.

Pseudo component 2 The second pseudo component contains all components with a molecular weight higher than 123 to a molecular weight of 158. This group includes C₁₀ and C₁₁.

Pseudo component 3 The third pseudo component includes components with a molecular weight higher than 158 to a molecular weight of 202. Therefore, this group includes C₁₂, C₁₃, and C₁₄.

Pseudo component 4 This pseudo component includes all the remaining components, that is, C₁₅ and C₁₆₊.

These are summarized below.

Group I	Component	z_i	z_I
1	C ₇	0.00347	0.00822
	C ₈	0.00268	
	C ₉	0.00207	
2	C ₁₀	0.001596	0.002826
	C ₁₁	0.00123	
3	C ₁₂	0.00095	0.002246
	C ₁₃	0.00073	
	C ₁₄	0.000566	
4	C ₁₅	0.000437	0.002108
	C ₁₆₊	0.001671	

It is convenient at this stage to present the mixing rules that can be employed to characterize the pseudo component in terms of its pseudo-physical and pseudo-critical properties.

Since the properties of the individual components can be mixed in numerous ways, each giving different properties for the pseudo components, the choice of a correct mixing rule is as important as the lumping scheme. Some of these mixing rules are given next.

Hong's Mixing Rules

Hong (1982) concluded that the weight fraction average, w_p , is the best mixing parameter in characterizing the C_{7+} fractions by the following mixing rules.

Defining the normalized weight fraction of a component, i , within the set of the lumped fraction, that is, $i \in L$, as

$$w_i^* = \frac{z_i M_i}{\sum_{i \in L} z_i M_i}$$

The proposed mixing rules are

$$\text{Pseudo-critical pressure } P_{cL} = \sum_{i \in L} w_i^* p_{ci}$$

$$\text{Pseudo-critical temperature } T_{cL} = \sum_{i \in L} w_i^* T_{ci}$$

$$\text{Pseudo-critical volume } V_{cL} = \sum_{i \in L} w_i^* V_{ci}$$

$$\text{Pseudo-acentric factor } \omega_L = \sum_{i \in L} w_i^* \omega_i$$

$$\text{Pseudo-molecular weight } M_L = \sum_{i \in L} w_i^* M_i$$

$$\text{Binary interaction coefficient } k_{kL} = 1 - \sum_{i \in L} \sum_{j \in L} w_i^* w_j^* (1 - k_{ij})$$

where

w_i^* = normalized weight fraction of component i in the lumped set

k_{kL} = binary interaction coefficient between the k th component and the lumped fraction

The subscript L in this relationship denotes the lumped fraction.

Lee's Mixing Rules

Lee et al. (1979), in their proposed regrouping model, employed Kay's mixing rules as the characterizing approach for determining the properties of the lumped fractions. Defining the normalized mole fraction of a component, i , within the set of the lumped fraction, that is $i \in L$, as

$$z_i^* = \frac{z_i}{\sum_{i \in L} z_i}$$

The following rules are proposed:

$$M_L = \sum_{i \in L}^L z_i^* M_i \quad (2-103)$$

$$\gamma_L = M_L / \sum_{i \in L}^L [z_i^* M_i / \gamma_i] \quad (2-104)$$

$$V_{cL} = \sum_{i \in L}^L [z_i^* M_i V_{ci} / M_L] \quad (2-105)$$

$$p_{cL} = \sum_{i \in L}^L [z_i^* p_{ci}] \quad (2-106)$$

$$T_{cL} = \sum_{i \in L}^L [z_i^* T_{ci}] \quad (2-107)$$

$$\omega_L = \sum_{i \in L}^L [z_i^* \omega_i] \quad (2-108)$$

EXAMPLE 2-16

Using Lee's mixing rules, determine the physical and critical properties of the four pseudo components in Example 2-15.

SOLUTION

Step 1 Assign the appropriate physical and critical properties to each component, as shown below.

Group	Comp.	z_i	z_I	M_i	γ_i	V_{ci}	p_{ci}	T_{ci}	ω_i
1	C ₇	0.00347	0.00822	96*	0.272*	0.06289*	453*	985*	0.280*
	C ₈	0.00268		107	0.749	0.06264	419	1,036	0.312
	C ₉	0.00207		121	0.768	0.06258	383	1,058	0.348
2	C ₁₀	0.001596	0.002826	134	0.782	0.06273	351	1,128	0.385
	C ₁₁	0.00123		147	0.793	0.06291	325	1,166	0.419
3	C ₁₂	0.00095	0.002246	161	0.804	0.06306	302	1,203	0.454
	C ₁₃	0.00073		175	0.815	0.06311	286	1,236	0.484
	C ₁₄	0.000566		190	0.826	0.06316	270	1,270	0.516
4	C ₁₅	0.000437	0.002108	206	0.826	0.06325	255	1,304	0.550
	C ₁₆₊	0.001671		259	0.908	0.0638**	215**	1,467	0.68**

*From Table 2-1.

**Calculated.

Step 2 Calculate the physical and critical properties of each group by applying equations (2-103) through (2-108) to give the results below.

Group	z_I	M_L	γ_L	V_{cL}	p_{cL}	T_{cL}	ω_L
1	0.00822	105.9	0.746	0.0627	424	1020	0.3076
2	0.002826	139.7	0.787	0.0628	339.7	1144.5	0.4000
3	0.002246	172.9	0.814	0.0631	288	1230.6	0.4794
4	0.002108	248	0.892	0.0637	223.3	1433	0.6531

Behrens and Sandler’s Lumping Scheme

Behrens and Sandler (1986) used the semicontinuous thermodynamic distribution theory to model the C_{7+} fraction for equation-of-state calculations. The authors suggested that the heptanes-plus fraction can be fully described with as few as two pseudo components.

A semicontinuous fluid mixture is defined as one in which the mole fractions of some components, such as C_1 through C_6 , have discrete values, while the concentrations of others, the unidentifiable components such as C_{7+} , are described as a *continuous distribution function*, $F(I)$. This continuous distribution function $F(I)$ describes the heavy fractions according to the index I , chosen to be a property of individual components, such as the carbon number, boiling point, or molecular weight.

For a hydrocarbon system with k discrete components, the following relationship applies:

$$\sum_{i=1}^{C_6} z_i + z_{7+} = 1.0$$

The mole fraction of C_{7+} in this equation is replaced with the selected distribution function, to give

$$\sum_{i=1}^{C_6} z_i + \int_A^B F(I)dI = 1.0 \tag{2-109}$$

where

- A = lower limit of integration (beginning of the continuous distribution, e.g., C_7)
- B = upper limit of integration (upper cutoff of the continuous distribution, e.g., C_{45})

This molar distribution behavior is shown schematically in Figure 2–10. The figure shows a semilog plot of the composition z_i versus the carbon number n of the individual components in a hydrocarbon system. The parameter A can be determined from the plot or defaulted to C_7 ; that is, $A = 7$. The value of the second parameter, B , ranges from 50 to

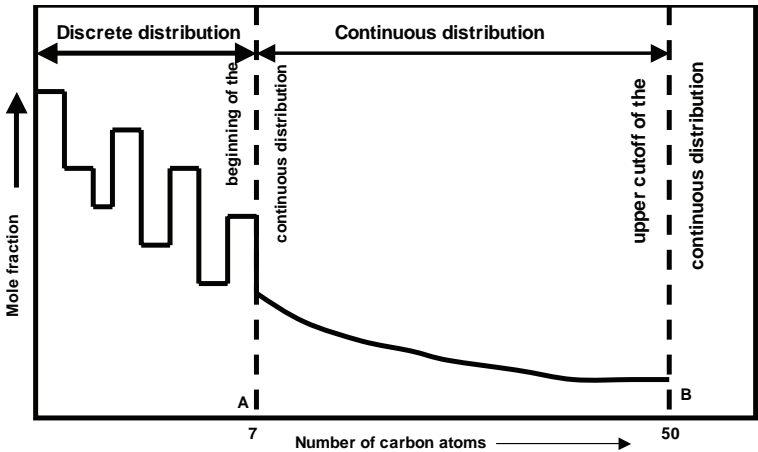


FIGURE 2–10 Schematic illustration of the semi-continuous distribution model.

infinity; that is, $50 \leq B \leq \infty$; however, Behrens and Sandler pointed out that the exact choice of the cutoff is not critical.

Selecting the index, I , of the distribution function $F(I)$ to be the carbon number, n , Behrens and Sandler proposed the following exponential form of $F(I)$:

$$F(n) = D(n) e^{\alpha n} \quad (2-110)$$

with

$$A \leq n \leq B$$

in which the parameter α is given by the following function $f(\alpha)$:

$$f(\alpha) = \frac{1}{\alpha} - \bar{c}_n + A - \frac{[A - B] e^{-B\alpha}}{e^{-A\alpha} - e^{-B\alpha}} = 0 \quad (2-111)$$

where \bar{c}_n is the average carbon number as defined by the relationship

$$\bar{c}_n = \frac{M_{C_{7+}} + 4}{14} \quad (2-112)$$

Equation (2-111) can be solved for α iteratively by using the method of successive substitutions or the Newton-Raphson method, with an initial value of α as

$$\alpha = [1/\bar{c}_n] - A$$

Substituting equation (2-112) into equation (2-111) yields

$$\sum_i^{C_6} z_i + \int_A^B D(n) e^{-\alpha n} dn = 1.0$$

or

$$z_{7+} = \int_A^B D(n) e^{-\alpha n} dn$$

By a transformation of variables and changing the range of integration from A and B to 0 and c , the equation becomes

$$z_{7+} = \int_0^c D(r) e^{-r} dr \quad (2-113)$$

where

$$c = (B - A)\alpha \quad (2-114)$$

r = dummy variable of integration

The authors applied the "Gaussian quadrature numerical integration method" with a two-point integration to evaluate equation (2-113), resulting in

$$z_{7+} = \sum_{i=1}^2 D(r_i) w_i = D(r_1) w_1 + D(r_2) w_2 \quad (2-115)$$

where r_i = roots for quadrature of integrals after variable transformation and w_i = weighting factor of Gaussian quadrature at point i . The values of r_1 , r_2 , w_1 , and w_2 are given in Table 2-7.

TABLE 2-7 *Behrens and Sandler Roots and Weights for Two-Point Integration*

c	r_1	r_2	w_1	w_2	c	r_1	r_2	w_1	w_2
0.30	0.0615	0.2347	0.5324	0.4676	4.40	0.4869	2.5954	0.7826	0.2174
0.40	0.0795	0.3101	0.5353	0.4647	4.50	0.4914	2.6304	0.7858	0.2142
0.50	0.0977	0.3857	0.5431	0.4569	4.60	0.4957	2.6643	0.7890	0.2110
0.60	0.1155	0.4607	0.5518	0.4482	4.70	0.4998	2.6971	0.7920	0.2080
0.70	0.1326	0.5347	0.5601	0.4399	4.80	0.5038	2.7289	0.7949	0.2051
0.80	0.1492	0.6082	0.5685	0.4315	4.90	0.5076	2.7596	0.7977	0.2023
0.90	0.1652	0.6807	0.5767	0.4233	5.00	0.5112	2.7893	0.8003	0.1997
1.00	0.1808	0.7524	0.5849	0.4151	5.10	0.5148	2.8179	0.8029	0.1971
1.10	0.1959	0.8233	0.5932	0.4068	5.20	0.5181	2.8456	0.8054	0.1946
1.20	0.2104	0.8933	0.6011	0.3989	5.30	0.5214	2.8722	0.8077	0.1923
1.30	0.2245	0.9625	0.6091	0.3909	5.40	0.5245	2.8979	0.8100	0.1900
1.40	0.2381	1.0307	0.6169	0.3831	5.50	0.5274	2.9226	0.8121	0.1879
1.50	0.2512	1.0980	0.6245	0.3755	5.60	0.5303	2.9464	0.8142	0.1858
1.60	0.2639	1.1644	0.6321	0.3679	5.70	0.5330	2.9693	0.8162	0.1838
1.70	0.2763	1.2299	0.6395	0.3605	5.80	0.5356	2.9913	0.8181	0.1819
1.80	0.2881	1.2944	0.6468	0.3532	5.90	0.5381	3.0124	0.8199	0.1801
1.90	0.2996	1.3579	0.6539	0.3461	6.00	0.5405	3.0327	0.8216	0.1784
2.00	0.3107	1.4204	0.6610	0.3390	6.20	0.5450	3.0707	0.8248	0.1754
2.10	0.3215	1.4819	0.6678	0.3322	6.40	0.5491	3.1056	0.8278	0.1722
2.20	0.3318	1.5424	0.6745	0.3255	6.60	0.5528	3.1375	0.8305	0.1695
2.30	0.3418	1.6018	0.6810	0.3190	6.80	0.5562	3.1686	0.8329	0.1671
2.40	0.3515	1.6602	0.6874	0.3126	7.00	0.5593	3.1930	0.8351	0.1649
2.50	0.3608	1.7175	0.6937	0.3063	7.20	0.5621	3.2170	0.8371	0.1629
2.60	0.3699	1.7738	0.6997	0.3003	7.40	0.5646	3.2388	0.8389	0.1611
2.70	0.3786	1.8289	0.7056	0.2944	7.70	0.5680	3.2674	0.8413	0.1587
2.80	0.3870	1.8830	0.7114	0.2886	8.10	0.5717	3.2992	0.8439	0.1561
2.90	0.3951	1.9360	0.7170	0.2830	8.50	0.5748	3.3247	0.8460	0.1540
3.00	0.4029	1.9878	0.7224	0.2776	9.00	0.5777	3.3494	0.8480	0.1520
3.10	0.4104	2.0386	0.7277	0.2723	10.00	0.5816	3.3811	0.8507	0.1493
3.20	0.4177	2.0882	0.7328	0.2672	11.00	0.5836	3.3978	0.8521	0.1479
3.30	0.4247	2.1367	0.7378	0.2622	12.00	0.5847	3.4063	0.8529	0.1471
3.40	0.4315	2.1840	0.7426	0.2574	14.00	0.5856	3.4125	0.8534	0.1466
3.50	0.4380	2.2303	0.7472	0.2528	16.00	0.5857	3.4139	0.8535	0.1465
3.60	0.4443	2.2754	0.7517	0.2483	18.00	0.5858	3.4141	0.8536	0.1464
3.70	0.4504	2.3193	0.7561	0.2439	20.00	0.5858	3.4142	0.8536	0.1464
3.80	0.4562	2.3621	0.7603	0.2397	25.00	0.5858	3.4142	0.8536	0.1464
3.90	0.4618	2.4038	0.7644	0.2356	30.00	0.5858	3.4142	0.8536	0.1464
4.00	0.4672	2.4444	0.7683	0.2317	40.00	0.5858	3.4142	0.8536	0.1464
4.10	0.4724	2.4838	0.7721	0.2279	60.00	0.5858	3.4142	0.8536	0.1464
4.20	0.4775	2.5221	0.7757	0.2243	100.00	0.5858	3.4142	0.8536	0.1464
4.30	0.4823	2.5593	0.7792	0.2208	∞	0.5858	3.4142	0.8536	0.1464

The computational sequences of the proposed method are summarized in the following steps.

Step 1 Find the endpoints A and B of the distribution. Since the endpoints are assumed to start and end at the midpoint between the two carbon numbers, the effective endpoints become

$$A = (\text{starting carbon number}) - 0.5 \quad (2-116)$$

$$B = (\text{ending carbon number}) + 0.5 \quad (2-117)$$

Step 2 Calculate the value of the parameter α by solving equation (2-111) iteratively.

Step 3 Determine the upper limit of integration c by applying equation (2-114).

Step 4 Find the integration points r_1 and r_2 and the weighting factors w_1 and w_2 from Table 2-7.

Step 5 Find the pseudo-component carbon numbers, n_p , and mole fractions, z_p , from the following expressions.

For the first pseudo component,

$$n_1 = \frac{r_1}{\alpha} + A$$

$$z_1 = w_1 z_{7+} \quad (2-118)$$

For the second pseudo component,

$$n_2 = \frac{r_2}{\alpha} + A$$

$$z_2 = w_2 z_{7+} \quad (2-119)$$

Step 6 Assign the physical and critical properties of the two pseudo components from Table 2-1.

EXAMPLE 2-17

A heptanes-plus fraction in a crude oil system has a mole fraction of 0.4608 with a molecular weight of 226. Using the Behrens and Sandler lumping scheme, characterize the C_{7+} by two pseudo components and calculate their mole fractions.

SOLUTION

Step 1 Assuming the starting and ending carbon numbers to be C_7 and C_{50} , calculate A and B from equations (2-116) and (2-117):

$$A = (\text{starting carbon number}) - 0.5$$

$$A = 7 - 0.5 = 6.5$$

$$B = (\text{ending carbon number}) + 0.5$$

$$B = 50 + 0.5 = 50.5$$

Step 2 Calculate \bar{c}_n from equation (2-112):

$$\bar{c}_n = \frac{M_{C_{7+}} + 4}{14}$$

$$\bar{c}_n = \frac{226 + 4}{14} = 16.43$$

Step 3 Solve equation (2-111) iteratively for α , to give

$$\frac{1}{\alpha} - \bar{c}_n + A - \frac{[A - B]e^{-B\alpha}}{e^{-A\alpha} - e^{-Ba}} = 0$$

$$\frac{1}{\alpha} - 16.43 + 6.5 - \frac{[6.5 - 50.5]e^{-50.5\alpha}}{e^{-6.5\alpha} - e^{-50.5\alpha}} = 0$$

Solving this expression iteratively for α gives $\alpha = 0.0938967$.

Step 4 Calculate the range of integration c from equation (2-114):

$$c = (B - A)\alpha$$

$$c = (50.5 - 6.5)0.0938967 = 4.13$$

Step 5 Find integration points r_i and weights w_i from Table 2-7:

$$r_1 = 0.4741$$

$$r_2 = 2.4965$$

$$w_1 = 0.7733$$

$$w_2 = 0.2267$$

Step 6 Find the pseudo-component carbon numbers n_i and mole fractions z_i by applying equations (2-118) and (2-119).

For the first pseudo component,

$$n_1 = \frac{r_1}{\alpha} + A$$

$$n_1 = \frac{0.4741}{0.0938967} + 6.5 = 11.55$$

$$z_1 = w_1 z_{7+}$$

$$z_1 = (0.7733)(0.4608) = 0.3563$$

For the second pseudo component,

$$n_2 = \frac{r_2}{\alpha} + A$$

$$n_2 = \frac{2.4965}{0.0938967} + 6.5 = 33.08$$

$$z_2 = w_2 z_{7+}$$

$$z_2 = (0.2267)(0.4608) = 0.1045$$

The C_{7+} fraction is represented then by the two pseudo components below.

Pseudo Component	Carbon Number	Mole Fraction
1	$C_{11.55}$	0.3563
2	$C_{33.08}$	0.1045

Step 7 Assign the physical properties of the two pseudo components according to their number of carbon atoms using the Katz and Firoozabadi generalized physical properties as given in Table 2-1 or by calculations from equation (2-6). The assigned physical properties for the two fractions are shown below.

Pseudo Component	n	T_b , °R	γ	M	T_c , °R	p_c , psia	ω
1	11.55	848	0.799	154	1185	314	0.437
2	33.08	1341	0.915	426	1629	134	0.921

Lee's Lumping Scheme

Lee et al. (1979) devised a simple procedure for regrouping the oil fractions into pseudo components. Lee and coworkers employed the physical reasoning that crude oil fractions having relatively close physico-chemical properties (such as molecular weight and specific gravity) can be accurately represented by a single fraction. Having observed that the closeness of these properties is reflected by the slopes of curves when the properties are plotted against the weight-averaged boiling point of each fraction, Lee et al. used the weighted sum of the slopes of these curves as a criterion for lumping the crude oil fractions. The authors proposed the following computational steps.

Step 1 Plot the available physico-chemical properties of each original fraction versus its weight-averaged boiling point.

Step 2 Calculate numerically the slope m_{ij} for each fraction at each WABP, where

m_{ij} = slope of the property curve versus boiling point

$i = 1, \dots, n_f$

$j = 1, \dots, n_p$

n_f = number of original oil fractions

n_p = number of available physico-chemical properties

Step 3 Compute the normalized absolute slope \bar{m}_{ij} as defined:

$$\bar{m}_{ij} = \frac{m_{ij}}{\max_{i=1, \dots, n_f} m_{ij}} \quad (2-120)$$

Step 4 Compute the weighted sum of slopes \bar{M}_i for each fraction as follows:

$$\bar{M}_i = \frac{\sum_{j=1}^{n_p} \bar{m}_{ij}}{n_p} \quad (2-121)$$

where \bar{M}_i represents the averaged change of physico-chemical properties of the crude oil fractions along the boiling-point axis.

Step 5 Judging the numerical values of \bar{M}_i for each fraction, group those fractions that have similar \bar{M}_i values.

Step 6 Using the mixing rules given by equations (2-103) through (2-108), calculate the physical properties of pseudo components.

EXAMPLE 2-18

The data in Table 2-8, as given by Hariu and Sage (1969), represent the average boiling point molecular weight, specific gravity, and molar distribution of 15 pseudo components in a crude oil system.

SOLUTION

Step 1 Plot the molecular weights and specific gravities versus the boiling points and calculate the slope m_{ij} for each pseudo component as in the following table.

Pseudo Component	T_b	$m_{i1} = \partial M / \partial T_b$	$m_{i2} = \partial \gamma / \partial T_b$
1	-600	0.1111	0.00056
2	-654	0.1327	0.00053
3	-698	0.1923	0.00051
4	-732	0.2500	0.00049
5	-770	0.3026	0.00041
6	-808	0.3457	0.00032
7	-851	0.3908	0.00022
8	-895	0.4253	0.00038
9	-938	0.4773	0.00041
10	-983	0.5000	0.00021
11	1052	0.6257	0.00027
12	1154	0.8146	0.00029
13	1257	0.9561	0.00025
14	1382	1.0071	0.00023
15	1540	1.0127	0.00022

Step 2 Calculate the normalized absolute slope m_{ij} and the weighted sum of slopes \bar{M}_i using equations (2-121) and (2-122), respectively. This is shown in Table 2-9. Note that the maximum of value of m_{i1} is 1.0127 and for m_{i2} is 0.00056.

Examining the values of \bar{M}_i , the pseudo components can be lumped into three groups:

- Group 1 Combine fractions 1-5 with a *total* mole fraction of 0.3403.
- Group 2 Combine fractions 6-10 with a *total* mole fraction of 0.2880.
- Group 3 Combine fractions 11-15 with a *total* mole fraction of 0.2805.

TABLE 2-8 Characteristics of Pseudo Components in Example 2-18

Pseudo Component	$T_b, ^\circ\text{R}$	M	γ	z_i
1	600	95	0.680	0.0681
2	654	101	0.710	0.0686
3	698	108	0.732	0.0662
4	732	116	0.750	0.0631
5	770	126	0.767	0.0743
6	808	139	0.781	0.0686
7	851	154	0.793	0.0628
8	895	173	0.800	0.0564
9	938	191	0.826	0.0528
10	983	215	0.836	0.0474
11	1052	248	0.850	0.0836
12	1154	322	0.883	0.0669
13	1257	415	0.910	0.0535
14	1382	540	0.940	0.0425
15	1540	700	0.975	0.0340

TABLE 2-9 Absolute Slope m_{ij} and Weighted Slopes \bar{M}_i

Pseudo Component	$\bar{m}_{i1} = m_{ij}/1.0127$	$\bar{m}_{i2} = m_{ij}/0.00056$	$\bar{M}_i = (\bar{m}_{i1} + \bar{m}_{i2})/2$
1	0.1097	1.0000	0.55485
2	0.1310	0.9464	0.53870
3	0.1899	0.9107	0.55030
4	0.2469	0.8750	0.56100
5	0.2988	0.7321	0.51550
6	0.3414	0.5714	0.45640
7	0.3859	0.3929	0.38940
8	0.4200	0.6786	0.54930
9	0.4713	0.7321	0.60170
10	0.4937	0.3750	0.43440
11	0.6179	0.4821	0.55000
12	0.8044	0.5179	0.66120
13	0.9441	0.4464	0.69530
14	0.9945	0.4107	0.70260
15	1.0000	0.3929	0.69650

Step 3 Calculate the physical properties of each group. This can be achieved by computing M and γ of each group by applying equations (2-103) and (2-104), respectively, followed by employing the Riazi-Daubert correlation (equation 2-6) to characterize each group. Results of the calculations are shown below.

Group I	Mole Fraction, z_i	M	γ	T_b	T_c	p_c	V_c
1	0.3403	109.4	0.7299	694	1019	404	0.0637
2	0.2880	171.0	0.8073	891	1224	287	0.0634
3	0.2805	396.5	0.9115	1383	1656	137	0.0656

The physical properties M , γ , and T_b reflect the chemical makeup of petroleum fractions. Some of the methods used to characterize the pseudo components in terms of their boiling point and specific gravity assume that a particular factor, called the *characterization factor*, C_f , is constant for all the fractions that constitute the C_{7+} . Soreide (1989) developed an accurate correlation for determining the specific gravity based on the analysis of 843 TBP fractions from 68 reservoir C_{7+} samples and introduced the characterization factor, C_f , into the correlation, as given by the following relationship:

$$\gamma_i = 0.2855 + C_f(M_i - 66)^{0.13} \quad (2-122)$$

Characterization factor C_f is adjusted to satisfy the following relationship:

$$(\gamma_{C_{7+}})_{\text{exp}} = \frac{z_{C_{7+}} M_{C_{7+}}}{\sum_{i=C_7}^{C_{N+}} \left[\frac{z_i M_i}{\gamma_i} \right]} \quad (2-123)$$

where $(\gamma_{C_{7+}})_{\text{exp}}$ is the measured specific gravity of the C_{7+} . Combining equation (2-122) with (2-123) gives

$$(\gamma_{C_{7+}})_{\text{exp}} = \frac{z_{C_{7+}} M_{C_{7+}}}{\sum_{i=C_7}^{C_{N+}} \left[\frac{z_i M_i}{0.2855 + C_f (M_i - 66)^{0.13}} \right]}$$

Rearranging,

$$f(C_f) = \sum_{i=C_7}^{C_{N+}} \left[\frac{z_i M_i}{0.2855 + C_f (M_i - 66)^{0.13}} \right] - \frac{z_{C_{7+}} M_{C_{7+}}}{(\gamma_{C_{7+}})_{\text{exp}}} = 0 \tag{2-124}$$

The optimum value of the characterization factor can be determined iteratively by solving this expression for C_f . The Newton-Raphson method is an efficient numerical technique that can be used conveniently to solve the preceding nonlinear equation by employing the relationship

$$C_f^{n+1} = C_f^n - \frac{f(C_f^n)}{\partial f(C_f^n) / \partial C_f^n}$$

with

$$\frac{\partial f(C_f^n)}{\partial C_f^n} = \sum_{i=C_7}^{C_{N+}} \left[\frac{-(M_i - 66)^{0.13}}{\left(0.2855 + C_f^n (M_i - 66)^{0.13} \right)^2} \right]$$

The method is based on assuming a starting value C_f^n and calculating an improved value C_f^{n+1} that can be used in the second iteration. The iteration process continues until the difference between the two, C_f^{n+1} and C_f^n , is small, say, 10^{-6} . The calculated value of C_f then can be used in equation (2-122) to determine specific gravity of any pseudo component γ_i .

Soreide also developed the following boiling-point temperature, T_b , correlation, which is a function of the molecular weight and specific gravity of the fraction:

$$T_b = 1928.3 - \frac{1.695(10^5) A \gamma^{3.266}}{M^{0.03522}}$$

with

$$A = \exp[0.003462 M \gamma - 0.004922 M - 4.7685 \gamma]$$

where T_b = boiling point temperature, °R, and M = molecular weight.

EXAMPLE 2-19

The molar distribution of a heptanes plus, as given by Whitson and Brule, is listed below, where $M_{C_{7+}} = 143$ and $(\gamma_{C_{7+}})_{\text{exp}} = 0.795$. Calculate the specific gravity of the five pseudo components.

C_{7+} Fraction, i	Mole Fraction, z_i	Molecular Weight, M_i
1	2.4228	95.55
2	2.8921	135.84
3	1.2852	296.65
4	0.2367	319.83
5	0.0132	500.00

SOLUTION

Step 1 Solve equation (2–124) for the characterization factor, C_f , by trial and error or Newton-Raphson method, to give

$$C_f = 0.26927$$

Step 2 Using equation (2–122), calculate the specific gravity of the five, shown in the following table, where

$$\gamma_i = 0.2855 + C_f(M_i - 66)^{0.13}$$

$$\gamma_i = 0.2855 + 0.26927(M_i - 66)^{0.13}$$

C_{7+} Fraction, i	Mole Fraction, z_i	Molecular Weight, M_i	Specific Gravity, $\gamma_i = 0.2855 + 0.26927(M_i - 66)^{0.13}$
1	2.4228	95.55	0.7407
2	2.8921	135.84	0.7879
3	1.2852	296.65	0.8358
4	0.2367	319.83	0.8796
5	0.0132	500.00	0.9226

Characterization of Multiple Hydrocarbon Samples

When characterizing multiple samples simultaneously for use in the equation-of-state applications, the following procedure is recommended:

1. Identify and select the *main* fluid sample among multiple samples from the same reservoir. In general, the sample that dominates the simulation process or has extensive laboratory data is chosen as the main sample.
2. Split the plus fractions of the main sample into several components using Whitson's method and determine the parameters M_N , η , and β^* , as outlined by equations (2–93) and (2–94).
3. Calculate the characterization factor, C_f , by solving equation (2–124) and calculate specific gravities of the C_{7+} fractions by using equation (2–122).
4. Lump the produced splitting fractions of the main sample into a number of pseudo components characterized by the physical properties p_c , T_c , M , γ , and ω .
5. Assign the gamma function parameters (M_N , η , and β^*) of the main sample to all the remaining samples; in addition, the characterization factor, C_f , must be the same for all mixtures. However, each sample can have a different $M_{C_{7+}}$ and α .
6. Using the same gamma function parameters of the main sample, split each of the remaining samples into a number of components.
7. For each of the remaining sample, group or lump the fractions into pseudo components with the condition that these pseudo components are lumped in a way to give similar or same molecular weights to those of the lumped fractions of the main sample.

The results of this characterization procedure are

- One set of molecular weights for the C_{7+} fractions.
- Each pseudo component has the same properties (i.e., M , γ , T_b , p_c , T_c , and ω) as those of the main sample but with a different mole fraction.

It should be pointed out that, when characterizing multiple samples, the outlier samples must be identified and treated separately. Assuming that these multiple samples are obtained from different depths and each is described by laboratory PVT measurements, the outlier samples can be identified by making the following plots:

- Saturation pressure versus depth.
- C_1 mol% versus depth.
- C_{7+} mol% versus depth.
- Molecular weight of C_{7+} versus depth.

Data deviating significantly from the general trend, as shown in Figures 2–11 through 2–14, should not be used in the multiple samples characterization procedure. Takahashi et al. (2002) point out that a single EOS model never predicts such outlier behavior using a common characterization. Also note that systematic deviation from a general trend may indicate a separate fluid system, requiring a separate equation-of-state model, while randomlike deviations from clear trends often are due to experimental data error or inconsistencies in reported compositional data as compared with the actual samples used in laboratory tests.

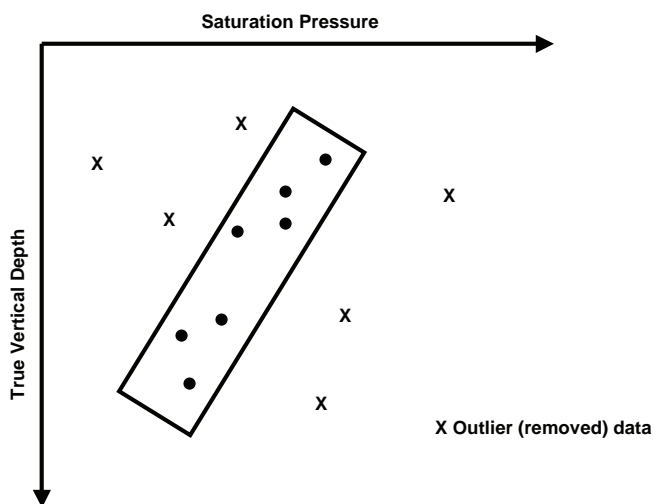


FIGURE 2-11 Measured saturation pressure versus depth.

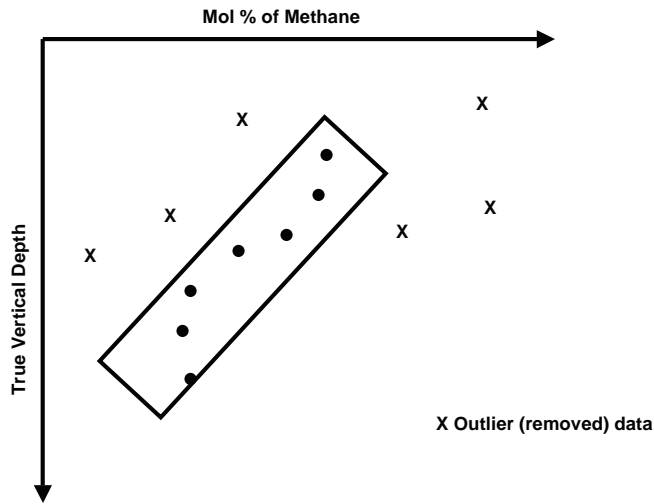


FIGURE 2-12 Measured methane content versus depth.

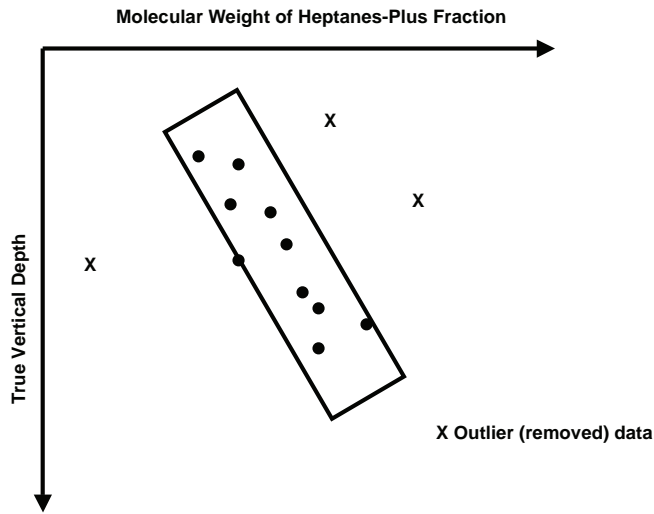


FIGURE 2-13 Measured C_{7+} molecular weight versus depth.

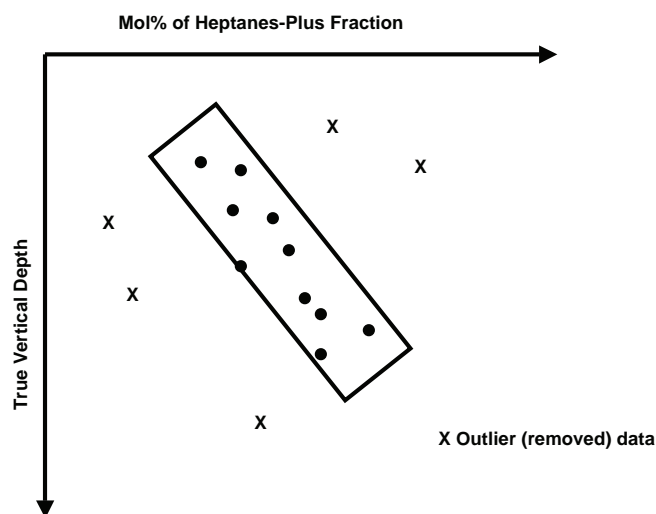


FIGURE 2-14 Measured mol% of C_{7+} versus depth.

Problems

- 1. A heptanes-plus fraction with a molecular weight of 198 and a specific gravity of 0.8135 presents a naturally-occurring condensate system. The reported mole fraction of the C_{7+} is 0.1145. Predict the molar distribution of the plus fraction using
 - a. Katz’s correlation.
 - b. Ahmed’s correlation.

Characterize the last fraction in the predicted extended analysis in terms of its physical and critical properties.

- 2. A naturally-occurring crude oil system has a heptanes-plus fraction with the following properties:

$M_{7+} = 213.0000$

$\gamma_{7+} = 0.8405$

$x_{7+} = 0.3497$

Extend the molar distribution of the plus fraction and determine the critical properties and acentric factor of the last component.

- 3. A crude oil system has the following composition:

COMPONENT	x_i
C_1	0.3100
C_2	0.1042
C_3	0.1187
C_4	0.0732
C_5	0.0441
C_6	0.0255
C_7	0.0571

COMPONENT	x_i
C ₈	0.0472
C ₉	0.0246
C ₁₀	0.0233
C ₁₁	0.0212
C ₁₂	0.0169
C ₁₃₊	0.1340

The molecular weight and specific gravity of C₁₃₊ are 325 and 0.842. Calculate the appropriate number of pseudo components necessary to adequately represent these components using

- Whitson's lumping method.
- Behrens-Sandler's method.

Characterize the resulting pseudo components in terms of their critical properties.

- If a petroleum fraction has a measured molecular weight of 190 and a specific gravity of 0.8762, characterize this fraction by calculating the boiling point, critical temperature, critical pressure, and critical volume of the fraction. Use Riazi-Daubert's correlation.
- Calculate the acentric factor and critical compressibility factor of the component in problem 4.
- A petroleum fraction has the following physical properties:
 $\text{API} = 50^\circ$
 $T_b = 400^\circ\text{F}$
 $M = 165$
 $\gamma = 0.79$
 Calculate p_c , T_c , V_c , ω , and Z_c using the following correlations:
 - Cavett.
 - Kesler-Lee.
 - Winn-Sim-Daubert.
 - Watansiri-Owens-Starling.
- An undefined petroleum fraction with 10 carbon atoms has a measured average boiling point of 791°R and a molecular weight of 134. If the specific gravity of the fraction is 0.78, determine the critical pressure, critical temperature, and acentric factor of the fraction using
 - Robinson-Peng's PNA method.
 - Bergman PNA's method.
 - Riazi-Daubert's method.
 - Cavett's correlation.
 - Kesler-Lee's correlation.
 - Willman-Teja's correlation.

8. A heptanes-plus fraction is characterized by a molecular weight of 200 and specific gravity of 0.810. Calculate p_c , T_c , T_b , and acentric factor of the plus fraction using
 - a. Riazi-Daubert's method.
 - b. Rowe's correlation.
 - c. Standing's correlation.
9. Using the data given in problem 8 and the boiling point as calculated by Riazi-Daubert's correlation, determine the critical properties and acentric factor employing
 - a. Cavett's correlation.
 - b. Kesler-Lee's correlation.Compare the results with those obtained in problem 8.

References

- Abramowitz, M., and J. Stegun. *Handbook of Mathematical Functions*. New York: Dover Publications, 1970.
- Ahmed, T. "Composition Modeling of Tyler and Mission Canyon Formation Oils with CO₂ and Lean Gasses." Final report submitted to Montanans on a New Track for Science (MONTs), Montana National Science Foundation Grant Program, 1985.
- Ahmed, T., G. Cady, and A. Story. "A Generalized Correlation for Characterizing the Hydrocarbon Heavy Fractions." Paper SPE 14266, presented at the 60th Annual Technical Conference of the Society of Petroleum Engineers, Las Vegas, September 22–25, 1985.
- Austad, T. "Practical Aspects of Characterizing Petroleum Fluids." Paper presented at the North Sea Condensate RTeserves, London, May 24–25, 1983.
- Behrens, R., and S. Sandler. "The Use of Semi-Continuous Description to Model the C₇₊ Fraction in Equation-of-State Calculation." Paper SPE/DOE 14925, presented at the Fifth Annual Symposium on EOR, held in Tulsa, OK, April 20–23, 1986.
- Bergman, D. F., M. R. Tek, and D. L. Katz. "Retrograde Condensation in Natural Gas Pipelines." Project PR 2-29 of Pipelines Research Committee, AGA, January 1977.
- Cavett, R. H. "Physical Data for Distillation Calculations—Vapor–Liquid Equilibrium." Proceedings of the 27th Meeting, API, San Francisco, 1962, pp. 351–366.
- Edmister, W. C. "Applied Hydrocarbon Thermodynamics, Part 4, Compressibility Factors and Equations of State." *Petroleum Refiner* 37 (April 1958): 173–179.
- Edmister, W. C., and B. I. Lee. *Applied Hydrocarbon Thermodynamics*, vol. 1. Houston: Gulf Publishing Company, 1984.
- Erbar, J. H., *Prediction of Absorber Oil K-Values and Enthalpies*. Research Report 13. Tulsa, OK: GPA, 1977.
- Gonzalez, E., P. Colonomos, and I. Rusinek. "A New Approach for Characterizing Oil Fractions and for Selecting Pseudo-Components of Hydrocarbons." *Canadian Journal of Petroleum Technology* (March–April 1986): 78–84.
- Hall, K. R., and L. Yarborough. "New Simple Correlation for Predicting Critical Volume." *Chemical Engineering* (November 1971): 76.
- Hariu, O., and R. Sage. "Crude Split Figured by Computer." *Hydrocarbon Processing* (April 1969): 143–148.
- Haugen, O. A., K. M. Watson, and R. A. Ragatz. *Chemical Process Principles*, 2nd ed. New York: Wiley, 1959, p. 577.
- Hong, K. S. "Lumped-Component Characterization of Crude Oils for Compositional Simulation." Paper SPE/DOE 10691, presented at the 3rd Joint Symposium on EOR, Tulsa, OK, April 4–7, 1982.

- Hopke, S. W., and C. J. Lin. "Application of BWRS Equation to Absorber Oil Systems." Proceedings 53rd Annual Convention GPA, Denver, CO, March 1974, pp. 63–71.
- Katz, D. "Overview of Phase Behavior of Oil and Gas Production." *Journal of Petroleum Technology* (June 1983): 1205–1214.
- Katz, D. L., and A. Firoozabadi. "Predicting Phase Behavior of Condensate/Crude-Oil Systems Using Methane Interaction Coefficients." *Journal of Petroleum Technology* (November 1978): 1649–1655.
- Kesler, M. G., and B. I. Lee. "Improve Prediction of Enthalpy of Fractions." *Hydrocarbon Processing* (March 1976): 153–158.
- Lee, S., et al., "Experimental and Theoretical Studies on the Fluid Properties Required for Simulation of Thermal Processes." Paper SPE 8393, presented at the 54th Annual Technical Conference of the Society of Petroleum Engineers, Las Vegas, September 23–26, 1979.
- Lohrenz, J., B. G. Bra, and C. R. Clark. "Calculating Viscosities of Reservoir Fluids from Their Compositions." *Journal of Petroleum Technology* (October 1964): 1171–1176.
- Maddox, R. N., and J. H. Erbar. *Gas Conditioning and Processing, Vol. 3: Advanced Techniques and Applications*. Norman, OK: Campbell Petroleum Series, 1982.
- Maddox, R., and J. H. Erbar. "A Statistical Approach for Combining Reservoir Fluids into Pseudo Components for Compositional Model Studies." Paper SPE 11201, presented at the 57th Annual Meeting of the SPE, New Orleans, September 26–29, 1983.
- Magoulas, S., and D. Tassios. *Predictions of Phase Behavior of HT-HP Reservoir Fluids*. Paper SPE no. 37294. Richardson, TX: Society of Petroleum Engineers, 1990.
- Matthews, T., C. Roland, and D. Katz. "High Pressure Gas Measurement." Proceedings of the Natural Gas Association of America (NGAA), 1942.
- Mehra, R. K., R. Heidemann, and K. Aziz. "Computation of Multi-Phase Equilibrium for Compositional Simulators." *Society of Petroleum Engineers Journal* (February 1980).
- Miquel, J., J. Hernandez, and F. Castells. "A New Method for Petroleum Fractions and Crude Oil Characterization." *SPE Reservoir Engineering* (May 1992): 265.
- Montel, F., and P. Gouel. "A New Lumping Scheme of Analytical Data for Composition Studies." Paper SPE 13119, presented at the 59th Annual Society of Petroleum Engineers Technical Conference, Houston, TX, September 16–19, 1984.
- Nath, J. "Acentric Factor and the Critical Volumes for Normal Fluids." *Industrial Engineering and Chemical. Fundamentals* 21, no. 3 (1985): 325–326.
- Pedersen, K., P. Thomassen, and A. Fredenslund. "Phase Equilibria and Separation Process." Report SEP 8207, Institute for Kemiteknik, Denmark Tekniske Højskole, July 1982.
- Reid, R., J. M. Prausnitz, and T. Sherwood. *The Properties of Gases and Liquids*, 3rd ed. New York: McGraw-Hill, 1977, p. 21.
- Riazi, M. R., and T. E. Daubert. "Simplify Property Predictions." *Hydrocarbon Processing* (March 1980): 115–116.
- Riazi, M. R., and T. E. Daubert. "Characterization Parameters for Petroleum Fractions." *Industrial Engineering and Chemical Research* 26, no. 24 (1987): 755–759.
- Robinson, D. B., and D. Y. Peng. "The Characterization of the Heptanes and Heavier Fractions." Research Report 28. Tulsa, OK: GPA, 1978.
- Rowe, A. M. "Internally Consistent Correlations for Predicting Phase Compositions for Use in Reservoir Compositional Simulators." Paper SPE 7475 presented at the 53rd Annual Society of Petroleum Engineers Fall Technical Conference and Exhibition, 1978.
- Salerno, S., et al. "Prediction of Vapor Pressures and Saturated Volumes." *Fluid Phase Equilibria* 27 (June 10, 1985): 15–34.
- Schlijper, A. G. "Simulation of Compositional Process: The Use of Pseudo-Components in Equation of State Calculations." Paper SPE/DOE 12633, presented at the SPE/DOE Fourth Symposium on EOR, Tulsa, OK, April 15–18, 1984.

- Silva, M. B., and F. Rodriguez. "Automatic Fitting of Equations of State for Phase Behavior Matching." Paper SPE 23703. Richardson, TX: Society of Petroleum Engineers, 1992.
- Sim, W. J., and T. E. Daubert. "Prediction of Vapor-Liquid Equilibria of Undefined Mixtures." *Ind. Eng. Chem. Process Des. Dev.* 19, no. 3 (1980): 380–393.
- Soreide, I. "Improved Phase Behavior Predictions of Petroleum Reservoir Fluids from a Cubic Equation of State." Doctor of Engineering dissertation, Norwegian Institute of Technology, Trondheim, 1989.
- Standing, M. B. *Volumetric and Phase Behavior of Oil Field Hydrocarbon Systems*. Dallas: Society of Petroleum Engineers, 1977.
- Takahashi, K., et al. *Fluid Characterization for Gas Injection Study Using Equilibrium Contact Mixing*. SPE paper 78483. Richardson, TX: Society of Petroleum Engineers, 2002.
- Twu, C. "An Internally Consistent Correlation for Predicting the Critical Properties and Molecular Weight of Petroleum and Coal-Tar Liquids." *Fluid Phase Equilibria*, no. 16 (1984): 137.
- Watansiri, S., V. H. Owens, and K. E. Starling. "Correlations for Estimating Critical Constants, Acentric Factor, and Dipole Moment for Undefined Coal-Fluid Fractions." *Ind. Eng. Chem. Process Des. Dev.* 24 (1985): 294–296.
- Watson, K. M., E. F. Nelson, and G. B. Murphy. "Characterization of Petroleum Fractions." *Ind. Eng. Chem.* 27 (1935): 1460.
- Whitson, C. "Characterizing Hydrocarbon-Plus Fractions." Paper EUR 183, presented at the European Offshore Petroleum Conference, London, October 21–24, 1980.
- Whitson, C. H. "Characterizing Hydrocarbon-Plus Fractions." *Society of Petroleum Engineers Journal* 275 (August 1983): 683; AIIME, 275.
- Whitson, C. H. "Effect of Physical Properties Estimation on Equation-of-State Predictions." *Society of Petroleum Engineers Journal* (Dec. 1984): 685–696.
- Whitson, C., T. Anderson, and J. Soreide. " C_{7+} Characteristics of Equilibrium Fluids Using the Gamma Distribution." In: *Advances in Thermodynamics*. New York: Taylor and Francis, 1989.
- Whitson, C. H., and M. R. Brule. *Phase Behavior*. Richardson, TX: Society of Petroleum Engineers, 2000.
- Willman, B., and A. Teja. "Prediction of Dew Points of Semicontinuous Natural Gas and Petroleum Mixtures." *Industrial Engineering and Chemical Research* 226, no. 5 (1987): 948–952.
- Winn, F. W. "Simplified Nomographic Presentation, Characterization of Petroleum Fractions." *Petroleum Refinery* 36, no. 2 (1957): 157.

3

Natural Gas Properties

LAWS THAT DESCRIBE the behavior of reservoir gases in terms of pressure, p , volume, V , and temperature, T , have been known for many years. These laws are relatively simple for a hypothetical fluid known as a *perfect* or *ideal gas*. This chapter reviews these laws and how they can be modified to describe the behavior of reservoir gases, which may deviate significantly from these simple laws.

Gas is defined as a homogeneous fluid of low viscosity and density, which has no definite volume but expands to completely fill the vessel in which it is placed. Generally, the natural gas is a mixture of hydrocarbon and nonhydrocarbon gases. The hydrocarbon gases normally found in a natural gas are methane, ethane, propane, butanes, pentanes, and small amounts of hexanes and heavier. The nonhydrocarbon gases, that is, impurities, include carbon dioxide, hydrogen sulfide, and nitrogen.

Knowledge of pressure-volume-temperature (PVT) relationships and other physical and chemical properties of gases are essential for solving problems in natural gas reservoir engineering. The properties of interest include

- Apparent molecular weight, M_a .
- Specific gravity, γ_g .
- Compressibility factor, Z .
- Gas density, ρ_g .
- Specific volume, v .
- Isothermal gas compressibility coefficient, c_g .
- Gas formation volume factor, B_g .
- Gas expansion factor, E_g .
- Viscosity, μ_g .

These gas properties may be obtained from direct laboratory measurements or by prediction from generalized mathematical expressions. This chapter reviews laws that describe the volumetric behavior of gases in terms of pressure and temperature and documents the mathematical correlations widely used in determining the physical properties of natural gases.

Behavior of Ideal Gases

The kinetic theory of gases postulates that the gas is composed of a very large number of particles called *molecules*. For an ideal gas, the volume of these molecules is insignificant compared with the total volume occupied by the gas. It is also assumed that these molecules have no attractive or repulsive forces between them, and it is assumed that all collisions of molecules are perfectly elastic.

Based on this kinetic theory of gases, a mathematical equation, called *equation of state*, can be derived to express the relationship existing between pressure, p , volume, V , and temperature, T , for a given quantity of moles of gas, n . This relationship for perfect gases, called the *ideal gas law*, is expressed mathematically by the following equation:

$$pV = nRT \quad (3-1)$$

where

p = absolute pressure, psia

V = volume, ft³

T = absolute temperature, °R

n = number of moles of gas, lb-mole

R = the universal gas constant that, for these units, has the value 10.73 psia ft³/lb-mole °R

The number of pound-moles of gas, that is, n , is defined as the weight of the gas, m , divided by the molecular weight, M , or

$$n = \frac{m}{M} \quad (3-2)$$

Combining equation (3-1) with (3-2) gives

$$pV = \left(\frac{m}{M} \right) RT \quad (3-3)$$

where

m = weight of gas, lb

M = molecular weight, lb/lb-mole

Since the density is defined as the mass per unit volume of the substance, equation (3-3) can be rearranged to estimate the gas density at any pressure and temperature:

$$\rho_g = \frac{m}{V} = \frac{pM}{RT} \quad (3-4)$$

where ρ_g = density of the gas, lb/ft³.

It should be pointed out that lb refers to *pounds mass* in all the subsequent discussions of density in this text.

EXAMPLE 3-1

Three pounds of n-butane are placed in a vessel at 120°F and 60 psia. Calculate the volume of the gas assuming an ideal gas behavior.

SOLUTION

Step 1 Determine the molecular weight of n-butane from Table 1-1 to give

$$M = 58.123$$

Step 2 Solve equation (3-3) for the volume of gas:

$$V = \left(\frac{m}{M} \right) \frac{RT}{p}$$

$$V = \left(\frac{3}{58.123} \right) \frac{(10.73)(120 + 460)}{60} = 5.35 \text{ ft}^3$$

EXAMPLE 3-2

Using the data given in the preceding example, calculate the density of n-butane.

SOLUTION

Solve for the density by applying equation (3-4) :

$$\rho_g = \frac{m}{V} = \frac{pM}{RT}$$

$$\rho_g = \frac{(60)(58.123)}{(10.73)(580)} = 0.56 \text{ lb/ft}^3$$

Petroleum engineers usually are interested in the behavior of mixtures and rarely deal with pure component gases. Because natural gas is a mixture of hydrocarbon components, the overall physical and chemical properties can be determined from the physical properties of the individual components in the mixture by using appropriate mixing rules.

The basic properties of gases commonly are expressed in terms of the apparent molecular weight, standard volume, density, specific volume, and specific gravity. These properties are defined as in the following sections.

Apparent Molecular Weight, M_a

One of the main gas properties frequently of interest to engineers is the apparent molecular weight. If y_i represents the mole fraction of the i th component in a gas mixture, the apparent molecular weight is defined mathematically by the following equation.

$$M_a = \sum_{i=1} y_i M_i \quad (3-5)$$

where

M_a = apparent molecular weight of a gas mixture

M_i = molecular weight of the i th component in the mixture

y_i = mole fraction of component i in the mixture

Conventionally, natural gas compositions can be expressed in three different forms: mole fraction, y_i , weight fraction, w_i , and volume fraction, v_i .

The mole fraction of a particular component, i , is defined as the number of moles of that component, n_i , divided by the total number of moles, n , of all the components in the mixture:

$$y_i = \frac{n_i}{n} = \frac{n_i}{\sum_i n_i}$$

The weight fraction of a particular component, i , is defined as the weight of that component, m_i , divided by the total weight of m , the mixture:

$$w_i = \frac{m_i}{m} = \frac{m_i}{\sum_i m_i}$$

Similarly, the volume fraction of a particular component, v_i , is defined as the volume of that component, V_i , divided by the total volume of V , the mixture:

$$v_i = \frac{V_i}{V} = \frac{V_i}{\sum_i V_i}$$

It is convenient in many engineering calculations to convert from mole fraction to weight fraction and vice versa. The procedure is given in the following steps.

1. Since the composition is one of the intensive properties and independent of the quantity of the system, assume that the total number of gas is 1; that is, $n = 1$.
2. From the definitions of mole fraction and number of moles (see equation 3-2),

$$y_i = \frac{n_i}{n} = \frac{n_i}{1} = n_i$$

$$m_i = n_i M_i = y_i M_i$$

3. From the above two expressions, calculate the weight fraction to give

$$w_i = \frac{m_i}{m} = \frac{m_i}{\sum_i m_i} = \frac{y_i M_i}{\sum_i y_i M_i} = \frac{y_i M_i}{M_a}$$

4. Similarly,

$$y_i = \frac{w_i / M_i}{\sum_i w_i / M_i}$$

Standard Volume, V_{sc}

In many natural gas engineering calculations, it is convenient to measure the volume occupied by 1 lb-mole of gas at a reference pressure and temperature. These reference conditions are usually 14.7 psia and 60°F and are commonly referred to as *standard conditions*. The standard volume then is defined as the volume of gas occupied by 1 lb-mole of gas at standard conditions. Applying these conditions to equation (3-1) and solving for the volume, that is, the standard volume, gives

$$V_{sc} = \frac{(1)RT_{sc}}{p_{sc}} = \frac{(1)(10.73)(520)}{14.7}$$

$$V_{sc} = 379.4 \text{ scf/lb-mole} \quad (3-6)$$

where

V_{sc} = standard volume, scf/lb-mole

scf = standard cubic feet

T_{sc} = standard temperature, °R

p_{sc} = standard pressure, psia

Gas Density, ρ_g

The density of an ideal gas mixture is calculated by simply replacing the molecular weight, M , of the pure component in equation (3-4) with the apparent molecular weight, M_a , of the gas mixture to give

$$\rho_g = \frac{pM_a}{RT} \quad (3-7)$$

where ρ_g = density of the gas mixture, lb/ft³, and M_a = apparent molecular weight.

Specific Volume, v

The specific volume is defined as the volume occupied by a unit mass of the gas. For an ideal gas, this property can be calculated by applying equation (3-3):

$$v = \frac{V}{m} = \frac{RT}{pM_a} = \frac{1}{\rho_g} \quad (3-8)$$

where v = specific volume, ft³/lb, and ρ_g = gas density, lb/ft³.

Specific Gravity, γ_g

The specific gravity is defined as the ratio of the gas density to that of the air. Both densities are measured or expressed at the same pressure and temperature. Commonly, the standard pressure, p_{sc} , and standard temperature, T_{sc} , are used in defining the gas specific gravity.

$$\gamma_g = \frac{\text{gas density @ 14.7 and 60}^\circ}{\text{air density @ 14.7 and 60}^\circ} = \frac{\rho_g}{\rho_{\text{air}}} \quad (3-9)$$

Assuming that the behavior of both the gas mixture and the air is described by the ideal gas equation, the specific gravity can be then expressed as

$$\gamma_g = \frac{\frac{p_{sc}M_a}{RT_{sc}}}{\frac{p_{sc}M_{\text{air}}}{RT_{sc}}}$$

or

$$\gamma_g = \frac{M_a}{M_{\text{air}}} = \frac{M_a}{28.96} \quad (3-10)$$

where

γ_g = gas specific gravity, $60^\circ/60^\circ$

ρ_{air} = density of the air

M_{air} = apparent molecular weight of the air = 28.96

M_a = apparent molecular weight of the gas

p_{sc} = standard pressure, psia

T_{sc} = standard temperature, $^\circ\text{R}$

EXAMPLE 3-3

A gas well is producing gas with a specific gravity of 0.65 at a rate of 1.1 MMscf/day. The average reservoir pressure and temperature are 1500 psi and 150°F. Calculate

1. The apparent molecular weight of the gas.
2. The gas density at reservoir conditions.
3. The flow rate in lb/day.

SOLUTION

From equation (3-10), solve for the apparent molecular weight:

$$M_a = 28.96 \gamma_g$$

$$M_a = (28.96)(0.65) = 18.82$$

Apply equation (3-7) to determine gas density:

$$\rho_g = \frac{(1500)(18.82)}{(10.73)(610)} = 4.31 \text{ lb/ft}^3$$

The following steps are used to calculate the flow rate.

Step 1 Because 1 lb-mole of any gas occupies 379.4 scf at standard conditions, then the daily number of moles, n , that the gas well is producing is

$$n = \frac{(1.1)(10)^6}{379.4} = 2899 \text{ lb-moles}$$

Step 2 Determine the daily mass, m , of the gas produced from equation (2-2):

$$m = nM_a$$

$$m = 2899(18.82) = 54,559 \text{ lb/day}$$

EXAMPLE 3-4

A gas well is producing a natural gas with the following composition:

COMPONENT	y_i
CO ₂	0.05
C ₁	0.90
C ₂	0.03
C ₃	0.02

Assuming an ideal gas behavior, calculate the apparent molecular weight, specific gravity, gas density at 2000 psia and 150°F, and specific volume at 2000 psia and 150°F.

SOLUTION

The table below describes the gas composition.

Component	y_i	M_i	$y_i M_i$
CO ₂	0.05	44.01	2.200
C ₁	0.90	16.04	14.436
C ₂	0.03	30.07	0.902
C ₃	0.02	44.11	0.882
			$M_a = 18.42$

Apply equation (3-5) to calculate the apparent molecular weight:

$$M_a = \sum_{i=1} y_i M_i$$

$$M_a = 18.42$$

Calculate the specific gravity by using equation (3-10):

$$\gamma_g = M_a / 28.96 = 18.42 / 28.96 = 0.636$$

Solve for the density by applying equation (3-7):

$$\rho_g = \frac{(2000)(18.42)}{(10.73)(610)} = 5.628 \text{ lb/ft}^3$$

Determine the specific volume from equation (3-8):

$$v = \frac{1}{\rho_g} = \frac{1}{5.628} = 0.178 \text{ ft}^3 / \text{lb}$$

Behavior of Real Gases

In dealing with gases at a very low pressure, the ideal gas relationship is a convenient and generally satisfactory tool. At higher pressures, the use of the ideal gas equation of state may lead to errors as great as 500%, as compared to errors of 2–3 % at atmospheric pressure.

Basically, the magnitude of deviations of real gases from the conditions of the ideal gas law increases with increasing pressure and temperature and varies widely with the composition of the gas. Real gases behave differently than ideal gases. The reason for this is that the perfect gas law was derived under the assumption that the volume of molecules is insignificant and neither molecular attraction or repulsion exists between them. This is not the case for real gases.

Numerous equations of state have been developed in the attempt to correlate the pressure-volume-temperature variables for real gases with experimental data. To express a more exact relationship between the variables p , V , and T , a correction factor, called the *gas compressibility factor*, *gas deviation factor*, or simply the *Z-factor*, must be introduced into equation (3-1) to account for the departure of gases from ideality. The equation has the following form:

$$pV = ZnRT \tag{3-11}$$

where the gas compressibility factor, Z , is a dimensionless quantity, defined as the ratio of the actual volume of n -moles of gas at T and p to the ideal volume of the same number of moles at the same T and p :

$$Z = \frac{V_{\text{actual}}}{V_{\text{ideal}}} = \frac{V}{(nRT)/p}.$$

Studies of the gas compressibility factors for natural gases of various compositions show that the compressibility factor can be generalized with sufficient accuracy for most engineering purposes when they are expressed in terms of the following two dimensionless properties: pseudo-reduced pressure, p_{pr} , and pseudo-reduced temperature, T_{pr} . These dimensionless terms are defined by the following expressions:

$$p_{\text{pr}} = \frac{p}{p_{\text{pc}}} \quad (3-12)$$

$$T_{\text{pr}} = \frac{T}{T_{\text{pc}}} \quad (3-13)$$

where

p = system pressure, psia

p_{pr} = pseudo-reduced pressure, dimensionless

T = system temperature, °R

T_{pr} = pseudo-reduced temperature, dimensionless

$p_{\text{pc}}, T_{\text{pc}}$ = pseudo-critical pressure and temperature, respectively, defined by the following relationships:

$$p_{\text{pc}} = \sum_{i=1} y_i p_{ci} \quad (3-14)$$

$$T_{\text{pc}} = \sum_{i=1} y_i T_{ci} \quad (3-15)$$

Matthews et al. (1942) correlated the critical properties of the C_{7+} fraction as a function of the molecular weight and specific gravity:

$$(p_c)_{C_{7+}} = 1188 - 431 \log(M_{C_{7+}} - 61.1) + [2319 - 852 \log(M_{C_{7+}} - 53.7)] (\gamma_{C_{7+}} - 0.8)$$

$$(T_c)_{C_{7+}} = 608 + 364 \log(M_{C_{7+}} - 71.2) + [2450 \log(M_{C_{7+}}) - 3800] \log(\gamma_{C_{7+}})$$

It should be pointed out that these pseudo-critical properties, that is, p_{pc} and T_{pc} , do not represent the actual critical properties of the gas mixture. These pseudo properties are used as correlating parameters in generating gas properties.

Based on the concept of pseudo-reduced properties, Standing and Katz (1942) presented a generalized gas compressibility factor chart as shown in Figure 3-1. The chart represents the compressibility factors of sweet natural gas as a function of p_{pr} and T_{pr} . This chart is generally reliable for natural gas with a minor amount of nonhydrocarbons. It is one of the most widely accepted correlations in the oil and gas industry.

EXAMPLE 3-5

A gas reservoir has the following gas composition:

COMPONENT	y_i
CO ₂	0.02
N ₂	0.01
C ₁	0.85

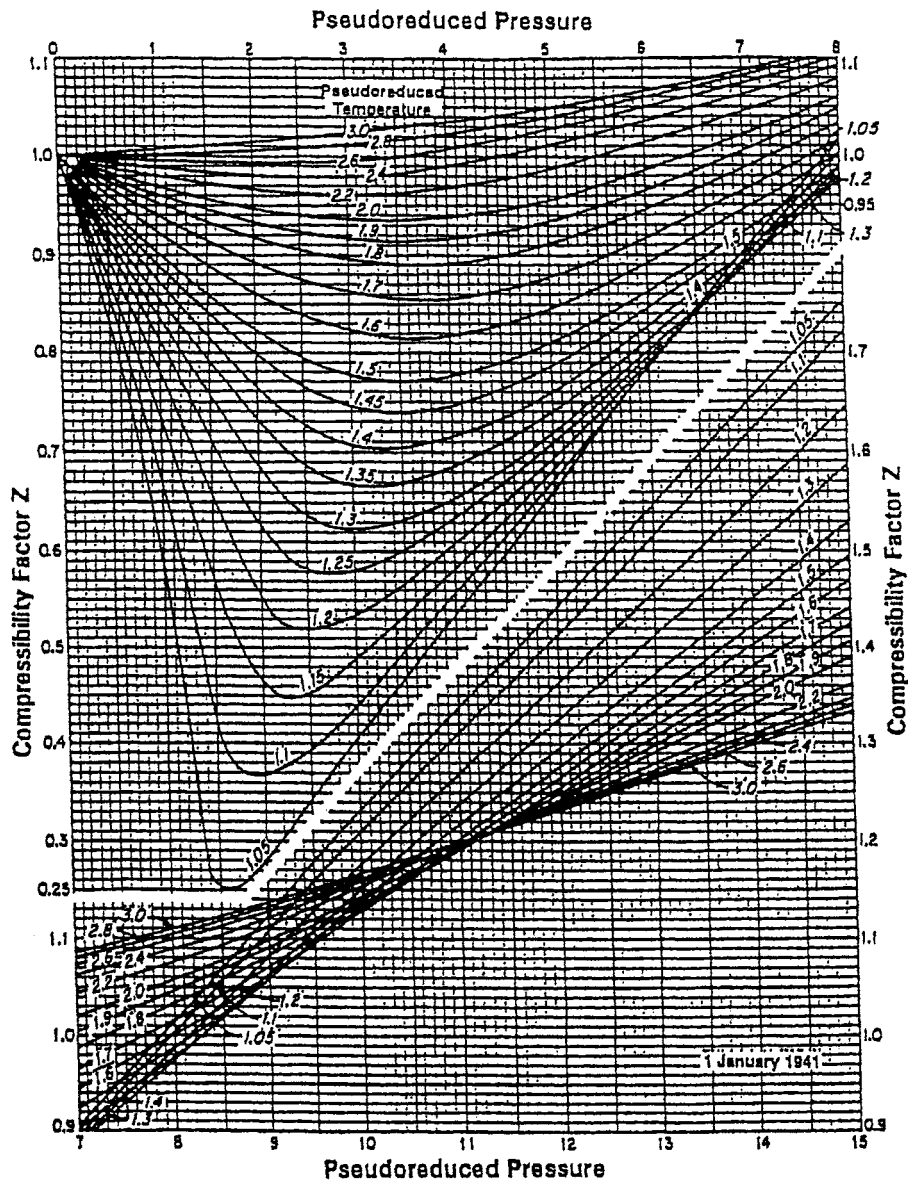


FIGURE 3–1 *Standing and Katz compressibility factors chart.*
Source: GPSA Engineering Data Book, 10th ed. Tulsa, OK: Gas Processors Suppliers Association, 1987. Courtesy of the Gas Processors Suppliers Association.

COMPONENT	y_i
C ₂	0.04
C ₃	0.03
i-C ₄	0.03
n-C ₄	0.02

The initial reservoir pressure and temperature are 3000 psia and 180°F, respectively. Calculate the gas compressibility factor under initial reservoir conditions.

SOLUTION

The table below describes the gas composition.

Component	y_i	$T_{ci}, ^\circ\text{R}$	$y_i T_{ci}$	p_{ci}	$y_i p_{ci}$
CO ₂	0.02	547.91	10.96	1071	21.42
N ₂	0.01	227.49	2.27	493.1	4.93
C ₁	0.85	343.33	291.83	666.4	566.44
C ₂	0.04	549.92	22.00	706.5	28.26
C ₃	0.03	666.06	19.98	616.40	18.48
i-C ₄	0.03	734.46	22.03	527.9	15.84
n-C ₄	0.02	765.62	15.31	550.6	11.01
$T_{pc} = 383.38$				$p_{pc} = 666.38$	

Step 1 Determine the pseudo-critical pressure from equation (3-14):

$$p_{pc} = \sum y_i p_{ci} = 666.38 \text{ psi}$$

Step 2 Calculate the pseudo-critical temperature from equation (3-15):

$$T_{pc} = \sum y_i T_{ci} = 383.38 ^\circ\text{R}$$

Step 3 Calculate the pseudo-reduced pressure and temperature by applying equations (3-12) and (3-13), respectively:

$$p_{pr} = \frac{p}{p_{pc}} = \frac{3000}{666.38} = 4.50$$

$$T_{pr} = \frac{T}{T_{pc}} = \frac{640}{383.38} = 1.67$$

Step 4 Determine the Z-factor from Figure 3-1, using the calculate values of p_{pr} and T_{pr} to give

$$Z = 0.85$$

Equation (3-11) can be written in terms of the apparent molecular weight, M_a , and the weight of the gas, m :

$$pV = Z \left(\frac{m}{M_a} \right) RT$$

Solving this relationship for the gas's specific volume and density give

$$v = \frac{V}{m} = \frac{ZRT}{pM_a} \quad (3-16)$$

$$\rho_g = \frac{1}{v} = \frac{pM_a}{ZRT} \quad (3-17)$$

where

v = specific volume, ft³/lb

ρ_g = density, lb/ft³

EXAMPLE 3-6

Using the data in Example 3-5 and assuming real gas behavior, calculate the density of the gas phase under initial reservoir conditions. Compare the results with that of ideal gas behavior.

SOLUTION

The table below describes the gas composition.

Component	y_i	M_i	$y_i M_i$	$T_{ci}, ^\circ\text{R}$	$y_i T_{ci}$	p_{ci}	$y_i p_{ci}$
CO ₂	0.02	44.01	0.88	547.91	10.96	1071	21.42
N ₂	0.01	28.01	0.28	227.49	2.27	493.1	4.93
C ₁	0.85	16.04	13.63	343.33	291.83	666.4	566.44
C ₂	0.04	30.1	1.20	549.92	22.00	706.5	28.26
C ₃	0.03	44.1	1.32	666.06	19.98	616.40	18.48
i-C ₄	0.03	58.1	1.74	734.46	22.03	527.9	15.84
n-C ₄	0.02	58.1	1.16	765.62	15.31	550.6	11.01
$M_a = 20.23$				$T_{pc} = 383.38$		$p_{pc} = 666.38$	

Step 1 Calculate the apparent molecular weight from equation (3-5):

$$M_a = \sum y_i M_i = 20.23$$

Step 2 Determine the pseudo-critical pressure from equation (3-14):

$$p_{pc} = \sum y_i p_{ci} = 666.38 \text{ psi}$$

Step 3 Calculate the pseudo-critical temperature from equation (3-15):

$$T_{pc} = \sum y_i T_{ci} = 383.38 ^\circ\text{R}$$

Step 4 Calculate the pseudo-reduced pressure and temperature by applying equations (3-12) and (3-13), respectively:

$$P_{pr} = \frac{P}{P_{pc}} = \frac{3000}{666.38} = 4.50$$

$$T_{pr} = \frac{T}{T_{pc}} = \frac{640}{383.38} = 1.67$$

Step 5 Determine the Z-factor from Figure 3-1 using the calculated values of P_{pr} and T_{pr} to give

$$Z = 0.85$$

Step 6 Calculate the density from equation (3-17).

$$\rho_g = \frac{p M_a}{Z R T}$$

$$\rho_g = \frac{(3000)(20.23)}{(0.85)(10.73)(640)} = 10.4 \text{ lb/ft}^3$$

Step 7 Calculate the density of the gas, assuming *ideal gas behavior*, from equation (3-7):

$$\rho_g = \frac{(3000)(20.23)}{(10.73)(640)} = 8.84 \text{ lb/ft}^3$$

The results of this example show that the ideal gas equation estimated the gas density with an absolute error of 15% when compared with the density value as predicted with the real gas equation.

In cases where the composition of a natural gas is not available, the pseudo-critical properties, p_{pc} and T_{pc} , can be predicted solely from the specific gravity of the gas. Brown et al. (1948) presented a graphical method for a convenient approximation of the pseudo-critical pressure and pseudo-critical temperature of gases when only the specific gravity of the gas is available. The correlation is presented in Figure 3–2. Standing (1977) expressed this graphical correlation in the following mathematical forms.

For Case 1, natural gas systems,

$$T_{pc} = 168 + 325\gamma_g - 12.5\gamma_g^2 \tag{3-18}$$

$$p_{pc} = 677 + 15.0\gamma_g - 37.5\gamma_g^2 \tag{3-19}$$

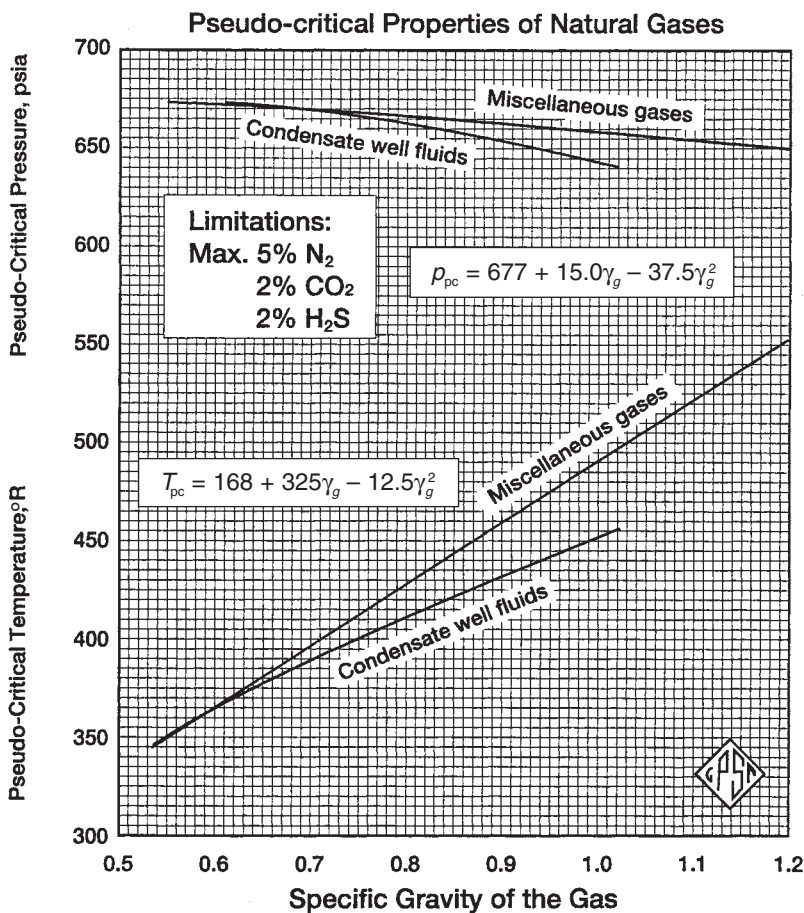


FIGURE 3–2 Pseudo-critical properties for natural gases.

Source: GPSA Engineering Data Book, 10th ed. Tulsa, OK: Gas Processors Suppliers Association, 1987. Courtesy of the Gas Processors Suppliers Association.

For Case 2, wet gas systems,

$$T_{pc} = 187 + 330\gamma_g - 71.5\gamma_g^2 \quad (3-20)$$

$$p_{pc} = 706 - 51.7\gamma_g - 11.1\gamma_g^2 \quad (3-21)$$

where

T_{pc} = pseudo-critical temperature, °R

p_{pc} = pseudo-critical pressure, psia

γ_g = specific gravity of the gas mixture

EXAMPLE 3-7

Using equations (3-18) and (3-19), calculate the pseudo-critical properties and rework Example 3-5.

SOLUTION

Step 1 Calculate the specific gravity of the gas:

$$\gamma_g = \frac{M_a}{28.96} = \frac{20.23}{28.96} = 0.699$$

Step 2 Solve for the pseudo-critical properties by applying equations (3-18) and (3-19):

$$T_{pc} = 168 + 325\gamma_g - 12.5(\gamma_g)^2$$

$$T_{pc} = 168 + 325(0.699) - 12.5(0.699)^2 = 389.1 \text{ °R}$$

$$p_{pc} = 677 + 15\gamma_g - 37.5(\gamma_g)^2$$

$$p_{pc} = 677 + 15(0.699) - 37.5(0.699)^2 = 669.2 \text{ psi}$$

Step 3 Calculate p_{pr} and T_{pr} :

$$p_{pr} = \frac{3000}{669.2} = 4.48$$

$$T_{pr} = \frac{640}{389.1} = 1.64$$

Step 4 Determine the gas compressibility factor from Figure 3-1:

$$Z = 0.824$$

Step 5 Calculate the density from equation (3-17):

$$\rho_g = \frac{pM_a}{ZRT}$$

$$\rho_g = \frac{(3000)(20.23)}{(0.845)(10.73)(640)} = 10.46 \text{ lb/ft}^3$$

Effect of Nonhydrocarbon Components on the Z-Factor

Natural gases frequently contain materials other than hydrocarbon components, such as nitrogen, carbon dioxide, and hydrogen sulfide. Hydrocarbon gases are classified as sweet or sour depending on the hydrogen sulfide content. Both sweet and sour gases may contain nitrogen, carbon dioxide, or both. A hydrocarbon gas is termed a sour gas if it contains 1 grain of H_2S per 100 cubic feet.

The common occurrence of small percentages of nitrogen and carbon dioxide, in part, is considered in the correlations previously cited. Concentrations of up to 5% of these nonhydrocarbon components do not seriously affect accuracy. Errors in compressibility factor calculations as large as 10% may occur in higher concentrations of nonhydrocarbon components in gas mixtures.

Nonhydrocarbon Adjustment Methods

Two methods were developed to adjust the pseudo-critical properties of the gases to account for the presence of the n-hydrocarbon components: the Wichert-Aziz method and the Carr-Kobayashi-Burrows method.

Wichert-Aziz's Correction Method

Natural gases that contain H_2S and/or CO_2 frequently exhibit different compressibility factors behavior than sweet gases. Wichert and Aziz (1972) developed a simple, easy-to-use calculation to account for these differences. This method permits the use of the Standing-Katz Z-factor chart (Figure 3-1), by using a pseudo-critical temperature adjustment factor ϵ , which is a function of the concentration of CO_2 and H_2S in the sour gas. This correction factor then is used to adjust the pseudo-critical temperature and pressure according to the following expressions:

$$T'_{pc} = T_{pc} - \epsilon \quad (3-22)$$

$$p'_{pc} = \frac{p_{pc} T'_{pc}}{T_{pc} + B(1-B)\epsilon} \quad (3-23)$$

where

T_{pc} = pseudo-critical temperature, °R

p_{pc} = pseudo-critical pressure, psia

T'_{pc} = corrected pseudo-critical temperature, °R

p'_{pc} = corrected pseudo-critical pressure, psia

B = mole fraction of H_2S in the gas mixture

ϵ = pseudo-critical temperature adjustment factor, defined mathematically by the following expression:

$$\epsilon = 120[A^{0.9} - A^{1.6}] + 15(B^{0.5} - B^{4.0}) \quad (3-24)$$

where the coefficient A is the sum of the mole fraction H_2S and CO_2 in the gas mixture:

$$A = y_{H_2S} + y_{CO_2}$$

The computational steps of incorporating the adjustment factor ϵ into the Z-factor calculations are summarized next.

Step 1 Calculate the pseudo-critical properties of the whole gas mixture by applying equations (3-18) and (3-19) or equations (3-20) and (3-21).

Step 2 Calculate the adjustment factor, ϵ , from equation (3-24).

Step 3 Adjust the calculated p_{pc} and T_{pc} (as computed in step 1) by applying equations (3-22) and (3-23).

Step 4 Calculate the pseudo-reduced properties, p_{pr} and T_{pr} , from equations (3-11) and (3-12).

Step 5 Read the compressibility factor from Figure 3-1.

EXAMPLE 3-8

A sour natural has a specific gravity of 0.70. The compositional analysis of the gas shows that it contains 5% CO₂ and 10% H₂S. Calculate the density of the gas at 3500 psia and 160°F.

SOLUTION

Step 1 Calculate the uncorrected pseudo-critical properties of the gas from equations (3-18) and (3-19):

$$\begin{aligned} T_{pc} &= 168 + 325\gamma_g - 12.5(\gamma_g)^2 \\ T_{pc} &= 168 + 325(0.7) - 12.5(0.7)^2 = 389.38^\circ\text{R} \\ p_{pc} &= 677 + 15\gamma_g - 37.5(\gamma_g)^2 \\ p_{pc} &= 677 + 15(0.7) - 37.5(0.7)^2 = 669.1 \text{ psia} \end{aligned}$$

Step 2 Calculate the pseudo-critical temperature adjustment factor from equation (3-24):

$$\varepsilon = 120(0.15^{0.9} - 0.15^{1.6}) + 15(0.5^{0.5} - 0.1^4) = 20.735$$

Step 3 Calculate the corrected pseudo-critical temperature by applying equation (3-22):

$$T'_{pc} = 389.38 - 20.735 = 368.64$$

Step 4 Adjust the pseudo-critical pressure p_{pc} by applying equation (3-23):

$$p'_{pc} = \frac{(669.1)(368.64)}{389.38 + 0.1(1 - 0.1)(20.635)} = 630.44 \text{ psia}$$

Step 5 Calculate p_{pr} and T_{pr} :

$$\begin{aligned} p_{pr} &= \frac{3500}{630.44} = 5.55 \\ T_{pr} &= \frac{160 + 460}{368.64} = 1.68 \end{aligned}$$

Step 6 Determine the Z-factor from Figure 3-1:

$$Z = 0.89$$

Step 7 Calculate the apparent molecular weight of the gas from equation (3-10):

$$M_a = 28.96\gamma_g = 28.96(0.7) = 20.27$$

Step 8 Solve for the gas density by applying equation (3-17):

$$\begin{aligned} \rho_g &= \frac{pM_a}{ZRT} \\ \rho_g &= \frac{(3500)(20.27)}{(0.89)(10.73)(620)} = 11.98 \text{ lb/ft}^3 \end{aligned}$$

Whitson and Brule (2000) point out that, when only the gas specific gravity and non-hydrocarbon content are known (including nitrogen, y_{N_2}), the following procedure is recommended:

- Calculate hydrocarbon specific gravity γ_{gHC} (excluding the nonhydrocarbon components) from the following relationship:

$$\gamma_{gHC} = \frac{28.96\gamma_g - (y_{N_2}M_{N_2} + y_{CO_2}M_{CO_2} + y_{H_2S}M_{H_2S})}{28.96(1 - y_{N_2} - y_{CO_2} - y_{H_2S})}$$

- Using the calculated hydrocarbon specific gravity, γ_{gHC} , determine the pseudo-critical properties from equations (3–18) and (3–19):

$$(T_{pc})_{HC} = 168 + 325\gamma_{gHC} - 12.5\gamma_{gHC}^2$$

$$(p_{pc})_{HC} = 677 + 150\gamma_{gHC} - 37.5\gamma_{gHC}^2$$

- Adjust these two values to account for the nonhydrocarbon components by applying the following relationships:

$$p_{pc} = (1 - y_{N_2} - y_{CO_2} - y_{H_2S})(p_{pc})_{HC} + y_{N_2}(p_c)_{N_2} + y_{CO_2}(p_c)_{CO_2} + y_{H_2S}(p_c)_{H_2S}$$

$$T_{pc} = (1 - y_{N_2} - y_{CO_2} - y_{H_2S})(T_{pc})_{HC} + y_{N_2}(T_c)_{N_2} + y_{CO_2}(T_c)_{CO_2} + y_{H_2S}(T_c)_{H_2S}$$

- Use the above calculated pseudo-critical properties in equations (3–22) and (3–23) to obtain the adjusted properties for Wichert-Aziz method of calculating the Z-factor.

Carr-Kobayashi-Burrows's Correction Method

Carr, Kobayashi, and Burrows (1954) proposed a simplified procedure to adjust the pseudo-critical properties of natural gases when nonhydrocarbon components are present. The method can be used when the composition of the natural gas is not available. The proposed procedure is summarized in the following steps.

Step 1 Knowing the specific gravity of the natural gas, calculate the pseudo-critical temperature and pressure by applying equations (3–18) and (3–19).

Step 2 Adjust the estimated pseudo-critical properties by using the following two expressions:

$$T'_{pc} = T_{pc} - 80y_{CO_2} + 130y_{H_2S} - 250y_{N_2} \quad (3-25)$$

$$p'_{pc} = p_{pc} + 440y_{CO_2} + 600y_{H_2S} - 170y_{N_2} \quad (3-26)$$

where:

T'_{pc} = the adjusted pseudo-critical temperature, °R

T_{pc} = the unadjusted pseudo-critical temperature, °R

y_{CO_2} = mole fraction of CO₂

y_{H_2S} = mole fraction of H₂S in the gas mixture

y_{N_2} = mole fraction of nitrogen

p'_{pc} = the adjusted pseudo-critical pressure, psia

p_{pc} = the unadjusted pseudo-critical pressure, psia

Step 3 Use the adjusted pseudo-critical temperature and pressure to calculate the pseudo-reduced properties.

Step 4 Calculate the Z -factor from Figure 3–1.

EXAMPLE 3–9

Using the data in Example 3–8, calculate the density by employing the preceding correction procedure.

SOLUTION

Step 1 Determine the corrected pseudo-critical properties from equations (3–25) and (3–26).

$$T'_{pc} = 389.38 - 80(0.05) + 130(0.10) - 250(0) = 398.38^\circ\text{R}$$

$$p'_{pc} = 669.1 + 440(0.05) + 600(0.01) - 170(0) = 751.1 \text{ psia}$$

Step 2 Calculate p_{pr} and T_{pr} :

$$p_{pr} = \frac{3500}{751.1} = 4.56$$

$$T_{pr} = \frac{620}{398.38} = 1.56$$

Step 3 Determine the gas compressibility factor from Figure 3–1:

$$Z = 0.820$$

Step 4 Calculate the gas density:

$$\rho_g = \frac{pM_a}{ZRT}$$

$$\gamma_g = \frac{(3500)(20.27)}{(0.82)(10.73)(620)} = 13.0 \text{ lb/ft}^3$$

The gas density as calculated in Example 3–8 with a Z -factor of 0.89 is

$$\rho_g = \frac{(3500)(20.27)}{(0.89)(10.73)(620)} = 11.98 \text{ lb/ft}^3$$

Correction for High-Molecular-Weight Gases

It should be noted that the Standing and Katz Z -factor chart (Figure 3–1) was prepared from data on binary mixtures of methane with propane, ethane, and butane and on natural gases, thus covering a wide range in composition of hydrocarbon mixtures containing methane. No mixtures having molecular weights in excess of 40 were included in preparing this plot.

Sutton (1985) evaluated the accuracy of the Standing-Katz compressibility factor chart using laboratory-measured gas compositions and Z -factors and found that the chart provides satisfactory accuracy for engineering calculations. However, Kay's mixing rules, that is, equations (3–13) and (3–14), or comparable gravity relationships for calculating pseudo-critical pressure and temperature, result in unsatisfactory Z -factors for high-molecular-weight reservoir gases. Sutton observed that large deviations occur to gases with high heptanes-plus concentrations. He pointed out that Kay's mixing rules should

not be used to determine the pseudo-critical pressure and temperature for reservoir gases with specific gravities greater than about 0.75.

Sutton proposed that this deviation can be minimized by utilizing the mixing rules developed by Stewart, Burkhardt, and Voo (1959), together with newly introduced empirical adjustment factors (F_J , E_J , and E_K) to account for the presence of the heptanes-plus fraction, C_{7+} , in the gas mixture. The proposed approach is outlined in the following steps.

Step 1 Calculate the parameters J and K from the following relationships:

$$J = \frac{1}{3} \left[\sum_i y_i \left(\frac{T_{ci}}{p_{ci}} \right) \right] + \frac{2}{3} \left[\sum_i y_i \left(\frac{T_{ci}}{p_{ci}} \right)^{0.5} \right]^2 \quad (3-27)$$

$$K = \sum_i \frac{y_i T_{ci}}{\sqrt{p_{ci}}} \quad (3-28)$$

where

J = Stewart-Burkhardt-Voo correlating parameter, °R/psia

K = Stewart-Burkhardt-Voo correlating parameter, °R/psia

y_i = mole fraction of component i in the gas mixture

Step 2 Calculate the adjustment parameters F_J , E_J , and E_K from the following expressions:

$$F_J = \frac{1}{3} \left[y \left(\frac{T_c}{p_c} \right) + \frac{2}{3} \left(y \sqrt{\frac{T_c}{p_c}} \right) \right]_{C_{7+}}^2 \quad (3-29)$$

$$E_J = 0.6081F_J + 1.1325F_J^2 - 14.004F_J y_{C_{7+}}^2 \quad (3-30)$$

$$E_K = \left[\frac{T}{\sqrt{p_c}} \right]_{C_{7+}} - \left[0.3129 y_{C_{7+}} - 4.8156 (y_{C_{7+}})^2 + 27.3751 (y_{C_{7+}})^3 \right] \quad (3-31)$$

where

$y_{C_{7+}}$ = mole fraction of the heptanes-plus component

$(T_c)_{C_{7+}}$ = critical temperature of the C_{7+}

$(p_c)_{C_{7+}}$ = critical pressure of the C_{7+}

Step 3 Adjust the parameters J and K by applying the adjustment factors E_J and E_K , according to these relationships:

$$J' = J - E_J \quad (3-32)$$

$$K' = K - E_K \quad (3-33)$$

where

J , K are calculated from equations (3-27) and (3-28)

E_J , E_K are calculated from equations (3-30) and (3-31)

Step 4 Calculate the adjusted pseudo-critical temperature and pressure from the expressions

$$T'_{pc} = \frac{(K')^2}{J'} \quad (3-34)$$

$$p'_{pc} = \frac{T'_{pc}}{J'} \quad (3-35)$$

Step 5 Having calculated the adjusted T_{pc} and p_{pc} , the regular procedure of calculating the compressibility factor from the Standing and Katz chart is followed.

Sutton's proposed mixing rules for calculating the pseudo-critical properties of high-molecular-weight reservoir gases, $\gamma_g > 0.75$, should significantly improve the accuracy of the calculated Z-factor.

EXAMPLE 3-10

A hydrocarbon gas system has the following composition:

COMPONENT	y_i
C ₁	0.83
C ₂	0.06
C ₃	0.03
n-C ₄	0.02
n-C ₅	0.02
C ₆	0.01
C ₇₊	0.03

The heptanes-plus fraction is characterized by a molecular weight and specific gravity of 161 and 0.81, respectively. Using Sutton's methodology, calculate the density of the gas 2000 psi and 150°F. Then, recalculate the gas density without adjusting the pseudo-critical properties.

SOLUTION USING SUTTON'S METHODOLOGY

Step 1 Calculate the critical properties of the heptanes-plus fraction by Riazi and Daubert correlation (Chapter 2, equation 2-6):

$$\begin{aligned}\theta &= a(M)^b \gamma^c \exp[d(M) + e\gamma + f(M)\gamma] \\ (T_c)_{C_{7+}} &= (544.2)(161)^{0.2998}(0.81)^{1.0555} \exp[-1.3478(10)^{-4}(150) - 0.61641(0.81)] = 1189^\circ\text{R} \\ (p_c)_{C_{7+}} &= 4.5203(10)^4 161^{-0.8063} 0.81^{1.6015} \exp[-1.8078(10)^{-3}(150) - 0.3084(0.81)] = 318.4 \text{ psia}\end{aligned}$$

Step 2 Construct the table below.

Component	y_i	M_i	T_{ci}	p_{ci}	$y_i M_i$	$y_i(T_{ci}/p_{ci})$	$y_i \sqrt{(T_{ci}/p_{ci})_i}$	$y_i [T_c / \sqrt{p_c}]_i$
C ₁	0.83	16.0	343.33	666.4	13.31	0.427	0.596	11.039
C ₂	0.06	30.1	549.92	706.5	1.81	0.047	0.053	1.241
C ₃	0.03	44.1	666.06	616.4	1.32	0.032	0.031	0.805
n-C ₄	0.02	58.1	765.62	550.6	1.16	0.028	0.024	0.653
n-C ₅	0.02	72.2	845.60	488.6	1.45	0.035	0.026	0.765
C ₆	0.01	84.0	923.00	483.0	0.84	0.019	0.014	0.420
C ₇₊	0.03	161.0	1189.0	318.4	4.83	0.112	0.058	1.999
Total					24.72	0.700	0.802	16.922

Step 2 Calculate the parameters J and K from equations (3-27) and (3-28) and using the values from the previous table.

$$J = \frac{1}{3}(0.700) + \frac{2}{3}(0.802)^2 = 0.662$$

$$J = \frac{1}{3} \left[\sum_i y_i \left(\frac{T_{ci}}{p_{ci}} \right) \right] + \frac{2}{3} \left[\sum_i y_i \left(\frac{T_{ci}}{p_{ci}} \right)^{0.5} \right]^2$$

$$K = \sum_i \frac{y_i T_{ci}}{\sqrt{p_{ci}}} = 16.922$$

Step 3 To account for the presence of the C_{7+} fraction, calculate the adjustment factors F_J , E_J , and E_K by applying equations (3–29) through (3–31):

$$F_J = \frac{1}{3} \left[y \left(\frac{T_c}{p_c} \right) + \frac{2}{3} \left(\sqrt{\frac{T_c}{p_c}} \right) \right]_{C_{7+}}^2$$

$$F_J = \frac{1}{3} [0.112] + \frac{2}{3} [0.058]^2 = 0.0396$$

$$E_J = 0.6081F_J + 1.1325F_J^2 - 14.004F_J y_{C_{7+}} + 64.434F_J y_{C_{7+}}^2$$

$$E_J = 0.6081(0.04) + 1.0352(0.04)^2 - 14.004(0.04)(0.03) + 64.434(0.04)(0.3)^2 = 0.012$$

$$E_K = \left[\frac{T}{\sqrt{p_c}} \right]_{C_{7+}} [0.3129 y_{C_{7+}} - 4.8156 (y_{C_{7+}})^2 + 27.2751 (0.03)^3]$$

$$E_K = 66.634 [0.3129(0.03) - 4.8156(0.03)^2 + 27.3751(0.03)^3] = 0.386$$

Step 4 Calculate the parameters J' and K' from equations (3–34) and (3–35):

$$J' = J - E_J = 0.662 - 0.012 = 0.650$$

$$K' = K - E_K = 16.922 - 0.386 = 16.536$$

Step 5 Determine the adjusted pseudo-critical properties from equations (3–34) and (3–35):

$$T'_{pc} = \frac{(K')^2}{J'} = \frac{(16.536)^2}{0.65} = 420.7$$

$$p'_{pc} = \frac{T'_{pc}}{J'} = \frac{420.7}{0.65} = 647.2$$

Step 6 Calculate the pseudo-reduced properties of the gas by applying equations (3–11) and (3–12) to give

$$p_{pr} = \frac{2000}{647.2} = 3.09$$

$$T_{pr} = \frac{610}{420.7} = 1.45$$

Step 7 Calculate the Z-factor from Figure 3–1 to give

$$Z = 0.745.$$

Step 8 From equation (3–17), calculate the density of the gas:

$$\rho_g = \frac{p M_a}{Z R T}$$

$$\rho_g = \frac{(2000)(24.73)}{(10.73)(610)(0.745)} = 10.14 \text{ lb/ft}^3$$

SOLUTION WITHOUT ADJUSTING THE PSEUDO-CRITICAL PROPERTIES

Step 1 Calculate the specific gravity of the gas:

$$\gamma_g = \frac{M_a}{28.96} = \frac{24.73}{28.96} = 0.854$$

Step 2 Solve for the pseudo-critical properties by applying equations (3-18) and (3-19):

$$T_{pc} = 168 + 325(0.84) - 12.5(0.854)^2 = 436.4^\circ\text{R}$$

$$p_{pc} = 677 + 15(0.854) - 37.5(0.854)^2 = 662.5 \text{ psia}$$

Step 3 Calculate p_{pr} and T_{pr} :

$$p_{pr} = \frac{2000}{662.5} = 3.02$$

$$T_{pr} = \frac{610}{436.4} = 1.40$$

Step 4 Calculate the Z-factor from Figure 3-1 to give

$$Z = 0.710$$

Step 5 From equation (3-17), calculate the density of the gas:

$$\rho_g = \frac{p M_a}{ZRT}$$

$$\rho_g = \frac{(2000)(24.73)}{(10.73)(610)(0.710)} = 10.64 \text{ lb/ft}^3$$

Direct Calculation of Compressibility Factors

After four decades of existence, the Standing-Katz Z-factor chart is still widely used as a practical source of natural gas compressibility factors. As a result, there was an apparent need for a simple mathematical description of that chart. Several empirical correlations for calculating Z-factors have been developed over the years. Papay (1985) proposed a simple expression for calculating the gas compressibility factor explicitly. Papay correlated the Z-factor with pseudo-reduced pressure p_{pr} and temperature T_{pr} as expressed next:

$$Z = 1 - \frac{3.53 p_{pr}}{10^{0.9813 T_{pr}}} + \frac{0.274 p_{pr}^2}{10^{0.8157 T_{pr}}}$$

For example, at $p_{pr} = 3$ and $T_{pr} = 2$, the Z-factor from the preceding equation is

$$Z = 1 - \frac{3.53 p_{pr}}{10^{0.9813 T_{pr}}} + \frac{0.274 p_{pr}^2}{10^{0.8157 T_{pr}}} = 1 - \frac{3.53(3)}{10^{0.9813(2)}} + \frac{0.274(3)^2}{10^{0.8157(2)}} = 0.9422$$

as compared with value obtained from the Standing and Katz chart of 0.954.

Numerous rigorous mathematical expressions have been proposed to accurately reproduce the Standing and Katz Z-factor chart. Most of these expressions are designed to solve for the gas compressibility factor at any p_{pr} and T_{pr} iteratively. Three of these empirical correlations are described next: Hall-Yarborough, Dranchuk-Abu-Kassem, and Dranchuk-Purvis-Robinson.

Hall-Yarborough's Method

Hall and Yarborough (1973) presented an equation of state that accurately represents the Standing and Katz Z-factor chart. The proposed expression is based on the Starling-Carnahan equation of state. The coefficients of the correlation were determined by fitting them to data taken from the Standing and Katz Z-factor chart. Hall and Yarborough proposed the following mathematical form:

$$Z = \left[\frac{0.06125tp_{\text{pr}}}{Y} \right] \exp[-1.2(1-t)^2] \quad (3-36)$$

where

p_{pr} = pseudo-reduced pressure

t = reciprocal of the pseudo-reduced temperature (i.e., T_{pc}/T)

Y = the reduced density, which can be obtained as the solution of the following equation:

$$F(Y) = X_1 + \frac{Y + Y^2 + Y^3 - Y^4}{(1-Y)} - (X_2)Y^2 + (X_3)Y^{X_4} = 0 \quad (3-37)$$

where

$$X_1 = -0.06125p_{\text{pr}}t \exp[-1.2(1-t)^2]$$

$$X_2 = (14.76t - 9.76t^2 + 4.58t^3)$$

$$X_3 = (90.7t - 242.2t^2 + 42.4t^3)$$

$$X_4 = (2.18 + 2.82t)$$

Equation (3-37) is a nonlinear equation and can be solved conveniently for the reduced density Y by using the Newton-Raphson iteration technique. The computational procedure of solving equation (3-37) at any specified pseudo-reduced pressure, p_{pr} , and temperature, T_{pr} , is summarized in the following steps.

Step 1 Make an initial guess of the unknown parameter, Y^k , where k is an iteration counter. An appropriate initial guess of Y is given by the following relationship:

$$Y^k = 0.0125 p_{\text{pr}} t \exp[-1.2(1-t)^2]$$

Step 2 Substitute this initial value in equation (3-37) and evaluate the nonlinear function. Unless the correct value of Y has been initially selected, equation (3-37) will have a nonzero value of $f(Y)$.

Step 3 A new improved estimate of Y , that is, Y^{k+1} , is calculated from the following expression:

$$Y^{k+1} = Y^k - \frac{f(Y^k)}{f'(Y^k)} \quad (3-38)$$

where $f'(Y^k)$ is obtained by evaluating the derivative of equation (3-37) at Y^k , or

$$f'(Y) = \frac{1 + 4Y + 4Y^2 - 4Y^3 + Y^4}{(1-Y)^4} - 2(X_2)Y + (X_3)(X_4)Y^{(X_4-1)} \quad (3-39)$$

Step 4 Steps 2 and 3 are repeated n times until the error, that is, $\text{abs}(Y^k - Y^{k+1})$, becomes smaller than a preset tolerance, say 10^{-12} .

Step 5 The correct value of Y is then used to evaluate equation (3-36) for the compressibility factor:

$$Z = \left[\frac{0.06125tp_{\text{pr}}}{Y} \right] \exp[-1.2(1-t)^2]$$

Hall and Yarborough pointed out that the method is not recommended for application if the pseudo-reduced temperature is less than 1.

Dranchuk and Abu-Kassem's Method

Dranchuk and Abu-Kassem (1975) derived an analytical expression for calculating the reduced gas density that can be used to estimate the gas compressibility factor. The reduced gas density ρ_r is defined as the ratio of the gas density at a specified pressure and temperature to that of the gas at its critical pressure or temperature:

$$\rho_r = \frac{\rho}{\rho_c} = \frac{[pM_a/(ZRT)]}{[p_cM_a/(Z_cRT_c)]} = \frac{[p/(ZT)]}{[p_c/(Z_cT_c)]}$$

The critical gas compressibility factor Z_c is approximately 0.27, which leads to the following simplified expression for the reduced gas density as expressed in terms of the reduced temperature T_r and reduced pressure p_r :

$$\rho_r = \frac{0.27p_{\text{pr}}}{ZT_{\text{pr}}} \quad (3-40)$$

The authors proposed the following 11-constant equation of state for calculating the reduced gas density:

$$f(\rho_r) = (R_1)\rho_r - \frac{R_2}{\rho_r} + (R_3)\rho_r^2 - (R_4)\rho_r^5 + (R_5)(1 + A_{11}\rho_r^2)\rho_r^2 \exp[-A_{11}\rho_r^2] + 1 = 0 \quad (3-41)$$

with the coefficients R_1 through R_5 as defined by the following relations:

$$R_1 = A_1 + \frac{A_2}{T_{\text{pr}}} + \frac{A_3}{T_{\text{pr}}^3} + \frac{A_4}{T_{\text{pr}}^4} + \frac{A_5}{T_{\text{pr}}^5}$$

$$R_2 = \frac{0.27p_{\text{pr}}}{T_{\text{pr}}}$$

$$R_3 = A_6 + \frac{A_7}{T_{\text{pr}}} + \frac{A_8}{T_{\text{pr}}^2}$$

$$R_4 = A_9 \left[\frac{A_7}{T_{\text{pr}}} + \frac{A_8}{T_{\text{pr}}^2} \right]$$

$$R_5 = \left[\frac{A_{10}}{T_{\text{pr}}^3} \right]$$

The constants A_1 through A_{11} were determined by fitting the equation, using nonlinear regression models, to 1500 data points from the Standing and Katz Z-factor chart. The coefficients have the following values:

$$\begin{aligned} A_1 &= 0.3265 & A_4 &= 0.01569 & A_7 &= -0.7361 & A_{10} &= 0.6134 \\ A_2 &= -1.0700 & A_5 &= -0.05165 & A_8 &= 0.1844 & A_{11} &= 0.7210 \\ A_3 &= -0.5339 & A_6 &= 0.5475 & A_9 &= 0.1056 \end{aligned}$$

Equation (3–41) can be solved for the reduced gas density ρ_r by applying the Newton-Raphson iteration technique as summarized in the following steps.

Step 1 Make an initial guess of the unknown parameter, ρ_r^k , where k is an iteration counter. An appropriate initial guess of ρ_r^k is given by the following relationship:

$$\rho_r = \frac{0.27 p_{\text{pr}}}{T_{\text{pr}}}$$

Step 2 Substitute this initial value in equation (3–41) and evaluate the nonlinear function. Unless the correct value of ρ_r^k has been initially selected, equation (3–41) will have a nonzero value for the function $f(\rho_r^k)$.

Step 3 A new improved estimate of ρ_r , that is, ρ_r^{k+1} , is calculated from the following expression:

$$\rho_r^{k+1} = \rho_r^k - \frac{f(\rho_r^k)}{f'(\rho_r^k)}$$

where

$$\begin{aligned} f'(\rho_r) &= (R_1) + \frac{R_2}{\rho_r^2} + 2(R_3)\gamma_r - 5(R_4)\rho_r^4 \\ &\quad + 2(R_5)\rho_r \exp(-A_{11}\rho_r^2) \left[(1 + 2A_{11}\rho_r^3) - A_{11}\rho_r^2 (1 + A_{11}\rho_r^2) \right] \end{aligned}$$

Step 4 Steps 2 and 3 are repeated n times, until the error, that is, $\text{abs}(\rho_r^k - \rho_r^{k+1})$, becomes smaller than a preset tolerance, say, 10^{-12} .

Step 5 The correct value of ρ_r is then used to evaluate equation (3–40) for the compressibility factor:

$$Z = \frac{0.27 p_{\text{pr}}}{\rho_r T_{\text{pr}}}$$

The proposed correlation was reported to duplicate compressibility factors from the Standing and Katz chart with an average absolute error of 0.585% and is applicable over the ranges

$$\begin{aligned} 0.2 &\leq p_{\text{pr}} < 30 \\ 1.0 &< T_{\text{pr}} \leq 3.0 \end{aligned}$$

Dranchuk-Purvis-Robinson Method

Dranchuk, Purvis, and Robinson (1974) developed a correlation based on the Benedict-Webb-Rubin type of equation of state. Fitting the equation to 1500 data points from the Standing and Katz Z-factor chart optimized the eight coefficients of the proposed equations. The equation has the following form:

$$1 + T_1 \rho_r + T_2 \rho_r^2 + T_3 \rho_r^5 + \left[T_4 \rho_r^2 (1 + A_8 \rho_r^2) \exp(-A_8 \rho_r^2) \right] - \frac{T_5}{\rho_r} = 0 \quad (3-42)$$

with

$$T_1 = A_1 + \frac{A_2}{T_{\text{pr}}} + \frac{A_3}{T_{\text{pr}}^3}$$

$$T_2 = A_4 + \frac{A_5}{T_{\text{pr}}}$$

$$T_3 = \frac{A_5 A_6}{T_{\text{pr}}}$$

$$T_4 = \frac{A_7}{T_{\text{pr}}^3}$$

$$T_5 = \frac{0.27 p_{\text{pr}}}{T_{\text{pr}}}$$

where ρ_r is defined by equation (3-41) and the coefficients A_1 through A_8 have the following values:

$$A_1 = 0.31506237 \quad A_5 = 0.31506237$$

$$A_2 = -1.0467099 \quad A_6 = -1.0467099$$

$$A_3 = -0.57832720 \quad A_7 = -0.57832720$$

$$A_4 = 0.53530771 \quad A_8 = 0.53530771$$

The solution procedure of equation (3-43) is similar to that of Dranchuk and Abu-Kassem.

The method is valid within the following ranges of pseudo-reduced temperature and pressure:

$$1.05 \leq T_{\text{pr}} < 3.0$$

$$0.2 \leq p_{\text{pr}} \leq 3.0$$

Compressibility of Natural Gases

Knowledge of the variability of fluid compressibility with pressure and temperature is essential in performing many reservoir engineering calculations. For a liquid phase, the compressibility is small and usually assumed to be constant. For a gas phase, the compressibility is neither small nor constant.

By definition, the isothermal gas compressibility is the change in volume per unit volume for a unit change in pressure, or in equation form,

$$c_g = \frac{1}{V} \left(\frac{\partial V}{\partial p} \right)_T \quad (3-43)$$

where c_g = isothermal gas compressibility, 1/psi.

From the real gas equation of state,

$$V = \frac{nRTZ}{p}$$

Differentiating this equation with respect to pressure at constant temperature T , gives

$$\left(\frac{\partial V}{\partial p}\right) = nRT \left[\frac{1}{p} \left(\frac{\partial Z}{\partial p} \right) - \frac{Z}{p^2} \right]$$

Substituting into equation (3-43) produces the following generalized relationship:

$$c_g = \frac{1}{p} - \frac{1}{Z} \left(\frac{\partial Z}{\partial p} \right)_T \quad (3-44)$$

For an ideal gas, $Z = 1$ and $(\partial Z / \partial p)_T = 0$; therefore,

$$c_g = \frac{1}{p} \quad (3-45)$$

It should be pointed out that equation (3-45) is useful in determining the expected order of magnitude of the isothermal gas compressibility.

Equation (3-44) can be conveniently expressed in terms of the pseudo-reduced pressure and temperature by simply replacing p with $(p_{pr} p_{pc})$:

$$c_g = \frac{1}{p_{pr} p_{pc}} - \frac{1}{Z} \left[\frac{\partial Z}{\partial (p_{pr} p_{pc})} \right]_{T_{pr}}$$

Multiplying this equation by p_{pc} yields

$$c_g p_{pc} = c_{pr} = \frac{1}{p_{pr}} - \frac{1}{Z} \left[\frac{\partial Z}{\partial p_{pr}} \right]_{T_{pr}} \quad (3-46)$$

The term c_{pr} is called the *isothermal pseudo-reduced compressibility*, defined by the relationship:

$$c_{pr} = c_g p_{pc} \quad (3-47)$$

where

c_{pr} = isothermal pseudo-reduced compressibility

c_g = isothermal gas compressibility, psi^{-1}

p_{pc} = pseudo-reduced pressure, psi

Values of $(\partial z / \partial p_{pr})_{T_{pr}}$ can be calculated from the slope of the T_{pr} isotherm on the Standing and Katz Z -factor chart.

EXAMPLE 3-11

A hydrocarbon gas mixture has a specific gravity of 0.72. Calculate the isothermal gas compressibility coefficient at 2000 psia and 140°F assuming, first, an ideal gas behavior, then a real gas behavior.

SOLUTION

Assuming an ideal gas behavior, determine c_g by applying equation (3-44)

$$c_g = \frac{1}{2000} = 500 \times 10^{-6} \text{psi}^{-1}$$

Assuming a real gas behavior, use the following steps.

Step 1 Calculate T_{pc} and p_{pc} by applying equations (3–17) and (3–18):

$$T_{pc} = 168 + 325(0.72) - 12.5(0.72)^2 = 395.5^\circ\text{R}$$

$$p_{pc} = 677 + 15(0.72) - 37.5(0.72)^2 = 668.4 \text{ psia}$$

Step 2 Compute p_{pr} and T_{pr} from equations (3–11) and (3–12):

$$p_{pr} = \frac{2000}{668.4} = 2.99$$

$$T_{pr} = \frac{600}{395.5} = 1.52$$

Step 3 Determine the Z -factor from Figure 3–1:

$$Z = 0.78$$

Step 4 Calculate the slope $[dZ/dp_{pr}]_{T_{pr}} = 1.52$:

$$\left[\frac{\partial Z}{\partial p_{pr}} \right]_{T_{pr}} = -0.022$$

Step 5 Solve for c_{pr} by applying equation (3–47):

$$c_{pr} = \frac{1}{2.99} - \frac{1}{0.78}[-0.022] = 0.3627$$

Step 6 Calculate c_g from equation (3–48):

$$c_{pr} = c_g p_{pc}$$

$$c_g = \frac{c_{pr}}{p_{pc}} = \frac{0.327}{668.4} = 543 \times 10^{-6} \text{ psi}^{-1}$$

Trube (1957a and 1957b) presented graphs from which the isothermal compressibility of natural gases may be obtained. The graphs, Figures 3–3 and 3–4, give the isothermal pseudo-reduced compressibility as a function of pseudo-reduced pressure and temperature.

EXAMPLE 3–12

Using Trube's generalized charts, rework Example 3–11.

SOLUTION

Step 1 From Figure 3–3, find c_{pr} to give

$$c_{pr} = 0.36$$

Step 2 Solve for c_g by applying equation (3–49):

$$c_g = \frac{0.36}{668.4} = 539 \times 10^{-6} \text{ psi}^{-1}$$

Mattar, Brar, and Aziz (1975) presented an analytical technique for calculating the isothermal gas compressibility. The authors expressed c_{pr} as a function of $\partial p / \partial \rho_r$, rather than $\partial p / \partial p_{pr}$.

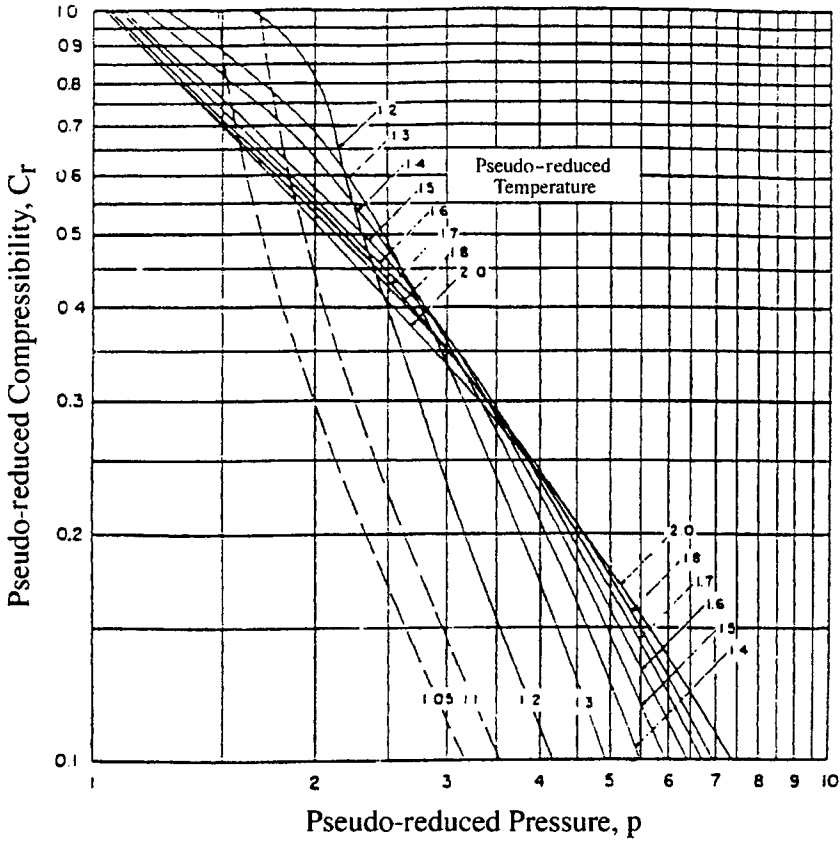


FIGURE 3-3 Trube's pseudo-reduced compressibility for natural gases.

Permission to publish from the Society of Petroleum Engineers of the AIME. © SPE-AIME.

Equation (3-41) is differentiated with respect to p_{pr} to give

$$\frac{\partial Z}{\partial p_{pr}} = \frac{0.27}{Z^2 T_{pr}} \left[\frac{(\partial Z / \partial \rho_r)_{T_{pr}}}{1 + \frac{\rho_r}{Z} (\partial Z / \partial \rho_r)_{T_{pr}}} \right] \quad (3-48)$$

Equation (3-48) may be substituted into equation (3-46) to express the pseudo-reduced compressibility as

$$c_{pr} = \frac{1}{p_r} - \frac{0.27}{Z^2 T_{pr}} \left[\frac{(\partial Z / \partial \rho_r)_{T_{pr}}}{1 + \frac{\rho_r}{Z} (\partial Z / \partial \rho_r)_{T_{pr}}} \right] \quad (3-49)$$

where ρ_r = pseudo-reduced gas density.

The partial derivative appearing in equation (3-49) is obtained from equation (3-42) to give

$$\left[\frac{\partial Z}{\partial \rho_r} \right]_{T_{pr}} = T_1 + 2T_2 \rho_r + 5T_3 \rho_r^4 + 2T_4 \rho_r (1 + A_8 \rho_r^2 - A_8^2 \rho_r^4) \exp(-A_8 \rho_r^2) \quad (3-50)$$

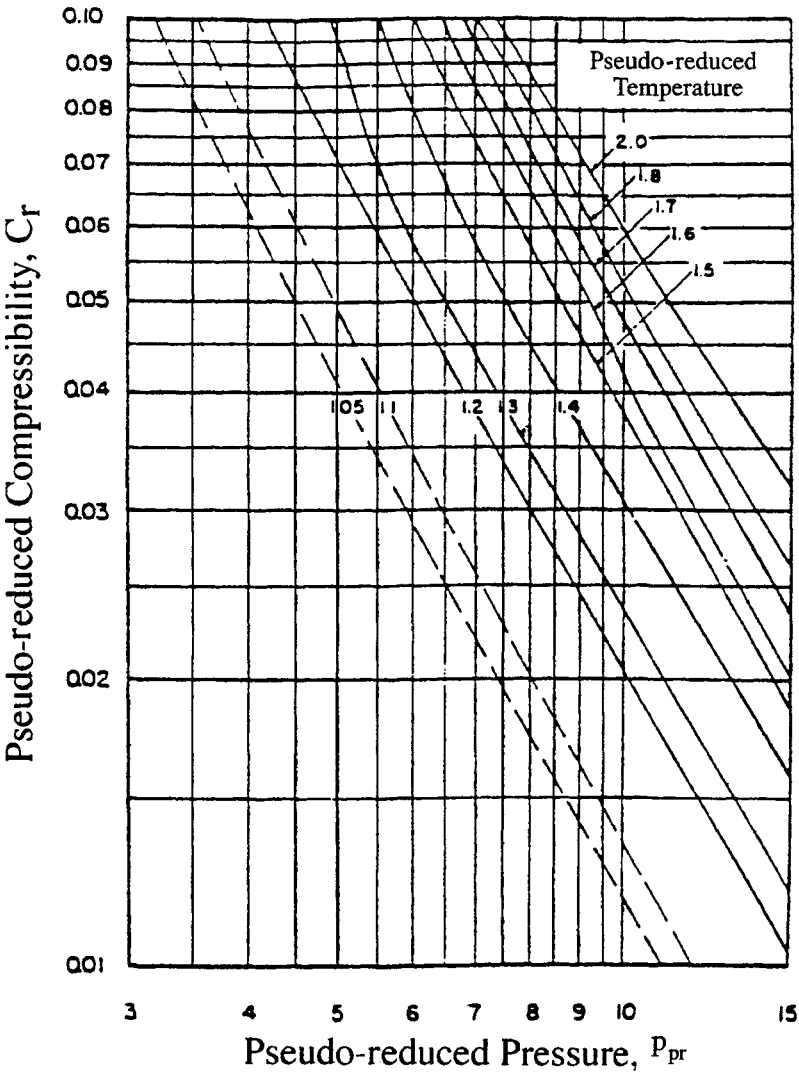


FIGURE 3-4 *Trube’s pseudo-reduced compressibility for natural gases.*
Permission to publish from the Society of Petroleum Engineers of the AIME. © SPE-AIME.

where the coefficients T_1 through T_4 and A_1 through A_8 are as defined previously by equation (3-42).

Gas Formation Volume Factor

The gas formation volume factor is used to relate the volume of gas, as measured at reservoir conditions, to the volume of the gas as measured at standard conditions, that is, 60°F and 14.7 psia. This gas property is then defined as the actual volume occupied by a certain amount of gas at a specified pressure and temperature, divided by the volume occupied by the same amount of gas at standard conditions. In equation form, the relationship is expressed as

$$B_g = \frac{(V)_{p,T}}{V_{sc}} \quad (3-51)$$

where

B_g = gas formation volume factor, ft³/scf

$V_{p,T}$ = volume of gas at pressure p and temperature T , ft³

V_{sc} = volume of gas at standard conditions

Applying the real gas equation of state, equation (3-11), and substituting for the volume V , gives

$$B_g = \frac{\frac{ZnRT}{p_{sc}}}{\frac{Z_{sc}nRT_{sc}}{p_{sc}}} = \frac{p_{sc}}{T_{sc}} \frac{ZT}{p}$$

where

Z_{sc} = Z-factor at standard conditions = 1.0

p_{sc}, T_{sc} = standard pressure and temperature

Assuming that the standard conditions are represented by $p_{sc} = 14.7$ psia and $T_{sc} = 520$, the preceding expression can be reduced to the following relationship:

$$B_g = 0.02827 \frac{ZT}{p} \quad (3-52)$$

where

B_g = gas formation volume factor, ft³/scf

Z = gas compressibility factor

T = temperature, °R

In other field units, the gas formation volume factor can be expressed in bbl/scf, to give

$$B_g = 0.005035 \frac{ZT}{p} \quad (3-53)$$

The reciprocal of the gas formation volume factor, called the *gas expansion factor*, is designated by the symbol E_g :

$$E_g = \frac{1}{B_g}$$

In terms of scf/ft³, the gas expansion factor is

$$E_g = 35.37 \frac{p}{ZT}, \text{ scf/ft}^3 \quad (3-54)$$

In other units,

$$E_g = 198.6 \frac{p}{ZT}, \text{ scf/bbl} \quad (3-55)$$

EXAMPLE 3-13

A gas well is producing at a rate of 15,000 ft³/day from a gas reservoir at an average pressure of 2000 psia and a temperature of 120°F. The specific gravity is 0.72. Calculate the gas flow rate in scf/day.

SOLUTION.

Step 1 Calculate the pseudo-critical properties from equations (3-17) and (3-18), to give:

$$T_{pc} = 168 + 325\gamma_g - 12.5\gamma_g^2 = 395.5^\circ\text{R}$$

$$p_{pc} = 677 + 15.0\gamma_g - 37.5\gamma_g^2 = 668.4 \text{ psia}$$

Step 2 Calculate the p_{pr} and T_{pr} :

$$p_{pr} = \frac{p}{p_{pc}} = \frac{2000}{668.4} = 2.99$$

$$T_{pr} = \frac{T}{T_{pc}} = \frac{600}{395.5} = 1.52$$

Step 3 Determine the Z-factor from Figure 3-1:

$$Z = 0.78$$

Step 4 Calculate the gas expansion factor from equation (3-54):

$$E_g = 35.37 \frac{p}{ZT} = 35.37 \frac{2000}{(0.78)(600)} = 151.15 \text{ scf/ft}^3$$

Step 5 Calculate the gas flow rate in scf/day by multiplying the gas flow rate (in ft³/day) by the gas expansion factor, E_g , as expressed in scf/ft³:

$$\text{Gas flow rate} = (151.15) (15,000) = 2.267 \text{ MMscf/day}$$

It is also convenient in many engineering calculations to express the gas density in terms of the B_g or E_g . From the definitions of gas density, the gas expansion factor, and gas formation volume factor,

$$\rho_g = \frac{M_a}{R} \left(\frac{p}{ZT} \right)$$

$$B_g = \frac{p_{sc}}{T_{sc}} \left(\frac{ZT}{P} \right)$$

$$E_g = \frac{T_{sc}}{p_{sc}} \left(\frac{p}{ZT} \right)$$

Combining the gas density equation with B_g and E_g gives

$$\rho_g = \frac{p_{sc} M_a}{T_{sc} R} \left(\frac{1}{B_g} \right) = \frac{0.002635 M_a}{B_g}$$

$$\rho_g = \frac{p_{sc} M_a}{T_{sc} R} (E_g) = 0.002635 M_a E_g$$

Gas Viscosity

The viscosity of a fluid is a measure of the internal fluid friction (resistance) to flow. If the friction between layers of the fluid is small, that is, low viscosity, an applied shearing force will result in a large velocity gradient. As the viscosity increases, each fluid layer exerts a larger frictional drag on the adjacent layers and velocity gradient decreases.

The viscosity of a fluid is generally defined as the ratio of the shear force per unit area to the local velocity gradient. Viscosities are expressed in terms of poises, centipoises, or micropoises. One poise equals a viscosity of 1 dyne-sec/cm² and can be converted to other field units by the following relationships:

$$\begin{aligned} 1 \text{ poise} &= 100 \text{ centipoises} \\ &= 1 \times 10^6 \text{ micropoises} \\ &= 6.72 \times 10^{-2} \text{ lb mass/ft-sec} \\ &= 20.9 \times 10^{-3} \text{ lbf-sec/ft}^2 \end{aligned}$$

The gas viscosity is not commonly measured in the laboratory because it can be estimated precisely from empirical correlations. Like all intensive properties, viscosity of a natural gas is completely described by the following function:

$$\mu_g = (p, T, y_i)$$

where μ_g = the viscosity of the gas phase. This relationship simply states that the viscosity is a function of pressure, temperature, and composition. Many of the widely used gas viscosity correlations may be viewed as modifications of that expression.

Two popular methods that are commonly used in the petroleum industry are the Carr-Kobayashi-Burrows correlation and the Lee-Gonzalez-Eakin method, which are described next.

Carr-Kobayashi-Burrows's Method

Carr, Kobayashi, and Burrows (1954) developed graphical correlations for estimating the viscosity of natural gas as a function of temperature, pressure, and gas gravity. The computational procedure of applying the proposed correlations is summarized in the following steps.

Step 1 Calculate the pseudo-critical pressure, pseudo-critical temperature, and apparent molecular weight from the specific gravity or the composition of the natural gas. Corrections to these pseudo-critical properties for the presence of the nonhydrocarbon gases (CO₂, N₂, and H₂S) should be made if they are present in concentration greater than 5 mole percent.

Step 2 Obtain the viscosity of the natural gas at one atmosphere and the temperature of interest from Figure 3–5. This viscosity, as denoted by μ_1 , *must be corrected for the presence of nonhydrocarbon components using the inserts of Figure 3–5*. The nonhydrocarbon fractions tend to increase the viscosity of the gas phase. The effect of nonhydrocarbon components on the viscosity of the natural gas can be expressed mathematically by the following relationship:

$$\mu_1 = (\mu_1)_{\text{uncorrected}} + (\Delta\mu)_{\text{N}_2} + (\Delta\mu)_{\text{CO}_2} + (\Delta\mu)_{\text{H}_2\text{S}} \quad (3-56)$$

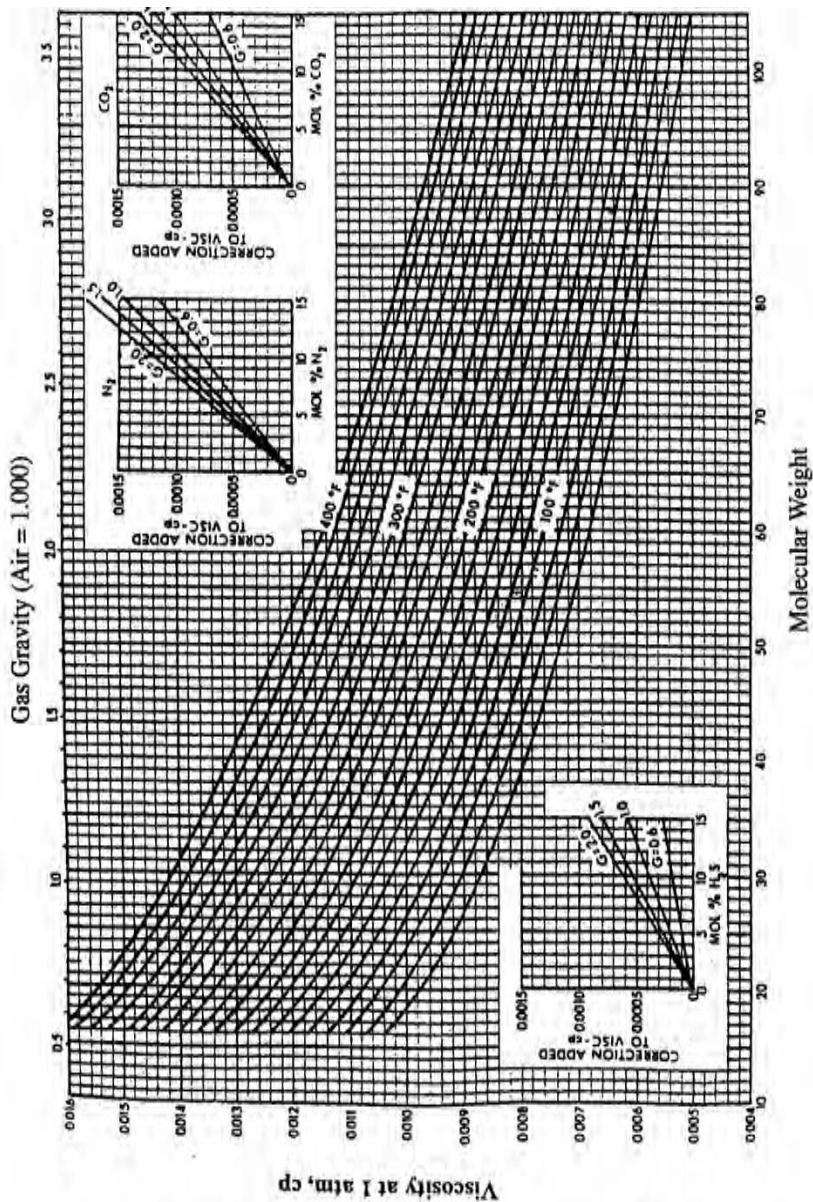


FIGURE 3-5 Carr et al.'s atmospheric gas viscosity correlation.

Source: Carr et al., "Viscosity of Hydrocarbon Gases under Pressure," *Transactions of the AIME* 201 (1954): 270-275. Permission to publish from the Society of Petroleum Engineers of the AIME. © SPE-AIME.

where

μ_1 = “corrected” gas viscosity at 1 atmospheric pressure and reservoir temperature,

cp

$(\Delta\mu)_{N_2}$ = viscosity corrections due to the presence of N_2

$(\Delta\mu)_{CO_2}$ = viscosity corrections due to the presence of CO_2

$(\Delta\mu)_{H_2S}$ = viscosity corrections due to the presence of H_2S

$(\mu_1)_{\text{uncorrected}}$ = uncorrected gas viscosity, cp

Step 3 Calculate the pseudo-reduced pressure and temperature.

Step 4 From the pseudo-reduced temperature and pressure, obtain the viscosity ratio (μ_g/μ_1) from Figure 3-6. The term μ_g represents the viscosity of the gas at the required conditions.

Step 5 The gas viscosity, μ_g , at the pressure and temperature of interest, is calculated by multiplying the viscosity at 1 atmosphere and system temperature, μ_1 , by the viscosity ratio.

The following examples illustrate the use of the proposed graphical correlations.

EXAMPLE 3-14

Using the data given in Example 3-13, calculate the viscosity of the gas.

SOLUTION

Step 1 Calculate the apparent molecular weight of the gas

$$M_a = (0.72)(28.96) = 20.85$$

Step 2 Determine the viscosity of the gas at 1 atm and 140°F from Figure 3-5:

$$\mu_1 = 0.0113$$

Step 3 Calculate p_{pr} and T_{pr} :

$$p_{pr} = 2.99$$

$$T_{pr} = 1.52$$

Step 4 Determine the viscosity rates from Figure 3-6:

$$\frac{\mu_g}{\mu_1} = 1.5$$

Step 5 Solve for the viscosity of the natural gas:

$$\mu_g = \frac{\mu_g}{\mu_1}(\mu_1) = (1.5)(0.0113) = 0.01695 \text{ cp}$$

Standing (1977) proposed a convenient mathematical expression for calculating the viscosity of the natural gas at atmospheric pressure and reservoir temperature, μ_1 . Standing also presented equations for describing the effects of N_2 , CO_2 , and H_2S on μ_1 . The proposed relationships are

$$\mu_1 = (\mu_1)_{\text{uncorrected}} + (\Delta\mu)_{N_2} + (\Delta\mu)_{CO_2} + (\Delta\mu)_{H_2S} \quad (3-57)$$

$$(\mu_1)_{\text{uncorrected}} = 8.118(10^{-3}) - 6.15(10^{-3}) \log(\gamma_g) + [1.709(10^{-5}) - 2.062(10^{-6})\gamma_g](T - 460) \quad (3-58)$$

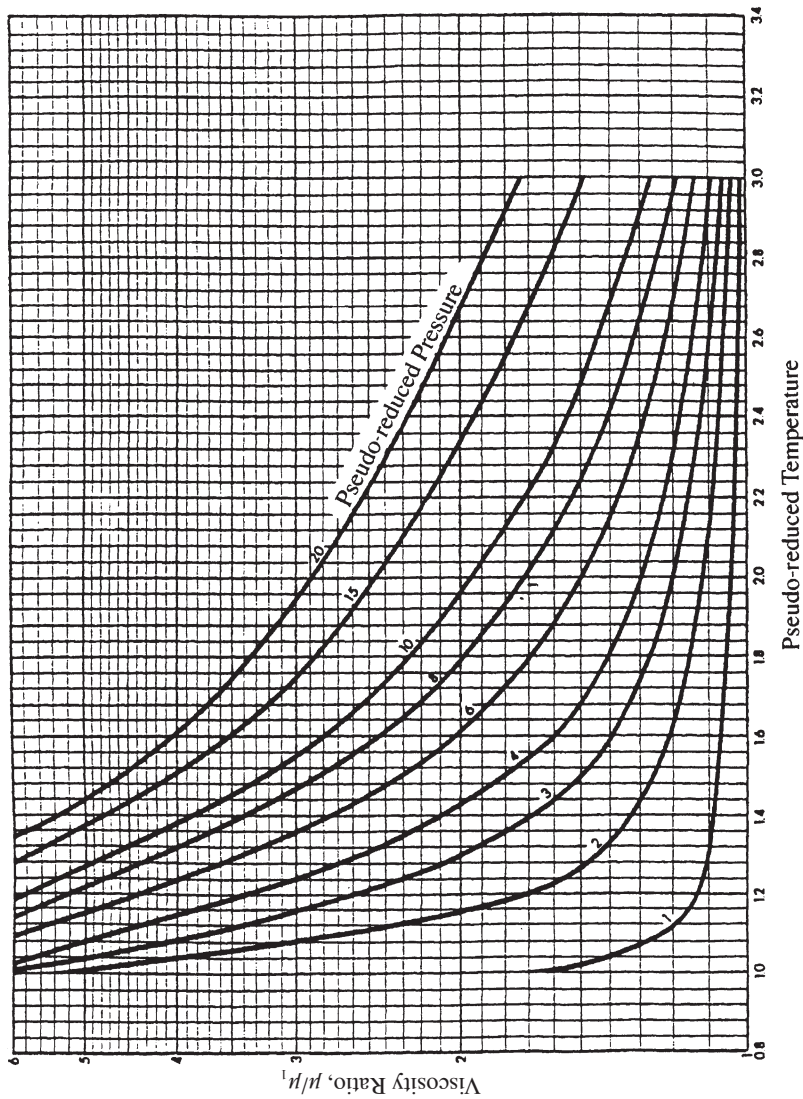


FIGURE 3-6 Carr et al.'s viscosity ratio correlation.

Source: Carr et al., "Viscosity of Hydrocarbon Gases under Pressure," *Transactions of the AIME* 201 (1954): 270-275. Permission to publish from the Society of Petroleum Engineers of the AIME. © SPE-AIME.

$$(\Delta\mu)_{N_2} = y_{N_2} [8.48(10^{-3}) \log(\gamma_g) + 9.59(10^{-3})] \quad (3-59)$$

$$(\Delta\mu)_{CO_2} = y_{CO_2} [9.08(10^{-3}) \log(\gamma_g) + 6.24(10^{-3})] \quad (3-60)$$

$$(\Delta\mu)_{H_2S} = y_{H_2S} [8.49(10^{-3}) \log(\gamma_g) + 3.73(10^{-3})] \quad (3-61)$$

where

μ_1 = viscosity of the gas at atmospheric pressure and reservoir temperature, cp

T = reservoir temperature, °R

γ_g = gas gravity; y_{N_2} , y_{CO_2} , y_{H_2S} = mole fraction of N_2 , CO_2 , and H_2S , respectively

Dempsey (1965) expressed the viscosity ratio μ_g/μ_1 by the following relationship:

$$\ln \left[T_{pr} \frac{\mu_g}{\mu_1} \right] = a_0 + a_1 p_{pr} + a_2 p_{pr}^2 + a_3 p_{pr}^3 + T_{pr} (a_4 + a_5 p_{pr} + a_6 p_{pr}^2 + a_7 p_{pr}^3) \\ + T_{pr}^2 (a_8 + a_9 p_{pr} + a_{10} p_{pr}^2 + a_{11} p_{pr}^3) + T_{pr}^3 (a_{12} + a_{13} p_{pr} + a_{14} p_{pr}^2 + a_{15} p_{pr}^3)$$

where

T_{pr} = pseudo-reduced temperature of the gas mixture

p_{pr} = pseudo-reduced pressure of the gas mixture

a_0, \dots, a_{17} = coefficients of the equations, as follows:

$a_0 = -2.46211820$	$a_8 = -7.93385648(10^{-1})$
$a_1 = 2.970547414$	$a_9 = 1.39643306$
$a_2 = -2.86264054(10^{-1})$	$a_{10} = -1.49144925(10^{-1})$
$a_3 = 8.05420522(10^{-3})$	$a_{11} = 4.41015512(10^{-3})$
$a_4 = 2.80860949$	$a_{12} = 8.39387178(10^{-2})$
$a_5 = -3.49803305$	$a_{13} = -1.86408848(10^{-1})$
$a_6 = 3.60373020(10^{-1})$	$a_{14} = 2.03367881(10^{-2})$
$a_7 = -1.044324(10^{-2})$	$a_{15} = -6.09579263(10^{-4})$

Lee-Gonzalez-Eakin's Method

Lee, Gonzalez, and Eakin (1966) presented a semi-empirical relationship for calculating the viscosity of natural gases. The authors expressed the gas viscosity in terms of the reservoir temperature, gas density, and the molecular weight of the gas. Their proposed equation is given by

$$\mu_g = 10^{-4} K \exp \left[X \left(\frac{\rho_g}{62.4} \right)^Y \right] \quad (3-62)$$

where

$$K = \frac{(9.4 + 0.02M_a)T^{1.5}}{209 + 19M_a + T} \quad (3-63)$$

$$X = 3.5 + \frac{986}{T} + 0.01M_a \quad (3-64)$$

$$Y = 2.4 - 0.2X \quad (3-65)$$

ρ = gas density at reservoir pressure and temperature, lb/ft³

T = reservoir temperature, °R

M_a = apparent molecular weight of the gas mixture

The proposed correlation can predict viscosity values with a standard deviation of 2.7% and a maximum deviation of 8.99%. The correlation is less accurate for gases with higher specific gravities. The authors pointed out that the method cannot be used for sour gases.

EXAMPLE 3-15

Rework Example 3-14 and calculate the gas viscosity by using the Lee-Gonzales-Eakin method.

SOLUTION

Step 1 Calculate the gas density from equation (3-17):

$$\rho_g = \frac{pM_a}{ZRT}$$

$$\rho_g = \frac{(2000)(20.85)}{(10.73)(600)(0.78)} = 8.3 \text{ lb/ft}^3$$

Step 2 Solve for the parameters K , X , and Y using equations (3-63), (3-64), and (3-65), respectively:

$$K = \frac{(9.4 + 0.02M_a)T^{1.5}}{209 + 19M_a + T}$$

$$K = \frac{[9.4 + 0.02(20.85)](600)^{1.5}}{209 + 19(20.85) + 600} = 119.72$$

$$X = 3.5 + \frac{986}{T} + 0.01M_a$$

$$X = 3.5 + \frac{986}{600} + 0.01(20.85) = 5.35$$

$$Y = 2.4 - 0.2X$$

$$Y = 2.4 - 0.2(5.35) = 1.33$$

Step 3 Calculate the viscosity from equation (3-62):

$$\mu_g = 10^{-4} K \exp \left[X \left(\frac{\rho_g}{62.4} \right)^Y \right]$$

$$\mu_g = 10^{-4} (119.72) \exp \left[5.35 \left(\frac{8.3}{62.4} \right)^{1.33} \right] = 0.0173 \text{ cp}$$

Specific Gravity Wet Gases

The specific gravity of a wet gas, γ_g , is described by the weighted-average of the specific gravities of the separated gas from each separator. This weighted average approach is based on the separator gas/oil ratio:

$$\gamma_g = \frac{\sum_{i=1}^n (R_{\text{sep}})_i (\gamma_{\text{sep}})_i + R_{\text{st}} \gamma_{\text{st}}}{\sum_{i=1}^n (R_{\text{sep}})_i + R_{\text{st}}} \quad (3-66)$$

where

n = number of separators

R_{sep} = separator gas/oil ratio, scf/STB

γ_{sep} = separator gas gravity

R_{st} = gas/oil ratio from the stock tank, scf/STB

γ_{st} = gas gravity from the stock tank

For wet gas reservoirs that produce liquid (condensate) at separator conditions, the produced gas mixtures normally exist as a “single” gas phase in the reservoir and production tubing. To determine the well-stream specific gravity, the produced gas and condensate (liquid) must be recombined in the correct ratio to find the average specific gravity of the “single-phase” gas reservoir. To calculate the specific gravity of the well-stream gas, let

γ_w = well-stream gas gravity

γ_o = condensate (oil) stock-tank gravity, 60°/60°

γ_g = average surface gas gravity as defined by equation (3–66)

M_o = molecular weight of the stock-tank condensate (oil)

r_p = producing oil/gas ratio (reciprocal of the gas/oil ratio, R_s), STB/scf

The average specific gravity of the well stream is given by

$$\gamma_w = \frac{\gamma_g + 4580 r_p \gamma_o}{1 + 133,000 r_p (\gamma_o / M_o)} \quad (3-67)$$

In terms of gas/oil ratio, R_s , equation (3–67) can be expressed as

$$\gamma_w = \frac{\gamma_g R_s + 4580 \gamma_o}{R_s + 133,000 \gamma_o / M_o} \quad (3-68)$$

Standing (1974) suggested the following correlation for estimating the molecular weight of the stock-tank condensate:

$$M_o = \frac{6084}{\text{API} - 5.9} \quad (3-69)$$

where API is the API gravity of the liquid as given by

$$\text{API} = \frac{141.5}{\gamma_o} - 131.5$$

Equation (3–70) should be used only in the range $45^\circ < \text{API} < 60^\circ$. Eilerts (1947) proposed an expression for the ratio γ_o / M_o as a function of the condensate stock-tank API gravity:

$$\gamma_o / M_o = 0.001892 + 7.35 (10^{-5}) \text{API} - 4.52 (10^{-8}) (\text{API})^2 \quad (3-70)$$

In retrograde and wet gas reservoirs calculations, it is convenient to express the produced separated gas as a fraction of the total system produced. This fraction f_g can be expressed in terms of the separated moles of gas and liquid as

$$f_g = \frac{n_g}{n_t} = \frac{n_g}{n_g + n_l} \quad (3-71)$$

where

f_g = fraction of the separated gas produced in the entire system

n_g = number of moles of the separated gas

n_l = number of moles of the separated liquid

n_t = total number of moles of the well stream

For a total producing gas/oil ratio of R_s scf/STB, the equivalent number of moles of gas as described by equation (3-6) is

$$n_g = R_s / 379.4 \quad (3-72)$$

The number of moles of 1 STB of the separated condensate is given by

$$n_o = \frac{\text{mass}}{\text{molecular weight}} = \frac{(\text{volume})(\text{density})}{M_o}$$

or

$$n_o = \frac{(1)(5.615)(62.4)\gamma_o}{M_o} = \frac{350.4\gamma_o}{M_o} \quad (3-73)$$

Substituting equations (3-72) and (3-73) into equation (3-71) gives

$$f_g = \frac{R_s}{R_s + 133,000(\gamma_o / M_o)} \quad (3-74)$$

When applying the material balance equation for a gas reservoir, it assumes that a volume of gas in the reservoir will remain as a gas at surface conditions. When liquid is separated, the cumulative liquid volume must be converted into an equivalent gas volume, V_{eq} , and *added to the cumulative gas production* for use in the material balance equation. If N_p STB of liquid (condensate) has been produced, the equivalent number of moles of liquid is given by equation (3-73) as

$$n_o = \frac{(N_p)(5.615)(62.4)\gamma_o}{M_o} = \frac{350.4\gamma_o N_p}{M_o}$$

Expressing this number of moles of liquid as an *equivalent gas volume* at standard conditions by applying the ideal gas equation of state gives

$$V_{eq} = \frac{n_o RT_{sc}}{p_{sc}} = \left(\frac{350.4\gamma_o N_p}{M_o} \right) \frac{(10.73)(520)}{14.7}$$

Simplifying the above expression to give V_{eq} ,

$$V_{eq} = 133,000 \frac{\gamma_o N_p}{M_o}$$

More conveniently, the equivalent gas volume can be expressed in scf/STB as

$$V_{eq} = 133,000 \frac{\gamma_o}{M_o} \quad (3-75)$$

where

V_{eq} = equivalent gas volume, scf/STB

N_p = cumulative, or daily, liquid volume, STB

γ_o = specific gravity of the liquid, 60°/60°

M_o = molecular weight of the liquid

EXAMPLE 3-16

The following data is available on a wet gas reservoir:

- Initial reservoir pressure $p_i = 3200$ psia.
- Reservoir temperature $T = 200^\circ\text{F}$.
- Average porosity $\phi = 18\%$.
- Average connate water saturation $S_{wi} = 30\%$.
- Condensate daily flow rate $Q_o = 400$ STB/day.
- API gravity of the condensate = 50°.
- Daily separator gas rate $Q_{gsep} = 4.20$ MM scf/day.
- Separator gas specific gravity $\gamma_{sep} = 0.65$.
- Daily stock-tank gas rate $Q_{gst} = 0.15$ MM scf/day.
- Stock-tank gas specific gravity $\gamma_{gst} = 1.05$.

Based on 1 acre-foot sand volume, calculate the initial oil (condensate) and gas in place and the daily well-stream gas flow rate in scf/day.

SOLUTION FOR INITIAL OIL AND GAS IN PLACE

Step 1 Use equation (3-66) to calculate the specific gravity of the separated gas:

$$\gamma_g = \frac{\sum_{i=1}^n (R_{sep})_i (\gamma_{sep})_i + R_{st} \gamma_{st}}{\sum_{i=1}^n (R_{sep})_i + R_{st}} = \frac{(R_{sep})_1 (\gamma_{sep})_1 + R_{st} \gamma_{st}}{(R_{sep})_1 + R_{st}}$$

$$\gamma_g = \frac{(4.2)(0.65) + (0.15)(1.05)}{4.2 + 0.15} = 0.664$$

Step 2 Calculate liquid specific gravity:

$$\gamma_o = \frac{141.5}{\text{API} + 131.5} = \frac{141.5}{50 + 131.5} = 0.780$$

Step 3 Estimate the molecular weight of the liquid by applying equation (3-69):

$$M_o = \frac{6084}{\text{API} - 5.9}$$

$$M_o = \frac{6084}{50 - 5.9} = 138 \text{ lb/lb-mole}$$

Step 4 Calculate the producing gas/oil ratio:

$$R_s = \frac{Q_g}{Q_o} = \frac{(4.2)(10^6) + (0.15)(10^6)}{400} = 10,875 \text{ scf/STB}$$

Step 5 Calculate the well-stream specific gravity from equation (3-68):

$$\gamma_w = \frac{(0.664)(10,875) + (4,580)(0.78)}{10,875 + (133,000)(0.78/138)} = 0.928$$

Step 6 Solve for the pseudo-critical properties of this wet gas using equations (3-20) and (3-21):

$$T_{pc} = 187 + 330(0.928) - 71.5(0.928)^2 = 432^\circ\text{R}$$

$$p_{pc} = 706 - 51.7(0.928) - 11.1(0.928)^2 = 648 \text{ psi}$$

Step 7 Calculate the pseudo-reduced properties by applying equations (3-12) and (3-13):

$$p_{pr} = \frac{3200}{648} = 4.9$$

$$T_{pr} = \frac{200 + 460}{432} = 1.53$$

Step 8 Determine the Z-factor from Figure 3-1 to give

$$Z = 0.81$$

Step 9 Calculate the hydrocarbon space per acre-foot at reservoir conditions:

$$V_{Hy} = 43,560(Ab)\phi(1 - S_{wi}), \text{ ft}^3$$

$$V_{Hy} = 43,560(1)(0.18)(1 - 0.2) = 6273 \text{ ft}^3/\text{ac-ft}$$

Step 10 Calculate total moles of gas per acre-foot at reservoir conditions by applying the real gas equation of state, equation (3-11):

$$n = \frac{PV}{ZRT} = \frac{(3200)(6273)}{(0.81)(10.73)(660)} = 3499 \text{ moles/ac-ft}$$

Step 11 Because 1 mole of gas occupies 379.4 scf (see equation 3-6) calculate the total gas initially in place per acre-foot, to give

$$G = (379.4)(3499) = 1328 \text{ Mscf/ac-ft}$$

If all this gas quantity is produced at the surface, a portion of it will be produced as stock-tank condensate.

Step 12 Calculate the fraction of the total that is produced as gas at the surface from equation (3-75):

$$f_g = \frac{10,875}{10,875 + 133,000(0.78/138)} = 0.935$$

Step 13 Calculate the initial gas and oil in place:

$$\text{Initial gas in place} = Gf_g = (1328)(0.935) = 1242 \text{ Mscf/ac-ft}$$

$$\text{Initial oil in place} = \frac{G}{R_s} = \frac{1328(10^3)}{10,875} = 122 \text{ STB/ac-ft}$$

SOLUTION FOR DAILY WELL-STREAM GAS RATE

Step 1 Calculate the equivalent gas volume from equation (3-75):

$$V_{eq} = 133,000 \frac{\gamma_o}{M_o}$$

$$V_{eq} = 133,000 \left(\frac{0.78}{138} \right) = 752 \text{ scf/STB}$$

Step 2 Calculate the total well-stream gas flow rate:

$$Q_g = \text{Total}(Q_g)_{sep} + V_{eq} Q_o$$

$$Q_g = (4.2 + 0.15)10^6 + (752)(400) = 4.651 \text{ MMscf/day}$$

Problems

1. Assuming an ideal gas behavior, calculate the density of n-butane at 200°F and 50 psia. Recalculate the density assuming real gas behavior.
2. Show that

$$y_i = \frac{w_i / M_i}{\sum_i (w_i / M_i)}$$

3. Given the following weight fractions of a gas:

COMPONENT	y_i
C ₁	0.60
C ₂	0.17
C ₃	0.13
n-C ₄	0.06
n-C ₅	0.04

Calculate

- a. Mole fraction of the gas.
 - b. Apparent molecular weight.
 - c. Specific gravity, and specific volume at 300 psia and 130°F, assuming an ideal gas behavior.
 - d. Density at 300 psia and 130°F, assuming real gas behavior.
 - e. Gas viscosity at 300 psia and 130°F.
4. An ideal gas mixture has a density of 2.15 lb/ft³ at 600 psia and 100°F. Calculate the apparent molecular weight of the gas mixture.
 5. Using the gas composition as given in problem 3 and assuming real gas behavior, calculate
 - a. Gas density at 2500 psia and 160°F.
 - b. Specific volume at 2500 psia and 160°F.
 - c. Gas formation volume factor in scf/ft³.
 - d. Gas viscosity.
 6. A natural gas with a specific gravity of 0.75 has a measured gas formation volume factor of 0.00529 ft³/scf at the current reservoir pressure and temperature. Calculate the density of the gas.

7. A natural gas has the following composition:

COMPONENT	y_i
C ₁	0.80
C ₂	0.07
C ₃	0.03
i-C ₄	0.04
n-C ₄	0.03
i-C ₅	0.02
n-C ₅	0.01

Reservoir conditions are 3500 psia and 200°F. Using, first, the Carr-Kobayashi-Burrows method, then the Lee-Gonzales-Eakin method, calculate

- Isothermal gas compressibility coefficient.
- Gas viscosity.

8. Given the following gas composition:

COMPONENT	y_i
CO ₂	0.06
N ₂	0.003
C ₁	0.80
C ₂	0.05
C ₃	0.03
n-C ₄	0.02
n-C ₅	0.01

If the reservoir pressure and temperature are 2500 psia and 175°F, respectively, calculate

- Gas density by accounting for the presence of nonhydrocarbon components using the Wichert-Aziz method, then the Carr-Kobayashi-Burrows method.
 - Isothermal gas compressibility coefficient.
 - Gas viscosity using the Carr-Kobayashi-Burrows method, then the Lee-Gonzales-Eakin method.
9. A high-pressure cell has a volume of 0.33 ft³ and contains gas at 2500 psia and 130°F, at which conditions its Z-factor is 0.75. When 43.6 scf of the gas are bled from the cell, the pressure drops to 1000 psia while the temperature remains at 130°F. What is the gas deviation factor at 1000 psia and 130°F.
10. A hydrocarbon gas mixture with a specific gravity of 0.65 has a density of 9 lb/ft³ at the prevailing reservoir pressure and temperature. Calculate the gas formation volume factor in bbl/scf.
11. A gas reservoir exists at a 150°F. The gas has the following composition:
- C₁ = 89 mol%
C₂ = 7 mol%
C₃ = 4 mol%

The gas expansion factory, E_g , was calculated as 210 scf/ft³ at the existing reservoir pressure and temperature. Calculate the viscosity of the gas.

12. A 20 ft³ tank at a pressure of 2500 psia and 200°F contains ethane gas. How many pounds of ethane are in the tank?
13. A gas well is producing dry gas with a specific gravity of 0.60. The gas flow rate is 1.2 MMft³/day at a bottom-hole flowing pressure of 1200 psi and temperature of 140°F. Calculate the gas flow rate in MMscf/day.
14. The following data are available on a wet gas reservoir:
 - Initial reservoir pressure, $P_i = 40,000$ psia
 - Reservoir temperature, $T = 150^\circ\text{F}$
 - Average porosity, $\phi = 15\%$
 - Average connate water saturation, $S_{wi} = 25\%$
 - Condensate daily flow rate, $Q_o = 350$ STB/day
 - API gravity of the condensate, $= 52^\circ$
 - Daily separator gas rate, $Q_{gsep} = 3.80$ MMscf/day
 - Separator gas specific gravity, $\gamma_{sep} = 0.71$
 - Daily stock-tank gas rate, $Q_{gst} = 0.21$ MMscf/day
 - Stock-tank gas specific gravity, $\gamma_{gst} = 1.02$
 Based on 1 acre-foot sand volume, calculate
 - a. Initial oil (condensate) and gas in place.
 - b. Daily well-stream gas flow rate in scf/day.

References

- Brown, et al. *Natural Gasoline and the Volatile Hydrocarbons*. Tulsa, OK: National Gas Association of America, 1948.
- Carr, N., R. Kobayashi, and D. Burrows. "Viscosity of Hydrocarbon Gases under Pressure." *Transactions of the AIME* 201 (1954): 270–275.
- Dempsey, J. R. "Computer Routine Treats Gas Viscosity as a Variable." *Oil and Gas Journal* (August 16, 1965): 141–143.
- Dranchuk, P. M., and J. H. Abu-Kassem. "Calculate of Z-factors for Natural Gases Using Equations-of-State." *Journal of Canadian Petroleum Technology* (July–September 1975): 34–36.
- Dranchuk, P. M., R. A. Purvis, and D. B. Robinson. "Computer Calculations of Natural Gas Compressibility Factors Using the Standing and Katz Correlation." Technical Series, no. IP 74-008. Alberta, Canada: Institute of Petroleum, 1974.
- Eilerts, C. "The Reservoir Fluid, Its Composition and Phase Behavior." *Oil and Gas Journal* (January 1, 1947).
- Hall, K. R., and L. Yarborough. "A New Equation of State for Z-factor Calculations." *Oil and Gas Journal* (June 18, 1973): 82–92.
- Lee, A. L., M. H. Gonzalez, and B. E. Eakin. "The Viscosity of Natural Gases." *Journal of Petroleum Technology* (August 1966): 997–1000.
- Mattar, L. G., S. Brar, and K. Aziz. "Compressibility of Natural Gases." *Journal of Canadian Petroleum Technology* (October–November 1975): 77–80.

- Matthews, T., C. Roland, and D. Katz. "High Pressure Gas Measurement." Proceedings of the Natural Gas Association of America (NGAA), 1942.
- Papay, J. "A Termelstechnologiai Parameterek Valtozasa a Gazlelepk Muvelese Soran." *OGIL MUSZ*, Tud, Kuzl. [Budapest] (1985): 267–273.
- Standing, M. *Petroleum Engineering Data Book*. Trondheim: Norwegian Institute of Technology, 1974.
- Standing, M. B. *Volumetric and Phase Behavior of Oil Field Hydrocarbon Systems*. Dallas: Society of Petroleum Engineers, 1977, pp. 125–126.
- Standing, M. B., and D. L. Katz. "Density of Natural Gases." *Transactions of the AIME* 146 (1942): 140–149.
- Stewart, W. F., S. F. Burkhard, and D. Voo. "Prediction of Pseudo-Critical Parameters for Mixtures." Paper presented at the AIChE Meeting, Kansas City, MO, 1959.
- Sutton, R. P. M. "Compressibility Factors for High-Molecular-Weight Reservoir Gases." Paper SPE 14265, presented at the 60th annual Technical Conference and Exhibition of the Society of Petroleum Engineers, Las Vegas, September 22–25, 1985.
- Trube, A. S. "Compressibility of Undersaturated Hydrocarbon Reservoir Fluids." *Transactions of the AIME* 210 (1957a): 341–344.
- Trube, A. S. "Compressibility of Natural Gases." *Transactions of the AIME* 210 (1957b): 355–357.
- Whitson, C. H., and M. R. Brule. *Phase Behavior*. Richardson, TX: Society of Petroleum Engineers, 2000.
- Wichert, E., and K. Aziz. "Calculation of Z's for Sour Gases." *Hydrocarbon Processing* 51, no. 5 (1972): 119–122.

4

PVT Properties of Crude Oils

PETROLEUM (an equivalent term is *crude oil*) is a complex mixture consisting predominantly of hydrocarbons and containing sulfur, nitrogen, oxygen, and helium as minor constituents. The physical and chemical properties of crude oils vary considerably and depend on the concentration of the various types of hydrocarbons and minor constituents present.

An accurate description of physical properties of crude oils is of a considerable importance in the fields of both applied and theoretical science and especially in the solution of petroleum reservoir engineering problems. Physical properties of primary interest in petroleum engineering studies include

- Fluid gravity.
- Specific gravity of the solution gas.
- Oil density.
- Gas solubility.
- Bubble-point pressure.
- Oil formation volume factor.
- Isothermal compressibility coefficient of undersaturated crude oils.
- Undersaturated oil properties.
- Total formation volume factor.
- Crude oil viscosity.
- Surface tension.

Data on most of these fluid properties is usually determined by laboratory experiments performed on samples of actual reservoir fluids. In the absence of experimentally

measured properties of crude oils, it is necessary for the petroleum engineer to determine the properties from empirically derived correlations.

Crude Oil Gravity

The crude oil density is defined as the mass of a unit volume of the crude at a specified pressure and temperature. It is usually expressed in pounds per cubic foot. The specific gravity of a crude oil is defined as the ratio of the density of the oil to that of water. Both densities are measured at 60°F and atmospheric pressure:

$$\gamma_o = \frac{\rho_o}{\rho_w} \quad (4-1)$$

where

γ_o = specific gravity of the oil

ρ_o = density of the crude oil, lb/ft³

ρ_w = density of the water, lb/ft³

It should be pointed out that the liquid specific gravity is dimensionless but traditionally is given the units 60°/60° to emphasize that both densities are measured at standard conditions. The density of the water is approximately 62.4 lb/ft³, or

$$\gamma_o = \frac{\rho_o}{62.4}, 60^\circ/60^\circ$$

Although the density and specific gravity are used extensively in the petroleum industry, the API gravity is the preferred gravity scale. This gravity scale is precisely related to the specific gravity by the following expression:

$$\text{API} = \frac{141.5}{\gamma_o} - 131.5 \quad (4-2)$$

This equation can be also rearranged to express the oil specific gravity in terms of the API gravity:

$$\gamma_o = \frac{141.5}{131.5 + \text{API}}$$

The API gravities of crude oils usually range from 47° API for the lighter crude oils to 10° API for the heavier asphaltic crude oils.

EXAMPLE 4-1

Calculate the specific gravity and the API gravity of a crude oil system with a measured density of 53 lb/ft³ at standard conditions.

SOLUTION

Step 1 Calculate the specific gravity from equation (4-1):

$$\gamma_o = \frac{\rho_o}{\rho_w}$$

$$\gamma_o = \frac{53}{62.4} = 0.849$$

Step 2 Solve for the API gravity:

$$\text{API} = \frac{141.5}{\gamma_o} - 131.5$$

$$\text{API} = \frac{141.5}{0.849} - 131.5 = 35.2^\circ \text{API}$$

Specific Gravity of the Solution Gas

The specific gravity of the solution gas, γ_g , is described by the weighted average of the specific gravities of the separated gas from each separator. This weighted average approach is based on the separator gas/oil ratio:

$$\gamma_g = \frac{\sum_{i=1}^n (R_{\text{sep}})_i (\gamma_{\text{sep}})_i + R_{\text{st}} \gamma_{\text{st}}}{\sum_{i=1}^n (R_{\text{sep}})_i + R_{\text{st}}} \quad (4-3)$$

where

n = number of separators

R_{sep} = separator gas/oil ratio, scf/STB

γ_{sep} = separator gas gravity

R_{st} = gas/oil ratio from the stock tank, scf/STB

γ_{st} = gas gravity from the stock tank

EXAMPLE 4-2

Separator tests were conducted on a crude oil sample. Results of the test in terms of the separator gas/oil ratio and specific gravity of the separated gas are given in the table below. Calculate the specific gravity of the separated gas.

Separator	Pressure (psig)	Temperature (°F)	Gas/Oil Ratio (scf/STB)	Gas Specific Gravity
Primary	660	150	724	0.743
Intermediate	75	110	202	0.956
Stock tank	0	60	58	1.296

SOLUTION

Estimate the specific gravity of the solution using equation (4-3):

$$\gamma_g = \frac{\sum_{i=1}^{n=2} (R_{\text{sep}})_i (\gamma_{\text{sep}})_i + R_{\text{st}} \gamma_{\text{st}}}{\sum_{i=1}^{n=2} (R_{\text{sep}})_i + R_{\text{st}}}$$

$$\gamma_g = \frac{(724)(0.743) + (202)(0.956) + (58)(1.296)}{724 + 202 + 58} = 0.819$$

Ostermann et al. (1987) proposed a correlation to account for the increase of the gas gravity of a solution gas drive reservoir with decreasing the reservoir pressure, p , below the bubble-point pressure, p_b . The authors expressed the correlation in the following form:

$$\gamma_g = \gamma_{gi} \left\{ 1 + \frac{a[1 - (p/p_b)]^b}{(p/p_b)} \right\}$$

Parameters a and b are functions of the bubble-point pressure, given by the following two polynomials:

$$a = 0.12087 - 0.06897p_b + 0.01461(p_b)^2$$

$$b = -1.04223 + 2.17073p_b - 0.68851(p_b)^2$$

where

γ_g = specific gravity of the solution gas at pressure p

γ_{gi} = initial specific gravity of the solution gas at the bubble-point pressure p_b

p_b = bubble-point pressure, psia

p = reservoir pressure, psia

Crude Oil Density

The crude oil density is defined as the mass of a unit volume of the crude at a specified pressure and temperature, mass/volume. The density usually is expressed in pounds per cubic foot and it varies from 30 lb/ft³ for light volatile oil to 60 lb/ft³ for heavy crude oil with little or no gas solubility. It is one of the most important oil properties, because its value substantially affects crude oil volume calculations. This vital oil property is measured in the laboratory as part of routine PVT tests. When laboratory crude oil density measurement is not available, correlations can be used to generate the required density data under reservoir pressure and temperature. Numerous empirical correlations for calculating the density of liquids have been proposed over the years. Based on the available limited measured data on the crude, the correlations can be divided into the following two categories:

- Correlations that use the crude oil composition to determine the density at the prevailing pressure and temperature.
- Correlations that use limited PVT data, such as gas gravity, oil gravity, and gas/oil ratio, as correlating parameters.

Density Correlations Based on the Oil Composition

Several reliable methods are available for determining the density of saturated crude oil mixtures from their compositions. The best known and most widely used calculation methods are the following two: Standing-Katz (1942) and Alani-Kennedy (1960). These two methods, presented next, calculate oil densities from their compositions at or below the bubble-point pressure.

Standing-Katz's Method

Standing and Katz (1942) proposed a graphical correlation for determining the density of hydrocarbon liquid mixtures. The authors developed the correlation from evaluating experimental, compositional, and density data on 15 crude oil samples containing up to 60 mol% methane. The proposed method yielded an average error of 1.2% and maximum

error of 4% for the data on these crude oils. The original correlation had no procedure for handling significant amounts of nonhydrocarbons.

The authors expressed the density of hydrocarbon liquid mixtures as a function of pressure and temperature by the following relationship:

$$\rho_o = \rho_{sc} + \Delta\rho_p - \Delta\rho_T \quad (4-4)$$

where

ρ_o = crude oil density at p and T , lb/ft³

ρ_{sc} = crude oil density (with all the dissolved solution gas) at standard conditions, that is, 14.7 psia and 60°F, lb/ft³

$\Delta\rho_p$ = density correction for compressibility of oils, lb/ft³

$\Delta\rho_T$ = density correction for thermal expansion of oils, lb/ft³

Standing and Katz correlated graphically the liquid density at standard conditions ρ_{sc} with the density of the propane-plus fraction, $\rho_{C_{3+}}$, the weight percent of methane in the entire system, $(m_{C_1})_{C_{1+}}$, and the weight percent of ethane in the ethane plus, $(m_{C_2})_{C_{2+}}$.

This graphical correlation is shown in Figure 4-1. The proposed calculation procedure is performed on the basis of 1 lb-mole, that is, $n_t = 1$, of the hydrocarbon system. The following are the specific steps in the Standing and Katz procedure of calculating the liquid density at a specified pressure and temperature.

Step 1 Calculate the total weight and the weight of each component in 1 lb-mole of the hydrocarbon mixture by applying the following relationships:

$$m_i = x_i M_i$$

$$m_t = \sum x_i M_i$$

where

m_i = weight of component i in the mixture, lb/lb-mole

x_i = mole fraction of component i in the mixture

M_i = molecular weight of component i

m_t = total weight of 1 lb-mole of the mixture, lb/lb-mole

Step 2 Calculate the weight percent of methane in the entire system and the weight percent of ethane in the ethane-plus from the following expressions:

$$(m_{C_1})_{C_{1+}} = \left[\frac{x_{C_1} M_{C_1}}{\sum_{i=1}^n x_i M_i} \right] 100 = \left[\frac{m_{C_1}}{m_t} \right] 100 \quad (4-5)$$

and

$$(m_{C_2})_{C_{2+}} = \left[\frac{x_{C_2} M_{C_2}}{m_{C_{2+}}} \right] 100 = \left[\frac{m_{C_2}}{m_t - m_{C_1}} \right] 100 \quad (4-6)$$

where

$(m_{C_1})_{C_{1+}}$ = weight percent of methane in the entire system

m_{C_1} = weight of methane in 1 lb-mole of the mixture, that is, $x_{C_1} M_{C_1}$

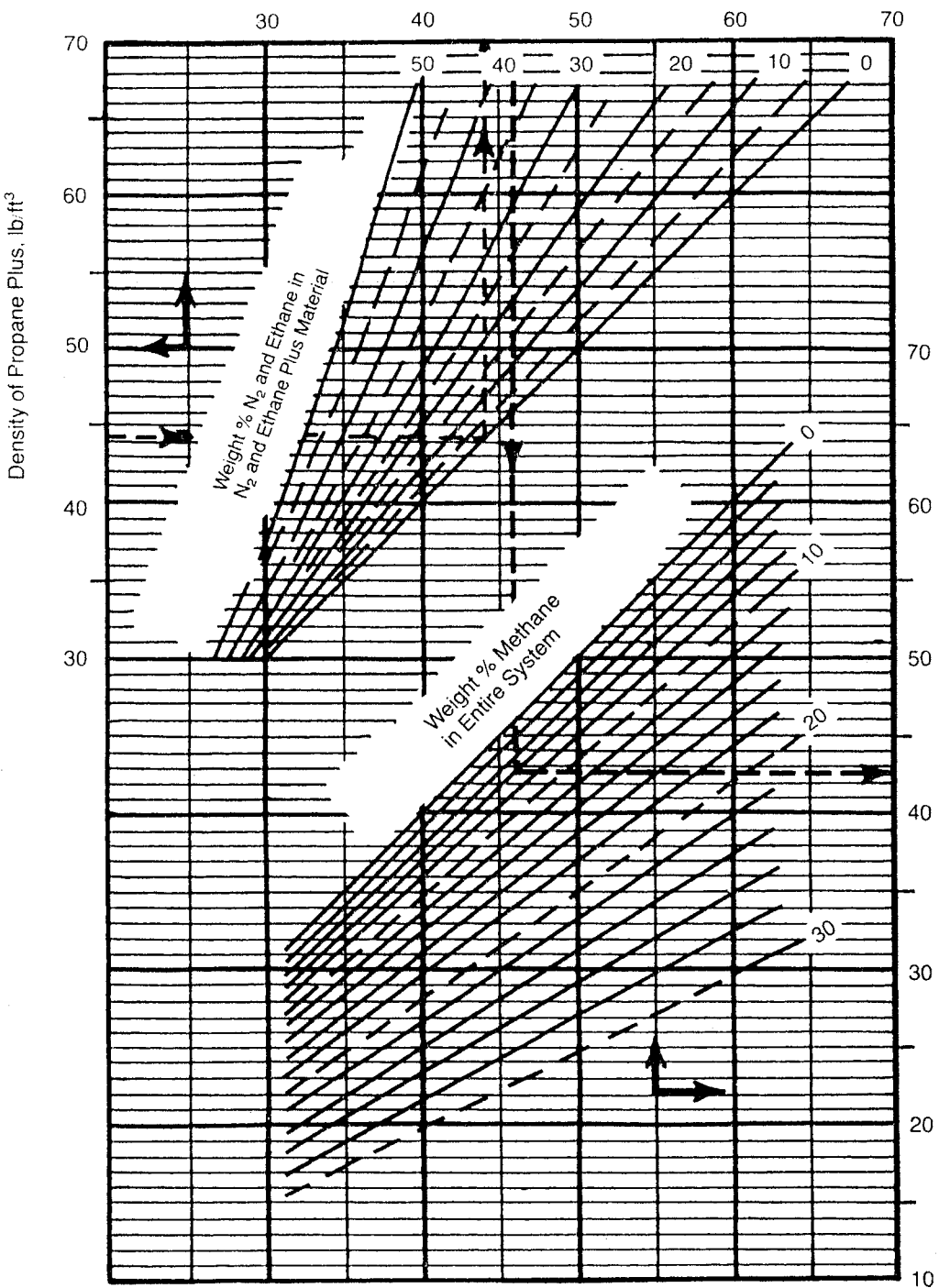


FIGURE 4-1 Standing and Katz density correlation.

Source: GPSA Engineering Data Book, 10th ed. Tulsa, OK: Gas Processors Suppliers Association, 1987. Courtesy of the Gas Processors Suppliers Association.

$(m_{C_2})_{C_{2+}}$ = weight percent of ethane in ethane-plus

m_{C_2} = weight of ethane in 1 lb-mole of the mixture, that is, $x_{C_{21}} M_{C_2}$

M_{C_1} = molecular weight of methane

M_{C_2} = molecular weight of ethane

Step 3 Calculate the density of the propane-plus fraction at standard conditions by using the following equations:

$$\rho_{C_{3+}} = \frac{m_{C_{3+}}}{V_{C_{3+}}} = \frac{\sum_{i=C_3}^n x_i M_i}{\sum_{i=C_3}^n \frac{x_i M_i}{\rho_{oi}}} = \frac{m_t - m_{C_1} - m_{C_2}}{\sum_{i=C_3}^n \frac{x_i M_i}{\rho_{oi}}} \quad (4-7)$$

with

$$m_{C_{3+}} = \sum_{i=C_3} x_i M_i \quad (4-8)$$

$$V_{C_{3+}} = \sum_{i=C_3} V_i = \sum_{i=C_3} \frac{m_i}{\rho_{oi}} \quad (4-9)$$

where

$\rho_{C_{3+}}$ = density of the propane and heavier components, lb/ft³

$m_{C_{3+}}$ = weight of the propane and heavier components, lb/ft³

$V_{C_{3+}}$ = volume of the propane-plus fraction, ft³/lb-mole

V_i = volume of component i in 1 lb-mole of the mixture

m_i = weight of component i , that is, $x_i M_i$, lb/lb-mole

ρ_{oi} = Density of component i at standard conditions, lb/ft³ (density values for pure components are tabulated in Table 1-1 in Chapter 1, but the density of the plus fraction must be measured)

Step 4 Using Figure 4-1, enter the $\rho_{C_{3+}}$ value into the left ordinate of the chart and move horizontally to the line representing $(m_{C_2})_{C_{2+}}$, then drop vertically to the line representing $(m_{C_1})_{C_{1+}}$. The density of the oil at standard condition is read on the right side of the chart. Standing (1977) expressed the graphical correlation in the following mathematical form:

$$\rho_{sc} = \rho_{C_{2+}} \left[1 - 0.012(m_{C_1})_{C_{1+}} - 0.000158(m_{C_1})_{C_{1+}}^2 \right] + 0.0133(m_{C_1})_{C_{1+}} + 0.00058(m_{C_1})_{C_{2+}}^2 \quad (4-10)$$

with:

$$\rho_{C_{2+}} = \rho_{C_{3+}} \left[1 - 0.01386(m_{C_2})_{C_{2+}} - 0.000082(m_{C_2})_{C_{2+}}^2 \right] + 0.379(m_{C_2})_{C_{2+}} + 0.0042(m_{C_2})_{C_{2+}}^2 \quad (4-11)$$

where $\rho_{C_{2+}}$ = density of the ethane-plus fraction.

Step 5 Correct the density at standard conditions to the actual pressure by reading the additive pressure correction factor, $\Delta\rho_p$, from Figure 4-2:

$$\rho_{p,60} = \rho_{sc} + \Delta\rho_p$$

The pressure correction term $\Delta\rho_p$ can be expressed mathematically by

$$\Delta\rho_p = [0.000167 + (0.016181)10^{-0.0425 \rho_{sc}}]p - (10^{-8})[0.299 + (263)10^{-0.0603 \rho_{sc}}]p^2 \quad (4-12)$$

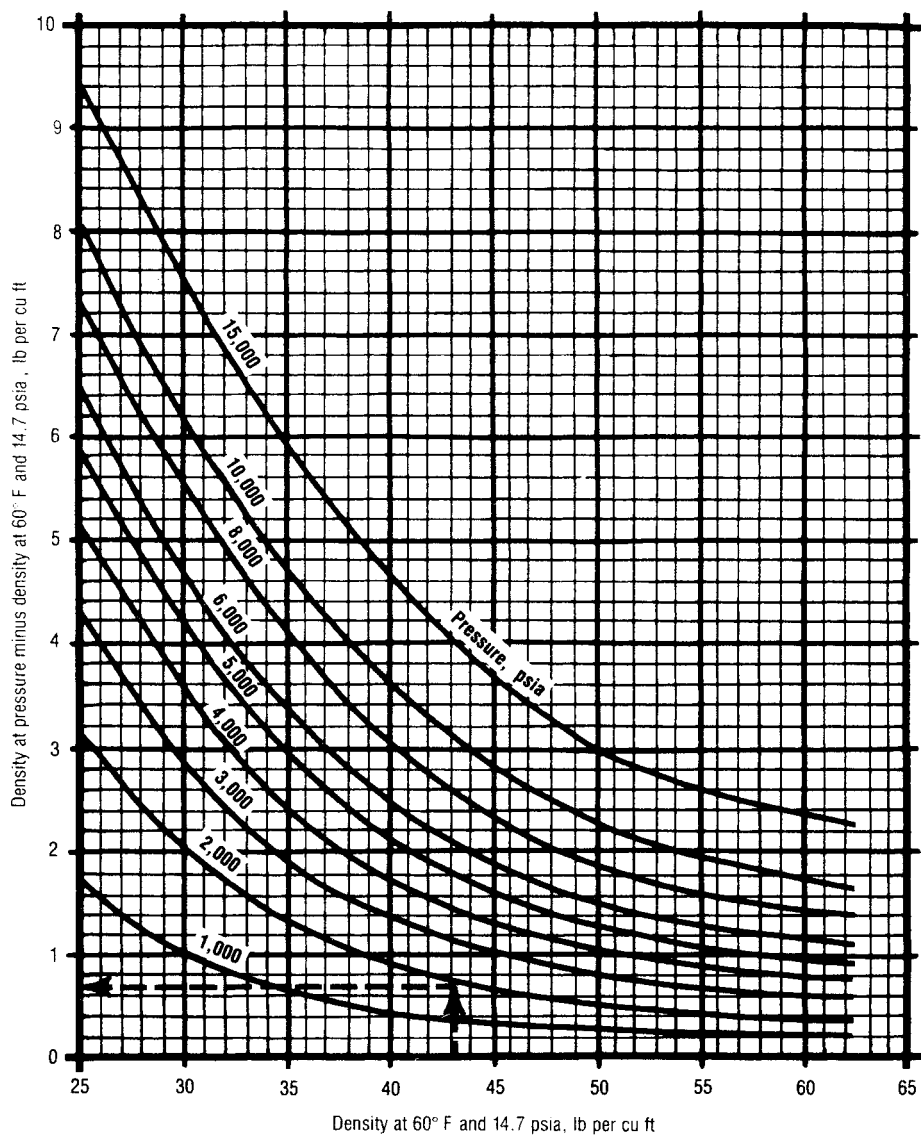


FIGURE 4-2 *Density correction for the compressibility of crude oils.*
Source: GPSA Engineering Data Book, 10th ed. Tulsa, OK: Gas Processors Suppliers Association, 1987. Courtesy of the Gas Processors Suppliers Association.

Step 6 Correct the density at 60°F and pressure to the actual temperature by reading the thermal expansion correction term, $\Delta\rho_T$, from Figure 4-3:

$$\rho_o = \rho_{p,60} - \Delta\rho_T$$

The thermal expansion correction term, $\Delta\rho_T$, can be expressed mathematically by

$$\Delta\rho_T = (T - 520) \left[0.0133 + 152.4(\rho_{sc} + \Delta\rho_p)^{-2.45} \right] - (T - 520)^2 \left[8.1(10^{-6}) - (0.0622)10^{-0.0764(\rho_{sc} + \Delta\rho_p)} \right] \tag{4-13}$$

where T is the system temperature in °R.

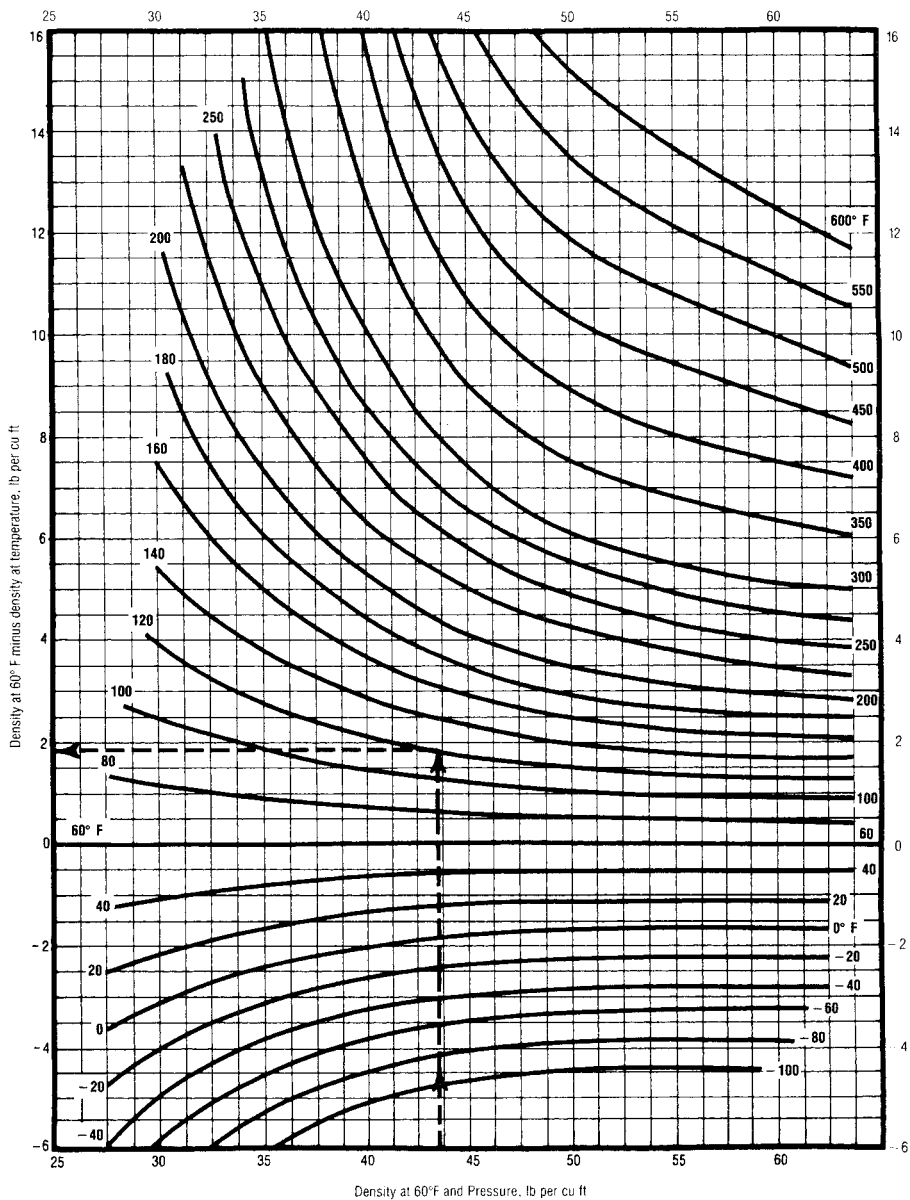


FIGURE 4-3 *Density correction for the isothermal expansion of crude oils.*

Source: GPSA Engineering Data Book, 10th ed. Tulsa, OK: Gas Processors Suppliers Association, 1987. Courtesy of the Gas Processors Suppliers Association.

EXAMPLE 4-3

A crude oil system has the following composition:

COMPONENT	x_i
C_1	0.45
C_2	0.05
C_3	0.05
C_4	0.03

COMPONENT	x_i
C ₅	0.01
C ₆	0.01
C ₇₊	0.40

If the molecular weight and specific gravity of the C₇₊ fractions are 215 and 0.87, respectively, calculate the density of the crude oil at 4000 psia and 160°F using the Standing and Katz method.

SOLUTION

The table below shows the values of the components.

Component	x_i	M_i	$m_i = x_i M_i$	ρ_{oi}^* , lb/ft ^{3*}	$V_i = m_i / \rho_{oi}$
C ₁	0.45	16.04	7.218	—	—
C ₂	0.05	30.07	1.5035	—	—
C ₃	0.05	44.09	2.2045	31.64	0.0697
C ₄	0.03	58.12	1.7436	35.71	0.0488
C ₅	0.01	72.15	0.7215	39.08	0.0185
C ₆	0.01	86.17	0.8617	41.36	0.0208
C ₇₊	0.40	215.0	86.00	54.288**	1.586
$\Sigma = m_t = 100.253$				$\Sigma = V_{C_{3+}} = 1.7418$	

*From Table 1-1.
** $\rho_{C_{7+}} = (0.87)(62.4) = 54.288$

Step 1 Calculate the weight percent of C₁ in the entire system and the weight percent of C₂ in the ethane-plus fraction:

$$\begin{aligned} (m_{C_1})_{C_{1+}} &= \left[\frac{x_{C_1} M_{C_1}}{\sum_{i=1}^n x_i M_i} \right] 100 = \left[\frac{m_{C_1}}{m_t} \right] 100 \\ (m_{C_1})_{C_{1+}} &= \left[\frac{7.218}{100.253} \right] 100 = 7.2\% \\ (m_{C_2})_{C_{2+}} &= \left[\frac{x_{C_2} M_{C_2}}{m_{C_{2+}}} \right] 100 = \left[\frac{m_{C_2}}{m_t - m_{C_1}} \right] 100 \\ (m_{C_2})_{C_{2+}} &= \left[\frac{1.5035}{100.253 - 7.218} \right] 100 = 1.616\% \end{aligned}$$

Step 2 Calculate the density of the propane and heavier:

$$\begin{aligned} \rho_{C_{3+}} &= \frac{m_{C_{3+}}}{V_{C_{3+}}} = \frac{m_t - m_{C_1} - m_{C_2}}{\sum_{i=C_3}^n \frac{x_i M_i}{\rho_{oi}}} \\ \rho_{C_{3+}} &= \frac{100.253 - 7.218 - 1.5035}{1.7418} = 52.55 \text{ lb/ft}^3 \end{aligned}$$

Step 3 Determine the density of the oil at standard conditions from Figure 4-1:

$$\rho_{sc} = 47.5 \text{ lb/ft}^3$$

Step 4 Correct for the pressure using Figure 4-2:

$$\Delta \rho_p = 1.18 \text{ lb/ft}^3$$

Density of the oil at 4000 psia and 60°F is then calculated by the expression

$$\rho_{p,60} = \rho_{sc} + \Delta \rho_p = 47.5 + 1.18 = 48.68 \text{ lb/ft}^3$$

Step 5 From Figure 4-3, determine the thermal expansion correction factor:

$$\Delta \rho_T = 2.45 \text{ lb/ft}^3$$

Step 6 The required density at 4000 psia and 160°F is

$$\rho_o = \rho_{p,60} - \Delta \rho_T$$

$$\rho_o = 48.68 - 2.45 = 46.23 \text{ lb/ft}^3$$

Alani-Kennedy's Method

Alani and Kennedy (1960) developed an equation to determine the molar liquid volume, V_m , of pure hydrocarbons over a wide range of temperatures and pressures. The equation then was adopted to apply to crude oils with heavy hydrocarbons expressed as a heptanes-plus fraction, that is, C_{7+} .

The Alani-Kennedy equation is similar in form to the Van der Waals equation, which takes the following form:

$$V_m^3 - \left[\frac{RT}{p} + b \right] V_m^2 + \frac{aV_m}{p} - \frac{ab}{p} = 0 \quad (4-14)$$

where

R = gas constant, 10.73 psia ft³/lb-mole, °R

T = temperature, °R

P = pressure, psia

V_m = molar volume, ft³/lb-mole

a, b = constants for pure substances

Alani and Kennedy considered the constants a and b functions of temperature and proposed the expressions for calculating the two parameters:

$$a = Ke^{n/T} \quad (4-15)$$

$$b = mT + c \quad (4-16)$$

where K, n, m , and c are constants for each pure component in the mixture and are tabulated in Table 4-1.

Table 4-1 contains no constants from which the values of the parameters a and b for heptanes-plus can be calculated. Therefore, Alani and Kennedy proposed the following equations for determining a and b of C_{7+} :

$$\begin{aligned} \ln(a_{C_{7+}}) &= 3.8405985(10^{-3})(M)_{C_{7+}} - 9.5638281(10^{-4}) \left(\frac{M}{\gamma} \right)_{C_{7+}} + \frac{261.80818}{T} \\ &\quad + 7.3104464(10^{-6})(M)_{C_{7+}}^2 + 10.753517 \\ b_{C_{7+}} &= 0.03499274(M)_{C_{7+}} - 7.2725403(\gamma)_{C_{7+}} + 2.232395(10^{-4})T \\ &\quad - 0.016322572 \left(\frac{M}{\gamma} \right)_{C_{7+}} + 6.2256545 \end{aligned}$$

TABLE 4-1 *Alani and Kennedy Coefficients*

Components	<i>K</i>	<i>n</i>	<i>m</i> × 10 ⁴	<i>c</i>
C ₁ 70–300°F	9160.6413	61.893223	3.3162472	0.50874303
C ₁ 301–460°F	147.47333	3247.4533	−14.072637	1.8326659
C ₂ 100–249°F	46,709.573	−404.48844	5.1520981	0.52239654
C ₂ 250–460°F	17,495.343	34.163551	2.8201736	0.62309877
C ₃	20,247.757	190.24420	2.1586448	0.90832519
i-C ₄	32,204.420	131.63171	3.3862284	1.1013834
n-C ₄	33,016.212	146.15445	2.902157	1.1168144
i-C ₅	37,046.234	299.62630	2.1954785	1.4364289
n-C ₅	37,046.234	299.62630	2.1954785	1.4364289
n-C ₆	52,093.006	254.56097	3.6961858	1.5929406
H ₂ S*	13,200.00	0	17.900	0.3945
N ₂ *	4300.00	2.293	4.490	0.3853
CO ₂ *	8166.00	126.00	1.8180	0.3872

*Values for nonhydrocarbon components as proposed by Lohrenz et al. (1964).

where

- $M_{C_{7+}}$ = molecular weight of C₇₊
- $\gamma_{C_{7+}}$ = specific gravity of C₇₊
- $a_{C_{7+}}, b_{C_{7+}}$ = constants of the heptanes-plus fraction
- T = temperature in °R

For hydrocarbon mixtures, the values of a and b of the mixture are calculated using the following mixing rules:

$$a_m = \sum_{i=1}^{C_{7+}} a_i x_i$$

(4-17)

$$b_m = \sum_{i=1}^{C_{7+}} b_i x_i$$

(4-18)

where the coefficients a_i and b_i refer to the values of pure hydrocarbon, i , as calculated from equations (4-15) and (4-16), at the existing temperature. x_i is the mole fraction of component i in the liquid phase. The values a_m and b_m are then used in equation (4-14) to solve for the molar volume V_m . The density of the mixture at the pressure and temperature of interest is determined from the following relationship:

$$\rho_o = \frac{M_a}{V_m}$$

(4-19)

where

- ρ_o = density of the crude oil, lb/ft³
- M_a = apparent molecular weight; that is, $M_a = \sum x_i M_i$
- V_m = molar volume, ft³/lb-mole

The Alani and Kennedy method for calculating the density of liquids is summarized in the following steps.

Step 1 Calculate the constants a and b for each pure component from equations (4-15) and (4-16):

$$a = Ke^{n/T}$$

$$b = mT + c$$

Step 2 Determine the C_{7+} parameters $a_{C_{7+}}$ and $b_{C_{7+}}$.

Step 3 Calculate values of the mixture coefficients a_m and b_m from equations (4-17) and (4-18).

Step 4 Calculate the molar volume V_m by solving equation (4-14) for the smallest real root. The equation can be solved iteratively by using the Newton-Raphson iterative method. In applying this technique, assume a starting value of $V_m = 2$ and evaluate equation (4-14) using the assumed value:

$$f(V_m) = V_m^3 - \left[\frac{RT}{p} + b_m \right] V_m^2 + \frac{a_m V_m}{p} - \frac{a_m b_m}{p}$$

If the absolute value of this function is smaller than a preset tolerance, say, 10^{-10} , then the assumed value is the desired volume. If not, a new assumed value of $(V_m)_{\text{new}}$ is used to evaluate the function. The new value can be calculated from the following expression:

$$(V_m)_{\text{new}} = (V_m)_{\text{old}} - \frac{f(V_m)_{\text{old}}}{f'(V_m)_{\text{old}}}$$

where the derivative $f'(V_m)$ is given by

$$f'(V_m) = 3V_m^2 - 2 \left[\frac{RT}{p} + b_m \right] V_m + \frac{a_m}{p}$$

Step 5 Compute the apparent molecular weight M_a from

$$M_a = \sum x_i M_i$$

Step 6 Determine the density of the crude oil from

$$\rho_o = \frac{M_a}{V_m}$$

EXAMPLE 4-4

A crude oil system has the composition:

COMPONENT	x_i
CO ₂	0.0008
N ₂	0.0164
C ₁	0.2840
C ₂	0.0716
C ₃	0.1048
i-C ₄	0.0420
n-C ₄	0.0420
i-C ₅	0.0191
n-C ₅	0.0191

COMPONENT	x_i
C_6	0.0405
C_{7+}	0.3597

Given the following additional data:

$$M_{C_{7+}} = 252$$

$$\gamma_{C_{7+}} = 0.8424$$

$$\text{Pressure} = 1708.7 \text{ psia}$$

$$\text{Temperature} = 591^\circ\text{R}$$

Calculate the density of the crude oil.

SOLUTION

Step 1 Calculate the parameters $a_{C_{7+}}$ and $b_{C_{7+}}$:

$$\ln(a_{C_{7+}}) = 3.8405985(10^{-3})M_{C_{7+}} - 9.5638281(10^{-4})\left(\frac{M}{\gamma}\right)_{C_{7+}} + \frac{261.80818}{T} \\ + 7.3104464(10^{-6})(M_{C_{7+}})^2 + 10.753517$$

$$\ln(a_{C_{7+}}) = 3.8405985(10^{-3})(252) - 9.5638281(10^{-4})\left(\frac{252}{0.8424}\right)_{C_{7+}} + \frac{261.80818}{591} \\ + 7.3104464(10^{-6})(252)^2 + 10.753517 = 12.34266$$

$$a_{C_{7+}} = \exp(12.34266) = 229269.9$$

and

$$b_{C_{7+}} = 0.03499274M_{C_{7+}} - 7.2725403(\gamma)_{C_{7+}} + 2.232395(10^{-4})T \\ - 0.016322572\left(\frac{M}{\gamma}\right)_{C_{7+}} + 6.2256545$$

$$b_{C_{7+}} = 0.03499274(252) - 7.2725403(0.8424) + 2.232395(10^{-4})591 \\ - 0.016322572\left(\frac{252}{0.8424}\right) + 6.2256545 = 4.165811$$

Step 2 Calculate the mixture parameters a_m and b_m :

$$a_m = \sum_{i=1}^{C_{7+}} a_i x_i = 99111.71$$

$$b_m = \sum_{i=1}^{C_{7+}} b_i x_i = 2.119383$$

Step 3 Solve equation (4-14) iteratively for the molar volume:

$$V_m^3 - \left[\frac{RT}{p} + b_m\right]V_m^2 + \frac{a_m V_m}{p} - \frac{a_m b_m}{p} = 0$$

$$V_m^3 - \left[\frac{10.73(591)}{1708.7} + 2.119383\right]V_m^2 + \frac{99111.71V_m}{1708.7} - \frac{99111.71(2.119383)}{1708.7} = 0$$

$$V_m^3 - 5.83064V_m^2 + 58.004V_m - 122.933 = 0$$

Solving this expression iteratively for V_m as outlined previously gives

$$V_m = 2.528417$$

Step 4 Determine the apparent molecular weight of this mixture:

$$M_a = \sum x_i M_i = 113.5102$$

Step 5 Compute the density of the oil system:

$$\rho_o = \frac{M_a}{V_m}$$

$$\rho_o = \frac{113.5102}{2.528417} = 44.896 \text{ lb/ft}^3$$

Density Correlations Based on Limited PVT Data

Several empirical correlations for calculating the density of liquids of unknown compositional analysis have been proposed. The correlations employ limited PVT data such as gas gravity, oil gravity, and gas solubility as correlating parameters to estimate liquid density at the prevailing reservoir pressure and temperature. Two methods are presented as representatives of this category: Katz's method and Standing's method.

Katz's Method

Density, in general, can be defined as the mass of a unit volume of material at a specified temperature and pressure. Accordingly, the density of a saturated crude oil (i.e., with gas in solution) at standard conditions can be defined mathematically by the following relationship:

$$\rho_{sc} = \frac{\text{weight of stock-tank oil} + \text{weight of solution gas}}{\text{volume of stock-tank oil} + \text{increase in stock-tank volume due to solution gas}}$$

or

$$\rho_{sc} = \frac{m_o + m_g}{(V_o)_{sc} + (\Delta V_o)_{sc}}$$

where

ρ_{sc} = density of the oil at standard conditions, lb/ft³

$(V_o)_{sc}$ = volume of oil at standard conditions, ft³/STB

m_o = total weight of one stock-tank barrel of oil, lb/STB

m_g = weight of the solution gas, lb/STB

$(\Delta V_o)_{sc}$ = increase in stock-tank oil volume due to solution gas, ft³/STB

The procedure of calculating the density at standard conditions is illustrated schematically in Figure 4-4. Katz (1942) expressed the increase in the volume of oil, $(\Delta V_o)_{sc}$, relative to the solution gas by introducing the apparent liquid density of the dissolved gas density, ρ_{ga} , to the preceding expression as

$$(\Delta V_o)_{sc} = \frac{m_g}{E_{ga}}$$

Combining the preceding two expressions gives

$$\rho_{sc} = \frac{m_o + m_g}{(V_o)_{sc} + \frac{m_g}{\rho_{ga}}}$$

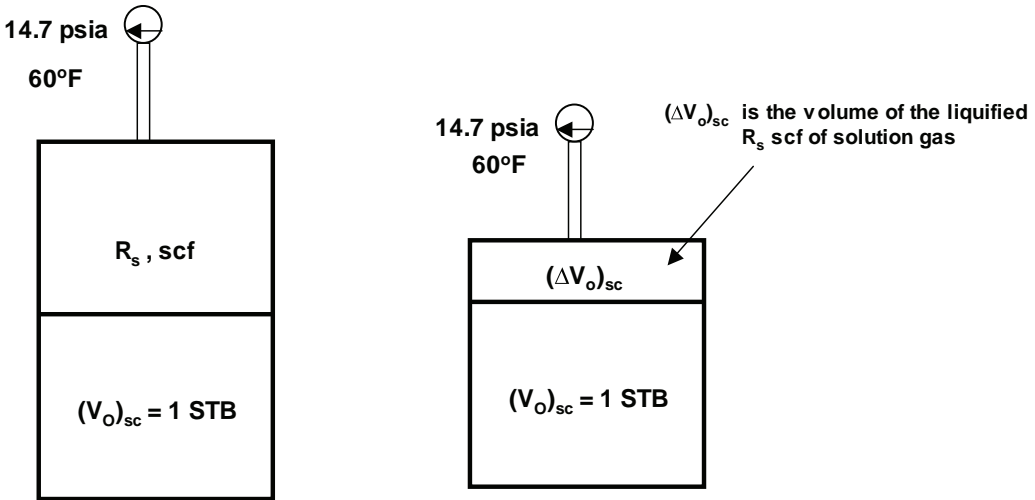


FIGURE 4-4 Schematic illustration of Katz's density model under standard conditions.

where ρ_{ga} , as introduced by Katz, is called the apparent density of the liquified dissolved gas at 60°F and 14.7 psia. Katz correlated the apparent gas density, in lb/ft³, graphically with gas specific gravity, γ_g , gas solubility (solution gas/oil ratio), R_s , specific gravity (or the API gravity) of the stock-tank oil, γ_o . This graphical correlation is presented in Figure 4-5. The proposed method does not require the composition of the crude oil.

Referring to the preceding equation, the weights of the solution gas and the stock tank can be determined in terms of the previous oil properties by the following relationships:

$$m_g = \frac{R_s}{379.4}(28.96)(\gamma_g), \text{ lb of solution gas/STB}$$

$$m_o = (5.615)(62.4)(\gamma_o), \text{ lb of oil/STB}$$

Substituting these terms into Katz's equation gives

$$\rho_{sc} = \frac{(5.615)(62.4)(\gamma_o) + \left(\frac{R_s}{379.4}\right)(28.96)(\gamma_g)}{5.615 + \left(\frac{R_s}{379.4}\right)(28.96)(\gamma_g / \rho_{ga})}$$

or

$$\rho_{sc} = \frac{350.376\gamma_o + \left(\frac{R_s \gamma_g}{13.1}\right)}{5.615 + \left(\frac{R_s \gamma_g}{13.1\rho_{ga}}\right)} \quad (4-20)$$

The pressure correction adjustment, $\Delta\rho_p$, and the thermal expansion adjustment, $\Delta\rho_T$, for the calculated ρ_{sc} can be made using Figures 4-2 and 4-3, respectively.

Standing (1981) showed that the apparent liquid density of the dissolved gas as represented by Katz's chart can be closely approximated by the following relationship:

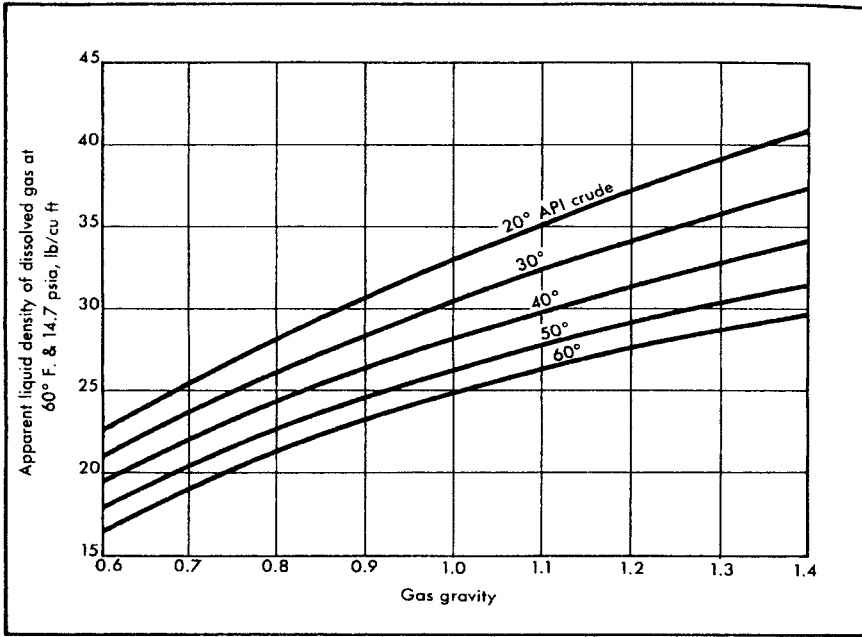


FIGURE 4-5 *Apparent liquid densities of natural gases.*

Source: D. Katz, *API Drilling and Production Practice*. Dallas: American Petroleum Institute, 1942, p. 137. Courtesy of the American Petroleum Institute.

$$\rho_{ga} = (38.52)10^{-0.00326 \text{ API}} + [94.75 - 33.93 \log(\text{API})] \log(\gamma_g)$$

EXAMPLE 4-5

A saturated crude oil exists at its bubble-point pressure of 4000 psia and a reservoir temperature of 180°F. Given

$$\text{API gravity} = 50^\circ$$

$$R_s = 650 \text{ scf/STB}$$

$$\gamma_g = 0.7$$

calculate the oil density at the specified pressure and temperature using Katz method.

SOLUTION

Step 1 From Figure 4-5 or the preceding equation, determine the apparent liquid density of dissolved gas:

$$\rho_{ga} = (38.52)10^{-0.00326 \text{ API}} + [94.75 - 33.93 \log(\text{API})] \log(\gamma_g)$$

$$\rho_{ga} = (38.52)10^{-0.00326(50)} + [94.75 - 33.93 \log(50)] \log(0.7) = 20.7 \text{ lb/ft}^3$$

Step 2 Calculate the stock-tank liquid gravity from equation (4-2):

$$\gamma_o = \frac{141.5}{\text{API} + 131.5} = \frac{141.5}{50 + 131.5} = 0.7796$$

Step 3 Apply equation (4–20) to calculate the liquid density at standard conditions:

$$\rho_{sc} = \frac{350.376\gamma_o + \left(\frac{R_s \gamma_g}{13.1}\right)}{5.615 + \left(\frac{R_s \gamma_g}{13.1 p_{ga}}\right)}$$

$$\rho_{sc} = \frac{(350.376)(0.7796) + \frac{(650)(0.7)}{13.1}}{5.615 + \frac{(650)(0.7)}{(13.1)(20.7)}} = 42.12 \text{ lb/ft}^3$$

Step 4 Determine the pressure correction factor from Figure 4–2:

$$\Delta\rho_p = 1.55 \text{ lb/ft}^3$$

Step 5 Adjust the oil density, as calculated at standard conditions, to reservoir pressure:

$$\rho_{p,60^\circ} = \rho_{sc} + \Delta\rho_p$$

$$\rho_{p,60^\circ F} = 42.12 + 1.55 = 43.67 \text{ lb/ft}^3$$

Step 6 Determine the *isothermal adjustment factor* from Figure 4–3:

$$\Delta\rho_T = 3.25 \text{ lb/ft}^3$$

Step 7 Calculate the oil density at 4000 psia and 180°F:

$$\rho_o = \rho_{p,60} - \Delta\rho_T$$

$$\rho_o = 43.67 - 3.25 = 40.42 \text{ lb/ft}^3$$

Standing's Method

Standing (1981) proposed an empirical correlation for estimating the oil formation volume factor as a function of the gas solubility, R_s , the specific gravity of stock-tank oil, γ_o , the specific gravity of solution gas, γ_g , and the system temperature, T . By coupling the mathematical definition of the oil formation volume factor (as discussed in a later section) with Standing's correlation, the density of a crude oil at a specified pressure and temperature can be calculated from the following expression:

$$\rho_o = \frac{62.4\gamma_o + 0.0136R_s \gamma_g}{0.972 + 0.000147 \left[R_s \left(\frac{\gamma_g}{\gamma_o} \right)^{0.5} + 1.25(T - 460) \right]^{1.175}} \quad (4-21)$$

where

T = system temperature, °R

γ_o = specific gravity of the stock-tank oil, 60°/60°

γ_g = specific gravity of the gas

R_s = gas solubility, scf/STB

ρ_o = oil density, lb/ft³

EXAMPLE 4-6

Rework Example 4–5 and solve for the density using Standing's correlation.

SOLUTION

$$\rho_o = \frac{62.4\gamma_o + 0.0136R_s\gamma_g}{0.972 + 0.000147 \left[R_s \left(\frac{\gamma_g}{\gamma_o} \right)^{0.5} + 1.25(T - 460) \right]^{1.175}}$$

$$\rho_o = \frac{62.4(0.7796) + 0.0136(650)(0.7)}{0.972 + 0.000147 \left[650 \left(\frac{0.7}{0.7796} \right)^{0.5} + 1.25(180) \right]^{1.175}} = 39.92 \text{ lb/ft}^3$$

The obvious advantage of using Standing's correlation is that it gives the density of the oil at the temperature and pressure at which the gas solubility is measured, and therefore, no further corrections are needed, that is, $\Delta\rho_p$ and $\Delta\rho_T$. Ahmed (1988) proposed another approach for estimating the crude oil density at standard conditions based on the apparent molecular weight of the stock-tank oil. The correlation calculates the apparent molecular weight of the oil from the readily available PVT on the hydrocarbon system. Ahmed expressed the apparent molecular weight of the crude oil with its dissolved solution gas by the following relationship:

$$M_a = \frac{0.0763R_s\gamma_g M_{st} + 350.376\gamma_o M_{st}}{0.0026537R_s M_{st} + 350.376\gamma_o}$$

where

M_a = apparent molecular weight of the oil

M_{st} = molecular weight of the stock-tank oil and can be taken as the molecular weight of the heptanes-plus fraction

γ_o = specific gravity of the stock-tank oil or the C_{7+} fraction, 60°/60°

The density of the oil at standard conditions can then be determined from the expression

$$\rho_{sc} = \frac{0.0763R_s\gamma_g + 350.376\gamma_o}{0.0026537R_s + \gamma_o \left(5.615 + \frac{199.71432}{M_{st}} \right)}$$

If the molecular weight of the stock-tank oil is not available, the density of the oil with its dissolved solution gas at standard conditions can be estimated from the following equation:

$$\rho_{sc} = \frac{0.0763R_s\gamma_g + 350.4\gamma_o}{0.0027R_s + 2.4893\gamma_o + 3.491}$$

The proposed approach requires the two additional steps of accounting for the effect of reservoir pressure and temperature.

EXAMPLE 4-7

Using the data given in Example 4-5, calculate the density of the crude oil by using the preceding simplified expression.

SOLUTION

Step 1 Calculate the density of the crude oil at standard conditions from

$$\rho_{sc} = \frac{0.0763R_s\gamma_g + 350.4\gamma_o}{0.0027R_s + 2.4893\gamma_o + 3.491}$$

$$\rho_{sc} = \frac{0.0763(650)(0.7) + 350.4(0.7796)}{0.0027(650) + 2.4893(0.7796) + 3.491} = 42.8 \text{ lb/ft}^3$$

Step 2 Determine $\Delta\rho_p$ from Figure 4-2:

$$\Delta\rho_p = 1.5 \text{ lb/ft}^3$$

Step 3 Determine $\Delta\rho_T$ from Figure 4-3:

$$\Delta\rho_T = 3.6 \text{ lb/ft}^3$$

Step 4 Calculate p_o at 4000 psia and 180°F:

$$\rho_o = \rho_{sc} + \Delta\rho_p - \Delta\rho_T$$

$$\rho_o = 42.8 + 1.5 - 3.6 = 40.7 \text{ lb/ft}^3$$

The oil density can also be calculated rigorously from the experimental measured PVT data at any specified pressure and temperature. The following expression (as derived later in this chapter) relates the oil density, ρ_o , to the gas solubility, R_s , specific gravity of the oil, gas gravity, and the oil formation volume factor:

$$\rho_o = \frac{62.4\gamma_o + 0.0136R_s\gamma_g}{B_o} \quad (4-22)$$

where

γ_o = specific gravity of the stock-tank oil, 60°/60°

R_s = gas solubility, scf/STB

ρ_o = oil density at pressure and temperature, lb/ft³

Gas Solubility

The gas solubility, R_s , is defined as the number of standard cubic feet of gas that dissolve in one stock-tank barrel of crude oil at certain pressure and temperature. The solubility of a natural gas in a crude oil is a strong function of the pressure, the temperature, the API gravity, and the gas gravity.

For a particular gas and crude oil to exist at a constant temperature, the solubility increases with pressure until the saturation pressure is reached. At the saturation pressure (bubble-point pressure), all the available gases are dissolved in the oil and the gas solubility reaches its maximum value. Rather than measuring the amount of gas that dissolves in a given stock-tank crude oil as the pressure is increased, it is customary to determine the amount of gas that comes out of a sample of reservoir crude oil as pressure decreases.

A typical gas solubility curve, as a function of pressure for an undersaturated crude oil, is shown in Figure 4-6. As the pressure is reduced from the initial reservoir pressure, p_r , to the bubble-point pressure, p_b , no gas evolves from the oil and consequently the gas solubility remains constant at its maximum value of R_{sb} . Below the bubble-point pressure, the solution gas is liberated and the value of R_s decreases with pressure.

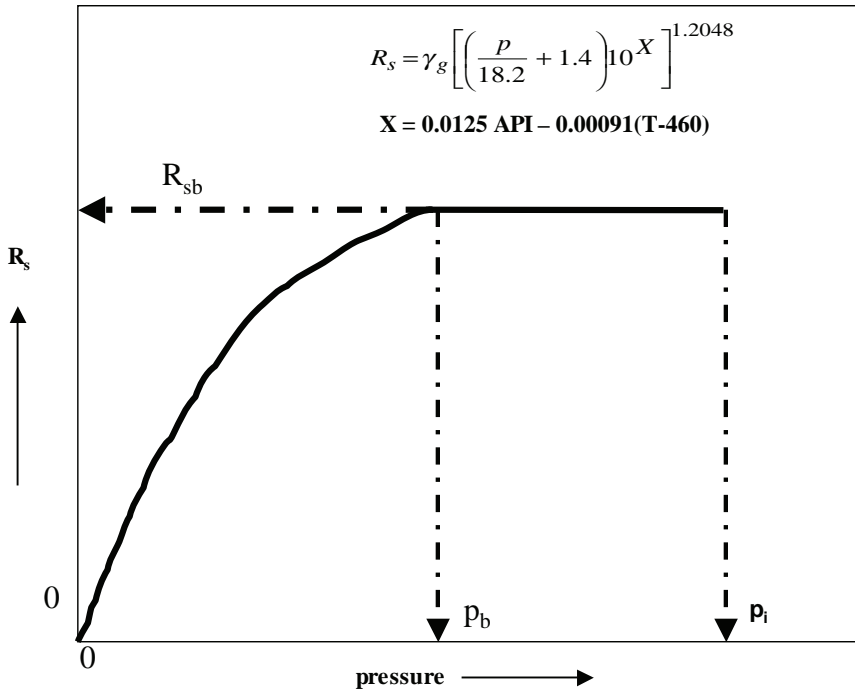


FIGURE 4-6 Typical gas solubility/pressure relationship.

In the absence of experimentally measured gas solubility on a crude oil system, it is necessary to determine this property from empirically derived correlations. Five empirical correlations for estimating the gas solubility are discussed here: Standing's correlation, Vasquez-Beggs's correlation, Glaso's correlation, Marhoun's correlation, and Petrosky-Farshad's correlation.

Standing's Correlation

Standing (1947) proposed a graphical correlation for determining the gas solubility as a function of pressure, gas specific gravity, API gravity, and system temperature. The correlation was developed from a total of 105 experimentally determined data points on 22 hydrocarbon mixtures from California crude oils and natural gases. The proposed correlation has an average error of 4.8%. In a mathematical form, Standing (1981) expressed his proposed graphical correlation in the following more convenient mathematical form:

$$R_s = \gamma_g \left[\left(\frac{p}{18.2} + 1.4 \right) 10^x \right]^{1.2048} \quad (4-23)$$

with

$$x = 0.0125 \text{ API} - 0.00091(T - 460)$$

where:

R_s = gas solubility, scf/STB

T = temperature, °R

p = system pressure, psia

γ_g = solution gas specific gravity
API = oil gravity, °API

It should be noted that Standing’s equation is valid for applications at and below the bubble-point pressure of the crude oil.

EXAMPLE 4–8

The following table shows experimental PVT data on six crude oil systems. Results are based on two-stage surface separation. Using Standing’s correlation, estimate the gas solubility at the bubble-point pressure and compare with the experimental value in terms of the absolute average error (AAE).

Oil	T , °F	p_b	R_s , Scf/	B_o	ρ_o , lb/ft ³	c_o at $p > p_b$	p_{sep}	T_{sep}	API	γ_g
			STB							
1	250	2377	751	1.528	38.13	22.14×10^{-6} at 2689	150	60	47.1	0.851
2	220	2620	768	0.474	40.95	18.75×10^{-6} at 2810	100	75	40.7	0.855
3	260	2051	693	1.529	37.37	22.69×10^{-6} at 2526	100	72	48.6	0.911
4	237	2884	968	1.619	38.92	21.51×10^{-6} at 2942	60	120	40.5	0.898
5	218	3045	943	1.570	37.70	24.16×10^{-6} at 3273	200	60	44.2	0.781
6	180	4239	807	1.385	46.79	11.45×10^{-6} at 4370	85	173	27.3	0.848

T = reservoir temperature, °F
 p_b = bubble-point pressure, psig
 B_o = oil formation volume factor, bbl/STB
 p_{sep} = separator pressure, psig
 T_{sep} = separator temperature, °F
 c_o = isothermal compressibility coefficient of the oil at a specified pressure, psi^{−1}

SOLUTION

Apply equation (4–23) to determine the gas solubility. Results of the calculations are given in the table below.

Oil	T , °F	API	x	10^x	Predicted R_s , Equation (4–23)	Measured R_s	% Error
1	250	47.1	0.361	2.297	838	751	11.6
2	220	40.7	0.309	2.035	817	768	6.3
3	260	48.6	0.371	2.349	774	693	11.7
4	237	40.5	0.291	1.952	914	968	5.5
5	218	44.2	0.322	2.097	1012	943	7.3
6	180	27.3	0.177	1.505	998	807	23.7
						AAE	9.7%

$x = 0.0125\text{API} - 0.00091(T - 460)$

$$R_s = \gamma_g \left[\left(\frac{p}{18.2} + 1.4 \right) 10^x \right]^{1.2048}$$

Vasquez-Beggs’s Correlation

Vasquez and Beggs (1980) presented an improved empirical correlation for estimating R_s . The correlation was obtained by regression analysis using 5008 measured gas solubility data points. Based on oil gravity, the measured data were divided into two groups. This division was made at a value of oil gravity of 30°API. The proposed equation has the following form:

$$R_s = C_1 \gamma_{gs} p^{C_2} \exp \left[C_3 \left(\frac{API}{T} \right) \right] \quad (4-24)$$

Values for the coefficients are as follows:

COEFFICIENTS	API ≤ 30	API > 30
C_1	0.362	0.0178
C_2	1.0937	1.1870
C_3	25.7240	23.931

Realizing that the value of the specific gravity of the gas depends on the conditions under which it is separated from the oil, Vasquez and Beggs proposed that the value of the gas specific gravity as obtained from a separator pressure of 100 psig be used in this equation. The reference pressure was chosen because it represents the average field separator conditions. The authors proposed the following relationship for adjustment of the gas gravity, γ_g , to the reference separator pressure:

$$\gamma_{gs} = \gamma_g \left[1 + 5.912(10^{-5})(API)(T_{sep} - 460) \log \left(\frac{p_{sep}}{114.7} \right) \right] \quad (4-25)$$

where

- γ_{gs} = gas gravity at the reference separator pressure
- γ_g = gas gravity at the actual separator conditions of p_{sep} and T_{sep}
- p_{sep} = actual separator pressure, psia
- T_{sep} = actual separator temperature, °R

The gas gravity used to develop all the correlations reported by the authors was that which would result from a two-stage separation. The first-stage pressure was chosen as 100 psig and the second stage was the stock tank. If the separator conditions are unknown, the unadjusted gas gravity may be used in equation (4-24).

An independent evaluation of this correlation by Sutton and Farashad (1984) shows that the correlation is capable of predicting gas solubilities with an average absolute error of 12.7%.

EXAMPLE 4-9

Using the PVT of the six crude oil systems of Example 4-8, solve for the gas solubility using the Vasquez and Beggs method.

SOLUTION

The results are shown in the following table.

Oil	γ_{gs} , Equation (4-25)	Predicted R_s , Equation (4-24)	Measured R_s	% Error
1	0.8731	779	751	3.76
2	0.855	733	768	-4.58
3	0.911	702	693	1.36
4	0.850	820	968	5.2
5	0.814	947	943	0.43

continued

Oil	γ_g , Equation (4-25)	Predicted R_s , Equation (4-24)	Measured R_s	% Error
6	0.834	841	807	4.30
			AAE	4.9%

$$\gamma_g = \gamma_g \left[1 + 5.912(10^{-5})(API)(T_{sep} - 460) \log \left(\frac{p_{sep}}{114.7} \right) \right]$$

$$R_s = C_1 \gamma_g p^{C_2} \exp \left[C_3 \left(\frac{API}{T} \right) \right]$$

Glaser’s Correlation

Glaser (1980) proposed a correlation for estimating the gas solubility as a function of the API gravity, the pressure, the temperature, and the gas specific gravity. The correlation was developed from studying 45 North Sea crude oil samples. Glaser reported an average error of 1.28% with a standard deviation of 6.98%. The proposed relationship has the following form:

$$R_s = \gamma_g \left\{ \left[\frac{API^{0.989}}{(T - 460)^{0.172}} \right] (A) \right\}^{1.2255} \tag{4-26}$$

The parameter A is a pressure-dependent coefficient defined by the following expression:

$$A = 10^X$$

with the exponent X as given by

$$X = 2.8869 - [14.1811 - 3.3093 \log(p)]^{0.5}$$

EXAMPLE 4-10

Rework Example 4-8 and solve for the gas solubility using Glaser’s correlation.

SOLUTION

The results are shown in the table below.

Oil	p	X	A	Predicted R_s , Equation (4-26)	Measured R_s	% Error
1	2377	1.155	14.286	737	751	-1.84
2	2620	1.196	15.687	714	768	-6.92
3	2051	1.095	12.450	686	693	-0.90
4	5884	1.237	17.243	843	968	-12.92
5	3045	1.260	18.210	868	943	-7.94
6	4239	1.413	25.883	842	807	4.34
					AAE	5.8%

$$X = 2.8869 - [14.1811 - 3.3093 \log(p)]^{0.5}$$

$$A = 10^X$$

$$R_s = \gamma_g \left[\left(\frac{API^{0.989}}{(T - 460)^{0.172}} \right) (A) \right]^{1.2255}$$

Marhoun’s Correlation

Marhoun (1988) developed an expression for estimating the saturation pressure of the Middle Eastern crude oil systems. The correlation originates from 160 experimental satu-

ration pressure data. The proposed correlation can be rearranged and solved for the gas solubility to give

$$R_s = \left[a \gamma_g^b \gamma_o^c T^d p \right]^e \tag{4-27}$$

where

γ_g = gas specific gravity

γ_o = stock-tank oil gravity

T = temperature, °R

$a-e$ = coefficients of the above equation having these values

$$a = 185.843208$$

$$b = 1.877840$$

$$c = -3.1437$$

$$d = -1.32657$$

$$e = 1.39844$$

EXAMPLE 4-11

Resolve Example 4-8 using Marhoun's correlation.

SOLUTION

The results are shown in the table below.

Oil	T , °F	p	Predicted R_s , Equation (4-27)	Measured R_s	% Error
1	250	2377	740	751	-1.43
2	220	2620	792	768	3.09
3	260	2051	729	693	5.21
4	237	2884	1041	968	7.55
5	218	3045	845	943	-10.37
6	180	4239	1186	807	47.03
				AAE	12.4%

$$R_s = \left[a \gamma_g^b \gamma_o^c T^d p \right]^e$$

$$a = 185.843208$$

$$b = 1.877840$$

$$c = -3.1437$$

$$d = -1.32657$$

$$e = 1.39844$$

Petrosky and Farshad's Correlation

Petrosky and Farshad (1993) used nonlinear multiple regression software to develop a gas solubility correlation. The authors constructed a PVT database from 81 laboratory analyses from the Gulf of Mexico crude oil system. Petrosky and Farshad proposed the following expression:

$$R_s = \left[\left(\frac{p}{112.727} + 12.340 \right) \gamma_g^{0.8439} 10^x \right]^{1.73184} \tag{4-28}$$

with

$$x = 7.916 (10^{-4})(\text{API})^{1.5410} - 4.561(10^{-5})(T - 460)^{1.3911}$$

where

- R_s = gas solubility, scf/STB
- T = temperature, °R
- p = system pressure, psia
- γ_g = solution gas specific gravity
- API = oil gravity, °API

EXAMPLE 4-12

Test the predictive capability of the Petrosky and Farshad equation by resolving Example 4-8.

SOLUTION

The results are shown in the table below.

Oil	API	T, °F	x	Predicted R_s , Equation (4-28)	Measured R_s	% Error
1	47.1	250	0.2008	772	751	2.86
2	40.7	220	0.1566	726	768	-5.46
3	48.6	260	0.2101	758	693	9.32
4	40.5	237	0.1579	875	968	-9.57
5	44.2	218	0.1900	865	943	-8.28
6	27.3	180	0.0667	900	807	11.57
				AAE		7.84%

$$x = 7.916(10^{-4})(\text{API})^{1.5410} - 4.561(10^{-5})(T - 460)^{1.3911}$$

$$R_s = \left[\left(\frac{p}{112.727} + 12.340 \right) \gamma_g^{0.8439} 10^x \right]^{1.73184}$$

As derived later in this chapter from the material balance approach, the gas solubility can also be calculated rigorously from the experimental, measured PVT data at the specified pressure and temperature. The following expression relates the gas solubility, R_s , to oil density, specific gravity of the oil, gas gravity, and the oil formation volume factor:

$$R_s = \frac{B_o \rho_o - 62.4 \gamma_o}{0.0136 \gamma_g} \tag{4-29}$$

where

- ρ_o = oil density at pressure and temperature, lb/ft³
- B_o = oil formation volume factor, bbl/STB
- γ_o = specific gravity of the stock-tank oil, 60°/60°
- γ_g = specific gravity of the solution gas

McCain (1991) pointed out that the weight average of separator and stock-tank gas specific gravities should be used for γ_g . The error in calculating R_s by using the preceding equation depends on the accuracy of only the available PVT data.

EXAMPLE 4-13

Using the data of Example 4-8, estimate R_s by applying equation (4-29).

SOLUTION

The results are shown in the table below.

Oil	p_b	B_o	ρ_o	API	γ_o	γ_g	Predicted R_s , Equation (4–29)	Measured R_s	% Error
1	2377	1.528	38.13	47.1	0.792	0.851	762	751	1.53
2	2620	1.474	40.95	40.7	0.822	0.855	781	768	1.73
3	2051	1.529	37.37	48.6	0.786	0.911	655	693	–5.51
4	2884	1.619	38.92	40.5	0.823	0.898	956	968	–1.23
5	3045	1.570	37.70	44.2	0.805	0.781	843	943	–10.57
6	4239	1.385	46.79	27.3	0.891	0.848	798	807	–1.13
								AAE	3.61%

$$\gamma_o = \frac{141.5}{131.5 + \text{API}}$$
$$R_s = \frac{B_o \rho_o - 62.4 \gamma_o}{0.0136 \gamma_g}$$

Bubble-Point Pressure

The bubble-point pressure, p_b , of a hydrocarbon system is defined as the highest pressure at which a bubble of gas is first liberated from the oil. This important property can be measured experimentally for a crude oil system by conducting a constant-composition expansion test.

In the absence of the experimentally measured bubble-point pressure, it is necessary for the engineer to make an estimate of this crude oil property from the readily available measured producing parameters. Several graphical and mathematical correlations for determining p_b have been proposed during the last four decades. These correlations are essentially based on the assumption that the bubble-point pressure is a strong function of gas solubility, R_s ; gas gravity, γ_g ; oil gravity, API; and temperature, T :

$$p_b = f(R_s, \gamma_g, \text{API}, T)$$

Ways of combining these parameters in a graphical form or a mathematical expression were proposed by several authors, including Standing, Vasquez and Beggs, Glaso, Marhoun, and Petrosky and Farshad. The empirical correlations for estimating the bubble-point pressure proposed by these authors follow.

Standing’s Correlation

Based on 105 experimentally measured bubble-point pressures on 22 hydrocarbon systems from California oil fields, Standing (1947) proposed a graphical correlation for determining the bubble-point pressure of crude oil systems. The correlating parameters in the proposed correlation are the gas solubility, R_s , gas gravity, γ_g , oil API gravity, and the system temperature. The reported average error is 4.8%.

In a mathematical form, Standing (1981) expressed the graphical correlation by the following expression:

$$p_b = 18.2[(R_s/\gamma_g)^{0.83}(10)^a - 1.4] \tag{4-30}$$

with

$$a = 0.00091(T - 460) - 0.0125(API) \tag{4-31}$$

where

- R_s = gas solubility, scf/STB
- p_b = bubble-point pressure, psia
- T = system temperature, °R

Standing’s correlation should be used with caution if nonhydrocarbon components are known to be present in the system.

Lasater (1958) used a different approach in predicting the bubble-point pressure by introducing and using the mole fraction of the solution gas, y_{gas} , in the crude oil as a correlating parameter, defined by

$$y_{gas} = \frac{M_o R_s}{M_o R_s + 133,000 \gamma_o}$$

where M_o = molecular weight of the stock-tank oil and γ_o = specific gravity of the stock-tank oil, 60°/60°.

If the molecular weight is not available, it can be estimated from Cragoe (1997) as

$$M_o = \frac{6084}{API - 5.9}$$

The bubble-point pressure as proposed by Lasater is given by the following relationship:

$$p_b = \left(\frac{T}{\gamma_g} \right) A$$

where T is the temperature in °R and A is a graphical correlating parameter that is a function of the mole fraction of the solution gas, y_{gas} . Whitson and Brule (2000) described this correlating parameter by

$$A = 0.83918 [10^{1.17664 y_{gas}}] y_{gas}^{0.57246}, \text{ when } y_{gas} \leq 0.6$$

$$A = 0.83918 [10^{1.08000 y_{gas}}] y_{gas}^{0.31109}; \text{ when } y_{gas} > 0.6$$

EXAMPLE 4-14

The experimental data given in Example 4-8 are repeated below for convenience. Predict the bubble-point pressure using Standing’s correlation.

Oil	$T, ^\circ F$	p_b	$R_s, \text{Scf/STB}$	B_o	$\rho_o, \text{lb/ft}^3$	$c_o \text{ at } p > p_b$	p_{sep}	T_{sep}	API	γ_g
1	250	2377	751	1.528	38.13	22.14×10^{-6} at 2689	150	60	47.1	0.851
2	220	2620	768	0.474	40.95	18.75×10^{-6} at 2810	100	75	40.7	0.855
3	260	2051	693	1.529	37.37	22.69×10^{-6} at 2526	100	72	48.6	0.911
4	237	2884	968	1.619	38.92	21.51×10^{-6} at 2942	60	120	40.5	0.898
5	218	3045	943	1.570	37.70	24.16×10^{-6} at 3273	200	60	44.2	0.781
6	180	4239	807	1.385	46.79	11.45×10^{-6} at 4370	85	173	27.3	0.848

SOLUTION

The results are shown in the following table.

Oil	API	γ_g	Coefficient a , Equation (4-31)	Predicted p_b , Equation (4-30)	Measured p_b	% Error
1	47.1	0.851	-0.3613	2181	2392	-8.8
2	40.7	0.855	-0.3086	2503	2635	-5.0
3	48.6	0.911	-0.3709	1883	2066	-8.8
4	40.5	0.898	-0.3115	2896	2899	-0.1
5	44.2	0.781	-0.3541	2884	3060	-5.7
6	27.3	0.848	-0.1775	3561	4254	-16.3
					AAE	7.4%

$$a = 0.00091(T - 460) - 0.0125(\text{API})$$

$$p_b = 18.2[(R/\gamma_g)^{0.83}(10)^a - 1.4]$$

McCain (1991) suggested that replacing the specific gravity of the gas in equation (4-30) with that of the separator gas, that is, excluding the gas from the stock tank, would improve the accuracy of the equation.

EXAMPLE 4-15

Using the data of Example 4-14 and given the following first separator gas gravities as observed by McCain, estimate the bubble-point pressure by applying Standing's correlation.

OIL	FIRST SEPARATOR GAS GRAVITY
1	0.755
2	0.786
3	0.801
4	0.888
5	0.705
6	0.813

SOLUTION

The results are shown in the table below.

Oil	API	First Separation γ_g	Coefficient a , Equation (4-31)	Predicted p_b , Equation (4-30)	Measured p_b	% Error
1	47.1	0.755	-0.3613	2411	2392	0.83
2	40.7	0.786	-0.3086	2686	2635	1.93
3	48.6	0.801	-0.3709	2098	2066	1.53
4	40.5	0.888	-0.3115	2923	2899	0.84
5	44.2	0.705	-0.3541	3143	3060	2.70
6	27.3	0.813	-0.1775	3689	4254	-13.27
					AAE	3.5%

$$a = 0.00091(T - 460) - 0.0125(\text{API})$$

$$p_b = 18.2[(R/\gamma_g)^{0.83}(10)^a - 1.4]$$

Vasquez-Beggs's Correlation

Vasquez and Beggs's gas solubility correlation as presented by equation (4-24) can be solved for the bubble-point pressure, p_b , to give

$$p_b = \left[\left(C_1 \frac{R_s}{\gamma_{gs}} \right) (10)^a \right]^{C_2}$$

(4-32)

with exponent a as given by

$$a = C_3 \left(\frac{API}{T} \right)$$

where the temperature, T , is in °R.

The coefficients C_1 , C_2 , and C_3 of equation (4-32) have the following values:

COEFFICIENT	API ≤ 30	API > 30
C_1	27.624	56.18
C_2	10.914328	0.84246
C_3	-11.172	-10.393

The gas specific gravity γ_{gs} at the reference separator pressure is defined by equation (4-25) as

$$\gamma_{gs} = \gamma_g \left[1 + 5.912(10^{-5})(API)(T_{sep} - 460) \log \left(\frac{p_{sep}}{114.7} \right) \right]$$

EXAMPLE 4-16

Rework Example 4-14 by applying equation (4-32).

SOLUTION

The results are shown in the table below.

Oil	T	R_s	API	γ_{gs} , Equation (4-25)	a	Predicted p_b	Measured p_b	% Error
1	250	751	47.1	0.873	-0.689	2319	2392	-3.07
2	220	768	40.7	0.855	-0.622	2741	2635	4.03
3	260	693	48.6	0.911	-0.702	2043	2066	-1.14
4	237	968	40.5	0.850	-0.625	3331	2899	14.91
5	218	943	44.2	0.814	-0.678	3049	3060	-0.36
6	180	807	27.3	0.834	-0.477	4093	4254	-3.78
							AAE	4.5%

$$a = C_3 \left(\frac{API}{T} \right)$$

$$p_b = \left[\left(C_1 \frac{R_s}{\gamma_{gs}} \right) (10)^a \right]^{C_2}$$

Glaser’s Correlation

Glaser (1980) used 45 oil samples, mostly from the North Sea hydrocarbon system, to develop an accurate correlation for bubble-point pressure prediction. Glaser proposed the following expression:

$$\log(p_b) = 1.7669 + 1.7447 \log(A) - 0.30218 [\log(A)]^2$$

(4-33)

The correlating parameter A in the equation is defined by the following expression:

$$A = \left(\frac{R_s}{\gamma_g} \right)^{0.816} \frac{(T - 460)^{0.172}}{(\text{API})^{0.989}} \quad (4-34)$$

where

R_s = gas solubility, scf/STB

T = system temperature, °R

γ_g = average specific gravity of the total surface gases

For volatile oils, Glaso recommends that the temperature exponent of equation (4-34) be slightly changed from 0.172 to the value of 0.130, to give

$$A = \left(\frac{R_s}{\gamma_g} \right)^{0.816} \frac{(T - 460)^{0.1302}}{(\text{API})^{0.989}}$$

EXAMPLE 4-17

Resolve Example 4-14 using Glaso's correlation.

SOLUTION

The results are shown in the table below.

Oil	T	R_s	API	A , Equation (3-34)	p_b , Equation (4-33)	Measured p_b	% Error
1	250	751	47.1	14.51	2431	2392	1.62
2	220	768	40.7	16.63	2797	2635	6.14
3	260	693	48.6	12.54	2083	2066	0.82
4	237	968	40.5	19.30	3240	2899	11.75
5	218	943	44.2	19.48	3269	3060	6.83
6	180	807	27.3	25.00	4125	4254	-3.04
						AAE	5.03%

$$A = \left(\frac{R_s}{\gamma_g} \right)^{0.816} \frac{(T - 460)^{0.172}}{(\text{API})^{0.989}}$$

$$\log(p_b) = 1.7669 + 1.7447 \log(A) - 0.30218 [\log(A)]^2$$

Marhoun's Correlation

Marhoun (1988) used 160 experimentally determined bubble-point pressures from the PVT analysis of 69 Middle Eastern hydrocarbon mixtures to develop a correlation for estimating p_b . The author correlated the bubble-point pressure with the gas solubility, R_s , the temperature, T , and the specific gravity of the oil and the gas. Marhoun proposed the following expression:

$$p_b = a R_s^b \gamma_g^c \gamma_o^d T^e \quad (4-35)$$

where

T = temperature, °R

R_s = gas solubility, scf/STB

γ_o = stock-tank oil specific gravity

γ_g = gas specific gravity

$a-e$ = coefficients of the correlation having the following values

$$a = 5.38088 \times 10^{-3}$$

$$b = 0.715082$$

$$c = -1.87784$$

$$d = 3.1437$$

$$e = 1.32657$$

The reported average absolute relative error for the correlation is 3.66% when compared with the experimental data used to develop the correlation.

EXAMPLE 4-18

Using equation (4-35), rework Example 4-13.

SOLUTION

The results are shown in the table below.

Oil	Predicted p_b	Measured p_b	% Error
1	2417	2392	1.03
2	2578	2635	-2.16
3	1992	2066	-3.57
4	2752	2899	-5.07
5	3309	3060	8.14
6	3229	4254	-24.09
			AAE = 7.3%

$$p_b = 0.00538033 R_s^{0.715082} \gamma_g^{-1.87784} \gamma_o^{3.1437} T^{1.32657}$$

Petrosky-Farshad's Correlation

Petrosky and Farshad's gas solubility equation, equation (4-28), can be solved for the bubble-point pressure to give

$$p_b = \left[\frac{112.727 R_s^{0.577421}}{\gamma_g^{0.8439} (10)^x} \right] - 1391.051 \quad (4-36)$$

where the correlating parameter, x , is as previously defined by the following expression:

$$x = 7.916(10^{-4})(\text{API})^{1.5410} - 4.561(10^{-5})(T - 460)^{1.3911}$$

where

R_s = gas solubility, scf/STB

T = temperature, °R

p = system pressure, psia

γ_g = solution gas specific gravity

API = oil gravity, °API

The authors concluded that the correlation predicts measured bubble-point pressures with an average absolute error of 3.28%.

EXAMPLE 4-19

Use the Petrosky and Farshad correlation to predict the bubble-point pressure data given in Example 4-14.

SOLUTION

The results are shown in the table below.

Oil	T	R_s	API	x	p_b , Equation (4-36)	Measured p_b	% Error
1	250	751	47.1	0.2008	2331	2392	-2.55
2	220	768	40.7	0.1566	2768	2635	5.04
3	260	693	48.6	0.2101	1893	2066	-8.39
4	237	968	40.5	0.1579	3156	2899	8.86
5	218	943	44.2	0.1900	3288	3060	7.44
6	180	807	27.3	0.0667	3908	4254	-8.13
						AAE	6.74%

$$x = 7.916(10^{-4})(\text{API})^{1.5410} - 4.561(10^{-5})(T - 460)^{1.3911}$$

$$p_b = \left[\frac{112.727 R_s^{0.577421}}{\gamma_g^{0.8439} (10)^x} \right] - 1391.051$$

Using the neural network approach, Al-Shammasi (1999) proposed the following expression that estimated the bubble-point pressure with an average absolute error of 18%:

$$P_b = \gamma_o^{5.527215} e^{-1.841408[\gamma_o \gamma_g]} [R_s T \gamma_g]^{0.783716}$$

where T is the temperature in °R.

Oil Formation Volume Factor

The oil formation volume factor, B_o , is defined as the ratio of the volume of oil (plus the gas in solution) at the prevailing reservoir temperature and pressure to the volume of oil at standard conditions. Evidently, B_o always is greater than or equal to unity. The oil formation volume factor can be expressed mathematically as

$$B_o = \frac{(V_o)_{p,T}}{(V_o)_{sc}} \quad (4-37)$$

where

B_o = oil formation volume factor, bbl/STB

$(V_o)_{p,T}$ = volume of oil under reservoir pressure, p , and temperature, i , bbl

$(V_o)_{sc}$ = volume of oil is measured under standard conditions, STB

A typical oil formation factor curve, as a function of pressure for an undersaturated crude oil ($p_i > p_b$), is shown in Figure 4-7. As the pressure is reduced below the initial reservoir pressure, p_i , the oil volume increases due to the oil expansion. This behavior results in an increase in the oil formation volume factor and continues until the bubble-point pressure is reached. At p_b , the oil reaches its maximum expansion and consequently attains a maximum value of B_{ob} for the oil formation volume factor. As the pressure is reduced below p_b , volume of the oil and B_o are decreased as the solution gas is liberated. When the pressure is reduced to atmospheric pressure and the temperature to 60°F, the value of B_o is equal to 1.

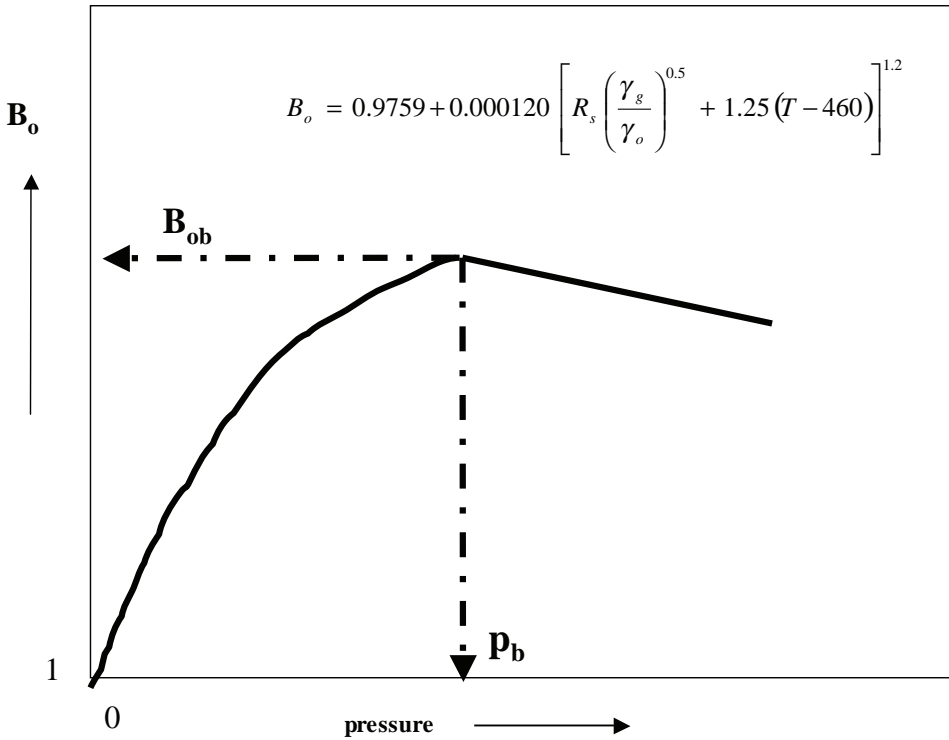


FIGURE 4-7 Typical oil formation volume factor/pressure relationship.

Most of the published empirical B_o correlations utilize the following generalized relationship:

$$B_o = f(R_s, \gamma_g, \gamma_o, T)$$

Six methods of predicting the oil formation volume factor are presented here: Standing's correlation, Vasquez and Beggs's correlation, Glaso's correlation, Marhoun's correlation, Petrosky and Farshad's correlation, and the material balance equation. It should be noted that all the correlations could be used for any pressure equal to or below the bubble-point pressure.

Standing's Correlation

Standing (1947) presented a graphical correlation for estimating the oil formation volume factor with the gas solubility, gas gravity, oil gravity, and reservoir temperature as the correlating parameters. This graphical correlation originated from examining 105 experimental data points on 22 California hydrocarbon systems. An average error of 1.2% was reported for the correlation.

Standing (1981) showed that the oil formation volume factor can be expressed more conveniently in a mathematical form by the following equation:

$$B_o = 0.9759 + 0.000120 \left[R_s \left(\frac{\gamma_g}{\gamma_o} \right)^{0.5} + 1.25 (T - 460) \right]^{1.2} \quad (4-38)$$

where

T = temperature, °R

γ_o = specific gravity of the stock-tank oil, 60°/60°

γ_g = specific gravity of the solution gas

Vasquez and Beggs's Correlation

Vasquez and Beggs (1980) developed a relationship for determining B_o as a function of R_s , γ_o , γ_g , and T . The proposed correlation was based on 6000 measurements of B_o at various pressures. Using the regression analysis technique, Vasquez and Beggs found the following equation to be the best form to reproduce the measured data:

$$B_o = 1.0 + C_1 R_s + (T - 520) \left(\frac{\text{API}}{\gamma_{gs}} \right) [C_2 + C_3 R_s] \quad (4-39)$$

where

R = gas solubility, scf/STB

T = temperature, °R

γ_{gs} = gas specific gravity as defined by equation 4-25:

$$\gamma_{gs} = \gamma_g \left[1 + 5.912(10^{-5})(\text{API})(T_{\text{sep}} - 460) \log \left(\frac{p_{\text{sep}}}{114.7} \right) \right]$$

Values for the coefficients C_1 , C_2 , and C_3 of equation (4-39) follow:

COEFFICIENT	API ≤ 30	API > 30
C_1	4.677×10^{-4}	4.670×10^{-4}
C_2	1.751×10^{-5}	1.100×10^{-5}
C_3	-1.811×10^{-8}	1.337×10^{-9}

Vasquez and Beggs reported an average error of 4.7% for the proposed correlation.

Glaser's Correlation

Glaser (1980) proposed the following expressions for calculating the oil formation volume factor:

$$B_o = 1.0 + 10^A \quad (4-40)$$

where

$$A = -6.58511 + 2.91329 \log B_{ob}^* - 0.27683(\log B_{ob}^*)^2 \quad (4-41)$$

B_{ob}^* is a "correlating number," defined by the following equation:

$$B_{ob}^* = R_s \left(\frac{\gamma_g}{\gamma_o} \right)^{0.526} + 0.968(T - 460) \quad (4-42)$$

where T = temperature, °R, and γ_o = specific gravity of the stock-tank oil, 60°/60°. These correlations were originated from studying PVT data on 45 oil samples. The average error of the correlation was reported at -0.43% with a standard deviation of 2.18%.

Sutton and Farshad (1984) concluded that Glaser's correlation offers the best accuracy when compared with Standing's and Vasquez-Beggs's correlations. In general, Glaser's correlation underpredicts formation volume factor, Standing's expression tends to overpredict oil

formation volume factors, while Vasquez-Beggs's correlation typically overpredicts the oil formation volume factor.

Marhoun's Correlation

Marhoun (1988) developed a correlation for determining the oil formation volume factor as a function of the gas solubility, stock-tank oil gravity, gas gravity, and temperature. The empirical equation was developed by use of the nonlinear multiple regression analysis on 160 experimental data points. The experimental data were obtained from 69 Middle Eastern oil reserves. The author proposed the following expression:

$$B_o = 0.497069 + 0.000862963T + 0.00182594F + 0.00000318099F^2 \quad (4-43)$$

with the correlating parameter F as defined by the following equation:

$$F = R_s^a \gamma_g^b \gamma_o^c \quad (4-44)$$

where T is the system temperature in °R and the coefficients a , b , and c have the following values:

$$a = 0.742390$$

$$b = 0.323294$$

$$c = -1.202040$$

Petrosky and Farshad's Correlation

Petrosky and Farshad (1993) proposed a new expression for estimating B_o . The proposed relationship is similar to the equation developed by Standing; however, the equation introduces three additional fitting parameters to increase the accuracy of the correlation.

The authors used a nonlinear regression model to match experimental crude oil from the Gulf of Mexico hydrocarbon system. Their correlation has the following form:

$$B_o = 1.0113 + 7.2046(10^{-5})A \quad (4-45)$$

with the term A as given by

$$A = \left[R_s^{0.3738} \left(\frac{\gamma_g^{0.2914}}{\gamma_o^{0.6265}} \right) + 0.24626(T - 460)^{0.5371} \right]^{3.0936}$$

where T = temperature, °R, and γ_o = specific gravity of the stock-tank oil, 60°/60°.

Material Balance Equation

From the definition of B_o as expressed mathematically by equation (4-37),

$$B_o = \frac{(V_o)_{p,T}}{(V_o)_{sc}}$$

The oil volume under p and T can be replaced with total weight of the hydrocarbon system divided by the density at the prevailing pressure and temperature:

$$B_o = \frac{\left[\frac{m_t}{\rho_o} \right]}{(V_o)_{sc}}$$

where the total weight of the hydrocarbon system is equal to the sum of the stock-tank oil plus the weight of the solution gas:

$$m_t = m_o + m_g$$

or

$$B_o = \frac{m_o + m_g}{\rho_o (V_o)_{sc}}$$

Given the gas solubility, R_s , per barrel of the stock-tank oil and the specific gravity of the solution gas, the weight of R_s scf of the gas is calculated as

$$m_g = \frac{R_s}{379.4} (28.96) (\gamma_g)$$

where m_g = weight of solution gas, lb of solution gas/STB.

The weight of one barrel of the stock-tank oil is calculated from its specific gravity by the following relationship:

$$m_o = (5.615)(62.4)(\gamma_o)$$

Substituting for m_o and m_g ,

$$B_o = \frac{(5.615)(62.4)\gamma_o + \frac{R_s}{379.4}(28.96)\gamma_g}{5.615\rho_o}$$

or

$$B_o = \frac{62.4\gamma_o + 0.0136R_s\gamma_g}{\rho_o} \quad (4-46)$$

where ρ_o = density of the oil at the specified pressure and temperature, lb/ft³.

The error in calculating B_o by using equation (4-46) depends on the accuracy of only the input variables (R_s , γ_g , and γ_o) and the method of calculating ρ_o .

EXAMPLE 4-20

The table below shows experimental PVT data on six crude oil systems. Results are based on two-stage surface separation. Calculate the oil formation volume factor at the bubble-point pressure using the preceding six different correlations. Compare the results with the experimental values and calculate the absolute average error.

Oil	T	p_b	R_s	B_o	ρ_o	c_o at $p > p_b$	p_{sep}	T_{sep}	API	γ_g
1	250	2377	751	1.528	38.13	22.14×10^{-6} at 2689	150	60	47.1	0.851
2	220	2620	768	1.474	40.95	18.75×10^{-6} at 2810	100	75	40.7	0.855
3	260	2051	693	0.529	37.37	22.69×10^{-6} at 2526	100	72	48.6	0.911
4	237	2884	968	1.619	38.92	21.51×10^{-6} at 2942	60	120	40.5	0.898
5	218	3065	943	0.570	37.70	24.16×10^{-6} at 3273	200	60	44.2	0.781
6	180	4239	807	0.385	46.79	11.65×10^{-6} at 4370	85	173	27.3	0.848

SOLUTION

For convenience, these six correlations follow:

Method 1

$$B_o = 0.9759 + 0.000120 \left[R_s \left(\frac{\gamma_g}{\gamma_o} \right)^{0.5} + 1.25(T - 460) \right]^{1.2}$$

Method 2

$$B_o = 1.0 + C_1 R_s + (T - 520) \left(\frac{API}{\gamma_{gs}} \right) [C_2 + C_3 R_s]$$

Method 3

$$B_o = 1.0 + 10^{-4}$$

Method 4

$$B_o = 0.497069 + 0.000862963T + 0.00182594F + 0.00000318099F^2$$

Method 5

$$B_o = 1.0113 + 7.2046(10^{-5})A$$

Method 6

$$B_o = \frac{62.4\gamma_o + 0.0136R_s\gamma_g}{\rho_o}$$

Results of applying these correlations for calculating B_o are tabulated in the table below.

Crude Oil	B_o	Method					
		1	2	3	4	5	6
1	1.528	1.506	1.474	1.473	1.516	1.552	1.525
2	1.474	1.487	1.450	1.459	1.477	1.508	1.470
3	1.529	1.495	1.451	1.461	1.511	1.556	1.542
4	1.619	1.618	1.542	1.589	1.575	1.632	1.623
5	1.570	1.571	1.546	1.541	1.554	1.584	1.599
6	1.385	1.461	1.389	1.438	1.414	1.433	1.387
%AAE	—	1.7	2.8	2.8	1.3	1.8	0.6

Method 1 = Standing’s correlation.
Method 2 = Vasquez and Beggs’s correlation.
Method 3 = Glaso’s correlation.
Method 4 = Marhoun’s correlation.
Method 5 = Petrosky and Farshad correlation.
Method 6 = Material balance equation.

Al-Shammasi (1999) used the neural network approach to generate an expression for predicting B_o . The relationship, as given below, gives an average absolute error of 1.81%:

$$B_o = 1 + [5.53(10^{-7})(T - 520)R_s] + 0.000181(R_s/\gamma_o) + [0.000449(T - 520)/\gamma_o]$$

$$+ [0.000206R_s\gamma_g/\gamma_o]$$

where T is the temperature in °R.

Isothermal Compressibility Coefficient of Crude Oil

The isothermal compressibility coefficient is defined as the rate of change in volume with respect to pressure increase per unit volume, all variables other than pressure being constant, including temperature. Mathematically, the isothermal compressibility, c , of a substance is defined by the following expression:

$$c = -\frac{1}{V} \left(\frac{\partial V}{\partial p} \right)_T$$

Isothermal compressibility coefficients are required in solving many reservoir engineering problems, including transient fluid flow problems; also they are required in the determination of the physical properties of the undersaturated crude oil.

For a crude oil system, the isothermal compressibility coefficient of the oil phase, c_o , is categorized into the following two types based on reservoir pressure:

1. At reservoir pressures that are greater than or equal to the bubble-point pressure ($p \geq p_b$), the crude oil exists as a single phase with all its dissolved gas still in solution. The isothermal compressibility coefficient of the oil phase, c_o , above the bubble point reflects the changes in the volume associated with oil expansion or compression of the single-phase oil with changing the reservoir pressure. The oil compressibility in this case is termed *undersaturated isothermal compressibility coefficient*.
2. Below the bubble-point pressure, the solution gas is liberated with decreasing reservoir pressure or redissolved with increasing the pressure. The changes of the oil volume as the result of changing the gas solubility must be considered when determining the isothermal compressibility coefficient. The oil compressibility in this case is termed *saturated isothermal compressibility coefficient*.

Undersaturated Isothermal Compressibility Coefficient

Generally, isothermal compressibility coefficients of an undersaturated crude oil are determined from a laboratory PVT study. A sample of the crude oil is placed in a PVT cell at the reservoir temperature and a pressure greater than the bubble-point pressure of the crude oil. At these initial conditions, the reservoir fluid exists as a single-phase liquid. The volume of the oil is allowed to expand as its pressure declines. This volume is recorded and plotted as a function of pressure. If the experimental pressure/volume diagram for the oil is available, the *instantaneous* compressibility coefficient, c_o , at any pressure can be calculated by graphically determining the volume, V , and the corresponding slope, $(\partial V/\partial p)_T$, at this pressure. At pressures above the bubble point, any of following equivalent expressions is valid in defining c_o :

$$c_o = -\frac{1}{V} \left(\frac{\partial V}{\partial p} \right)_T \quad (4-47)$$

$$c_o = -\frac{1}{B_o} \left(\frac{\partial B_o}{\partial p} \right)_T$$

$$c_o = \frac{1}{\rho_o} \left(\frac{\partial \rho_o}{\partial p} \right)_T$$

where

c_o = isothermal compressibility of the crude oil, psi^{-1}

$\left(\frac{\partial V}{\partial p} \right)_T$ = slope of the isothermal pressure/volume curve at p

ρ_o = oil density, lb/ft^3

B_o = oil formation volume factor, bbl/STB

Craft and Hawkins (1959) introduced the cumulative or average isothermal compressibility coefficient, which defines the compressibility from the initial reservoir pressure to current reservoir pressure. Craft and Hawkins's average compressibility, as defined here, is used in all material balance calculations:

$$\bar{c}_o = \frac{V \int_p^{p_i} c_o dp}{V[p_i - p]} = \frac{V - V_i}{V[p_i - p]}$$

where the subscript i represents initial condition. Equivalently, the average compressibility can be expressed in terms of B_o and ρ_o by the expressions

$$\bar{c}_o = \frac{B_o - B_{oi}}{B_o[p_i - p]}$$

$$\bar{c}_o = \frac{\rho_{oi} - \rho_o}{\rho_o[p_i - p]}$$

Several correlations were developed to estimate the oil compressibility at pressures above the bubble-point pressure, that is, an undersaturated crude oil system. Four of these correlations follow: Trube's correlation, Vasquez-Beggs's correlation, Petrosky-Farshad's correlation, and Standing's correlation.

Trube's Correlation

Trube (1957) introduced the concept of the isothermal pseudo-reduced compressibility, c_r , of undersaturated crude oils as defined by the relationship

$$c_r = c_o p_{pc} \quad (4-48)$$

Trube correlated this property graphically with the pseudo-reduced pressure and temperature, p_{pr} and T_{pr} , as shown in Figure 4-8.

Additionally, Trube presented two graphical correlations, as shown in Figures 4-9 and 4-10, to estimate the pseudo-critical properties of crude oils. The calculation procedure of the proposed method is summarized in the following steps.

Step 1 From the bottom-hole pressure measurements and pressure-gradient data, calculate the average density of the undersaturated reservoir oil, in gm/cm^3 , from the following expression:

$$(\rho_o)_T = \frac{dp/dh}{0.433}$$

where $(\rho_o)_T$ = oil density at reservoir pressure and temperature T , gm/cm^3 , and dp/dh = pressure gradient as obtained from a pressure buildup test.

Step 2 Adjust the calculated undersaturated oil density to its value at 60°F using the following equation:

$$(\rho_o)_{60} = (\rho_o)_T = 0.00046(T - 520) \quad (4-49)$$

where $(\rho_o)_{60}$ = adjusted undersaturated oil density to 60°F, gm/cm^3 , and T = reservoir temperature, °R.

Step 3 Determine the bubble-point pressure, p_b , of the crude oil at reservoir temperature. If the bubble-point pressure is not known, it can be estimated from Standing (1981), equation (4-30), written in a compacted form as

$$p_b = 18.2 \left[\left(\frac{R_s}{\gamma_g} \right)^{0.83} \left(\frac{10^{0.00091(T-460)}}{10^{0.0125^\circ \text{ API}}} \right) - 1.4 \right]$$

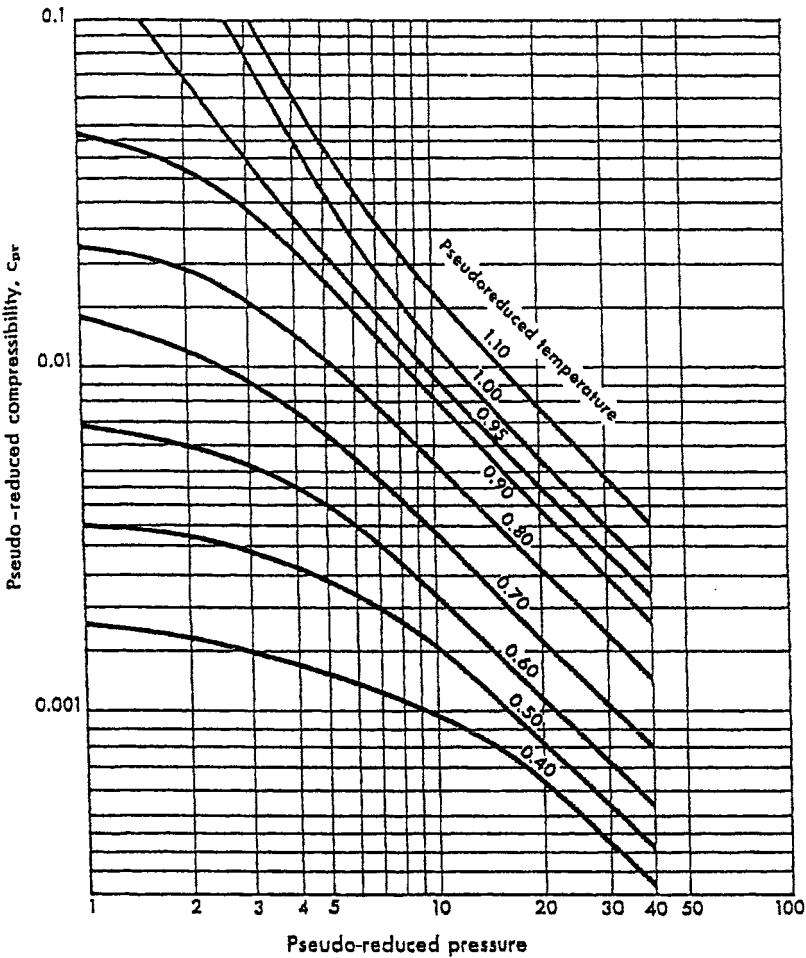


FIGURE 4-8 *Trube's pseudo-reduced compressibility of under-saturated crude oil.*

Source: A. S. Trube, "Compressibility of Under-saturated Hydrocarbon Reservoir Fluids," *Transactions of the AIME* 210 (1957): 341–344. Permission to publish from the Society of Petroleum Engineers of the AIME. © SPE-AIME.

Step 4 Correct the calculated bubble-point pressure, p_b , at reservoir temperature to its value at 60°F using the following equation as proposed by Standing (1942):

$$(p_b)_{60} = \frac{1.134 p_b}{10^{0.00091(T - 460)}} \tag{4-50}$$

where

- $(p_b)_{60}$ = bubble-point pressure at 60°F, psi
- p_b = bubble-point pressure at reservoir temperature, psia
- T = reservoir temperature, °R

Step 5 Enter in Figure 4-9 the values of $(p_b)_{60}$ and $(\rho_o)_{60}$ and determine the pseudo-critical temperature, T_{pc} , of the crude.

Step 6 Enter the value of T_{pc} in Figure 4-10 and determine the pseudo-critical pressure, p_{pc} , of the crude.

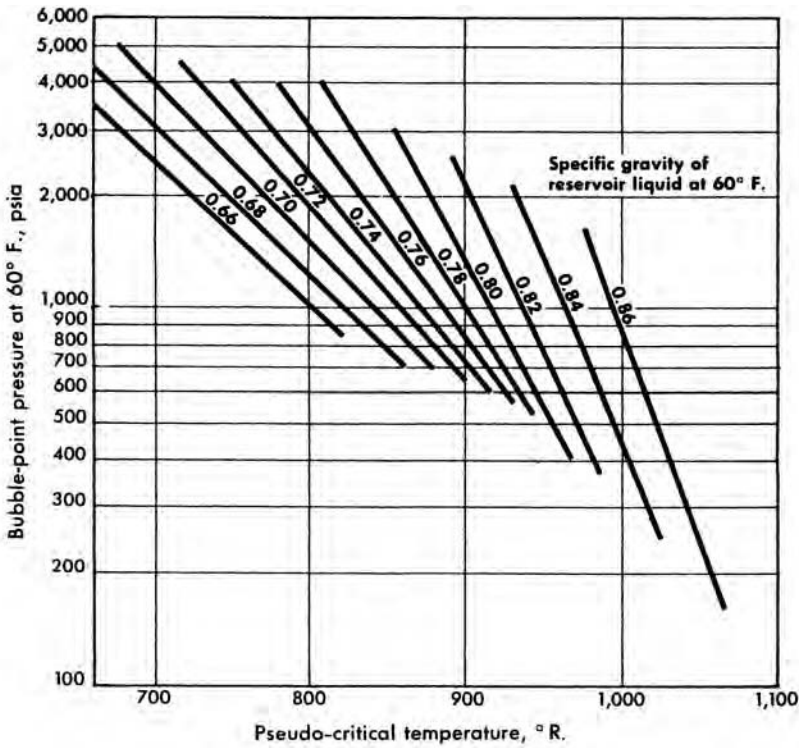


FIGURE 4-9 *Trube's pseudo-critical temperature correlation.*

Source: A. S. Trube, "Compressibility of Understaturated Hydrocarbon Reservoir Fluids," *Transactions of the AIME* 210 (1957): 341-344. Permission to publish from the Society of Petroleum Engineers of the AIME. © SPE-AIME.

Step 7 Calculate the pseudo-reduced pressure, p_{pr} , and temperature, T_{pr} , from the following relationships:

$$T_{pr} = \frac{T}{T_{pc}}$$

$$p_{pr} = \frac{p}{p_{pc}}$$

Step 8 Determine c_r by entering into Figure 4-8 the values of T_{pr} and p_{pr} .

Step 9 Calculate c_o from equation (4-48):

$$c_o = \frac{c_r}{p_{pc}}$$

Trube did not specify the data used to develop the correlation nor did he allude to their accuracy, although the examples presented in his paper showed an average absolute error of 7.9% between calculated and measured values. Trube's correlation can be best illustrated through the following example.

EXAMPLE 4-21

Given the following data:

Oil gravity = 45°

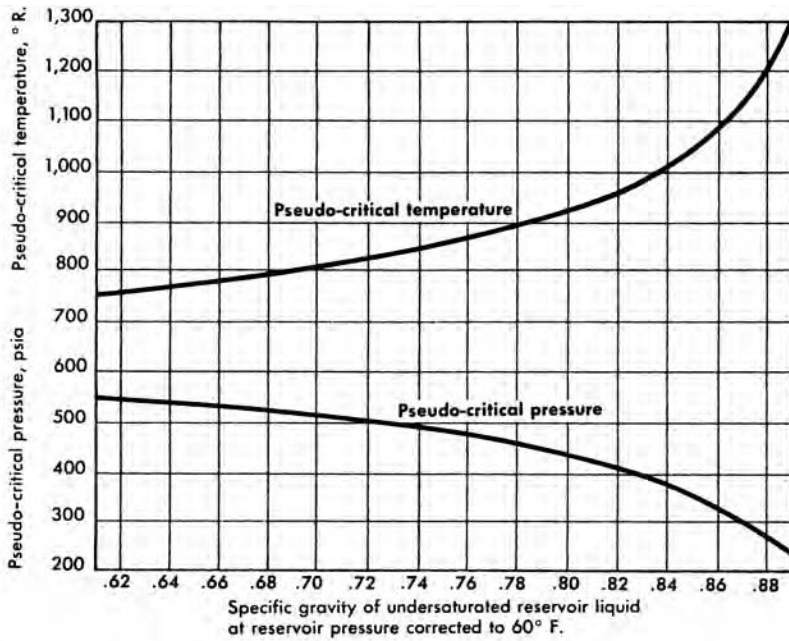


FIGURE 4-10 Trube's pseudo-critical properties correlation.

Source: A. S. Trube, "Compressibility of Understaturated Hydrocarbon Reservoir Fluids," *Transactions of the AIME* 210 (1957): 341-344. Permission to publish from the Society of Petroleum Engineers of the AIME. © SPE-AIME.)

Gas solubility = 600 scf/STB

Solution gas gravity = 0.8

Reservoir temperature = 212°F

Reservoir pressure = 2000 psia

Pressure gradient of reservoir liquid at 2000 psia and 212°F = 0.032 psi/ft

find c_o at 2000, 3000, and 4000 psia.

SOLUTION

Step 1 Determine $(\rho_o)_T$:

$$(\rho_o)_T = \frac{dp/dh}{0.433} = \frac{0.32}{0.433} = 0.739 \text{ gm/cm}^3$$

Step 2 Correct the calculated oil specific gravity to its value at 60°F by applying equation (4-49):

$$\begin{aligned} (\rho_o)_{60} &= (\rho_o)_T + 0.00046(T - 520) \\ (\rho_o)_{60} &= 0.739 + 0.00046(152) = 0.8089 \end{aligned}$$

Step 3 Calculate the bubble-point pressure from Standing's correlation (equation 4-40):

$$\begin{aligned} p_b &= 18.2 \left[\left(\frac{R_s}{\gamma_g} \right)^{0.83} \left(\frac{10^{0.00091(T-460)}}{10^{0.0125 \text{ API}}} \right) - 1.4 \right] \\ p_b &= 18.2 \left[\left(\frac{600}{0.8} \right)^{0.83} \frac{10^{0.00091(T-212)}}{10^{0.0125(45)}} - 1.4 \right] = 1866 \text{ psia} \end{aligned}$$

Step 4 Adjust p_b to its value at 60°F by applying equation (4–50):

$$(p_b)_{60} = \frac{1.134 p_b}{10^{0.00091(T-460)}}$$

$$(p_b)_{60} = \frac{1.134(1866)}{10^{0.00091(212)}} = 1357.1 \text{ psia}$$

Step 5 Estimate the pseudo-critical temperature, T_{pc} , of the crude oil from Figure 4–9, to give:

$$T_{pc} = 840^\circ\text{R}$$

Step 6 Estimate the pseudo-critical pressure, p_{pc} , of the crude oil from Figure 4–10, to give:

$$p_{pc} = 500 \text{ psia}$$

Step 7 Calculate the pseudo-reduced temperature:

$$T_{pr} = \frac{672}{840} = 0.8$$

Step 8 Calculate the pseudo-reduced pressure, p_{pr} , the pseudo-reduced isothermal compressibility coefficient, c_r , and tabulate values of the corresponding isothermal compressibility coefficient as shown in the table below.

p	$p_{pr} = p/500$	c_r	$c_o = c_r/p_{pr} 10^{-6} \text{ psia}^{-1}$
2000	4	0.0125	25.0
3000	6	0.0089	17.8
4000	8	0.0065	13.0

Vasquez-Beggs's Correlation

From a total of 4036 experimental data points used in a linear regression model, Vasquez and Beggs (1980) correlated the isothermal oil compressibility coefficients with R_s , T , $^\circ\text{API}$, γ_g , and p . They proposed the following expression:

$$c_o = \frac{-1433 + 5R_{sb} + 17.2(T-460) - 1180\gamma_{gs} + 12.61^\circ\text{API}}{10^5 p} \quad (4-51)$$

where

T = temperature, $^\circ\text{R}$

p = pressure above the bubble-point pressure, psia

R_{sb} = gas solubility at the bubble-point pressure

γ_{gs} = corrected gas gravity as defined by equation (4–3)

Petrosky-Farshad's Correlation

Petrosky and Farshad (1993) proposed a relationship for determining the oil compressibility for undersaturated hydrocarbon systems. The equation has the following form:

$$c_o = 1.705 \times 10^{-7} R_{sb}^{0.69357} \gamma_g^{0.1885} \text{API}^{0.3272} (T-460)^{0.6729} P^{-0.5906} \quad (4-52)$$

where T = temperature, $^\circ\text{R}$, and R_{sb} = gas solubility at the bubble-point pressure, scf/STB.

Standing’s Correlation

Standing (1974) proposed a graphical correlation for determining the oil compressibility for undersaturated hydrocarbon systems. Whitson and Brule expressed his relationship in the following mathematical form:

$$c_o = 10^{-6} \exp \left[\frac{\rho_{ob} + 0.004347(p - p_b) - 79.1}{0.0007141(p - p_b) - 12.938} \right] \tag{4-53}$$

where

- ρ_{ob} = oil density at the bubble-point pressure, lb/ft³
- p_b = bubble-point pressure, psia
- c_o = oil compressibility, psia⁻¹

EXAMPLE 4-22

Using the experimental data given in Example 4-20, estimate the undersaturated oil compressibility coefficient using the Vasquez-Beggs, Petrosky-Farshad, and Standing correlations. The data given in Example 4-20 is reported in the following table for convenience.

Oil	<i>T</i>	<i>p_b</i>	<i>R_s</i>	<i>B_o</i>	ρ_o	<i>c_o</i> at <i>p</i> > <i>p_b</i>	<i>p_{sep}</i>	<i>T_{sep}</i>	API	γ_g
1	250	2377	751	1.528	38.13	22.14 × 10 ⁻⁶ at 2689	150	60	47.1	0.851
2	220	2620	768	1.474	40.95	18.75 × 10 ⁻⁶ at 2810	100	75	40.7	0.855
3	260	2051	693	0.529	37.37	22.69 × 10 ⁻⁶ at 2526	100	72	48.6	0.911
4	237	2884	968	1.619	38.92	21.51 × 10 ⁻⁶ at 2942	60	120	40.5	0.898
5	218	3065	943	0.570	37.70	24.16 × 10 ⁻⁶ at 3273	200	60	44.2	0.781
6	180	4239	807	0.385	46.79	11.65 × 10 ⁻⁶ at 4370	85	173	27.3	0.848

SOLUTION

The results are shown in the table below.

Oil	Pressure	Measured <i>c_o</i> 10 ⁻⁶ psi	Standing’s 10 ⁻⁶ psi	Vasquez-Beggs 10 ⁻⁶ psi	Petrosky-Farshad 10 ⁻⁶ psi
1	2689	22.14	22.54	22.88	22.24
2	2810	18.75	18.46	20.16	19.27
3	2526	22.60	23.30	23.78	22.92
4	2942	21.51	22.11	22.31	21.78
5	3273	24.16	23.72	20.16	20.39
6	4370	11.45	11.84	11.54	11.77
AAE			2.0%	6.18%	4.05%

Vasquez-Beggs: $c_o = \frac{-1433 + 5R_{sb} + 17.2(T - 460) - 1180\gamma_{gs} + 12.61^\circ\text{API}}{10^5 p}$

Petrosky-Farshad: $c_o = 1.705 \times 10^{-7} R_{sb}^{0.69357} \gamma_g^{0.1885} \text{API}^{0.3272} (T - 460)^{0.6729} P^{-0.5906}$

Standing’s : $c_o = 10^{-6} \exp \left[\frac{\rho_{ob} + 0.004347(p - p_b) - 79.1}{0.0007141(p - p_b) - 12.938} \right]$

Saturated Isothermal Compressibility Coefficient

At pressures below the bubble-point pressure, the isothermal compressibility coefficient of the oil must be modified to account for the shrinkage associated with the liberation of the solution gas with decreasing reservoir pressure or swelling of the oil with repressurizing

the reservoir and redissolving the solution gas. These changes in the oil volume as the result of changing the gas solubility must be considered when determining the isothermal compressibility coefficient of the oil compressibility. Below the bubble-point pressure, c_o , is defined by the following expression:

$$c_o = \frac{-1}{B_o} \frac{\partial B_o}{\partial p} + \frac{B_g}{B_o} \frac{\partial R_s}{\partial p} \quad (4-54)$$

where B_g = gas formation volume factor, bbl/scf.

Analytically, Standing's correlations for R_s (equation 4-23) and B_o (equation 4-38) can be differentiated with respect to the pressure, p , to give

$$\frac{\partial R_s}{\partial p} = \frac{R_s}{0.83p + 21.75}$$

$$\frac{\partial B_o}{\partial p} = \left[\frac{0.000144 R_s}{0.83p + 21.75} \right] \left(\frac{\gamma_g}{\gamma_o} \right)^{0.5} \left[R_s \left(\frac{\gamma_g}{\gamma_o} \right)^{0.5} + 1.25(T - 46) \right]^{0.2}$$

These two expressions can be substituted into equation (4-54) to give the following relationship:

$$c_o = \frac{-R_s}{B_o(0.83p + 21.75)} \left\{ 0.000144 \sqrt{\frac{\gamma_g}{\gamma_o}} \left[R_s \sqrt{\frac{\gamma_g}{\gamma_o}} + 1.25(T - 460) \right]^{0.2} - B_g \right\} \quad (4-55)$$

where

p = pressure, psia

T = temperature, °R

B_g = gas formation volume factor at pressure p , bbl/scf

R_s = gas solubility at pressure p , scf/STB

B_o = oil formation volume factor at p , bbl/STB

γ_o = specific gravity of the stock-tank oil

γ_g = specific gravity of the solution gas

McCain and coauthors (1988) correlated the oil compressibility with pressure, p , psia; oil API gravity; gas solubility at the bubble-point, R_{sb} , in scf/STB; and temperature, T , in °R. Their proposed relationship has the following form:

$$c_o = \exp(A) \quad (4-56)$$

where the correlating parameter A is given by the following expression:

$$A = -7.633 - 1.497 \ln(p) + 1.115 \ln(T) + 0.533 \ln(\text{API}) + 0.184 \ln(R_{sp}) \quad (4-57)$$

The authors suggested that the accuracy of equation (4-56) can be substantially improved if the bubble-point pressure is known. They improved correlating parameter, A , by including the bubble-point pressure, p_b , as one of the parameters in the preceding equation, to give

$$A = -7.573 - 1.45 \ln(p) - 0.383 \ln(p_b) + 1.402 \ln(T) + 0.256 \ln(\text{API}) + 0.449 \ln(R_{sb}) \quad (4-58)$$

EXAMPLE 4-23

A crude oil system exists at 1650 psi and a temperature of 250°F. The system has the following PVT properties:

$$API = 47.1$$

$$p_b = 2377 \text{ psi}$$

$$\gamma_g = 0.851$$

$$\gamma_{gs} = 0.873$$

$$R_{sb} = 751 \text{ scf/STB}$$

$$B_{ob} = 1.528 \text{ bbl/STB}$$

The laboratory-measured oil PVT data at 1650 psig follow:

$$B_o = 1.393 \text{ bbl/STB}$$

$$R_s = 515 \text{ scf/STB}$$

$$B_g = 0.001936 \text{ bbl/scf}$$

$$c_o = 324.8 \times 10^{-6} \text{ psi}^{-1}$$

Estimate the oil compressibility using McCain's correlation, then equation (4-55).

SOLUTION

Calculate the correlating parameter A by applying equation (4-58):

$$A = -7.573 - 1.45 \ln(p) - 0.383 \ln(p_b) + 1.402 \ln(T) + 0.256 \ln(API) + 0.449 \ln(R_{sb})$$

$$A = -7.573 - 1.45 \ln(1665) - 0.383 \ln(2392) + 1.402 \ln(710) + 0.256 \ln(47.1) + 0.449 \ln(451) = -8.1445$$

Solve for c_o using equation (4-56):

$$c_o = \exp(A)$$

$$c_o = \exp(-8.1445) = 290.3 \times 10^{-6} \text{ psi}^{-1}$$

Solve for c_o using equation (4-55):

$$c_o = \frac{-R_s}{B_o(0.83p + 21.75)} \left\{ 0.000144 \sqrt{\frac{\gamma_g}{\gamma_o}} \left[R_s \sqrt{\frac{\gamma_g}{\gamma_o}} + 1.25(T - 460) \right]^{0.2} - B_g \right\}$$

$$c_o = \frac{-515}{1.393[0.83(1665) + 21.75]} \left\{ 0.000144 \sqrt{\frac{0.851}{0.792}} \left[515 \sqrt{\frac{0.851}{0.792}} + 1.25(250) \right]^{0.2} - 0.001936 \right\}$$

$$c_o = 358 \times 10^{-6} \text{ psi}^{-1}$$

It should be pointed out that, when it is necessary to establish PVT relationships for the hydrocarbon system through correlations or by extrapolation below the bubble-point pressure, care should be exercised to see that the PVT functions are consistent. This consistency is assured if the increase in oil volume with increasing pressure is less than the decrease in volume associated with the gas going into solution. Since the oil compressibility coefficient, c_o , as expressed by equation (4-54) must be positive, that leads to the following consistency criteria:

$$\frac{\partial B_o}{\partial p} < B_g \frac{\partial R_s}{\partial p}$$

This consistency can easily be checked in the tabular form of PVT data. The PVT consistency errors most frequently occur at higher pressures, where the gas formation volume factor, B_g , assumes relatively small values.

Undersaturated Oil Properties

Figure 4–11 shows the volumetric behavior of the gas solubility, R_s , oil formation volume factor, B_o , and oil density, ρ_o , as a function of pressure. As previously defined, the gas solubility, R_s , measures the tendency of the gas to dissolve in the oil at a particular temperature with increasing pressure. This solubility tendency, as measured in standard cubic feet of gas per one stock-tank barrel of oil, increases with pressure until the bubble-point pressure is reached. With increasing of the gas solubility in the crude oil, the oil swells with the resulting increase in the oil formation volume factor and an associated decrease in both its density and viscosity, as shown in Figure 4–11. With increasing the pressure above the bubble-point pressure, p_b , the gas solubility remains constant with a maximum value that is denoted by R_{sb} (gas solubility at the bubble-point pressure). However, as the pressure increases above p_b , the crude oil system experiences a reduction in its volume (V_o)_{p,T} during this isothermal compression. From the mathematical definition of B_o and ρ_o ,

$$B_o = \frac{(V_o)_{p,T}}{(V_o)_{sc}}$$

$$\rho_o = \frac{\text{mass}}{(V_o)_{p,T}}$$

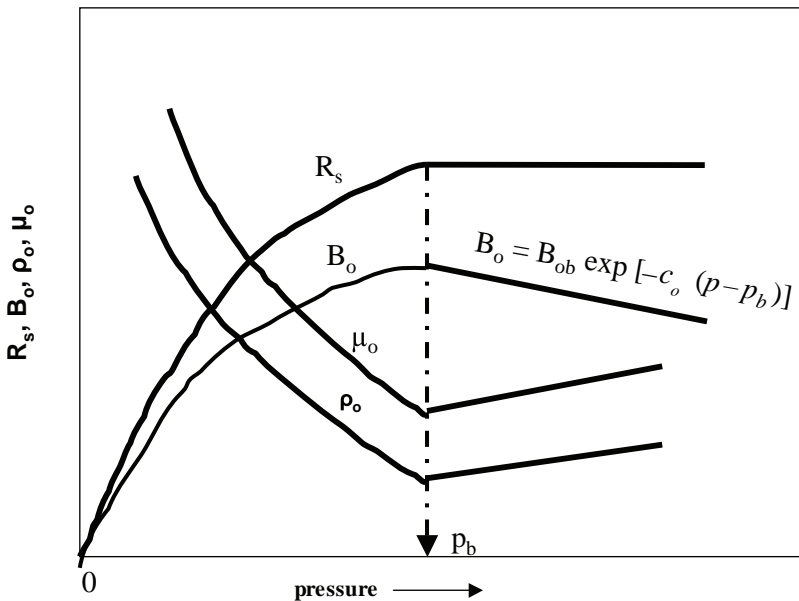


FIGURE 4–11 Undersaturated fluid properties versus pressure.

These two expressions indicate that, with increasing the pressure above p_b , the associated reduction in the volume oil $(V_o)_{p,T}$ results in a decrease in B_o and an increase in ρ_o .

The magnitude of the changes in the oil volume above the bubble-point pressure is a function of its isothermal compressibility coefficient c_o . To account for the effect of oil compression on the oil formation volume factor and oil density, these two properties are first calculated at the bubble-point pressure as B_{ob} and ρ_{ob} using any of the methods previously described and then adjusted to reflect the increase in p over p_b .

Undersaturated Oil-Formation Volume Factor

The isothermal compressibility coefficient (as expressed mathematically by equation 4-47) can be equivalently written in terms of the oil-formation volume factor:

$$c_o = \frac{-1}{V_o} \frac{\partial V_o}{\partial p}$$

This relationship can be equivalently expressed in terms of B_o as

$$c_o = \frac{-1}{V_o / (V_o)_{sc}} \frac{\partial [V_o / (V_o)_{sc}]}{\partial p} = \frac{-1}{B_o} \frac{\partial B_o}{\partial P} \quad (4-59)$$

This relationship can be rearranged and integrated to produce

$$\int_{p_b}^p -c_o dp = \int_{B_{ob}}^{B_o} \frac{1}{B_o} dB_o \quad (4-60)$$

Evaluating c_o at the arithmetic average pressure and concluding the integration procedure to give

$$B_o = B_{ob} \exp[-c_o (p - p_b)] \quad (4-61)$$

where

B_o = oil formation volume factor at the pressure of interest, bbl/STB

B_{ob} = oil formation volume factor at the bubble-point pressure, bbl/STB

p = pressure of interest, psia

p_b = bubble-point pressure, psia

Replacing the isothermal compressibility coefficient in equation (4-60) with the Vasquez-Beggs's c_o expression, equation (4-51), and integrating the resulting equation gives

$$B_o = B_{ob} \exp \left[-A \ln \left(\frac{p}{p_b} \right) \right] \quad (4-62)$$

where

$$A = 10^{-5} [-1433 + 5R_{sb} + 17.2(T - 460) - 1180\gamma_{gs} + 12.61 \text{ API}]$$

Similarly, replacing c_o in equation (4-60) with the Petrosky and Farshad expression (equation 4-52) and integrating gives

$$B_o = B_{ob} \exp[-A(p^{0.4094} - p_b^{0.4094})] \quad (4-63)$$

with the correlating parameter A as defined by

$$A = 4.1646(10^{-7})R_{sb}^{0.69357}\gamma_g^{0.1885}(\text{API})^{0.3272}(T - 460)^{0.6729} \quad (4-64)$$

where

T = temperature, °R

p = pressure, psia

R_{sb} = gas solubility at the bubble-point pressure

EXAMPLE 4-24

Using the PVT data given in Example 4-23, calculate the oil formation volume factor at 5000 psig using equation (4-62) then equation (4-64). The experimental measured B_o is 1.457 bbl/STB.

SOLUTION USING EQUATION (4-62)

Step 1 Calculate parameter A of equation (4-62):

$$A = 10^{-5}[-1433 + 5R_{sb} + 17.2(T - 460) - 1180\gamma_{gs} + 12.61 \text{ API}]$$

$$A = 10^{-5}[-1433 + 5(751) + 17.2(250) - 1180(0.873) + 12.61(47.1)] = 0.061858$$

Step 2 Apply equation (4-62):

$$B_o = B_{ob} \exp\left[-A \ln\left(\frac{p}{p_b}\right)\right]$$

$$B_o = 1.528 \exp\left[-0.061858 \ln\left(\frac{5015}{2392}\right)\right] = 1.459 \text{ bbl/STB}$$

SOLUTION USING EQUATION (4-64)

Step 1 Calculate the correlating parameter, A , from equation (4-64):

$$A = 4.1646(10^{-7})R_{sb}^{0.69357}\gamma_g^{0.1885}(\text{API})^{0.3272}(T - 460)^{0.6729}$$

$$A = 4.1646 \times 10^{-7}(751)^{0.69357}(0.851)^{0.1885}(47.1)^{0.3272}(250)^{0.6729} = 0.005778$$

Step 2 Solve for B_o by applying equation (4-63):

$$B_o = B_{ob} \exp[-A(p^{0.4094} - p_b^{0.4094})]$$

$$B_o = (1.528) \exp[-0.005778(5015^{0.4094} - 2392^{0.4094})] = 1.453 \text{ bbl/STB}$$

Undersaturated Oil Density

Oil density ρ_o is defined as mass, m , over volume, V_o , at any specified pressure and temperature, or the volume can be expressed as

$$V_o = \frac{m}{\rho_o}$$

Differentiating density with respect to pressure gives

$$\left(\frac{\partial V_o}{\partial p}\right)_T = \frac{-m}{\rho_o^2} \frac{\partial \rho_o}{\partial p}$$

Substituting these two relations into equation (4-47) gives

$$c_o = \frac{-1}{V_o} \frac{\partial V_o}{\partial p} = \frac{-1}{(m/\rho_o)} \left[\frac{-m}{\rho_o^2} \frac{\partial \rho_o}{\partial p} \right]$$

or, in terms of density,

$$c_o = \frac{1}{\rho_o} \frac{\partial \rho_o}{\partial p}$$

Rearranging and integrating yields

$$\int_{p_b}^p c_o dp = \int_{p_b}^p \frac{d\rho_o}{\rho_o}$$

$$c_o(p - p_b) = \ln \left(\frac{\rho_o}{\rho_{ob}} \right)$$

Solving for the density of the oil at pressures above the bubble-point pressure,

$$\rho_o = \rho_{ob} \exp[c_o(p - p_b)] \quad (4-65)$$

where

ρ_o = density of the oil at pressure p , lb/ft³

ρ_{ob} = density of the oil at the bubble-point pressure, lb/ft³

c_o = isothermal compressibility coefficient at average pressure, psi⁻¹

Vasquez-Beggs's oil compressibility correlation and Petrosky-Farshad's c_o expression can be incorporated in equation (4-65) to give the following.

For Vasquez-Beggs's c_o equation,

$$\rho_o = \rho_{ob} \exp \left[A \ln \left(\frac{p}{p_b} \right) \right] \quad (4-66)$$

where

$$A = 10^{-5} [-1433 + 5R_{sb} + 17.2(T - 460) - 1180\gamma_{gs} + 12.61^\circ\text{API}]$$

For Petrosky-Farshad's c_o expression,

$$\rho_o = \rho_{ob} \exp \left[A \left(p^{0.4094} - p_b^{0.4094} \right) \right] \quad (4-67)$$

with the correlating parameter A given by equation (4-64):

$$A = 4.1646(10^{-7})R_{sb}^{0.69357}\gamma_g^{0.1885}(\text{API})^{0.3272}(T - 460)^{0.6729}$$

Total-Formation Volume Factor

To describe the pressure/volume relationship of hydrocarbon systems below their bubble-point pressure, it is convenient to express this relationship in terms of the total-formation volume factor as a function of pressure. This property defines the total volume of a system regardless of the number of phases present. The total formation volume factor, denoted B_t , is defined as the ratio of the total volume of the hydrocarbon mixture, that is, oil and gas, if present, at the prevailing pressure and temperature per unit volume of the stock-tank oil. Because naturally-occurring hydrocarbon systems usually exist in either one or two

phases, the term two-phase formation volume factor has become synonymous with the total-formation volume.

Mathematically, B_t is defined by the following relationship:

$$B_t = \frac{(V_o)_{p,T} + (V_g)_{p,T}}{(V_o)_{sc}} \quad (4-68)$$

where

B_t = total formation volume factor, bbl/STB

$(V_o)_{p,T}$ = volume of the oil at p and T , bbl

$(V_g)_{p,T}$ = volume of the liberated gas at p and T , bbl

$(V_o)_{sc}$ = volume of the oil at standard conditions, STB

Note that, when reservoir pressures are greater than or equal to the bubble-point pressure, no free gas will exist in the reservoir and, therefore, $(V_g)_{p,T} = 0$. At these conditions, equation (4-68) is reduced to the equation that describes the oil formation volume factor:

$$B_t = \frac{(V_o)_{p,T} + 0}{(V_o)_{sc}} = \frac{(V_o)_{p,T}}{(V_o)_{sc}} = B_o$$

A typical plot of B_t as a function of pressure for an undersaturated crude oil is shown in Figure 4-12. The oil formation volume factor curve is also included in the illustration. As pointed out, B_o and B_t are identical at pressures above or equal to the bubble-point pressure because only one phase, the oil phase, exists at these pressures. It should also be noted that at pressures below the bubble-point pressure, the difference in the values of the two oil properties represents the volume of the evolved solution gas as measured at system conditions per stock-tank barrel of oil.

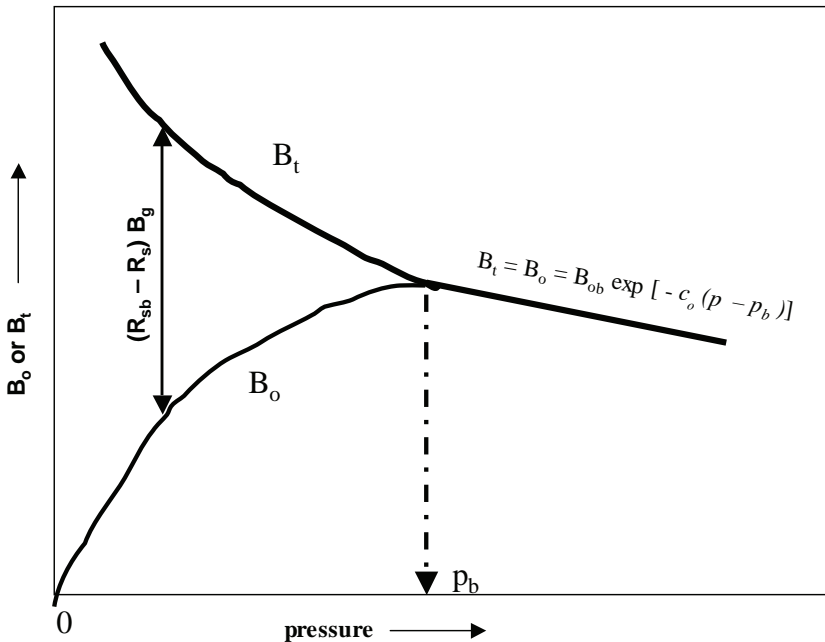


FIGURE 4-12 B_o and B_t versus pressure.

Consider a crude oil sample placed in a PVT cell at its bubble-point pressure, p_b , and reservoir temperature, as shown schematically in Figure 4–13. Assume that the volume of the oil sample is sufficient to yield one stock-tank barrel of oil at standard conditions. Let R_{sb} represent the gas solubility at p_b . By lowering the cell pressure to p , a portion of the solution gas is evolved and occupies a certain volume of the PVT cell. Let R_s and B_o represent the corresponding gas solubility and oil formation volume factor at p . Obviously, the term $(R_{sb} - R_s)$ represents the volume of the free gas as measured in scf per sock-tank barrel of the oil. The volume of the free gas at the cell conditions is then

$$(V_g)_{p,T} = (R_{sb} - R_s)B_g$$

where $(V_g)_{p,T}$ = volume of the free gas at p and T , bbl of gas/STB of oil, and B_g = gas formation volume factor, bbl/scf.

The volume of the remaining oil at the cell condition is

$$(V_o)_{p,T} = B_o$$

From the definition of the two-phase formation volume factor,

$$B_t = B_o + (R_{sb} - R_s) B_g \tag{4-69}$$

where

R_{sb} = gas solubility at the bubble-point pressure, scf/STB

R_s = gas solubility at any pressure, scf/STB

B_o = oil formation volume factor at any pressure, bbl/STB

B_g = gas formation volume factor, bbl/scf

It is important to note from the previously described laboratory procedure that no gas or oil has been removed from the PVT cell with declining pressure, that is, *no changes in*

Constant Composition Expansion (CCE)

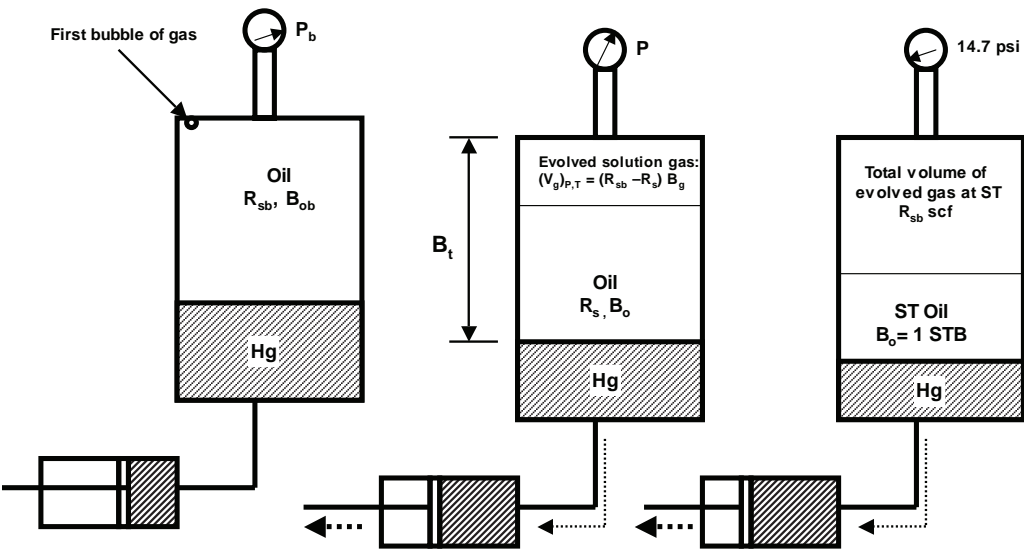


FIGURE 4–13 The concept of the two-phase formation volume factor.

the overall composition of the hydrocarbon mixture. As described later in this chapter, this is a property determined from the *constant composition expansion* test. It should be pointed out that the accuracy of estimating B_t by equation (4-69) depends largely on the accuracy of the other PVT parameters used in the equation: B_o , R_{sb} , R_s , and B_g .

Several correlations can be used to estimate the two-phase formation volume factor when the experimental data are not available; three of these methods follow: Standing's correlation, Glaso's correlation, and Marhoun's correlation.

Standing's Correlation

Standing (1947) used 387 experimental data points to develop a graphical correlation for predicting the two-phase formation volume factor with a reported average error of 5%. The proposed correlation uses the following parameters for estimating the two-phase formation volume factor:

- The gas solubility at pressure of interest, R_s .
- Solution gas gravity, γ_g .
- Oil gravity, γ_o , 60°/60°.
- Reservoir temperature, T .
- Pressure of interest, p .

In developing his graphical correlation, Standing used a combined correlating parameter that is given by

$$\log(A^*) = \log \left[R_s \frac{(T - 460)^{0.5} (\gamma_o)^C}{(\gamma_g)^{0.3}} \right] - \left(10.1 - \frac{96.8}{6.604 + \log(p)} \right) \quad (4-70)$$

with the exponent C as defined by

$$C = (2.9)10^{-0.00027R_s} \quad (4-71)$$

Whitson and Brule (2000) expressed Standing's graphical correlation by the following mathematical form:

$$\log(B_t) = -5.223 - \frac{47.4}{\log(A^*) - 12.22} \quad (4-72)$$

Glaso's Correlation

Experimental data on 45 crude oil samples from the North Sea were used by Glaso (1980) in developing a generalized correlation for estimating B_t . Glaso modified Standing's correlating parameter A^* as given by equation (4-70) and used it in a regression analysis model to develop the following expression for B_t :

$$\log(B_t) = 0.080135 + 0.47257 \log(A^*) + 0.17351 [\log(A^*)]^2 \quad (4-73)$$

The author included the pressure in Standing's correlating parameter A^* to give:

$$A^* = \left[\frac{R_s (T - 460)^{0.5} (\gamma_o)^C}{(\gamma_g)^{0.3}} \right] p^{-1.1089} \quad (4-74)$$

with the exponent C as given by equation (4-71):

$$C = (2.9)10^{-0.00027R_s}$$

Glaser reported a standard deviation of 6.54% for the total formation volume factor correlation.

Marhoun's Correlation

Based on 1556 experimentally determined total-formation volume factors, Marhoun (1988) used a nonlinear multiple regression model to develop a mathematical expression for B_t . The empirical equation has the following form:

$$B_t = 0.314693 + 0.106253 \times 10^{-4}F + 0.18883 \times 10^{-10}F^2 \quad (4-75)$$

with the correlating parameter F as given by

$$F = R_s^a \gamma_g^b \gamma_o^c T^d p^e$$

where T is the temperature in $^{\circ}\text{R}$ and the coefficients a – e as given below:

$$a = 0.644516$$

$$b = -1.079340$$

$$c = 0.724874$$

$$d = 2.006210$$

$$e = -0.761910$$

Marhoun reported an average absolute error of 4.11% with a standard deviation of 4.94% for the correlation.

EXAMPLE 4-25

Given the following PVT data:

$$p_b = 2744 \text{ psia}$$

$$T = 600^{\circ}\text{R}$$

$$\gamma_g = 0.6744$$

$$R_s = 444 \text{ scf/STB}$$

$$R_{sb} = 603 \text{ scf/STB}$$

$$\gamma_o = 0.843 \text{ } 60^{\circ}/60^{\circ}$$

$$p = 2000 \text{ psia}$$

$$B_o = 1.1752 \text{ bbl/STB}$$

calculate B_t at 2000.7 psia using equation (4-69), Standing's correlation, Glasco's correlation, and Marhoun's correlation.

SOLUTION USING EQUATION (4-69)

Step 1 Calculate T_{pc} and p_{pc} of the solution gas from its specific gravity by applying equations (3-18) and (3-19):

$$T_{pc} = 168 + 325\gamma_g - 12.5(\gamma_g)^2$$

$$T_{pc} = 168 + 325(0.6744) - 12.5(0.6744)^2 = 381.49^{\circ}\text{R}$$

$$p_{pc} = 677 + 15\gamma_g - 37.5(\gamma_g)^2 = 670.06 \text{ psia}$$

Step 2 Calculate p_{pr} and T_{pr} :

$$p_{pr} = \frac{p}{p_{pc}} = \frac{2000}{670.00} = 2.986$$

$$T_{pr} = \frac{T}{T_{pc}} = \frac{600}{381.49} = 1.57$$

Step 3 Determine the gas compressibility factor from Figure 3-1:

$$Z = 0.81$$

Step 4 Calculate B_g from equation (3-54):

$$B_g = 0.00504 \frac{(0.81)(600)}{2000} = 0.001225 \text{ bbl/scf}$$

Step 5 Solve for B_t by applying equation (4-69):

$$B_t = B_o + (R_{sb} - R_s)B_g$$

$$B_t = 1.1752 + 0.0001225(603 - 444) = 1.195 \text{ bbl/STB}$$

SOLUTION USING STANDING'S CORRELATION

Calculate the correlating parameters C and A^* by applying equations (4-71) and (4-70), respectively:

$$C = (2.9)10^{-0.00027R_s}$$

$$C = (2.9)10^{-0.00027(444)} = 2.20$$

$$\log(A^*) = \log \left[R_s \frac{(T - 460)^{0.5} (\gamma_o)^C}{(\gamma_g)^{0.3}} \right] - \left(10.1 - \frac{96.8}{6.604 + \log(p)} \right)$$

$$\log(A^*) = \log \left[(444) \frac{(140)^{0.5} (0.843)^{2.2}}{(0.6744)^{0.3}} \right] - \left(10.1 - \frac{96.8}{6.604 + \log(2000)} \right) = 3.281$$

Estimate B_t from equation (4-72):

$$\log(B_t) = -5.223 - \frac{47.4}{\log(A^*) - 12.22}$$

$$\log(B_t) = -5.223 - \frac{47.4}{3.281 - 12.22} = 0.0792$$

to give

$$B_t = 10^{0.0792} = 1.200 \text{ bbl/STB}$$

SOLUTION USING GLASO'S CORRELATION

Step 1 Determine the coefficient C from equation (4-71):

$$C = (2.9)10^{-0.00027(444)} = 2.2$$

Step 2 Calculate the correlating parameter A^* from equation (4-74):

$$A^* = \left[\frac{R_s (T - 460)^{0.5} (\gamma_o)^C}{(\gamma_g)^{0.3}} \right] p^{-1.1089}$$

$$A^* = \left[\frac{(444)(140)^{0.5} (0.843)^{2.2}}{(0.6744)^{0.3}} \right] 2000^{-1.1089} = 0.8873$$

Step 3 Solve for B_t by applying equation (4-73) to yield:

$$\begin{aligned}\log(B_t) &= 0.080135 + 0.47257 \log(A^*) + 0.17351 [\log(A^*)]^2 \\ \log(B_t) &= 0.080135 + 0.47257 \log(0.8873) + 0.17351 [\log(0.8873)]^2 = 0.0561\end{aligned}$$

to give

$$B_t = 10^{0.0561} = 1.138$$

SOLUTION USING MARHOUN'S CORRELATION

Step 1 Determine the correlating parameter F of equation (4-75) to give

$$\begin{aligned}F &= R_s^a \gamma_g^b \gamma_o^c T^d p^e \\ F &= 444^{0.644516} 0.6744^{-1.07934} 0.843^{0.724874} 600^{2.00621} 2000^{-0.76191} = 78590.6789\end{aligned}$$

Step 2 Solve for B_t from equation (4-75):

$$\begin{aligned}B_t &= 0.314693 + 0.106253 \times 10^{-4}F + 0.18883 \times 10^{-10}F^2 \\ B_t &= 0.314693 + 0.106253 \times 10^{-4}(78590.6789) + 0.18883 \times 10^{-10}(78590.6789)^2 \\ B_t &= 1.2664 \text{ bbl/STB}\end{aligned}$$

Crude Oil Viscosity

Crude oil viscosity is an important physical property that controls the flow of oil through porous media and pipes. The viscosity, in general, is defined as the internal resistance of the fluid to flow. It ranges from 0.1 cp for near critical to over 100 cp for heavy oil. It is considered the most difficult oil property to calculate with a reasonable accuracy from correlations.

Oil's viscosity is a strong function of the temperature, pressure, oil gravity, gas gravity, gas solubility, and composition of the crude oil. Whenever possible, oil viscosity should be determined by laboratory measurements at reservoir temperature and pressure. The viscosity usually is reported in standard PVT analyses. If such laboratory data are not available, engineers may refer to published correlations, which usually vary in complexity and accuracy, depending on the available data on the crude oil. Based on the available data on the oil mixture, correlations can be divided into the following two types: correlations based on other measured PVT data, such as API or R_s , and correlations based on oil composition. Depending on the pressure, p , the viscosity of crude oils can be classified into three categories:

- *Dead oil viscosity*, μ_{od} . The dead oil viscosity (oil with no gas in the solution) is defined as the viscosity of crude oil at *atmospheric pressure* and system temperature, T .
- *Saturated oil viscosity*, μ_{ob} . The saturated (bubble-point) oil viscosity is defined as the viscosity of the crude oil at any pressure less than or equal to the bubble-point pressure.
- *Undersaturated oil viscosity*, μ_o . The undersaturated oil viscosity is defined as the viscosity of the crude oil at a pressure above the bubble-point and reservoir temperature.

The definition of the three categories of oil viscosity is illustrated conceptually in Figure 4-14. At atmospheric pressure and reservoir temperature, there is no dissolved gas in the oil (i.e., $R_s = 0$) and therefore the oil has its highest viscosity value of μ_{od} . As the

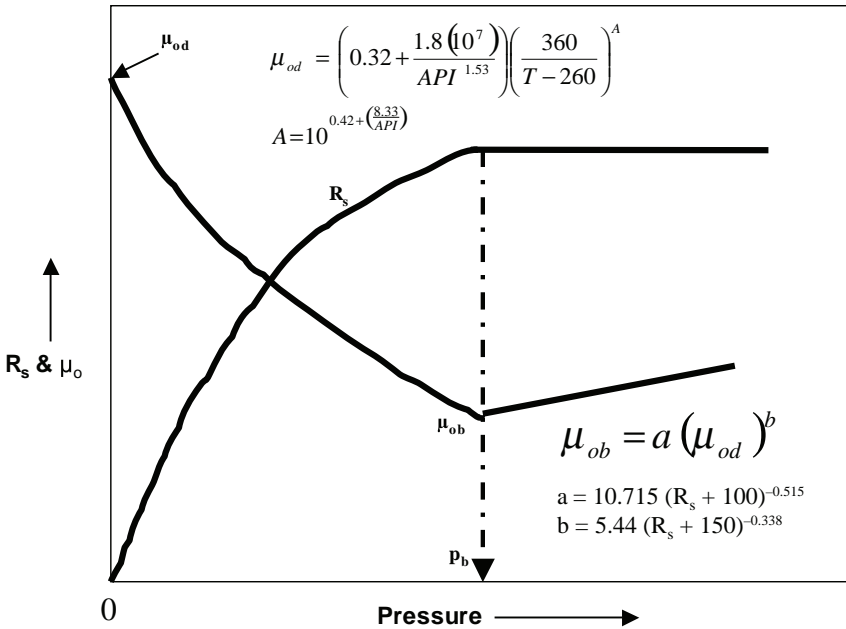


FIGURE 4-14 Crude oil viscosity as a function of R_s and p .

pressure increases, the solubility of the gas increases accordingly, with the resulting decrease in the oil viscosity. The oil viscosity at any pressure $\leq p_b$ is considered “saturated oil at this p .” As the pressure reaches the bubble-point pressure, the amount of gas in solution reaches its maximum at R_{sb} and the oil viscosity at its minimum of μ_{ob} . With increasing the pressure above p_b , the viscosity of the undersaturated crude oil μ_o increases with pressure due to the compression of the oil.

Based on these three categories, predicting the oil’s viscosity follows a similar three-step procedure.

Step 1 Calculate the dead oil viscosity, μ_{od} , at the specified reservoir temperature and atmospheric pressure without dissolved gas: $R_s = 0$.

Step 2 Adjust the dead oil viscosity to any specified reservoir pressure ($p \leq p_b$) according to the gas solubility at p .

Step 3 For pressures above the bubble-point pressure, a further adjustment is made to μ_{ob} to account for the compression of the oil above p_b .

Viscosity Correlations Based on PVT Data

Dead Oil Correlations

Several empirical methods are proposed to estimate the viscosity of the dead oil, including Beal’s correlation, Beggs-Robinson’s correlation, and Glaso’s correlation. Discussion of the three methods follows.

Beal's Correlation

From a total of 753 values for dead oil viscosity at and above 100°F, Beal (1946) developed a graphical correlation for determining the viscosity of the dead oil as a function of temperature and the API gravity of the crude. Standing (1981) expressed the proposed graphical correlation in a mathematical relationship as follows:

$$\mu_{od} = 0.32 + \frac{18(10^7)}{API^{4.53}} \left(\frac{360}{T - 260} \right)^A \quad (4-76)$$

with

$$A = 10^{0.42 + \left(\frac{8.33}{API} \right)}$$

where μ_{od} = viscosity of the dead oil as measured at 14.7 psia and reservoir temperature, cp, and T = temperature, °R.

Beggs-Robinson's Correlation

Beggs and Robinson (1975) developed an empirical correlation for determining the viscosity of the dead oil. The correlation originated from analyzing 460 dead oil viscosity measurements. The proposed relationship is expressed mathematically as follows:

$$\mu_{od} = 10^{A(T-460)^{-1.163}} - 1.0 \quad (4-77)$$

where

$$A = 10^{3.0324 - 0.02023 \text{ API}}$$

$$T = \text{temperature in } ^\circ\text{R}$$

An average error of -0.64% with a standard deviation of 13.53% was reported for the correlation when tested against the data used for its development. However, Sutton and Farshad (1984) reported an error of 114.3% when the correlation was tested against 93 cases from the literature.

Glazo's Correlation

Glazo (1980) proposed a generalized mathematical relationship for computing the dead oil viscosity. The relationship was developed from experimental measurements on 26 crude oil samples. The correlation has the following form:

$$\mu_{od} = [3.141(10^{10})](T - 460)^{-3.444} [\log(API)]^A \quad (4-78)$$

The temperature T is expressed in °R and the coefficient A is given by

$$A = 10.313[\log(T - 460)] - 36.447$$

This expression can be used within the range of 50–300°F for the system temperature and 20–48° for the API gravity of the crude. Sutton and Farshad (1984) concluded that Glazo's correlation showed the best accuracy of the three previous correlations.

Methods of Calculating the Saturated Oil Viscosity

Several empirical methods are proposed to estimate the viscosity of the saturated oil, including the Chew-Connally and Beggs-Robinson correlations, which are discussed next.

Chew-Connally Correlation

Chew and Connally (1959) presented a graphical correlation to account for the reduction of the dead oil viscosity due to gas solubility. The proposed correlation was developed from 457 crude oil samples. Standing (1981) expressed the correlation in a mathematical form as follows:

$$\mu_{ob} = (10)^a (\mu_{od})^b \quad (4-79)$$

with

$$a = R_s[2.2(10^{-7})R_s - 7.4(10^{-4})]$$

$$b = 0.68(10)^c + 0.25(10)^d + 0.062(10)^e$$

$$c = -0.0000862R_s$$

$$d = -0.0011R_s$$

$$e = -0.00374R_s$$

where μ_{ob} = viscosity of the oil at the bubble-point pressure, cp, and μ_{od} = viscosity of the dead oil at 147.7 psia and reservoir temperature, cp.

The experimental data used by Chew and Connally to develop their correlation encompassed the following ranges of values for the independent variables:

Pressure: 132–5645 psia

Temperature: 72–292°F

Gas solubility: 51–3544 scf/STB

Dead oil viscosity: 0.377–50 cp

Beggs-Robinson Correlation

From 2073 saturated oil viscosity measurements, Beggs and Robinson (1975) proposed an empirical correlation for estimating the saturated oil viscosity. The proposed mathematical expression has the following form:

$$\mu_{ob} = a(\mu_{od})^b \quad (4-80)$$

where:

$$a = 10.715(R_s + 100)^{-0.515}$$

$$b = 5.44(R_s + 150)^{-0.338}$$

The reported accuracy of the correlation is –1.83% with a standard deviation of 27.25%. The ranges of the data used to develop Beggs and Robinson's equation are

Pressure: 132–5265 psia

Temperature: 70–295°F

API gravity: 16–58

Gas solubility: 20–2070 scf/STB

An observation by Abu-Khamsim and Al-Marhoun (1991) suggests that the saturated oil viscosity, μ_{ob} , correlates very well with the saturated oil density, ρ_{ob} , as given by

$$\ln(\mu_{ob}) = 8.484462\rho_{ob}^4 - 2.652294$$

where the saturated oil density, ρ_{ob} , is expressed in gm/cm^3 , that is, $\rho_{ob}/62.4$.

Methods of Calculating the Viscosity of the Undersaturated Oil

Oil viscosity at pressures above the bubble point is estimated by first calculating the oil viscosity at its bubble-point pressure and adjusting the bubble-point viscosity to higher pressures. Three methods for estimating the oil viscosity at pressures above saturation pressure follow.

Beal's Correlation

Based on 52 viscosity measurements, Beal (1946) presented a graphical correlation for the variation of the undersaturated oil viscosity with pressure where it has been curve-fit by Standing (1981) by

$$\mu_o = \mu_{ob} + 0.001(p - p_b)[0.024\mu_{ob}^{1.6} + 0.038\mu_{ob}^{0.56}] \quad (4-81)$$

where μ_o = undersaturated oil viscosity at pressure p and μ_{ob} = oil viscosity at the bubble-point pressure, cp. The reported average error for Beal's expression is 2.7%.

Khan's Correlation

From 1500 experimental viscosity data points on Saudi Arabian crude oil systems, Khan et al. (1987) developed the following equation with a reported absolute average relative error of 2%:

$$\mu_o = \mu_{ob} \exp[9.6(10^{-6})(p - p_b)] \quad (4-82)$$

Vasquez-Beggs's Correlation

Vasquez and Beggs proposed a simple mathematical expression for estimating the viscosity of the oil above the bubble-point pressure. From 3593 data points, Vasquez and Beggs (1980) proposed the following expression for estimating the viscosity of undersaturated crude oil:

$$\mu_o = \mu_{ob} \left(\frac{p}{p_b} \right)^m \quad (4-83)$$

where

$$m = 2.6p^{1.187}10^{-4}$$

$$A = -3.9(10^{-5})p - 5$$

The data used in developing the above correlation have the following ranges:

Pressure: 141–9151 psia

Gas solubility: 9.3–2199 scf/STB

Viscosity: 0.117–148 cp

Gas gravity: 0.511–1.351

API gravity: 15.3–59.5

The average error of the viscosity correlation is reported as –7.54%.

EXAMPLE 4-26

The experimental PVT data given in Example 4-22 are repeated below. In addition to this information, viscosity data are presented in the next table. Using all the oil viscosity correlations discussed in this chapter, calculate μ_{od} , μ_{ob} , and the viscosity of the undersaturated oil.

Oil	T	p_b	R_s	B_o	ρ_o	c_o at $p > p_b$	p_{sep}	T_{sep}	API	γ_g
1	250	2377	751	1.528	38.13	22.14×10^{-6} at 2689	150	60	47.1	0.851
2	220	2620	768	1.474	40.95	18.75×10^{-6} at 2810	100	75	40.7	0.855
3	260	2051	693	0.529	37.37	22.69×10^{-6} at 2526	100	72	48.6	0.911
4	237	2884	968	1.619	38.92	21.51×10^{-6} at 2942	60	120	40.5	0.898
5	218	3065	943	0.570	37.70	24.16×10^{-6} at 3273	200	60	44.2	0.781
6	180	4239	807	0.385	46.79	11.65×10^{-6} at 4370	85	173	27.3	0.848

Oil	Dead Oil, μ_{od} @ T	Saturated Oil, μ_{ob} , cp	Undersaturated Oil, μ_o @ p
1	0.765 @ 250°F	0.224	0.281 @ 5000 psi
2	1.286 @ 220°F	0.373	0.450 @ 5000 psi
3	0.686 @ 260°F	0.221	0.292 @ 5000 psi
4	1.014 @ 237°F	0.377	0.414 @ 6000 psi
5	1.009 @ 218°F	0.305	0.394 @ 6000 psi
6	4.166 @ 180°F	0.950	1.008 @ 5000 psi

SOLUTION FOR DEAD OIL VISCOSITY

The results are shown in the table below.

Oil	Measured μ_{od}	Beal	Beggs-Robinson	Glaso
1	0.765	0.322	0.568	0.417
2	1.286	0.638	1.020	0.775
3	0.686	0.275	0.493	0.363
4	1.014	0.545	0.917	0.714
5	1.009	0.512	0.829	0.598
6	4.166	4.425	4.246	4.536
AAE		44.9%	17.32%	35.26%

Beal: $\mu_{od} = \left(0.32 + \frac{1.8(10^7)}{API^{4.53}} \right) \left(\frac{360}{T - 260} \right)^{.4}$

Beggs-Robinson: $\mu_{od} = 10^{.4(T-460)^{-1.163}} - 1.0$

Glaso: $\mu_{od} = [3.141(10^{10})](T-460)^{-3.444} [\log(API)]^{.4}$

SOLUTION FOR SATURATED OIL VISCOSITY

The results are shown in the table below.

Oil	Measured ρ_{ob} , gm/cm ³	Measured μ_{ob}	Chew-Connally	Beggs-Robinson	Abu Khamsin-Al Marhoun
1	0.6111	0.224	0.313*	0.287*	0.230
2	0.6563	0.373	0.426	0.377	0.340
3	0.5989	0.221	0.308	0.279	0.210
4	0.6237	0.377	0.311	0.297	0.255
5	0.6042	0.305	0.316	0.300	0.218
6	0.7498	0.950	0.842	0.689	1.030
AAE			21%	17%	14%

*Using the measured μ_{od} .

Chew-Connally: $\mu_{ob} = (10)^a (\mu_{od})^b$

Beggs-Robinson: $\mu_{ob} = a(\mu_{od})^b$

Abu-Khamsin and Al-Marhoun: $\ln(\mu_{ob}) = 8.484462p_{ob}^4 - 2.652294$

SOLUTION FOR UNDERSATURATED OIL VISCOSITY

The results are shown in the table below.

Oil	Measured μ_o	Beal	Vasquez-Beggs
1	0.281	0.273*	0.303*
2	0.45	0.437	0.485
3	0.292	0.275	0.318
4	0.414	0.434	0.472
5	0.396	0.373	0.417
6	1.008	0.945	1.016
AAE		3.8%	7.5%

*Using the measured μ_{ob} .

Beals: $\mu_o = \mu_{ob} + 0.001(p - p_b)[0.024\mu_{ob}^{1.6} + 0.038\mu_{ob}^{0.56}]$

Vasquez-Beggs: $\mu_o = \mu_{ob} \left(\frac{p}{p_b} \right)^m$

Viscosity Correlations Oil Composition

Like all intensive properties, viscosity is a strong function of the pressure, temperature, and composition of the oil, x_i . In general, this relationship can be expressed mathematically by the following function:

$$\mu_o = f(p, T, x_1, \dots, x_n)$$

In compositional reservoir simulation of miscible gas injection, the compositions of the reservoir gases and oils are calculated based on the equation-of-state approach and used to perform the necessary volumetric behavior of the reservoir hydrocarbon system. The calculation of the viscosities of these fluids from their compositions is required for a true and complete compositional material balance.

Two empirical correlations of calculating the viscosity of crude oils from their compositions are widely used: the Lohrenz-Bray-Clark correlation and the Little-Kennedy correlation.

Lohrenz-Bray-Clark's Correlation

Lohrenz, Bray, and Clark (1964) (LBC) developed an empirical correlation for determining the viscosity of the saturated oil from its composition. The proposed correlation has been enjoying great acceptance and application by engineers in the petroleum industry. The authors proposed the following generalized form of the equation:

$$\mu_{ob} = \mu_o + \frac{[a_1 + a_2\rho_r + a_3\rho_r^2 + a_4\rho_r^3 + a_5\rho_r^4]^4 - 0.0001}{\xi_m} \quad (4-84)$$

Coefficients a_1 through a_5 follow:

$$a_1 = 0.1023$$

$$\begin{aligned}
a_2 &= 0.023364 \\
a_3 &= 0.058533 \\
a_4 &= -0.040758 \\
a_5 &= 0.0093324
\end{aligned}$$

with the mixture viscosity parameter, ξ_m , the viscosity parameter, μ_o , and the reduced density, ρ_r , given mathematically by

$$\xi_m = \frac{5.4402(T_{pc})^{1/6}}{\sqrt{M_a}(p_{pc})^{2/3}} \quad (4-85)$$

$$\mu_o = \frac{\sum_{i=1}^n (x_i \mu_i \sqrt{M_i})}{\sum_{i=1}^n (x_i \sqrt{M_i})} \quad (4-86)$$

$$\rho_r = \frac{\left(\sum_{\substack{i=1 \\ i \notin C_{7+}}}^n [(x_i M_i V_{ci})] + x_{C_{7+}} V_{C_{7+}} \right) \rho_o}{M_a} \quad (4-87)$$

where

- μ_o = oil viscosity parameter, cp
- μ_i = viscosity of component i , cp
- T_{pc} = pseudo-critical temperatures of the crude, °R
- p_{pc} = pseudo-critical pressure of the crude, psia
- M_a = apparent molecular weight of the mixture
- ρ_o = oil density at the prevailing system condition, lb/ft³
- x_i = mole fraction of component i
- M_i = molecular weight of component i
- V_{ci} = critical volume of component i , ft³/lb
- $x_{C_{7+}}$ = mole fraction of C_{7+}
- $V_{C_{7+}}$ = critical volume of C_{7+} , ft³/lb-mole
- n = number of components in the mixture

The oil viscosity parameter, μ_o , essentially represents the oil viscosity at reservoir temperature and atmospheric pressure. The viscosity of the individual component, μ_i , in the mixture is calculated from the following relationships:

$$\text{when } T_{ri} \leq 1.5: \quad \mu_i = \frac{34(10^{-5})(T_{ri})^{0.94}}{\xi_i} \quad (4-88)$$

$$\text{when } T_{ri} > 1.5: \quad \mu_i = \frac{17.78(10^{-5})[4.58T_{ri} - 1.67]^{0.625}}{\xi_i} \quad (4-89)$$

where

$$\begin{aligned}
T_{ri} &= \text{reduced temperature of component } i; T/T_{ci} \\
\xi_i &= \text{viscosity parameter of component } i, \text{ given by } \xi_i = \frac{5.4402(T_{ci})^{1/6}}{\sqrt{M_i}(p_{ci})^{2/3}}
\end{aligned} \quad (4-90)$$

It should be noted that, when applying equation (4-86), the viscosity of the n th component, C_{7+} , must be calculated by any of the dead oil viscosity correlations discussed before.

Lohrenz and coworkers proposed the following expression for calculating $V_{C_{7+}}$:

$$V_{C_{7+}} = a_1 + a_2 M_{C_{7+}} + a_3 \gamma_{C_{7+}} + a_4 M_{C_{7+}} \gamma_{C_{7+}} \quad (4-91)$$

where

$M_{C_{7+}}$ = molecular weight of C_{7+}

$\gamma_{C_{7+}}$ = specific gravity of C_{7+}

$a_1 = 21.572$

$a_2 = 0.015122$

$a_3 = -27.656$

$a_4 = 0.070615$

Experience with the Lohrenz et al. equation has shown that the correlation is extremely sensitive to the density of the oil and the critical volume of C_{7+} . When observed viscosity data are available, values of the coefficients a_1 – a_5 in equation (4-84) and the critical volume of C_{7+} usually are adjusted and used as tuning parameters until a match with the experimental data is achieved.

Little-Kennedy's Correlation

Little and Kennedy (1968) proposed an empirical equation for predicting the viscosity of the saturated crude oil. The correlation was originated from studying the behavior of 828 distinct crude oil systems representing 3349 viscosity measurements.

The equation is similar in form to van der Waals's equation of state. The authors expressed the equation in the following form:

$$\mu_{\text{ob}}^3 - \left(b_m + \frac{p}{T}\right) \mu_{\text{ob}}^2 + \left(\frac{a_m}{T}\right) \mu_{\text{ob}} - \left(\frac{a_m b_m}{T}\right) = 0 \quad (4-92)$$

where

μ_{ob} = viscosity of the saturated crude oil, cp

p = system pressure, psia

T = system temperature, °R

a_m, b_m = mixture coefficient parameters

Little and Kennedy proposed the following relationships for calculating the parameters a_m and b_m :

$$a_m = \exp(A) \quad (4-93)$$

$$b_m = \exp(B) \quad (4-94)$$

The authors correlated the coefficients A and B with

Temperature, T .

Molecular weight of the C_{7+} .

Specific gravity of the C_{7+} .

Apparent molecular weight of the crude oil, M_a .

Density of the oil, ρ_o , at p and T .

The coefficients are given by the following equations:

$$A = A_0 + \frac{A_1}{T} + A_2 M_{C_{7+}} + \frac{A_3 M_{C_{7+}}}{\gamma_{C_{7+}}} + \frac{A_4 \rho_o}{T} + \frac{A_5 \rho_o^2}{T^2} + A_6 M_a \quad (4-95)$$

$$+ A_7 M_a^3 + A_8 M_a \rho_o + A_9 (M_a \rho_o)^3 + A_{10} E_o^2$$

$$B = B_0 + \frac{B_1}{T} + \frac{B_2}{T^4} + B_3 \gamma_{C_{7+}}^3 + B_4 \gamma_{C_{7+}}^4 + \frac{B_5 M_{C_{7+}}^4}{\gamma_{C_{7+}}^4} + \frac{B_6 \rho_o^4}{T^4} + B_7 M_a \quad (4-96)$$

$$+ B_8 M_a \rho_o + B_9 (M_a \rho_o)^4 + B_{10} \rho_o^3 + B_{11} \rho_o^4$$

where

$M_{C_{7+}}$ = molecular weight of C_{7+}

$\gamma_{C_{7+}}$ = specific gravity of C_{7+}

ρ_o = density of the saturated crude oil, lb/ft³

T = temperature, °R

M_a = apparent molecular weight of the oil

$A_0 - A_{10}$, $B_0 - B_{11}$ = coefficients of equations (4-95) and (4-96) are tabulated below.

$A_0 = 21.918581$	$B_0 = -2.6941621$
$A_1 = -16,815.621$	$B_1 = 3757.4919$
$A_2 = 0.0233159830$	$B_2 = -0.31409829(10^{12})$
$A_3 = -0.0192189510$	$B_3 = -33.744827$
$A_4 = 479.783669$	$B_4 = 31.333913$
$A_5 = -719.808848$	$B_5 = 0.24400196(10^{-10})$
$A_6 = -0.0968584490$	$B_6 = 4.632634$
$A_7 = 0.5432455400(10^{-6})$	$B_7 = -0.0370221950$
$A_8 = 0.0021040196$	$B_8 = 0.0011348044$
$A_9 = -0.4332274341(10^{-11})$	$B_9 = -0.0547665355(10^{-15})$
$A_{10} = -0.0081362043$	$B_{10} = 0.0893548761(10^{-3})$
	$B_{11} = -2.0501808400(10^{-6})$

Equation (4-92) can be solved for the viscosity of the saturated crude oil and the pressure and temperature of interest by extracting the minimum real root of the equation. An iterative technique, such as the Newton-Raphson iterative method, can be employed to solve the proposed equation.

Surface/Interfacial Tension

The surface tension is defined as the force exerted on the boundary layer between a liquid phase and a vapor phase per unit length. This force is caused by differences between the molecular forces in the vapor phase and those in the liquid phase and also by the imbalance of these forces at the interface. The surface can be measured in the laboratory and usually is expressed in dynes per centimeter.

The surface tension is an important property in reservoir engineering calculations and designing enhanced oil recovery projects.

Sugden (1924) suggested a relationship that correlates the surface tension of a pure liquid in equilibrium with its own vapor. The correlating parameters of the proposed relationship are the molecular weight, M , of the pure component; the densities of both phases; and a newly introduced temperature independent parameter, P_{ch} . The relationship is expressed mathematically in the following form:

$$\sigma = \left[\frac{P_{ch}(\rho_L - \rho_v)}{M} \right]^4 \quad (4-97)$$

where σ is the surface tension and P_{ch} is a temperature independent parameter, called the *parachor*.

The parachor is a dimensionless constant characteristic of a pure compound, calculated by imposing experimentally measured surface tension and density data on equation (4-97) and solving for P_{ch} . The parachor values for a selected number of pure compounds are given in the table below, as reported by Weinaug and Katz (1943).

Component	Parachor	Component	Parachor
CO ₂	49.0	n-C ₄	189.9
N ₂	41.0	i-C ₅	225.0
C ₁	77.0	n-C ₅	231.5
C ₂	108.0	n-C ₆	271.0
C ₃	150.3	n-C ₇	312.5
i-C ₄	181.5	n-C ₈	351.5

Fanchi (1985) correlated the parachor with molecular weight with a simple linear equation. This linear equation is valid only for components heavier than methane. Fanchi's linear equation has the following form:

$$(P_{ch})_i = 69.9 + 2.3M_i \quad (4-98)$$

where M_i = molecular weight of component i and $(P_{ch})_i$ = parachor of component i .

Firoozabadi et al. (1988) developed a correlation that can be used to approximate the parachor of pure hydrocarbon fractions from C₁ through C₆ and for C₇₊ fractions:

$$(P_{ch})_i = 11.4 + 3.23M_i - 0.0022(M_i)^2$$

Katz and Saltman (1939) suggested the following expression for estimating the parachor for C₇₊ fractions as

$$(P_{ch})_{C_{7+}} = 25.2 + 2.86M_{C_{7+}}$$

For a complex hydrocarbon mixture, Katz et al. (1943) employed the Sugden correlation for mixtures by introducing the compositions of the two phases into equation (4-97). The modified expression has the following form:

$$\sigma^{1/4} = \sum_{i=1}^n \left[(P_{ch})_i (Ax_i - By_i) \right] \quad (4-99)$$

with the parameters A and B defined by

$$A = \frac{\rho_o}{62.4 M_o}$$

$$B = \frac{\rho_g}{62.4 M_g}$$

where

- ρ_o = density of the oil phase, lb/ft³
- M_o = apparent molecular weight of the oil phase
- ρ_g = density of the gas phase, lb/ft³
- M_g = apparent molecular weight of the gas phase
- x_i = mole fraction of component i in the oil phase
- y_i = mole fraction of component i in the gas phase
- n = total number of components in the system

The interfacial tension varies between 72 dynes/cm for a water/gas system to 20–30 dynes/cm for water/oil system. Ramey (1973) proposed a graphical correlation for estimating water/hydrocarbon interfacial tension that was curve-fit by Whitson and Brule (2000) by the following expression:

$$\sigma_{w-b} = 20 + 0.57692(\rho_w - \rho_b)$$

where

- σ_{w-b} = interfacial tension, dynes/cm
- ρ_w = density of the water phase, lb/ft³
- ρ_b = density of the hydrocarbon phase, lb/ft³

EXAMPLE 4-27

The composition of a crude oil and the associated equilibrium gas follows. The reservoir pressure and temperature are 4000 psia and 160°F, respectively.

COMPONENT	x_i	y_i
C ₁	0.45	0.77
C ₂	0.05	0.08
C ₃	0.05	0.06
n-C ₄	0.03	0.04
n-C ₅	0.01	0.02
C ₆	0.01	0.02
C ₇₊	0.40	0.01

The following additional PVT data are available:

- Oil density, $\rho_o = 46.23$ lb/ft³
- Gas density, $\rho_g = 18.21$ lb/ft³
- Molecular weight of C₇₊ = 215

Calculate the surface tension.

SOLUTION

Step 1 Calculate the apparent molecular weight of the liquid and gas phases:

$$M_o = \sum x_i M_i = 100.253$$

$$M_g = \sum y_i M_i = 24.99$$

Step 2 Calculate the coefficients A and B :

$$A = \frac{\rho_o}{62.4 M_o} = \frac{46.23}{(62.4)(100.253)} = 0.00739$$

$$B = \frac{\rho_g}{62.4 M_g} = \frac{18.21}{(62.4)(24.99)} = 0.01168$$

Step 3 Calculate the parachor of C_{7+} from equation (4–98):

$$(P_{ch})_i = 69.9 + 2.3 M_i$$

$$(P_{ch})_{C_{7+}} = 69.9 + (2.3)(215) = 564.4$$

Step 4 Construct a working table as shown in the table below.

Component	P_{ch}	$Ax_i = 0.00739 x_i$	$By_i = 0.01169 y_i$	$P_{ch}(Ax_i - By_i)$
C_1	77.0	0.00333	0.0090	-0.4361
C_2	108.0	0.00037	0.00093	-0.0605
C_3	150.3	0.00037	0.00070	-0.0497
n- C_4	189.9	0.00022	0.00047	-0.0475
n- C_5	231.5	0.00007	0.00023	-0.0370
C_6	271.0	0.000074	0.00023	-0.0423
C_{7+}	564.4	0.00296	0.000117	1.6046
				$\Sigma = 0.9315$

Step 5 Calculate the surface tension from equation (4–99):

$$\sigma^{1/4} = \sum_{i=1}^n [(P_{ch})_i (Ax_i - By_i)] = 0.9315$$

$$\sigma = (0.9315)^4 = 0.753 \text{ dynes/cm}$$

PVT Correlations for Gulf of Mexico Oil

Dindoruk and Christman (2004) developed a set of PVT correlations for Gulf of Mexico (GOM) crude oil systems. These correlations have been developed for the following properties:

- Bubble-point pressure.
- Solution gas/oil ratio (GOR) at bubble-point pressure.
- Oil formation volume factor (FVF) at bubble-point pressure.
- Undersaturated isothermal oil compressibility.
- Dead oil viscosity.
- Saturated oil viscosity.
- Undersaturated oil viscosity.

In developing their correlations, the authors used the solver tool built in Microsoft Excel to match data on more than 100 PVT reports from the GOM. Dindoruk and

Christman suggest that the proposed correlations can be tuned for other basins and areas or certain classes of oils. The authors' correlations, as briefly summarized here, employ the following field units:

Temperature, T , in 0176°R .

Pressure, p , in psia.

FVF, B_o , in bbl/STB.

Gas solubility, R_s , in scf/STB.

Viscosity, μ_o , in cp.

For the bubble-point pressure correlation,

$$p_b = a_8 \left(\frac{R_s^{a_9}}{\gamma_g^{a_{10}}} 10^A + a_{11} \right)$$

The correlating parameter A is given by

$$A = \frac{a_1 T^{a_2} + a_3 \text{API}^{a_4}}{\left(a_5 + \frac{2R_s^{a_6}}{\gamma_g^{a_7}} \right)^2}$$

The p_b correlation coefficients a_1 – a_{11} are

$$a_1 = 1.42828(10^{-10})$$

$$a_2 = 2.844591797$$

$$a_3 = -6.74896(10^{-4})$$

$$a_4 = 1.225226436$$

$$a_5 = 0.033383304$$

$$a_6 = -0.272945957$$

$$a_7 = -0.084226069$$

$$a_8 = 1.869979257$$

$$a_9 = 1.221486524$$

$$a_{10} = 1.370508349$$

$$a_{11} = 0.011688308$$

For the gas solubility correlation, R_{sb} ,

$$R_{sb} = \left[\left(\frac{p_b}{a_8} + a_9 \right) \gamma_g^{a_{10}} 10^A \right]^{a_{11}}$$

with

$$A = \frac{a_1 \text{API}^{a_2} + a_3 T^{a_4}}{\left(a_5 + \frac{2\text{API}^{a_6}}{p_b^{a_7}} \right)^2}$$

The coefficients (R_{sb} correlation) a_1 – a_{11} are

$$a_1 = 4.86996(10^{-6})$$

$$a_2 = 5.730982539$$

$$a_3 = 9.92510(10^{-3})$$

$$a_4 = 1.776179364$$

$$a_5 = 44.25002680$$

$$a_6 = 2.702889206$$

$$a_7 = 0.744335673$$

$$a_8 = 3.359754970$$

$$a_9 = 28.10133245$$

$$a_{10} = 1.579050160$$

$$a_{11} = 0.928131344$$

For the oil formation volume factor (B_{ob}),

$$B_{ob} = a_{11} + a_{12}A + a_{13}A^2 + a_{14}(T - 60)\frac{API}{\gamma_g}$$

with the parameter A given by

$$A = \frac{\left[\frac{R_s^{a_1} \gamma_g^{a_2}}{\gamma_o^{a_3}} + a_4(T - 60)^{a_5} + a_6 R_s \right]^{a_7}}{\left[a_8 + \frac{2R_s^{a_9}}{\gamma_g^{a_{10}}}(T - 60) \right]^2}$$

The coefficients a_1 – a_{14} for the proposed B_{ob} correlation are

$$a_1 = 2.510755(10^0)$$

$$a_2 = -4.852538(10^0)$$

$$a_3 = 1.183500(10^1)$$

$$a_4 = 1.365428(10^5)$$

$$a_5 = 2.252880(10^0)$$

$$a_6 = 1.007190(10^1)$$

$$a_7 = 4.450849(10^{-1})$$

$$a_8 = 5.352624(10^0)$$

$$a_9 = -6.308052(10^{-1})$$

$$a_{10} = 9.000749(10^{-1})$$

$$a_{11} = 9.871766(10^{-7})$$

$$a_{12} = 7.865146(10^{-4})$$

$$a_{13} = 2.689173(10^{-6})$$

$$a_{14} = 1.100001(10^{-5})$$

When the pressure is above the bubble-point pressure, the authors proposed the following expression for undersaturated isothermal oil compressibility:

$$c_o = (a_{11} + a_{12}A + a_{13}A^2)10^{-6}$$

with

$$A = \frac{\left[\frac{R_s^{a_1} \gamma_g^{a_2}}{\gamma_o^{a_3}} + a_4 (T - 60)^{a_5} + a_6 R_s \right]^{a_7}}{\left[a_8 + \frac{2R_s^{a_9}}{\gamma_g^{a_{10}}} (T - 60) \right]^2}$$

The coefficients a_1 – a_{13} of the proposed c_o correlation are

$$\begin{aligned} a_1 &= 0.980922372 \\ a_2 &= 0.021003077 \\ a_3 &= 0.338486128 \\ a_4 &= 20.00006368 \\ a_5 &= 0.300001059 \\ a_6 &= -0.876813622 \\ a_7 &= 1.759732076 \\ a_8 &= 2.749114986 \\ a_9 &= -1.713572145 \\ a_{10} &= 9.999932841 \\ a_{11} &= 4.487462368 \\ a_{12} &= 0.005197040 \\ a_{13} &= 0.000012580 \end{aligned}$$

Normally, the dead oil viscosity (μ_{od}) at reservoir temperature is expressed in terms of reservoir temperature, T , and the oil API gravity. However, the authors introduced two additional parameters: the bubble-point pressure, p_b , and gas solubility, R_{sb} , at the bubble-point pressure. Dindoruk and Christman justify this approach because the same amount of solution gas can cause different levels of bubble-point pressures for paraffinic and aromatic oils. The authors point out that using this methodology will capture some information about the oil type without requiring additional data. The proposed correlation has the following form:

$$\mu_{od} = \frac{a_3 T^{a_4} (\log \text{API})^A}{a_5 p_b^{a_6} + a_7 R_{sb}^{a_8}}$$

with

$$A = a_1 \log(T) + a_2$$

The coefficients (μ_{od} correlation) a_1 – a_8 for the dead oil viscosity are

$$\begin{aligned} a_1 &= 14.505357625 \\ a_2 &= -44.868655416 \\ a_3 &= 9.36579(10^{-9}) \\ a_4 &= -4.194017808 \\ a_5 &= -3.1461171(10^{-9}) \\ a_6 &= 1.517652716 \\ a_7 &= 0.010433654 \\ a_8 &= -0.000776880 \end{aligned}$$

For the saturated oil viscosity (μ_{ob}),

$$\mu_{ob} = A(\mu_{od})^B$$

with the parameters A and B given by

$$A = \frac{a_1}{\exp(a_2 R_s)} + \frac{a_3 R_s^{a_4}}{\exp(a_5 R_s)}$$

$$B = \frac{a_6}{\exp(a_7 R_s)} + \frac{a_8 R_s^{a_9}}{\exp(a_{10} R_s)}$$

with the following coefficients a_1 – a_{10} of the proposed saturated oil viscosity correlation:

$$\begin{aligned} a_1 &= 1.000000(10^0) \\ a_2 &= 4.740729(10^{-4}) \\ a_3 &= -1.023451(10^{-2}) \\ a_4 &= 6.600358(10^{-1}) \\ a_5 &= 1.075080(10^{-3}) \\ a_6 &= 1.000000(10^0) \\ a_7 &= -2.191172(10^{-5}) \\ a_8 &= -1.660981(10^{-2}) \\ a_9 &= 4.233179(10^{-1}) \\ a_{10} &= -2.273945(10^{-4}) \end{aligned}$$

For the undersaturated oil viscosity (μ_o),

$$\mu_o = \mu_{ob} + a_6 (p - p_b) 10^A$$

with

$$A = a_1 + a_2 \log \mu_{ob} + a_3 \log(R_s) + a_4 \mu_{ob} \log(R_s) + a_5 (p - p_b)$$

The coefficients (μ_o correlation) a_1 – a_6 are

$$\begin{aligned} a_1 &= 0.776644115 \\ a_2 &= 0.987658646 \\ a_3 &= -0.190564677 \\ a_4 &= 0.009147711 \\ a_5 &= -0.0000191111 \\ a_6 &= 0.000063340 \end{aligned}$$

Properties of Reservoir Water

Like hydrocarbon systems, the properties of the formation water depend on the pressure, temperature, and composition of the water. The compressibility of the connate water contributes materially in some cases to the production of undersaturated volumetric reservoirs and accounts for much of the water influx in water drive reservoir. The formation water usually contains salts, mainly sodium chloride (NaCl), and dissolved gas that affect its properties. Generally, formation water contains a much higher concentration of NaCl, ranges, from 10,000 to 300,000 ppm, than the seawater concentration of approximately

30,000 ppm. Hass (1976) points out that there is a limit on the maximum concentration of salt in the water that is given by

$$(C_{sw})_{max} = 262.18 + 72.0T + 1.06T^2$$

where $(C_{sw})_{max}$ = maximum salt concentration, ppm by weight, and T = temperature, °C.

In addition of describing the salinity of the water in terms of ppm by weight, it can be also expressed in terms of the weight fraction, w_s , or as ppm by volume, C_{sv} . The conversion rules between these expressions are

$$C_{sv} = \frac{\rho_w C_{sw}}{62.4}$$
$$C_{sw} = 10^6 w_s$$

where ρ_w is the density of the brine at standard conditions in lb/ft³ and can be estimated from the Rowe-Chou (1970) correlation as

$$\rho_w = \frac{1}{0.01604 - 0.011401w_s + 0.0041755w_s^2}$$

The solubility of gas in water is normally less than 30 scf/STB; however, when combined with the concentration of salt, it can significantly affect the properties of the formation water. Methods of estimating the PVT properties, as documented next, are based on reservoir pressure, p , reservoir temperature, T , and salt concentration, C_{sw} .

Water Formation Volume Factor

The water formation volume factor can be calculated by the following mathematical expression (Hewlett-Packard, *Petroleum Fluids PAC Manual*, H.P. 41C, 1982):

$$B_w = A_1 + A_2p + A_3p^2 \tag{4-100}$$

where the coefficients A_1 – A_3 are given by the following expression:

$$A_i = a_1 + a_2(T - 460) + a_3(T - 460)^2$$

with a_1 – a_3 for gas-free and gas-saturated water given in the table below. The temperature T in equation (4-100) is in °R.

A_i	a_1	a_2	a_3
Gas-free water			
A_1	0.9947	$5.8(10^{-6})$	$1.02(10^{-6})$
A_2	$-4.228(10^{-6})$	$1.8376(10^{-8})$	$-6.77(10^{-11})$
A_3	$1.3(10^{-10})$	$-1.3855(10^{-12})$	$4.285(10^{-15})$
Gas-saturated water			
A_1	0.9911	$6.35(10^{-5})$	$8.5(10^{-7})$
A_2	$-1.093(10^{-6})$	$-3.497(10^{-9})$	$4.57(10^{-12})$
A_3	$-5.0(10^{-11})$	$-6.429(10^{-13})$	$-1.43(10^{-15})$

Source: Hewlett-Packard, *Petroleum Fluids PAC Manual*, H.P. 41C, 1982.

McCain et al. (1988) developed the following correlation for calculating B_w :

$$B_w = (1 + \Delta V_{wt})(1 + \Delta V_{wp})$$

with

$$\Delta V_{wt} = -0.01 + 1.33391 \times 10^{-6} T + 5.50654 \times 10^{-7} T^2$$

$$\Delta V_{wp} = pT(-1.95301 \times 10^{-9} - 1.72834 \times 10^{-13} p) - p(3.58922 \times 10^{-7} + 2.25341 \times 10^{-10} p)$$

where T = temperature, °F, and p = pressure, psi.

The correlation does not account for the salinity of the water, however, McCain et al. observed that variations in salinity caused offsetting errors in terms ΔV_{wt} and ΔV_{wp} .

Water Viscosity

The viscosity of the water is a function of its pressure, temperature, and salinity. Meehan (1980) proposed a water viscosity correlation that accounts for both the effects of pressure and salinity:

$$\mu_w = \mu_{wD}[1 + 3.5 \times 10^{-2} p^2(T - 40)] \quad (4-101)$$

with

$$\mu_{wD} = A + B/T$$

$$A = 4.518 \times 10^{-2} + 9.313 \times 10^{-7} Y - 3.93 \times 10^{-12} Y^2$$

$$B = 70.634 + 9.576 \times 10^{-10} Y^2$$

where

μ_w = brine viscosity at p and T , cp

μ_{wD} = brine viscosity at $p = 14.7$ and reservoir temperature, cp

p = pressure of interest, psia

T = temperature of interest, °F

Y = water salinity, ppm

Brill and Beggs (1973) presented a simpler equation, which considers only the temperature effects:

$$\mu_w = \exp(1.003 - 1.479 \times 10^{-2} T + 1.982 \times 10^{-5} T^2) \quad (4-102)$$

where T is in °F and μ_w is in cp.

McCain et al. (1988) developed the following correlation for estimating the water viscosity at atmospheric pressure and reservoir temperature:

$$\mu_{w1} = AT^B$$

with

$$A = 109.574 - 0.0840564 w_s + 0.313314(w_s)^2 + 0.00872213(w_s)^3$$

$$B = -1.12166 + 0.0263951 w_s - 0.000679461(w_s)^2 - 0.0000547119(w_s)^3 + 1.55586$$

$$\times 10^{-6}(w_s)^4$$

where

T = temperature, °F

μ_{w1} = water viscosity at 1 atm and reservoir temperature, cp

w_s = water salinity, percent by weight, solids

McCain et al. adjusted μ_{w1} to account for the increase of the pressure from 1 atm to p by the following correlation:

$$\frac{\mu_w}{\mu_{w1}} = 0.9994 + 0.0000450295 p + 3.1062 \times 10^{-9} p^2$$

Gas Solubility in Water

The gas solubility in pure saltwater ($R_{sw, \text{pure}}$), as expressed in scf/STB, can be estimated from the following correlation:

$$(R_{sw})_{\text{pure}} = A + Bp + Cp^2 \quad (4-103)$$

where

$$A = 2.12 + 3.45(10^{-3})T - 3.59(10^{-5})T^2$$

$$B = 0.0107 - 5.26(10^{-5})T + 1.48(10^{-7})T^2$$

$$C = 8.75(10^{-7}) + 3.9(10^{-9})T - 1.02(10^{-11})T^2$$

P = pressure, psi

The temperature, T , in these equations is expressed in °F. To account for the salinity of the water, McKetta and Wehe (1962) proposed the following adjustment:

$$R_{sw} = D(R_{sw, \text{pure}})$$

where

$$D = 10^{-0.0840655T - 0.285854}$$

Water Isothermal Compressibility

Brill and Beggs (1973) proposed the following equation for estimating water isothermal compressibility, ignoring the corrections for dissolved gas and solids:

$$c_w = (C_1 + C_2T + C_3T^2)10^{-6} \quad (4-104)$$

where

$$C_1 = 3.8546 - 0.000134p$$

$$C_2 = -0.01052 + 4.77 \times 10^{-7}p$$

$$C_3 = 3.9267 \times 10^{-5} - 8.8 \times 10^{-10}p$$

T = temperature in °F

p = pressure in psia

c_w = water compressibility coefficient in psi^{-1}

McCain (1991) suggested the following approximation for water isothermal compressibility:

$$c_w = \frac{1}{7.033p + 541.55C_{sw} - 537.0T + 403,300}$$

where C_{sw} is the salinity of the water in mg/L and the temperature in °F.

Laboratory Analysis of Reservoir Fluids

Accurate laboratory studies of PVT and phase-equilibria behavior of reservoir fluids are necessary for characterizing these fluids and evaluating their volumetric performance at

various pressure levels by conducting laboratory tests on a reservoir fluid sample. The amount of data desired determines the number of tests performed in the laboratory. In general, three types of laboratory tests are used to measure hydrocarbon reservoir samples:

1. *Primary tests* These are simple field (on-site) routine tests involving the measurements of the specific gravity and the gas/oil ratio of the produced hydrocarbon fluids.
2. *Routine laboratory tests* Several laboratory tests are routinely conducted to characterize the reservoir hydrocarbon fluid. These tests include
 - Compositional analysis of the system.
 - Constant-composition expansion.
 - Differential liberation.
 - Separator tests.
 - Constant-volume depletion.
3. *Special laboratory PVT tests* These types of tests are performed for very specific applications. If a reservoir is to be depleted under miscible gas injection or gas cycling scheme, the following tests may be performed: slim-tube test or swelling test.

The remainder of this chapter focuses on discussing well conditioning procedures and fluid sampling methods, reviewing the PVT laboratory tests and the proper use of the information contained in PVT reports, and describing details of several of the routine and special laboratory tests.

Well Conditioning and Fluid Sampling

Improved estimates of the PVT properties of the reservoir fluids at measure in the laboratory can be made by obtaining samples that are representative of the reservoir fluids. The proper sampling of the sampling of fluids is of greatest importance in securing accurate data. A prerequisite step for obtaining a representative fluid sample is a proper well conditioning.

Well Conditioning

Proper well conditioning is essential to obtain representative samples from the reservoir. The best procedure is to use the lowest rate that results in smooth well operation and the most dependable measurements of surface products. Minimum drawdown of bottom-hole pressure during the conditioning period is desirable and the produced gas/liquid ratio should remain constant (within about 2%) for several days; less-permeable reservoirs require longer periods. The further the well deviates from the constant produced gas/liquid ratio, the greater the likelihood that the samples will not be representative.

The following procedure is usually adequate in the preparation (conditioning) of an oil well for subsurface sampling. However, in many situations special procedures must be used to prepare a well for the collection of proper fluid samples. Before collecting fluid samples, the tested well is allowed to produce for a sufficient amount of time to remove the drilling fluids, acids, and other well stimulation materials. The pressure drawdown should be controlled to ensure that bottom-hole pressure does not fall below the bubble-point pressure. After the cleaning period, the flow rate is reduced to one-half the flow rate used during that period. The well should be allowed to flow at this reduced rate for at least

24 hours. If, however, the formation has low permeability or the oil is very viscous, the 24-hour reduced-flow rate period must be extended to 48 hours (or even four days in extreme cases) to stabilize the various parameters monitored. During this period, the well should be closely monitored to establish when the wellhead pressure, production rate, and gas/oil ratio have stabilized.

Fluid Sampling

Reservoir fluid analysis provides some of the important basic data to the petroleum engineer. The fluid studies performed by a competent and unbiased PVT laboratory are such that precise control can be maintained through the use of accepted analytical procedures, data evaluation techniques, and a series of built-in quality control checks. Unfortunately, the resulting definition of the type of reservoir fluid, the overall quality of the study, and the subsequent engineering calculations based on that study are no better than the quality of the fluid samples originally collected during the field sampling process.

For proper definition of the type of reservoir fluid and the performance of a proper fluid study, the collection of reservoir fluid samples must occur before the reservoir pressure is allowed to deplete below the saturation pressure of the reservoir fluid. Therefore, it usually is essential that the reservoir fluid samples be collected immediately after the hydrocarbon discovery, the only production to be a result of well cleanout. In addition to early sample collection, equally important are well conditioning and use of the proper sampling method for the type of fluid.

Having established that the activities surrounding the sampling process are very important elements for a successful reservoir fluid analysis, the recommended well conditioning procedures that should precede the actual collection of the samples are presented next. Following the discussion on well conditioning, the two basic methods of sample collection are subsurface (bottom-hole) sampling and surface (separator) sampling.

Subsurface Samples

Subsurface samples can be taken with a subsurface sampling chamber, called a *sampling bomb*, or with a repeat formation testing (RFT, the name used by Schlumberger) tool or modular dynamic testing tool (MDT, also a Schlumberger tool), both of which run on a wireline to the reservoir depth. The sampling bomb requires the well to be flowing, and the flowing bottom-hole pressure (p_{wf}) should be above the bubble-point pressure of the fluid (p_b) to avoid phase segregation. If this condition can be achieved, a sample of oil containing the correct amount of gas (R_{gi}) (scf/STB; the initial solution gas/oil ratio) is collected. If the reservoir pressure is close to the bubble point, this means sampling at low rates to maximize the sampling pressure. The valves on the sampling bomb are open to allow the fluid to flow through the tool then are hydraulically or electrically closed to trap a volume (typically 600 cm³) of fluid. This small sample volume is one of the drawbacks of traditional subsurface sampling, which has been overcome in the MDT.

Sampling saturated reservoirs with this technique requires special care to obtain a representative sample; and in any case, when the flowing bottom-hole pressure is lower than the bubble point, the validity of the sample remains doubtful. Multiple subsurface samples

usually are taken by running sample bombs in tandem or performing repeat runs. The samples are checked for consistency by measuring their bubble-point pressure in surface temperatures. Samples whose bubble point lies within 2% of each other are considered reliable and may be sent to the laboratory for PVT analysis.

There are limitations of subsurface fluid sampling. Subsurface sampling generally is not recommended for gas-condensate reservoirs or oil reservoirs producing substantial quantities of water. The liquid phase in the tubing of a shut-in gas-condensate reservoir is not representative of the reservoir fluid. A large water column in the tubing of a shut-in oil well prevents sampling at the proper depth and usually creates a situation where the collection of representative subsurface fluid is impossible.

Water frequently remains at the bottom of the hole. This often is true even in wells that normally produce no water. For this reason, a static pressure gradient should be run and interpreted to determine the gas/oil level and oil/water level in the tubing. In the actual run of the bottom-hole sampler, the sampler should be lowered through the gas/oil interface with care. Lack of due care can result in the premature tripping of some of the mechanisms that actuate the sample collection process. A nonrepresentative sample is the result of early collection of the sample. To prevent the collection of reservoir water, the sampler should not be lowered below the oil/water interface.

Surface Samples

Accurate measurement of hydrocarbon gas and liquid production rates during the well conditioning and well sampling tests are necessary because the laboratory tests will be based on fluid compositions recombined in the same ratios as the hydrocarbon streams measured in the field. The original reservoir fluid cannot be simulated in the laboratory unless accurate field measurements of all the separator streams are taken. (Gas/liquid ratios may be reported and used in several different forms.) Surface sampling involves taking samples of the two phases (gas and liquid) flowing through the surface separators and recombining the two fluids in an appropriate ratio such that the recombined sample is representative of the reservoir fluid. Separator pressure and temperatures should remain as constant as possible during the well conditioning period; this will help maintain constancy of the stream rates and thus the observed hydrocarbon gas/liquid ratio.

The oil and gas samples are taken from the appropriate flow lines of the same separator, whose pressure, temperature, and flow rate must be carefully recorded to allow the recombination ratios to be calculated. The oil and gas samples are sent separately to the laboratory, where they are recombined before the PVT analysis is performed. A quality check on the sampling technique is that the bubble point of the recombined sample at the temperature of the separator from which the samples were taken should be equal to the separator pressure.

The advantages of surface sampling and recombination are that large samples may be taken, stabilized conditions can be established over a number of hours prior to sampling, and costly wireline entry into the well is avoided. The subsurface sampling requirements also apply to surface sampling: If p_{wf} is below p_b , then it is probable that an excess volume of gas will enter the wellbore and even good surface sampling practice will not obtain a true reservoir fluid sample.

The following laboratory tests are routinely conducted to characterize the reservoir hydrocarbon fluid:

- Compositional analysis of the system.
- Constant-composition expansion.
- Differential liberation.
- Separator tests.
- Constant-volume depletion.

These routine laboratory PVT experiments are described next.

Routine Laboratory PVT Tests

Composition of the Reservoir Fluid

It is desirable to obtain a fluid sample as early in the life of a field as possible so that the sample closely approximates the original reservoir fluid. Collection of a fluid sample early in the life of a field reduces the chances of free gas in the oil zone of the reservoir.

Most of the parameters measured in a reservoir fluid study can be calculated with some degree of accuracy from the composition. It is the most complete description of reservoir fluid that can be made. In the past, reservoir fluid compositions were usually measured to include separation of the component methane through hexane, with the heptanes and heavier components grouped as a single component and reported with the average molecular weight and density. With the development of more-sophisticated equations of state to calculate fluid properties, it was learned that a more-complete description of the heavy components was necessary. It is now recommended that compositional analyses of the reservoir fluid include a separation of components through C_{10} as a minimum. The more sophisticated research laboratories now use equations of state that require compositions through C_{30} or higher.

Table 4-2 shows a chromatographic “fingerprint” compositional analysis of the Big Butte crude oil system. The table includes the mole fraction, weight fraction, density, and molecular weight of the individual component.

Constant-Composition Expansion Tests

Constant-composition expansion experiments are performed on gas condensates or crude oil to simulate the pressure/volume relations of these hydrocarbon systems. The test is conducted to determine saturation pressure (bubble-point or dew-point pressure), isothermal compressibility coefficients of the single-phase fluid in excess of saturation pressure, compressibility factors of the gas phase, and total hydrocarbon volume as a function of pressure.

The experimental procedure, shown schematically in Figure 4-15 involves placing a hydrocarbon fluid sample (oil or gas) in a visual PVT cell at reservoir temperature and at a pressure in excess of the initial reservoir pressure (Figure 4-15A). The pressure is reduced in steps at constant temperature by removing mercury from the cell, and the change in the total hydrocarbon volume, V_t , is measured for each pressure increment. The saturation

TABLE 4-2 *Hydrocarbon Analysis of Reservoir Fluid Sample*

Component	Mol%	Wt%	Liquid Density, gm/cc	MW
Hydrogen sulfide	0.00	0.00	0.8006	34.08
Carbon dioxide	0.25	0.11	0.8172	44.01
Nitrogen	0.88	0.25	0.8086	28.013
Methane	23.94	3.82	0.2997	16.043
Ethane	11.67	3.49	0.3562	30.07
Propane	9.36	4.11	0.5070	44.097
iso-Butane	1.39	0.81	0.5629	58.123
n-Butane	4.61	2.66	0.5840	58.123
iso-Pentane	1.50	1.07	0.6244	72.15
n-Pentane	2.48	1.78	0.6311	72.15
Hexanes	3.26	2.73	0.6850	84
Heptanes	5.83	5.57	0.7220	96
Octanes	5.52	5.88	0.7450	107
Nonanes	3.74	4.50	0.7640	121
Decanes	3.38	4.50	0.7780	134
Undecanes	2.57	3.76	0.7890	147
Dodecanes	2.02	3.23	0.8000	161
Tridecanes	2.02	3.52	0.8110	175
Tetradecanes	1.65	3.12	0.8220	190
Pentadecanes	1.48	3.03	0.8320	206
Hexadecanes	1.16	2.57	0.8390	222
Heptadecanes	1.06	2.50	0.8470	237
Octadecanes	0.93	2.31	0.8520	251
Nonadecanes	0.88	2.31	0.8570	263
Eicosanes	0.77	2.11	0.8620	275
Heneicosanes	0.68	1.96	0.8670	291
Docosanes	0.60	1.83	0.8720	305
Tricosanes	0.55	1.74	0.8770	318
Tetracosanes	0.48	1.57	0.8810	331
Pentacosanes	0.47	1.60	0.8850	345
Hexacosanes	0.41	1.46	0.8890	359
Heptacosanes	0.36	1.33	0.8930	374
Octacosanes	0.37	1.41	0.8960	388
Nonacosanes	0.34	1.34	0.8990	402
Triacotanes-plus	3.39	16.02	1.0440	474
Total	100.00	100.00		
Plus fractions:				
Heptanes-plus	40.66	79.17	0.8494	196
Undecanes-plus	22.19	58.72	0.8907	266
Pentadecanes-plus	13.93	45.09	0.9204	326
Eicosanes-plus	8.42	32.37	0.9540	387
Pentacosanes-plus	5.34	23.16	0.9916	437
Triacotanes-plus	3.39	16.02	1.0440	474

Note: Composition of reservoir fluid sample analyzed by flash test and extended-capillary chromatography. Total sample properties: molecular weight = 100.55 and equivalent liquid density = 0.7204 gm/cc.

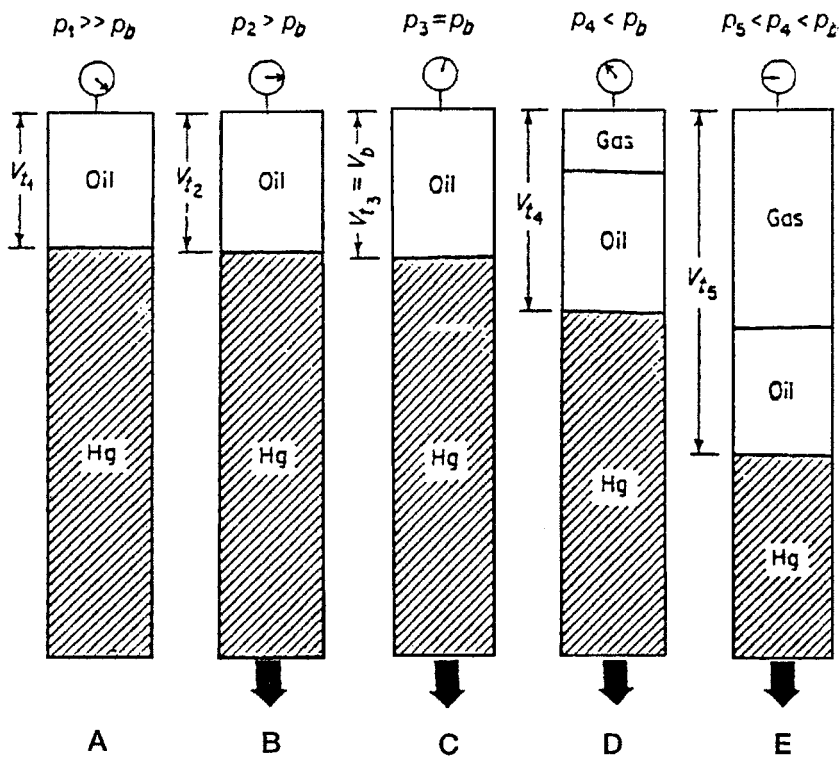


FIGURE 4-15 Constant-composition expansion test.

pressure (bubble-point or dew-point pressure) and the corresponding volume are observed and recorded and used as a reference volume, V_{sat} (Figure 4-15C). The volume of the hydrocarbon system as a function of the cell pressure is reported as the ratio of the reference volume. This volume, termed the relative volume, is expressed mathematically by the following equation:

$$V_{\text{rel}} = \frac{V_t}{V_{\text{sat}}}, \tag{4-105}$$

where

- V_{rel} = relative volume
- V_t = total hydrocarbon volume
- V_{sat} = volume at the saturation pressure

The relative volume is equal to 1 at the saturation pressure. This test is commonly called *pressure/volume relations*, *flash liberation*, *flash vaporization*, or *flash expansion*.

It should be noted that no hydrocarbon material is removed from the cell, therefore, the composition of the total hydrocarbon mixture in the cell remains fixed at the original composition.

Table 4–3 shows the results of the flash liberation test (constant-composition expansion test) for the Big Butte crude oil system. The bubble-point pressure of the hydrocarbon system is 1930 psi at 247°F. In addition to the reported values of the relative volume, the table includes the measured values of the oil density at and above the saturation pressure.

TABLE 4–3 *Constant Composition Expansion Data (Pressure/Volume Relations at 247°F*

Pressure, psig	Relative Volume*	Y-Function**	Density, gm/cc
6500	0.9371		0.6919
6000	0.9422		0.6882
5500	0.9475		0.6843
5000	0.9532		0.6803
4500	0.9592		0.6760
4000	0.9657		0.6714
3500	0.9728		0.6665
3000	0.9805		0.6613
2500	0.9890		0.6556
2400	0.9909		0.6531
2300	0.9927		0.6519
2200	0.9947		0.6506
2100	0.9966		0.6493
2000	0.9987		0.6484
<i>b</i> > 1936	1.0000		
1930	1.0014		
1928	1.0018		
1923	1.0030		
1918	1.0042		
1911	1.0058		
1878	1.0139		
1808	1.0324		
1709	1.0625	2.108	
1600	1.1018	2.044	
1467	1.0611	1.965	
1313	1.2504	1.874	
1161	1.3694	1.784	
1035	1.5020	1.710	
782	1.9283	1.560	
600	2.4960	1.453	
437	3.4464	1.356	

*Relative volume: V/V_{sat} or volume at indicated pressure per volume at saturated pressure.

**Where Y -function =
$$\frac{(p_{\text{sat}} - p)}{(p_{\text{abs}}) \times (V/V_{\text{sat}} - 1)}$$

The density of the oil at the saturation pressure is 0.6484 gm/cc, determined from direct weight/volume measurements on the sample in the PVT cell. Above the bubble-point pressure, the density of the oil can be calculated by using the recorded relative volume:

$$\rho = \frac{\rho_{\text{sat}}}{V_{\text{rel}}} \quad (4-106)$$

where

ρ = density at any pressure above the saturation pressure

ρ_{sat} = density at the saturation pressure

V_{rel} = relative volume at the pressure of interest

EXAMPLE 4-28

Given the experimental data in Table 4-3, verify the oil density values at 4000 and 6500 psi.

SOLUTION

Using equation (4-106) gives the following results.

At 4000 psi,

$$\begin{aligned} \rho_o &= \frac{\rho_{\text{sat}}}{V_{\text{rel}}} \\ \rho_o &= \frac{0.6484}{0.9657} = 1.6714 \text{ gm/cc} \end{aligned}$$

At 6500 psi,

$$\begin{aligned} \rho_o &= \frac{\rho_{\text{sat}}}{V_{\text{rel}}} \\ \rho_o &= \frac{0.6484}{0.9371} = 0.6919 \end{aligned}$$

The relative volume data frequently require smoothing to correct for laboratory inaccuracies in measuring the total hydrocarbon volume just below the saturation pressure and also at lower pressures. A dimensionless compressibility function, commonly called the *Y-function*, is used to smooth the values of the relative volume. The function in its mathematical form is defined only below the saturation pressure and given by the following expression:

$$Y = \frac{p_{\text{sat}} - p}{p(V_{\text{rel}} - 1)} \quad (4-107)$$

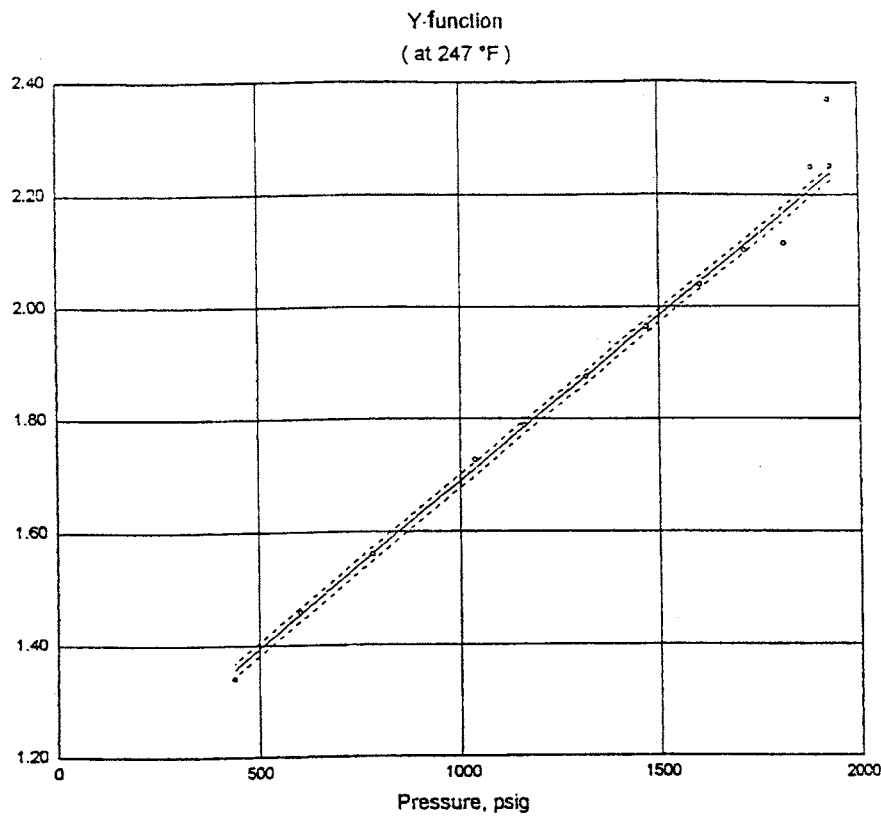
where

p_{sat} = saturation pressure, psia

p = pressure, psia

V_{rel} = relative volume at pressure p

Column three in Table 4-3 lists the computed values of the *Y-function* as calculated using equation (4-107). To smooth the relative volume data below the saturation pressure, the *Y-function* is plotted as a function of pressure on a Cartesian scale. When plotted, the *Y-function* forms a straight line or has only a small curvature. Figure 4-16 shows the



Y-fuction Expression : $y= a + b (X_d)^i$	LEGEND
where: $a= 1.09810e+ 00$ $b= 1.14439e+ 00$ $i= 1.000$	<div><div>○</div>Laboratory Data</div> <div><div>----</div>Confidence Limits</div> <div><div>————</div>Analytical Expression</div> <div>Saturation Pressure: 1936 psig</div> <div>Current Reservoir Pressure: 2900 psig</div>
Note: X_d (dimensionless 'X') = P_i / P_{sat} , psig	
Confidence level: 99 % Confidence interval: ± 0.012 'r squared': .999133	Pressure-Volume Relations

FIGURE 4-16 *Y-function versus pressure.*

Y-function versus pressure for the Big Butte crude oil system. The figure illustrates the erratic behavior of the data near the bubble-point pressure.

The following steps summarize the simple procedure of smoothing and correcting the relative volume data.

Step 1 Calculate the *Y*-function for all pressures below the saturation pressure using equation (4-107).

Step 2 Plot the *Y*-function versus pressure on a Cartesian scale.

Step 3 Determine the coefficients of the best straight fit of the data:

$$Y = a + bp \quad (4-108)$$

where a and b are the intercept and slope of the lines, respectively.

Step 4 Recalculate the relative volume at all pressures below the saturation pressure from the following expression:

$$V_{\text{rel}} = 1 + \frac{p_{\text{sat}} - p}{p(a + bp)} \quad (4-109)$$

EXAMPLE 4-29

The best straight fit of the Y -function as a function of pressure for the Big Butte oil system is given by

$$Y = a + bp$$

where

$$a = 1.0981$$

$$b = 0.000591$$

Smooth the recorded relative volume data of Table 4-3.

SOLUTION

The results are shown in the table below.

Pressure	Measured V_{rel}	Smoothed V_{rel} , Equation (4-109)
1936	—	—
1930	—	1.0014
1928	—	1.0018
1923	—	1.0030
1918	—	1.0042
1911	—	1.0058
1878	—	1.0139
1808	—	1.0324
1709	1.0625	1.0630
1600	1.1018	1.1028
1467	1.1611	1.1626
1313	1.2504	1.2532
1161	1.3696	1.3741
1035	1.5020	1.5091
782	1.9283	1.9458
600	2.4960	2.5328
437	3.4464	3.5290

The oil compressibility coefficient, c_o , above the bubble-point pressure is also obtained from the relative volume data as listed in the following table for the Big Butte oil system.

Pressure Range, psig	Single-Phase Compressibility, $V/V/\text{psi}$
6500–6000	10.73(10^{-6})
6000–5500	11.31(10^{-6})
5500–5000	11.96(10^{-6})
5000–4500	12.70(10^{-6})
4500–4000	13.57(10^{-6})
4000–3500	14.61(10^{-6})
3500–3000	15.86(10^{-6})
3000–2500	17.43(10^{-6})
2500–2000	19.47(10^{-6})
2000–1936	20.79(10^{-6})

Saturation pressure (p_{sat}) = 1936 psig

Density at p_{sat} = 0.6484 gm/cc

Thermal expansion at 6500 psig = $1.10401V$ at 247°F/ V at 60°F

The oil compressibility is defined by equations (2–94) through (2–96) and equivalently can be written in terms of the relative volume:

$$c_o = \frac{-1}{V_{\text{rel}}} \frac{\partial V_{\text{rel}}}{\partial p} \quad (4-110)$$

Commonly, the relative volume data above the bubble-point pressure is plotted as a function of pressure, as shown in Figure 4–17. To evaluate c_o at any pressure p , it is necessary only to graphically differentiate the curve by drawing a tangent line and determining the slope of the line, that is, $\partial V_{\text{rel}}/\partial p$.

EXAMPLE 4-30

Using Figure 4-17, evaluate c_o at 3000 psi.

SOLUTION

Draw a tangent line to the curve and determine the slope:

$$\partial V_{\text{rel}}/\partial p = 14.92 \times 10^{-6}$$

Apply equation (4-110) to give

$$c_o = \frac{-1}{V_{\text{rel}}} \frac{\partial V_{\text{rel}}}{\partial p}$$

$$c_o = \left(\frac{-1}{0.98} \right) (-14.92 \times 10^{-6}) = 15.23 \times 10^{-6} \text{ psi}^{-1}$$

It should be noted that the table above lists the compressibility coefficient at several ranges of pressure, such as 6500–6000. These values are determined by calculating the changes in the relative volume at the indicated pressure interval and evaluating the relative volume at the lower pressure:

$$c_o = \frac{-1}{[V_{\text{rel}}]_2} \frac{(V_{\text{rel}})_1 - (V_{\text{rel}})_2}{p_1 - p_2} \quad (4-111)$$

The subscripts 1 and 2 represent the corresponding values at the higher and lower pressure ranges, respectively.

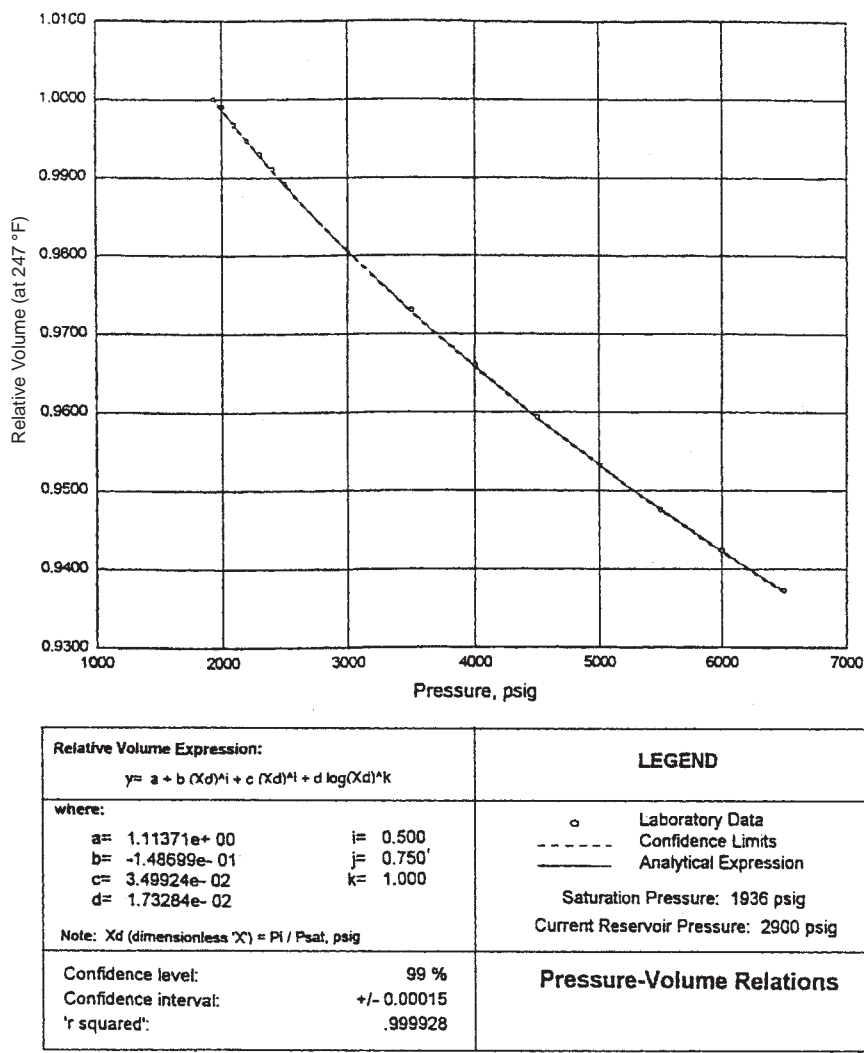


FIGURE 4-17 Relative volume data above the bubble-point pressure.

EXAMPLE 4-31

Using the measured relative volume data in Table 4-3 for the Big Butte crude oil system, calculate the average oil compressibility in the pressure range of 2500 to 2000 psi.

SOLUTION

Apply equation (4-111) to give

$$c_o = \frac{-1}{[V_{rel}]_2} \frac{(V_{rel})_1 - (V_{rel})_2}{p_1 - p_2}$$
$$c_o = \frac{-1}{0.9987} \frac{0.9890 - 0.9987}{2500 - 2000} = 19.43 \times 10^{-6} \text{ psi}^{-1}$$

Differential Liberation (Vaporization) Test

In the differential liberation process, the solution gas liberated from an oil sample during a decline in pressure is continuously removed from contact with the oil, before establishing equilibrium with the liquid phase. This type of liberation is characterized by a varying composition of the total hydrocarbon system. The experimental data obtained from the test include

- Amount of gas in solution as a function of pressure.
- The shrinkage in the oil volume as a function of pressure.
- Properties of the evolved gas, including the composition of the liberated gas, the gas compressibility factor, and the gas specific gravity.
- Density of the remaining oil as a function of pressure.

The differential liberation test is considered to better describe the separation process taking place in the reservoir and is considered to simulate the flowing behavior of hydrocarbon systems at conditions above the critical gas saturation. As the saturation of the liberated gas reaches the critical gas saturation, the liberated gas begins to flow, leaving behind the oil that originally contained it. This is attributed to the fact that gases, in general, have higher mobility than oils. Consequently, this behavior follows the differential liberation sequence.

The test is carried out on reservoir oil samples and involves charging a visual PVT cell with a liquid sample at the bubble-point pressure and reservoir temperature. As shown schematically in Figure 4-18, the pressure is reduced in steps, usually 10 to 15 pressure levels, then all the liberated gas is removed and its volume is measured at standard conditions. The volume of oil remaining, V_L , also is measured at each pressure level. It should be noted that the remaining oil is subjected to continual compositional changes as it becomes progressively richer in the heavier components.

This procedure is continued to atmospheric pressure, where the volume of the residual (remaining) oil is measured and converted to a volume at 60°F, V_{sc} . The differential oil formation volume factors, B_{od} (commonly called the relative oil volume factors), at all the various pressure levels are calculated by dividing the recorded oil volumes, V_L , by the volume of residual oil, V_c :

$$B_{od} = \frac{V_L}{V_{sc}} \quad (4-112)$$

The differential solution gas/oil ratio, R_{sd} , is calculated by dividing the volume of gas in solution by the residual oil volume.

Table 4-4 shows the results of the differential liberation test for the Big Butte crude. The test indicates that the differential gas/oil ratio and differential relative oil volume at the bubble-point pressure are 933 scf/STB and 1.730 bbl/STB, respectively. The symbols R_{sdb} and B_{odb} are used to represent these two values:

$$\begin{aligned} R_{sdb} &= 933 \text{ scf/STB} \\ B_{odb} &= 1.730 \text{ bbl/STB} \end{aligned}$$

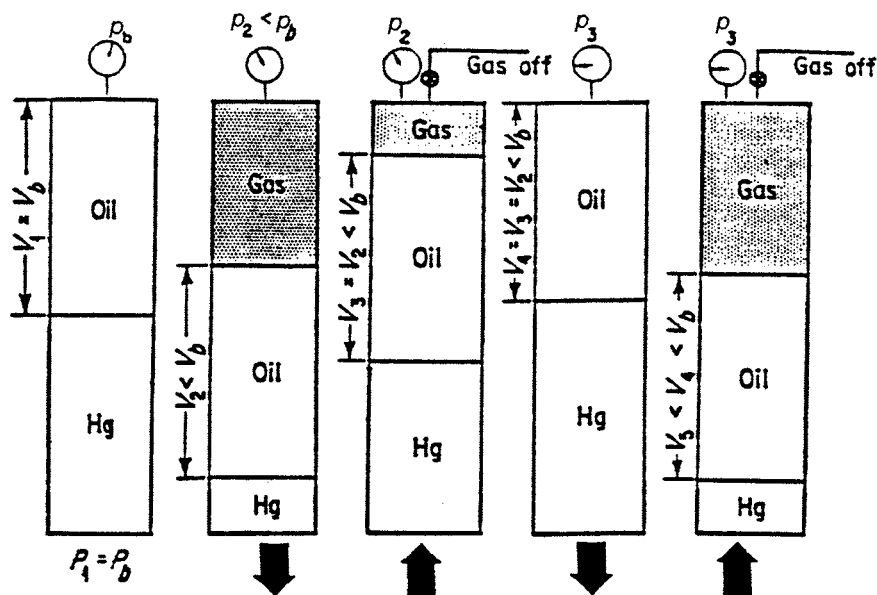


FIGURE 4-18 Differential vaporization test.

TABLE 4-4 Differential Liberation Data (Differential Vaporization at 247°F)

Pressure, psig	Solution Gas/Oil Ratio, ^a R_{sd}	Relative Oil Volume, ^b B_{od}	Relative Total Volume, ^c B_{td}	Oil Density, gm/cc	Deviation Factor, Z	Gas Formation Volume Factor ^d	Incremental Gas Gravity (Air = 1.000)
$b > 1936$	933	1.730	1.730	0.6484			
1700	841	1.679	1.846	0.6577	0.864	0.01009	0.885
1500	766	1.639	1.982	0.6650	0.869	0.01149	0.894
1300	693	1.600	2.171	0.6720	0.876	0.01334	0.901
1100	622	1.563	2.444	0.6790	0.885	0.01591	0.909
900	551	1.525	2.862	0.6863	0.898	0.01965	0.927
700	479	1.486	3.557	0.6944	0.913	0.02559	0.966
500	400	1.440	4.881	0.7039	0.932	0.03626	1.051
300	309	1.382	8.138	0.7161	0.955	0.06075	1.230
185	242	1.335	13.302	0.7256	0.970	0.09727	1.423
120	195	1.298	20.439	0.7328	0.979	0.14562	1.593
0	0	1.099		0.7745			2.375
At 60°F = 1.000							

Gravity of residual oil = 34.6°API at 60°F

Density of residual oil = 0.8511 gm/cc at 60°F

^aCubic feet of gas at 14.73 psia and 60°F per barrel of residual oil at 60°F.

^bBarrels of oil at indicated pressure and temperature per barrel of residual oil at 60°F.

^cBarrels of oil and liberated gas at indicated pressure and temperature per barrel of residual oil at 60°F.

^dCubic feet of gas at indicated pressure and temperature per cubic feet at 14.73 psia and at 60°F.

Column 4 of Table 4-4 shows the relative total volume, B_{td} , from differential liberation as calculated from the following expression:

$$B_{td} = B_{od} + (R_{sdb} - R_{sd})B_g \quad (4-113)$$

where B_{td} = relative total volume, bbl/STB, and B_g = gas formation volume factor, bbl/scf.

The gas deviation factor, Z , listed in column 6 represents the Z -factor of the liberated (removed) solution gas at the specific pressure. These values are calculated from the recorded gas volume measurements as follows:

$$Z = \left(\frac{Vp}{T} \right) \left(\frac{T_{sc}}{V_{sc}p_{sc}} \right) \quad (4-114)$$

where

V = volume of the liberated gas in the PVT cell at p and T

V_{sc} = volume of the removed gas at standard column 7 of Table 4-4 that contains the gas formation volume factor, B_g , as expressed by

$$B_g = \left(\frac{p_{sc}}{T_{sc}} \right) \frac{ZT}{p} \quad (4-115)$$

where

B_g = gas formation volume factor, ft³/scf

T = temperature, °R

p = cell pressure, psia

T_{sc} = standard temperature, °R

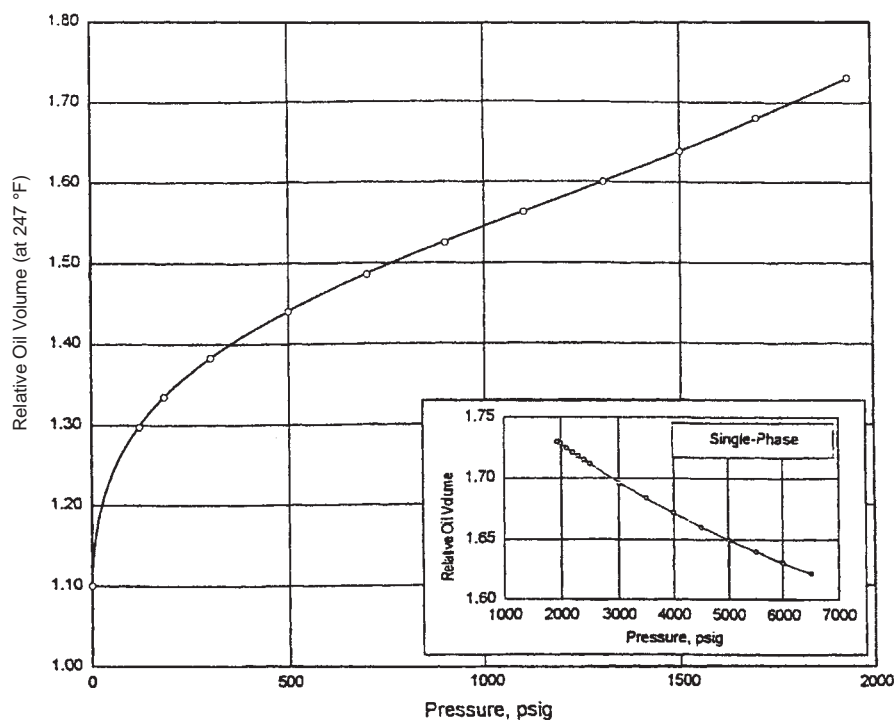
p_{sc} = standard pressure, psia

Moses (1986) pointed out that reporting the experimental data in relation to the residual oil volume at 60°F (as shown graphically in Figures 4-19 and 4-20) gives the relative oil volume, B_{od} , and the differential gas/oil ratio, R_{sc} , curves the appearance of the oil formation volume factor, B_g , and the solution gas solubility, R_s , curves, leading to their misuse in reservoir calculations.

It should be pointed out that the differential liberation test represents the behavior of the oil in the reservoir as the pressure declines. We must find a way of bringing this oil to the surface through separators and into the stock tank. This is a flash or separator process.

Separator Tests

Separator tests are conducted to determine the changes in the volumetric behavior of the reservoir fluid as the fluid passes through the separator (or separators) and then into the stock tank. The resulting volumetric behavior is influenced to a large extent by the operating conditions, that is pressures and temperatures, of the surface separation facilities. The primary objective of conducting separator tests, therefore, is to provide the essential laboratory information necessary for determining the optimum surface separation conditions, which in turn maximize the stock-tank oil production. In addition, the results of the test, when appropriately combined with the differential liberation test data, provide a means of

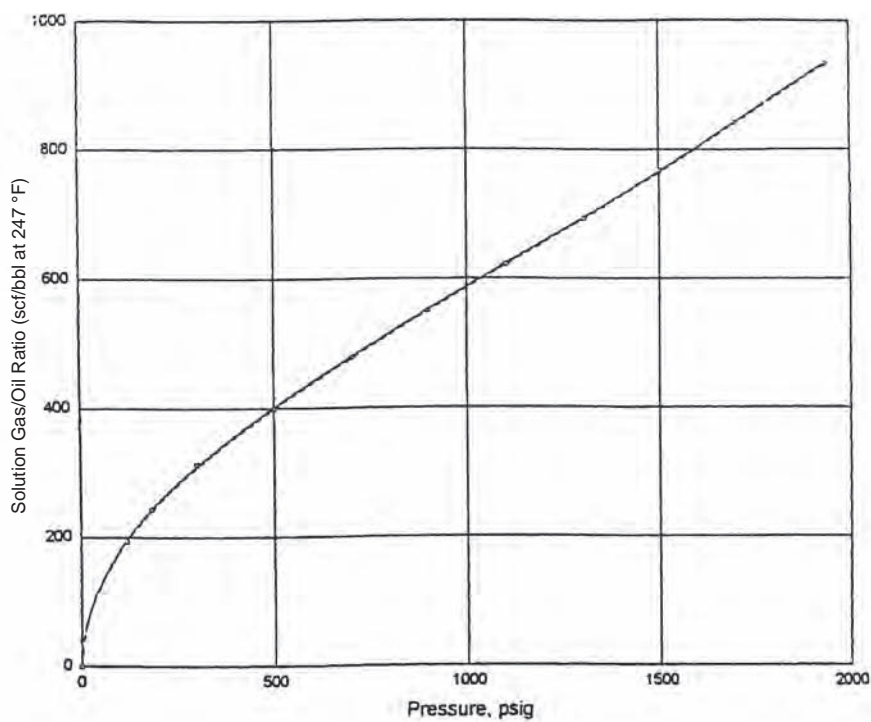


Relative Oil Volume Expression:		LEGEND	
$y= a + b (Xi)^i + c (Xi)^j + d (Xi)^k$			
where:			
a= 1.09883e+ 00	i= 1.075	<div><div>○</div>Laboratory Data</div> <div><div>-----</div>Confidence Limits</div> <div><div>—————</div>Analytical Expression</div> <div>Saturation Pressure: 1936 psig</div>	
b= -1.08945e- 04	j= 0.449		
c= 2.52865e- 02	k= 2.000		
d= 6.59813e- 08			
Note: Xi (incremental 'X') = pressure, psig			
Confidence level:		99 %	
Confidence interval:		+/- 0.00028	
'r squared':		.999997	
		Differential Vaporization	

FIGURE 4-19 Relative volume versus pressure.

obtaining the PVT parameters (B_o , R_s , and B_g) required for petroleum engineering calculations. These separator tests are performed only on the original oil at the bubble point.

The test involves placing a hydrocarbon sample at its saturation pressure and reservoir temperature in a PVT cell. The volume of the sample is measured as V_{sat} . The hydrocarbon sample then is displaced and flashed through a laboratory multistage separator system, commonly one to three stages. The pressure and temperature of these stages are set to represent the desired or actual surface separation facilities. The gas liberated from each stage is removed to measure its specific gravity and volume at standard conditions. The volume of the remaining oil in the last stage (representing the stock-tank condition) is measured and recorded as $(V_o)_{st}$. These experimental measured data can then be used to



Solution Gas/Oil Ratio Expression: $y = a + b (Xi)^i + c (Xi)^j + d (Xi)^k$	LEGEND
where: $a = -2.13685e-01$ $b = 1.69108e+01$ $c = -5.05326e-03$ $d = 2.58392e-04$ $i = 0.515$ $j = 1.482$ $k = 1.906$ Note: Xi (incremental 'X') = pressure, psig	\circ Laboratory Data - - - - - Confidence Limits ————— Analytical Expression Saturation Pressure: 1936 psig
Confidence level: 99 % Confidence interval: +/- 1.47 scf/bbl 'r squared': .999966	Differential Vaporization

FIGURE 4-20 Solution gas/oil ratio versus pressure.

determine the oil formation volume factor and gas solubility at the bubble-point pressure as follows:

$$B_{\text{ofb}} = \frac{V_{\text{sat}}}{(V_o)_{\text{st}}} \tag{4-116}$$

$$R_{\text{sfb}} = \frac{(V_g)_{\text{sc}}}{(V_o)_{\text{st}}} \tag{4-117}$$

where

B_{ofb} = bubble-point oil formation volume factor, as measured by flash liberation, bbl of the bubble-point oil/STB

R_{sfb} = bubble-point solution gas/oil ratio as measured by flash liberation, scf/STB
 $(V_g)_{\text{sc}}$ = total volume of gas removed from separators, scf

This laboratory procedure is repeated at a series of different separator pressures and a fixed temperature. It usually is recommended that four of these tests be used to determine the optimum separator pressure, which usually is considered the separator pressure that results in minimum oil formation volume factor. At the same pressure, the stock-tank oil gravity is at a maximum and the total evolved gas, that is, the separator gas and the stock-tank gas, at a minimum.

A typical example of a set of separator tests for a two-stage separation system, as reported by Moses (1986), is shown in Table 4-5. By examining the laboratory results reported in Table 4-5, it should be noted that the optimum separator pressure is 100 psia, considered to be the separator pressure that results in the minimum oil formation volume factor. It is important to note that the oil formation volume factor varies from 1.474 bbl/STB to 1.495 bbl/STB, while the gas solubility ranges from 768 scf/STB to 795 scf/STB. Table 4-5 indicates that the values of the crude oil PVT data depend on the method of surface separation. Table 4-6 presents the results of performing a separator test on the Big Butte crude oil. The differential liberation data, as expressed in Table 4-4, shows that the solution gas/oil ratio at the bubble point is 933 scf/STB, as compared with the measured value of 646 scf/STB from the separator test. This significant difference is attributed to the fact that the processes of obtaining residual oil and stock-tank oil from bubble-point oil are different. The differential liberation is considered a multiple series of flashes at the elevated reservoir temperatures; the separator test generally is a one- or two-stage flash at low pressure and low temperature. The quantity of gas released is different, and the quantity of final liquid is different. Again, it should be pointed out that oil formation volume factor, as expressed by equation (4-116), is defined as “the volume of oil at reservoir pressure and temperature divided by the resulting stock-tank oil volume after it passes through the surface separators.”

TABLE 4-5 Separator Tests

Separator Pressure, psig	Temperature, °F	GOR, ^a R_{sfb}	Stock-Tank Oil Gravity, °API at 60°F	FVF, ^b B_{oib}
50	75	737	40.5	1.481
0	75	41		
Total		778		
100	75	676	40.7	1.474
0	75	92		
Total		768		
200	75	602	40.4	1.483
0	75	178		
Total		780		
300	75	549	40.1	1.495
0	75	246		
Total		795		

^aGOR in cubic feet of gas at 17.65 psia and 60°F per barrel of stock-tank oil at 60°F.

^bFVF is barrels of saturated oil at 2.620 psig and 220°F per barrel of stock-tank oil at 60°F.

TABLE 4-6 Separator Test Data, Separator Flash Analysis

Flash Conditions		Gas/Oil Ratio		Stock-Tank Oil Gravity at 60°F, °API	Formation Volume Factor, ^c B _{oib}	Separator Volume Factor ^d	Specific Gravity of Flashed Gas, Air = 1.000	Oil Phase Density
psig	°F	scf/bbl ^a	scf/STbbl ^b					
1936	247							0.6484
28	130	593	632			1.066	1.132 ^e	0.7823
0	80	13	13	38.8	1.527	1.010	— ^f	0.8220
R _{sb} = 646								

^aCubic feet of gas at 14.73 psia and 60°F per barrel of oil at indicated pressure and temperature.

^bCubic feet of gas at 14.73 psia and 60°F per barrel of stock-tank oil at 60°F.

^cBarrels of saturated oil at 1936 psig and 247°F per barrel of stock-tank oil at 60°F.

^dBarrels of oil at indicated pressure and temperature per barrel of stock-tank oil at 60°F.

^eCollected and analyzed in the laboratory by gas chromatography.

^fInsufficient quantity for measurement.

Adjustment of Differential Liberation Data to Separator Conditions

To perform material balance calculations, the oil formation volume factor, B_o , and gas solubility, R_s , as a function of the reservoir pressure, must be available. The ideal method of obtaining this data is to place a large sample of reservoir oil in a PVT all at reservoir temperature and pressure-deplete it with a differential process to simulate reservoir depletion. At some pressure a few hundred psi below the bubble point, a portion of the oil is removed from the cell and pumped through the separators to obtain B_o and R at the lower reservoir pressure. This process should be repeated at several progressively lower reservoir pressures until complete curves of B_o and R versus reservoir pressure have been obtained. These data are occasionally measured in the laboratory. The method was originally proposed by Dodson, Goodwill, and Mayer (1953) and is called the *Dodson method*.

Amyx, Bass, and Whiting (1960) and Dake (1978) proposed a procedure for constructing the oil formation volume factor and gas solubility curves using the differential liberation data (as shown in the table on p. 267 in the solution to Example 4-29) in conjunction with the experimental separator flash data (as shown in Table 4-6) for a given set of separator conditions. The method is summarized in the following steps.

Step 1 Calculate the differential shrinkage factors at various pressure by dividing each relative oil volume factors, B_{od} , by the relative oil volume factor at the bubble point, B_{odb} :

$$S_{od} = \frac{B_{od}}{B_{odb}} \quad (4-118)$$

where

B_{od} = differential relative oil volume factor at pressure p , bbl/STB

B_{odb} = differential relative oil volume factor at the bubble-point pressure p_b , psia, bbl/STB

S_{od} = differential oil shrinkage factor, bbl/bbl of bubble-point oil

The differential oil shrinkage factor has a value of 1 at the bubble point and a value less than 1 at subsequent pressures below p_b .

Step 2 Adjust the relative volume data by multiplying the separator (flash) formation volume factor at the bubble point, B_{ofb} (as defined by equation 4-116), by the differential oil shrinkage factor, S_{od} (as defined by equation 4-118), at various reservoir pressures. Mathematically, this relationship is expressed as follows:

$$B_o = B_{\text{ofb}} \frac{B_{\text{od}}}{B_{\text{odb}}} = B_{\text{ofb}} S_{\text{od}} \quad (4-119)$$

where

B_o = oil formation volume factor, bbl/STB

B_{ofb} = bubble-point oil formation volume factor, bbl of the bubble-point oil/STB (as obtained from the separator test)

S_{od} = differential oil shrinkage factor, bbl/bbl of bubble-point oil

Step 3 Calculate the oil formation volume factor at pressures above the bubble-point pressure by multiplying the relative oil volume data, V_{rel} , as generated from the constant-composition expansion test, by B_{ofb} :

$$B_o = (V_{\text{rel}})(B_{\text{ofb}}) \quad (4-120)$$

where B_o = oil formation volume factor above the bubble-point pressure, bbl/STB, and V_{rel} = relative oil volume, bbl/bbl.

Step 4 Adjust the differential gas solubility data, R_{sd} , to give the required gas solubility factor, R_s :

$$R_s = R_{\text{sfb}} - (R_{\text{sdb}} - R_{\text{sd}}) \frac{B_{\text{ofb}}}{B_{\text{odb}}} \quad (4-121)$$

where

R_s = gas solubility, scf/STB

R_{sfb} = bubble-point solution gas/oil ratio from the separator test, scf/STB

R_{sdb} = solution gas/oil ratio at the bubble-point pressure as measured by the differential liberation test, scf/STB

R_{sd} = solution gas/oil ratio at various pressure levels as measured by the differential liberation test, scf/STB

These adjustments typically produce lower formation volume factors and gas solubilities than the differential liberation data.

Examining equations (4-119) and (4-121), McCain (2002) indicated that the ratio $B_{\text{ofb}}/B_{\text{odb}}$ in equation (4-119) takes into account the differences in the oils from the separator test and differential liberation test; however, the difference in the gases from the two tests are ignored in equation (4-121). Based on this observation, McCain suggested the following simple expression for adjusting the differential gas solubility data, R_{sd} , to give the required gas solubility factor, R_s :

$$R_s = R_{\text{sd}} \frac{R_{\text{sfb}}}{R_{\text{sdb}}}$$

Step 5 Obtain the two-phase (total) formation volume factor, B_t , by multiplying values of the relative oil volume, V_{rel} , below the bubble-point pressure by B_{ofb} :

$$B_t = (B_{ofb})(V_{rel}) \quad (4-122)$$

where B_t = two-phase formation volume factor, bbl/STB, and V_{rel} = relative oil volume below the p_b , bbl/bbl.

Similar values for B_t can be obtained from the differential liberation test by multiplying the relative total volume, B_{td} (see Table 4-4) by b_{ofb} :

$$B_t = (B_{td})(B_{ofb})/B_{odb} \quad (4-123)$$

It should be pointed out the equations (4-120) and (4-121) usually produce values less than 1 for B_o and negative values for R_s at low pressures. The calculated curves of B_o and R_s versus pressures must be manually drawn to $B_o = 1.0$ and $R_s = 0$ at atmospheric pressure.

EXAMPLE 4-32

The constant-composition expansion test, differential liberation test, and separator test for the Big Butte crude oil system are given in Tables 4-3, 4-4, and 4-6, respectively. Calculate the oil formation volume factor at 4000 and 1100 psi, the gas solubility at 1100 psi, and the two-phase formation volume factor at 1300 psi.

SOLUTION

Step 1 Determine B_{odb} , R_{sdb} , B_{ofb} , and R_{sfb} from Tables 4-5 and 4-7:

$$B_{odb} = 1.730 \text{ bbl/STB}$$

$$R_{sdb} = 933 \text{ scf/STB}$$

$$B_{ofb} = 1.527 \text{ bbl/STB}$$

$$R_{sfb} = 646 \text{ scf/STB}$$

Step 2 Calculate B_o at 4000 by applying equation (4-120):

$$B_o = (V_{rel})(B_{ofb})$$

$$B_o = (0.9657)(1.57) = 1.4746 \text{ bbl/STB}$$

Step 3 Calculate B_o at 1100 psi by applying equations (4-118) and (4-119):

$$S_{od} = \frac{B_{od}}{B_{odb}}$$

$$S_{od} = \frac{1.563}{1.730} = 0.9035$$

and

$$B_o = B_{ofb} S_{od}$$

$$B_o = (0.9035)(1.527) = 1.379 \text{ bbl/STB}$$

Step 4 Calculate the gas solubility at 1100 psi using equation (4-121):

$$R_s = R_{sfb} - (R_{sdb} - R_{sd}) \frac{B_{ofb}}{B_{odb}}$$

$$R_s = 646 - (933 - 622) \left(\frac{1.527}{1.730} \right) = 371 \text{ scf/STB}$$

Note: Using the correction proposed by McCain gives

$$R_s = R_{sd} \frac{R_{sfb}}{R_{sdb}} = 622 \left(\frac{646}{933} \right) = 431 \text{ scf/STB}$$

Step 5 From the pressure/volume relations (i.e., constant-composition data) of Table 4-3, the relative volume at 1300 psi is 1.2579 bbl/bbl. Using equation (4-122), calculate B_t to give

$$B_t = (B_{ofb})(V_{rel})$$

$$B_t = (1.527)(1.2579) = 1.921 \text{ bbl/STB}$$

Equivalently applying equation (4-123) gives

$$B_t = (B_{td})(B_{ofb})/B_{odb}$$

$$B_t = (2.171)(1.527)/1.73 = 1.916 \text{ bbl/STB}$$

Table 4-7 presents a complete documentation of the adjusted differential vaporization data for the Big Butte crude oil system. Figures 4-21 and 4-22 compare graphically the adjusted values of R_s and B_o with those of unadjusted values. Note that no adjustments are needed for the gas formation volume factor, oil density, or viscosity data.

Extrapolation of Reservoir Fluid Data

In partially depleted reservoirs or fields that originally existed at the bubble-point pressure, it is difficult to obtain a fluid sample that represents the oil in the reservoir at the time of discovery. Also, in collecting fluid samples from oil wells, the possibility exists of obtaining samples with a saturation pressure that might be lower than or higher than the actual saturation pressure of the reservoir. In these cases, it is necessary to correct or adjust the laboratory PVT measured data to reflect the actual saturation pressure. The proposed correction procedure for adjusting the following laboratory test data is described in the following sections: constant-composition expansion (CCE), differential expansion test (DE), oil viscosity test, and separator tests.

Correcting Constant-Composition Expansion Data

The correction procedure summarized in the following steps is based on calculating the Y -function value for each point below the “old” saturation pressure.

Step 1 Calculate the Y -function, as expressed by equation (4-107), for each point by using the old saturation pressure:

$$Y = \frac{p_{sat} - p}{p(V_{rel} - 1)}$$

Step 2 Plot the values of the Y -function versus pressure on a Cartesian scale and draw the best straight line. Points in the neighborhood of the saturation pressure may be erratic and need not be used.

Step 3 Calculate the coefficients a and b of the straight-line equation:

$$Y = a + bp$$

Step 4 Recalculate the relative volume, V_{rel} , values by applying equation (4-5) and using the “new” saturation pressure:

TABLE 4-7 *Differentiation Liberation Data Adjusted to Separator Conditions*

Pressure, psig	Solution Gas/Oil Ratio, ^a R_s	Formation Volume Factor, ^b B_o	Formation Volume Factor ^c	Oil Density, gm/cc	Oil/Gas Viscosity Ratio
6500	646	1.431		0.6919	
6000	646	1.439		0.6882	
5500	646	1.447		0.6843	
5000	646	1.456		0.6803	
4500	646	1.465		0.6760	
4000	646	1.475		0.6714	
3500	646	1.486		0.6665	
3000	646	1.497		0.6613	
2500	646	1.510		0.6556	
2100	646	1.513		0.6544	
2300	646	1.516		0.6531	
2200	646	1.519		0.6519	
2100	646	1.522		0.6506	
2000	646	1.525		0.6493	
$b > 1936$	646	1.527		0.6484	
1700	564	1.482	0.01009	0.6577	19.0
1500	498	1.446	0.01149	0.6650	21.3
1300	434	1.412	0.01334	0.6720	23.8
1100	371	1.379	0.01591	0.6790	26.6
900	309	1.346	0.01965	0.6863	29.8
700	244	1.311	0.02559	0.6944	33.7
500	175	1.271	0.03626	0.7039	38.6
300	95	1.220	0.06075	0.7161	46.0
185	36	1.178	0.09727	0.7256	52.8
120		1.146	0.14562	0.7328	58.4
0				0.7745	

Separator conditions:

First stage = 28 psig at 130°F

Stock tank = 0 psig at 80°F

^aCubic feet of gas at 14.73 psia and 60°F per barrel of stock-tank oil at 60°F.

^bBarrel of oil at indicated pressure and temperature per barrel of stock-tank oil at 60°F.

^cCubic feet of gas at indicated pressure and temperature per cubic feet at 14.73 psia and 60°F.

$$V_{\text{rel}} = 1 + \frac{p_{\text{sat}}^{\text{new}} - p}{p(a + bp)} \quad (4-124)$$

To determine points above the “new” saturation pressure, proceed by the following steps:

Step 1 Plot the “old” relative volume values above the “old” saturation pressure versus pressure on a regular scale and draw the best straight line through these points.

Step 2 Calculate the slope of line S. Note that the slope is negative; that is, $S < 0$.

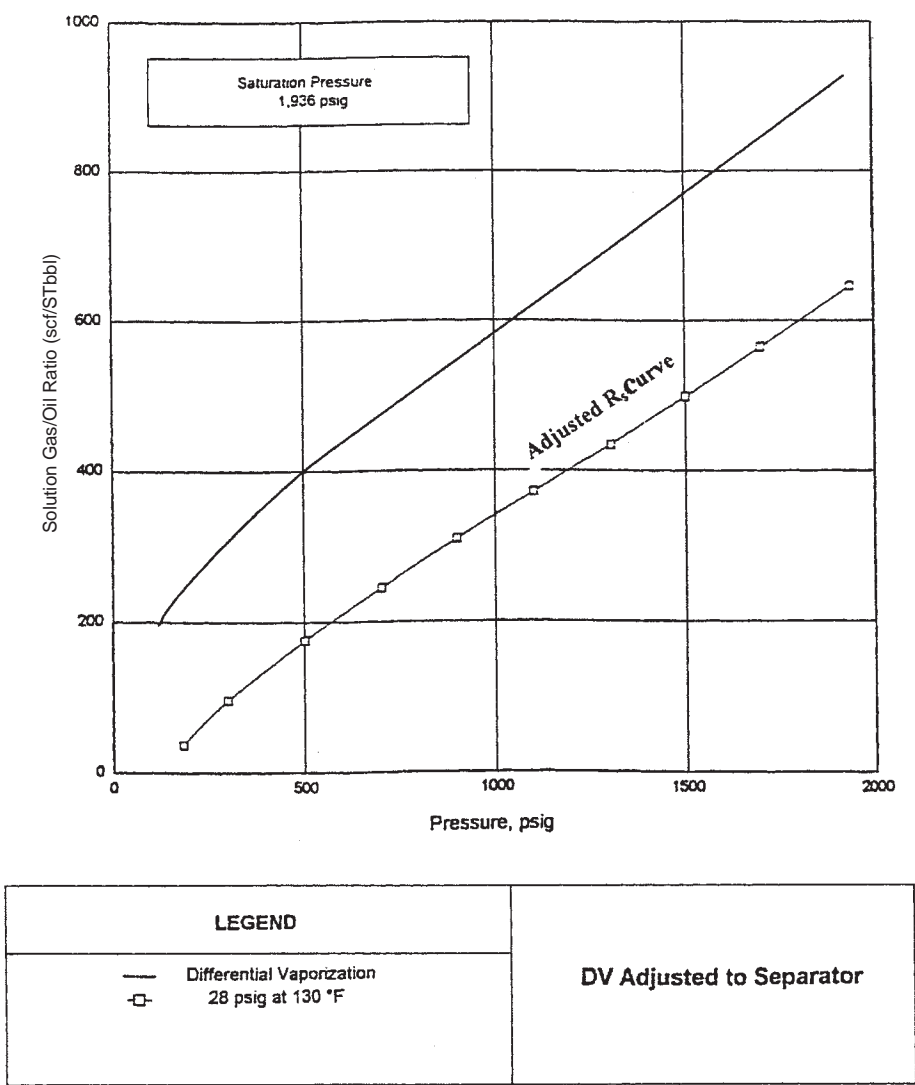


FIGURE 4-21 Adjusted gas solubility and pressure.

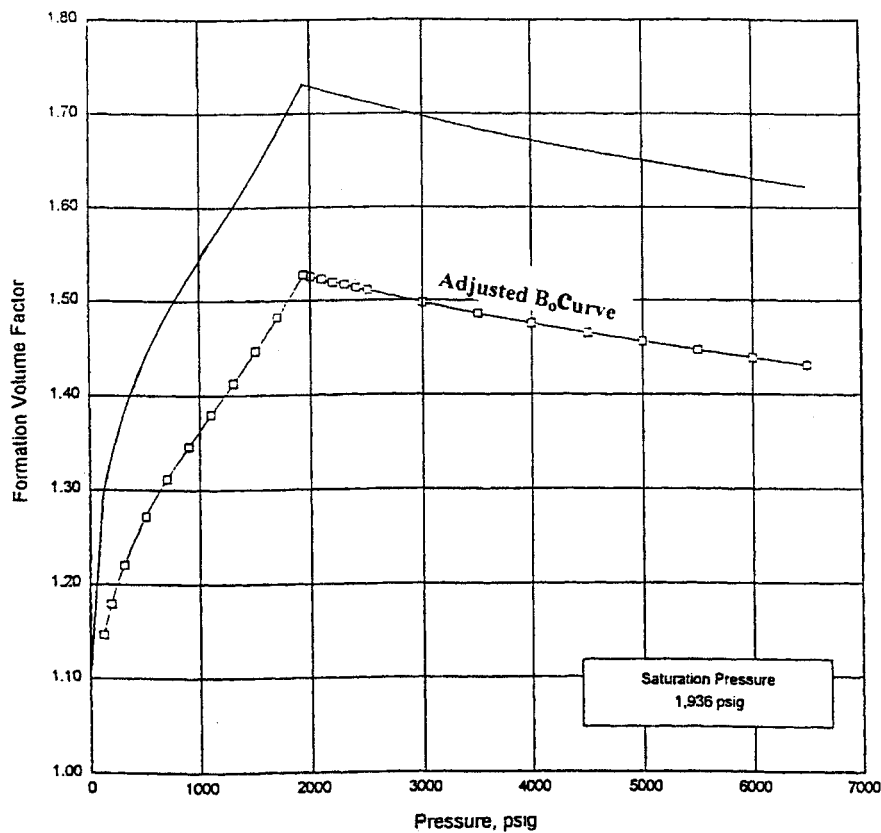
Step 3 Draw a straight line that passes through the point ($V_{rel} = 1, p_{sat}^{new}$) and parallel to the line of step 1.

Step 4 Relative volume data above the new saturation pressure are read from the straight line or determined from the following expression at any pressure p :

$$V_{rel} = 1 - S(p_{sat}^{new} - p)$$

(4-125)

where S = slope of the line and p = pressure.



LEGEND		DV Adjusted to Separator
—	Differential Vaporization	
□	28 psig at 130 °F	

FIGURE 4-22 Adjusted oil formation volume factor versus pressure.

EXAMPLE 4-33

The pressure/volume relations of the Big Butte crude oil system are given in Table 4-3. The test indicates that the oil has a bubble-point pressure of 1930 psig at 247°F. The *Y*-function for the oil system is expressed by the following linear equation:

$$Y = 1.0981 + 0.000591p$$

Above the bubble-point pressure, the relative volume data versus pressure exhibits a straight-line relationship with a slope, *S*, of −0.0000138.

The surface production data of the field suggests that the actual bubble-point pressure is approximately 2500 psig. Please reconstruct the pressure/volume data using the new reported saturation pressure.

SOLUTION

Use equations (4-124) and (4-125):

$$\text{Equation (4-124): } V_{\text{rel}} = 1 + \frac{p_{\text{sat}}^{\text{new}} - p}{p(a + bp)} = 1 + \frac{2500 - p}{p(1.0981 + 0.000591p)}$$

$$\text{Equation (4-125): } V_{\text{rel}} = 1 - S(p_{\text{sat}}^{\text{new}} - p) = 1 - (-0.0000138)(2500 - p)$$

to give the results in the table below.

Pressure, psig	Old V_{rel}	New V_{rel}	Comments
6500	0.9371	0.9448	Equation (4-125)
6000	0.9422	0.9517	Equation (4-125)
5000	0.9532	0.9655	Equation (4-125)
4000	0.9657	0.9793	Equation (4-125)
3000	0.9805	0.9931	Equation (4-125)
$p_b^{\text{new}} = 2500$	0.9890	1.0000	
2000	0.9987	1.1096	Equation (4-124)
$p_b^{\text{old}} = 1936$	1.0000	1.1299	Equation (4-124)
1911	1.0058	1.1384	Equation (4-124)
1808	1.0324	1.1767	Equation (4-124)
1600	1.1018	1.1018	Equation (4-124)
600	2.4960	2.4960	Equation (4-124)
437	3.4404	3.4404	Equation (4-124)

Correcting Differential Liberation Data

Relative Oil Volume, B_{od} , versus Pressure

The laboratory measured B_{od} data must be corrected to account for the new bubble-point pressure p_b^{new} . The proposed procedure is summarized in the following steps.

Step 1 Plot the B_{od} data versus gauge pressure on a regular scale.

Step 2 Draw the best straight line through the *middle pressure range* of 30–90% p_b .

Step 3 Extend the straight line to the new bubble-point pressure, as shown schematically in Figure 4-23.

Step 4 Transfer any curvature at the end of the original curve, that is, ΔB_{o1} at p_b^{old} , to the new bubble-point pressure by placing ΔB_{o1} above or below the straight line at p_b^{new} .

Step 5 Select any differential pressure Δp below the p_b^{old} and transfer the corresponding curvature ΔB_{o1} to the pressure $(p_b^{\text{new}} - \Delta p)$.

Step 6 Repeat this process and draw a curve that connects the generated B_{od} points with the original curve at the point of intersection with the straight line. Below this point no change is needed.

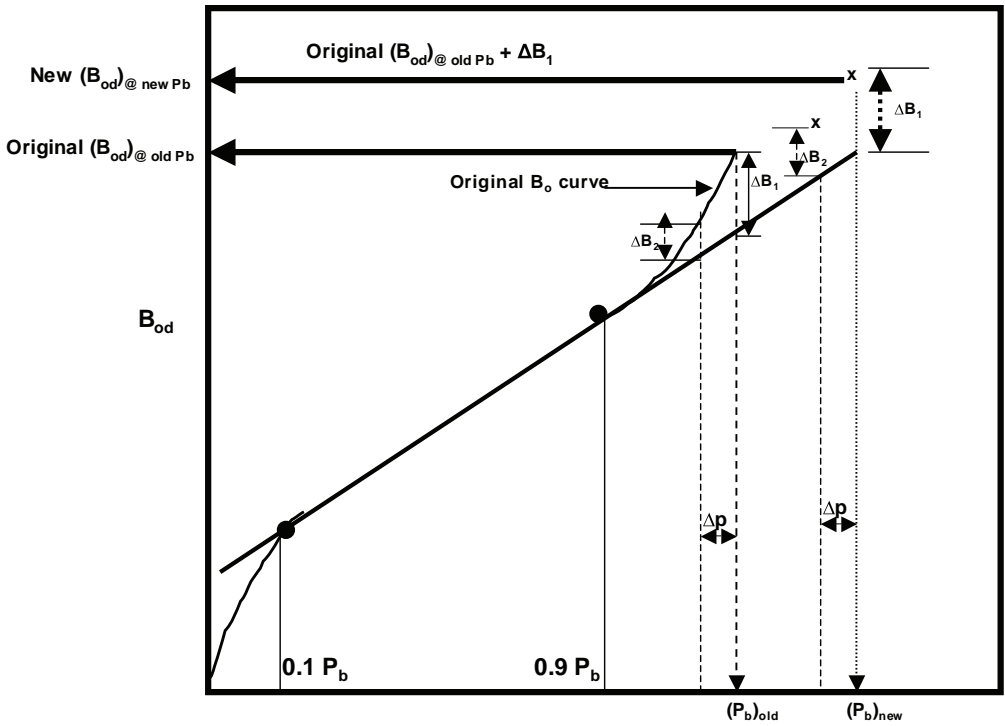


FIGURE 4-23 Adjusting the B_{od} curve to reflect the new bubble-point pressure.

Solution to the Gas/Oil Ratio

The correction procedure for the isolation gas/oil ratio, R_{sd} , data is identical to that of the relative oil volume data.

Correcting Oil Viscosity Data

The oil viscosity data can be extrapolated to a new, higher bubble-point pressure by applying the following steps.

Step 1 Defining the “fluidity” as the reciprocal of the oil viscosity, that is, $1/\mu_o$, calculate the fluidity for each point *below* the original saturation pressure.

Step 2 Plot fluidity versus pressure on a Cartesian scale (see Figure 4–24).

Step 3 Draw the best straight line through the points and extend it to the new saturation pressure, p_b^{old} .

Step 4 New oil viscosity values above p_b^{old} are read from the straight line.

To obtain the oil viscosity for pressures above the new bubble-point pressure p_b^{new} , follow the following steps.

Step 1 Plot the viscosity values for all points *above* the old saturation pressure on a Cartesian coordinate, as shown schematically in Figure 4–25, and draw the best straight line through them, line *A*.

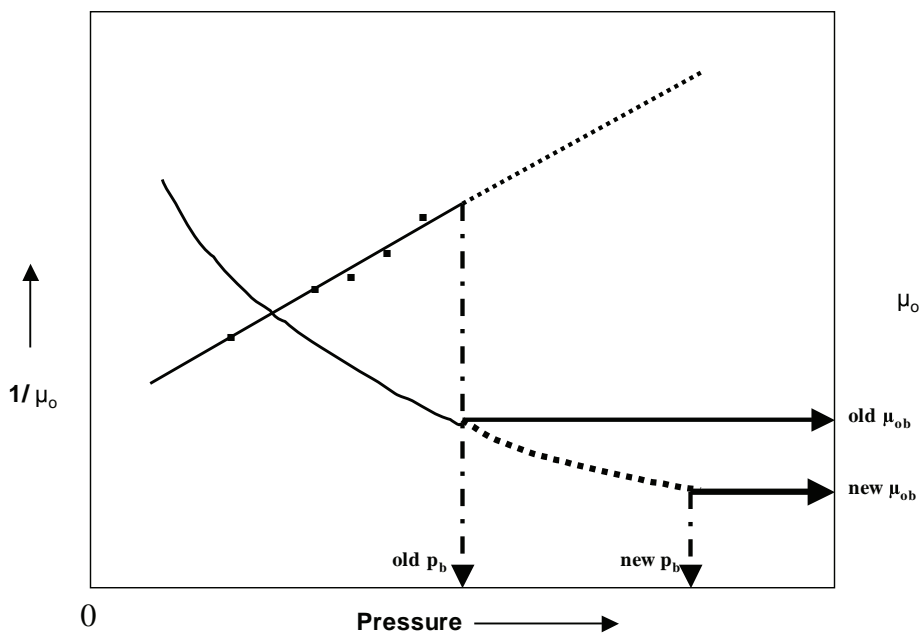


FIGURE 4-24 *Extrapolation of a new oil viscosity to a new p_b .*

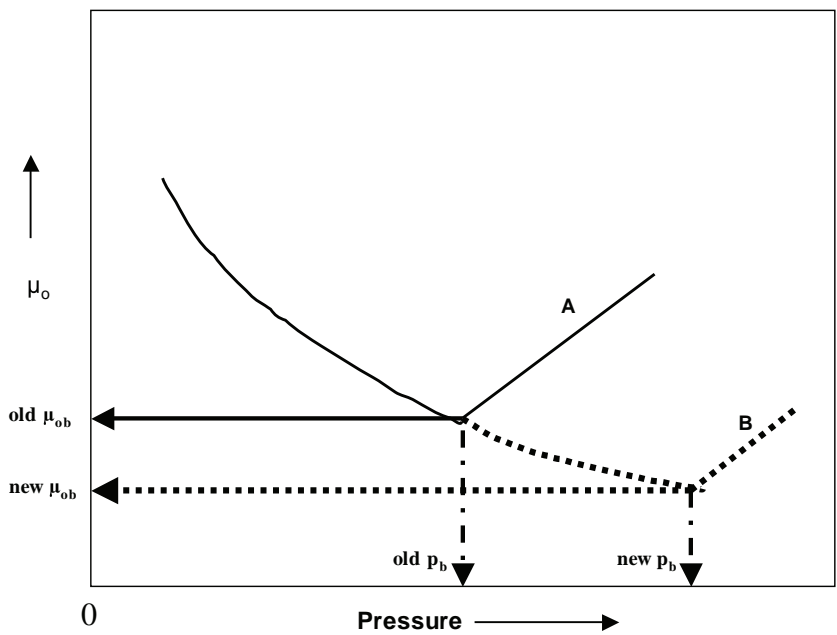


FIGURE 4-25 *Extrapolation of a new oil viscosity to above the new p_b .*

Step 2 Through the point on the extended viscosity curve at p_b^{new} , draw a straight line (line B) parallel to A .

Step 3 Viscosities above the new saturation pressure then are read from line A .

Correcting the Separator Tests Data

Stock-Tank Gas/Oil Ratio and Gravity

No corrections are needed for the stock-tank gas/oil ratio and the stock-tank API gravity.

Separator Gas/Oil Ratio

The total gas-oil ratio, R_{sfb} , is changed in the same proportion as the differential ratio was changed:

$$R_{\text{sfb}}^{\text{new}} = R_{\text{sfb}}^{\text{old}} \left(\frac{R_{\text{sdb}}^{\text{new}}}{R_{\text{sdb}}^{\text{old}}} \right) \quad (4-126)$$

The separator gas/oil ratio then is the difference between the new (corrected) gas solubility $R_{\text{sfb}}^{\text{new}}$ and the unchanged stock-tank gas/oil ratio.

Formation Volume Factor

The separator oil formation volume factor, B_{ofb} , is adjusted in the same proportion as the differential liberation values:

$$B_{\text{ofb}}^{\text{new}} = B_{\text{ofb}}^{\text{old}} \left(\frac{B_{\text{odb}}^{\text{new}}}{B_{\text{odb}}^{\text{old}}} \right) \quad (4-127)$$

EXAMPLE 4-34

Results of the differential liberation and the separator tests on the Big Butte crude oil system are given in Tables 4-4 and 4-6, respectively. The field data indicates that the actual bubble-point value is 1936 psi. The correction procedure for B_{od} and R_{sd} as described previously was applied, to give the following values at the new bubble point:

$$B_{\text{odb}}^{\text{new}} = 2.013 \text{ bbl/STB}$$

$$R_{\text{sdb}}^{\text{new}} = 1134 \text{ scf/STB}$$

Using the separator test data given in Table 4-6, calculate the gas solubility and the oil formation volume factor at the new bubble-point pressure.

SOLUTION

Gas solubility is found from equation (4-126):

$$R_{\text{sfb}}^{\text{new}} = R_{\text{sfb}}^{\text{old}} \left(\frac{R_{\text{sdb}}^{\text{new}}}{R_{\text{sdb}}^{\text{old}}} \right) = 646 \left(\frac{1134}{933} \right) = 785 \text{ scf/STB}$$

$$\text{Separator GOR} = 785 - 13 = 772 \text{ scf/STB}$$

The oil formation volume factor is found by applying equation (4-127):

$$B_{\text{ofb}}^{\text{new}} = B_{\text{ofb}}^{\text{old}} \left(\frac{B_{\text{odb}}^{\text{new}}}{B_{\text{odb}}^{\text{old}}} \right)$$

$$B_{ob} = 1.527 \left(\frac{2.013}{1.730} \right) = 1.777 \text{ bbl/STB}$$

Laboratory Analysis of Gas-Condensate Systems

In the laboratory, a standard analysis on a gas-condensate sample consists of recombination and analysis of the separator samples; measuring the pressure/volume relationship, that is, the constant-composition expansion test; and the constant-volume depletion test.

Recombination of Separator Samples

Obtaining a representative sample of the reservoir fluid is considerably more difficult for a gas-condensate fluid than for a conventional black-oil reservoir. The principal reason for this difficulty is that the liquid may condense from the reservoir fluid during the sampling process, and if representative proportions of both liquid and gas are not recovered, then an erroneous composition is calculated. Because of the possibility of erroneous compositions and the limited volumes obtainable, subsurface sampling is seldom used in gas-condensate reservoirs. Instead, surface sampling techniques are used, and samples are obtained only after long-stabilized flow periods. During this stabilized flow period, volumes of liquid and gas produced in the surface separation facilities are accurately measured, and the fluid samples then recombined in these proportions. The hydrocarbon composition of separator samples also are determined by chromatography, low-temperature fractional distillation, or a combination of both. Table 4-7 shows the hydrocarbon analyses of the separator liquid and gas samples taken from the Nameless field. The gas and liquid samples are recombined in the proper ratio to obtain the well-stream composition as given in Table 4-8. The laboratory data indicate that the overall well-stream system contains 63.71 mol% methane and 10.75 mol% hexanes-plus.

Constant-Composition Test

This test involves measuring the pressure/volume relations of the reservoir fluid at reservoir temperature with a visual cell. The usual PVT cell allows the visual observation of the condensation process resulting from changing the pressures. The experimental test procedure is similar to that conducted on crude oil systems. The CCE test is designed to provide the dew-point pressure, p_d , at the reservoir temperature and the total relative volume, V_{rel} , of the reservoir fluid (relative to the dew-point volume) as a function of pressure. The relative volume is equal to 1 at p_d . The gas compressibility factor at pressures greater than or equal to the saturation pressure also is reported. It is necessary to experimentally measure the Z -factor at only one pressure, p_1 , and determine the gas deviation factor at the other pressure, p , from

$$Z = Z_1 \left(\frac{p}{p_1} \right) \frac{V_{rel}}{(V_{rel})_1} \quad (4-128)$$

where

Z = gas deviation factor at p

TABLE 4-8 *Hydrocarbon Analyses of Separator Products and Calculated Well Stream*

Component	Separator	Separator Gas		Well Stream	
	mol%	mol%	GPM	mol%	GPM
Hydrogen sulfide	0.00	0.00		0.00	
Carbon dioxide	0.29	1.17		0.92	
Nitrogen	0.13	0.38		0.31	
Methane	18.02	81.46		63.71	
Ethane	12.08	11.46		11.63	
Propane	11.40	3.86	1.083	5.97	1.675
iso-Butane	30.5	0.49	0.163	1.21	0.404
n-Butane	5.83	0.71	0.228	2.14	0.688
iso-Pentane	3.07	0.18	0.067	0.99	0.369
Pentane	2.44	0.12	0.044	0.77	0.284
Hexanes	5.50	0.09	0.037	1.60	0.666
Hexanes-plus	38.19	0.08	0.037	10.75	7.944
Total	100.00	100.00	1.659	100.00	12.030
Hexanes-plus properties:					
API gravity at 60°F	43.4				
Specific gravity at 60/60°F	0.8091			0.809	
Molecular weight	185	103		185	

Calculated separator gas gravity (air = 1.00) = 0.687

Calculated gross heating value for separator gas = 1209 Btu

Primary separator gas collected at 745 psig and 74°F and primary separator liquid collected at 745 psig and 74°F:

Primary separator gas/separated liquid ratio = 2413 scf/bbl at 60°F

Primary separator liquid/stock-tank liquid ratio = 1.360 bbl at 60°F

Primary separator gas/well-stream ratio = 720.13 Mscf/MMscf

Stock-tank liquid/well-stream ratio = 219.4 bbl/MMscf

V_{rel} = relative volume at pressure p

$(V_{\text{rel}})_1$ = relative volume at pressure p_1

If the gas compressibility factor is measured at the dew-point pressure, then

$$Z = Z_d \left(\frac{p}{p_d} \right) (V_{\text{rel}}) \quad (4-129)$$

where

Z_d = gas compressibility factor at the dew-point pressure, p_d

p_d = dew-point pressure, psia

p = pressure, psia

Table 4-9 shows the dew-point determination and the pressure/volume relations of the Nameless field. The dew-point pressure of the system is reported as 4968 psi at 262°F. The measured gas compressibility factor at the dew point is 1.043.

TABLE 4-9 *Pressure/Volume Relations of Reservoir Fluid at 262°F (Constant-Composition Expansion)*

Pressure, psig	Relative Volume	Deviations Factor Z
8100	0.8733	1.484
7800	0.8806	1.441
7500	0.8880	1.397
7000	0.9036	1.327
6500	0.9195	1.254
6000	0.9397	1.184
5511	0.9641	1.116
5309	0.9764	1.089
5100	0.9909	1.061
5000	0.9979	1.048
4968 (dew-point pressure)	1.0000	1.048
4905	1.0057	
4800	1.0155	
1600	1.0369	
4309	1.0725	
4000	1.1177	
3600	1.1938	
3200	1.2970	
2830	1.4268	
2400	1.6423	
2010	1.9312	
1600	2.4041	
1230	3.1377	
1000	3.8780	
861	4.5249	
770	5.0719	

Note: Gas expansion factor = 1.2854 Mscf/bbl.

EXAMPLE 4-35

Using equation (4-130) and the data in Table 4-9, calculate the gas deviation factor at 6000 and 8100 psi.

SOLUTION

At 6000 psi,

$$Z = 1.043 \left(\frac{8100 + 15.025}{4968 + 15.025} \right) (0.9397) = 1.183$$

At 8100 psi,

$$Z = 1.043 \left(\frac{8100 + 15.025}{4968 + 15.025} \right) (0.8733) = 1.483$$

Constant-Volume Depletion Test

Constant-volume depletion (CVD) experiments are performed on gas condensates and volatile oils to simulate reservoir depletion performance and compositional variation. The test provides a variety of useful and important information that are used in reservoir engineering calculations. The laboratory procedure of the test is shown schematically in Figure 4-26 and summarized in the following steps.

Step 1 A measured amount of a representative sample of the original reservoir fluid with a known overall composition of z_i is charged to a visual PVT cell at the dew-point pressure, p_d (Figure 4-26(a)). The temperature of the PVT cell is maintained at the reservoir temperature, T , throughout the experiment. The initial volume, V_i , of the saturated fluid is used as a reference volume.

Step 2 The initial gas compressibility factor is calculated from the real gas equation:

$$Z_d = \frac{p_d V_i}{n_i R T} \quad (4-130)$$

where

p_d = dew-point pressure, psia

V_i = initial gas volume, ft³

n_i = initial number of moles of the gas = m/M_a

R = gas constant, 10.73

T = temperature, °R

Z_d = compressibility factor at dew-point pressure

m = weight of the gas sample, lb

M_a = apparent molecular weight of the gas sample

Step 3 The cell pressure is reduced from the saturation pressure to a predetermined level, p . This can be achieved by withdrawing mercury from the cell, as illustrated in Figure 4-26(b). During the process, a second phase (retrograde liquid) is formed. The fluid in the cell is

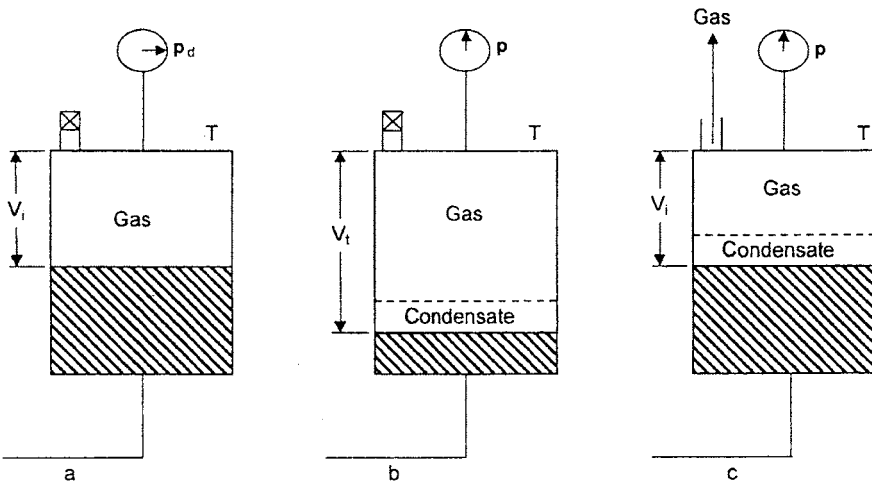


FIGURE 4-26 Schematic illustration of the constant-volume depletion test.

brought to equilibrium and the gas volume, V_g , and volume of the retrograde liquid, V_L , are visually measured. This retrograde volume is reported as a percent of the initial volume, V_i , which basically represents the retrograde liquid saturation, S_L , during depletion of retrograde gas reservoir as calculated by

$$S_L = \left(\frac{V_L}{V_i} \right)$$

where V_L = liquid volume in the PVT cell at any depletion pressure and V_i = cell volume.

This saturation can be corrected to account for water saturation, S_w , with

$$S_o = (1 - S_w)S_L$$

For most of retrograde reservoirs, the maximum liquid dropout (LDO) occurs near 2000 psi to 2500 psi. Cho, Civan, and Starting (1985) correlated the maximum LDO with reservoir temperature (in °F) and mole fraction of the C_{7+} , that is, $z_{C_{7+}}$, in the dew-point mixture by the expression, to give the following expression:

$$(\text{LDO})_{\max} = 93.404 + 479.9z_{C_{7+}} - 19.73 \ln(T)$$

Step 4 Mercury is reinjected into the PVT cell at constant pressure, p , while an equivalent volume of gas is simultaneously removed. When the initial volume, V_i , is reached, mercury injection is ceased, as illustrated in Figure 4-26(c). This step simulates a reservoir producing only gas, with retrograde liquid remaining immobile in the reservoir.

Step 5 The removed gas is charged to analytical equipment, where its composition y_i is determined and its volume is measured at standard conditions and recorded as $(V_{gp})_{sc}$. The corresponding moles of gas produced can be calculated from the expression

$$n_p = \frac{p_{sc}(V_{gp})_{sc}}{RT_{sc}} \quad (4-131)$$

where

n_p = moles of gas produced

$(V_{gp})_{sc}$ = volume of gas produced measured at standard conditions, scf

T_{sc} = standard temperature, °R

p_{sc} = standard pressure, psia

$R = 10.73$

Step 6 The gas compressibility factor at cell pressure and temperature is calculated from the real gas equation of state as follows:

$$Z = \frac{p(V_g)_{p,T}}{(n_i - n_p)RT} \quad (4-132)$$

where $(V_g)_{p,T}$ is the measured remaining gas volume in the cell at p and T , as expressed in ft³.

Another property, the *two-phase compressibility factor*, also is calculated. The two-phase compressibility factor represents the total compressibility of all the remaining fluid (gas and retrograde liquid) in the cell and is computed from the real gas law as

$$Z_{\text{two-phase}} = \frac{pV_i}{(n_i - n_p)RT} \quad (4-133)$$

where

$(n_i - n_p)$ = represents the remaining moles of fluid in the cell

n_i = initial moles in the cell

n_p = cumulative moles of gas removed

The two-phase Z-factor is a significant property, because it is used when the p/Z versus cumulative gas produced plot is constructed for evaluating gas-condensate production.

Equation (4-133) can be expressed in a more convenient form by replacing moles of gas, that is, n_i and n_p , with their equivalent gas volumes:

$$Z_{\text{two-phase}} = \left(\frac{Z_d}{p_d} \right) \left[\frac{p}{1 - (G_p / \text{GIIP})} \right] \quad (4-134)$$

where

Z_d = gas deviation factor at the dew-point pressure

p_d = dew-point pressure, psia

p = reservoir pressure, psia

GIIP = initial gas in place, scf

G_p = cumulative gas produced at pressure p , scf

Step 7 The volume of gas produced as a percentage of gas initially in place is calculated by dividing the cumulative volume of the produced gas by the gas initially in place, both at standard conditions:

$$\%G_p = \left[\frac{\sum (V_{\text{gp}})_{\text{sc}}}{\text{GIIP}} \right] 100 \quad (4-135)$$

or

$$\%G_p = \left[\frac{\sum n_p}{(n_i)_{\text{original}}} \right] 100$$

This experimental procedure is repeated several times until a minimum test pressure is reached, after which the quantity and composition of the gas and retrograde liquid remaining in the cell are determined.

The test procedure can also be conducted on a volatile oil sample. In this case, the PVT cell initially contains liquid, instead of gas, at its bubble-point pressure.

The results of the pressure-depletion study for the Nameless field are illustrated in Tables 4-10 and 4-11. Note that the composition listed in the 4968 psi pressure column in Table 4-11 is the composition of the reservoir fluid at the dew point and exists in the reservoir in the gaseous state. Table 4-10 and Figure 4-27 show the changing composition of the well stream during depletion. Note the progressive reduction of C_{7+} below the dew point and increase in the methane fraction, C_1 . The concentrations of intermediates, C_2 – C_6 , are also seen to decrease (they condense) as pressure drops down to about 2000 psi, then increase as they revaporize at the lower pressures. The final column shows the composition

TABLE 4-10 Depletion Study at 262°F (Hydrocarbon Analyses of Produced Well Stream, mol%)

Component	Reservoir Pressure, psig							
	4968	4300	3500	2800	2000	1300	700	700 ^a
Carbon dioxide	0.92	0.97	0.99	0.01	1.02	1.03	1.03	0.30
Nitrogen	0.31	0.34	0.37	0.39	0.39	0.37	0.31	0.02
Methane	63.71	69.14	71.96	73.24	73.44	72.48	69.74	12.09
Ethane	11.63	11.82	11.87	11.92	12.25	12.67	13.37	5.86
Propane	5.97	5.77	5.59	5.54	5.65	5.98	6.80	5.61
iso-Butane	1.21	1.14	1.07	1.04	1.04	1.13	1.32	1.61
n-Butane	2.14	1.99	1.86	1.79	1.76	1.88	2.24	3.34
iso-Pentane	0.99	0.88	0.79	0.72	0.72	0.77	0.92	2.17
n-Pentane	0.77	0.68	0.59	0.53	0.53	0.56	0.68	1.88
Hexanes	1.60	1.34	1.12	0.90	0.90	0.91	1.07	5.34
Heptanes-plus	10.75	5.93	3.79	2.82	2.30	2.22	2.52	61.78
Total	100.00	100.00	100.00	100.00	100.00	100.00	100.00	100.000
Heptanes-plus								
Molecular weight	185	143	133	125	118	114	112	203
Specific gravity	0.809	0.777	0.768	0.760	0.753	0.749	0.747	0.819
Deviation factor Z								
Equilibrium gas	1.043	0.927	0.874	0.862	0.879	0.908	0.946	
Two phase	1.043	0.972	0.897	0.845	0.788	0.720	0.603	
Well-stream produced, cumulative % of initial GPM, smooth compositions	0.000	7.021	17.957	30.268	46.422	61.745	75.172	
Propane-plus	12.030	7.303	5.623	4.855	4.502	4.624	5.329	
Butanes-plus	10.354	5.682	4.054	3.301	2.916	2.946	3.421	
Pentanes-plus	9.263	4.664	3.100	2.378	2.004	1.965	2.261	

^aEquilibrium liquid phase, representing 13.323% of original well stream.

TABLE 4-11 Retrograde Condensation during Gas Depletion at 262°F

Pressure, psig	Retrograde Liquid Volume, % of Hydrocarbon Pore Space
4968 (dew-point pressure)	0.0
4905	19.3
4800	25.0
4600	29.9
4300 (first-depletion level)	33.1
3500	34.4
2800	34.1
2000	32.5
1300	30.2
700	27.3
0	21.8

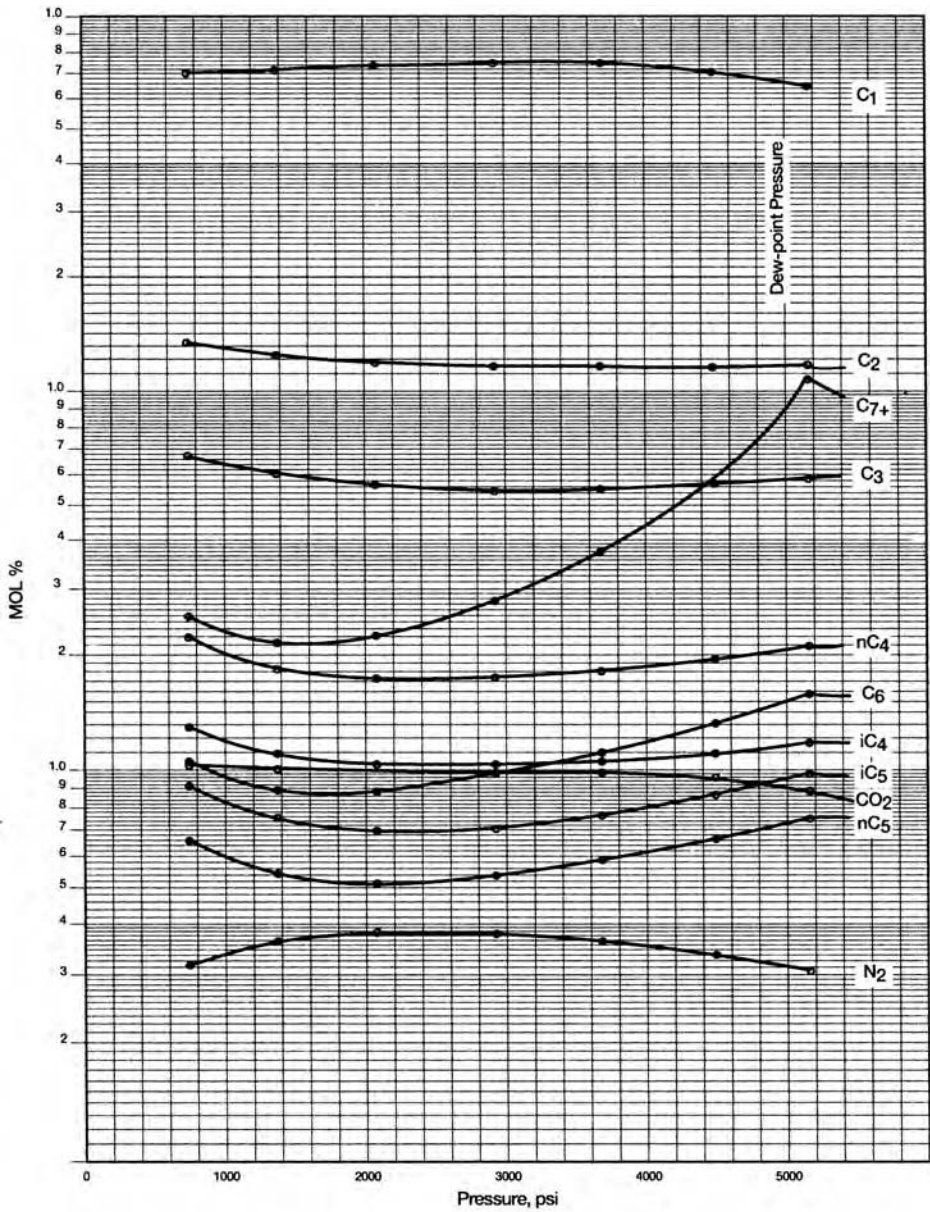


FIGURE 4-27 Hydrocarbon analysis during depletion.

of the liquid remaining in the cell (or reservoir) at the abandonment pressure of 700 psi; the predominance of C_{7+} components in the liquid is apparent.

The Z -factor of the equilibrium gas and the two-phase Z are presented. (*Note:* If a (p/Z) versus G_p analysis is to be done, the two-phase compressibility factors are the appropriate values to use.)

The row in Table 4-10, “Well-stream produced, % of initial,” gives the fraction of the total moles (or scf) in the cell (or reservoir) that has been produced. This is the *total* recovery of well stream and has not been separated here into surface gas and oil recoveries.

In addition to the composition of the produced well stream at the final depletion pressure, the composition of the retrograde liquid is measured. The composition of the liquid is reported in the last column of Table 4–10 at 700 psi. These data are included as a control composition in the event the study is used for compositional material-balance purposes.

The volume of the retrograde liquid, that is, liquid dropout, measured during the course of the depletion study is shown in Table 4–11. The data are reshown as a percent of hydrocarbon pore space. The measurements indicate that the maximum liquid dropout of 34.4% occurs at 3500 psi. The liquid dropout can be expressed as a percent of the pore volume (saturation) by adjusting the reported values to account for the presence of the initial water saturation:

$$S_o = (\text{LDO})(1 - S_{wi}) \quad (4-136)$$

where

S_o = retrograde liquid (oil) saturation, %

LDO = liquid dropout, %

S_{wi} = initial water saturation, fraction

EXAMPLE 4-36

Using the experimental data of the Nameless gas-condensate field given in Table 4–10, calculate the two-phase compressibility factor at 2000 psi by applying equation (4–134).

SOLUTION

The laboratory report indicates that the base (standard) pressure is 15.025 psia. Applying equation (4–134) gives

$$Z_{\text{two-phase}} = \left(\frac{Z_d}{P_d} \right) \left[\frac{p}{1 - (G_p / \text{GIIP})} \right]$$

$$Z_{\text{two-phase}} = \left[\frac{1.043}{4968 + 15.025} \right] \left[\frac{2000 + 15.025}{1 - 0.46422} \right] = 0.787$$

Frequently, the surface gas is processed to remove and liquify all hydrocarbon components that are heavier than methane, such as ethane and propane. These liquids are called *plant products* or the *liquid yield*. The quantities of liquid products are expressed in gallons of liquid per thousand standard cubic feet of gas processed, gal/Mscf, and denoted GPM. It usually is reported for C_{3+} through C_{5+} groups in the produced well streams at each pressure-depletion stage. The following expression can be used for calculating the anticipated GPM for each component in the gas phase:

$$\text{GPM}_i = 11.173 \left(\frac{p_{sc}}{T_{sc}} \right) \left(\frac{y_i M_i}{\gamma_{oi}} \right) \quad (4-137)$$

Assuming $p_{sc} = 14.7$ psia and $T_{sc} = 520^\circ\text{R}$, equation (4–137) is reduced to

$$\text{GPM}_i = 0.31585 \left(\frac{y_i M_i}{\gamma_{oi}} \right)$$

with a total plant product GPM as given by the summation of GPM of individual components:

$$\text{GPM} = \sum_i \text{GPM}_i$$

For example, the liquid yield of the C_{3+} group at CVD depletion stage k is given by

$$(\text{GPM})_{C_{3+}} = \sum_{i=C_3}^{C_{7+}} (\text{GPM}_i)_k = 0.31585 \sum_{i=C_3}^{C_{7+}} \left(\frac{y_i M_i}{\gamma_{oi}} \right)_k$$

where

p_{sc} = standard pressure, psia

T_{sc} = standard temperature, °R

y_i = mole fraction of component i in the gas phase

M_i = molecular weight of component i

γ_{oi} = specific gravity of component i as a liquid at standard conditions (Chapter 1, Table 1-1, column E)

It should be pointed out that the complete recovery of these products is not feasible. However, it is proposed that, as a rule of thumb, 5–25% of ethane, 80–90% of the propane, 95% or more of the butanes, and 100% of the heavier components can be recovered from a simple surface facility:

$$(\text{GPM})_{C_{3+}} = \sum_{i=C_3}^{C_{7+}} (\text{GPM}_i)_k = 0.31585 \sum_{i=C_3}^{C_{7+}} \left[\left(\frac{y_i M_i}{\gamma_{oi}} \right) E_p \right]_k$$

where E_p is the plant efficiency.

EXAMPLE 4-37

Table 4-8 shows the well-stream compositional analysis of the Nameless field. Using equation (4-137), calculate the maximum available liquid products, assuming 5% of the ethane, 80% of the propane, 95% of the butanes, and 100% of the heavier components can be recovered from the surface facility.

SOLUTION

Using the values of p_{sc} and T_{sc} given in Table 4-8, calculate the GPM:

$$\begin{aligned} \text{GPM}_i &= 11.173 \left(\frac{p_{sc}}{T_{sc}} \right) \left(\frac{y_i M_i}{\gamma_{oi}} \right) \\ \text{GPM}_i &= 11.173 \left(\frac{15.025}{520} \right) \left(\frac{y_i M_i}{\gamma_{oi}} \right) = 0.3228 \left(\frac{y_i M_i}{\gamma_{oi}} \right) \end{aligned}$$

Then, construct the working Table 4-12.

More detailed CVD test data are given in Tables 4-13 and 4-14 and shown graphically in Figures 4-28 and 4-29. Table 4-14 gives various calculated cumulative recoveries based on the reservoir initially being at its dew-point pressure. The basis for the calculation is 1 MMscf of dew-point gas in place; that is, $G = 1.0$ MMscf with the corresponding initial moles in place is given by

TABLE 4-12 Working Table for Example 4-37

Component	y_i	M_i	γ_{oi}	GPM_i	$(GPM_i)E_p$
CO ₂	0.0092				
N ₂	0.0031				
C ₁	0.6371				
C ₂	0.1163	30.070	0.35619	1.069	0.267
C ₃	0.0597	44.097	0.50699	1.676	1.341
i-C ₄	0.0121	58.123	0.56287	0.403	0.383
n-C ₄	0.0214	58.123	0.58401	0.688	0.653
i-C ₅	0.0099	72.150	0.62470	0.369	0.369
n-C ₅	0.0077	72.150	0.63112	0.284	0.284
C ₆	0.0160	86.177	0.66383	0.670	0.670
C ₇₊	0.1075	185.00	0.809	7.936	7.936

GPM = 11.90

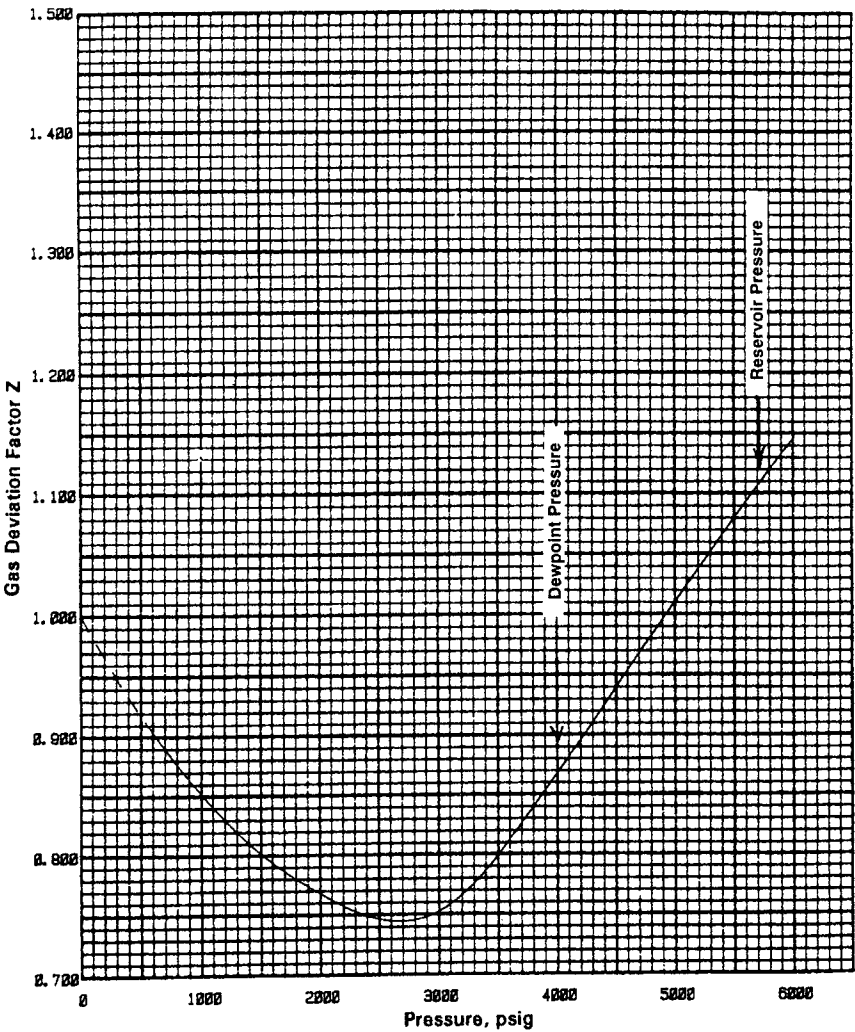


FIGURE 4-28 CVD data for the gas condensate sample from Good Oil Company Well 7, equilibrium gas factor, Z_g . Source: After C. H. Whitson and M. R. Brule, *Phase Behavior*. Richardson, TX: SPE, 2000.

TABLE 4-13 CVD Data for Good Oil Company Well 7, Gas Condensate Sample 2

Component, mol%	Reservoir Pressure, psig							0 ^c
	5713 ^a	4000 ^b	3500	2900	2100	1300	605	
CO ₂	0.18	0.18	0.18	0.18	0.18	0.19	0.21	
N ₂	0.13	0.13	0.13	0.14	0.15	0.15	0.14	
C ₁	61.72	61.72	63.10	65.21	69.79	70.77	66.59	
C ₂	14.10	14.10	14.27	14.10	14.12	14.63	16.06	
C ₃	8.37	8.37	8.26	8.10	7.57	7.73	9.11	
i-C ₄	0.98	0.98	0.91	0.95	0.81	0.79	1.01	
n-C ₄	3.45	3.45	3.40	1.39	2.71	2.59	3.31	
i-C ₅	0.91	0.91	0.86	3.16	0.67	0.55	0.68	
n-C ₅	1.52	1.52	1.40	1.39	0.97	0.81	1.02	
C ₆	1.79	1.79	1.60	1.52	1.03	0.73	0.80	
C ₇₊	6.85	6.85	5.90	4.41	2.00	1.06	1.07	
Total	100.000	100.000	100.000	100.000	100.000	100.000	100.000	
Properties								
C ₇₊ molecular weight	143	143	138	128	116	111	110	
C ₇₊ specific gravity	0.795	0.795	0.790	0.780	0.767	0.762	0.761	
Equilibrium gas deviation factor, Z	1.07	0.867	0.799	0.748	0.762	0.819	0.902	
Two-phase deviation factor, Z	1.07	0.867	0.802	0.744	0.707	0.671	0.576	
Well-stream produced, cumulative % of initial		0.000	5.374	15.438	35.096	57.695	76.787	93.515
From smooth compositions:								
C ₃ , gal/Mscf	9.218	9.218	8.476	7.174	5.171	4.490	5.307	
C ₄₊ , gal/Mscf	6.922	6.922	6.224	4.980	3.095	2.370	2.808	
C ₅₊ , gal/Mscf	5.519	5.519	4.876	3.692	1.978	1.294	1.437	
Retrograde liquid volume, % hydro-carbon pore space		0.0	3.3	19.4	23.9	22.5	18.1	12.6

Note: Study conducted at 186°F.
^aOriginal reservoir pressure.
^bDew-point pressure.
^c0 psig residual liquid properties: 47.5°API oil gravity at 60°F, 0.7897 specific gravity at 60/60°F, and molecular weight of 140.

TABLE 4–14 *Calculated Recoveries from CVD Report for Good Oil Company Well 7, Gas Condensate Sample*

	Initial in place	Reservoir Pressure, psig						
		4000 ^a	3500	2900	2100	1300	605	0
Well stream, Mscf	1000	0	53.74	154.38	350.96	576.95	767.87	935.15
Normal temperature separation ^b								
Stock-tank liquid, bbl	135.7	0	6.4	15.4	24.0	29.7	35.1	
Primary separator gas, Mscf	757.87	0	41.95	124.78	301.57	512.32	658.02	
Second-stage gas, Mscf	96.68	0	4.74	12.09	20.75	27.95	37.79	
Stock-tank gas, Mscf	24.23	0	1.21	3.16	5.61	7.71	10.4	
Total plant products in primary separator ^c								
Propane, gal	1198	0	67	204	513	910	1276	
Butanes, gal	410	0	23	72	190	346	491	
Pentanes, gal	180	0	10	31	81	144	192	
Total plant products in second-stage separator ^c								
Propane, gal	669	0	33	86	149	205	286	
Butanes, gal	308	0	15	41	76	108	159	
Pentanes, gal	138	0	7	19	35	49	69	
Total plant products in well stream ^c								
Propane, gal	2296	0	121	342	750	1229	1706	
Butanes, gal	1403	0	73	202	422	665	927	
Pentanes, gal	5519	0	262	634	1022	1315	1589	

Note: Cumulative recovery per MMscf of original fluid calculated during depletion.

^aDew-point pressure.

^bRecovery basis: primary separation at 500 psia and 70°F, second-stage separation at 50 psia and 70°F, stock tank at 14.7 psia and 70°F.

^cRecovery assumes 100% plant efficiency.

$$n_i = \frac{G}{379.4} = \frac{1 \times 10^6}{379.4} = 2636.16 = \text{mol}$$

The first row in Table 4–14 represents cumulative moles produced, that is, n_p/n_i , expressed as gas volume, G_p , in Mscf:

$$G_p = 2363 \left(\frac{n_p}{n_i} \right) \left(\frac{379.4}{1000} \right) = 1000 \left(\frac{n_p}{n_i} \right)$$

where

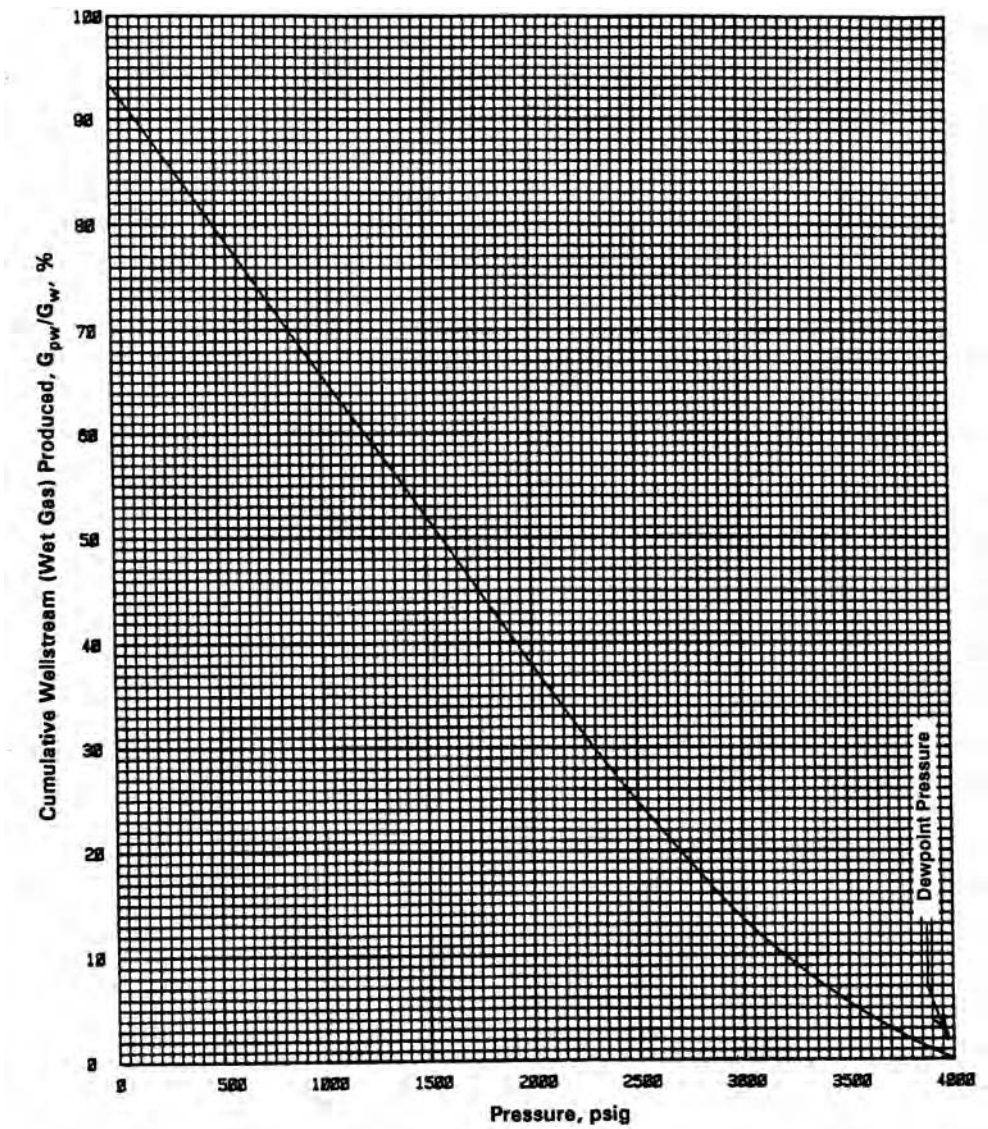


FIGURE 4-29 CVD data for the gas condensate sample from Good Oil Company Well 7, wet-gas material balance.

Source: After C. H. Whitson and M. R. Brule, *Phase Behavior*. Richardson, TX: SPE, 2000.

- G_p = cumulative gas produced, Mscf
- n_p = cumulative moles produced
- G = initial gas in place, MMscf
- n_i = initial moles in place

Recall that 1 lb mole of gas occupies 379.4 scf and $n_p/n_i = G_p/G$.

Recoveries in rows 2 through 4 in Table 4-14 refer to production when the reservoir is produced through a three-stage separator. Whitson and Brule (2000) illustrated the separation process schematically as shown in Figure 4-30.

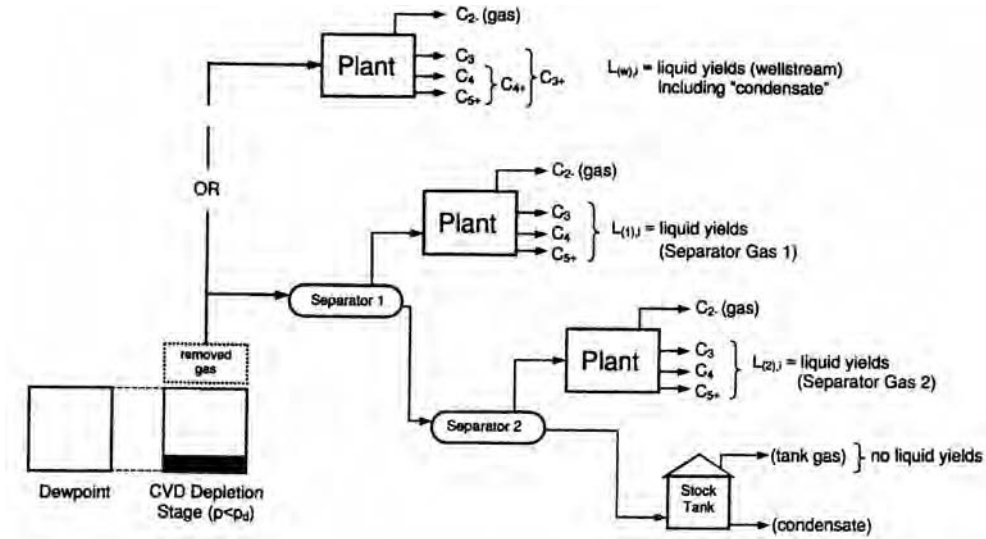


FIGURE 4-30 Schematic of method of calculating plant recoveries in a CVD report for a gas condensate.

Source: After C. H. Whitson and M. R. Brule, *Phase Behavior*, Richardson, TX: SPE, 2000.

Referring to Table 4-14, the stock-tank liquid in initial dew-point fluid, $n = 135.7$ STB, is determined by flashing 1 MMscf of the original gas through a three-stage separator. The values 757.87, 96.68, and 24.23 Mscf represent volumes of the “dry” separator gas at each stage of the separation and reference to G_D . The mole fraction of the well stream resulting as surface gas, y_D , is given by

$$y_D = \frac{G_D}{G} = \frac{(757.87 + 96.68 + 24.23)10^3}{10^6} = 0.8788$$

Whitson and Brule point out that y_D should be used to calculate the “dry” gas formation volume factor B_{gD} from

$$B_{gD} = \left(\frac{1}{y_D} \right) \left[0.00504 \frac{ZT}{P} \right], \text{ bbl/scf}$$

or

$$B_{gD} = \left(\frac{1}{y_D} \right) \left[0.02827 \frac{ZT}{P} \right], \text{ ft}^3/\text{scf} \quad (4-138)$$

For the dew-point pressure, B_{gD} ,

$$B_{gD} = \left(\frac{1}{0.8788} \right) \left[0.02827 \frac{(0.867)(646)}{4015} \right] = 0.004487 \text{ ft}^3/\text{scf}$$

The producing GOR of the dew-point mixture for the specified separator conditions can be calculated on

$$R_p = \frac{G_D}{N} = \frac{(757.87 + 96.68 + 24.23)10^3}{135.7} = 6476 \text{ scf/STB}$$

The dew-point solution oil/gas ratio, r_s , is simply the inverse of R_p ; that is,

$$r_s = \frac{1}{R_p} = \frac{1}{6476} = 1.544 \times 10^{-4} \text{ STB/scf} = 1544 \text{ STB/MMscf}$$

The table also gives cumulative volume of separation products at each depletion stage: N_p , G_{D_1} , G_{D_2} , and G_{D_3} . The producing GOR of the well stream during a depletion stage, such as stage k , is given by

$$(R_p) = \frac{[(301.57 + 20.75 + 5.61) - (124.78 + 12.09 + 3.16)]10^3}{24 - 15.4} = 21.850 \text{ scf/STB}$$

and in terms of solution oil/gas ratio,

$$r_s = \frac{1}{21,850} = 4.58 \times 10^{-5} \text{ STB/scf} = 45.8 \text{ STB/MMscf}$$

The mole fraction of the removed gas at stage k is given by

$$y_D = \frac{(G_{D_1} + G_{D_2} + G_{D_3}) - (G_{D_1} + G_{D_2} + G_{D_3})_{k-1}}{G \left[\left(\frac{n_p}{n} \right)_k - \left(\frac{n_p}{n} \right)_{k-1} \right]}$$

For $P = 2100$ psig, this gives

$$y_D = \frac{[(301.57 + 20.75 + 5.61) - (124.78 + 12.09 + 3.16)]10^3}{1 \times 10^6 (0.35096 - 0.15478)} = 0.9558$$

The dry gas formation volume factor is

$$B_{gD} = \left(\frac{1}{0.9558} \right) \left[0.2827 \frac{(0.762)(646)}{2115} \right] = 6.884 \times 10^{-3} \text{ ft}^3/\text{scf}$$

Recovery Adjustment

All recoveries given in Table 4-14 assume that the reservoir pressure is initially at the dew point. Whitson and Brule (2000) point out that, if the initial reservoir pressure does not equal the dew-point pressure, the tabulated recovery values can be adjusted by using the following methodology.

Step 1 Calculate the additional gas recovery from initial reservoir pressure to dew-point pressure by applying the following expression:

$$\Delta G_p = G \left[\frac{(P/Z)_i}{(P/Z)_d} - 1 \right]$$

where

ΔG_p = additional recovery from the initial reservoir pressure to the dew-point pressure

G = gas initially in place at the dew point, that is, 1 MMscf

$(P/Z)_i$ = value of (P/Z) at initial reservoir pressure

$(P/Z)_d$ = value of (P/Z) at dew-point pressure

For the example reported,

$$\Delta G_p = (10^6) \left[\frac{(5728/1.107)}{(4015/0.867)} - 1 \right] = 0.1173 \text{ MMscf} = 117.3 \text{ Mscf}$$

Step 2 Calculate wet gas initially in place at initial reservoir pressure from

$$G_w = G + \Delta G_p$$

For the example reported, the initial reservoir pressure is 5728 psig; therefore, the wet gas initially in place is

$$G_w = 1.0 + 0.1173 = 1.1173 \text{ MMscf}$$

Step 3 Based on initial reservoir pressure, p_{id} , adjust the tabulated cumulative gas production data by applying the following expressions:

$$\text{For } p > p_d: (G_p)_{adj} = G \left[\frac{(P/Z)_i}{(P/Z)_d} - \frac{(P/Z)}{(P/Z)_d} \right]$$

$$\text{For } p \leq p_d: (G_p)_{adj} = (G_p) + \Delta G_p$$

When $p < p_d$, this expression suggests that the entire tabulated cumulative gas production “cap” for all depletion pressures should be increased by ΔG_p . For the example reported, $\Delta G_p = 117.3 \text{ Mscf}$; therefore, the adjusted cumulative gas production at 4000 and 3500 psig are

$$\text{At 4000 psig: } (G_p)_{adj} = 0 + 117.3 = 117.3 \text{ Mscf}$$

$$\text{At 3500 psig: } (G_p)_{adj} = 53.74 + 117.3 = 171 \text{ Mscf}$$

Step 4 Similarly, the reported stock-tank liquid recovery should be adjusted by calculating the additional liquid recovery ΔN_{sep} from the following expression:

$$\Delta N_{sep} = N_{sep} \left[\frac{(P/Z)_i}{(P/Z)_d} - 1 \right]$$

For the example reported:

$$\Delta N_{sep} = 135.7 \left[\frac{(5728/1.107)}{(4015/0.867)} - 1 \right] = 15.9 \text{ STB}$$

Step 5 Adjust stock-tank oil recovery at $p < p_d$ by using

$$(N_{sep})_{adj} = N_{sep} + \Delta N_{sep}$$

Therefore,

$$\text{At 4000 psig: } (N_{sep})_{adj} = 0 + 15.9 = 15.9 \text{ STB}$$

$$\text{At 3500 psig: } (N_{sep})_{adj} = 6.4 + 15.9 = 22.3 \text{ STB}$$

$$\text{At 2900 psig: } (N_{sep})_{adj} = 15.4 + 15.9 + 31.3 \text{ STB}$$

Liquid Dropout

Figure 4–31 shows the liquid dropout volume in the CVD test as a fraction of cell volume at the dew point. The cell volume at the dew-point pressure is used as a reference volume that essentially represents the reservoir pore volume. The figure shows the dropped out liq-

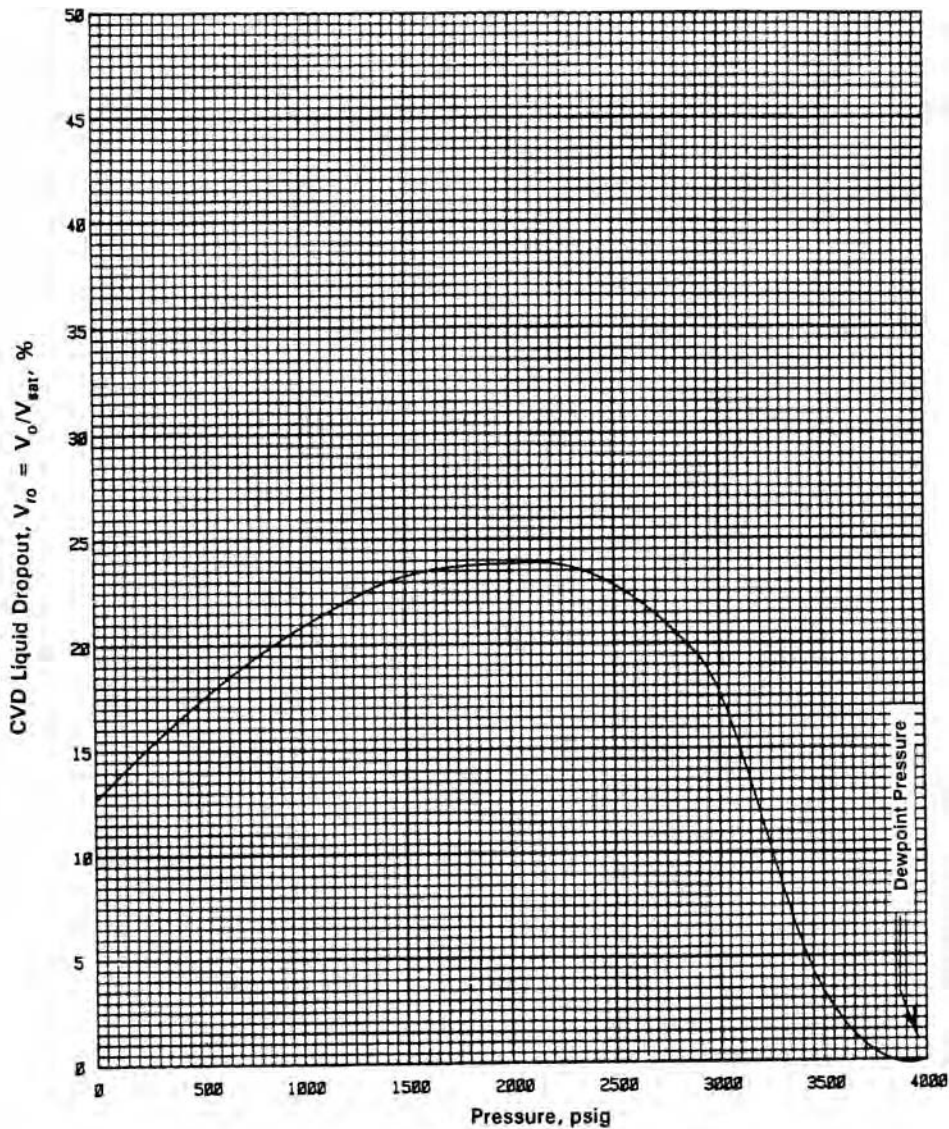


FIGURE 4-31 CVD data for the gas condensate sample from Good Oil Company Well 7, liquid dropout curve, V_{ro} .

Source: After C. H. Whitson and M. R. Brule, *Phase Behavior*. Richardson, TX: SPE, 2000.

uid is vaporized back into the gas phase at lower pressure conditions. This behavior occurs as a result of the transfer of components between the liquid dropout phase and gas phase.

Some gas condensate systems exhibit what is referred to as a tail, where the liquid drops out very slowly before increasing toward a maximum. This trailing behavior in the liquid dropout curve has been the subject of considerable interest, with diverse views on its cause. The initial gradual and small buildup of the condensate phase has been attributed to the contamination of collected samples with hydraulic fluids from various sources during drilling, production, and sampling. There is no firm evidence, however, that the trailing cannot be the true characteristic of a real reservoir fluid.

Liquid Blockage in Gas-Condensate Reservoirs

Well productivity is a key parameter in the development of gas-condensate reservoirs. However, accurate prediction of well productivity can be difficult because of the need to understand and account for the complex processes that occur in the near-well region. When the bottom-hole flowing pressure drops below the dew point, a region of high liquid saturation might build up around the well bore, causing a “liquid blockage” that reduces the gas flow and well productivity. Ahmed (2000) studied the effectiveness of lean gas, N_2 , and CO_2 injection in reducing the liquid blockage. The author suggested the use of the Huff-n-Puff injection. The results indicated the importance of selecting the optimum gas volume and pressure. Fevang and Whitson (1994) identified three flowing zones, as shown in Figure 4-32.

Zone 1 An inner near-well-bore region where both gas and oil flow simultaneously but at different velocities. This zone has a constant flowing gas/oil ratio equal to the well-producing GOR (assuming all the condensate that flows into the well bore is lifted to the surface and no liquid holdups are at the bottom of the well bore). The size of zone 1 increases with time and stabilizes when the single-phase gas entering this zone has sufficient mobility to flow with no net accumulation. As shown by lab experiments, most of the deliverability loss is caused by the reduced gas permeability in zone 1.

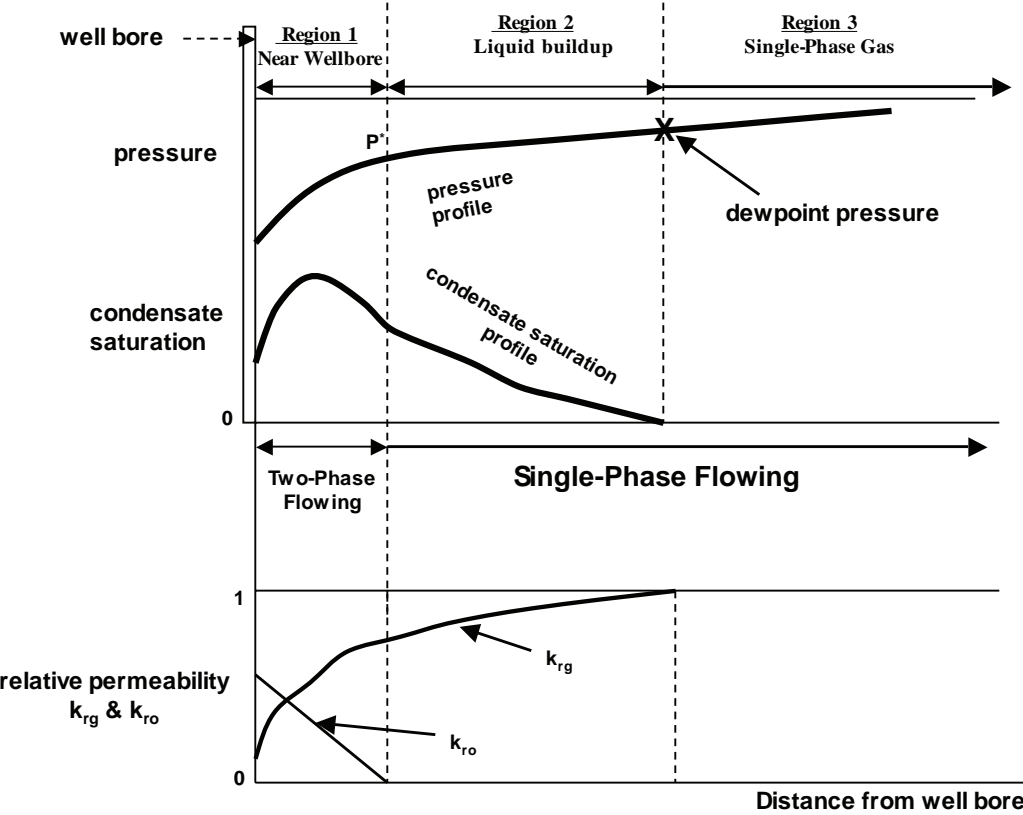


FIGURE 4-32 Condensate liquid blockage.

Zone 2 This zone defines the net accumulation of condensate in sections of the reservoir, where the pressure is below the gas dew-point pressure. There is only gas flow (no liquid flow as the condensate is immobile) in this zone. This is a zone of liquid saturation buildup. The size of zone 2 is largest at early times, just after the reservoir pressure drops below the dew point. It decreases in size with time, because zone 1 is expanding. The size and importance of zone 2 is greater for lean gas condensate.

Zone 3 This zone consists of single-phase gas, as the pressure in this zone is above the dew-point pressure. There is no hydrocarbon liquid in this zone. This will always exist in a gas-condensate reservoir that is currently undersaturated.

The gas rate can be expressed by

$$Q_g = \frac{kb}{1422 \left[\ln \left(\frac{r_e}{r_w} \right) - 0.75 + s \right]} \int_{p_{wf}}^{p_r} \left[\left(\frac{k_{ro}}{\mu_o B_o} \right) R_s + \frac{k_{rg}}{\mu_g B_{gd}} \right] dp$$

or

$$Q_g = C \int_{p_{wf}}^{p_r} \left[\left(\frac{k_{ro}}{\mu_o B_o} \right) R_s + \frac{k_{rg}}{\mu_g B_E} \right] dp \quad (4-139)$$

The performance coefficient C is defined by

$$C = \frac{kb}{1422 \left[\ln \left(\frac{r_e}{r_w} \right) - 0.75 + s \right]}$$

where:

Q_g = gas flow rate, scf/day

k = absolute permeability, md

b = thickness, ft

r_e = drainage radius

r_w = well base radius

p_r = reservoir pressure, psi

p_{wf} = bottom-hole flow pressure

B_{gd} = dry gas formation volume factor, bbl/scf as defined by equation (4-138)

B_o = oil formation volume factor, bbl/STB

s = skin factor

In calculating the pseudo-pressure integral, Fevang and Whitson (1994) proposed dividing the integral into three parts, corresponding to the three flow zones:

$$(\Delta p)_{\text{Total}} = (\Delta p)_{\text{zone1}} + (\Delta p)_{\text{zone2}} + (\Delta p)_{\text{zone3}}$$

$$\text{Total } \Delta p = \int_{p_{wf}}^{p_r} \left(\frac{k_{rg}}{B_{gd} \mu_g} + \frac{k_{ro}}{B_o \mu_o} R_s \right) dp =$$

$$\text{Zone 1: } \int_{p^*}^{p_r} \left(\frac{k_{rg}}{B_{gd} \mu_g} + \frac{k_E}{B_{gd} \mu_g} R_s \right) dp +$$

$$\begin{aligned}
 \text{Zone 2: } & \int_{p^*}^{p_d} \frac{k_{rg}}{B_{gd} \mu_g} dp + \\
 \text{Zone 3: } & k_{rg}(s_{wi}) \int_{p_d}^{p_r} \frac{1}{B_{gd} \mu_g} dp
 \end{aligned} \tag{4-140}$$

The pressure, p^* , is defined as the pressure at the outer boundary of zone 1 and essentially represents the dew-point pressure of the producing stream. Ferang and Whitson proposed the following methodology for evaluating equation (4-140).

Step 1 From the laboratory relative permeability values, plot the relative permeability ratio k_{rg}/k_{ro} versus k_{rg} .

Step 2 Generate the pressure-dependent PVT properties of the gas-condensate system, which include the solution oil/gas ratio, r_s , solution gas/oil ratio, R_s , oil (liquid-dropout) FVF, B_o , and gas FVF, B_{gd} , as given by equation (4-138):

$$B_{gd} = \left(\frac{1}{y_D} \right) \left[0.02827 \frac{ZT}{P} \right]$$

oil (liquid-dropout) viscosity, μ_o ; and gas viscosity, μ_g .

Step 3 Given the initial producing GOR, R_p , calculate

$$r_s = \frac{1}{R_p}$$

and locate the pressure that corresponds to r_s from the PVT table. This pressure is set equal to the dew-point pressure of the producing well stream, p^* .

Step 4 For zone 1, the flowing composition is constant, the combined flow in both the oil and gas phases. The equation that defines the producing gas/oil ratio, R_p , is given by

$$R_p = R_s + \left(\frac{k_{rg}}{k_{ro}} \right) \left(\frac{\mu_o B_o}{\mu_g B_{gd}} \right) (1 - r_s R_p)$$

Rearranging this equation to solve for k_{rg}/k_{ro} as a function of pressure gives

$$\frac{k_{rg}}{k_{ro}}(p) = \left(\frac{R_p - R_s}{1 - r_s R_p} \right) \frac{E_g B_{gd}}{\mu_o B_o} \tag{4-141}$$

The PVT properties used in evaluating the equation can be found directly from the PVT table generated in step 2.

The authors show that the condensate blockage occurring in zone 1 is dictated primarily by the relative permeability ratio, k_{rg}/k_{ro} , of equation (4-141). Ferang and Whitson show that the k_{rg}/k_{ro} ratio is given explicitly by the PVT behavior as modeled by the CCE test. The explicit relationship is given by

$$\frac{k_{rg}}{k_{ro}}(p) = \left[\frac{1}{(V_{rel})_o} - 1 \right] \left(\frac{\mu_g}{\mu_o} \right) \tag{4-142}$$

where $(V_{rel})_o$ is the ratio of oil volume to the total gas + oil volume from CCE test:

$$(V_{rel})_o = \frac{V_o}{V_g + V_o}$$

Combining equations (4-141) and (4-142), $(V_{\text{rel}})_o$ can be expressed in terms of black-oil PVT properties at any producing gas/oil ratio, R_p , by

$$(V_{\text{rel}})_o = \frac{1}{1 + \left(\frac{R_p - R_s}{1 - r_s R_p} \right) \frac{B_{\text{gd}}}{B_o}} \quad (4-143)$$

Values of the ratio $k_{\text{rg}}/k_{\text{ro}}$ as calculated from equation (4-142) are used to determine the corresponding values of k_{rg} from the plot generated in step 1. The corresponding values of k_{ro} are simply given by

$$k_{\text{ro}} = (k_{\text{rg}}/k_{\text{ro}})(k_{\text{rg}})$$

For zone 2, when it exists ($p^* < p_r$), the zone 2 integral,

$$\text{Zone 2: } \int_{p^*}^{p_d} \frac{k_{\text{rg}}}{B_{\text{gd}} \mu_g} dp$$

is evaluated by determining the gas relative permeability value, k_{rg} , at S_o , which is estimated as a function pressure from the CVD liquid dropout volume, LDO.

The liquid dropout saturation after correcting for initial water saturation is given by

$$S_o(p) = (\text{LDO})(1 - S_{\text{wi}})$$

and

$$S_g(p) = (\text{LDO})[1 - S_o(p) - S_{\text{wi}}]$$

where $S_o(p)$ and $S_g(p)$ are the saturation of oil and gas at pressure i .

For zone 3, the only gas PVT properties are found in this zone's integral, where the traditional single-phase pseudo-pressure functions can be used.

Special Laboratory PVT Tests

In addition to the previously described routine laboratory tests, a number of other projects may be performed for very specific applications. If a reservoir is to be depleted under gas injection, miscible gas injection, or a dry-gas cycling scheme, any number of the following tests are conducted: the swelling test, slim-tube test, rising bubble test, or core flood. It should be pointed out that miscible gas injection is characterized by high recoveries in slim-tube tests. These recoveries are usually greater than 90% but less than the 100% recovery expected from first-contact miscible displacement by liquid solvent or chemical slug. The classical thermodynamics definition of *miscibility* is the condition of pressure and temperature at which two fluids, when mixed in any proportion, form a single phase. For example, kerosene and crude oil are miscible at room conditions, whereas stock tank and water are clearly immiscible.

The first three of the listed tests are briefly discussed here.

Swelling Test

The swelling test is the most common multicontact PVT test. During a swelling test, gas with a known composition (usually similar to proposed injection gas) is added to the original reservoir oil at varying proportions in a series of steps. After each addition of certain measured

volume of gas, the overall mixture is quantified in terms of the molar percentage of the injection gas, such as 10 mol% of N_2 . The PVT cell then is pressured to the saturation pressure of the new mixture (only one phase is present). The gas addition starts at the saturation pressure of the reservoir fluid (bubble-point pressure if an oil sample or dew-point pressure if a gas sample) and the addition of the gas continues to perhaps 80 mol% injected gas in the fluid sample.

The data obtained from such a test include

- The relationship of saturation pressure to volume of gas injected.
- The saturation pressure may change from bubble point to dew point after significant volumes of gas injection.
- The volume of the saturated fluid mixture in relation to the volume of the original saturated reservoir oil. This data is essential since it reveals the ability of the injected gas to dissolve in the reservoir fluid and the associated swelling of the resulting mixture.

These data may be used to characterize the mixing of the individual hydrocarbon components and the effect of mixing on the volume increase of the saturated fluid and examine the ability of the hydrocarbon mixture to dissolve injection gas.

Slim Tube

Gas injection experiments are conducted with several objectives. Most tests have been designed to directly measure the minimum miscibility pressure or enrichment. Tests also are conducted to generate volumetric and compositional data for specific studies, such as oil vaporization by gas injection or evaluation and tuning of phase behavior models for numerical simulation of the reservoir performance.

Displacement of oil by gas through a porous medium simulates the gas injection process more closely than other tests, and it is considered the definitive test. The displacement is conducted either in a core, extracted from the reservoir, or more often in a long and narrow sand pack, known as the *slim tube*. Static tests, where the injection gas and the reservoir oil are equilibrated in a cell, also are conducted to determine the mixture phase behavior. Although these tests do not closely simulate the dynamic reservoir conditions, they provide accurate, well-controlled data that are quite valuable, particularly for tuning the equation of state used in modeling the process.

Unlike the previously described laboratory tests that concentrate specifically on fluid property variations with pressure and composition, the slim tube test is conducted to examine the flushing efficiency and fluid mixing during a miscible displacement process. Its purpose is solely to examine the phase behavior properties for a given gas displacement by eliminating reservoir heterogeneities, water, and gravity. Slim tube results are interpreted by plotting cumulative oil recovery versus pore volume of gas injected. Two recoveries are usually reported: recovery at breakthrough and recovery after injection of 1.2 pore volume of gas.

Recovery at 1.2 pore volume of gas injected is then plotted versus injection pressure. For immiscible displacements, relative permeabilities and viscosities influence the recovery process. It should be noted that the point at which the recovery/pressure curve starts

to flatten, as the displacement becomes near miscibility and eventually forms a straight line starting at certain pressure, is called *minimum miscibility pressure* (MMP).

The laboratory test is performed in a long tube (i.e., 20 ft or longer) with a relatively small diameter (i.e., less than 0.25 in.) packed with glass beads or sand. This apparatus is saturated with reservoir oil and pressured up to the anticipated pressure level of the miscible flood scheme. The reservoir oil is then displaced, at a regulated pressure, with the fluid proposed for the miscible flood. Volumes of produced fluids are recorded as functions of the number of pore volumes of fluid injected. Some component in the injection stream is selected as a tracer, and its concentration in the produced stream is recorded as a function of the pore volumes of fluid injected. This enables detection of the displacement front at the exit end of the slim tube. A schematic diagram of the tube and the auxiliary equipment as illustrated by Danesh (2003) is shown in Figure 4–33.

The displacement often is terminated after injecting 1.2 pore volume (PV) gases. The recovery at that point is referred to as the *ultimate recovery*. The test also may be terminated at a preselected high-producing gas and oil ratio, around 8000 vol/vol (40,000–50,000 scf/STB), with the ultimate recovery determined at those conditions.

The volume of produced stabilized oil in the separator generally is converted to that at reservoir conditions, using the volume ratio measured on the original oil. Under high-pressure conditions, particularly in rich-gas injection, a significant amount of the liquid collected in the separator can be due to condensate dropout from the produced gas. The volume factor for such a liquid is different from that of the original oil. Furthermore, the liquid recovery at such conditions is not totally by displacement.

Figure 4–34 shows typical recovery plot from a slim tube experiment.

Different recovery levels, such as 80% at the gas breakthrough, or 90–95% ultimate recovery have been suggested as the criteria for miscible displacement. The oil recovery, however, depends on the tube design and operating conditions. A slim tube may deliver only 80% oil recovery at miscible conditions. The evaluation of recovery changes with displacement pressure, or gas enrichment is more appropriate to determine miscibility

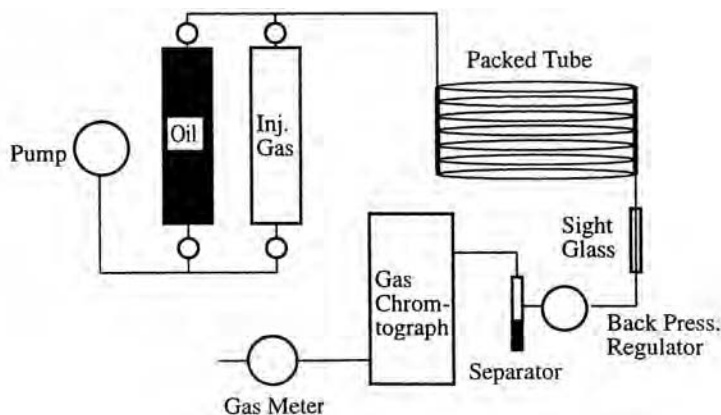


FIGURE 4–33 Schematic diagram of a slim-tube apparatus.

Source: After Danesh (2003).

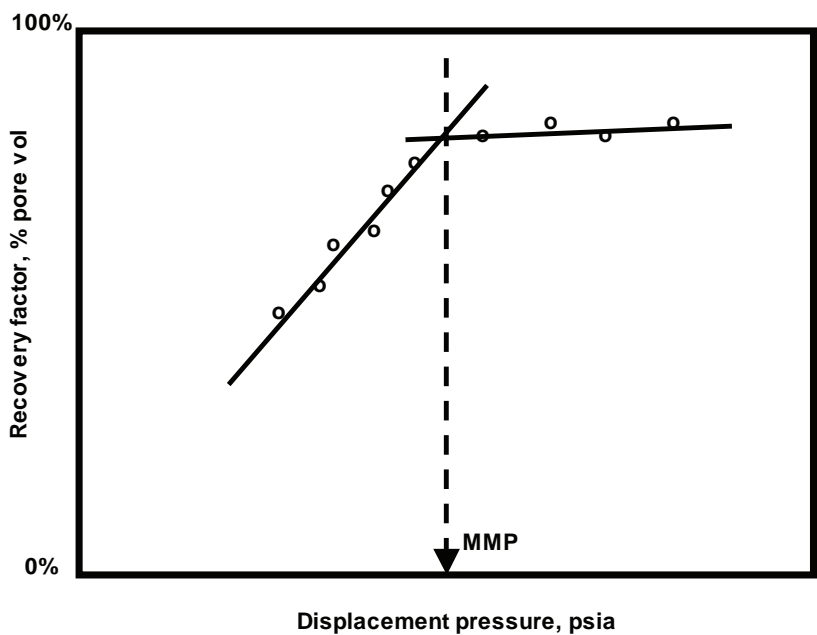


FIGURE 4-34 *Determination of MMP from the slim-tube oil recovery data.*

conditions than searching for a high recovery. The most acceptable definition is the pressure, or enrichment level, at the breakover point of the ultimate oil recovery, as shown in Figure 4-34. The recovery is expected to increase by increasing the displacement pressure, but the additional recovery above MMP is generally minimal.

Rising Bubble Experiment

Rising bubble apparatus is employed in another experimental technique, which is commonly used for quick and reasonable estimates of gas/oil miscibility. In this method, the miscibility is determined from the visual observations of changes in the shape and appearance of bubbles of injected gas as they rise through a visual high-pressure cell filled with the reservoir crude oil. A series of tests are conducted at different pressures or enrichment levels of the injected gas, and the bubble shape is continuously monitored to determine miscibility. This test is qualitative in nature, as miscibility is inferred from visual observations. Hence, some subjectivity is associated with the miscibility interpretation of this technique.

Therefore, the results obtained from this test are somewhat arbitrary, however, this test is quite rapid and requires less than two hours to determine miscibility. This method also is cheaper and requires smaller quantities of fluids, compared to the slim tube. The subjective interpretations of miscibility from visual observations, lack of quantitative information to support the results, and some arbitrariness associated with miscibility interpretation are some of the disadvantages of this technique. Also no strong theoretical background appears to be associated with this technique and it provides only reasonable estimates of gas/oil miscibility conditions.

On Miscibility Pressure

The displacement efficiency of oil by gas depends highly on pressure, and miscible displacement is achieved only at pressures greater than a certain minimum, the minimum miscibility pressure. Slim-tube displacement tests are commonly used to determine the MMP for a given crude oil. The minimum miscibility pressure is defined as the pressure at which the oil recovery versus pressure curve (as generated from the slim-tube test) shows a sharp change in slope, the inflection point.

There are several factors that affect MMP, including:

- Reservoir temperature.
- Oil characteristics and properties, including the API gravity.
- Injected gas composition.
- Concentration of C_1 and N_2 in the crude oil.
- Oil molecular weight.
- Concentration of intermediate components (C_2 – C_5) in the oil phase.

There exists a distinct possibility between reservoir temperature and MMP because MMP increases as the reservoir temperature increases. The MMP also increases with high-molecular-weight oil and oils containing higher concentrations of C_1 and N_2 . However, the MMP decreases with increasing the percentage of the intermediates in the oil phase.

To facilitate screening procedures and gain insight into the miscible displacement process, many correlations relating the MMP to the physical properties of the oil and the displacing gas have been proposed. It should be noted that, ideally, any MMP's correlation should

- Account for each parameter known to affect the MMP.
- Be based on thermodynamic or physical principles that affect the miscibility of fluids.
- Be directly related to the multiple-contact miscibility process.

A variety of correlations or estimations of the MMP developed from regressions of slim-tube data. Although less accurate, these correlations are quick and easy to use and generally require only a few input parameters. Hence, they are very useful for a fast screening of a reservoir for various types of gas injection. They also are useful when detailed fluid characterizations are not available. One significant disadvantage of current MMP correlations is that the regressions use MMPs from slim-tube data, which themselves are uncertain.

Some MMP correlations require only the input of reservoir temperature and the API gravity of the reservoir fluid. Other, more accurate, correlations require reservoir temperature and the total C_2 – C_6 content of the reservoir fluid. In nearly all the correlations, the methane content of the oil is assumed to not affect the MMP significantly.

In general, the MMP correlations fall into the following two categories: those dedicated to pure and impure CO_2 and those that examine the MMPs of other gases. The following section briefly reviews the correlations associated with each of these categories.

Pure and Impure CO₂ MMP

It is well documented that the development of miscibility in a CO₂ crude oil displacement is the result of extraction of some hydrocarbons from the oil by dense CO₂. Many authors found considerable evidence that the extraction of hydrocarbons from a crude oil is strongly influenced by the density of CO₂. Improvement of extraction with the increase in CO₂ density that accompanies increasing pressure accounts for the development of miscibility. The presence of impurities can affect the pressure required to achieve miscible displacement.

Orr and Silva Correlation Orr and Silva (1987) developed a methodology for determining the MMP for pure and contaminated CO₂/crude oil systems. Orr and Silva pointed out that the distribution of molecular sizes present in a crude oil has a significantly larger impact on the MMP than variations in hydrocarbon structure. The carbon-number distributions of the crude oil system are the only data needed to use the correlation. The authors introduced a weighted composition parameter, F , based on a normalized partition coefficient, K_i , for the components C₂ through C₃₇ fractions. The specific steps of the method are summarized next.

Step 1 From the chromatographic or the simulated compositional distribution of the crude oil, omit C₁ and all the nonhydrocarbon components (i.e., CO₂, N₂, and H₂S) from the oil composition. Normalize the weight fractions (w_i) of the remaining components (C₂ to C₃₇).

Step 2 Calculate the partition coefficient K_i for each component in the remaining oil fractions, that is, C₂ to C₃₇, using the following equation:

$$\log(K_i) = 0.761 - 0.04175C_i$$

where C_i is the number of carbon atoms of component i .

Step 3 Evaluate the weighted-composition parameter, F , from

$$F = \sum_{i=2}^{37} K_i w_i$$

Step 4 Calculate the density of CO₂ required to achieve miscibility from the following expressions:

$$\rho_{\text{mmp}} = 1.189 - 0.542F, \quad \text{for } F < 1.467$$

$$\rho_{\text{mmp}} = 0.42, \quad \text{for } F > 1.467$$

Step 5 Given the reservoir temperature, find the pressure, which is assigned to the MMP, at which the CO₂ density is equal to the required ρ_{mmp} . Figure 4-35 shows a graphical presentation of the density of CO₂ as a function of pressure and temperature. This graphical CO₂ density presentation can be used to estimate the MMP by entering the graph with the calculated value of ρ_{mmp} and reservoir temperature to read the pressure that corresponds to the MMP. Kennedy (1954) presented the relationship of the density of CO₂ as a function of pressure and temperature in a tabulated and graphical form as shown in Table 4-15.

Extrapolated Vapor Pressure Method Orr and Jensen (1986) suggested that the vapor pressure curve of CO₂ can be extrapolated and equated with the minimum miscibility pressure to estimate the MMP for low-temperature reservoirs ($T < 120^\circ\text{F}$). A convenient equation for the vapor pressure has been given by Newitt et al. (1996):

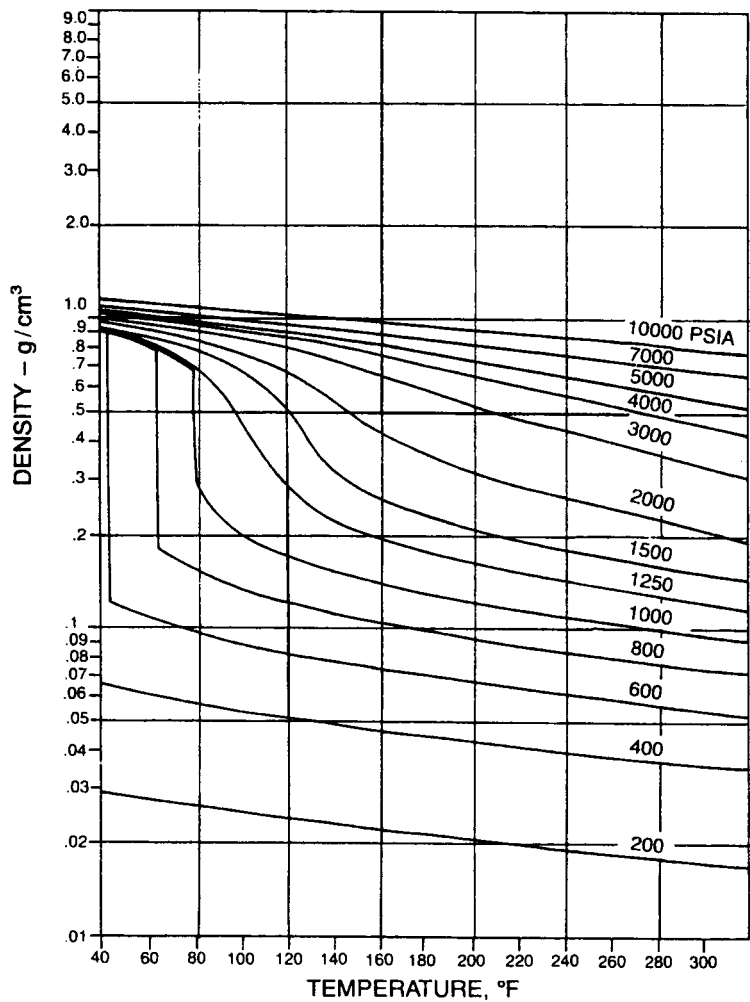


FIGURE 4-35 *CO₂ density versus temperature at various pressures.*
Source: After Sage and Lacey (1955).

$$\text{EVP} = 14.7 \exp \left[10.91 - \frac{2015}{255.372 + 0.5556(T - 460)} \right]$$

with the extrapolated vapor pressure (EVP) in psia and the temperature, T , in °R.

EXAMPLE 4-38

Estimate the MMP for pure CO₂ at 610°R using the EVP method.

SOLUTION

Estimate the MMP for pure CO₂ at 610°R using the EVP method:

$$\text{EVP} = 14.7 \exp \left[10.91 - \frac{2015}{255.372 + 0.5556(610 - 460)} \right] \approx 2098 \text{ psi}$$

TABLE 4-15 *Density of CO₂ as a Function of Pressure and Temperature*

Temperature (°F)	CO ₂ Density (gm/cm ³), Pressure (bar)							
	25	50	75	100	150	200	250	300
68	0.0527	0.1423	0.8100	0.8550	0.9010	0.9335	0.9600	0.9832
86	0.0499	0.1251	0.6550	0.7820	0.8500	0.8887	0.9190	0.9460
104	0.0476	0.1135	0.2305	0.6380	0.7850	0.8415	0.8771	0.9077
122	0.0456	0.1052	0.1932	0.3901	0.7050	0.7855	0.8347	0.8687
140	0.0437	0.0984	0.1726	0.2868	0.6040	0.7240	0.7889	0.8292
158	0.0421	0.0930	0.1584	0.2478	0.5040	0.6605	0.7379	0.7882
176	0.0406	0.0883	0.1469	0.2215	0.4300	0.5935	0.6872	0.7466
194	0.0391	0.0845	0.1381	0.2019	0.3730	0.5325	0.6359	0.7040
212	0.0378	0.0810	0.1305	0.1877	0.3330	0.4815	0.5880	0.6630
230	0.0366	0.0778	0.1239	0.1765	0.3040	0.4378	0.5443	0.6230
248	0.0354	0.0749	0.1187	0.1673	0.2800	0.4015	0.5053	0.5855
266	0.0344	0.0722	0.1141	0.1595	0.2620	0.3718	0.4718	0.5517
284	0.0334	0.0697	0.1094	0.1525	0.2465	0.3470	0.4419	0.5200
302	0.0325	0.0674	0.1054	0.1461	0.2337	0.3267	0.4151	0.4925
320	0.0316	0.0653	0.1018	0.1403	0.2229	0.3089	0.3918	0.4680

Researchers in the Petroleum Recovery Institute suggest equating the MMP with the vapor pressure of CO₂ when the system temperature is below the critical temperature, *T_c*, of CO₂. For temperatures greater than *T_c*, they proposed the following expression:

MMP = 1071.82893(10^{*b*})

with the coefficient *b* as defined by

b = [2.772 – (1519/*T*)]

where MMP is in psia and *T* in °R.

EXAMPLE 4-39

Estimate the MMP for pure CO₂ at 610°R using the method proposed by Petroleum Recovery Institute.

SOLUTION

Step 1 Calculate the coefficient *b*:

b = [2.772 – (1519/*T*)]
b = [2.772 – (1519/610)] = 0.28184

Step 2 Calculate MMP from

MMP = 1071.82893(10^{*b*})
MMP = 1071.82893(10^{0.28184}) = 2051 psi

Yellig and Metcalfe Correlation From their experimental study, Yellig and Metcalfe (1980) proposed a correlation for predicating the CO₂ MMPs that uses the temperature, *T*, in °R, as the only correlating parameter. The proposed expression follows:

$$\text{MMP} = 1833.7217 + 2.2518055(T - 460) + 0.01800674(T - 460)^2 - \frac{103949.93}{T - 460}$$

Yellig and Metcalfe pointed out that, if the bubble-point pressure of the oil is greater than the predicted MMP, then the CO_2 MMP is set equal to the bubble-point pressure.

EXAMPLE 4-40

Estimate the MMP for pure CO_2 at 610°R using Yellig and Metcalfe method.

SOLUTION

$$\begin{aligned}\text{MMP} &= 1833.7217 + 2.2518055(T - 460) + 0.01800674(T - 460)^2 - \frac{103949.93}{T - 460} \\ \text{MMP} &= 1833.7217 + 2.2518055(610 - 460) + 0.01800674(610 - 460)^2 \\ &\quad - \frac{103949.93}{610 - 460} = 1884 \text{ psi}\end{aligned}$$

Alston's Correlation Alston, Kokolis, and James (1985) developed an empirically derived correlation for estimating the MMPs for pure or impure CO_2 /oil systems. Alston and coworkers used the temperature, oil C_{5+} molecular weight, volatile oil fraction, intermediate oil fraction, and the composition of the CO_2 stream as the correlating parameters. The MMP for pure CO_2 /oil systems is given by

$$\text{MMP} = 0.000878(T - 460)^{1.06} (M_{C_{5+}})^{1.78} \left[\frac{X_{\text{vol}}}{X_{\text{int}}} \right]^{0.136}$$

where

T = system temperature, $^\circ\text{R}$

$M_{C_{5+}}$ = molecular weight of pentane and heavier fractions in the oil phase

X_{int} = mole fraction of intermediate oil components (C_2 – C_4 , CO_2 , and H_2S)

X_{vol} = mole fraction of the volatile (C_1 and N_2) oil components

Contamination of CO_2 with N_2 or C_1 has been shown to adversely affect the minimum miscibility pressure of carbon dioxide. Conversely, the addition of C_2 , C_3 , C_4 , or H_2S to CO_2 has shown to lower the MMP. To account for the effects of the presence of contaminants in the injected CO_2 , the authors correlated impure CO_2 MMP with the weighted-average pseudo-critical temperature, T_{pc} , of the injected gas and the pure CO_2 MMP by the following expression:

$$\text{MMP}_{\text{imp}} = \text{MMP} \left[\frac{87.8}{T_{\text{pc}}} \right]^{\frac{168.893}{T_{\text{pc}} - 460}}$$

The pseudo-critical temperature of the injected gas is given by

$$T_{\text{pc}} = \sum w_i T_{\text{ci}} - 460$$

where

MMP = minimum miscibility pressure of pure CO_2

MMP_{imp} = minimum miscibility pressure of the contaminated CO_2

- w_i = weight fraction of component i in the injected gas
- T_{ci} = critical temperatures of component in the injected gas, in °R
- T = system temperature, in °R

It should be pointed out that the authors assigned a uniform critical temperature value of 585°R for H₂S and C₂ in the injected gas.

Sebastian’s Method Sebastian, Wenger, and Renner (1985) proposed a similar corrective step that adjusts the pure CO₂ MMP by an amount related to the mole average critical temperature, T_{cm} , of the injected gas by

$$MMP_{imp} = [C]MMP$$

where the correction parameter, C , is given by

$$C = 1.0 - A[0.0213 - 0.000251A - 2.35(10^{-7})A^2]$$

with

$$A = [T_{cm} - 87.89]/1.8$$
$$T_{cm} = \sum y_i(T_{ci} - 460)$$

where

- MMP = minimum miscibility pressure of pure CO₂
- MMP_{imp} = minimum miscibility pressure of the contaminated CO₂
- y_i = mole fraction of component i in the injected gas
- T_{ci} = critical temperature of component i in the injected gas, °R

To give a better fit to their data, the authors adjusted T_c of H₂S from 212°F to 125°F.

National Petroleum Council Method The National Petroleum Council (NPC) proposed an empirical correlation that provides rough estimates of the pure CO₂ MMPs. The correlation uses the API gravity and the temperature as the correlating parameters, as follows:

GRAVITY, API	MMP
<27°	4000 psi
27–30°	3000 psi
>30°	1200 psi

Reservoir temperature correction:

$T(^{\circ}F)$	ADDITIONAL PRESSURE
< 120	0 psi
120–150	200 psi
150–200	350 psi
200–250	500 psi

Cronquist’s Correlation Cronquist (1978) proposed an empirical equation that was generated from a regression fit on 58 data points. Cronquist characterizes the miscibility pressure as a function of T , molecular weight of the oil pentanes-plus fraction, and the mole percentage of methane and nitrogen. The correlation has the following form:

$$MMP = 15.988(T - 460)^A$$

with:

$$A = 0.744206 + 0.0011038M_{C_{5+}} + 0.0015279y_{c_1-N_2}$$

where T = reservoir temperature, °R, and $y_{c_1-N_2}$ = mole percentage of methane and nitrogen in the injected gas.

Yuan's Correlation Yuan et al. (2005) developed a correlation for predicting minimum miscibility pressure for pure CO₂ based on matching 41 experimental slim-tube MMP values. The authors correlated the MMP with the molecular weight of the heptanes-plus fraction, $M_{C_{7+}}$; temperature T , in °R; and mole percent of the intermediate components, C_{Mp} that is, C_2 – C_6 .

The correlation has the following form:

$$\begin{aligned} (\text{MMP})_{\text{pure CO}_2} = & a_1 + a_2 M_{C_{7+}} + a_3 C_M + \left[a_4 + a_5 M_{C_{7+}} + \frac{a_6 C_M}{(M_{C_{7+}})^2} \right] (T - 460) \\ & + (a_7 + a_8 M_{C_{7+}} + a_9 (M_{C_{7+}})^2 + a_{10} C_M) (T - 460)^2 \end{aligned}$$

with the coefficients as follows:

$$\begin{aligned} a_1 &= -1463.4 & a_6 &= 8166.1 \\ a_2 &= 6.612 & a_7 &= -0.12258 \\ a_3 &= -44.979 & a_8 &= 0.0012283 \\ a_4 &= 21.39 & a_9 &= -4.052(10^{-6}) \\ a_5 &= 0.11667 & a_{10} &= -9.2577(10^{-4}). \end{aligned}$$

The authors proposed an additional correlation to account for the contamination of CO₂ with methane. The correlation is valid for methane contents in the gas only up to 40%. The proposed expression takes the form:

$$\frac{(\text{MMP})_{\text{impure}}}{(\text{MMP})_{\text{pure CO}_2}} = 1 + m(y_{\text{CO}_2} - 100)$$

with

$$\begin{aligned} m = & a_1 + a_2 M_{C_{7+}} + a_3 C_M + \left[a_4 + a_5 M_{C_{7+}} + \frac{a_6 C_M}{(M_{C_{7+}})^2} \right] (T - 460) \\ & + [a_7 + a_8 M_{C_{7+}} + a_9 (M_{C_{7+}})^2 + a_{10} C_M] (T - 460)^2 \end{aligned}$$

with the coefficients as follows:

$$\begin{aligned} a_1 &= -0.065996 & a_6 &= -0.027344 \\ a_2 &= -1.524(10^{-4}) & a_7 &= -2.6953(10^{-6}) \\ a_3 &= 0.0013807 & a_8 &= 1.7279(10^{-8}) \\ a_4 &= 6.2384(10^{-4}) & a_9 &= -43.1436(10^{-11}) \\ a_5 &= -6.7725(10^{-7}) & a_{10} &= -1.9566(10^{-8}) \end{aligned}$$

Lean-Gas and Nitrogen Miscibility Correlations

High-pressure lean gases and N₂ injection have been successfully used as displacing fluids for enhanced oil recovery (EOR) projects and also are widely used in gas cycling and pressure maintenance. In general, miscibility pressure with lean gas (e.g., methane) increases

with increasing temperature because the solubility of methane in hydrocarbons decreases with increasing temperature, which in turn causes the size of the two-phase region to increase. However, miscibility pressure with nitrogen decreases with increasing temperatures because the solubility of nitrogen in hydrocarbons increases. Firoozabadi and Aziz documented the successful use of lean gas/ N_2 as a high-pressure miscible gas injection in several oil fields.

Firoozabadi and Aziz's Correlation Firoozabadi and Aziz (1986) proposed a generalized correlation that can predict MMP for N_2 and lean gases. They used the concentration of oil intermediate components, temperature, and the molecular weight of C_{7+} as the correlating parameters. The authors defined the intermediate components as the sum of the mol% of C_2 – C_5 , CO_2 , and H_2S in the crude oil. The correlation has the following form:

$$MMP = 9433 - 188 (10^3)F + 1430(10^3)F^2$$

with

$$F = \frac{I}{M_{C_{7+}} (T - 460)^{0.25}}$$

$$I = x_{C_2-C_5} + x_{CO_2} + x_{H_2S}$$

where

I = concentration of intermediates in the oil phase, mol%

T = temperature, °R

$M_{C_{7+}}$ = molecular weight of C_{7+}

Conrard (1987) points out that most of nitrogen and lean gas miscibility correlations overestimate the MMP as compared with experimental MMP. The author attributed this departure to the difference between MMP and saturation pressure and suggested the following expression to improve the predictive capability of the Firoozabadi and Aziz correlation:

$$MMP = 0.6909(MMP)_{F-A} + 0.3091 p_b$$

where

MMP = corrected minimum miscibility pressure, psi

MMP_{F-A} = Firoozabadi and Aziz MMP, psi

p_b = bubble-point pressure, psi

A very simplified expression that uses the Firoozabadi and Aziz form is given below for estimating MMP for a nitrogen-crude oil system:

$$MMP = 75.652 \left(\frac{1.8I}{TM_{C_{7+}}} \right)^{-0.5236}$$

Hudgins's Correlation Hudgins, Liave, and Chung (1990) performed a comprehensive laboratory study of N_2 miscible flooding for enhanced recovery of light crude oil. They stated that the reservoir fluid composition, especially the amounts of C_1 through C_5 fractions in the oil phase, is the major determining factor for miscibility. For pure N_2 the authors proposed the following expression:

$$\text{MMP} = 5568 e^{R1} + 3641 e^{R2}$$

with

$$R1 = \frac{-792.06 x_{C_2-C_5}}{M_{C_{7+}} T^{0.25}}$$

$$R2 = \frac{-2.158(10^6)(C_1)^{5.632}}{M_{C_{7+}} T^{0.25}}$$

where

T = temperature, °F

C_1 = mole fraction of methane

$x_{C_2-C_5}$ = sum of the mole fraction of C_2 – C_5 in the oil phase

Glaso's Correlation Glaso (1990) investigated the effect of reservoir fluid composition, displacement velocity, column length of the slim tube, and temperature on slim-tube oil recovery with N_2 . Glaso used the following correlating parameters in developing his MMP relationship:

- Molecular weight of C_{7+} ; that is, $M_{C_{7+}}$.
- Temperature T , in °R.
- Sum of the mol% intermediates (C_2 – C_6) in the oil phase; that is, $x_{C_2-C_6}$.
- Mol% of methane in the oil phase; that is, x_{C_1} .

Glaso proposed the following relationships:

For API < 40:

$$\text{MMP} = 80.14 + 35.35H + 0.76H^2$$

where

$$H = \frac{M_{C_{7+}}^{0.88} (T - 460)^{0.11}}{(x_{C_2-C_6})^{0.64} (x_{C_1})^{0.33}}$$

For API > 40:

$$\text{MMP} = -648.5 + 2619.5H - 1347.6H^2$$

where

$$H = \frac{M_{C_{7+}}^{0.48} (T - 460)^{0.25}}{(x_{C_2-C_6})^{0.12} (x_{C_1})^{0.42}}$$

Sebastian and Lawrence Correlation Sebastian and Lawrence (1992) developed a correlation for predicting the MMP for nitrogen, N_2 . The authors used the following variables to develop their correlation:

- Molecular weight of C_{7+} in the oil phase, $M_{C_{7+}}$.
- Mole fraction of methane in the oil phase, x_{C_1} .

- Mole fraction of intermediate components (C_2 – C_6 and CO_2) in the oil phase, x_m .
- Reservoir temperature, T , in °R.

The proposed correlation has the following form:

$$MMP_{N_2} = 4603 - \left[\frac{3283x_{C_1}T - 4.776(x_{C_1})^2T^2 + 4.008x_mT^2}{M_{C_{7+}}} \right] + 2.05M_{C_{7+}} + 7.541T$$

Lange's Correlation Lange (1998) developed a generalized MMP correlation that can be used for a wide range of injected gases, crude oils, temperatures, and pressures. The correlation is based on representation of the physical and chemical properties of crude oil and injected gas through the well-known Hildebrand solubility parameters. The solubility parameter concept is widely used to judge the “goodness” of a solvent for a solute, such that a small difference in solubility parameters between a solute and solvent suggests that the solute may dissolve in the solvent. The solubility parameter of a high-pressure gas depends primarily on its reduced density ρ_r , which can be estimated with an equation-of-state calculation and is expressed by the following relationship:

$$\delta_{gi} = 0.122\rho_{ri}\sqrt{p_{ci}}$$

where

ρ_{ri} = reduced density of component i in the injected gas, lb/ft³

p_{ci} = critical pressure of component i in the injected gas, psia

δ_{gi} = solubility parameter of component i in the injected gas, (cal/cm³)^{0.5}

The reduced density as defined previously is given by

$$\rho_r = \rho_i/\rho_{ci}$$

or

$$\delta_{gi} = 0.122\frac{\rho_i}{\rho_{ci}}\sqrt{p_{ci}}$$

The solubility parameter of the injected gas, δ_{gas} , can be calculated by using the following mixing rules, based on individual component's solubility, δ_{gi} , and its volume fraction in the injected gas:

$$\delta_{gas} = \sum_{i=1}^N (v_i\delta_{gi}) \quad (4-144)$$

where

δ_{gas} = solubility parameter of the injected gas, (cal/cm³)^{0.5}

δ_{gi} = solubility parameter of component i in the injected gas, (cal/cm³)^{0.5}

v_i = volume fraction of component i in the injected gas, psia

p_{ci} = critical pressure of component i in the injected gas, psia

ρ_i = density of component i in the injected gas at injection pressure and temperature, lb/ft³

ρ_{ci} = critical density of component i in the injected gas, lb/ft³

The solubility of a crude oil depends primarily on its molecular weight and can be approximated by the following expression:

$$\delta_{\text{oil}} = (6.97)0.01M - 0.00556(T - 460) \quad (4-145)$$

where M = molecular weight of the reservoir oil and T = reservoir temperature, °R.

Lange points out that miscibility occurs when the solubility difference between the oil injected gas is around $3(\text{cal/cm}^3)^{0.5}$, or

$$\text{Miscibility criterion: } |\delta_{\text{oil}} - \delta_{\text{gas}}| \leq 3 \pm 0.4$$

The process of determining the MMP using Lange's correlation is essentially a trial and-error approach. A pressure is assumed and δ_{gas} is calculated; if the miscibility criterion, as just defined, is met, then the assumed pressure is the MMP, otherwise the process is repeated.

Lange also developed an expression for estimating the residual oil saturation to miscible displacement, S_{orm} , which is very useful as a screening parameter. The correlation is based on data from a large pool of core floods with the following form:

$$S_{\text{orm}} = S_{\text{orw}}[0.12(|\delta_{\text{oil}} - \delta_{\text{gas}}|) - 0.11]$$

where S_{orw} is residual oil saturation to water flood.

Problems

- Tables 4-16 through 4-18 show the experimental results performed on a crude oil sample taken from the MTech field. The results include the CCE, DE, and separator tests.
 - Select the optimum separator conditions and generate B_o , R_s , and B_t values for the crude oil system. Plot your results and compare with the unadjusted values.
 - Assume that new field indicates that the bubble-point pressure is better described by a value of 2500 psi. Adjust the PVT to reflect for the new bubble-point pressure.
- A crude oil system exists at its bubble-point pressure of 1708.7 psia and a temperature of 131°F. Given the following data:
 API = 40°
 Average specific gravity of separator gas = 0.85
 Separator pressure = 100 psig
 - Calculate R_{sb} using
 - Standing's correlation.
 - Vasquez-Beggs's method.
 - Glaser's correlation.
 - Marhoun's equation.
 - Petrosky and Farshad's correlation.
 - Calculate B_{ob} by applying methods listed in part a.

TABLE 4–16 *Pressure/Volume Relations of a Reservoir Fluid at 260°F (Constant-Composition Expansion)*

Pressure, psig	Relative Volume
5000	0.9460
4500	0.9530
4000	0.9607
3500	0.9691
3000	0.9785
2500	0.9890
2300	0.9938
2200	0.9962
2100	0.9987
2051	1.0000
2047	1.0010
2041	1.0025
2024	1.0069
2002	1.0127
1933	1.0320
1843	1.0602
1742	1.0966
1612	1.1524
1467	1.2299
1297	1.3431
1102	1.5325
863	1.8992
653	2.4711
482	3.4050

3. Estimate the bubble-point pressure of a crude oil system with the following limited PVT data:
- API = 35°
- T = 160°F
- R_{sb} = 700 scf/STB
- γ_g = 0.75
- Use the five different methods listed in problem 2, part a.
4. A crude oil system exists at an initial reservoir pressure of 3000 psi and 185°F. The bubble-point pressure is estimated at 2109 psi. The oil properties at the bubble-point pressure are as follows:
- B_{ob} = 1.406 bbl/STB
- R_{sb} = 692 scf/STB
- γ_g = 0.876
- API = 41.9°

TABLE 4-17 *Differential Vaporization at 260°*

Pressure, psig	Solution Gas/Oil Ratio ^a	Relative Oil Volume ^b	Relative Total Volume ^c	Oil Density, gm/cc	Deviation Factor Z	Gas Formation Volume Factor ^d	Incremental Gas Gravity
2051	1004	1.808	1.808	0.5989			
1900	930	1.764	1.887	0.6063	0.880	0.00937	0.843
1700	838	1.708	2.017	0.6165	0.884	0.01052	0.840
1500	757	1.660	2.185	0.6253	0.887	0.01194	0.844
1300	678	1.612	2.413	0.6348	0.892	0.01384	0.857
1100	601	1.566	2.743	0.6440	0.899	0.01644	0.876
900	529	1.521	3.229	0.6536	0.906	0.02019	0.901
700	456	1.476	4.029	0.6635	0.917	0.02616	0.948
500	379	1.424	5.537	0.6755	0.933	0.03695	0.018
300	291	1.362	9.214	0.6896	0.955	0.06183	1.373
170	223	1.309	16.246	0.7020	0.974	0.10738	2.230
0	0	1.110		0.7298			

Notes: Solution gas/oil ratio at 60°F = 1.000
Gravity of residual oil = 43.1° API at 60°F
^aCubic feet of gas at 14.73 psia and 60°F per barrel of residual oil at 60°F.
^bBarrels of oil at indicated pressure and temperature per barrel of residual oil at 60°F.
^cBarrels of oil plus liberated gas at indicated pressure and temperature per barrel of residual oil at 60°F.
^dCubic feet of gas at indicated pressure and temperature per cubic foot at 14.73 psia and 60°F.

TABLE 4-18 *Separator Tests of Reservoir Fluid Sample*

Separator Pressure, psi Gauge	Separator Temperature, °F	Gas/Oil Ratio ^a	Gas/Oil Ratio ^b	Stock- Tank Gravity, °API at 60°F	Formation Volume Factor ^c	Separator Volume Factor ^d	Specific Gravity of Flashed Gas
2000 to 0	71	431	490			1.138	0.739 ^e
	71	222	223	48.2	0.549	1.006	1.367
100 to 0	72	522	566			1.083	0.801 ^e
	72	126	127	48.6	1.529	1.006	1.402
50 to 0	71	607	632			1.041	0.869 ^e
	71	54	54	48.6	1.532	1.006	1.398
25 to 0	70	669	682			1.020	0.923 ^e
	70	25	25	48.4	1.558	1.006	1.340

^aGas/oil ratio in cubic feet of gas at 60°F and 14.75 psi absolute per barrel of oil at indicated pressure and temperature.
^bGas/oil ratio in cubic feet of gas at 60°F and 14.75 psi absolute per barrel of stock-tank oil at 60°F.
^cFormation volume factor in barrels of saturated oil at 2051 psi gauge and 260°F per barrel of stock-tank oil at 60°F.
^dSeparator volume factor in barrels of oil at indicated pressure and temperature per barrel of stock-tank oil at 60°F.
^eCollected and analyzed in the laboratory.

Calculate

- a. Oil density at the bubble-point pressure.
 - b. Oil density at 3000 psi.
 - c. B_o at 3000 psi.
5. The PVT data as shown in Table 4–19 were obtained on a crude oil sample taken from the Nameless field. The initial reservoir pressure was 3600 psia at 160°F. The average specific gravity of the solution gas is 0.65. The reservoir contains 250 MMbbl of oil initially in place. The oil has a bubble-point pressure of 2500 psi.
- a. Calculate the two-phase oil formation volume factor at
 - 1. 3200 psia.
 - 2. 2800 psia.
 - 3. 1800 psia.
 - b. Calculate the initial oil in place as expressed in MMSTB.
 - c. What is the initial volume of dissolved gas in the reservoir?
 - d. Calculate the oil compressibility coefficient at 3200 psia.
6. The PVT data below was obtained from the analysis of a bottom-hole sample.

p , psia	Relative Volume, V/V_{sat}
3000	1.0000
2927	1.0063
2703	1.0286
2199	1.1043
1610	1.2786
1206	1.5243
999	1.7399

- a. Plot the Y -function versus pressure on rectangular coordinate paper.
- b. Determine the constants in the equation $Y = mp + b$ using the method of least squares.
- c. Recalculate relative oil volume from the equation.

TABLE 4–19 *PVT Data for Problem 5*

Pressure, psia	Solution Gas, scf/STB at 14.7 psia and 60°F	Formation Volume Factor, bbl/STB
3600		1.310
3200		1.317
2800		1.325
2500	567	1.333
2400	554	1.310
1800	436	1.263
1200	337	1.210
600	223	1.140
200	143	1.070

7. A 295 cc of a crude oil sample was placed in a PVT at an *initial* pressure of 3500 psi. The cell temperature was held at a constant temperature of 220°F. A differential liberation test was then performed on the crude oil sample with the recorded measurements as given in Table 4–20. Using the *recorded* measurements and assuming an oil gravity of 40°API, calculate the following PVT properties:
 - a. Oil formation volume factor at 3500 psi.
 - b. Gas solubility at 3500 psi.
 - c. Oil viscosity at 3500 psi.
 - d. Isothermal compressibility coefficient at 3300 psi.
 - e. Oil density at 1000 psi.
8. Experiments were made on a bottom-hole crude oil sample taken from the North Grieve field to determine the gas solubility and oil formation volume factor as a function of pressure. The initial reservoir pressure was recorded as 3600 psia and reservoir temperature was 130°F. The data in Table 4–21 were obtained from the measurements. At the end of the experiments, the API gravity of the oil was measured as 40°. If the average specific gravity of the solution gas is 0.7, calculate
 - a. Total formation volume factor at 3200 psia.
 - b. Oil viscosity at 3200 psia.
 - c. Isothermal compressibility coefficient at 1800 psia.

TABLE 4–20 *Crude Oil Sample for Problem 7*

p, psi	T, °F	Total Volume, cc	Volume of Liquids, cc	Volume of Liberated Gas, scf	Specific Gravity of Liberated Gas
3500	220	290	290	0	—
3300	220	294	294	0	—
3000*	220	300	300	0	—
2000	220	323.2	286.4	0.1627	0.823
1000	220	375.2	271.5	0.1840	0.823
14.7	60	—	179.53	0.5488	0.823

*Bubble-point pressure.

TABLE 4–21 *Data for Problem 8*

Pressure, psia	R_s , scf/STB	B_g , bbl/STB
3600	567	1.310
3200	567	1.317
2800	567	1.325
2500	567	1.333
2400	554	1.310
1800	436	1.263
1200	337	1.210
600	223	1.140
200	143	1.070

9. You are producing a 35°API crude oil from a reservoir at 5000 psia and 140°F. The bubble-point pressure of the reservoir liquids is 4000 psia at 140°F. Gas with a gravity of 0.7 is produced with the oil at a rate of 900 scf/STB. Calculate
- a. Density of the oil at 5000 psia and 140°F.
 - b. Total formation volume factor at 5000 psia and 140°F.
10. An undersaturated oil reservoir exists at an initial reservoir pressure 3112 psia and a reservoir temperature of 125°F. The bubble-point of the oil is 1725 psia. The crude oil has the pressure versus oil formation volume factor relationship found in Table 4–22. The API gravity of the crude oil and the specific gravity of the solution gas are 40° and 0.65, respectively. Calculate the density of the crude oil at 3112 psia and 125°F.
11. A PVT cell contains 320 cc of oil and its bubble-point pressure of 2500 psia and 200°F. When the pressure was reduced to 2000 psia, the volume increased to 335.2 cc. The gas was bled off and found to occupy a volume of 0.145 scf. The volume of the oil was recorded as 303 cc. The pressure was reduced to 14.7 psia and the temperature to 60°F while 0.58 scf of gas was evolved, leaving 230 cc of oil with a gravity of 42°API. Calculate
- a. Gas compressibility factor at 2000 psia.
 - b. Gas solubility at 2000 psia.
12. The composition of a crude oil and the associated equilibrium gas is given below. The reservoir pressure and temperature are 3000 psia and 140°F, respectively.

COMPONENT	x_i	y_i
C ₁	0.40	0.79
C ₂	0.08	0.06
C ₃	0.07	0.05
n-C ₄	0.03	0.04
n-C ₅	0.01	0.02
C ₆	0.01	0.02
C ₇₊	0.40	0.02

TABLE 4–22 *Pressure versus Oil Relationship for Problem 10*

Pressure, psia	B_o , bbl/STB
3112	1.4235
2800	1.4290
2400	1.4370
2000	1.4446
1725	1.4509
1700	1.4468
1600	1.4303
1500	1.4139
1400	1.3978

The following additional PVT data are available:

Molecular weight of $C_{7+} = 215$

Specific gravity of $C_{7+} = 0.77$

Calculate the surface tension.

13. Estimate the MMP for pure CO_2 at 630°R using the following methods:

- a. EVP method.
- b. Petroleum Recovery Institute method.
- c. Yellig and Metcalfe's method.

References

- Abu-Khamsin, A., and M. Al-Marhoun. "Development of a New Correlation for Bubblepoint Viscosity." *Arabian Journal of Science and Engineering* 16, no. 2A (April 1991): 99.
- Ahmed, T. "Compositional Modeling of Tyler and Mission Canyon Formation Oils with CO_2 and Lean Gases." Final report submitted to Montana's On a New Track for Science (MONTs), Montana National Science Foundation Grant Program, 1988.
- Ahmed, T. "Removing Well Bore Liquid Blockage by Gas Injection." Paper 002-00 presented at the Rio Oil and Gas Expo and Conference, Rio de Janeiro, Brazil, October 16–19, 2000.
- Alani, G. H., and H. T. Kennedy. "Volume of Liquid Hydrocarbons at High Temperatures and Pressures." *Transactions of the AIME* 219 (1960): 288–292.
- Al-Shammasi, A. "Bubble-point Pressure and Formation Volume Factor Correlations." SPE Paper 53185, Presented at the SPE Middle East Conference, Bahrain, February 20–23, 1999.
- Alston, R. B., G. P. Kokolis, and C. F. James. " CO_2 Minimum Miscibility Pressure: A Correlation for Impure CO_2 Streams and Live Oil Streams." *Society of Petroleum Engineers Journal* (April 1985): 268–274.
- Amyx, J. M., D. M. Bass, and R. Whiting. *Petroleum Reservoir Engineering—Physical Properties*. New York: McGraw-Hill, 1960.
- Beal, C. "The Viscosity of Air, Water, Natural Gas, Crude Oils and Its Associated Gases at Oil Field Temperatures and Pressures." *Transactions of the AIME* 165 (1946): 94–112.
- Beggs, H. D., and J. R. Robinson. "Estimating the Viscosity of Crude Oil Systems." *Journal of Petroleum Technology* (September 1975): 1140–1141.
- Brill, J., and D. Beggs. "A Study of Two-Phase Flow in Inclined Pipes." *Journal of Petroleum Technology* (May 1973).
- Chew, J., and C. A. Connally, Jr. "A Viscosity Correlation for Gas-Saturated Crude Oils." *Transactions of the AIME* 216 (1959): 23–25.
- Cho, S., F. Civan, and K. Starting. "A Correlation to Predict Maximum Condensation for Retrograde Fluids." Paper SPE 14268 presented at the SPE annual meeting, Las Vegas, September 22–25, 1985.
- Conrard, P. "Discussion of Analysis and Correlation of Nitrogen and Lean Gas Miscibility Pressure." *SPE Reservoir Engineering* (May 1987).
- Craft, B., and M. Hawkins. *Applied Petroleum Reservoir Engineering*. Englewood Cliffs, NJ: Prentice-Hall, 1959.
- Cragoe, C. *Thermodynamic Properties of Petroleum Products*. Washington, DC: U.S. Department of Commerce, 1997, p. 97.
- Cronquist, C. "Carbon Dioxide Dynamic Displacement with Light Reservoir Oils." Paper presented at the U.S. Department of Energy annual symposium, Tulsa, August 28–30, 1978.
- Dake, L. P. *Fundamentals of Reservoir Engineering*. Amsterdam: Elsevier, 1978.
- Danesh, A. *PVT and Phase Behavior of Petroleum Reservoir Fluids*, 3d ed. Burlington, MA: Elsevier, 2003.

- Dindoruk, B., and P. Christman. "PVT Properties and Viscosity Correlations for Gulf of Mexico Oils." *SPE Reservoir Evaluation and Engineering* (December 2004).
- Dodson, C., D. Goodwill, and E. Mayer. "Application of Laboratory PVT Data to Engineering Problems." *Journal of Petroleum Technology* (December 1953).
- Fanchi, J. R. "Calculation of Parachors for Composition Simulation." *Journal of Petroleum Technology* (November 1985): 2049–2050.
- Fevang, D., and C. Whitson. "Accurate In-Situ Compositions in Petroleum Reservoirs." Paper SPE 28829 presented at the European Petroleum Conference, London, October 25–27, 1994.
- Firoozabadi, A., and K. Aziz. "Analysis and Correlation of Nitrogen and Lean Gas Miscibility Pressure." *SPE Reservoir Engineering* (August 1986): 100–110.
- Firoozabadi, A., et al. "Surface Tension of Reservoir Crude Oil/Gas Systems." *SPE Reservoir Engineering* (February 1988).
- Glaser, O. "Generalized Pressure-Volume-Temperature Correlations." *Journal of Petroleum Technology* (May 1980): 785–795.
- Glaser, O. "Miscible Displacement: Recovery Tests with Nitrogen." *SPE Reservoir Engineering* (February 1990): 61–68.
- Haas, J. "Physical Properties of the Coexisting Phases and Thermochemical Properties of H_2O ." *Geological Survey Bulletin* (1976).
- Hudgins, D. A., F. Liave, and F. Chung. "Nitrogen Miscible Displacement of Light Crude Oil," *SPE Reservoir Engineering* (February 1990): 100–106.
- Katz, D. *Drilling and Production Practice*. Dallas: American Petroleum Institute, 1942.
- Katz, D., and W. Saltman. "Surface Tension of Hydrocarbons." *Industrial Engineering and Chemistry* 31 (1939): 91.
- Katz, D., et al. *Handbook of Natural Gas Engineering*. New York: McGraw-Hill, 1959.
- Kennedy, G. "Pressure-Volume-Temperature Relations in CO_2 ." *American Journal of Science* 252 (April 1954): 225.
- Khan, S., et al. *Viscosity Correlations for Saudi Arabia Oils*. SPE Paper 15720. Dallas: Society of Petroleum Engineers, 1987.
- Lange, E. "Correlation and Prediction of Residual Oil Saturation for Gas-Injection-Enhanced Oil-Recovery Processes." *SPE Reservoir Evaluation and Engineering* (April 1998).
- Lasater, J. A. "Bubble-Point Pressure Correlation." *Transactions of the AIME* 213 (1958): 379–381.
- Little, J. E., and H. T. Kennedy. "A Correlation of the Viscosity of Hydrocarbon Systems with Pressure, Temperature, and Composition." *Society of Petroleum Engineers Journal* (June 1968): 157–162.
- Lohrenz, J., B. G. Bra, and C. R. Clark. "Calculating Viscosities of Reservoir Fluids from Their Compositions." *Journal of Petroleum Technology* (October 1964): 1171–1176.
- Marhoun, M. A. "PVT Correlation for Middle East Crude Oils." *Journal of Petroleum Technology* (May 1988): 650–665.
- McCain, W. *The Properties of Petroleum Fluids*. Tulsa: PennWell Publishing Company, 1991.
- McCain, W. "Analysis of Black Oil PVT Reports Revisited." Paper SPE 77386 presented at the SPE annual meeting, San Antonio, TX, September 29–October 2, 2002.
- McCain, W., et al. "The Coefficient of Isothermal Compressibility of Black Oils at Pressures below Bubble Point." SPE Formation Evaluation (September 1988).
- McKetta, J., and A. Wehe. "Hydrocarbon/Water and Formation Water Correlations." In *Petroleum Production Handbook*, 2d ed., ed. T. C. Frick and R. W. Taylor. Richardson, TX: Society of Petroleum Engineers, 1962.
- Meehan, D. N. "A Correlation for Water Compressibility." *Petroleum Engineer* (November 1980): 125–126.
- Moses, P. "Engineering Application of Phase Behavior of Crude Oil and Condensate Systems." *Journal of Petroleum Technology* (July 1986): 715–723.

- Newitt, D. M., et al. "Carbon Dioxide." In *Thermodynamic Functions of Gases*, vol. 1, ed F. Din, pp. 102–134. London: Butterworths, 1996.
- Orr, F. M., and C. M. Jensen. "Interpretation of Pressure-Composition Phase Diagram for CO₂/Crude-Oil systems." *Society of Petroleum Engineers Journal* (October 1986): 485–497.
- Orr, F. M., and M. K. Silva. "Effect of Oil Composition on MMP—Part 2. Correlation." *SPE Reservoir Engineering* (November 1987): 479–492.
- Ostermann, R., et al. "A Correlation for Increased Gas Gravity during Pressure Depletion." Paper SPE 16962 presented at the SPE annual conference, Dallas, September 27–30, 1987.
- Petrosky, G. E., and F. Farshad. "Pressure-Volume-Temperature Correlations for Gulf of Mexico Crude Oils." SPE paper 26644, presented at the 68th Annual Technical Conference of the Society of Petroleum Engineers, Houston, October 3–6, 1993.
- Ramey, H. *Correlation of Surface and Interfacial Tensions of Reserve Fluids*. SPE paper no. 4429. Richardson, TX: Society of Petroleum Engineers, 1973.
- Rowe, A., and J. Chou. "Pressure-Volume-Temperature Correlation Relation of Aqueous NaCl Solutions." *Journal of Chemical Engineering Data* 15 (1970).
- Sage, B., and W. Lacey. "Some Properties of the Lighter Hydrocarbons and Carbon Dioxide." API research project 37. New York: API, 1955.
- Sebastian, H., and D. Lawrence. "Nitrogen Minimum Miscibility Pressures." Paper SPE 24134 presented at the SPE/DOE meeting, Tulsa, OK, April 22–24, 1992.
- Sebastian, H. M., R. S. Wenger, and T. A. Renner. "Correlation of Minimum Miscibility Pressure for Impure CO₂ Streams." *Journal of Petroleum Technology* (November 1985): 2076–2082.
- Standing, M. B. "A Pressure-Volume-Temperature Correlation for Mixtures of California Oils and Gases." *Drilling and Production Practice* [API] (1947): 275–287.
- Standing, M. B. *Petroleum Engineering Data Book*. Trondheim: Norwegian Institute of Technology, 1974.
- Standing, M. B. *Volumetric and Phase Behavior of Oil Field Hydrocarbon Systems*. Dallas: Society of Petroleum Engineers, 1977, pp. 125–126.
- Standing, M. B. *Volumetric and Phase Behavior of Oil Field Hydrocarbon Systems*, 9th ed. Dallas: Society of Petroleum Engineers, 1981.
- Standing, M. B., and D. L. Katz. "Density of Natural Gases." *Transactions of the AIME* 146 (1942): 140–149.
- Sugden, S. "The Variation of Surface Tension. VI. The Variation of Surface Tension with Temperature and Some Related Functions." *Journal of the Chemistry Society* 125 (1924): 32–39.
- Sutton, R. P., and F. F. Farashad. "Evaluation of Empirically Derived PVT Properties for Gulf of Mexico Crude Oils." Paper SPE 13172, presented at the 59th Annual Technical Conference, Houston, 1984.
- Trube, A. S. "Compressibility of Undersaturated Hydrocarbon Reservoir Fluids." *Transactions of the AIME* 210 (1957): 341–344.
- Vasquez, M., and H. D. Beggs. "Correlations for Fluid Physical Property Prediction." *Journal of Petroleum Technology* (June 1980): 968–970.
- Weinaug, C., and D. L. Katz. "Surface Tension of Methane-Propane Mixtures." *Industrial Engineering and Chemistry* 25 (1943): 35–43.
- Whitson, C. H., and M. R. Brule. *Phase Behavior*. Richardson, TX: SPE, 2000.
- Yellig, W. F., and R. S. Metcalfe. "Determination and Prediction of CO₂ Minimum Miscibility Pressures." *Journal of Petroleum Technology* (January 1980): 160–168.
- Yuan, H., et al. *Simplified Method for Calculation of MMP*. SPE paper 77381. Dallas: Society of Petroleum Engineers, 2005.

5

Equations of State and Phase Equilibria

A PHASE IS THE PART OF A SYSTEM that is uniform in physical and chemical properties, homogeneous in composition, and separated from other, coexisting phases by definite boundary surfaces. The most important phases occurring in petroleum production are the hydrocarbon liquid phase and gas phase. Water is also commonly present as an additional liquid phase. These can coexist in equilibrium when the variables describing change in the entire system remain constant in time and position. The chief variables that determine the state of equilibrium are system temperature, system pressure, and composition.

The conditions under which these different phases can exist are a matter of considerable practical importance in designing surface separation facilities and developing compositional models. These types of calculations are based on the following two concepts, equilibrium ratios and flash calculations, which are discussed next.

Equilibrium Ratios

As indicated in Chapter 1, a system that contains only one component is considered the simplest type of hydrocarbon system. The word *component* refers to the number of molecular or atomic species present in the substance. A single-component system is composed entirely of one kind of atom or molecule. We often use the word *pure* to describe a single-component system. The qualitative understanding of the relationship that exists between temperature, T , pressure, p , and volume, V , of pure components can provide an excellent basis for understanding the phase behavior of complex hydrocarbon mixtures.

In a multicomponent system, the equilibrium ratio, K_i , of a given component is defined as the ratio of the mole fraction of the component in the gas phase, y_i , to the mole

fraction of the component in the liquid phase, x_i . Mathematically, the relationship is expressed as

$$K_i = \frac{y_i}{x_i} \quad (5-1)$$

where

K_i = equilibrium ratio of component i

y_i = mole fraction of component i in the gas phase

x_i = mole fraction of component i in the liquid phase

At pressures below 100 psia, Raoult's and Dalton's laws for ideal solutions provide a simplified means of predicting equilibrium ratios. Raoult's law states that the partial pressure, p_i , of a component in a multicomponent system is the product of its mole fraction in the liquid phase, x_i , and the vapor pressure of the component, p_{vi} :

$$p_i = x_i p_{vi} \quad (5-2)$$

where

p_i = partial pressure of a component i , psia

p_{vi} = vapor pressure of component i , psia

x_i = mole fraction of component i in the liquid phase

Dalton's law states that the partial pressure of a component is the product of its mole fraction in the gas phase, y_i , and the total pressure of the system, p :

$$p_i = y_i p \quad (5-3)$$

where p = total system pressure, psia.

At equilibrium and in accordance with the previously cited laws, the partial pressure exerted by a component in the gas phase must be equal to the partial pressure exerted by the same component in the liquid phase. Therefore, equating the equations describing the two laws yields the following:

$$x_i p_{vi} = y_i p$$

Rearranging the preceding relationship and introducing the concept of the equilibrium ratio gives

$$\frac{y_i}{x_i} = \frac{p_{vi}}{p} = K_i \quad (5-4)$$

Equation (5-4) shows that, for ideal solutions and regardless of the overall composition of the hydrocarbon mixture, the equilibrium ratio is a function of only the system pressure, p , and the temperature, T , since the vapor pressure of a component is only a function of temperature (see Figure 1-3, reproduced as Figure 5-1 for convenience).

Taking the logarithm of both sides of equation (5-4) and rearranging gives

$$\log(K_i) = \log(p_{vi}) - \log(p)$$

This relationship indicates that under constant temperature, T (implying a constant p_{vi}), the equilibrium ratio for a component is a linear function of pressure with a slope of -1 when plotted on a log-log scale.

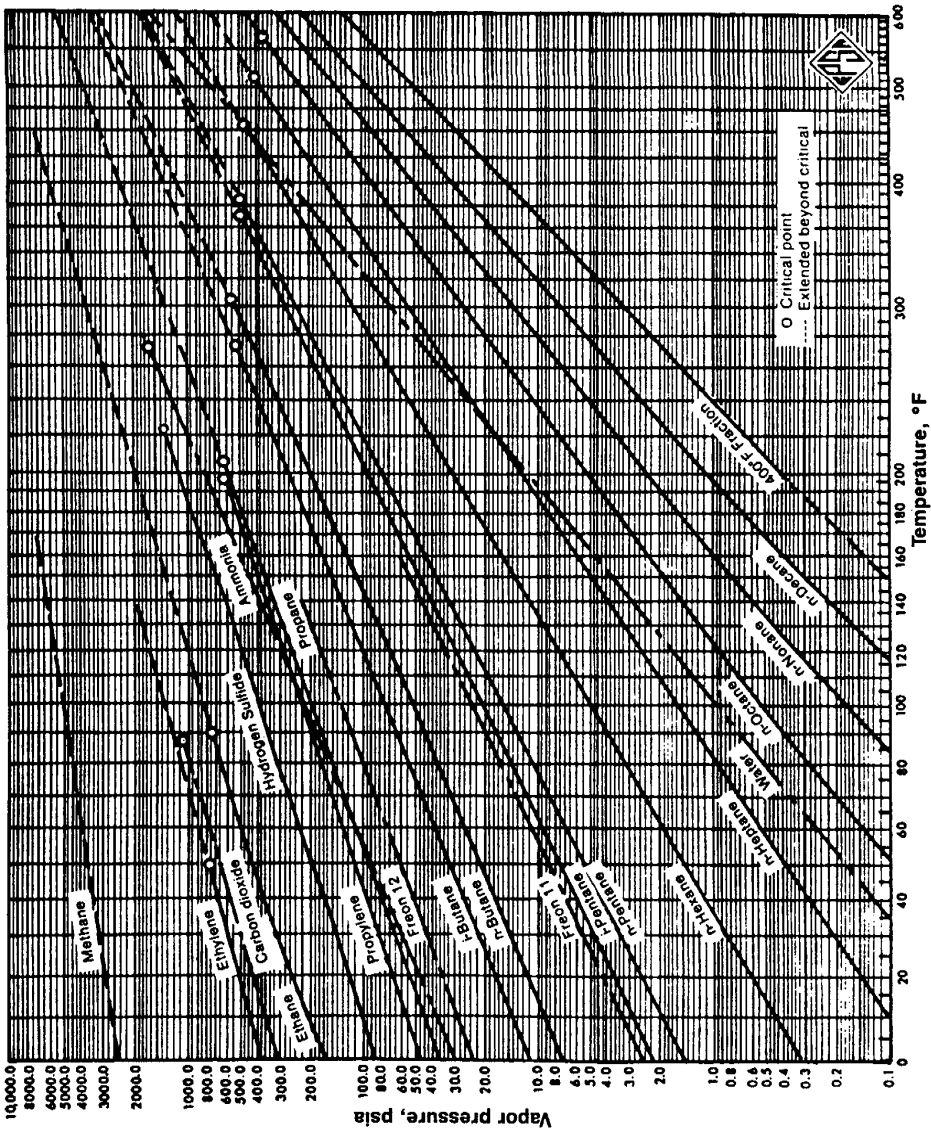


FIGURE 5-1 Vapor pressure chart for hydrocarbon components.
Source: GPSA Engineering Data Book, 10th ed. Tulsa, OK: Gas Processors Suppliers Association, 1987. Courtesy of the Gas Processors Suppliers Association.

It is appropriate at this stage to introduce and define the following nomenclatures:

z_i = mole fraction of component i in the entire hydrocarbon mixture

n = total number of moles of the hydrocarbon mixture, lb-mole

n_L = total number of moles in the liquid phase

n_v = total number of moles in the vapor (gas) phase

By definition,

$$n = n_L + n_v \quad (5-5)$$

Equation (5-5) indicates that the total number of moles in the system is equal to the total number of moles in the liquid phase plus the total number of moles in the vapor phase. A material balance on the i th component results in

$$z_i n = x_i n_L + y_i n_v \quad (5-6)$$

where

$z_i n$ = total number of moles of component i in the system

$x_i n_L$ = total number of moles of component i in the liquid phase

$y_i n_v$ = total number of moles of component i in the vapor phase

Also by the definition of the total mole fraction in a hydrocarbon system, we may write

$$\sum_i z_i = 1 \quad (5-7)$$

$$\sum_i x_i = 1 \quad (5-8)$$

$$\sum_i y_i = 1 \quad (5-9)$$

It is convenient to perform all the phase-equilibria calculations on the basis of 1 mole of the hydrocarbon mixture; that is, $n = 1$. That assumption reduces equations (5-5) and (5-6) to

$$n_L + n_v = 1 \quad (5-10)$$

$$x_i n_L + y_i n_v = z_i \quad (5-11)$$

Combining equations (5-4) and (5-11) to eliminate y_i from equation (5-11) gives

$$x_i n_L + (x_i K_i) n_v = z_i$$

Solving for x_i yields

$$x_i = \frac{z_i}{n_L + n_v K_i} \quad (5-12)$$

Equation (5-11) can also be solved for y_i by combining it with equation (5-4) to eliminate x_i , which gives

$$y_i = \frac{z_i K_i}{n_L + n_v K_i} = x_i K_i \quad (5-13)$$

Combining equation (5-12) with (5-8) and equation (5-13) with (5-9) results in

$$\sum_i x_i = \sum_i \frac{z_i}{n_L + n_v K_i} = 1 \quad (5-14)$$

$$\sum_i y_i = \sum_i \frac{z_i K_i}{n_L + n_v K_i} = 1 \quad (5-15)$$

Since

$$\sum_i y_i - \sum_i x_i = 0$$

then

$$\sum_i \frac{z_i K_i}{n_L + n_v K_i} - \sum_i \frac{z_i}{n_L + n_v K_i} = 0$$

Rearranging gives

$$\sum_i \frac{z_i (K_i - 1)}{n_L + n_v K_i} = 0$$

Replacing n_L with $(1 - n_v)$ yields

$$f(n_v) = \sum_i \frac{z_i (K_i - 1)}{n_v (K_i - 1) + 1} = 0 \quad (5-16)$$

This set of equations provides the necessary phase relationships to perform volumetric and compositional calculations on a hydrocarbon system. These calculations are referred to as *flash calculations*, as described next.

Flash Calculations

Flash calculations are an integral part of all reservoir and process engineering calculations. They are required whenever it is desirable to know the amounts (in moles) of hydrocarbon liquid and gas coexisting in a reservoir or a vessel at a given pressure and temperature. These calculations also are performed to determine the composition of the existing hydrocarbon phases.

Given the overall composition of a hydrocarbon system at a specified pressure and temperature, flash calculations are performed to determine the moles of the gas phase, n_v , moles of the liquid phase, n_L , composition of the liquid phase, x_i , and composition of the gas phase, y_i . The computational steps for determining n_L , n_v , y_i , and x_i of a hydrocarbon mixture with a known overall composition of z_i and characterized by a set of equilibrium ratios, K_i , are summarized in the following steps.

Step 1 Calculate n_v . Equation (5-16) can be solved for the number of moles of the vapor phase n_v by using the Newton-Raphson iteration technique. In applying this iterative technique, do the following.

Assume any arbitrary value of n_v between 0 and 1, such as $n_v = 0.5$. A good assumed value may be calculated from the following relationship:

$$n_v = A/(A + B)$$

where

$$A = \sum_i [z_i (K_i - 1)]$$

$$B = \sum_i \left[z_i \left(\frac{1}{K_i} - 1 \right) \right]$$

These expressions could yield a starting value for n_v , *providing that the values of the equilibrium ratios are accurate*. Note that the assumed value of n_v must be between 0 and 1; that is, $0 < n_v < 1$.

Evaluate the function $f(n_v)$ as given by equation (5-16) using the assumed (old) value of n_v :

$$f(n_v) = \sum_i \frac{z_i(K_i - 1)}{n_v(K_i - 1) + 1}$$

If the absolute value of the function $f(n_v)$ is smaller than a preset tolerance, such as 10^{-6} , then the assumed value of n_v is the desired solution.

If the absolute value of $f(n_v)$ is greater than the preset tolerance, then a new value of $(n_v)_{\text{new}}$ is calculated from the following expression:

$$(n_v)_{\text{new}} = n_v - \frac{f(n_v)}{f'(n_v)}$$

with the derivative $f'(n_v)$ as given by

$$f'(n_v) = - \sum_i \left\{ \frac{z_i(K_i - 1)^2}{[n_v(K_i - 1) + 1]^2} \right\}$$

where $(n_v)_n$ is the new value of n_v to be used for the next iteration.

This procedure is repeated with the new value of n_v until convergence is achieved, that is, when

$$|f(n_v)| \leq \text{eps}$$

or

$$|(n_v)_{\text{new}} - (n_v)| \leq \text{eps}$$

in which eps is a selected tolerance, such as $\text{eps} = 10^{-6}$.

Step 2 Calculate n_L . The number of moles of the liquid phase can be calculated by applying equation (5-10) to give

$$n_L + n_v = 1$$

or

$$n_L = 1 - n_v$$

Step 3 Calculation of x_i . Calculate the composition of the liquid phase by applying equation (5-12):

$$x_i = \frac{z_i}{n_L + n_v K_i}$$

Step 4 Calculation of y_i . Determine the composition of the gas phase from equation (5-13):

$$y_i = \frac{z_i K_i}{n_L + n_v K_i} = x_i K_i$$

EXAMPLE 5-1

A hydrocarbon mixture with the following overall composition is flashed in a separator at 50 psia and 100°F:

COMPONENT	z_i
C ₃	0.20
i-C ₄	0.10
n-C ₄	0.10
i-C ₅	0.20
n-C ₅	0.20
C ₆	0.20

Assuming an ideal solution behavior, perform flash calculations.

SOLUTION

Step 1 Determine the vapor pressure p_{vi} from the Cox chart (Figure 5-1) and calculate the equilibrium ratios using equation (5-4). The results are shown below.

COMPONENT	z_i	p_{vi} at 100°F	$K_i = p_{vi}/50$
C ₃	0.20	190	3.80
i-C ₄	0.10	72.2	1.444
n-C ₄	0.10	51.6	1.032
i-C ₅	0.20	20.44	0.4088
n-C ₅	0.20	15.57	0.3114
C ₆	0.20	4.956	0.09912

Step 2 Solve equation (5-16) for n_v using the Newton-Raphson method:

$$(n_v)_n = n_v - \frac{f(n_v)}{f'(n_v)}$$

ITERATION	n_v	$f(n_v)$
0	0.08196579	3.073(10 ⁻²)
1	0.1079687	8.894(10 ⁻⁴)
2	0.1086363	7.60(10 ⁻⁷)
3	0.1086368	1.49(10 ⁻⁸)
4	0.1086368	0.0

to give $n_v = 0.1086368$.

Step 3 Solve for n_L :

$$n_L = 1 - n_v$$

$$n_L = 1 - 0.1086368 = 0.8913631$$

Step 4 Solve for x_i and y_i to yield

$$x_i = \frac{z_i}{n_L + n_v K_i}$$

$$y_i = x_i K_i$$

The component results are shown below.

COMPONENT	z_i	K_i	$x_i = z_i / (0.8914 + 0.1086 K_i)$	$y_i = x_i K_i$
C ₃	0.20	3.80	0.1534	0.5829
i-C ₄	0.10	1.444	0.0954	0.1378
n-C ₄	0.10	1.032	0.0997	0.1029
i-C ₅	0.20	0.4088	0.2137	0.0874
n-C ₅	0.20	0.3114	0.2162	0.0673
C ₆	0.20	0.09912	0.2216	0.0220

Note that, for a *binary system*, that is, a two-component system, flash calculations can be performed without restoring to the preceding iterative technique. Flash calculations can be performed by applying the following steps.

Step 1 Solve for the composition of the liquid phase, x_i . For a two-component system, equations (5–8) and (5–9) can be expanded as

$$\sum_i x_i = x_1 + x_2 = 1$$
$$\sum_i y_i = y_1 + y_2 = K_1 x_1 + K_2 x_2 = 1$$

Solving these expressions for the liquid composition, x_1 and x_2 , gives

$$x_1 = \frac{1 - K_2}{K_1 - K_2}$$

and

$$x_2 = 1 - x_1$$

where

- x_1 = mole fraction of the first component in the liquid phase
- x_2 = mole fraction of the second component in the liquid phase
- K_1 = equilibrium ratio of the first component
- K_2 = equilibrium ratio of the first component

Step 2 Solve for the composition of the gas phase, y_i . From the definition of the equilibrium ratio, calculate the composition of the liquid as follows:

$$y_1 = x_1 K_1$$
$$y_2 = x_2 K_2 = 1 - y_1.$$

Step 3 Solve for the number of moles of the vapor phase, n_v , and liquid phase, n_l . Arrange equation (5–12) to solve for n_v by using the mole fraction and K -value of one of the two components to give

$$n_v = \frac{z_1 - x_1}{x_1 (K_1 - 1)}$$

and

$$n_L = 1 - n_v$$

Exact results will be obtained if selecting the second component; that is,

$$n_v = \frac{z_2 - x_2}{x_2(K_2 - 1)}$$

and

$$n_L = 1 - n_v$$

where

z_1 = mole fraction of the first component in the binary system

x_1 = mole fraction of the first component in the liquid phase

z_2 = mole fraction of the second component in the binary system

x_2 = mole fraction of the second component in the liquid phase

K_1 = equilibrium ratio of the first component

K_2 = equilibrium ratio of the second component

The equilibrium ratios, which indicate the partitioning of each component between the liquid phase and gas phases, as calculated by equation (5-4) in terms of vapor pressure and system pressure, proved inadequate. The basic assumptions behind equation (5-4) are that:

- The vapor phase is an ideal gas as described by Dalton's law.
- The liquid phase is an ideal solution as described by Raoult's law.

The combination of assumptions is unrealistic and results in inaccurate predictions of equilibrium ratios at high pressures.

Equilibrium Ratios for Real Solutions

For a real solution, the equilibrium ratios are no longer a function of the pressure and temperature alone but also the composition of the hydrocarbon mixture. This observation can be stated mathematically as

$$K_i = K(p, T, z_i)$$

Numerous methods have been proposed for predicting the equilibrium ratios of hydrocarbon mixtures. These correlations range from a simple mathematical expression to a complicated expression containing several compositional dependent variables. The following methods are presented: Wilson's correlation, Standing's correlation, the convergence pressure method, and Whitson and Torp's correlation.

Wilson's Correlation

Wilson (1968) proposed a simplified thermodynamic expression for estimating K -values. The proposed expression has the following form:

$$K_i = \frac{p_{ci}}{p} \exp \left[5.37(1 + \omega_i) \left(1 - \frac{T_{ci}}{T} \right) \right] \quad (5-17)$$

where

p_{ci} = critical pressure of component i , psia

p = system pressure, psia

T_{ci} = critical temperature of component i , °R

T = system temperature, °R

This relationship generates reasonable values for the equilibrium ratio when applied at low pressures.

Standing's Correlation

Hoffmann, Crump, and Hocott (1953), Brinkman and Sicking (1960), Kehn (1964), and Dykstra and Mueller (1965) suggested that any pure hydrocarbon or nonhydrocarbon component could be uniquely characterized by combining its boiling point temperature, critical temperature, and critical pressure into a characterization parameter, which is defined by the following expression:

$$F_i = b_i [1/T_{bi} - 1/T] \quad (5-18)$$

with

$$b_i = \frac{\log(p_{ci}/14.7)}{[1/T_{bi} - 1/T_{ci}]} \quad (5-19)$$

where F_i = component characterization factor and T_{bi} = *normal* boiling point of component i , °R.

Standing (1979) derived a set of equations that fit the equilibrium ratio data of Katz and Hachmuth (1937) at pressures less than 1000 psia and temperatures below 200°F, which are basically appropriate for surface-separator conditions. The proposed form of the correlation is based on an observation that plots of $\log(K_i p)$ versus F_i at a given pressure often form straight lines with a slope of c and intercept of a . The basic equation of the straight-line relationship is given by

$$\log(K_i p) = a + cF_i$$

Solving for the equilibrium ratio, K_p , gives

$$K_i = \frac{1}{p} 10^{(a+cF_i)} \quad (5-20)$$

where the coefficients a and c in the relationship are the intercept and the slope of the line, respectively.

From six isobar plots of $\log(K_i p)$ versus F_i for 18 sets of equilibrium ratio values, Standing correlated the coefficients a and c with the pressure, to give

$$a = 1.2 + 0.00045p + 15(10^{-8})p^2 \quad (5-21)$$

$$c = 0.89 - 0.00017p - 3.5(10^{-8})p^2 \quad (5-22)$$

Standing pointed out that the predicted values of the equilibrium ratios of N_2 , CO_2 , H_2S , and C_1 through C_6 can be improved considerably by changing the correlating parameter, b_p , and the boiling point of these components. The author proposed the following modified values:

COMPONENT	b_i	T_{bi} , °R
N_2	470	109
CO_2	652	194

COMPONENT	b_i	$T_{b_i}, ^\circ\text{R}$
H ₂ S	1136	331
C ₁	300	94
C ₂	1145	303
C ₃	1799	416
i-C ₄	2037	471
n-C ₄	2153	491
i-C ₅	2368	542
n-C ₅	2480	557
C ₆	2738	610
n-C ₆	2780	616
n-C ₇	3068	616
n-C ₈	3335	718
n-C ₉	3590	763
n-C ₁₀	3828	805

When making flash calculations, the question of the equilibrium ratio to use for the lumped plus fraction always arises. One rule of thumb proposed by Katz and Hachmuth (1937) is that the K -value for C_{7+} can be taken as 15% of the K of C_7 , or

$$K_{C_{7+}} = 0.15K_{C_7}$$

Standing offered an alternative approach for determining the K -value of the heptanes and heavier fractions. By imposing experimental equilibrium ratio values for C_{7+} on equation (5-20), Standing calculated the corresponding characterization factors, F_p , for the plus fraction. The calculated F_i values were used to specify the pure normal paraffin hydrocarbon having the K -value of the C_{7+} fraction.

Standing suggested the following computational steps for determining the parameters b and T_b of the *heptanes-plus fraction*.

Step 1 Determine, from the following relationship, the number of carbon atoms, n , of the normal paraffin hydrocarbon having the K -value of the C_{7+} fraction:

$$n = 7.30 + 0.0075(T - 460) + 0.0016p \quad (5-23)$$

Step 2 Calculate the correlating parameter, b , and the boiling point, T_b , from the following expression:

$$b = 1013 + 324n - 4.256n^2 \quad (5-24)$$

$$T_b = 301 + 59.85n - 0.971n^2 \quad (5-25)$$

The calculated values can then be used in equation (5-18) to evaluate F_i for the heptanes-plus fraction, that is, $F_{C_{7+}}$. It is interesting to note that numerous experimental phase-equilibria data suggest that the equilibrium ratio for carbon dioxide can be closely approximated by the following relationship:

$$K_{\text{CO}_2} = \sqrt{K_{C_1} K_{C_2}}$$

where

K_{CO_2} = equilibrium ratio of CO_2 at system pressure p and temperature T
 K_{C_1} = equilibrium ratio of methane at p and T
 K_{C_2} = equilibrium ratio of ethane at p and T

Note that the methane and the plus fraction are perhaps the most important two components in a hydrocarbon mixture, due to their high concentration in the system. The C_1 and C_{7+} fractions essentially are the two components that when defined, can categorize the hydrocarbon system. These two components in particular must be well defined, and their K -values must be accurately estimated. When the system pressure is below 1000 psia, the following correlation for determining the K -values for C_1 can be used:

$$K_{\text{C}_1} = \frac{\exp\left(A - \frac{B}{T}\right)}{p}$$

with

$$A = 2.0(10^{-7})p^2 - 0.0005p + 9.4633$$
$$B = 0.0001p^2 - 0.456p + 855.89$$

where P = pressure, psi, and T = temperature, °R.

It is possible to correlate the equilibrium ratios of C_2 through C_6 with that of C_1 at low pressures by the following relationship:

$$K_i = \frac{K_{\text{C}_1} F_i}{\ln(p K_{\text{C}_1})}$$

with the parameter F_i as defined by

$$F_i = a_i T - b_i$$

The temperature, T , is in °R. Values of the coefficients a_i and b_i for C_2 through C_6 follow:

COMPONENT	a_i	b_i
C_2	0.0057	1.3166
C_3	0.0043	1.7111
i- C_4	0.0028	1.1818
n- C_4	0.0025	1.1267
i- C_5	0.0018	0.9004
n- C_5	0.0016	0.8237
C_6	0.0009	0.4919

This correlation provides a very rough estimate of the K -values for the listed components at pressures below 1000 psia.

EXAMPLE 5-2

A hydrocarbon mixture with the following composition is flashed at 1000 psia and 150°F.

COMPONENT	z_i
CO_2	0.009
N_2	0.003
C_1	0.535

COMPONENT	z_i
C ₂	0.115
C ₃	0.088
i-C ₄	0.023
n-C ₄	0.023
i-C ₅	0.015
n-C ₅	0.015
C ₆	0.015
C ₇₊	0.159

If the molecular weight and specific gravity of C₇₊ are 150.0 and 0.78, respectively, calculate the equilibrium ratios using Wilson's correlation then Standing's correlation.

SOLUTION USING WILSON'S CORRELATION

Step 1 Calculate the critical pressure, critical temperature, and acentric factor of C₇₊ by using the characterization method of Riazi and Daubert discussed in Chapter 2. Example 2-1 gives

$$T_c = 1139.4^\circ\text{R}$$

$$p_c = 320.3 \text{ psia}$$

$$\omega = 0.5067$$

Step 2 Apply equation (5-17) to get the results shown below.

Component	P_c , psia	T_c , °R	ω	$K_i = \frac{p_{ci}}{1000} \exp \left[5.37(1 + \omega_i) \left(1 - \frac{T_{ci}}{610} \right) \right]$
CO ₂	1071	547.9	0.225	2.0923
N ₂	493	227.6	0.040	16.343
C ₁	667.8	343.37	0.0104	7.155
C ₂	707.8	550.09	0.0986	1.263
C ₃	616.3	666.01	0.1524	0.349
i-C ₄	529.1	734.98	0.1848	0.144
n-C ₄	550.7	765.65	0.2010	0.106
i-C ₅	490.4	829.1	0.2223	0.046
n-C ₅	488.6	845.7	0.2539	0.036
C ₆	436.9	913.7	0.3007	0.013
C ₇₊	320.3	1139.4	0.5069	0.00029

SOLUTION USING STANDING'S CORRELATION

Step 1 Calculate the coefficients a and c from equations (5-21) and (5-22) to give

$$a = 1.2 + 0.00045p + 15(10^{-8})p^2$$

$$a = 1.2 + 0.00045(1000) + 15(10^{-8})(1000)^2 = 1.80$$

$$c = 0.89 - 0.00017p - 3.5(10^{-8})p^2$$

$$c = 0.89 - 0.00017(1000) - 3.5(10^{-8})(1000)^2 = 0.685$$

Step 2 Calculate the number of carbon atoms, n , from equation (5-23) to give

$$n = 7.30 + 0.0075(T - 460) + 0.0016p$$

$$n = 7.3 + 0.0075(150) + 0.0016(1000) = 10.025$$

Step 3 Determine the parameter b and the boiling point, T_b , for the hydrocarbon component with n carbon atoms by using equations (5–24) and (5–25). The calculated values of b and T_b , as given below, are assigned to the C_{7+} :

$$\begin{aligned} b &= 1013 + 324\,n - 4.256n^2 \\ b &= 1013 + 324(10.025) - 4.256(10.025)^2 = 3833.369 \\ T_b &= 301 + 59.85n - 0.971n^2 \\ T_b &= 301 + 59.85(10.025) - 0.971(10.025)^2 = 803.41^\circ\text{R} \end{aligned}$$

Step 4 Apply equation (5–20), to give the results shown below.

Component	b_i	T_{bi}	F_i , Equation (5–18)	K_i , Equation (5–20)
CO ₂	652	194	2.292	2.344
N ₂	470	109	3.541	16.811
C ₁	300	94	2.700	4.462
C ₂	1145	303	1.902	1.267
C ₃	1799	416	1.375	0.552
i-C ₄	2037	471	0.985	0.298
n-C ₄	2153	491	0.855	0.243
i-C ₅	2368	542	0.487	0.136
n-C ₅	2480	557	0.387	0.116
C ₆	2738	610	0	0.063
C ₇₊	3833.369	803.41	–1.513	0.0058

The Convergence Pressure Method

Early high-pressure phase-equilibria studies revealed that, when a hydrocarbon mixture of a fixed overall composition is held at a constant temperature as the pressure increases, the equilibrium values of all components converge toward a *common value of unity* at certain pressure. This pressure is termed the *convergence pressure*, p_k , of the hydrocarbon mixture. The convergence pressure essentially is used to correlate the effect of the composition on equilibrium ratios.

The concept of the convergence pressure can be better appreciated by examining Figure 5–2. The figure is a schematic diagram of a typical set of equilibrium ratios plotted versus pressure on log-log paper for a hydrocarbon mixture held at a constant temperature. The illustration shows a tendency of the equilibrium ratios to converge isothermally to a value of $K_i = 1$ for all components at a specific pressure, that is, convergence pressure. A different hydrocarbon mixture may exhibit a different convergence pressure.

The Natural Gas Processors Suppliers Association (NGPSA) correlated a considerable quantity of K -factor data as a function of temperature, pressure, component identity, and convergence pressure. These correlation charts, available through the NGPSA’s Engineering Data Book (1978), are considered to be the most extensive set of published equilibrium ratios for hydrocarbons. They include the K -values for a number of convergence pressures, specifically 800, 1000, 1500, 2000, 3000, 5000, and 10,000 psia. Equilibrium ratios for methane through decane and for a convergence pressure of 5000 psia are given in the Appendix of this book.

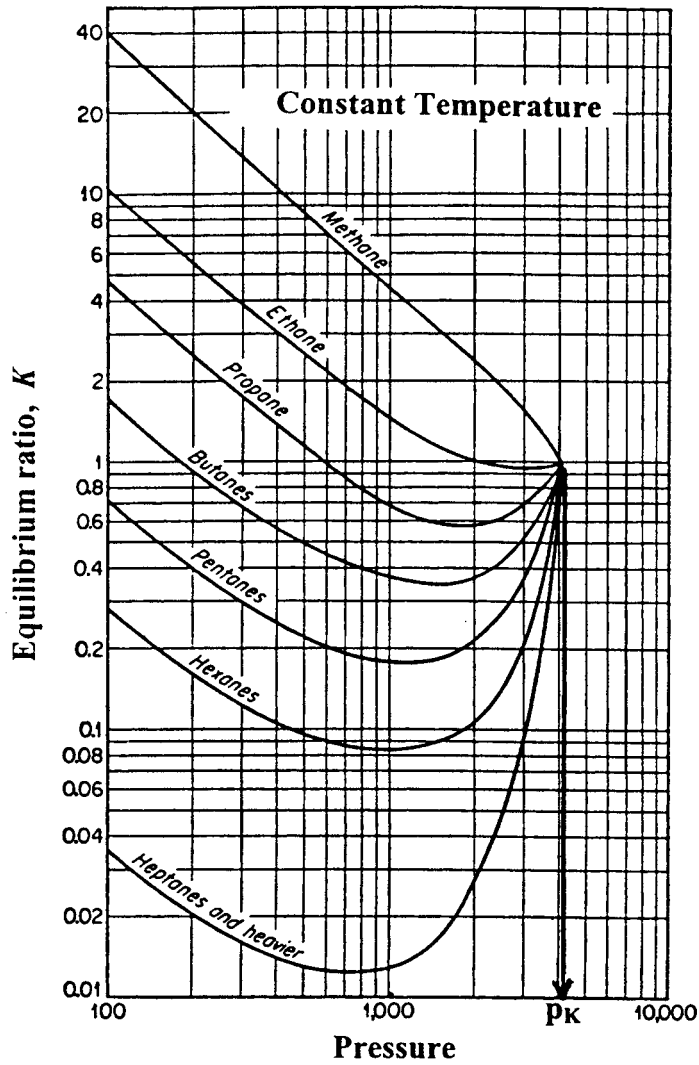


FIGURE 5-2 Equilibrium ratios for a hydrocarbon system.

Several investigators observed that, for hydrocarbon mixtures with convergence pressures of 4000 psia or greater, the values of the equilibrium ratio are essentially the same for hydrocarbon mixtures with system pressures less than 1000 psia. This observation led to the conclusion that the overall composition of the hydrocarbon mixture has little effect on equilibrium ratios when the system pressure is less than 1000 psia.

The problem with using the NGPSA equilibrium ratio graphical correlations is that the convergence pressure must be known before selecting the appropriate charts. The following three methods of determining the convergence pressure are commonly used: Hadden's method, Standing's method, and Rzasa's method. Brief discussions of these methods are presented next.

$$p_{pc} = \sum_{i=2} w_i^* p_{ci}$$

where

w_i^* = normalized weight fraction of component i

T_{pc} = pseudo-critical temperature, °R

p_{pc} = pseudo-critical pressure, psi

Step 8 Enter into Figure 5-3 the critical properties of the pseudo component and trace the critical locus of the binary consisting of the light component and the pseudo component.

Step 9 Read the new convergence pressure (ordinate) from the point at which the locus crosses the temperature of interest.

Step 10 If the calculated new convergence pressure is not reasonably close to the assumed value, repeat steps 2 through 9.

Note that, when the calculated new convergence pressure is between values for which charts are provided, interpolation between charts might be necessary. If the K -values do not change rapidly with the convergence pressure, then the set of charts nearest to the calculated p_k may be used.

Standing's Method

Standing (1977) suggested that the convergence pressure could be roughly correlated linearly with the molecular weight of the heptanes-plus fraction. Whitson and Torp (1981) expressed this relationship by the following equation:

$$p_k = 60M_{C_{7+}} - 4200 \quad (5-26)$$

where $M_{C_{7+}}$ is the molecular weight of the heptanes-plus fraction.

Rzasa's Method

Rzasa, Glass, and Opfell (1952) presented a simplified graphical correlation for predicting the convergence pressure of light hydrocarbon mixtures. They used the temperature and the product of the molecular weight and specific gravity of the heptane-plus fraction as correlating parameters. A graphical illustration of the proposed correlation is shown in Figure 5-4.

The graphical correlation is expressed mathematically by the following equation:

$$p_k = -2381.8542 + 46.341487[M\gamma]_{C_{7+}} + \sum_{i=1}^3 a_i \left[\frac{(M\gamma)_{C_{7+}}}{T - 460} \right]^i \quad (5-27)$$

where

$(M)_{C_{7+}}$ = molecular weight of C_{7+}

$(\gamma)_{C_{7+}}$ = specific gravity of C_{7+}

T = temperature, in °R

a_1 - a_3 = coefficients of the correlation with the following values:

$$a_1 = 6124.3049$$

$$a_2 = -2753.2538$$

$$a_3 = 415.42049$$

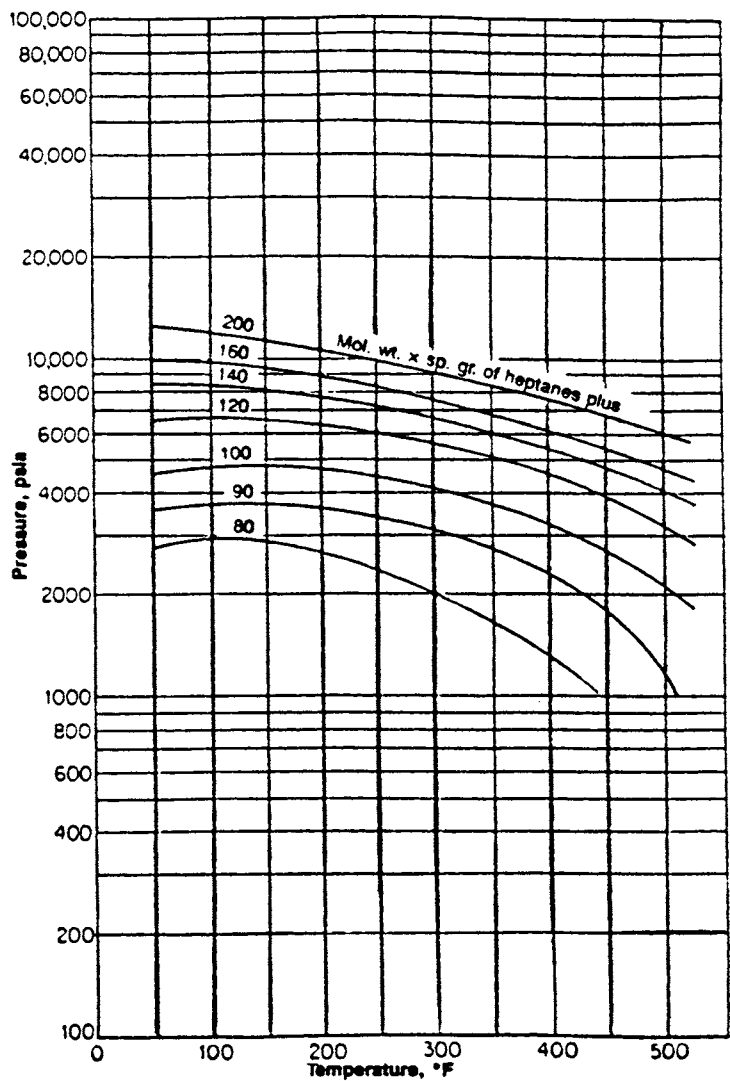


FIGURE 5-4 Rza et al.'s convergence pressure correlation.

Source: M. J. Rza et al. "Prediction of Critical Properties and Equilibrium Vaporization Constants for Complex Hydrocarbon Systems," *Chemical Engineering Program Symposium* Series 48, no. 2 (1952): 28. Courtesy of the American Institute of Chemical Engineers.

This mathematical expression can be used for determining the convergence pressure of hydrocarbon mixtures at temperatures in the range of 50°F to 300°F.

Whitson and Torp's Correlation

Whitson and Torp (1981) reformulated Wilson's equation (equation 5-17) to yield accurate results at higher pressures. Wilson's equation was modified by incorporating the convergence pressure into the correlation, to give:

$$K_i = \left(\frac{p_{ci}}{p_k}\right)^{A-1} \left(\frac{p_{ci}}{p}\right) \exp \left[5.37 A (1 + \omega_i) \left(1 - \frac{T_{ci}}{T} \right) \right] \tag{5-28}$$

with

$$A = 1 - \left(\frac{p}{p_k} \right)^{0.7}$$

where

- p = system pressure, psig
- p_k = convergence pressure, psig
- T = system temperature, °R
- ω_i = acentric factor of component i

EXAMPLE 5-3

Rework Example 5-2 and calculate the equilibrium ratios by using Whitson and Torp's method.

SOLUTION

Step 1 Determine the convergence pressure from equation (5-27) to give

$$p_k = 9473.89$$

Step 2 Calculate the coefficient A :

$$A = 1 - \left(\frac{1000}{9474} \right)^{0.7} = 0.793$$

Step 3 Calculate the equilibrium ratios from equation (5-28) to give the results shown below.

Component	p_c , psia	T_c , °R	ω	$K_i = \left(\frac{p_{ci}}{9474} \right)^{0.793-1} \frac{p_{ci}}{1000} \exp \left[5.37 A (1 + \omega_i) \left(1 - \frac{T_c}{610} \right) \right]$
CO ₂	1071	547.9	0.225	2.9
N ₂	493	227.6	0.040	14.6
C ₁	667.8	343.37	0.0104	7.6
C ₂	707.8	550.09	0.0986	2.1
C ₃	616.3	666.01	0.1524	0.7
i-C ₄	529.1	734.98	0.1848	0.42
n-C ₄	550.7	765.65	0.2010	0.332
i-C ₅	490.4	829.1	0.2223	0.1794
n-C ₅	488.6	845.7	0.2539	0.150
C ₆	436.9	913.7	0.3007	0.0719
C ₇₊	320.3	1139.4	0.5069	0.683(10 ⁻³)

Equilibrium Ratios for the Plus Fractions

The equilibrium ratios of the plus fractions often behave in a manner different from the other components of a system. This is because the plus fraction, in itself, is a mixture of components. Several techniques have been proposed for estimating the K -value of the plus fractions. Three methods are presented next: Campbell's method, Winn's method, and Katz's method.

Campbell's Method

Campbell (1976) proposed that the plot of the log of K_i versus T_{ci}^2 for each component is a linear relationship for any hydrocarbon system. Campbell suggested that, by drawing the best straight line through the points for propane through hexane components, the resulting line can be extrapolated to obtain the K -value of the plus fraction. He pointed out that the plot of $\log K_i$ versus $1/T_{bi}$ of each heavy fraction in the mixture also is a straight line. The line can be extrapolated to obtain the equilibrium ratio of the plus fraction from the reciprocal of its average boiling point.

Winn's Method

Winn (1954) proposed the following expression for determining the equilibrium ratio of heavy fractions with a boiling point above 210°F:

$$K_{C_+} = \frac{K_{C_7}}{(K_{C_2}/K_{C_7})^b} \quad (5-29)$$

where

K_{C_+} = value of the plus fraction

K_{C_+} = K -value of n-heptane at system pressure, temperature, and convergence pressure

K_{C_7} = K -value of ethane

b = volatility exponent

Winn correlated, graphically, the volatility component, b , of the heavy fraction, with the atmosphere boiling point, as shown in Figure 5-5.

This graphical correlation can be expressed mathematically by the following equation:

$$b = a_1 + a_2(T_b - 460) + a_3(T_b - 460)^2 + a_4(T_b - 460)^3 + a_5/(T - 460) \quad (5-30)$$

where

T_b = boiling point, °R

a_1 – a_5 = coefficients with the following values:

$$a_1 = 1.6744337$$

$$a_2 = -3.4563079 \times 10^{-3}$$

$$a_3 = 6.1764103 \times 10^{-6}$$

$$a_4 = 2.4406839 \times 10^{-9}$$

$$a_5 = 2.9289623 \times 10^2$$

Katz's Method

Katz et al. (1959) suggested that a factor of 0.15 times the equilibrium ratio for the heptane component gives a reasonably close approximation to the equilibrium ratio for heptanes and heavier. This suggestion is expressed mathematically by the following equation:

$$K_{C_{7+}} = 0.15K_{C_7} \quad (5-31)$$

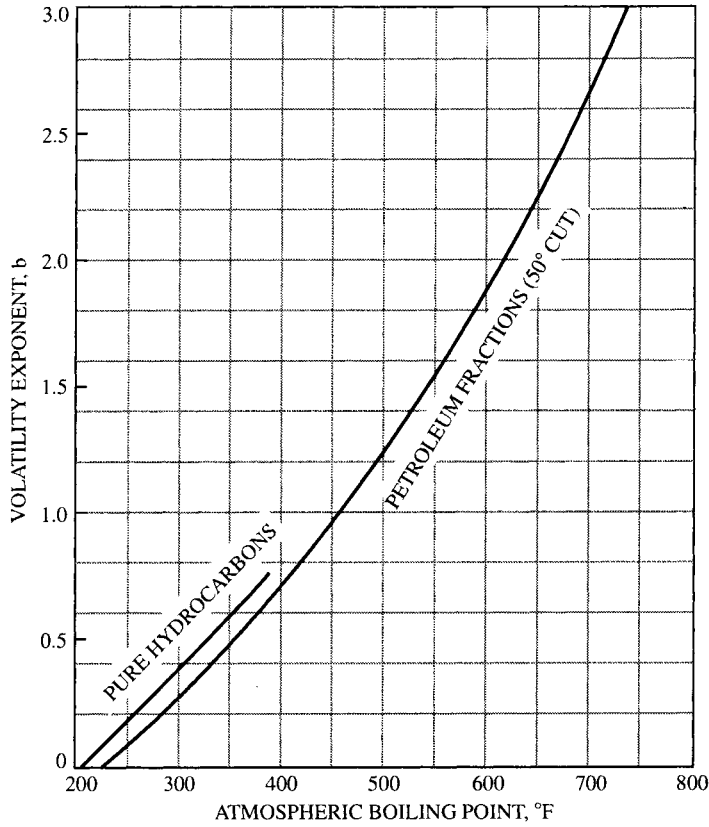


FIGURE 5-5 Volatility exponent.

Source: Courtesy of the Petroleum Refiner.

K-Values for Nonhydrocarbon Components

Lohrenze, Clark, and Francis (1963) developed the following set of correlations that express the K -values of H_2S , N_2 , and CO_2 as a function of pressure, temperature, and the convergence pressure, p_k .

For H_2S

$$\ln(K_{H_2S}) = \left(1 - \frac{p}{p_k}\right)^{0.8} \left[6.3992127 + \frac{1399.2204}{T} - \ln(p) \left(0.76885112 + \frac{18.215052}{T} \right) - \frac{1112446.2}{T^2} \right]$$

For N_2

$$\ln(K_{N_2}) = \left(1 - \frac{p}{p_k}\right)^{0.4} \left[11.294748 - \frac{1184.2409}{T} - 0.90459907 \ln(p) \right]$$

For CO_2

$$\ln(K_{CO_2}) = \left(1 - \frac{p}{p_k}\right)^{0.6} \left[7.0201913 - \frac{152.7291}{T} - \ln(p) \left(1.8896974 - \frac{1719.2956}{T} + \frac{644740.69}{T^2} \right) \right]$$

where

T = temperature, °R

p = pressure, psia

p_k = convergence pressure, psia

Vapor-Liquid Equilibrium Calculations

The vast amount of experimental and theoretical work performed on equilibrium ratio studies indicates their importance in solving phase equilibrium problems in reservoir and process engineering. The basic phase equilibrium calculations include the dew-point pressure, p_d , bubble-point pressure, p_b , and separator calculations. The use of the equilibrium ratio in performing these applications is discussed next.

Dew-Point Pressure

The dew-point pressure, p_d , of a hydrocarbon system is defined as the pressure at which an infinitesimal quantity of liquid is in equilibrium with a large quantity of gas. For a total of 1 lb-mole of a hydrocarbon mixture, that is, $n = 1$, the following conditions are applied at the dew-point pressure:

$$n_l \approx 0$$

$$n_v \approx 1$$

Under these conditions, the composition of the vapor phase, y_i , is equal to the overall composition, z_i . Applying these constraints to equation (5-14) yields

$$\sum_i \frac{z_i}{n_l + n_v K_i} = \sum_i \frac{z_i}{0 + (1.0) K_i} = \sum_i \frac{z_i}{K_i} = 1 \quad (5-32)$$

where z_i = total composition of the system under consideration.

The solution of equation (5-32) for the dew-point pressure, p_d , involves a trial-and-error process. The process is summarized in the following steps.

Step 1 Assume a trial value of p_d . A good starting value can be obtained by applying Wilson's equation (equation 5-17) for calculating K_i to equation (5-32), to give

$$\sum_i \frac{z_i}{K_i} = \sum_i \left\{ \frac{z_i}{\frac{p_{ci}}{p_d} \exp \left[5.37(1 + \omega_i) \left(1 - \frac{T_{ci}}{T} \right) \right]} \right\} = 1$$

Solving this expression for p_d gives an initial estimate of p_d as

$$p_d = \frac{1}{\sum_i \left\{ \frac{z_i}{p_{ci} \exp \left[5.37(1 + \omega_i) \left(1 - \frac{T_{ci}}{T} \right) \right]} \right\}} \quad (5-33)$$

Another approach is to treat the hydrocarbon mixture as an ideal system with the equilibrium ratio K_i as given by equation (5-4):

$$K_i = \frac{p_{vi}}{p}$$

Substituting the preceding expression into equation (5-29), gives

$$\sum_i \frac{z_i}{K_i} = \sum_i \frac{z_i}{(p_{vi}/p_d)} = 1.0$$

Solving this relationship for p_d yields an initial assumed value for p_d :

$$p_d = \frac{1}{\sum_{i=1} \left(\frac{z_i}{p_{vi}} \right)} \quad (5-34)$$

Step 2 Using the assumed dew-point pressure, calculate the equilibrium ratio, K_i , for each component at the system temperature.

Step 3 Calculate the summation of equation (5-32), that is, $\sum_i z_i/K_i$.

Step 4 If the sum is less than 1, repeat steps 2 and 3 at a higher initial value of pressure; conversely, if the sum is greater than 1, repeat the calculations with a lower initial value of p_d . The correct value of the dew-point pressure is obtained when the sum is equal to 1.

EXAMPLE 5-4

A natural gas reservoir at 250°F has the following composition:

COMPONENT	z_i
C ₁	0.80
C ₂	0.05
C ₃	0.04
i-C ₄	0.03
n-C ₄	0.02
i-C ₅	0.03
n-C ₅	0.02
C ₆	0.005
C ₇₊	0.005

If the molecular weight and specific gravity of C₇₊ are 140 and 0.8, calculate the dew-point pressure.

SOLUTION

Step 1 Calculate the convergence pressure of the mixture from Rzasa's correlation (equation 5-26) to give

$$p_k = 5000 \text{ psia}$$

Step 2 Determine an initial value for the dew-point pressure from equation (5-33), to give

$$P_d = 207 \text{ psia}$$

Step 3 Using the K -value curves in this book’s Appendix, solve for the dew-point pressure by applying the iterative procedure discussed previously and using equation (5–32), to give the results in the table below. The dew-point pressure, therefore, is 222 psia at 250°F.

Component	z_i	K_i at 207 psia	z_i/K_i	K_i at 300 psia	z_i/K_i	K_i at 222.3 psia	z_i/K_i
C ₁	0.78	19	0.0411	13	0.06	18	0.0433
C ₂	0.05	6	0.0083	4.4	0.0114	5.79	0.0086
C ₃	0.04	3	0.0133	2.2	0.0182	2.85	0.0140
i-C ₄	0.03	1.8	0.0167	1.35	0.0222	1.75	0.0171
n-C ₄	0.02	1.45	0.0138	1.14	0.0175	1.4	0.0143
i-C ₅	0.03	0.8	0.0375	0.64	0.0469	0.79	0.0380
n-C ₅	0.02	0.72	0.0278	0.55	0.0364	0.69	0.029
C ₆	0.005	0.35	0.0143	0.275	0.0182	0.335	0.0149
C ₇₊	0.02	0.255*	0.7843	0.02025*	0.9877	0.0243*	0.8230
Σ			0.9571		1.2185		1.0022

*Equation (5–29).

Bubble-Point Pressure

At the bubble-point p_b , the hydrocarbon system is essentially liquid, except for an infinitesimal amount of vapor. For a total of 1 lb-mole of the hydrocarbon mixture, the following conditions are applied at the bubble-point pressure:

$$n_l \approx 1$$
$$n_v \approx 0$$

Obviously, under these conditions, $x_i = z_i$. Applying these constraints to equation (5–15) yields

$$\sum_i \frac{z_i K_i}{n_l + n_v K_i} = \sum_i \frac{z_i K_i}{1 + (0)K_i} = \sum_i (z_i K_i) = 1 \tag{5-35}$$

Following the procedure outlined in the dew-point pressure determination, equation (5–35) is solved for the bubble-point pressure, p_b , by assuming various pressures and determining the pressure that produces K -values satisfying equation (5–35).

During the iterative process, if

$$\sum_i (z_i K_i) < 1, \text{ then the assumed pressure is high}$$
$$\sum_i (z_i K_i) > 1, \text{ then the assumed pressure is low}$$

Wilson’s equation can be used to give a good starting value for the iterative process:

$$\sum_i \left\{ z_i \frac{p_{ci}}{p_b} \exp \left[5.37(1 + \omega) \left(1 - \frac{T_{ci}}{T} \right) \right] \right\} = 1$$

Solving for the bubble-point pressure gives

$$p_b = \sum_i \left\{ z_i p_{ci} \exp \left[5.37(1 + \omega) \left(1 - \frac{T_{ci}}{T} \right) \right] \right\} \tag{5-36}$$

Assuming an ideal solution behavior, an initial guess for the bubble-point pressure can also be calculated by replacing the K_i in equation (5-35) with that of equation (5-4), to give

$$\sum_i \left[z_i \left(\frac{p_{vi}}{p_b} \right) \right] = 1$$

or

$$p_b = \sum_i (z_i p_{vi}) \quad (5-37)$$

EXAMPLE 5-5

A crude oil reservoir has a temperature of 200°F and a composition as follows. Calculate the bubble-point pressure of the oil.

COMPONENT	x_i
C ₁	0.80
C ₂	0.05
C ₃	0.04
i-C ₄	0.03
n-C ₄	0.02
i-C ₅	0.03
n-C ₅	0.02
C ₆	0.005
C ₇₊	0.005

For C₇₊,

$$\begin{aligned} (M)_{C_{7+}} &= 216.0 \\ (\gamma)_{C_{7+}} &= 0.8605 \\ (T_b)_{C_{7+}} &= 977^\circ\text{R} \end{aligned}$$

SOLUTION

Step 1 Calculate the convergence pressure of the system by using Standing's correlation, equation (5-26):

$$\begin{aligned} p_k &= 60M_{C_{7+}} - 4200 \\ p_k &= (60)(216) - 4200 = 8760 \text{ psia} \end{aligned}$$

Step 2 Calculate the critical pressure and temperature of the C₇₊ by the Riazi and Daubert equation, equation (2-4), to give

$$\begin{aligned} p_c &= 3.12281 \times 10^9 (977)^{-2.3125} (0.8605)^{2.3201} = 230.4 \text{ psi} \\ T_c &= 24.27870 (977)^{0.58848} (0.8605)^{0.3596} = 1279.8^\circ\text{R} \end{aligned}$$

Step 3 Calculate the acentric factor by employing the Edmister correlation (equation 2-21) to yield

$$\omega = \frac{3[\log(p_c / 14.70)]}{7[(T_c / T_b - 1)]} - 1 = 0.653$$

Step 4 Estimate the bubble-point pressure from equation (5–36) to give

$$p_b = \sum_i (z_i p_{vi}) = 3924 \text{ psia}$$

Step 5 Employing the iterative procedure outlined previously and using Whitson and Torp’s equilibrium ratio correlation gives the results in the table below. The calculated bubble-point pressure = 4330 psia.

Component	z_i	At 3924 psia		At 3950 psia		At 4329 psia	
		K_i	$z_i K_i$	K_i	$z_i K_i$	K_i	$z_i K_i$
C ₁	0.42	2.257	0.9479	2.242	0.9416	2.0430	0.8581
C ₂	0.05	1.241	0.06205	2.137	0.0619	1.1910	0.0596
C ₃	0.05	0.790	0.0395	0.7903	0.0395	0.793	0.0397
i-C ₄	0.03	0.5774	0.0173	0.5786	0.0174	0.5977	0.0179
n-C ₄	0.02	0.521	0.0104	0.5221	0.0104	0.5445	0.0109
i-C ₅	0.01	0.3884	0.0039	0.3902	0.0039	0.418	0.0042
n-C ₅	0.01	0.3575	0.0036	0.3593	0.0036	0.3878	0.0039
C ₆	0.01	0.2530	0.0025	0.2549	0.0025	0.2840	0.0028
C ₇₊	0.40	0.0227	0.0091	0.0232	0.00928	0.032	0.0138
Σ			1.09625		1.09008		1.0099

Separator Calculations

Produced reservoir fluids are complex mixtures of different physical characteristics. As a well stream flows from the high-temperature, high-pressure petroleum reservoir, it experiences pressure and temperature reductions. Gases evolve from the liquids and the well stream changes in character. The physical separation of these phases is by far the most common of all field-processing operations and one of the most critical. The manner in which the hydrocarbon phases are separated at the surface influences the stock-tank oil recovery. The principal means of surface separation of gas and oil is the conventional stage separation.

Stage separation is a process in which gaseous and liquid hydrocarbons are flashed (separated) into vapor and liquid phases by two or more separators. These separators usually are operated in a series at consecutively lower pressures. Each condition of pressure and temperature at which hydrocarbon phases are flashed is called a *stage of separation*. Examples of one- and two-stage separation processes are shown in Figure 5–6.

Traditionally, the stock tank is considered a separate stage of separation. Mechanically, there are two types of gas/oil separation: *differential* and *flash* or *equilibrium* separation. To explain the various separation processes, it is convenient to define the composition of a hydrocarbon mixture by three groups of components:

- The very volatile components, the “lights,” such as nitrogen, methane, and ethane.
- The components of intermediate volatility, that is, “intermediates,” such as propane through hexane.
- The components of less volatility, the “heavies,” such as heptane and heavier components.

In the differential separation, the liberated gas (which is composed mainly of lighter components) is removed from contact with the oil as the pressure on the oil is reduced. As pointed out by Clark (1960), when the gas is separated in this manner, the maximum amount of heavy and intermediate components remain in the liquid, and there is minimum shrinkage of the oil, and therefore, greater stock-tank oil recovery. This is due to the fact that the gas liberated earlier at higher pressures is not present at lower pressures to attract the intermediate and heavy components and pull them into the gas phase.

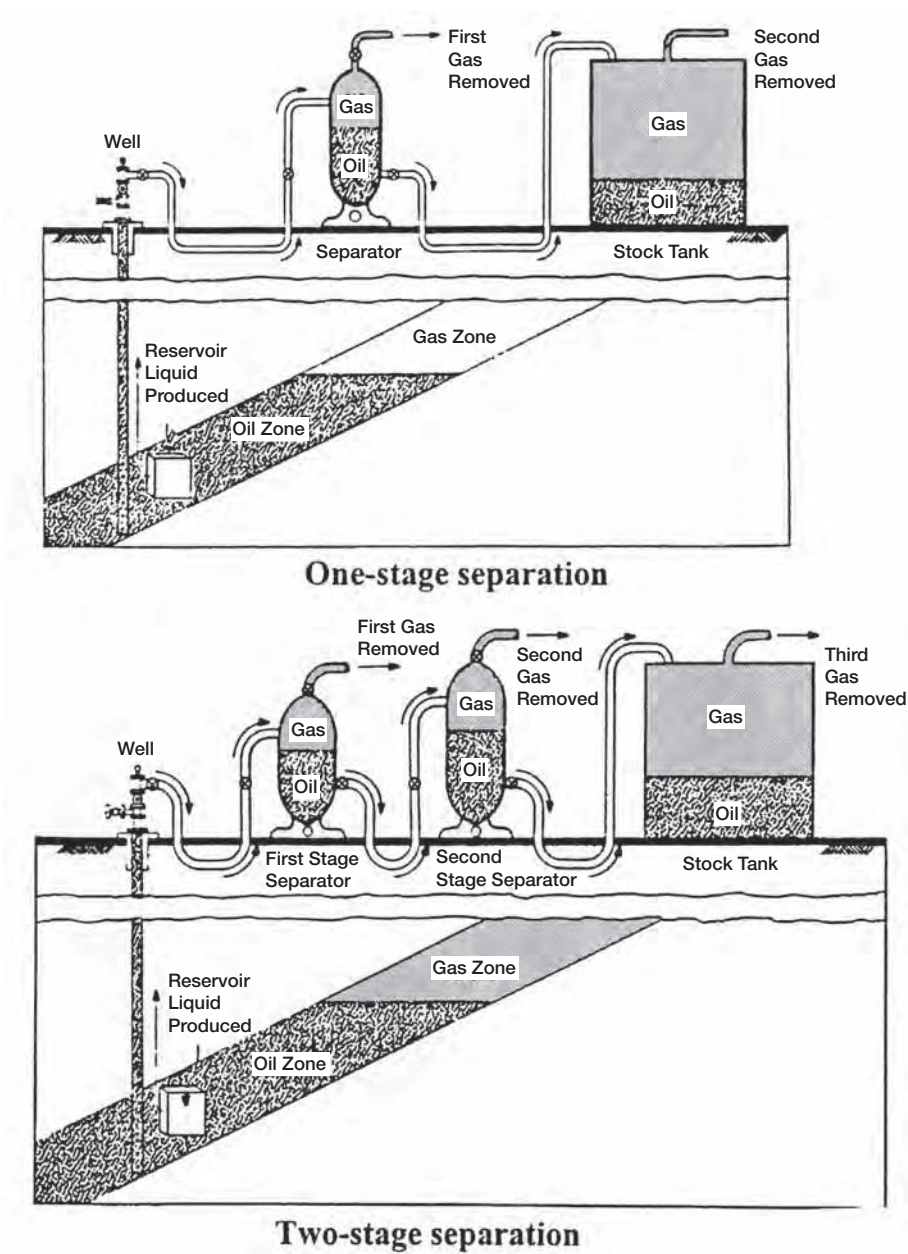


FIGURE 5-6 Schematic illustration of one- and two-stage separation processes.
Source: After N. Clark, *Elements of Petroleum Reservoirs*. Dallas: Society of Petroleum Engineers, 1960.

In the flash (equilibrium) separation, the liberated gas remains in contact with the oil until its instantaneous removal at the final separation pressure. A maximum proportion of intermediate and heavy components are attracted into the gas phase by this process, and this results in maximum oil shrinkage and, therefore, lower oil recovery.

In practice, the differential process is introduced first in field separation, when gas or liquid is removed from the primary separator. In each subsequent stage of separation, the liquid initially undergoes a flash liberation followed by a differential process as actual separation occurs. As the number of stages increases, the differential aspect of the overall separation becomes greater.

The purpose of stage separation then is to reduce the pressure on the produced oil in steps so that more stock-tank oil recovery results.

Separator calculations are basically performed to determine

- Optimum separation conditions: separator pressure and temperature.
- Composition of the separated gas and oil phases.
- Oil formation volume factor.
- Producing gas/oil ratio.
- API gravity of the stock-tank oil.

Note that, if the separator pressure is high, large amounts of light components remain in the liquid phase at the separator and are lost along with other valuable components to the gas phase at the stock tank. On the other hand, if the pressure is too low, large amounts of light components are separated from the liquid, and they attract substantial quantities of intermediate and heavier components. An intermediate pressure, called the optimum separator pressure, should be selected to maximize the oil volume accumulation in the stock tank. This optimum pressure also yields

- A maximum in the stock-tank API gravity.
- A minimum in the oil formation volume factor (i.e., less oil shrinkage).
- A minimum in the producing gas/oil ratio (gas solubility).

The concept of determining the optimum separator pressure by calculating the API gravity, B_o , and R_s is shown graphically in Figure 5–7.

The computational steps of the “separator calculations” are described next in conjunction with Figure 5–8, which schematically shows a bubble-point reservoir flowing into a surface separation unit consisting of n -stages operating at successively lower pressures.

Step 1 Calculate the volume of oil occupied by 1 lb-mole of the crude oil at the reservoir pressure and temperature. This volume, denoted V_o , is calculated by recalling and applying the equation that defines the number of moles, to give

$$n = \frac{m}{M_a} = \frac{\rho_o V_o}{M_a} = 1$$

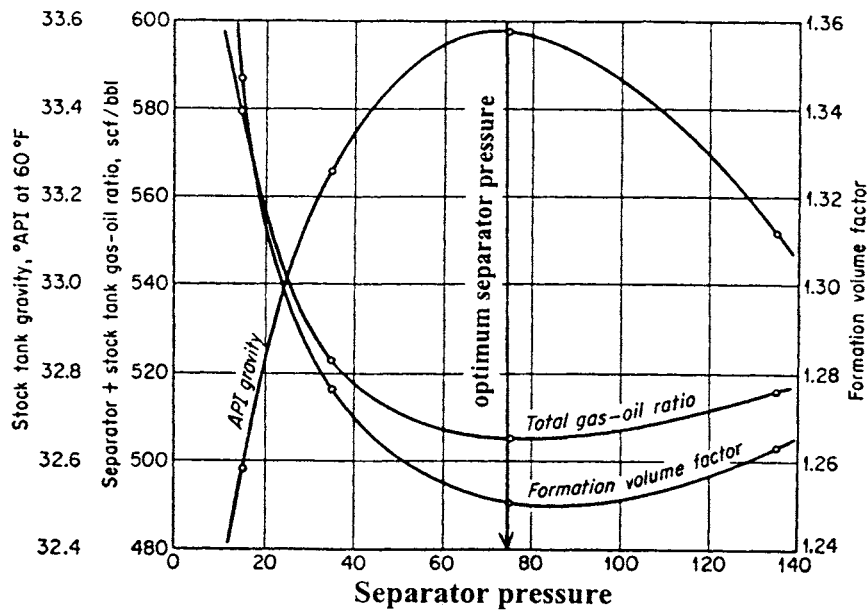


FIGURE 5-7 Effect of separator pressure on API, B_o , and GOR.
Source: After J. M. Amyx, D. M. Bass, and R. Whiting, *Petroleum Reservoir Engineering—Physical Properties*. New York: McGraw-Hill, 1960.

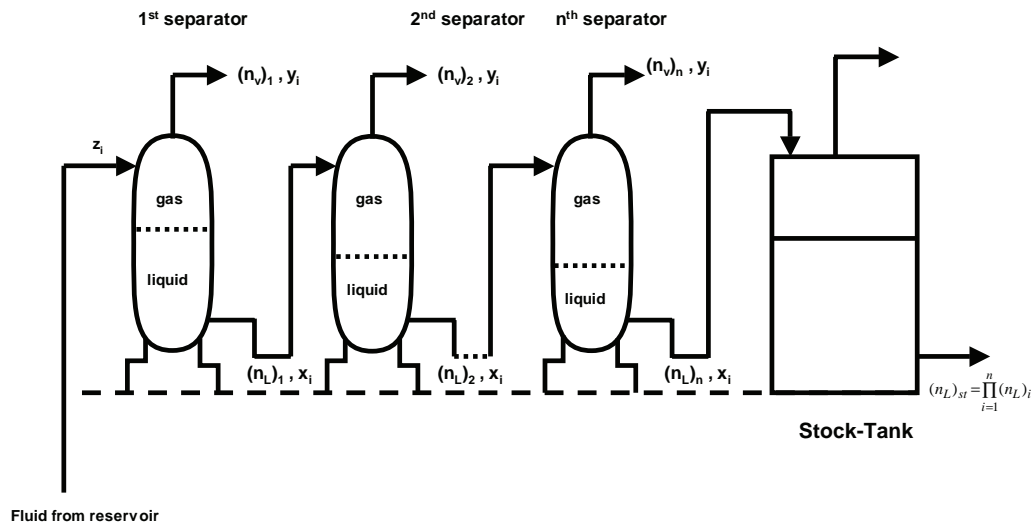


FIGURE 5-8 Schematic illustration of n separation stages.

Solving for the oil volume gives

$$V_o = \frac{M_a}{\rho_o} \quad (5-38)$$

where

m = total weight of 1 lb-mole of the crude oil, lb/mole

V_o = volume of 1 lb-mole of the crude oil at reservoir conditions, ft³/mole

M_a = apparent molecular weight

ρ_o = density of the reservoir oil, lb/ft³

Step 2 Given the composition of the feed stream, z_i , to the first separator and the operating conditions of the separator, that is, separator pressure and temperature, calculate the equilibrium ratios of the hydrocarbon mixture.

Step 3 Assuming a total of 1 mole of the feed entering the first separator and using the preceding calculated equilibrium ratios, perform flash calculations to obtain the compositions and quantities, in moles, of the gas and the liquid leaving the first separator. Designating these moles as $(n_L)_1$ and $(n_v)_1$, the actual number of moles of the gas and the liquid leaving the first separation stage are

$$\begin{aligned} [n_{v1}]_a &= (n)(n_v)_1 = (1)(n_v)_1 \\ [n_{L1}]_a &= (n)(n_L)_1 = (1)(n_L)_1 \end{aligned}$$

where $[n_{v1}]_a$ = actual number of moles of vapor leaving the first separator and $[n_{L1}]_a$ = actual number of moles of liquid leaving the first separator.

Step 4 Using the composition of the liquid leaving the first separator as the feed for the second separator, that is, $z_i = x_i$, calculate the equilibrium ratios of the hydrocarbon mixture at the prevailing pressure and temperature of the separator.

Step 5 Based on 1 mole of the feed, perform flash calculations to determine the compositions and quantities of the gas and liquid leaving the second separation stage. The actual number of moles of the two phases then is calculated from

$$\begin{aligned} [n_{v2}]_a &= [n_{L1}]_a(n_v)_2 = (1)(n_L)_1(n_v)_2 \\ [n_{L2}]_a &= [n_{L1}]_a(n_L)_2 = (1)(n_L)_1(n_L)_2 \end{aligned}$$

where

$$\begin{aligned} [n_{v2}]_a, [n_{L2}]_a &= \text{actual moles of gas and liquid leaving separator 2} \\ (n_v)_2, (n_L)_2 &= \text{moles of gas and liquid as determined from flash calculations} \end{aligned}$$

Step 6 The previously outlined procedure is repeated for each separation stage, including the stock-tank storage, and the calculated moles and compositions are recorded. The total number of moles of gas given off in all stages then are calculated as

$$(n_v)_t = \sum_{i=1}^n (n_{vi})_i = (n_v)_1 + (n_L)_1(n_v)_2 + (n_L)_1(n_L)_2(n_v)_3 + \dots + (n_L)_1 \dots (n_L)_{n-1}(n_v)_n$$

In a more compact form, this expression can be written as

$$(n_v)_t = (n_v)_1 + \sum_{i=2}^n \left[(n_v)_i \prod_{j=1}^{i-1} (n_L)_j \right] \quad (5-39)$$

where $(n_v)_t$ = total moles of gas given off in all stages, lb-mole/mole of feed, and n = number of separation stages.

The total moles of liquid remaining in the stock tank can also be calculated as

$$(n_L)_{st} = n_{L1} n_{L2} \cdots n_{Ln}$$

or

$$(n_L)_{st} = \prod_{i=1}^n (n_L)_i \quad (5-40)$$

where $(n_L)_{st}$ = number of moles of liquid remaining in the stock tank.

Step 7 Calculate the volume, in scf, of all the liberated solution gas from

$$V_g = 379.4(n_v)_t \quad (5-41)$$

where V_g = total volume of the liberated solution gas scf/mole of feed.

Step 8 Determine the volume of stock-tank oil occupied by $(n_L)_{st}$ moles of liquid from

$$(V_o)_{st} = \frac{(n_L)_{st} (M_a)_{st}}{(\rho_o)_{st}} \quad (5-42)$$

where

$(V_o)_{st}$ = volume of stock-tank oil, ft³/mole of feed

$(M_a)_{st}$ = apparent molecular weight of the stock-tank oil

$(\rho_o)_{st}$ = density of the stock-tank oil, lb/ft³

Step 9 Calculate the specific gravity and the API gravity of the stock-tank oil by applying the expression

$$\gamma_o = \frac{(\rho_o)_{st}}{62.4}$$

Step 10 Calculate the total gas/oil ratio (or gas solubility, R_g):

$$\begin{aligned} \text{GOR} &= \frac{V_g}{(V_o)_{st} / 5.615} = \frac{(5.615)(379.4)(n_v)_t}{(n_L)_{st} (M)_{st} (\rho_o)_{st}} \\ \text{GOR} &= \frac{2130.331(n_v)_t (\rho_o)_{st}}{(n_L)_{st} (M)_{st}} \end{aligned} \quad (5-43)$$

where GOR = gas/oil ratio, scf/STB.

Step 11 Calculate the oil formation volume factor from the relationship

$$B_o = \frac{V_o}{(V_o)_{st}}$$

Combining equations (5–38) and (5–42) with the preceding expression gives

$$B_o = \frac{M_a (\rho_o)_{st}}{\rho_o (n_L)_{st} (M_a)_{st}}$$

(5–44)

where

- B_o = oil formation volume factor, bbl/STB
- M_a = apparent molecular weight of the feed
- $(M_a)_{st}$ = apparent molecular weight of the stock-tank oil
- ρ_o = density of crude oil at reservoir conditions, lb/ft³

The separator pressure can be optimized by calculating the API gravity, GOR, and B_o in the manner just outlined at different assumed pressures. The optimum pressure corresponds to a maximum in the API gravity and a minimum in gas/oil ratio and oil formation volume factor.

EXAMPLE 5–6

A crude oil, with the composition as follows, exists at its bubble-point pressure of 1708.7 psia and a temperature of 131°F. The crude oil is flashed through two-stage and stock-tank separation facilities. The operating conditions of the three separators are:

SEPARATOR	PRESSURE, PSIA	TEMPERATURE, °F
1	400	72
2	350	72
Stock tank	14.7	60

The composition of the crude oil follows:

COMPONENT	z_i	M_i
CO ₂	0.0008	44.0
N ₂	0.0164	28.0
C ₁	0.2840	164.0
C ₂	0.0716	30.0
C ₃	0.1048	44.0
i-C ₄	0.0420	584.0
n-C ₄	0.0420	58.0
i-C ₅	0.0191	72.0
n-C ₅	0.1912	72.0
C ₆	0.0405	86.0
C ₇₊	0.3597	252

The molecular weight and specific gravity of C₇₊ are 252 and 0.8429. Calculate B_o , R_s , stock-tank density, and the API gravity of the hydrocarbon system.

SOLUTION

Step 1 Calculate the apparent molecular weight of the crude oil to give

$$M_a = \sum z_i M_i = 113.5102$$

Step 2 Calculate the density of the bubble-point crude oil by using the Standing and Katz correlations to yield

$$\rho_o = 44.794 \text{ lb/ft}^3$$

Step 3 Flash the original composition through the first separator by generating the equilibrium ratios using the Standing correlation (equation 5–20) to give the results in the following table, with $n_L = 0.7209$ and $n_v = 0.29791$.

Component	z_i	K_i	x_i	y_i	M_i
CO ₂	0.0008	3.509	0.0005	0.0018	44.0
N ₂	0.0164	39.90	0.0014	0.0552	28.0
C ₁	0.2840	8.850	0.089	0.7877	16.0
C ₂	0.0716	1.349	0.0652	0.0880	30.0
C ₃	0.1048	0.373	0.1270	0.0474	44.0
i-C ₄	0.0420	0.161	0.0548	0.0088	58.0
n-C ₄	0.0420	0.120	0.0557	0.0067	58.0
i-C ₅	0.0191	0.054	0.0259	0.0014	72.0
n-C ₅	0.0191	0.043	0.0261	0.0011	72.0
C ₆	0.0405	0.018	0.0558	0.0010	86.0
C ₇₊	0.3597	0.0021	0.4986	0.0009	252

Step 4 Use the calculated liquid composition as the feed for the second separator or flash the composition at the operating condition of the separator. The results are shown in the table below, with $n_L = 0.9851$ and $n_v = 0.0149$.

Component	z_i	K_i	x_i	y_i	M_i
CO ₂	0.0005	3.944	0.0005	0.0018	44.0
N ₂	0.0014	46.18	0.0008	0.0382	28.0
C ₁	0.089	10.06	0.0786	0.7877	16.0
C ₂	0.0652	1.499	0.0648	0.0971	30.0
C ₃	0.1270	0.4082	0.1282	0.0523	44.0
i-C ₄	0.0548	0.1744	0.0555	0.0097	58.0
n-C ₄	0.0557	0.1291	0.0564	0.0072	58.0
i-C ₅	0.0259	0.0581	0.0263	0.0015	72.0
n-C ₅	0.0261	0.0456	0.0264	0.0012	72.0
C ₆	0.0558	0.0194	0.0566	0.0011	86.0
C ₇₊	0.4986	0.00228	0.5061	0.0012	252

Step 5 Repeat the calculation for the stock-tank stage, to give the results in the following table, with $n_L = 0.6837$ and $n_v = 0.3163$.

Component	z_i	K_i	x_i	y_i
CO ₂	0.0005	81.14	0000	0.0014
N ₂	0.0008	1159	0000	0.026
C ₁	0.0784	229	0.0011	0.2455
C ₂	0.0648	27.47	0.0069	0.1898
C ₃	0.1282	6.411	0.0473	0.3030
i-C ₄	0.0555	2.518	0.0375	0.0945
n-C ₄	0.0564	1.805	0.0450	0.0812
i-C ₅	0.0263	0.7504	0.0286	0.0214
n-C ₅	0.0264	0.573	0.02306	0.0175
C ₆	0.0566	0.2238	0.0750	0.0168
C ₇₊	0.5061	0.03613	0.7281	0.0263

Step 6 Calculate the actual number of moles of the liquid phase at the stock-tank conditions from equation (5–40):

$$(n_L)_{st} = \prod_{i=1}^n (n_L)_i$$

$$(n_L)_{st} = (1)(0.7209)(0.9851)(0.6837) = 0.48554$$

Step 7 Calculate the total number of moles of the liberated gas from the entire surface separation system:

$$n_v = 1 - (n_L)_{st} = 1 - 0.48554 = 0.51446$$

Step 8 Calculate apparent molecular weight of the stock-tank oil from its composition, to give

$$(M_a)_{st} = \sum M_i x_i = 200.6$$

Step 9 Using the composition of the stock-tank oil, calculate the density of the stock-tank oil by using Standing's correlation, to give

$$(\rho_o)_{st} = 50.920$$

Step 10 Calculate the API gravity of the stock-tank oil from the specific gravity:

$$\gamma = \rho_o / 62.4 = 50.920 / 62.4 = 0.816 \text{ } 60^\circ / 60^\circ$$

$$\text{API} = (141.5 / \gamma) - 131.5 = (141.5 / 0.816) - 131.5 = 41.9$$

Step 11 Calculate the gas solubility from equation (5–43) to give

$$R_s = \frac{2130.331(n_v)_t(\rho_o)_{st}}{(n_L)_{st}(M)_{st}}$$

$$R_s = \frac{2130.331(0.51446)(50.92)}{0.48554(200.6)} = 573.0 \text{ scf/STB}$$

Step 12 Calculate B_o from equation (5–44) to give

$$B_o = \frac{M_a(\rho_o)_{st}}{\rho_o(n_L)_{st}(M_a)_{st}}$$

$$B_o = \frac{(113.5102)(50.92)}{(44.794)(0.48554)(200.6)} = 1.325 \text{ bbl/STB}$$

To optimize the operating pressure of the separator, these steps should be repeated several times under different assumed pressures and the results, in terms of API, B_o , and R_s , should be expressed graphically and used to determine the optimum pressure.

Equations of State

An equation of state (EOS) is an analytical expression relating the pressure, p , to the temperature, T , and the volume, V . A proper description of this PVT relationship for real hydrocarbon fluids is essential in determining the volumetric and phase behavior of petroleum reservoir fluids and predicting the performance of surface separation facilities; these can be described accurately by equations of state. In general, most equations of state require only the critical properties and acentric factor of individual components. The main advantage of using an EOS is that the same equation can be used to model the behavior of all phases, thereby assuring consistency when performing phase equilibria calculations.

The best known and the simplest example of an equation of state is the ideal gas equation, expressed mathematically by the expression

$$p = \frac{RT}{V} \quad (5-45)$$

where V = gas volume in ft^3 per 1 mole of gas, ft^3/mol .

This PVT relationship is used to describe the volumetric behavior only of real hydrocarbon gases at pressures close to the atmospheric pressure for which it was experimentally derived.

The extreme limitations of the applicability of equation (5-45) prompted numerous attempts to develop an equation of state suitable for describing the behavior of real fluids at extended ranges of pressures and temperatures.

A review of recent developments and advances in the field of empirical cubic equations of state are presented next, along with samples of their applications in petroleum engineering. Four equations of state are discussed here, those by van der Waals, Redlich-Kwong, Soave-Redlich-Kwong, and Peng-Robinson.

Van der Waals's Equation of State

In developing the ideal gas EOS, equation (5-45), two assumptions were made:

1. The volume of the gas molecules is insignificant compared to both the volume of the container and distance between the molecules.
2. There are no attractive or repulsive forces between the molecules or the walls of the container.

Van der Waals (1873) attempted to eliminate these two assumptions in developing an empirical equation of state for real gases. In his attempt to eliminate the first assumption, van der Waals pointed out that the gas molecules occupy a significant fraction of the volume at higher pressures and proposed that the volume of the molecules, denoted by the parameter b , be subtracted from the actual molar volume, V , in equation (5-45), to give

$$p = \frac{RT}{V - b}$$

where the parameter b is known as the covolume and considered to reflect the volume of molecules. The variable V represents the actual volume in ft^3 per 1 mole of gas.

To eliminate the second assumption, van der Waals subtracted a corrective term, denoted by a/V^2 , from this equation to account for the attractive forces between molecules. In a mathematical form, van der Waals proposed the following expression:

$$p = \frac{RT}{V - b} - \frac{a}{V^2} \quad (5-46)$$

where

p = system pressure, psia

T = system temperature, °R

R = gas constant, $10.73 \text{ psi-ft}^3/\text{lb-mole, °R}$

V = volume, ft^3/mole

a = “attraction” parameter

b = “repulsion” parameter

The two parameters, a and b , are constants characterizing the molecular properties of the individual components. The symbol a is considered a measure of the intermolecular attractive forces between the molecules. Equation (5-46) shows the following important characteristics:

1. At low pressures, the volume of the gas phase is large in comparison with the volume of the molecules. The parameter b becomes negligible in comparison with V and the attractive forces term, a/V^2 , becomes insignificant; therefore, the van der Waals equation reduces to the ideal gas equation (equation 5-45).
2. At high pressure, that is, $p \rightarrow \infty$, the volume, V , becomes very small and approaches the value b , which is the actual molecular volume, mathematically given by

$$\lim_{p \rightarrow \infty} V(p) = b$$

The van der Waals or any other equation of state can be expressed in a more generalized form as follows:

$$p = p_{\text{repulsion}} - p_{\text{attraction}} \quad (5-47)$$

where the repulsion pressure term, $p_{\text{repulsion}}$, is represented by the term $RT/(V - b)$, and the attraction pressure term, $p_{\text{attraction}}$, is described by a/V^2 .

In determining the values of the two constants, a and b , for any pure substance, van der Waals observed that the critical isotherm has a horizontal slope and an inflection point at the critical point, as shown in Figure 5-9. This observation can be expressed mathematically as follows:

$$\begin{aligned} \left[\frac{\partial p}{\partial V} \right]_{T_c, p_c} &= 0 \\ \left[\frac{\partial^2 p}{\partial V^2} \right]_{T_c, p_c} &= 0 \end{aligned} \quad (5-48)$$

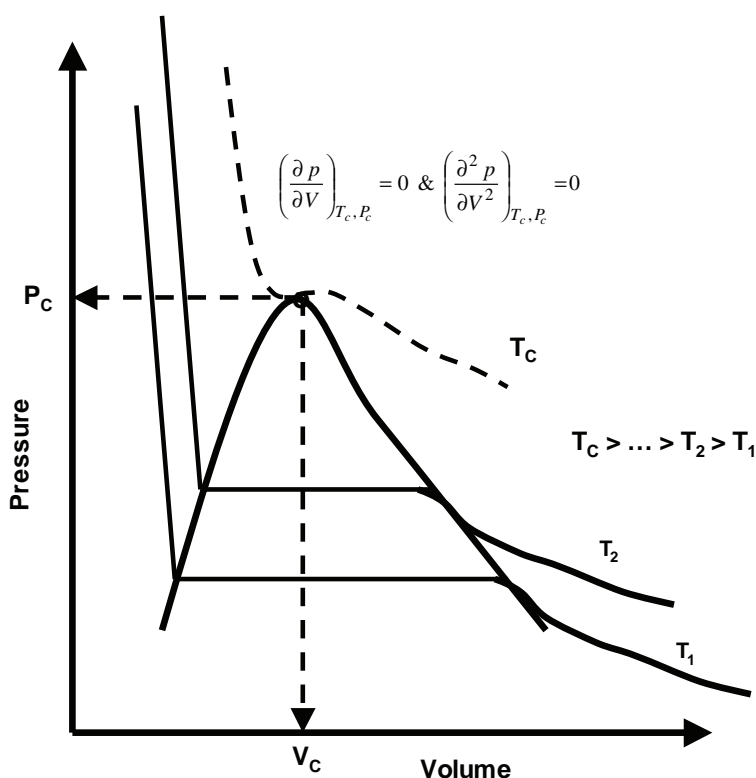


FIGURE 5-9 An idealized pressure/volume relationship for a pure component.

Differentiating equation (5-46) with respect to the volume at the critical point results in

$$\left[\frac{\partial p}{\partial V}\right]_{T_c, P_c} = \frac{-RT_c}{(V_c - b)^2} + \frac{2a}{V_c^3} = 0 \quad (5-49)$$

$$\left[\frac{\partial^2 p}{\partial V^2}\right]_{T_c, P_c} = \frac{2RT_c}{(V_c - b)^3} + \frac{6a}{V_c^4} = 0 \quad (5-50)$$

Solving equations (5-49) and (5-50) simultaneously for the parameters a and b gives

$$b = \left(\frac{1}{3}\right)V_c \quad (5-51)$$

$$a = \left(\frac{8}{9}\right)RT_c V_c \quad (5-52)$$

Equation (5-51) suggests that the volume of the molecules, b , is approximately 0.333 of the critical volume, V_c , of the substance. Experimental studies reveal that the covolume, b , is in the range 0.24–0.28 of the critical volume and pure component.

By applying equation (5-48) to the critical point (i.e., by setting $T = T_c$, $p = p_c$ and $V = V_c$) and combining with equations (5-51) and (5-52) yields

$$p_c V_c = (0.375)RT_c \quad (5-53)$$

Equation (5-53) shows that, regardless of the type of the substance, the van der Waals EOS produces a universal *critical gas compressibility factor*, Z_c , of 0.375. Experimental studies show that Z_c values for substances range between 0.23 and 0.31.

Equation (5-53) can be combined with equations (5-51) and (5-52) to give more convenient and traditional expressions for calculating the parameters a and b , to yield

$$a = \Omega_a \frac{R^2 T_c^2}{p_c} \quad (5-54)$$

$$b = \Omega_b \frac{RT_c}{p_c} \quad (5-55)$$

where

R = gas constant, 10.73 psia-ft³/lb-mole-°R

p_c = critical pressure, psia

T_c = critical temperature, °R

$\Omega_a = 0.421875$

$\Omega_b = 0.125$

Equation (5-46) can also be expressed in a cubic form in terms of the volume, V , as follows:

$$p = \frac{RT}{V-b} - \frac{a}{V^2}$$

Rearranging gives

$$V^3 - \left(b + \frac{RT}{p}\right)V^2 + \left(\frac{a}{p}\right)V - \left(\frac{ab}{p}\right) = 0 \quad (5-56)$$

Equation (5-56) usually is referred to as the van der Waals *two-parameter cubic equation of state*. The term *two-parameter* refers to parameters a and b . The term *cubic equation of state* implies an equation that, if expanded, would contain volume terms to the first, second, and third powers.

Perhaps the most significant features of equation (5-56) is that it describes the liquid-condensation phenomenon and the passage from the gas to the liquid phase as the gas is compressed. These important features of the van der Waals EOS are discussed next in conjunction with Figure 5-10.

Consider a pure substance with a p - V behavior as shown in Figure 5-10. Assume that the substance is kept at a constant temperature, T , below its critical temperature. At this temperature, equation (5-56) has three real roots (volumes) for each specified pressure, p . A typical solution of equation (5-56) at constant temperature, T , is shown graphically by the dashed isotherm, the constant temperature curve *DWEZB*, in Figure 5-10. The three values of V are the intersections B , E , and D on the horizontal line, corresponding to a fixed value of the pressure. This dashed calculated line (*DWEZB*) then appears to give a continuous transition from the gaseous phase to the liquid phase, but in reality, the transition is abrupt and discontinuous, with both liquid and vapor existing along the straight horizontal line *DB*. Examining the graphical solution of equation (5-56) shows that the largest root (volume), indicated by point D , corresponds to the volume of the saturated

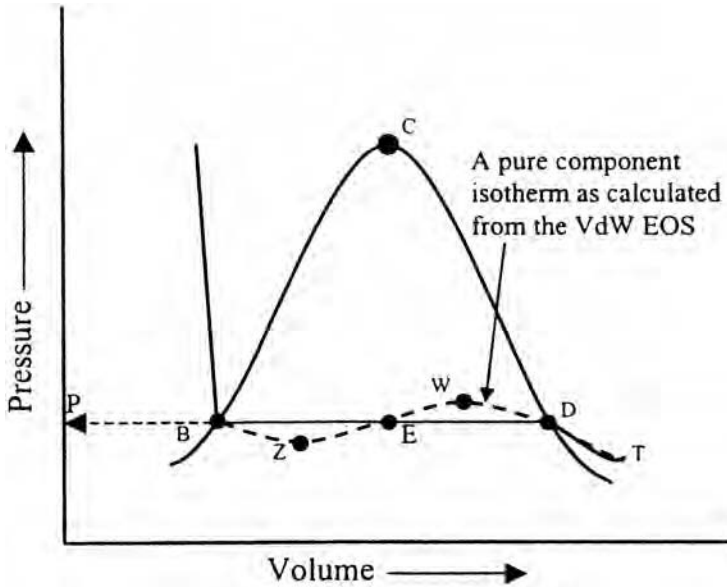


FIGURE 5-10 Pressure/volume diagram for a pure component.

vapor, while the smallest positive volume, indicated by point *B*, corresponds to the volume of the saturated liquid. The third root, point *E*, has no physical meaning. Note that these values become identical as the temperature approaches the critical temperature, T_c , of the substance.

Equation (5-56) can be expressed in a more practical form in terms of the compressibility factor, Z . Replacing the molar volume, V , in equation (5-56) with ZRT/p gives

$$V^3 - \left(b + \frac{RT}{p}\right)V^2 + \left(\frac{a}{p}\right)V - \left(\frac{ab}{p}\right) = 0$$

$$V^3 - \left(b + \frac{RT}{p}\right)\left(\frac{ZRT}{p}\right)^2 + \left(\frac{a}{p}\right)\left(\frac{ZRT}{p}\right) - \left(\frac{ab}{p}\right) = 0$$

or

$$Z^3 - (1 + B)Z^2 + AZ - AB = 0 \quad (5-57)$$

where

$$A = \frac{ap}{R^2T^2} \quad (5-58)$$

$$B = \frac{bp}{RT} \quad (5-59)$$

Z = compressibility factor

p = system pressure, psia

T = system temperature, °R

Equation (5-57) yields one real root* in the one-phase region and three real roots in the two-phase region (where system pressure equals the vapor pressure of the substance). In the two-phase region, the *largest positive root* corresponds to the compressibility factor of the *vapor phase*, Z^v , while the *smallest positive root* corresponds to that of the *liquid phase*, Z^L .

An important practical application of equation (5-57) is density calculations, as illustrated in the following example.

EXAMPLE 5-7

A pure propane is held in a closed container at 100°F. Both gas and liquid are present. Calculate, using the van der Waals EOS, the density of the gas and liquid phases.

SOLUTION

Step 1 Determine the vapor pressure, p_v , of the propane from the Cox chart. This is the only pressure at which two phases can exist at the specified temperature:

$$p_v = 185 \text{ psi}$$

Step 2 Calculate parameters a and b from equations (5-54) and (5-55), respectively:

$$a = \Omega_a \frac{R^2 T_c^2}{p_c} = 0.421875 \frac{(10.73)^2 (666)^2}{616.3} = 34,957.4$$

and

$$b = \Omega_b \frac{RT_c}{p_c} = 0.125 \frac{10.73(666)}{616.3} = 1.4494$$

Step 3 Compute the coefficients A and B by applying equations (5-58) and (5-59), respectively:

$$A = \frac{ap}{R^2 T^2} = \frac{(34,957.4)(185)}{(10.73)^2 (560)^2} = 0.179122$$

$$B = \frac{bp}{RT} = \frac{(1.4494)(185)}{(10.73)(560)} = 0.044625$$

Step 4 Substitute the values of A and B into equation (5-57), to give

$$Z^3 - (1 + B)Z^2 + AZ - AB = 0$$

$$Z^3 - 1.044625Z^2 + 0.179122Z - 0.007993 = 0$$

Step 5 Solve the above third-degree polynomial by extracting the *largest* and *smallest* roots of the polynomial using the appropriate direct or iterative method, to give

$$Z^v = 0.72365$$

$$Z^L = 0.07534$$

Step 6 Solve for the density of the gas and liquid phases using equation (2-17):

$$\rho_g = \frac{pM}{Z^v RT} = \frac{(185)(44.0)}{(0.72365)(10.73)(560)} = 1.87 \text{ lb/ft}^3$$

*In some super critical regions, equation (5-57) can yield three real roots for Z . From the three real roots, the largest root is the value of the compressibility with physical meaning.

and

$$\rho_L = \frac{pM}{Z^L RT} = \frac{(185)(44)}{(0.07534)(10.73)(560)} = 17.98 \text{ lb/ft}^3$$

The van der Waals equation of state, despite its simplicity, provides a correct description, at least qualitatively, of the PVT behavior of substances in the liquid and gaseous states. Yet, it is not accurate enough to be suitable for design purposes.

With the rapid development of computers, the equation-of-state approach for calculating physical properties and phase equilibria proved to be a powerful tool, and much energy was devoted to the development of new and accurate equations of state. These equations, many of them a modification of the van der Waals equation of state, range in complexity from simple expressions containing 2 or 3 parameters to complicated forms containing more than 50 parameters. Although the complexity of any equation of state presents no computational problem, most authors prefer to retain the simplicity found in the van der Waals cubic equation while improving its accuracy through modifications.

All equations of state generally are developed for pure fluids first and then extended to mixtures through the use of mixing rules. These mixing rules are simply means of calculating mixture parameters equivalent to those of pure substances.

Redlich-Kwong's Equation of State

Redlich and Kwong (1949) demonstrated that, by a simple adjustment of the van der Waals's attraction pressure term, a/V^2 , and explicitly including the system temperature, they could considerably improve the prediction of the volumetric and physical properties of the vapor phase. Redlich and Kwong replaced the attraction pressure term with a generalized temperature dependence term, as given in following form:

$$p = \frac{RT}{V-b} - \frac{a}{V(V+b)\sqrt{T}} \quad (5-60)$$

in which T is the system temperature, in °R.

Redlich and Kwong noted that, as the system pressure becomes very large, that is, $p \rightarrow \infty$, the molar volume, V , of the substance shrinks to about 26% of its critical volume, V_c , regardless of the system temperature. Accordingly, they constructed equation (5-60) to satisfy the following condition:

$$b = 0.26V_c \quad (5-61)$$

Imposing the critical point conditions (as expressed by equation 5-48) on equation (5-60) and solving the resulting two equations simultaneously, gives

$$\begin{aligned} \left[\frac{\partial p}{\partial V} \right]_{T_c, p_c} &= 0 \\ \left[\frac{\partial^2 p}{\partial V^2} \right]_{T_c, p_c} &= 0 \\ a &= \Omega_a \frac{R^2 T_c^{2.5}}{p_c} \end{aligned} \quad (5-62)$$

$$b = \Omega_b \frac{RT_c}{p_c} \quad (5-63)$$

where $\Omega_a = 0.42747$ and $\Omega_b = 0.08664$.

Equating equation (5-63) with (5-61) gives

$$0.26V_c = \Omega_b \frac{RT_c}{p_c}$$

or

$$p_c V_c = 0.333RT_c \quad (5-64)$$

Equation (5-64) shows that the Redlich-Kwong EOS produces a universal critical compressibility factor (Z_c) of 0.333 for all substances. As indicated earlier, the critical gas compressibility ranges from 0.23 to 0.31 for most of the substances.

Replacing the molar volume, V , in equation (5-60) with ZRT/p and rearranging gives

$$Z^3 - Z^2 + (A - B - B^2)Z - AB = 0 \quad (5-65)$$

where

$$A = \frac{ap}{R^2 T^{2.5}} \quad (5-66)$$

$$B = \frac{bp}{RT} \quad (5-67)$$

As in the van der Waals EOS, equation (5-65) yields one real root in the one-phase region (gas-phase region or liquid-phase region) and three real roots in the two-phase region. In the latter case, the *largest root* corresponds to the compressibility factor of the gas phase, Z^v , while the *smallest positive root* corresponds to that of the liquid, Z^L .

EXAMPLE 5-8

Rework Example 5-7 using the Redlich-Kwong equation of state.

SOLUTION

Step 1 Calculate the parameters a , b , A , and B .

$$a = \Omega_a \frac{R^2 T_c^{2.5}}{p_c} = 0.42747 \frac{(10.73)^2 (666)^{2.5}}{616.3} = 914,110.1$$

$$b = \Omega_b \frac{RT_c}{p_c} = 0.08664 \frac{(10.73)(666)}{616.3} = 1.0046$$

$$A = \frac{ap}{R^2 T^{2.5}} = \frac{(914,110.1)(185)}{(10.73)^2 (560)^{2.5}} = 0.197925$$

$$B = \frac{bp}{RT} = \frac{(1.0046)(185)}{(10.73)(560)} = 0.03093$$

Step 2 Substitute the parameters A and B into equation (5-65) and extract the largest and the smallest roots, to give

$$Z^3 - Z^2 + (A - B - B^2)Z - AB = 0$$

$$Z^3 - Z^2 + 0.1660384Z - 0.0061218 = 0$$

$$\text{Largest root: } Z^v = 0.802641$$

$$\text{Smallest root: } Z^L = 0.0527377$$

Step 3 Solve for the density of the liquid phase and gas phase:

$$\rho^L = \frac{pM}{Z^L RT} = \frac{(185)(44)}{(0.0527377)(10.73)(560)} = 25.7 \text{ lb/ft}^3$$

$$\rho^v = \frac{pM}{Z^v RT} = \frac{(185)(44)}{(0.802641)(10.73)(560)} = 1.688 \text{ lb/ft}^3$$

Redlich and Kwong extended the application of their equation to hydrocarbon liquid and gas mixtures by employing the following mixing rules:

$$a_m = \left[\sum_{i=1}^n x_i \sqrt{a_i} \right]^2 \quad (5-68)$$

$$b_m = \sum_{i=1}^n [x_i b_i] \quad (5-69)$$

where

n = number of components in the mixture

a_i = Redlich-Kwong a parameter for the i th component as given by equation (5-62)

b_i = Redlich-Kwong b parameter for the i th component as given by equation (5-63)

a_m = parameter a for mixture

b_m = parameter b for mixture

x_i = mole fraction of component i in the liquid phase

To calculate a_m and b_m for a hydrocarbon gas mixture with a composition of y_i , use equations (5-68) and (5-69) and replace x_i with y_i :

$$a_m = \left[\sum_{i=1}^n y_i \sqrt{a_i} \right]^2$$

$$b_m = \sum_{i=1}^n [y_i b_i]$$

Equation (5-65) gives the compressibility factor of the gas phase or the liquid with the coefficients A and B as defined by equations (5-66) and (5-67). The application of the Redlich and Kwong equation of state for hydrocarbon mixtures can be best illustrated through the following two examples.

EXAMPLE 5-9

Calculate the density of a crude oil with the composition at 4000 psia and 160°F given in the table below. Use the Redlich-Kwong EOS.

Component	x_i	M	p_c	T_c
C_1	0.45	16.043	666.4	343.33
C_2	0.05	30.070	706.5	549.92
C_3	0.05	44.097	616.0	666.06
n- C_4	0.03	58.123	527.9	765.62
n- C_5	0.01	72.150	488.6	845.8
C_6	0.01	84.00	453	923
C_{7+}	0.40	215	285	1287

SOLUTION

Step 1 Determine the parameters a_i and b_i for each component using equations (5–62) and (5–63):

$$a_i = 0.47274 \frac{R^2 T_c^{2.5}}{p_c}$$
$$b_i = 0.08664 \frac{RT_c}{p_c}$$

The results are shown in the table below.

Component	x_i	M	p_c	T_c	a_i	b_i
C ₁	0.45	16.043	666.4	343.33	161,044.3	0.4780514
C ₂	0.05	30.070	706.5	549.92	493,582.7	0.7225732
C ₃	0.05	44.097	616.0	666.06	914,314.8	1.004725
n-C ₄	0.03	58.123	527.9	765.62	1,449,929	1.292629
n-C ₅	0.01	72.150	488.6	845.8	2,095,431	1.609242
C ₆	0.01	84.00	453	923	2,845,191	1.945712
C ₇₊	0.40	215	285	1287	1.022348(10 ⁷)	4.191958

Step 2 Calculate the mixture parameters, a_m and b_m , from equations (5–68) and (5–69), to give

$$a_m = \left[\sum_{i=1}^n x_i \sqrt{a_i} \right]^2 = 2,591,967$$

and

$$b_m = \sum_{i=1}^n [x_i b_i] = 2.0526$$

Step 3 Compute the coefficients A and B by using equations (5–66) and (5–67), to produce

$$A = \frac{a_m p}{R^2 T^{2.5}} = \frac{2,591,967(4000)}{10.73^2 (620)^{2.5}} = 9.406539$$
$$B = \frac{b_m p}{RT} = \frac{2.0526(4000)}{10.73(620)} = 1.234049$$

Step 4 Solve equation (5–65) for the *largest positive root*, to yield

$$Z^3 - Z^2 + 6.93845Z - 11.60813 = 0$$
$$Z^L = 1.548126$$

Step 5 Calculate the apparent molecular weight of the crude oil:

$$M_a = \sum x_i M_i = 110.2547$$

Step 6 Solve for the density of the crude oil:

$$\rho^L = \frac{p M_a}{Z^L RT} = \frac{(4000)(100.2547)}{(10.73)(620)(1.548120)} = 38.93 \text{ lb/ft}^3$$

Note that calculating the liquid density as by Standing’s method gives a value of 46.23 lb/ft³.

EXAMPLE 5-10

Calculate the density of a gas phase with the composition at 4000 psia and 160°F shown in the following table. Use the RK EOS.

Component	y_i	M	p_c	T_c
C ₁	0.86	16.043	666.4	343.33
C ₂	0.05	30.070	706.5	549.92
C ₃	0.05	44.097	616.0	666.06
C ₄	0.02	58.123	527.9	765.62
C ₅	0.01	72.150	488.6	845.8
C ₆	0.005	84.00	453	923
C ₇₊	0.005	215	285	1287

SOLUTION

Step 1 Determine the parameters a_i and b_i for each component using equations (5-62) and (5-63):

$$a_i = 0.47274 \frac{R^2 T_c^{2.5}}{p_c}$$

$$b_i = 0.08664 \frac{RT_c}{p_c}$$

The results are shown in the table below.

Component	y_i	M	p_c	T_c	a_i	b_i
C ₁	0.86	16.043	666.4	343.33	161,044.3	0.4780514
C ₂	0.05	30.070	706.5	549.92	493,582.7	0.7225732
C ₃	0.05	44.097	616.0	666.06	914,314.8	1.004725
C ₄	0.02	58.123	527.9	765.62	1,449,929	1.292629
C ₅	0.01	72.150	488.6	845.8	2,095,431	1.609242
C ₆	0.005	84.00	453	923	2,845,191	1.945712
C ₇₊	0.005	215	285	1287	1.022348(10 ⁷)	4.191958

Step 2 Calculate a_m and b_m using equations (5-68) and (5-69), to give

$$a_m = \left[\sum_{i=1}^n y_i \sqrt{a_i} \right]^2 = 241,118$$

$$b_m = \sum b_i x_i = 0.5701225$$

Step 3 Calculate the coefficients A and B by applying equations (5-66) and (5-67), to yield

$$A = \frac{a_m p}{R^2 T^{2.5}} = \frac{241,118(4000)}{10.73^2 (620)^{2.5}} = 0.8750$$

$$B = \frac{b_m p}{RT} = \frac{0.5701225(4000)}{10.73(620)} = 0.3428$$

Step 4 Solve equation (5-65) for Z^v , to give

$$Z^3 - Z^2 + 0.414688Z - 0.29995 = 0$$

$$Z^v = 0.907$$

Step 5 Calculate the apparent molecular weight and density of the gas mixture:

$$M_a = \sum y_i M_i = 20.89$$

$$\rho^v = \frac{p M_a}{Z^v R T} = \frac{(4000)(20.89)}{(10.73)(620)(0.907)} = 13.85 \text{ lb/ft}^3$$

Soave-Redlich-Kwong Equation of State and Its Modifications

One of the most significant milestones in the development of cubic equations of state was the report by Soave (1972) of a modification in the evaluation of the parameter a in the attraction pressure term of the Redlich-Kwong equation of state (equation 5–60). Soave replaced the term $(a/T^{0.5})$ in equation (5–60) with a more general *temperature-dependent term*, denoted by $a\alpha(T)$, to give

$$p = \frac{RT}{V - b} - \frac{a\alpha(T)}{V(V + b)} \quad (5-70)$$

where $\alpha(T)$ is a dimensionless factor that becomes unity when the *reduced temperature*, T_r , = 1; that is, $\alpha(T) = 1$ when $T/T_c = 1$. Soave used vapor pressures of pure components to develop a generalized expression for the temperature correction parameter $\alpha(T)$. At system temperatures other than the critical temperature, the correction parameter $\alpha(T)$ is defined by the following relationship:

$$\alpha(T) = \left[1 + m \left(1 - \sqrt{T_r} \right) \right]^2 \quad (5-71)$$

Soave correlated the parameter m with the acentric factor, ω , to give

$$m = 0.480 + 1.574\omega - 0.176\omega^2 \quad (5-72)$$

where

T_r = reduced temperature, T/T_c

ω = acentric factor of the substance

T = system temperature, °R

For simplicity and convenience, the temperature-dependent term $\alpha(T)$ is replaced by the symbol α for the remainder of this chapter.

For any pure component, the constants a and b in equation (5–70) are found by imposing the classical van der Waals's critical point constraints (equation 5–48), on equation (5–70) and solving the resulting two equations:

$$a = \Omega_a \frac{R^2 T_c^2}{p_c} \quad (5-73)$$

$$b = \Omega_b \frac{RT_c}{p_c} \quad (5-74)$$

where Ω_a and Ω_b are the Soave-Redlich-Kwong (SRK) dimensionless pure component parameters and have the following values:

$$\Omega_a = 0.42747$$

$$\Omega_b = 0.08664$$

Edmister and Lee (1986) showed that the two parameters, a and b , can be determined by a more convenient method. For the critical isotherm,

$$(V - V_c)^3 = V^3 - [3V_c]V^2 + [3V_c^2]V - [V_c^3] = 0 \quad (5-75)$$

Equation (5-70) also can be expressed into a cubic form, to give

$$V^3 - \left[\frac{RT}{p} \right] V^2 + \left[\frac{a\alpha}{p} - \frac{bRT}{p} - b^2 \right] V - \left[\frac{(a\alpha)b}{p} \right] = 0 \quad (5-76)$$

At the critical point, equations (5-75) and (5-76) are identical when $\alpha = 1$. Equating the *coefficients* of the volume, V , of both equations gives

$$3V_c = \frac{RT_c}{p_c} \quad (5-77)$$

$$3V_c^2 = \frac{a}{p_c} - \frac{bRT_c}{p_c} - b^2 \quad (5-78)$$

$$V_c^3 = \frac{ab}{p_c} \quad (5-79)$$

Solving these equations simultaneously for parameters a and b gives relationships identical to those given by equations (5-73) and (5-74).

Rearranging equation (5-77) gives

$$p_c V_c = \frac{1}{3} RT_c$$

which indicates that the SRK equation of state gives a universal critical gas compressibility factor, Z_c , of 0.333. Note that combining equation (5-74) with (5-77), gives a covolume value of 26% of the critical volume; that is,

$$b = 0.26V_c$$

Introducing the compressibility factor, Z , into equation (5-33) by replacing the molar volume, V , in the equation with (ZRT/p) and rearranging gives

$$Z^3 - Z^2 + (A - B - B^2)Z - AB = 0 \quad (5-80)$$

with

$$A = \frac{(a\alpha)p}{(RT)^2} \quad (5-81)$$

$$B = \frac{bp}{RT} \quad (5-82)$$

where

p = system pressure, psia

T = system temperature, °R

R = 10.730 psia ft³/lb-mole °R

EXAMPLE 5-11

Rework Example 5-7 and solve for the density of the two phases using the SRK EOS.

SOLUTION

Step 1 Determine the critical pressure, critical temperature, and acentric factor from Table 1-1 of Chapter 1, to give

$$T_c = 666.01^\circ\text{R}$$

$$p_c = 616.3 \text{ psia}$$

$$\omega = 0.1524$$

Step 2 Calculate the reduced temperature:

$$T_r = T/T_c = 560/666.01 = 0.8408$$

Step 3 Calculate the parameter m by applying equation (5-72), to yield

$$m = 0.480 + 1.574\omega - 0.176\omega^2$$

$$m = 0.480 + 1.574(0.1524) - 0.176(0.1524)^2$$

Step 4 Solve for parameter α using equation (5-71), to give

$$\alpha = \left[1 + m(1 - \sqrt{T_r}) \right]^2$$

$$\alpha = \left[1 + 0.7052(1 - \sqrt{0.8408}) \right]^2 = 1.120518$$

Step 5 Compute the coefficients a and b by applying equations (5-73) and (5-74), to yield

$$a = \Omega_a \frac{R^2 T_c^2}{p_c} = 0.42747 \frac{10.73^2 (666.01)^2}{616.3} = 35,427.6$$

$$b = \Omega_b \frac{RT_c}{p_c} = 0.08664 \frac{10.73(666.01)}{616.3} = 1.00471$$

Step 6 Calculate the coefficients A and B from equations (5-81) and (5-82), to produce

$$A = \frac{(a\alpha)p}{R^2 T^2} = \frac{(35,427.6)(1.120518)(185)}{10.73^2 (560)^2} = 0.203365$$

$$B = \frac{bp}{RT} = \frac{(1.00471)(185)}{(10.73)(560)} = 0.034658$$

Step 7 Solve equation (5-80) for Z^L and Z^v :

$$Z^3 - Z^2 + (A - B - B^2)Z + AB = 0$$

$$Z^3 - Z^2 + (0.203365 - 0.034658 - 0.034658^2)Z + (0.203365)(0.034658) = 0$$

Solving this third-degree polynomial gives

$$Z^L = 0.06729$$

$$Z^v = 0.80212$$

Step 8 Calculate the gas and liquid density, to give

$$\rho^v = \frac{pM}{Z^v RT} = \frac{(185)(44.0)}{(0.80212)(10.73)(560)} = 1.6887 \text{ lb/ft}^3$$

$$\rho^L = \frac{pM}{Z^L RT} = \frac{(185)(44.0)}{(0.06729)(10.73)(560)} = 20.13 \text{ lb/ft}^3$$

To use equation (5-80) with mixtures, mixing rules are required to determine the terms $(a\alpha)$ and b for the mixtures. Soave adopted the following mixing rules:

$$(a\alpha)_m = \sum_i \sum_j \left[x_i x_j \sqrt{a_i a_j \alpha_i \alpha_j} (1 - k_{ij}) \right] \quad (5-83)$$

$$b_m = \sum_i [x_i b_i] \quad (5-84)$$

with

$$A = \frac{(a\alpha)_m p}{(RT)^2} \quad (5-85)$$

and

$$B = \frac{b_m p}{RT} \quad (5-86)$$

The parameter k_{ij} is an empirically determined correction factor (called the *binary interaction coefficient*) designed to characterize any binary system formed by components i and j in the hydrocarbon mixture.

These binary interaction coefficients are used to model the intermolecular interaction through empirical adjustment of the $(a\alpha)_m$ term as represented mathematically by equation (5-83). They are dependent on the difference in molecular size of components in a binary system and they are characterized by the following properties:

- The interaction between hydrocarbon components increases as the relative difference between their molecular weights increases:

$$k_{i,j+1} > k_{i,j}$$

- Hydrocarbon components with the same molecular weight have a binary interaction coefficient of zero:

$$k_{i,j} = 0$$

- The binary interaction coefficient matrix is symmetric:

$$k_{ij} = k_{ji}$$

Slot-Petersen (1987) and Vidal and Daubert (1978) presented theoretical background to the meaning of the interaction coefficient and techniques for determining their values. Graboski and Daubert (1978) and Soave (1972) suggested that no binary interaction coefficients are required for hydrocarbon systems. However, with nonhydrocarbons present, binary interaction parameters can greatly improve the volumetric and phase behavior predictions of the mixture by the SRK EOS.

In solving equation (5-75) for the compressibility factor of the liquid phase, the composition of the liquid, x_i , is used to calculate the coefficients A and B of equations (5-85) and (5-86) through the use of the mixing rules as described by equations (5-83) and (5-84). For determining the compressibility factor of the gas phase, Z^v , the previously outlined procedure is used with composition of the gas phase, y_i , replacing x_i .

EXAMPLE 5-12

A two-phase hydrocarbon system exists in equilibrium at 4000 psia and 160°F. The system has the composition shown in the following table.

Component	x_i	y_i	p_c	T_c	ω_i
C ₁	0.45	0.86	666.4	343.33	0.0104
C ₂	0.05	0.05	706.5	549.92	0.0979
C ₃	0.05	0.05	616.0	666.06	0.1522
C ₄	0.03	0.02	527.9	765.62	0.1852
C ₅	0.01	0.01	488.6	845.8	0.2280
C ₆	0.01	0.005	453	923	0.2500
C ₇₊	0.40	0.0005	285	1160	0.5200

The heptanes-plus fraction has the following properties:

$m = 215$
 $P_c = 285 \text{ psia}$
 $T_c = 700^\circ\text{F}$
 $\omega = 0.52$

Assuming $k_{ij} = 0$, calculate the density of each phase by using the SRK EOS.

SOLUTION

Step 1 Calculate the parameters α , a , and b by applying equations (5–71), (5–73), and (5–74):

$$\alpha = \left[1 + m \left(1 - \sqrt{T_r} \right) \right]^2$$
$$a = 0.42747 \frac{R^2 T_c^2}{p_c}$$
$$b = 0.08664 \frac{RT_c}{p_c}$$

The results are shown in the table below.

Component	p_c	T_c	ω_i	α_i	a_i	b_i
C ₁	666.4	343.33	0.0104	0.6869	8689.3	0.4780
C ₂	706.5	549.92	0.0979	0.9248	21,040.8	0.7225
C ₃	616.0	666.06	0.1522	1.0502	35,422.1	1.0046
C ₄	527.9	765.62	0.1852	1.1616	52,390.3	1.2925
C ₅	488.6	845.8	0.2280	1.2639	72,041.7	1.6091
C ₆	453	923	0.2500	1.3547	94,108.4	1.9455
C ₇₊	285	1160	0.5200	1.7859	232,367.9	3.7838

Step 2 Calculate the mixture parameters $(a\alpha)_m$ and b_m for the gas phase and liquid phase by applying equations (5–83) and (5–84), to give the following.

For the gas phase, using y_i ,

$$(a\alpha)_m = \sum_i \sum_j \left[y_i y_j \sqrt{a_i a_j \alpha_i \alpha_j} (1 - k_{ij}) \right] = 9219.3$$
$$b_m = \sum_i [y_i b_i] = 0.5680$$

For the liquid phase, using x_i ,

$$(a\alpha)_m = \sum_i \sum_j \left[x_i x_j \sqrt{a_i a_j \alpha_i \alpha_j} (1 - k_{ij}) \right] = 104,362.9$$

$$b_m = \sum_i [x_i b_i] = 1.8893$$

Step 3 Calculate the coefficients A and B for each phase by applying equations (5–85) and (5–86), to yield the following.

For the gas phase,

$$A = \frac{(a\alpha)_m p}{R^2 T^2} = \frac{(9219.3)(4000)}{(10.73)^2 (620)^2} = 0.8332$$

$$B = \frac{b_m p}{RT} = \frac{(0.5680)(4000)}{(10.73)(620)} = 0.3415$$

For the liquid phase,

$$A = \frac{(a\alpha)_m p}{R^2 T^2} = \frac{(104,362.9)(4000)}{(10.73)^2 (620)^2} = 9.4324$$

$$B = \frac{b_m p}{RT} = \frac{(1.8893)(4000)}{(10.73)(620)} = 1.136$$

Step 4 Solve equation (5–80) for the compressibility factor of the gas phase, to produce

$$Z^3 - Z^2 + (A - B - B^2)Z + AB = 0$$

$$Z^3 - Z^2 + (0.8332 - 0.3415 - 0.3415^2)Z + (0.8332)(0.3415) = 0$$

Solving this polynomial for the largest root gives

$$Z^v = 0.9267$$

Step 5 Solve equation (5–80) for the compressibility factor of the liquid phase, to produce

$$Z^3 - Z^2 + (A - B - B^2)Z + AB = 0$$

$$Z^3 - Z^2 + (9.4324 - 1.136 - 1.136^2)Z + (9.4324)(1.136) = 0$$

Solving the polynomial for the smallest root gives

$$Z^L = 1.4121$$

Step 6 Calculate the apparent molecular weight of the gas phase and liquid phase from their composition, to yield the following.

$$\text{For the gas phase: } M_a = \sum y_i M_i = 20.89$$

$$\text{For the liquid phase: } M_a = \sum x_i M_i = 100.25$$

Step 7 Calculate the density of each phase:

$$\rho = \frac{p M_a}{RT Z}$$

$$\text{For the gas phase: } \rho^v = \frac{(4000)(20.89)}{(10.73)(620)(0.9267)} = 13.556 \text{ lb/ft}^3$$

$$\text{For the liquid phase: } \rho^L = \frac{(4000)(100.25)}{(10.73)(620)(1.4121)} = 42.68 \text{ lb/ft}^3$$

It is appropriate at this time to introduce and define the concept of the fugacity and the fugacity coefficient of the component.

The *fugacity*, f , is a measure of the molar Gibbs energy of a real gas. It is evident from the definition that the fugacity has the units of pressure; in fact, the fugacity may be looked

on as a vapor pressure modified to correctly represent the *tendency of the molecules from one phase to escape into the other*. In a mathematical form, the fugacity of a *pure component* is defined by the following expression:

$$f^o = p \exp \left[\int_0^p \left(\frac{Z-1}{p} \right) dp \right] \quad (5-87)$$

where

f^o = fugacity of a pure component, psia

p = pressure, psia

Z = compressibility factor

The ratio of the fugacity to the pressure, f/p , called the *fugacity coefficient*, Φ , is calculated from equation (5-87) as

$$\frac{f^o}{p} = \Phi = \exp \left[\int_0^p \left(\frac{Z-1}{p} \right) dp \right]$$

Soave applied this generalized thermodynamic relationship to equation (5-70) to determine the fugacity coefficient of a pure component, to give

$$\ln \left(\frac{f^o}{p} \right) = \ln(\Phi) = Z - 1 - \ln(Z - B) - \frac{A}{B} \ln \left[\frac{Z + B}{Z} \right] \quad (5-88)$$

In practical petroleum engineering applications, we are concerned with the phase behavior of the hydrocarbon liquid mixture, which at a specified pressure and temperature, is in equilibrium with a hydrocarbon gas mixture at the same pressure and temperature.

In a hydrocarbon multicomponent mixture, the component fugacity in each phase is introduced to develop a criterion for thermodynamic equilibrium. Physically, the fugacity of a component i in one phase with respect to the fugacity of the component in a second phase is a measure of the potential for transfer of the component between phases. The phase with the lower component fugacity accepts the component from the phase with a higher component fugacity. Equal fugacities of a component in the two phases results in a zero net transfer. A zero transfer for all components implies a hydrocarbon system in thermodynamic equilibrium. Therefore, the condition of the thermodynamic equilibrium can be expressed mathematically by

$$f_i^v = f_i^L, \quad 1 \leq i \leq n \quad (5-89)$$

where

f_i^v = fugacity of component i in the gas phase, psi

f_i^L = fugacity of component i in the liquid phase, psi

n = number of components in the system

The fugacity coefficient of component i in a hydrocarbon liquid mixture or hydrocarbon gas mixture is a function of the system pressure, mole fraction, and fugacity of the component. The fugacity coefficient is defined as:

$$\text{For a component } i \text{ in the gas phase: } \Phi_i^v = \frac{f_i^v}{y_i p} \quad (5-90)$$

For a component i in the liquid phase: $\Phi_i^L = \frac{f_i^L}{x_i p}$ (5-91)

where Φ_i^v = fugacity coefficient of component i in the vapor phase and Φ_i^L = fugacity coefficient of component i in the liquid phase.

It is clear that, at equilibrium ($f_i^L = f_i^v$), the equilibrium ratio, K_i , as previously defined by equation (5-1), that is, $K_i = y_i/x_i$, can be redefined in terms of the fugacity of components as

$$K_i = \frac{[f_i^L / (x_i p)]}{[f_i^v / (y_i p)]} = \frac{\Phi_i^L}{\Phi_i^v} \quad (5-92)$$

Reid, Prausnitz, and Sherwood (1987) defined the fugacity coefficient of component i in a hydrocarbon mixture by the following generalized thermodynamic relationship:

$$\ln(\Phi_i) = \left(\frac{1}{RT} \right) \left[\int_V^\infty \left(\frac{\partial p}{\partial n_i} - \frac{RT}{V} \right) dV \right] - \ln(Z) \quad (5-93)$$

where

V = total volume of n moles of the mixture

n_i = number of moles of component i

Z = compressibility factor of the hydrocarbon mixture

By combining the above thermodynamic definition of the fugacity with the SRK EOS (equation 5-70), Soave proposed the following expression for the fugacity coefficient of component i in the liquid phase:

$$\ln \left(\frac{f_i^L}{x_i p} \right) = \ln(\Phi_i^L) = \frac{b_i(Z^L - 1)}{b_m} - \ln(Z^L - B) - \left(\frac{A}{B} \right) \left[\frac{2\Psi_i}{(a\alpha)_m} - \frac{b_i}{b_m} \right] \ln \left[1 + \frac{B}{Z^L} \right] \quad (5-94)$$

where

$$\Psi_i = \sum_j \left[x_j \sqrt{a_i a_j \alpha_i \alpha_j} (1 - k_{ij}) \right] \quad (5-95)$$

$$(a\alpha)_m = \sum_i \sum_j \left[x_i x_j \sqrt{a_i a_j \alpha_i \alpha_j} (1 - k_{ij}) \right] \quad (5-96)$$

Equation (5-94) also is used to determine the fugacity coefficient of component in the gas phase, Φ_i^v , by using the composition of the gas phase, y_i , in calculating A , B , Z^v , and other composition-dependent terms; that is,

$$\ln(\Phi_i^v) = \frac{b_i(Z^v - 1)}{b_m} - \ln(Z^v - B) - \left(\frac{A}{B} \right) \left[\frac{2\Psi_i}{(a\alpha)_m} - \frac{b_i}{b_m} \right] \ln \left[1 + \frac{B}{Z^v} \right]$$

where

$$\Psi_i = \sum_j \left[y_j \sqrt{a_i a_j \alpha_i \alpha_j} (1 - k_{ij}) \right]$$

$$(a\alpha)_m = \sum_i \sum_j \left[y_i y_j \sqrt{a_i a_j \alpha_i \alpha_j} (1 - k_{ij}) \right]$$

It is important to note that, in solving the cubic Z -factor equation for hydrocarbon mixtures, one or three real roots may exist. When three roots exist with different values

that are denoted as Z_{Largest} , Z_{Middle} , and Z_{Smallest} , the middle root, Z_{Middle} , always is discarded as a nonphysical value or meaning. However, the choice of the correct root between the remaining two roots is not a priori and the correct root is chosen as the one with the lowest normalized Gibbs energy function, g^* . The normalized Gibbs energy function, g^* , is defined in terms of the composition of the system and the individual component fugacity in the system; mathematically, it is defined by

$$\text{Normalized Gibbs energy for gas: } g_{\text{gas}}^* = \sum_{i=1}^n y_i \ln(f_i^v)$$

$$\text{Normalized Gibbs energy for liquid: } g_{\text{Liquid}}^* = \sum_{i=1}^n x_i \ln(f_i^L)$$

Therefore, assume that a liquid phase with a composition of x_i has multiple Z -factor roots; the middle root is *discarded* automatically, and the remaining two are designated Z_{L1} and Z_{L2} . To select the correct root, calculate the normalized Gibbs energy function using the two remaining roots:

$$g_{Z_{L1}}^* = \sum_{i=1}^n x_i \ln(f_i^L)$$

$$g_{Z_{L2}}^* = \sum_{i=1}^n x_i \ln(f_i^L)$$

In which the fugacity f_i^L is determined from equation (5–94) using the two remaining roots, Z_{L1} and Z_{L2} :

$$(f_i^L)_{Z_{L1}} = x_i p + \exp \left\{ \frac{b_i(Z_{L1}-1)}{b_m} - \ln(Z_{L1}-B) - \left(\frac{A}{B} \right) \left[\frac{2\Psi_i}{(a\alpha)_m} - \frac{b_i}{b_m} \right] \ln \left[1 + \frac{B}{Z_{L1}} \right] \right\}$$

$$(f_i^L)_{Z_{L2}} = x_i + \exp \left\{ \frac{b_i(Z_{L2}-1)}{b_m} - \ln(Z_{L2}-B) - \left(\frac{A}{B} \right) \left[\frac{2\Psi_i}{(a\alpha)_m} - \frac{b_i}{b_m} \right] \ln \left[1 + \frac{B}{Z_{L2}} \right] \right\}$$

If $g_{Z_{L1}}^* < g_{Z_{L2}}^*$ then Z_{L1} is chosen as the correct root; otherwise, Z_{L2} is chosen.

It should be pointed out that the partial Gibbs free energy plays an equally important role in determining the equilibrium of mixtures. The partial Gibbs energy is given the name *chemical potential*, μ_i , as defined by

$$\mu_i = \left(\frac{\partial G}{\partial n_i} \right)_{p, T, n_j}$$

The chemical potential, μ_p , essentially is a quantity that measures how much energy a component brings to a mixture. As was defined mathematically, this property can be used to measure the change of Gibbs free energy, G , in the system with the change in the amount of substance i as a constant: pressure, p ; temperature, T ; and amount of other components, n_j , where n_i is the amount of component i in the mixture and $i \neq j$. In a mixture, the normalized Gibbs free energy, g , is not the same in both phases because their compositions are different. Instead, the criterion for equilibrium is that the total Gibbs free energy, G , is at minimum with respect to all transfers of components from one phase to another at constant pressure and temperature; that is

$$\partial G = [\mu_i^{\text{gas}} - \mu_i^{\text{liquid}}] \partial n_i = 0$$

This criterion implies that, at equilibrium, the chemical potential of each component μ_i has the same value in each phase:

$$\mu_i^{\text{gas}} = \mu_i^{\text{liquid}}$$

The chemical potential of component i is related to the activity \hat{a}_i by

$$\mu_i = \mu_i^o + RT \ln(\hat{a}_i)$$

with

$$\hat{a}_i = \frac{f_i}{f_i^o}$$

where

\hat{a}_i = activity of component i in mixture at p and T

μ_i^o = chemical potential of pure of component i at p and T

f_i^o = fugacity of pure component i at p and T

f_i = fugacity of component i in mixture at p and T

Modifications of the SRK EOS

To improve the pure component vapor pressure predictions by the SRK equation of state, Groboski and Daubert (1978) proposed a new expression for calculating parameter m of equation (5-72). The proposed relationship, which originated from analyzing extensive experimental data for pure hydrocarbons, has the following form:

$$m = 0.48508 + 1.55171\omega - 0.15613\omega^2 \quad (5-97)$$

Sim and Daubert (1980) pointed out that, because the coefficients of equation (5-97) were determined by analyzing vapor pressure data of low-molecular-weight hydrocarbons, it is unlikely that equation (5-97) will suffice for high-molecular-weight petroleum fractions. Realizing that the acentric factors for the heavy petroleum fractions are calculated from an equation such as the Edmister correlation or the Lee and Kesler correlation, the authors proposed the following expressions for determining parameter m :

- If the acentric factor is determined using the Edmister correlation, then

$$m = 0.431 + 1.57\omega_i - 0.161\omega_i^2 \quad (5-98)$$

- If the acentric factor is determined using the Lee and Kesler correction, then

$$m = 0.315 + 1.60\omega_i - 0.166\omega_i^2 \quad (5-99)$$

Elliot and Daubert (1985) stated that the optimal binary interaction coefficient, k_{ij} , would minimize the error in the representation of all the thermodynamic properties of a mixture. Properties of particular interest in phase-equilibrium calculations include bubble-point pressure, dew-point pressure, and equilibrium ratios. The authors proposed a set of relationships for determining interaction coefficients for asymmetric mixtures* that contain methane, N_2 , CO_2 , and H_2S . Referring to the principal component as i and other fractions as j , Elliot and Daubert proposed the following expressions:

*An asymmetric mixture is defined as one in which two of the components are considerably different in their chemical behavior. Mixtures of methane with hydrocarbons of 10 or more carbon atoms can be considered asymmetric. Mixtures containing gases such as nitrogen or hydrogen are asymmetric.

For N_2 systems,

$$k_{ij} = 0.107089 + 2.9776k_{ij}^{\infty} \quad (5-100)$$

For CO_2 systems,

$$k_{ij} = 0.08058 - 0.77215k_{ij}^{\infty} - 1.8404(k_{ij}^{\infty})^2 \quad (5-101)$$

For H_2S systems,

$$k_{ij} = 0.07654 + 0.017921k_{ij}^{\infty} \quad (5-102)$$

For methane systems with compounds of 10 carbons or more,

$$k_{ij} = 0.17985 + 2.6958k_{ij}^{\infty} + 10.853(k_{ij}^{\infty})^2 \quad (5-103)$$

where

$$k_{ij}^{\infty} = \frac{-(\epsilon_i - \epsilon_j)^2}{2\epsilon_i\epsilon_j} \quad (5-104)$$

and

$$\epsilon_i = \frac{0.480453\sqrt{a_i}}{b_i} \quad (5-105)$$

The two parameters, a_i and b_i , of equation (5-105) were defined previously by equations (5-73) and (5-74).

The major drawback in the SRK EOS is that the critical compressibility factor takes on the unrealistic universal critical compressibility of 0.333 for all substances. Consequently, the molar volumes typically are overestimated; that is, densities are underestimated.

Peneloux, Rauzy, and Freze (1982) developed a procedure for improving the volumetric predictions of the SRK EOS by introducing a volume correction parameter, c_i , into the equation. This third parameter *does not change* the vapor/liquid equilibrium conditions determined by the unmodified SRK equation, that is, the equilibrium ratio K_i , but it modifies the liquid and gas volumes. The proposed methodology, known as the *volume translation method*, uses the following expressions:

$$V_{\text{corr}}^L = V^L - \sum_i (x_i c_i) \quad (5-106)$$

$$V_{\text{corr}}^v = V^v - \sum_i (y_i c_i) \quad (5-107)$$

where

V^L = uncorrected liquid molar volume (i.e., $V^L = Z^L RT/p$), ft^3/mole

V^v = uncorrected gas molar volume $V^v = Z^v RT/p$, ft^3/mole

V_{corr}^L = corrected liquid molar volume, ft^3/mole

V_{corr}^v = corrected gas molar volume, ft^3/mole

x_i = mole fraction of component i in the liquid phase

y_i = mole fraction of component i in the gas phase

The authors proposed six schemes for calculating the correction factor, c_i , for each component. For petroleum fluids and heavy hydrocarbons, Peneloux and coworkers suggested that the best correlating parameter for the volume correction factor c_i is the Rackett compressibility factor, Z_{RA} . The correction factor then is defined mathematically by the following relationship:

$$c_i = 4.43797878(0.29441 - Z_{\text{RA}})T_{\text{ci}}/p_{\text{ci}} \quad (5-108)$$

where

- c_i = correction factor for component i , ft³/lb-mole
- T_{ci} = critical temperature of component i , °R
- p_{ci} = critical pressure of component i , psia

The parameter Z_{RA} is a unique constant for each compound. The values of Z_{RA} , in general, are not much different from those of the critical compressibility factors, Z_c . If their values are not available, Peneloux et al. proposed the following correlation for calculating c_i :

$$c_i = (0.0115831168 + 0.411844152\omega_i) \left(\frac{T_{ci}}{p_{ci}} \right) \quad (5-109)$$

where ω_i = acentric factor of component i .

EXAMPLE 5-13

Rework Example 5-12 by incorporating the Peneloux et al. volume correction approach in the solution. Key information from Example 5-12 includes:

- For gas: $Z^v = 0.9267$, $M_a = 20.89$
- For liquid: $Z^L = 1.4121$, $M_a = 100.25$
- $T = 160^\circ\text{F}$, and $p = 4000$ psi

SOLUTION

Step 1 Calculate the correction factor c_i using equation (5-109):

$$c_i = (0.0115831168 + 0.411844152\omega_i) \left(\frac{T_{ci}}{p_{ci}} \right)$$

The results are shown in the table below.

Component	x_i	p_c	T_c	ω_i	c_i	$c_i x_i$	y_i	$c_i y_i$
C ₁	0.45	666.4	343.33	0.0104	0.00839	0.003776	0.86	0.00722
C ₂	0.05	706.5	549.92	0.0979	0.03807	0.001903	0.05	0.00190
C ₃	0.05	616.0	666.06	0.1522	0.07729	0.003861	0.05	0.00386
C ₄	0.03	527.9	765.62	0.1852	0.1265	0.00379	0.02	0.00253
C ₅	0.01	488.6	845.8	0.2280	0.19897	0.001989	0.01	0.00198
C ₆	0.01	453	923	0.2500	0.2791	0.00279	0.005	0.00139
C ₇₊	0.40	285	1160	0.5200	0.91881	0.36752	0.005	0.00459
Σ						0.38564		0.02349

Step 2 Calculate the uncorrected volume of the gas and liquid phase using the compressibility factors as calculated in Example 5-12.

$$V^v = \frac{RTZ^v}{p} = \frac{(10.73)(620)(0.9267)}{4000} = 1.54119 \text{ ft}^3/\text{mole}$$

$$V^L = \frac{RTZ^L}{p} = \frac{(10.73)(620)(1.4121)}{4000} = 2.3485 \text{ ft}^3/\text{mole}$$

Step 3 Calculate the corrected gas and liquid volumes by applying equations (5-106) and (5-107):

$$V_{\text{corr}}^L = V^L - \sum_i (x_i c_i) = 2.3485 - 0.38564 = 1.962927 \text{ ft}^3/\text{mole}$$

$$V_{\text{corr}}^v = V^v - \sum_i (y_i c_i) = 1.54119 - 0.02349 = 1.5177 \text{ ft}^3/\text{mole}$$

Step 4 Calculate the corrected compressibility factors:

$$Z_{\text{corr}}^v = \frac{(4000)(1.5177)}{(10.73)(620)} = 0.91254$$

$$Z_{\text{corr}}^L = \frac{(4000)(1.962927)}{(10.73)(620)} = 1.18025$$

Step 5 Determine the corrected densities of both phases:

$$\rho = \frac{pM_a}{RTZ}$$

$$\rho^v = \frac{(4000)(20.89)}{(10.73)(620)(0.91254)} = 13.767 \text{ lb/ft}^3$$

$$\rho^L = \frac{(4000)(100.25)}{(10.73)(620)(1.18025)} = 51.07 \text{ lb/ft}^3$$

As pointed out by Whitson and Brule (2000), when the volume shift is introduced to the EOS for mixtures, the resulting expressions for fugacity are

$$(f_i^L)_{\text{modified}} = (f_i^L)_{\text{original}} \exp \left[-c_i \frac{p}{RT} \right]$$

and

$$(f_i^v)_{\text{modified}} = (f_i^v)_{\text{original}} \exp \left[-c_i \frac{p}{RT} \right]$$

This implies that the fugacity ratios are unchanged by the volume shift:

$$\frac{(f_i^L)_{\text{modified}}}{(f_i^v)_{\text{modified}}} = \frac{(f_i^L)_{\text{original}}}{(f_i^v)_{\text{original}}}$$

Peng-Robinson's Equation of State and Its Modifications

Peng and Robinson (1976a) conducted a comprehensive study to evaluate the use of the SRK equation of state for predicting the behavior of naturally-occurring hydrocarbon systems. They illustrated the need for an improvement in the ability of the equation of state to predict liquid densities and other fluid properties, particularly in the vicinity of the critical region. As a basis for creating an improved model, Peng and Robinson (PR) proposed the following expression:

$$p = \frac{RT}{V-b} - \frac{a\alpha}{(V+b)^2 - cb^2}$$

where a , b , and α have the same significance as they have in the SRK model, and parameter c is a whole number optimized by analyzing the values of the terms Z_c and b/V_c as obtained from the equation. It is generally accepted that Z_c should be close to 0.28 and b/V_c

should be approximately 0.26. An optimized value of $c = 2$ gives $Z_c = 0.307$ and $(b/V_c) = 0.253$. Based on this value of c , Peng and Robinson proposed the following equation of state (commonly referred to as PR EOS):

$$p = \frac{RT}{V-b} - \frac{a\alpha}{V(V+b)+b(V-b)} \quad (5-110)$$

Imposing the classical critical point conditions (equation 5-48) on equation (5-110) and solving for parameters a and b yields

$$a = \Omega_a \frac{R^2 T_c^2}{p_c} \quad (5-111)$$

$$b = \Omega_b \frac{RT_c}{p_c} \quad (5-112)$$

where

$$\Omega_a = 0.45724$$

$$\Omega_b = 0.07780$$

This equation predicts a universal critical gas compressibility factor, Z_c , of 0.307, compared to 0.333 for the SRK model. Peng and Robinson also adopted Soave's approach for calculating parameter α :

$$\alpha = \left[1 + m(1 - \sqrt{T_r}) \right]^2 \quad (5-113)$$

where $m = 0.3796 + 1.54226\omega - 0.2699\omega^2$.

Peng and Robinson (1978) proposed the following modified expression for m that is recommended for heavier components with acentric values $\omega > 0.49$:

$$m = 0.379642 + 1.48503\omega - 0.1644\omega^2 + 0.016667\omega^3 \quad (5-114)$$

Rearranging equation (5-110) into the compressibility factor form, gives

$$Z^3 + (B-1)Z^2 + (A-3B^2-2B)Z - (AB-B^2-B^3) = 0 \quad (5-115)$$

where A and B are given by equations (5-81) and (5-82) for pure component and by equations (5-85) and (5-86) for mixtures; that is,

$$A = \frac{(a\alpha)_m p}{(RT)^2}$$

$$B = \frac{b_m p}{RT}$$

with

$$(a\alpha)_m = \sum_i \sum_j \left[x_i x_j \sqrt{a_i a_j \alpha_i \alpha_j} (1 - k_{ij}) \right]$$

$$b_m = \sum_i [x_i b_i]$$

EXAMPLE 5-14

Using the composition given in Example 5-12, calculate the density of the gas phase and liquid phase by using the Peng-Robinson EOS. Assume $k_{ij} = 0$. The components are described in the following table.

Component	x_i	y_i	p_c	T_c	ω_i
C ₁	0.45	0.86	666.4	343.33	0.0104
C ₂	0.05	0.05	706.5	549.92	0.0979
C ₃	0.05	0.05	616.0	666.06	0.1522
C ₄	0.03	0.02	527.9	765.62	0.1852
C ₅	0.01	0.01	488.6	845.8	0.2280
C ₆	0.01	0.005	453	923	0.2500
C ₇₊	0.40	0.0005	285	1160	0.5200

The heptanes-plus fraction has the following properties:

$M = 215$
 $p_c = 285 \text{ psia}$
 $T_c = 700^\circ\text{F}$
 $\omega = 0.582$

SOLUTION

Step 1 Calculate the parameters a , b , and α for each component in the system by applying equations (5–111) through (5–113):

$$a = 0.45724 \frac{R^2 T_c^2}{p_c}$$
$$b = 0.07780 \frac{RT_c}{p_c}$$
$$\alpha = \left[1 + m \left(1 - \sqrt{T_r} \right) \right]^2$$

The results are shown in the table below.

Component	p_c	T_c	ω_i	m	α_i	a_i	b_i
C ₁	666.4	343.33	0.0104	1.8058	0.7465	9294.4	0.4347
C ₂	706.5	549.92	0.0979	1.1274	0.9358	22,506.1	0.6571
C ₃	616.0	666.06	0.1522	0.9308	1.0433	37,889.0	0.9136
C ₄	527.9	765.62	0.1852	0.80980	1.1357	56,038.9	1.1755
C ₅	488.6	845.8	0.2280	0.73303	1.2170	77,058.9	1.6091
C ₆	453	923	0.2500	0.67172	1.2882	100,662.3	1.4635
C ₇₊	285	1160	0.5200	0.53448	1.6851	248,550.5	3.4414

Step 2 Calculate the mixture parameters $(a\alpha)_m$ and b_m for the gas and liquid phase, to give the following.

For the gas phase,

$$(a\alpha)_m = \sum_i \sum_j \left[y_i y_j \sqrt{a_i a_j \alpha_i \alpha_j} (1 - k_{ij}) \right] = 10,423.54$$
$$b_m = \sum_i (y_i b_i) = 0.862528$$

For the liquid phase,

$$(a\alpha)_m = \sum_i \sum_j \left[x_i x_j \sqrt{a_i a_j \alpha_i \alpha_j} (1 - k_{ij}) \right] = 107,325.4$$

$$b_m = \sum_i (x_i b_i) = 1.696543$$

Step 3 Calculate the coefficients A and B , to give the following.

For the gas phase,

$$A = \frac{(a\alpha)_m p}{R^2 T^2} = \frac{(10,423.54)(4000)}{(10.73)^2 (620)^2} = 0.94209$$

$$B = \frac{b_m p}{RT} = \frac{(0.862528)(4000)}{(10.73)(620)} = 0.30669$$

For the liquid phase,

$$A = \frac{(a\alpha)_m p}{R^2 T^2} = \frac{(107,325.4)(4000)}{(10.73)^2 (620)^2} = 9.700183$$

$$B = \frac{b_m p}{RT} = \frac{(1.696543)(4000)}{(10.73)(620)} = 1.020078$$

Step 4 Solve equation (5–115) for the compressibility factor of the gas and liquid phases, to give

$$Z^3 + (B - 1)Z^2 + (A - 3B^2 - 2B)Z - (AB - B^2 - B^3) = 0$$

For the gas phase:

Substituting for $A = 0.94209$ and $B = 0.30669$ in the above equation gives

$$Z^3 + (B - 1)Z^2 + (A - 3B^2 - 2B)Z - (AB - B^2 - B^3) = 0$$

$$Z^3 + (0.30669 - 1)Z^2 + [0.94209 - 3(0.30669)^2 - 2(0.30669)]Z - [(0.94209)(0.30669) - (0.30669)^2 - (0.30669)^3] = 0$$

Solving for Z gives

$$Z^v = 0.8625$$

For the liquid phase:

Substituting $A = 9.700183$ and $B = 1.020078$ in equation (5–115) gives

$$Z^3 + (B - 1)Z^2 + (A - 3B^2 - 2B)Z - (AB - B^2 - B^3) = 0$$

$$Z^3 + (1.020078 - 1)Z^2 + [(9.700183) - 3(1.020078)^2 - 2(1.020078)]Z - [(9.700183)(1.020078) - (1.020078)^2 - (1.020078)^3] = 0$$

Solving for Z gives

$$Z^L = 1.2645$$

Step 5 Calculate the density of both phases.

Density of the vapor phase:

$$\rho^v = \frac{pM_a}{Z^v RT}$$

$$\rho^v = \frac{(4000)(20.89)}{(10.73)(620)(0.8625)} = 14.566 \text{ lb/ft}^3$$

Density of the liquid phase:

$$\rho^L = \frac{pM_a}{Z^L RT}$$

$$\rho^L = \frac{(4000)(100.25)}{(10.73)(620)(1.2645)} = 47.67 \text{ lb/ft}^3$$

Applying the thermodynamic relationship, as given by equation (5–88), to equation (5–111) yields the following expression for the fugacity of a pure component:

$$\ln\left(\frac{f}{p}\right) = \ln(\Phi) = Z - 1 - \ln(Z - B) - \left[\frac{A}{2\sqrt{2}B}\right] \ln\left[\frac{Z + (1 + \sqrt{2})B}{Z - (1 - \sqrt{2})B}\right] \tag{5-116}$$

The fugacity coefficient of component *i* in a hydrocarbon liquid mixture is calculated from the following expression:

$$\begin{aligned} \ln\left(\frac{f^L}{x_i p}\right) = \ln(\Phi_i^L) = & \frac{b_i(Z^L - 1)}{b_m} - \ln(Z^L - B) \\ & - \frac{A}{2\sqrt{2}B} \left[\frac{2\Psi_i}{(a\alpha)_m} - \frac{b_i}{b_m} \right] \ln\left[\frac{Z^L + (1 + \sqrt{2})B}{Z^L - (1 - \sqrt{2})B}\right] \end{aligned} \tag{5-117}$$

where the mixture parameters *b_m*, *B*, *A*, *Ψ_i*, and (*aα*)_{*m*} are defined previously.

Equation (5–117) also is used to determine the fugacity coefficient of any component in the gas phase by replacing the composition of the liquid phase, *x_i*, with the composition of the gas phase, *y_i*, in calculating the composition-dependent terms of the equation:

$$\begin{aligned} \ln\left(\frac{f^v}{y_i p}\right) = \ln(\Phi_i^L) = & \frac{b_i(Z^v - 1)}{b_m} - \ln(Z^v - B) - \frac{A}{2\sqrt{2}B} \left[\frac{2\Psi_i}{(a\alpha)_m} - \frac{b_i}{b_m} \right] \\ & \ln\left[\frac{Z^v + (1 + \sqrt{2})B}{Z^v - (1 - \sqrt{2})B}\right] \end{aligned}$$

The table below shows the set of binary interaction coefficient, *k_{ij}*, traditionally used when predicting the volumetric behavior of hydrocarbon mixture with the Peng-Robinson equation of state.

	CO ₂	N ₂	H2S	C ₁	C ₂	C ₃	i-C ₄	n-C ₄	i-C ₅	n-C ₅	C ₆	C ₇	C ₈	C ₉	C ₁₀
CO ₂	0	0	0.135	0.105	0.130	0.125	0.120	0.115	0.115	0.115	0.115	0.115	0.115	0.115	0.115
N ₂		0	0.130	0.025	0.010	0.090	0.095	0.095	0.100	0.100	0.110	0.115	0.120	0.120	0.125
H ₂ S			0	0.070	0.085	0.080	0.075	0.075	0.070	0.070	0.070	0.060	0.060	0.060	0.055
C ₁				0	0.005	0.010	0.035	0.025	0.050	0.030	0.030	0.035	0.040	0.040	0.045
C ₂					0	0.005	0.005	0.010	0.020	0.020	0.020	0.020	0.020	0.020	0.020
C ₃						0	0.000	0.000	0.015	0.015	0.010	0.005	0.005	0.005	0.005
i-C ₄							0	0.005	0.005	0.005	0.005	0.005	0.005	0.005	0.005
n-C ₄								0	0.005	0.005	0.005	0.005	0.005	0.005	0.005
i-C ₅									0	0.000	0.000	0.000	0.000	0.000	0.000
n-C ₅										0	0.000	0.000	0.000	0.000	0.000
C ₆											0	0.000	0.000	0.000	0.000
C ₇												0	0.000	0.000	0.000
C ₈													0	0.000	0.000
C ₉														0	0.00
C ₁₀															0

Note that *k_{ij}* = *k_{ji}*.

To improve the predictive capability of the PR EOS when describing mixtures containing N_2 , CO_2 , and CH_4 , Nikos et al. (1986) proposed a generalized correlation for generating the binary interaction coefficient, k_{ij} . The authors correlated these coefficients with system pressure, temperature, and the acentric factor. These generalized correlations originated with all the binary experimental data available in the literature. The authors proposed the following generalized form for k_{ij} :

$$k_{ij} = \partial_2 T_{ij}^2 + \partial_1 T_{ij} + \partial_0 \quad (5-118)$$

where i refers to the principal component, N_2 , CO_2 , or CH_4 , and j refers to the other hydrocarbon component of the binary. The acentric-factor-dependent coefficients, ∂_0 , ∂_1 , and ∂_2 , are determined for each set of binaries by applying the following expressions:

For nitrogen-hydrocarbons,

$$\partial_0 = 0.1751787 - 0.7043 \log(\omega_j) - 0.862066[\log(\omega_j)]^2 \quad (5-119)$$

$$\partial_1 = -0.584474 + 1.328 \log(\omega_j) + 2.035767[\log(\omega_j)]^2 \quad (5-120)$$

$$\partial_2 = 2.257079 + 7.869765 \log(\omega_j) + 13.50466[\log(\omega_j)]^2 + 8.3864[\log(\omega)]^3 \quad (5-121)$$

They also suggested the following pressure correction:

$$k'_{ij} = k_{ij}(1.04 - 4.2 \times 10^{-5} p) \quad (5-122)$$

where p is the pressure in pounds per square inch.

For methane-hydrocarbons,

$$\partial_0 = -0.01664 - 0.37283 \log(\omega_j) + 1.31757[\log(\omega_j)]^2 \quad (5-123)$$

$$\partial_1 = 0.48147 + 3.35342 \log(\omega_j) - 1.0783[\log(\omega_j)]^2 \quad (5-124)$$

$$\partial_2 = -0.4114 - 3.5072 \log(\omega_j) - 0.78798[\log(\omega_j)]^2 \quad (5-125)$$

For CO_2 -hydrocarbons,

$$\partial_0 = 0.4025636 + 0.1748927 \log(\omega_j) \quad (5-126)$$

$$\partial_1 = -0.94812 - 0.6009864 \log(\omega_j) \quad (5-127)$$

$$\partial_2 = 0.741843368 + 0.441775 \log(\omega_j) \quad (5-128)$$

For the CO_2 interaction parameters, the following pressure correction is suggested:

$$k'_{ij} = k_{ij}(1.044269 - 4.375 \times 10^{-5} p) \quad (5-129)$$

Stryjek and Vera (1986) proposed an improvement in the reproduction of vapor pressures of a pure component by the PR EOS in the reduced temperature range from 0.7 to 1.0, by replacing the m term in equation (5-113) with the following expression:

$$m_0 = 0.378893 + 1.4897153 - 0.17131848\omega^2 + 0.0196554\omega^3 \quad (5-130)$$

To reproduce vapor pressures at reduced temperatures below 0.7, Stryjek and Vera further modified the m parameter in the PR equation by introducing an adjustable parameter, m_1 , characteristic of each compound to equation (5-113). They proposed the following generalized relationship for the parameter m :

$$m = m_0 + \left[m_1 \left(1 + \sqrt{T_r} \right) (0.7 - T_r) \right] \quad (5-131)$$

where

- T_r = reduced temperature of the pure component
- m_0 = defined by equation (5-130)
- m_1 = adjustable parameter

For all components with a reduced temperature above 0.7, Stryjek and Vera recommended setting $m_1 = 0$. For components with a reduced temperature greater than 0.7, the optimum values of m_1 for compounds of industrial interest are tabulated below:

COMPONENT	m_1
Nitrogen	0.01996
Carbon dioxide	0.04285
Water	-0.06635
Methane	-0.00159
Ethane	0.02669
Propane	0.03136
Butane	0.03443
Pentane	0.03946
Hexane	0.05104
Heptane	0.04648
Octane	0.04464
Nonane	0.04104
Decane	0.04510
Undecane	0.02919
Dodecane	0.05426
Tridecane	0.04157
Tetradecane	0.02686
Pentadecane	0.01892
Hexadecane	0.02665
Heptadecane	0.04048
Octadecane	0.08291

Due to the totally empirical nature of the parameter m_1 , Stryjek and Vera could not find a generalized correlation for m_1 in terms of pure component parameters. They pointed out that these values of m_1 should be used without changes.

Jhaveri and Youngren (1984) pointed out that, when applying the Peng-Robinson equation of state to reservoir fluids, the error associated with the equation in the prediction of gas-phase Z-factors ranged from 3 to 5% and the error in the liquid density predictions ranged from 6 to 12%. Following the procedure proposed by Peneloux and coworkers (see the SRK EOS), Jhaveri and Youngren introduced the volume correction parameter, c_i , to the PR EOS. This third parameter has the same units as the second parameter, b_i , of the unmodified PR equation and is defined by the following relationship:

$$c_i = S_i b_i$$

(5-132)

where S_i is a dimensionless parameter, called the shift parameter, and b_i is the Peng-Robinson covolume, as given by equation (5-112).

As in the SRK EOS, the volume correction parameter, c_p , does not change the vapor/liquid equilibrium conditions, equilibrium ratio K_i . The corrected hydrocarbon phase volumes are given by the following expressions:

$$V_{\text{corr}}^L = V^L - \sum_{i=1} (x_i c_i)$$

$$V_{\text{corr}}^v = V^v - \sum_{i=1} (y_i c_i)$$

where

V^L, V^v = volumes of the liquid phase and gas phase as calculated by the unmodified PR EOS, ft³/mole
 $V_{\text{corr}}^L, V_{\text{corr}}^v$ = corrected volumes of the liquid and gas phase, ft³/mole

Whitson and Brule (2000) point out that the volume translation (correction) concept can be applied to any two-constant cubic equation, thereby eliminating the volumetric deficiency associated with the application of EOS. Whitson and Brule extended the work of Jhaveri and Youngren and tabulated the shift parameters, S_i , for a selected number of pure components. These tabulated values, which follow, are used in equation (5-132) to calculate the volume correction parameter, c_p , for the Peng-Robinson and SRK equations of state:

COMPONENT	PR EOS	SRK EOS
N ₂	-0.1927	-0.0079
CO ₂	-0.0817	0.0833
H ₂ S	-0.1288	0.0466
C ₁	-0.1595	0.0234
C ₂	-0.1134	0.0605
C ₃	-0.0863	0.0825
i-C ₄	-0.0844	0.0830
n-C ₄	-0.0675	0.0975
i-C ₅	-0.0608	0.1022
n-C ₅	-0.0390	0.1209
n-C ₆	-0.0080	0.1467
n-C ₇	0.0033	0.1554
n-C ₈	0.0314	0.1794
n-C ₉	0.0408	0.1868
n-C ₁₀	0.0655	0.2080

Jhaveri and Youngren proposed the following expression for calculating the shift parameter for the C₇₊:

$$S_{C_{7+}} = 1 - \frac{d}{(M)^e}$$

where M = molecular weight of the heptanes-plus fraction and d, e = positive correlation coefficients.

The authors proposed that, in the absence of the experimental information needed for calculating e and d , the power coefficient e could be set equal to 0.2051 and the coefficient

d adjusted to match the C_{7+} density with the values of d ranging from 2.2 to 3.2. In general, the following values may be used for C_{7+} fractions, by hydrocarbon family:

HYDROCARBON FAMILY	d	e
Paraffins	2.258	0.1823
Naphthenes	3.044	0.2324
Aromatics	2.516	0.2008

To use the Peng-Robinson equation of state to predict the phase and volumetric behavior of mixtures, one must be able to provide the critical pressure, the critical temperature, and the acentric factor for each component in the mixture. For pure compounds, the required properties are well defined and known. Nearly all naturally-occurring petroleum fluids contain a quantity of heavy fractions that are not well defined. These heavy fractions often are lumped together as a heptanes-plus fraction. The problem of how to adequately characterize the C_{7+} fractions in terms of their critical properties and acentric factors has been long recognized in the petroleum industry. Changing the characterization of C_{7+} fractions present in even small amounts can have a profound effect on the PVT properties and the phase equilibria of a hydrocarbon system as predicted by the Peng-Robinson equation of state.

The usual approach for such situations is to “tune” the parameters in the EOS in an attempt to improve the accuracy of prediction. During the tuning process, the critical properties of the heptanes-plus fraction and the binary interaction coefficients are adjusted to obtain a reasonable match with experimental data available on the hydrocarbon mixture.

Recognizing that the inadequacy of the predictive capability of the PR EOS lies with the improper procedure for calculating the parameters a , b , and α of the equation for the C_{7+} fraction, Ahmed (1991) devised an approach for determining these parameters from the following two readily measured physical properties of C_{7+} : the molecular weight, M_{7+} , and the specific gravity, γ_{7+} .

The approach is based on generating 49 density values for the C_{7+} by applying the Riazi and Daubert correlation. These values were subsequently subjected to 10 temperature and 10 pressure values in the range of 60–300°F and 14.7–7000 psia, respectively. The Peng-Robinson EOS was then applied to match the 4900 generated density values by optimizing the parameters a , b , and α , using a nonlinear regression model. The optimized parameters for the heptanes-plus fraction are given by the following expressions.

For the parameter α of C_{7+} ,

$$\alpha = \left[1 + m \left(1 - \sqrt{\frac{520}{T}} \right) \right]^2 \quad (5-133)$$

with m as defined by

$$m = \frac{D}{A_0 + A_1 D} + A_2 M_{7+} + A_3 M_{7+}^2 + \frac{A_4}{M_{7+}} + A_5 \gamma_{7+} + A_6 \gamma_{7+}^2 + \frac{A_7}{\gamma_{7+}} \quad (5-134)$$

with parameter D as defined by the ratio of the molecular weight to the specific gravity of the heptanes-plus fraction:

$$D = \frac{M_{7+}}{\gamma_{7+}}$$

where

- M_{7+} = molecular weight of C_{7+}
- γ_{7+} = specific gravity of C_{7+}
- A_0 – A_7 = coefficients as given in the table below

Coefficient	<i>a</i>	<i>b</i>	<i>m</i>
A_0	-2.433525×10^7	-6.8453198	-36.91776
A_1	8.3201587×10^3	1.730243×10^{-2}	$-5.2393763 \times 10^{-2}$
A_2	-0.18444102×10^2	$-6.2055064 \times 10^{-6}$	1.7316235×10^{-2}
A_3	3.6003101×10^{-2}	9.0910383×10^{-9}	$-1.3743308 \times 10^{-5}$
A_4	3.4992796×10^7	13.378898	12.718844
A_5	2.838756×10^7	7.9492922	10.246122
A_6	-1.1325365×10^7	-3.1779077	-7.6697942
A_7	6.418828×10^6	1.7190311	-2.6078099

For parameters *a* and *b* of C_{7+} , the following generalized correlation is proposed:

$$a \text{ or } b = \left[\sum_{i=0}^3 (A_i D^i) \right] + \frac{A_4}{D} + \left[\sum_{i=5}^6 (A_i \gamma_{7+}^{i-4}) \right] + \frac{A_7}{\gamma_{7+}} \quad (5-135)$$

The coefficients A_0 through A_7 are included in the table above.

To further improve the predictive capability of the Peng-Robinson EOS, the author optimized the coefficients *a*, *b*, and *m* for nitrogen, CO₂, and methane by matching 100 Z-factor values for each of these components. Using a nonlinear regression model, the optimized values in the table below are recommended.

Component	<i>a</i>	<i>b</i>	<i>m</i> (Equation 5-133)
CO ₂	1.499914×10^4	0.41503575	-0.73605717
N ₂	4.5693589×10^3	0.4682582	-0.97962859
C ₁	7.709708×10^3	0.46749727	-0.549765

To provide the modified PR EOS with a consistent procedure for determining the binary interaction coefficient, k_{ij} , the following computational steps are proposed.

Step 1 Calculate the binary interaction coefficient between methane and the heptanes-plus fraction from

$$k_{C_1-C_{7+}} = 0.00189T - 1.167059$$

where the temperature, *T*, is in °R.

Step 2 Set

$$\begin{aligned} k_{CO_2-N_2} &= 0.12 \\ k_{CO_2\text{-hydrocarbon}} &= 0.10 \\ k_{N_2\text{-hydrocarbon}} &= 0.10 \end{aligned}$$

Step 3 Adopting the procedure recommended by Petersen, Thomassen, and Fredenslund (1989), calculate the binary interaction coefficients between components heavier than methane (i.e., C₂, C₃, etc.) and the heptanes-plus fraction from

$$k_{C_n-C_{7+}} = 0.8k_{C_{(n-1)}-C_{7+}}$$

where n is the number of carbon atoms of component C_n ; for example,

Binary interaction coefficient between C_2 and C_{7+} : $k_{C_2-C_{7+}} = 0.8k_{C_1-C_{7+}}$

Binary interaction coefficient between C_3 and C_{7+} : $k_{C_3-C_{7+}} = 0.8k_{C_2-C_{7+}}$

Step 4 Determine the remaining k_{ij} from

$$k_{ij} = k_{i-C_{7+}} \left[\frac{(M_j)^5 - (M_i)^5}{(M_{C_{7+}})^5 - (M_i)^5} \right]$$

where M is the molecular weight of any specified component. For example, the binary interaction coefficient between propane, C_3 , and butane, C_4 , is

$$k_{C_3-C_4} = k_{C_3-C_{7+}} \left[\frac{(M_{C_4})^5 - (M_{C_3})^5}{(M_{C_{7+}})^5 - (M_{C_3})^5} \right]$$

A summary of the different equations of state discussed in this chapter are listed in the table below in the form of

$$p = p_{\text{repulsion}} - p_{\text{attraction}}$$

EOS	$p_{\text{repulsion}}$	$p_{\text{attraction}}$	a	b
Ideal	$\frac{RT}{V}$	0	0	0
vdW	$\frac{RT}{V-b}$	$\frac{a}{V^2}$	$\Omega_a \frac{R^2 T_c^2}{p_c}$	$\Omega_b \frac{RT_c}{p_c}$
RK	$\frac{RT}{V-b}$	$\frac{a}{V(V+b)\sqrt{T}}$	$\Omega_a \frac{R^2 T_c^{2.5}}{p_c}$	$\Omega_b \frac{RT_c}{p_c}$
SRK	$\frac{RT}{V-b}$	$\frac{a\alpha(T)}{V(V+b)}$	$\Omega_a \frac{R^2 T_c^2}{p_c}$	$\Omega_b \frac{RT_c}{p_c}$
PR	$\frac{RT}{V-b}$	$\frac{a\alpha(T)}{V(V+b) + b(V-b)}$	$\Omega_a \frac{R^2 T_c^2}{p_c}$	$\Omega_b \frac{RT_c}{p_c}$

Equation-of-State Applications

Most petroleum engineering applications rely on the use of the equation of state due to its simplicity, consistency, and accuracy when properly tuned. Cubic equations of state have found widespread acceptance as tools that permit the convenient and flexible calculation of the complex phase behavior of reservoir fluids. Some of these applications are presented in this section and include the determination of the equilibrium ratio, K_i ; dew-point pressure, p_d ; bubble-point pressure, p_b ; three-phase flash calculations; vapor pressure, p_v ; and PVT laboratory experiments.

Equilibrium Ratio, K_i

A flow diagram is presented in Figure 5–11 to illustrate the procedure of determining equilibrium ratios of a hydrocarbon mixture. For this type of calculation, the system temperature, T , the system pressure, p , and the overall composition of the mixture, z_i , must be known. The procedure is summarized in the following steps in conjunction with Figure 5–11.

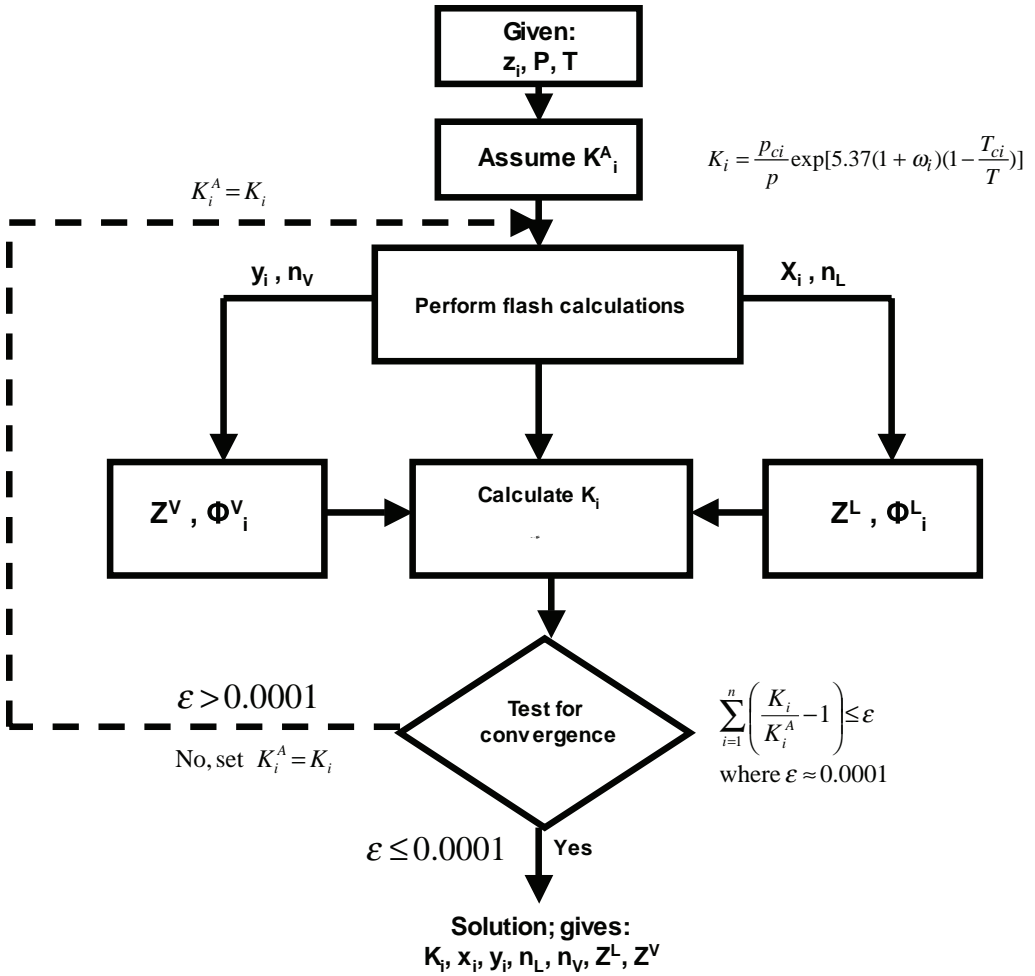


FIGURE 5-11 Flow diagram of equilibrium ratio determination by an EOS.

Step 1 Assume an initial value of the equilibrium ratio for each component in the mixture at the specified system pressure and temperature. Wilson’s equation can provide the starting values of K_i :

$$K_i^A = \frac{p_{ci}}{p} \exp[5.37 (1 + \omega_i) (1 - T_{ci} / T)]$$

where K_i^A is an assumed equilibrium ratio for component i .

Step 2 Using the overall composition and the assumed K -values, perform flash calculations to determine x_i , y_i , n_L , and n_v .

Step 3 Using the calculated composition of the liquid phase, x_i , determine the fugacity coefficient Φ_i^L for each component in the liquid phase by applying equation (5-117):

$$\ln(\Phi_i^L) = \frac{b_i(Z^L - 1)}{b_m} - \ln(Z^L - B) - \frac{A}{2\sqrt{2}B} \left[\frac{2\Psi_i}{(a\alpha)_m} - \frac{b_i}{b_m} \right] \ln \left[\frac{Z^L + (1 + \sqrt{2})B}{Z^L - (1 - \sqrt{2})B} \right]$$

Step 4 Repeat step 3 using the calculated composition of the gas phase, y_i , to determine Φ_i^v .

$$\ln(\Phi_i^L) = \frac{b_i(Z^v - 1)}{b_m} - \ln(Z^v - B) - \frac{A}{2\sqrt{2}B} \left[\frac{2\Psi_i}{(a\alpha)_m} - \frac{b_i}{b_m} \right] \ln \left[\frac{Z^v + (1 + \sqrt{2})B}{Z^v - (1 - \sqrt{2})B} \right]$$

Step 5 Calculate the new set of equilibrium ratios from

$$K_i = \frac{\Phi_i^L}{\Phi_i^v}$$

Step 6 Check for the solution by applying the following constraint:

$$\sum_{i=1}^n [K_i / K_i^A - 1]^2 \leq \epsilon$$

where ϵ = preset error tolerance, such as 0.0001, and n = number of components in the system.

If these conditions are satisfied, then the solution has been reached. If not, steps 1 through 6 are repeated using the calculated equilibrium ratios as initial values.

Dew-Point Pressure, p_d

A saturated vapor exists for a given temperature at the pressure at which an infinitesimal amount of liquid first appears. This pressure is referred to as the *dew-point pressure*, p_d . The dew-point pressure of a mixture is described mathematically by the following two conditions:

$$y_i = z_i, \text{ for } 1 \leq i \leq n \text{ and } n_v = 1 \quad (5-136)$$

$$\sum_{i=1}^n \left[\frac{z_i}{K_i} \right] = 1 \quad (5-137)$$

Applying the definition of K_i in terms of the fugacity coefficient to equation (5-137) gives

$$\sum_{i=1}^n \left[\frac{z_i}{k_i} \right] = \sum_{i=1}^n \left[\frac{z_i}{(\Phi_i^L / \Phi_i^v)} \right] = \sum_{i=1}^n \left[\left(\frac{z_i}{\Phi_i^L} \right) \frac{f_i^v}{z_i p_d} \right] = 1$$

or

$$p_d = \sum_{i=1}^n \left[\frac{f_i^v}{\Phi_i^L} \right]$$

This above equation is arranged to give

$$f(p_d) = \sum_{i=1}^n \left[\frac{f_i^v}{\Phi_i^L} \right] - p_d = 0 \quad (5-138)$$

where

p_d = dew-point pressure, psia

f_i^v = fugacity of component i in the vapor phase, psia

Φ_i^L = fugacity coefficient of component i in the liquid phase

Equation (5-35) can be solved for the dew-point pressure by using the Newton-Raphson iterative method. To use the iterative method, the derivative of equation (5-138) with respect to the dew-point pressure, p_d , is required. This derivative is given by the following expression:

$$\frac{\partial f}{\partial p_d} = \sum_{i=1}^n \left[\frac{\Phi_i^L (\partial f_i^v / \partial p_d) - f_i^v (\partial \Phi_i^L / \partial p_d)}{(\Phi_i^L)^2} \right] - 1 \quad (5-139)$$

The two derivatives in this equation can be approximated numerically as follows:

$$\frac{\partial f^v}{\partial p_d} = \left[\frac{f_i^v(p_d + \Delta p_d) - f_i^v(p_d - \Delta p_d)}{2\Delta p_d} \right] \quad (5-140)$$

and

$$\frac{\partial \Phi_i^L}{\partial p_d} = \left[\frac{\Phi_i^L(p_d + \Delta p_d) - \Phi_i^L(p_d - \Delta p_d)}{2\Delta p_d} \right] \quad (5-141)$$

where

Δp_d = pressure increment (e.g., 5 psia)

$f_i^v(p_d + \Delta p_d)$ = fugacity of component i at $(p_d + \Delta p_d)$

$f_i^v(p_d - \Delta p_d)$ = fugacity of component i at $(p_d - \Delta p_d)$

$\Phi_i^L(p_d + \Delta p_d)$ = fugacity coefficient of component i at $(p_d + \Delta p_d)$

$\Phi_i^L(p_d - \Delta p_d)$ = fugacity coefficient of component i at $(p_d - \Delta p_d)$

Φ_i^L = fugacity coefficient of component i at p_d

The computational procedure of determining p_d is summarized in the following steps.

Step 1 Assume an initial value for the dew-point pressure, p_d^A .

Step 2 Using the assumed value of p_d^A , calculate a set of equilibrium ratios for the mixture by using any of the previous correlations, such as Wilson's correlation.

Step 3 Calculate the composition of the liquid phase, that is, the composition of the droplets of liquid, by applying the mathematical definition of K_i , to give

$$x_i = \frac{z_i}{K_i}$$

It should be noted that $y_i = z_i$.

Step 4 Calculate p_d^A using the composition of the gas phase, z_i and Φ_i^L , using the composition of liquid phase, x_i , at the following three pressures:

1. p_d^A
2. $p_d^A + \Delta p_d$
3. $p_d^A - \Delta p_d$

where p_d^A is the assumed dew-point pressure and Δp_d is a selected pressure increment of 5 to 10 psi.

Step 5 Evaluate the function $f(p_d)$, that is, equation (5-138), and its derivative using equations (5-139) through (5-141).

Step 6 Using the values of the function $f(p_d)$ and the derivative $\partial f / \partial p_d$ as determined in step 5, calculate a new dew-point pressure by applying the Newton-Raphson formula:

$$p_d = p_d^A - f(p_d) / [\partial f / \partial p_d] \quad (5-142)$$

Step 7 The calculated value of p_d is checked numerically against the assumed value by applying the following condition:

$$|p_d - p_d^A| \leq 5$$

If this condition is met, then the correct dew-point pressure, p_d , has been found. Otherwise, steps 3 through 6 are repeated using the calculated p_d as the new value for the next iteration. A set of equilibrium ratios must be calculated at the new assumed dew-point pressure from

$$k_i = \frac{\Phi_i^L}{\Phi_i^V}$$

Bubble-Point Pressure, p_b

The bubble-point pressure, p_b , is defined as the pressure at which the first bubble of gas is formed. Accordingly, the bubble-point pressure is defined mathematically by the following equations:

$$y_i = z_i, \text{ for } 1 \leq i \leq n \text{ and } n_L = 1.0 \quad (5-143)$$

$$\sum_{i=1}^n [z_i K_i] = 1 \quad (5-144)$$

Introducing the concept of the fugacity coefficient into equation (5-144) gives

$$\sum_{i=1}^n \left[z_i \frac{\Phi_i^L}{\Phi_i^V} \right] = \sum_{i=1}^n \left[z_i \frac{\left(\frac{f_i^L}{z_i p_b} \right)}{\Phi_i^V} \right] = 1$$

Rearranging,

$$p_b = \sum_{i=1}^n \left[\frac{f_i^L}{\Phi_i^V} \right]$$

or

$$f(p_b) = \sum_{i=1}^n \left[\frac{f_i^L}{\Phi_i^V} - p_b \right] = 0 \quad (5-145)$$

The iteration sequence for calculation of p_b from the preceding function is similar to that of the dew-point pressure, which requires differentiating that function with respect to the bubble-point pressure:

$$\frac{\partial f}{\partial p_b} = \sum_{i=1}^n \left[\frac{\Phi_i^V (\partial f_i^L / \partial p_b) - f_i^L (\partial \Phi_i^V / \partial p_b)}{(\Phi_i^V)^2} \right] - 1 \quad (5-146)$$

The phase envelope can be constructed by either calculating the saturation pressures, p_b and p_d , as a function of temperature or calculating the bubble-point and dew-point temperatures at selected pressures. The selection to calculate a pressure or temperature depends on how steep or flat is the phase envelope at a given point. In terms of the slope of the envelope at a point, the criteria are

- Calculate the bubble-point or dew-point *pressure* if

$$\left| \frac{\partial \ln(p)}{\partial \ln(T)} \right| \approx \left| \frac{\ln(p_2) - \ln(p_1)}{\ln(T_2) - \ln(T_1)} \right| < 2$$

- Calculate the bubble-point or dew-point *temperature* if

$$\left| \frac{\partial \ln(p)}{\partial \ln(T)} \right| \approx \left| \frac{\ln(p_2) - \ln(p_1)}{\ln(T_2) - \ln(T_1)} \right| > 20$$

Three-Phase Equilibrium Calculations

Two- and three-phase equilibria occur frequently during the processing of hydrocarbon and related systems. Peng and Robinson (1976b) proposed a three-phase equilibrium calculation scheme of systems that exhibit a water-rich liquid phase, a hydrocarbon-rich liquid phase, and a vapor phase.

In applying the principle of mass conversation to 1 mole of a water-hydrocarbon in a three-phase state of thermodynamic equilibrium at a fixed temperature, T , and pressure, p , gives

$$n_L + n_w + n_v = 1 \quad (5-147)$$

$$n_L x_i + n_w x_{wi} + n_v y_i = z_i \quad (5-148)$$

$$\sum_i^n x_i = \sum_{i=1}^n x_{wi} = \sum_{i=1}^n y_i = \sum_{i=1}^n z_i = 1 \quad (5-149)$$

where

n_L, n_w, n_v = number of moles of the hydrocarbon-rich liquid, the water-rich liquid, and the vapor, respectively

x_i, x_{wi}, y_i = mole fraction of component i in the hydrocarbon-rich liquid, the water-rich liquid, and the vapor, respectively

The equilibrium relations between the compositions of each phase are defined by the following expressions:

$$K_i = \frac{y_i}{x_i} = \frac{\Phi_i^L}{\Phi_i^v} \quad (5-150)$$

and

$$K_{wi} = \frac{y_i}{x_{wi}} = \frac{\Phi_i^w}{\Phi_i^v} \quad (5-151)$$

where

K_i = equilibrium ratio of component i between vapor and hydrocarbon-rich liquid

K_{wi} = equilibrium ratio of component i between the vapor and water-rich liquid

Φ_i^L = fugacity coefficient of component i in the hydrocarbon-rich liquid

Φ_i^v = fugacity coefficient of component i in the vapor phase

Φ_i^w = fugacity coefficient of component i in the water-rich liquid

Combining equations (5-147) through (5-151) gives the following conventional non-linear equations:

$$\sum_{i=1} x_i = \sum_{i=1} \left[\frac{z_i}{n_L(1 - K_i) + n_w \left(\frac{K_i}{K_{wi}} - K_i \right) + K_i} \right] = 1 \quad (5-152)$$

$$\sum_{i=1} x_{wi} = \sum_{i=1} \left[\frac{z_i(K_i/K_{wi})}{n_L(1 - K_i) + n_w \left(\frac{K_i}{K_{wi}} - K_i \right) + K_i} \right] = 1 \quad (5-153)$$

$$\sum_{i=1} y_i = \sum_{i=1} \left[\frac{z_i K_i}{n_L(1 - K_i) + n_w \left(\frac{K_i}{K_{wi}} - K_i \right) + K_i} \right] = 1 \quad (5-154)$$

Assuming that the equilibrium ratios between phases can be calculated, these equations are combined to solve for the two unknowns, n_L and n_w , and hence x_p , x_{wi} , and y_i . The nature of the specific equilibrium calculation is what determines the appropriate combination of equations (5-152) through (5-154). The combination of these three expressions then can be used to determine the phase and volumetric properties of the three-phase system.

There are essentially three types of phase behavior calculations for the three-phase system: bubble-point prediction, dew-point prediction, and flash calculation. Peng and Robinson (1980) proposed the following combination schemes of equations (5-152) through (5-154).

For the bubble-point pressure determination,

$$\sum_i x_i - \sum_i x_{wi} = 0$$

and

$$\left[\sum_i y_i \right] - 1 = 0$$

Substituting equations (5-152) through (5-154) in these relationships gives

$$f(n_L, n_w) = \sum_i \left[\frac{z_i(1 - K_i/K_{wi})}{n_L(1 - K_i) + n_w(K_i/K_{wi} - K_i) + K_i} \right] = 0 \quad (5-155)$$

and

$$g(n_L, n_w) = \sum_i \left[\frac{z_i K_i}{n_L(1 - K_i) + n_w(K_i/K_{wi} - K_i) + K_i} \right] - 1 = 0 \quad (5-156)$$

For the dew-point pressure,

$$\sum_i x_{wi} - \sum_i y_i = 0$$

$$\left[\sum_i x_i \right] - 1 = 0$$

Combining with equations (5-152) through (5-154) yields

$$f(n_L, n_w) = \sum_i \left[\frac{z_i K_i (1/K_{wi} - 1)}{n_L (1 - K_i) + n_w (K_i/K_{wi} - K_i) + K_i} \right] = 0 \quad (5-157)$$

and

$$g(n_L, n_w) = \sum_i \left[\frac{z_i}{n_L (1 - K_i) + n_w (K_i/K_{wi} - K_i) + K_i} \right] - 1 = 0 \quad (5-158)$$

For flash calculations,

$$\sum_i x_i - \sum_i y_i = 0$$

$$\left[\sum_i x_{wi} \right] - 1 = 0$$

or

$$f(n_L, n_w) = \sum_i \left[\frac{z_i (1 - K_i)}{n_L (1 - K_i) + n_w (K_i/K_{wi} - K_i) + K_i} \right] = 0 \quad (5-159)$$

and

$$g(n_L, n_w) = \sum_i \left[\frac{z_i K_i / K_{wi}}{n_L (1 - K_i) + n_w (K_i/K_{wi} - K_i) + K_i} \right] - 1.0 = 0 \quad (5-160)$$

Note that, in performing any of these property predictions, we always have two unknown variables, n_L and n_w , and between them, two equations. Providing that the equilibrium ratios and the overall composition are known, the equations can be solved simultaneously using the appropriate iterative technique, such as the Newton-Raphson method. The application of this iterative technique for solving equations (5-159) and (5-160) is summarized in the following steps.

Step 1 Assume initial values for the unknown variables n_L and n_w .

Step 2 Calculate new values of n_L and n_w by solving the following two linear equations:

$$\begin{bmatrix} n_L \\ n_w \end{bmatrix}^{\text{new}} = \begin{bmatrix} n_L \\ n_w \end{bmatrix} - \begin{bmatrix} \partial f / \partial n_L & \partial f / \partial n_w \\ \partial g / \partial n_L & \partial g / \partial n_w \end{bmatrix}^{-1} \begin{bmatrix} f(n_L, n_w) \\ g(n_L, n_w) \end{bmatrix}$$

where $f(n_L, n_w)$ = value of the function $f(n_L, n_w)$ as expressed by equation (5-159) and $g(n_L, n_w)$ = value of the function $g(n_L, n_w)$ as expressed by equation (5-160).

The first derivative of these functions with respect to n_L and n_w is given by the following expressions:

$$\begin{aligned} (\partial f / \partial n_L) &= \sum_{i=1} \left\{ \frac{-z_i (1 - K_i)^2}{[n_L (1 - K_i) + n_w (K_i/K_{wi} - K_i) + K_i]^2} \right\} \\ (\partial f / \partial n_w) &= \sum_{i=1} \left\{ \frac{-z_i (1 - K_i)(K_i/K_{wi} - K_i)}{[n_L (1 - K_i) + n_w (K_i/K_{wi} - K_i) + K_i]^2} \right\} \end{aligned}$$

$$\begin{aligned} (\partial g / \partial n_L) &= \sum_{i=1} \left\{ \frac{-z_i (K_i / K_{wi}) (1 - K_i)}{[n_L (1 - K_i) + n_w (K_i / K_{wi} - K_i) + K_i]^2} \right\} \\ (\partial g / \partial n_w) &= \sum_{i=1} \left\{ \frac{-z_i (K_i K_{wi}) (K_i / K_{wi} - K_i)}{[n_L (1 - K_i) + n_w (K_i / K_{wi} - K_i) + K_i]^2} \right\} \end{aligned}$$

Step 3 The new calculated values of n_L and n_w then are compared with the initial values. If no changes in the values are observed, then the correct values of n_L and n_w have been obtained. Otherwise, the steps are repeated with the new calculated values used as initial values.

Peng and Robinson (1980) proposed two modifications when using their equation of state for three-phase equilibrium calculations. The first modification concerns the use of the parameter α as expressed by equation (5-113) for the water compound. Peng and Robinson suggested that, when the reduced temperature of this compound is less than 0.85, the following equation is applied:

$$\alpha_w = [1.0085677 + 0.82154(1 - T_{rw}^{0.5})]^2 \quad (5-161)$$

where T_{rw} is the reduced temperature of the water component; that is, $T_{rw} = T/T_{cw}$.

The second important modification of the PR EOS is the introduction of alternative mixing rules and new interaction coefficients for the parameter ($a\alpha$). A temperature-dependent binary interaction coefficient was introduced into the equation, to give:

$$(a\alpha)_{\text{water}} = \sum_i \sum_j [x_{wi} x_{wj} (a_i a_j \alpha_i \alpha_j)^{0.5} (1 - \tau_{ij})] \quad (5-162)$$

where τ_{ij} = temperature-dependent binary interaction coefficient and x_{wi} = mole fraction of component i in the water phase.

Peng and Robinson proposed graphical correlations for determining this parameter for each aqueous binary pair. Lim et al. (1984) expressed these graphical correlations mathematically by the following generalized equation:

$$\tau_{ij} = a_1 \left[\frac{T}{T_{ci}} \right]^2 \left[\frac{p_{ci}}{p_{cj}} \right] + a_2 \left[\frac{T}{T_{ci}} \right] \left[\frac{p_{ci}}{p_{cj}} \right] + a_3 \quad (5-163)$$

where

T = system temperature, °R

T_{ci} = critical temperature of the component of interest, °R

p_{ci} = critical pressure of the component of interest, psia

p_{cj} = critical pressure of the water compound, psia

Values of the coefficients a_1 , a_2 , and a_3 of this polynomial are given in the table below for selected binaries.

Component i	a_1	a_2	a_3
C ₁	0	1.659	-0.761
C ₂	0	2.109	-0.607
C ₃	-18.032	9.441	-1.208
n-C ₄	0	2.800	-0.488
n-C ₆	49.472	-5.783	-0.152

For selected nonhydrocarbon components, values of interaction parameters are given by the following expressions.

For N_2 - H_2O binary,

$$\tau_{ij} = 0.402(T/T_{ci}) - 1.586 \quad (5-164)$$

where τ_{ij} = binary parameter between nitrogen and the water compound and T_{ci} = critical temperature of nitrogen, °R.

For CO_2 - H_2O binary,

$$\tau_{ij} = -0.074 \left[\frac{T}{T_{ci}} \right]^2 + 0.478 \left[\frac{T}{T_{ci}} \right] - 0.503 \quad (5-165)$$

where T_{ci} is the critical temperature of CO_2 .

In the course of making phase equilibrium calculations, it is always desirable to provide initial values for the equilibrium ratios so the iterative procedure can proceed as reliably and rapidly as possible. Peng and Robinson adopted Wilson's equilibrium ratio correlation to provide initial K -values for the hydrocarbon/vapor phase:

$$K_i = \frac{p_{ci}}{p} \exp \left[5.3727(1 + \omega_i) \left(1 - \frac{T_{ci}}{T} \right) \right]$$

While for the water-vapor phase, Peng and Robinson proposed the following expression for K_{wi} :

$$K_{wi} = 10^6 [p_{ci} T / (T_{ci} p)]$$

Vapor Pressure, p_v

The calculation of the vapor pressure of a pure component through an equation of state usually is made by the same trial-and-error algorithms used to calculate vapor-liquid equilibria of mixtures. Soave (1972) suggests that the van der Waals (vdW), Soave-Redlich-Kwong (SRK), and the Peng-Robinson (PR) equations of state can be written in the following generalized form:

$$p = \frac{RT}{V - b} - \frac{a\alpha}{V^2 + uVb + wb^2} \quad (5-166)$$

with

$$a = \Omega_a \frac{R^2 T_c^2}{p_c}$$

$$b = \Omega_b \frac{RT_c}{p_c}$$

where the values of u , w , Ω_a , and Ω_b for three different equations of state are given in the table below.

EOS	u	w	Ω_a	Ω_b
vdW	0	0	0.421875	0.125
SRK	1	0	0.42748	0.08664
PR	2	-1	0.45724	0.07780

Soave introduced the reduced pressure, p_r , and reduced temperature, T_r , to these equations, to give

$$A = \frac{a\alpha p}{R^2 T^2} = \Omega_a \frac{\alpha p_r}{T_r} \quad (5-167)$$

$$B = \frac{bp}{RT} = \Omega_b \frac{p_r}{T_r} \quad (5-168)$$

and

$$\frac{A}{B} = \frac{\Omega_a}{\Omega_b} \left(\frac{\alpha}{T_r} \right) \quad (5-169)$$

where

$$\begin{aligned} p_r &= p/p_c \\ T_r &= T/T_c \end{aligned}$$

In the cubic form and in terms of the Z -factor, the three equations of state can be written as

$$\text{vdW: } Z^3 - Z^2(1 + B) + ZA - AB = 0$$

$$\text{SRK: } Z^3 - Z^2 + Z(A - B - B^2) - AB = 0$$

$$\text{PR: } Z^3 - Z^2(1 - B) + Z(A - 3B^2 - 2B) - (AB - B^2 - B^3) = 0$$

And the *pure component* fugacity coefficient is given by

$$\text{vdW: } \ln\left(\frac{f^o}{p}\right) = Z - 1 - \ln(Z - B) - \frac{A}{Z}$$

$$\text{SRK: } \ln\left(\frac{f^o}{p}\right) = Z - 1 - \ln(Z - B) - \left(\frac{A}{B}\right) \ln\left(1 + \frac{B}{Z}\right)$$

$$\text{PR: } \ln\left(\frac{f^o}{p}\right) = Z - 1 - \ln(Z - B) - \left(\frac{A}{2\sqrt{2}B}\right) \ln\left[\frac{Z + (1 + \sqrt{2})B}{Z - (1 - \sqrt{2})B}\right]$$

A typical iterative procedure for the calculation of pure component vapor pressure at any temperature, T , through one of these EOS is summarized next.

Step 1 Calculate the reduced temperature; that is, $T_r = T/T_c$.

Step 2 Calculate the ratio A/B from equation (5-169).

Step 3 Assume a value for B .

Step 4 Solve the selected equation of state, such as SRK EOS, to obtain Z^L and Z , that is, smallest and largest roots, for both phases.

Step 5 Substitute Z^L and Z^v into the pure component fugacity coefficient and obtain $\ln(f^o/p)$ for both phases.

Step 6 Compare the two values of f/p . If the isofugacity condition is not satisfied, assume a new value of B and repeat steps 3 through 6.

Step 7 From the final value of B , obtain the vapor pressure from equation (5-168):

$$B = \Omega_b \frac{(p_v / p_c)}{T_r}$$

Solving for p_v gives

$$p_v = \frac{BT_r p_c}{\Omega_b}$$

Simulation of Laboratory PVT Data by Equations of State

Before attempting to use an EOS-based compositional model in a full-field simulation study, it is essential the selected equation of state is capable of achieving a satisfactory match between EOS results and all the available PVT test data. It should be pointed out that an equation of state generally is not predictive without tuning its parameters to match the relevant experimental data. Several PVT laboratory tests were presented in Chapter 4 and are repeated here for convenience to illustrate the procedure of applying an EOS to simulate these experiments, including

- Constant-volume depletion.
- Constant-composition expansion.
- Differential liberation.
- Flash separation tests.
- Composite liberation.
- Swelling tests.
- Compositional gradients.
- Minimum-miscibility pressure.

Constant-Volume Depletion Test

A reliable prediction of the pressure depletion performance of a gas-condensate reservoir is necessary in determining reserves and evaluating field-separation methods. The predicted performance is also used in planning future operations and studying the economics of projects for increasing liquid recovery by gas cycling. Such predictions can be performed with aid of the experimental data collected by conducting constant-volume-depletion (CVD) tests on gas condensates. These tests are performed on a reservoir fluid sample in such a manner as to simulate depletion of the actual reservoir, assuming that retrograde liquid appearing during production remains *immobile* in the reservoir.

The CVD test provides five important laboratory measurements that can be used in a variety of reservoir engineering predictions:

1. Dew-point pressure.
2. Composition changes of the gas phase with pressure depletion.
3. Compressibility factor at reservoir pressure and temperature.
4. Recovery of original in-place hydrocarbons at any pressure.

5. Retrograde condensate accumulation, that is, liquid saturation.

The laboratory procedure of the CVD test (with immobile condensate), as shown schematically in Figure 5–12, is summarized in the following steps.

Step 1 A measured amount m of a representative sample of the original reservoir fluid with a known overall composition of z_i is charged to a visual PVT cell at the dew-point pressure, p_d (section A). The temperature of the PVT cell is maintained at the reservoir temperature, T , throughout the experiment. The initial volume, V_i , of the saturated fluid is used as a reference volume.

Step 2 The initial gas compressibility factor is calculated from the real gas equation:

$$Z_{\text{dew}} = \frac{p_d V_i}{n_i R T} \quad (5-170)$$

with

$$n_i = \frac{m}{M_a}$$

where

p_d = dew-point pressure, psia

V_i = initial gas volume, ft³

n_i = initial number of moles of the gas

M_a = apparent molecular weight, lb/lb-mole

m = mass of the initial gas in place, lb

R = gas constant, 10.73

T = temperature, °R

z_d = compressibility factor at dew-point pressure

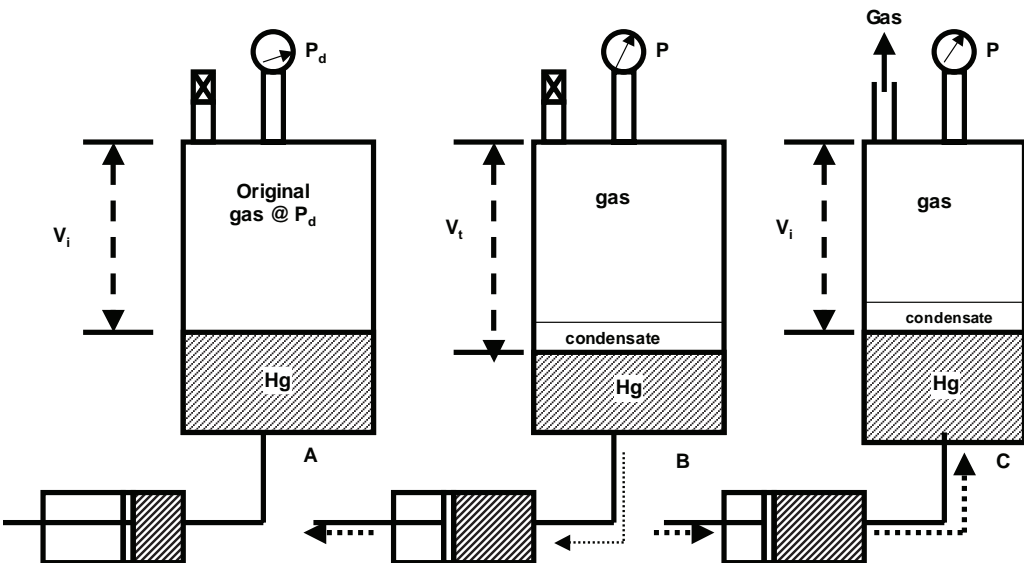


FIGURE 5–12 Schematic illustration of the CVD test.

with the gas initially in place as expressed in standard units, scf, given by

$$G = 379.4n_i \quad (5-171)$$

Step 3 The cell pressure is reduced from the saturation pressure to a predetermined level, p . This can be achieved by withdrawing mercury from the cell, as illustrated in Figure 5-12, section B. During the process, a second phase (retrograde liquid) is formed. The fluid in the cell is brought to equilibrium and the total volume, V_t , and volume of the retrograde liquid, V_L , are visually measured. This retrograde volume is reported as a percent of the initial volume, V_i :

$$S_L = \left(\frac{V_L}{V_i} \right) 100$$

This value can be translated into condensate saturation in the presence of water saturation by

$$S_o = (1 - S_w)S_L/100$$

Step 4 Mercury is reinjected into the PVT cell at constant pressure p while an equivalent volume of gas is removed. When the initial volume, V_i , is reached, mercury injection ceases, as illustrated in Figure 5-12, section C. The volume of the removed gas is measured at the cell conditions and recorded as $(V_{gp})_{p,T}$. This step simulates a reservoir producing only gas, with retrograde liquid *remaining immobile* in the reservoir.

Step 5 The removed gas is charged to analytical equipment, where its composition, y_i , is determined and its volume is measured at standard conditions and recorded as $(V_{gp})_{sc}$. The corresponding moles of gas produced can be calculated from the expression:

$$n_p = \frac{(V_{gp})_{sc}}{379.4} \quad (5-172)$$

where n_p = moles of gas produced and $(V_{gp})_{sc}$ = volume of gas produced measured at standard conditions, scf.

Step 6 The compressibility factor of the gas phase at cell pressure and temperature is calculated by

$$Z = \frac{V_{\text{actual}}}{V_{\text{ideal}}} = \frac{(V_{gp})_{p,T}}{V_{\text{ideal}}} \quad (5-173)$$

where

$$V_{\text{ideal}} = \frac{RTn_p}{p}$$

Combining equations (5-172) and (5-173) and solving for the compressibility factor Z gives

$$Z = \frac{379.4p(V_{gp})_{p,T}}{RT(V_{gp})_{sc}} \quad (5-174)$$

Another property, the *two-phase compressibility factor*, also is calculated. The two-phase Z -factor represents the total compressibility of all the remaining fluid (gas and retrograde liquid) in the cell and is computed from the real gas law as

$$Z_{\text{two-phase}} = \frac{pV_i}{(n_i - n_p)(RT)} \quad (5-175)$$

where

$(n_i - n_p)$ = represents the remaining moles of fluid in the cell

n_i = initial moles in the cell

n_p = cumulative moles of gas removed

Step 7 The volume of gas produced as a percentage of gas initially in place is calculated by dividing the cumulative volume of the produced gas by the gas initially in place, both at standard conditions:

$$\%G_p = \left[\frac{\sum (V_{gp})_{sc}}{G} \right] 100 \quad (5-176)$$

Equivalently as

$$\%G_p = \left[\frac{\sum n_p}{(n_i)_{\text{original}}} \right] 100$$

This experimental procedure is repeated several times, until a minimum test pressure is reached, after which the quantity and composition of the gas and retrograde liquid remaining in the cell are determined.

This test procedure also can be conducted on a volatile oil sample. In this case, the PVT cell initially contains liquid, instead of gas, at its bubble-point pressure.

Simulation of the CVD Test by EOS

In the absence of the CVD test data on a specific gas-condensate system, predictions of pressure-depletion behavior can be obtained by using any of the well-established equations of state to compute the phase behavior when the composition of the total gas-condensate system is known. The stepwise computational procedure using the Peng-Robinson EOS as a representative equation of state now is summarized in conjunction with the flow diagram shown in Figure 5-13.

Step 1 Assume that the original hydrocarbon system with a total composition z_i occupies an initial volume of 1 ft³ at the dew-point pressure p_d and system temperature T :

$$V_i = 1$$

Step 2 Using the initial gas composition, calculate the gas compressibility factor Z_{dew} at the dew-point pressure from equation (5-115):

$$Z^3 + (B - 1)Z^2 + (A - 3B^2 - 2B)Z - (AB - B^2 - B^3) = 0$$

Step 3 Calculate the initial moles in place by applying the real gas law:

$$n_i = \frac{(1)(p_d)}{Z_{\text{dew}} RT} \quad (5-177)$$

where p_d = dew-point pressure, psi, and Z_{dew} = gas compressibility factor at the dew-point pressure.

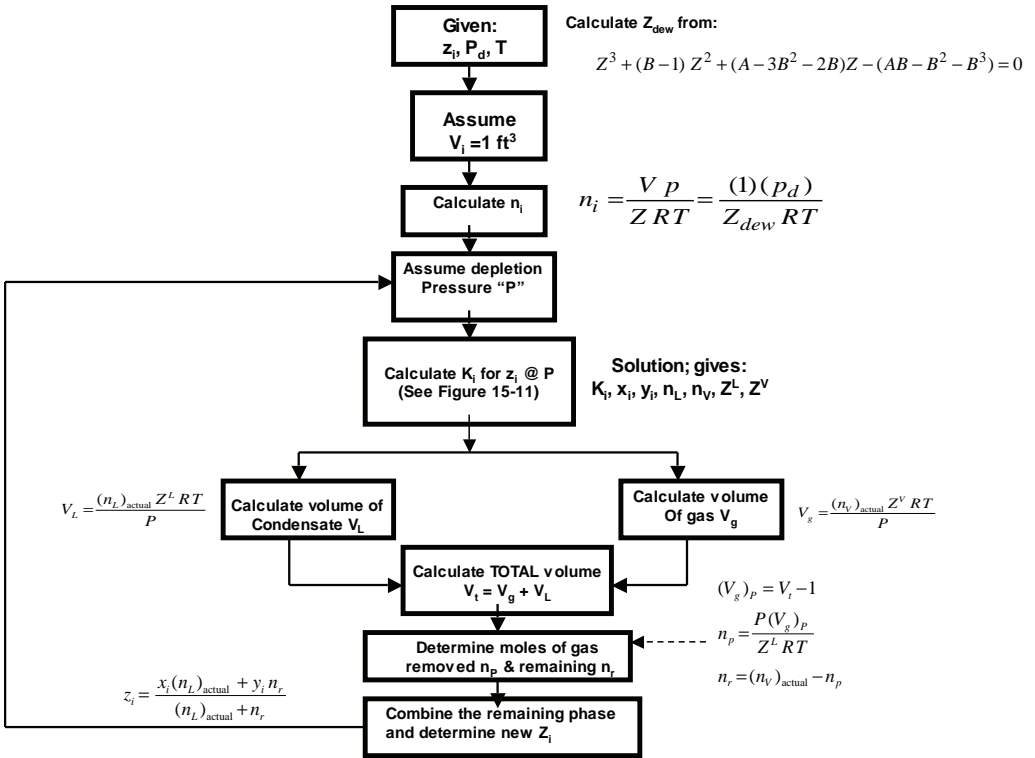


FIGURE 5-13 Flow diagram for EOS simulating a CVD test.

Step 4 Reduce the pressure to a predetermined value p . At this pressure level, the equilibrium ratios (K -values) are calculated from EOS. Results of the calculation at this stage include

- Equilibrium ratios (K -values).
- Composition of the liquid phase (i.e., retrograde liquid), x_i .
- Moles of the liquid phase, n_L .
- Composition of the gas phase, y_i .
- Moles of the gas phase, n_V .
- Compressibility factor of the liquid phase, Z^L .
- Compressibility factor of the gas phase, Z^V .

The composition of the gas phase, y_i , should reasonably match the experimental gas composition at pressure, p .

Step 5 Because flash calculations, as part of the K -value results, are usually performed assuming the total moles are equal to 1, calculate the actual moles of the liquid and gas phases from

$$(n_L)_{actual} = n_i n_L \quad (5-178)$$

$$(n_V)_{actual} = n_i n_V \quad (5-179)$$

where n_L and n_V are moles of liquid and gas, respectively, as determined from flash calculations.

Step 6 Calculate the volume of each hydrocarbon phase by applying the expression

$$V_L = \frac{(n_L)_{\text{actual}} Z^L RT}{p} \quad (5-180)$$

$$V_g = \frac{(n_v)_{\text{actual}} Z^v RT}{p} \quad (5-181)$$

where

V_L = volume of the retrograde liquid, ft³/ft³

V_g = volume of the gas phase, ft³/ft³

Z^L, Z^v = compressibility factors of the liquid and gas phase

T = cell (reservoir) temperature, °R

Since $V_i = 1$, then

$$S_L = (V_L)100$$

This value should match the experimental value if the equation of state is properly tuned.

Step 7 Calculate the total volume of fluid in the cell:

$$V_t = V_L + V_g \quad (5-182)$$

where V_t = total volume of the fluid, ft³.

Step 8 Since the volume of the cell is constant at 1 ft³, remove the following excess gas volume from the cell:

$$(V_{gp})_{p,T} = V_t - 1 \quad (5-183)$$

Step 9 Calculate the number of moles of gas removed:

$$n_p = \frac{p(V_{gp})_{p,T}}{Z^v RT} \quad (5-184)$$

Step 10 Calculate cumulative gas produced as a percentage of gas initially in place by dividing cumulative moles of gas removed, $\sum n_p$ by the original moles in place:

$$\%G_p = \left[\frac{\sum (n_p)}{(n_i)_{\text{original}}} \right] 100$$

Step 11 Calculate the two-phase gas deviation factor from the relationship:

$$Z_{\text{two-phase}} = \frac{(p)(1)}{(n_i - n_p)RT} \quad (5-185)$$

Step 12 Calculate the remaining moles of gas $(n_v)_r$ by subtracting the moles produced (n_p) from the actual number of moles of the gas phase $(n_v)_{\text{actual}}$:

$$(n_v)_r = (n_v)_{\text{actual}} - n_p \quad (5-186)$$

Step 13 Calculate the new total moles and new composition remaining in the cell by applying the molal and component balances, respectively:

$$n_i = (n_L)_{\text{actual}} + (n_v)_r, \quad (5-187)$$

$$z_i = \frac{x_i(n_L)_{\text{actual}} + y_i(n_v)_r}{n_i} \quad (5-188)$$

Step 14 Consider a new lower pressure and repeat steps 4 through 13.

Constant-Composition Expansion Test

Constant-composition expansion experiments, commonly called *pressure/volume tests*, are performed on gas condensates or crude oil to simulate the pressure/volume relations of these hydrocarbon systems. The test is conducted for the purposes of determining

- Saturation pressure (bubble-point or dew-point pressure).
- Isothermal compressibility coefficients of the single-phase fluid in excess of saturation pressure.
- Compressibility factors of the gas phase.
- Total hydrocarbon volume as a function of pressure.

The experimental procedure, shown schematically in Figure 5–14, involves placing a hydrocarbon fluid sample (oil or gas) in a visual PVT cell at reservoir temperature and a pressure in excess of the initial reservoir pressure (Figure 5–14, section A). The pressure is reduced in steps at constant temperature by removing mercury from the cell, and the change in the hydrocarbon volume, V , is measured for each pressure increment. The saturation pressure (bubble-point or dew-point pressure) and the corresponding volume are observed and recorded (Figure 5–14, section B). The volume at the saturation pressure is used as a reference

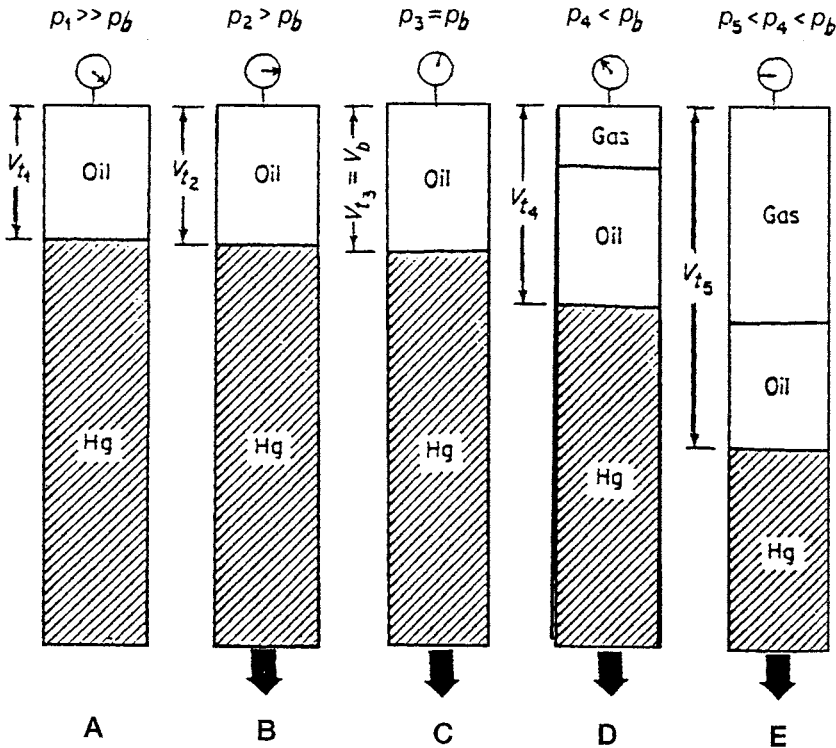


FIGURE 5–14 Schematic illustration of the constant-composition expansion test.

volume. At pressure levels higher than the saturation pressure, the volume of the hydrocarbon system is recorded as a ratio of the reference volume. This volume, commonly termed the *relative volume*, is expressed mathematically by the following equation:

$$V_{\text{rel}} = \frac{V}{V_{\text{sat}}} \quad (5-189)$$

where

V_{rel} = relative volume

V = volume of the hydrocarbon system

V_{sat} = volume at the saturation pressure

Also, above the saturation pressure, the isothermal compressibility coefficient of the single-phase fluid usually is determined from the expression

$$c = -\frac{1}{V_{\text{rel}}} \left[\frac{\partial V_{\text{rel}}}{\partial p} \right]_T \quad (5-190)$$

where c = isothermal compressibility coefficient, psi^{-1} .

For gas-condensate systems, the gas compressibility factor, Z , is determined in addition to the preceding experimentally determined properties.

Below the saturation pressure, the two-phase volume, V_t , is measured relative to the volume at saturation pressure and expressed as

$$\text{Relative total volume} = \frac{V_t}{V_{\text{sat}}} \quad (5-191)$$

where V_t = total hydrocarbon volume.

Note that no hydrocarbon material is removed from the cell, therefore, the composition of the total hydrocarbon mixture in the cell remains fixed at the original composition.

Simulation of the Constant Composition Expansion Test by EOS

The simulation procedure utilizing the Peng-Robinson equation of state is illustrated in the following steps.

Step 1 Given the total composition of the hydrocarbon system, z_i , and saturation pressure (p_b for oil systems, p_d for gas systems), calculate the total volume occupied by 1 mole of the system. This volume corresponds to the reference volume V_{sat} (volume at the saturation pressure). Mathematically, the volume is calculated from the relationship

$$V_{\text{sat}} = \frac{(1)ZRT}{p_{\text{sat}}} \quad (5-192)$$

where

V_{sat} = volume of saturation pressure, ft^3/mole

p_{sat} = saturation pressure (dew-point or bubble-point pressure), psia

T = system temperature, $^{\circ}\text{R}$

Z = compressibility factor, Z^L or Z^v depending on the type of system

Step 2 The pressure is increased in steps above the saturation pressure, where the single phase still exists. At each pressure, the compressibility factor, Z^L or Z^v , is calculated by solving equation (5-115) and used to determine the fluid volume.

$$V = \frac{(1)ZRT}{p}$$

where

V = compressed liquid or gas volume at the pressure level p , ft³/mole

Z = compressibility factor of the compressed liquid or gas, Z^L or Z^v

p = system pressure, $p > p_{\text{sat}}$, psia

R = gas constant; 10.73 psi ft³/lb-mol °R

The corresponding relative phase volume, V_{rel} , is calculated from the expression

$$V_{\text{rel}} = \frac{V}{V_{\text{sat}}}$$

Step 3 The pressure is then reduced in steps *below* the saturation pressure p_{sat} , where two phases are formed. The equilibrium ratios are calculated and flash calculations are performed at each pressure level. Results of the calculation at each pressure level include K_i , x_i , y_i , n_L , n_v , Z^v , and Z^L . Since no hydrocarbon material is removed during pressure depletion, the original moles ($n_i = 1$) and composition, z_i , remain constant. The volumes of the liquid and gas phases can then be calculated from the expressions

$$V_L = \frac{(1)(n_L)Z^L RT}{p} \quad (5-193)$$

$$V_g = \frac{(1)(n_v)Z^v RT}{p} \quad (5-194)$$

and

$$V_t = V_L + V_g$$

where

n_L , n_v = moles of liquid and gas as calculated from flash calculations

Z^L , Z^v = liquid and gas compressibility factors

V_t = total volume of the hydrocarbon system

Step 4 Calculate the relative total volume from the following expression:

$$\text{Relative total volume} = \frac{V_t}{V_{\text{sat}}}$$

Differential Liberation Test

The test is carried out on reservoir oil samples and involves charging a visual PVT cell with a liquid sample at the bubble-point pressure and reservoir temperature, as described in detail in Chapter 4. The pressure is reduced in steps, usually 10 to 15 pressure levels, and all the liberated gas is removed and its volume, G_p , is measured under standard conditions. The volume of oil remaining, V_L , also is measured at each pressure level. Note that the remaining oil is subjected to continual compositional changes as it becomes progressively richer in the heavier components.

This procedure is continued to atmospheric pressure, where the volume of the residual (remaining) oil is measured and converted to a volume at 60°F, V_{sc} . The differential oil formation volume factors B_{od} (commonly called the *relative oil volume factors*) at all the various pressure levels are calculated by dividing the recorded oil volumes, V_L , by the volume of residual oil V_{sc} :

$$B_{od} = \frac{V_L}{V_{sc}}$$

(5-195)

The differential solution gas/oil ratio R_{sd} is calculated by dividing the volume of gas in the solution by the residual oil volume. Typical laboratory results of the test are shown in the following table and in Figures 5-15 and 5-16.

Pressure (psig)	Solution GOR,* R_{sd}	Relative-Oil Volume, B_{od} **
2620	854	1.600
2350	763	1.554
2100	684	1.515
1850	612	1.479
1600	544	1.445
1350	479	1.412
1100	416	1.382
850	354	1.351
600	292	1.320
350	223	1.283
159	157	1.244
0	0	1.075
0	0	at 60°F = 1.000

*Cubic feet of gas at 14.65 psia and 60°F per barrel of residual oil at 60°F.
**Barrels of oil at indicated pressure and temperature per barrel of residual oil at 60°F.

It should be pointed out that reporting the experimental data relative to the residual oil volume at 60°F (as shown graphically in Figure 5-15) gives the relative-oil volume curve the appearance of the formation volume factor curve, leading to its misuse in reservoir calculations. Moses suggested that a better method of reporting these data is in the form of a shrinkage curve, as shown in Figure 5-17. The relative-oil volume data in Figure 5-15 and the table above can be converted to a shrinkage curve by dividing each relative-oil volume factor B_{od} by the relative-oil volume factor at the bubble point, B_{odb} :

$$S_{od} = \frac{B_{od}}{B_{odb}}$$

(5-196)

where

- B_{od} = differential relative-oil volume factor at pressure p , bbl/STB
- B_{odb} = differential relative-oil volume factor at the bubble-point pressure, p_b , psia, bbl/STB
- S_{od} = differential oil shrinkage factor, bbl/bbl, of bubble-point oil

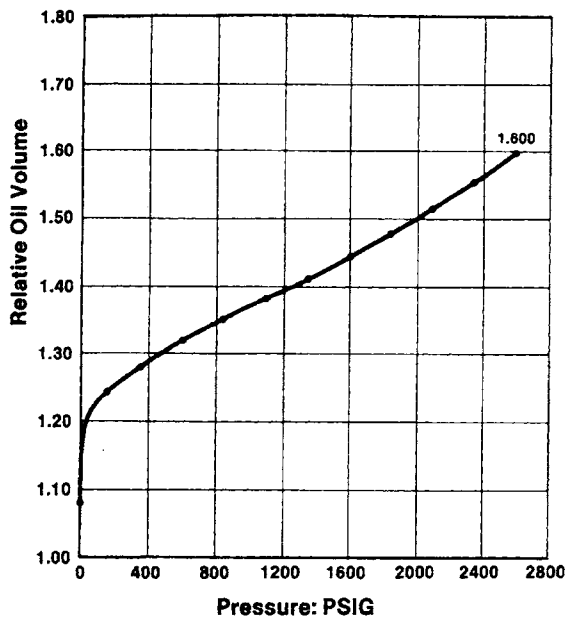


FIGURE 5-15 *Relative-oil volume versus pressure.*

Source: P. Moses, "Engineering Applications of Phase Behavior of Crude Oil and Condensate Systems," *Journal of Petroleum Technology* (July 1980). Reproduced by permission of the Society of Petroleum Engineers of AIME, © SPE-AIME.

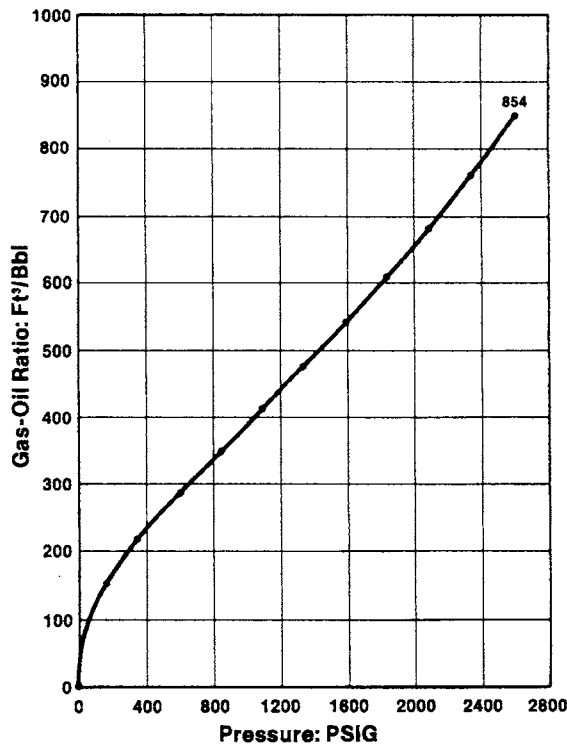


FIGURE 5-16 *Gas/oil ratio versus pressure.*

Source: P. Moses, "Engineering Applications of Phase Behavior of Crude Oil and Condensate Systems," *Journal of Petroleum Technology* (July 1980). Reproduced by permission of the Society of Petroleum Engineers of AIME, © SPE-AIME.

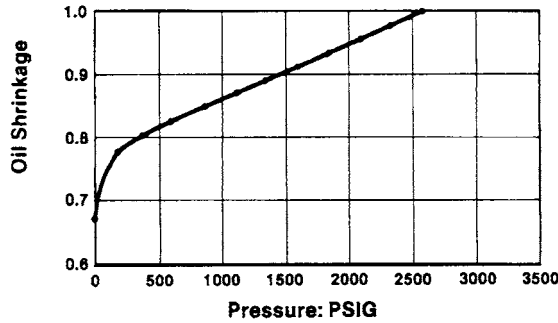


FIGURE 5-17 Oil shrinkage curve.

Source: P. Moses, "Engineering Applications of Phase Behavior of Crude Oil and Condensate Systems," *Journal of Petroleum Technology* (July 1980). Reproduced by permission of the Society of Petroleum Engineers of AIME, © SPE-AIME.

The shrinkage curve has a value of 1 at the bubble point and a value less than 1 at subsequent pressures below p_b . In this suggested form, the shrinkage describes the changes in the volume of the bubble-point oil as reservoir pressure declines.

The results of the differential liberation test, when combined with the results of the flash separation test, provide a means of calculating the oil formation volume factors and gas solubility as a function of reservoir pressure. These calculations are outlined in the next section.

Simulation of the Differential Liberation Test by EOS

The simulation procedure of the test by the Peng-Robinson EOS is summarized in the following steps and in conjunction with the flow diagram shown in Figure 5-18.

Step 1 Starting with the saturation pressure, p_{sat} , and reservoir temperature, T , calculate the volume occupied by a total of 1 mole, that is, $n_i = 1$, of the hydrocarbon system with an overall composition of z_i . This volume, V_{sat} , is calculated by applying equation (5-192):

$$V_{\text{sat}} = \frac{(1)ZRT}{p_{\text{sat}}}$$

Step 2 Reduce the pressure to a predetermined value of p at which the equilibrium ratios are calculated and used in performing flash calculations. The actual number of moles of the liquid phase, with a composition of x_i , and the actual number of moles of the gas phase, with a composition of y_i , then are calculated from the expressions

$$\begin{aligned} (n_L)_{\text{actual}} &= n_i n_L \\ (n_v)_{\text{actual}} &= n_i n_v \end{aligned}$$

where

$$\begin{aligned} (n_L)_{\text{actual}} &= \text{actual number of moles of the liquid phase} \\ (n_v)_{\text{actual}} &= \text{actual number of moles of the gas phase} \\ n_L, n_v &= \text{number of moles of the liquid and gas phases as computed by performing flash calculations} \end{aligned}$$

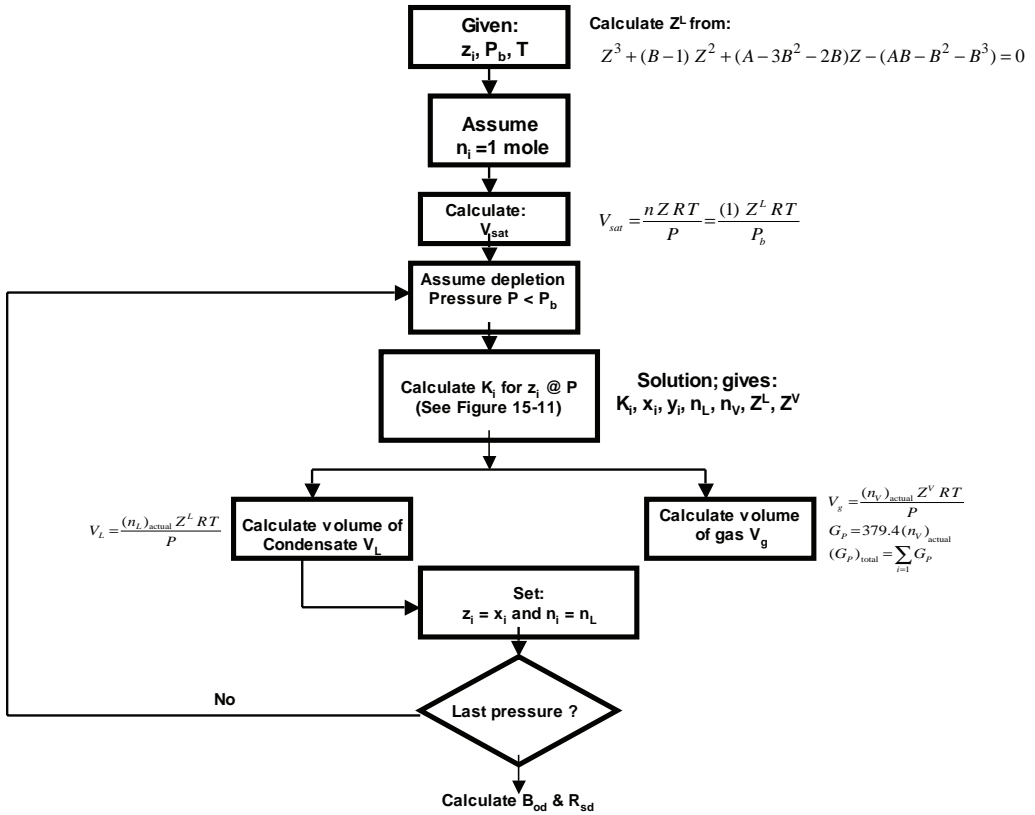


FIGURE 5-18 Flow diagram for EOS simulating the DE test.

Step 3 Determine the volume of the liquid and gas phase from

$$V_L = \frac{Z^L RT (n_L)_{actual}}{p} \quad (5-197)$$

$$V_g = \frac{Z^v RT (n_v)_{actual}}{p} \quad (5-198)$$

where V_L, V_g = volumes of the liquid and gas phases, ft^3 , and Z^L, Z^v = compressibility factors of the liquid and gas phases. The volume of the produced (liberated) solution gas as measured at standard conditions is determined from the relationship

$$G_p = 379.4 (n_v)_{actual} \quad (5-199)$$

where G_p = gas produced during depletion pressure p , scf.

The total cumulative gas produced at any depletion pressure, p , is the cumulative gas liberated from the crude oil sample during the pressure reduction process (sum of all the liberated gas from previous pressures and current pressure) as calculated from the expression

$$(G_p)_p = \sum_{P_{sat}}^p G_p$$

where $(G_p)_p$ is the cumulative produced solution gas at pressure level p .

Step 4 Assume that all the equilibrium gas is removed from contact with the oil. This can be achieved mathematically by setting the overall composition, z_i , equal to the composition of the liquid phase, x_i , and setting the total moles equal to the liquid phase:

$$z_i = x_i$$

$$n_i = (n_L)_{\text{actual}}$$

Step 5 Using the new overall composition and total moles, steps 2 through 4 are repeated. When the depletion pressure reaches the atmospheric pressure, the temperature is changed to 60°F and the residual-oil volume is calculated. This residual-oil volume, calculated by equation (5-197), is referred to as V_{sc} . The total volume of gas that evolved from the oil and produced $(G_p)_{\text{Total}}$ is the sum of the all-liberated gas including that at atmospheric pressure:

$$(G_p)_{\text{Total}} = \sum_{P_{\text{sat}}}^{14.7} G_p$$

Step 6 The calculated volumes of the oil and removed gas then are divided by the residual-oil volume to calculate the relative-oil volumes (B_{od}) and the solution GOR at all the selected pressure levels from

$$B_{od} = \frac{V_L}{V_{sc}} \quad (5-200)$$

$$R_{sd} = \frac{(5.615)(\text{remaining gas in solution})}{V_{sc}} = \frac{(5.615)[(G_p)_{\text{Total}} - (G_p)_p]}{V_{sc}}$$

Flash Separation Tests

Flash separation tests, commonly called *separator tests*, are conducted to determine the changes in the volumetric behavior of the reservoir fluid as the fluid passes through the separator (or separators) and then into the stock tank. The resulting volumetric behavior is influenced to a large extent by the operating conditions, that is, pressures and temperatures of the surface separation facilities. The primary objective of conducting separator tests, therefore, is to provide the essential laboratory information necessary for determining the optimum surface separation conditions, which in turn maximize the stock-tank oil production. In addition, the results of the test, when appropriately combined with the differential liberation test data, provide a means of obtaining the PVT parameters (B_o , R_s , and B_v) required for petroleum engineering calculations. The laboratory procedure of the flash separation test involves the following steps.

Step 1 The oil sample is charged into a PVT cell at reservoir temperature and its bubble-point pressure.

Step 2 A small amount of the oil sample, with a volume of $(V_o)_{pb}$, is removed from the PVT cell at constant pressure and flashed through a multistage separator system, with each separator at a fixed pressure and temperature. The gas liberated from each stage (separator) is removed and its volume and specific gravity measured. The volume of the remaining oil in the last stage (stock-tank condition) is recorded as $(V_o)_{st}$.

Step 3 The total solution gas/oil ratio and the oil formation volume factor at the bubble-point pressure are then calculated:

$$B_{\text{ofb}} = (V_o)_{\text{pb}} / (V_o)_{\text{st}} \quad (5-201)$$

$$R_{\text{sfb}} = (V_g)_{\text{sc}} / (V_o)_{\text{st}} \quad (5-202)$$

where

B_{ofb} = bubble-point oil formation volume factor, as measured by flash liberation, bbl of the bubble-point oil/STB

R_{sfb} = bubble-point solution gas/oil ratio, as measured by flash liberation, scf/STB

$(V_g)_{\text{sc}}$ = total volume of gas removed from separators, scf

Steps 1 through 3 are repeated at a series of different separator pressures and a fixed temperature.

A typical example of a set of separator tests for a two-stage separation is shown in the table below. By examining the laboratory results reported in the table, it should be noted that the optimum separator pressure is 100 psia, considered to be the separator pressure that results in the minimum oil formation volume factor.

Separator Pressure (psig)	Temperature (°F)	GOR, R_{sfb} *	Stock-Tank Oil Gravity (°API at 60°F)	FVF, B_{ofb} **
50	75	737	40.5	1.481
to 0	75	41		
		$\Sigma = 778$		
100	75	676	40.7	1.474
to 0	75	92		
		$\Sigma = 768$		
200	75	602	40.4	1.483
to 0	75	178		
		$\Sigma = 780$		
300	75	549	40.1	1.495
to 0	75	246		
		$\Sigma = 795$		

*GOR in cubic feet of gas at 14.65 psia and 60°F per barrel of stock-tank oil at 60°F.

**FVF in barrels of saturated oil at 2620 psig and 220°F per barrel of stock-tank oil at 60°F.

Amyx, Bass, and Whiting (1960) and Dake (1978) proposed a procedure for constructing the oil formation volume factor and gas solubility curves by using the differential liberation data (as shown in the table on p. 418) in conjunction with the experimental separator flash data (as shown in the table above) for a given set of separator conditions. The procedure calls for multiplying the flash oil formation factor at the bubble point, B_{ofb} (as defined by equation 5-201) by the differential oil shrinkage factor S_{od} (as defined by equation 5-196) at various reservoir pressures. Mathematically, this relationship is expressed as follows:

$$B_o = B_{\text{ofb}} S_{\text{od}} \quad (5-203)$$

where

B_o = oil formation volume factor, bbl/STB

B_{ofb} = bubble-point oil formation volume factor, bbl of the bubble-point oil/STB

S_{od} = differential oil shrinkage factor, bbl/bbl of bubble-point oil

Amyx et al. and Dake proposed the following expression for adjusting the differential gas solubility data, R_{sd} , to give the required gas solubility factor, R_s :

$$R_s = R_{\text{sfb}} - (R_{\text{sdb}} - R_{\text{sd}}) \frac{B_{\text{ofb}}}{B_{\text{odb}}} \quad (5-204)$$

where

R_s = gas solubility, scf/STB

R_{sfb} = bubble-point solution gas/oil ratio as defined by equation (5-202), scf/STB

R_{sdb} = solution gas/oil at the bubble-point pressure as measured by the differential liberation test, scf/STB

R_{sd} = solution gas/oil ratio at various pressure levels as measured by the differential liberation test, scf/STB

These adjustments typically produce lower formation volume factors and gas solubilities than the differential liberation data. This adjustment procedure is illustrated graphically in Figures 5-19 and 5-20.

Example 5-7 shows how the separator test can be simulated mathematically by applying the concept of equilibrium ratios. The same procedure can be applied using equations of state.

Composite Liberation Test

The laboratory procedures for conducting the differential liberation and flash liberation tests for the purpose of generating B_o and R_s versus p relationships are considered approximations to the actual relationships. Another type of test, called a *composite liberation test*, has been suggested by Dodson, Goodwill, and Mayer (1953) and represents a combination of differential and flash liberation processes. The laboratory test, commonly called the

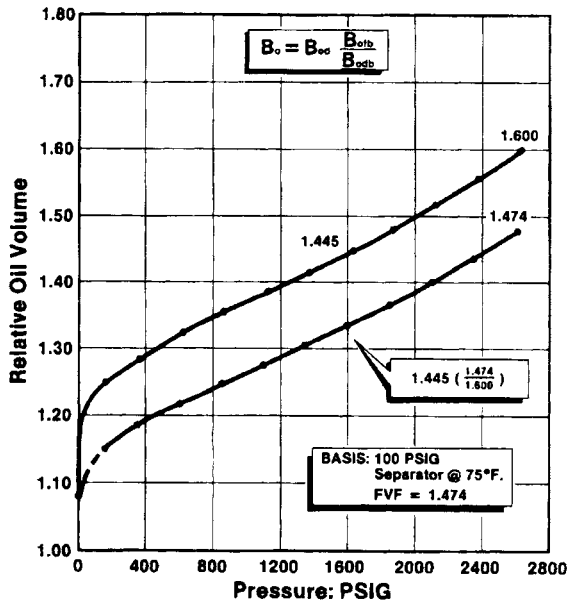


FIGURE 5-19 Adjustment of oil volume curve to separator conditions.

Source: P. Moses, "Engineering Applications of Phase Behavior of Crude Oil and Condensate Systems," *Journal of Petroleum Technology* (July 1980). Reproduced by permission of the Society of Petroleum Engineers of AIME, © SPE-AIME.

Dodson test, provides a better means of describing the PVT relationships. The experimental procedure for this composite liberation, as proposed by Dodson et al., is summarized in the following steps.

Step 1 A large representative fluid sample is placed into a cell at a pressure higher than the bubble-point pressure of the sample. The temperature of the cell then is raised to reservoir temperature.

Step 2 The pressure is reduced in steps by removing mercury from the cell, and the change in the oil volume is recorded. The process is repeated until the bubble point of the hydrocarbon is reached.

Step 3 A carefully measured small volume of oil is removed from the cell at constant pressure and flashed at temperatures and pressures equal to those in the surface separators and stock tank. The liberated gas volume and stock-tank oil volume are measured. The oil formation volume factor, B_o , and gas solubility, R_s , then are calculated from the measured volumes:

$$B_o = (V_o)_{p,T} / (V_o)_{st} \quad (5-205)$$

$$R_s = (V_g)_{sc} / (V_o)_{st} \quad (5-206)$$

where

$(V_o)_{p,T}$ = volume of oil removed from the cell at constant pressure p

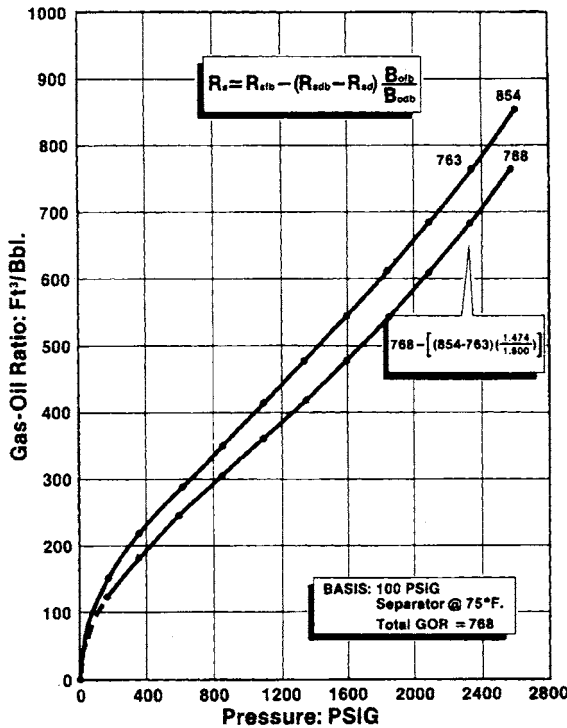


FIGURE 5-20 Adjustment of gas-in-solution curve to separator conditions.

Source: P. Moses, "Engineering Applications of Phase Behavior of Crude Oil and Condensate Systems," *Journal of Petroleum Technology* (July 1980). Reproduced by permission of the Society of Petroleum Engineers of AIME, © SPE-AIME.

$(V_g)_{sc}$ = total volume of the liberated gas as measured under standard conditions
 $(V_o)_{st}$ = volume of the stock-tank oil

Step 4 The volume of the oil remaining in the cell is allowed to expand through a pressure decrement and the gas evolved is removed, as in the differential liberation.

Step 5 Following the gas removal, step 3 is repeated and B_o and R_s calculated.

Step 6 Steps 3 through 5 are repeated at several progressively lower reservoir pressures to secure a complete PVT relationship.

Note that this type of test, while more accurately representing the PVT behavior of complex hydrocarbon systems, is more difficult and costly to perform than other liberation tests. Consequently, these experiments usually are not included in a routine fluid property analysis.

Simulation of the Composite Liberation Test by EOS

The stepwise computational procedure for simulating the composite liberation test using the Peng-Robinson EOS is summarized next in conjunction with the flow chart shown in Figure 5–21.

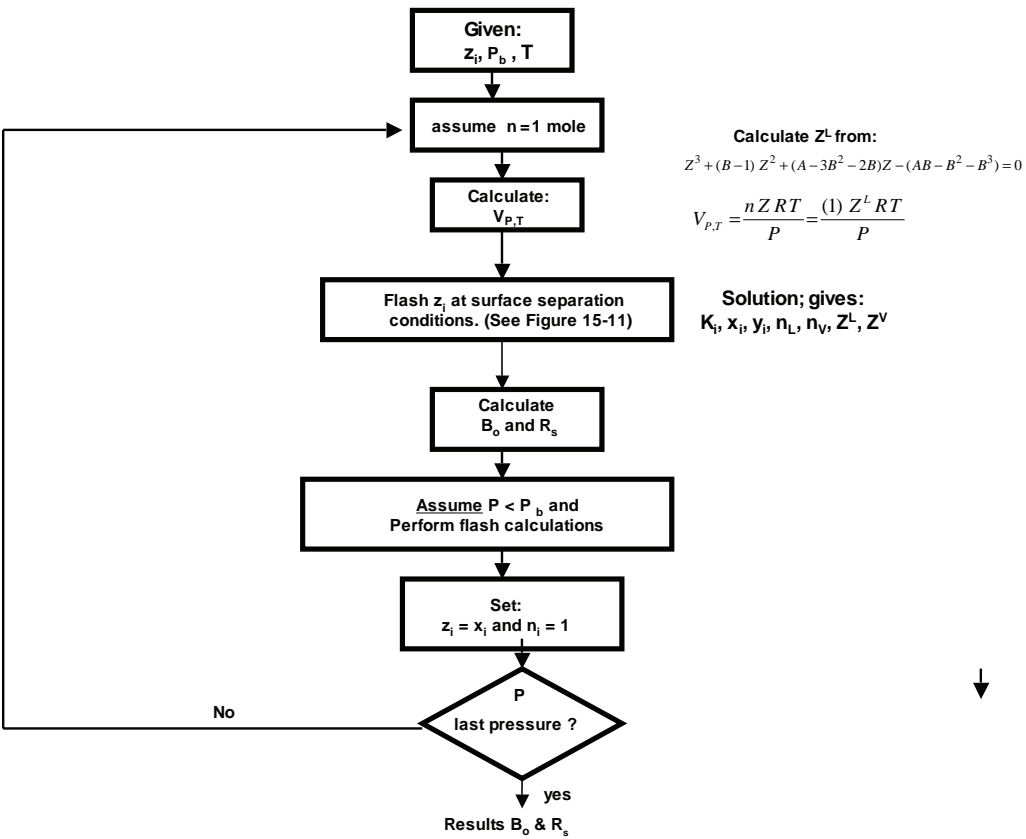


FIGURE 5–21 Flow chart for EOS simulating the composite liberation test.

Step 1 Assume a large reservoir fluid sample with an overall composition of z_i is placed in a cell at the bubble-point pressure, p_b , and reservoir temperature, T .

Step 2 Remove 1 lb-mole $n_i = 1$, of the liquid from the cell and calculate the corresponding volume at p_b and T by applying the Peng-Robinson EOS to estimate the liquid compressibility factor, Z^L :

$$(V_o)_{p,T} = \frac{(1)Z^L RT}{p_b} \quad (5-207)$$

where $(V_o)_{p,T}$ = volume of 1 mole of the oil, ft^3 .

Step 3 Flash the resulting volume (step 2) at temperatures and pressures equal to those in the surface separators and stock tank. Designating the resulting total liberated gas volume $(V_g)_{sc}$ and the volume of the stock-tank oil $(V_o)_{st}$, calculate the B_o and R_s by applying equations (5-205) and (5-206), respectively:

$$B_o = (V_o)_{p,T} / (V_o)_{st}$$

$$R_s = (V_g)_{sc} / (V_o)_{st}$$

Step 4 Set the cell pressure to a lower pressure level, p , and using the original composition z_i , generate the K_i values through the application of the PR EOS.

Step 5 Perform flash calculations based on z_i and the calculated k_i values.

Step 6 To simulate the differential liberation step of removing the equilibrium liberated gas from the cell at constant pressure, simply set the overall composition, z_i , equal to the mole fraction of the equilibrium liquid, x_i , and the bubble-point pressure, p_b , equal to the new pressure level, p . Mathematically, this step is summarized by the following relationships:

$$z_i = x_i$$

$$p_b = p$$

Step 7 Repeat steps 2 through 6.

Swelling Tests

Swelling tests should be preformed if a reservoir is to be depleted under gas injection or a dry gas cycling scheme. The swelling test can be conducted on gas condensate or crude oil samples. The purpose of this laboratory experiment is to determine the degree to which the proposed injection gas will dissolve in the hydrocarbon mixture. The data that can be obtained during a test of this type include

- The relationship of saturation pressure and volume of gas injected.
- The volume of the saturated fluid mixture compared to the volume of the original saturated fluid.

The test procedure, as shown schematically in Figure 5-22, is summarized in the following steps.

Step 1 A representative sample of the hydrocarbon mixture with a known overall composition, z_i , is charged to a visual PVT cell at saturation pressure and reservoir temperature.

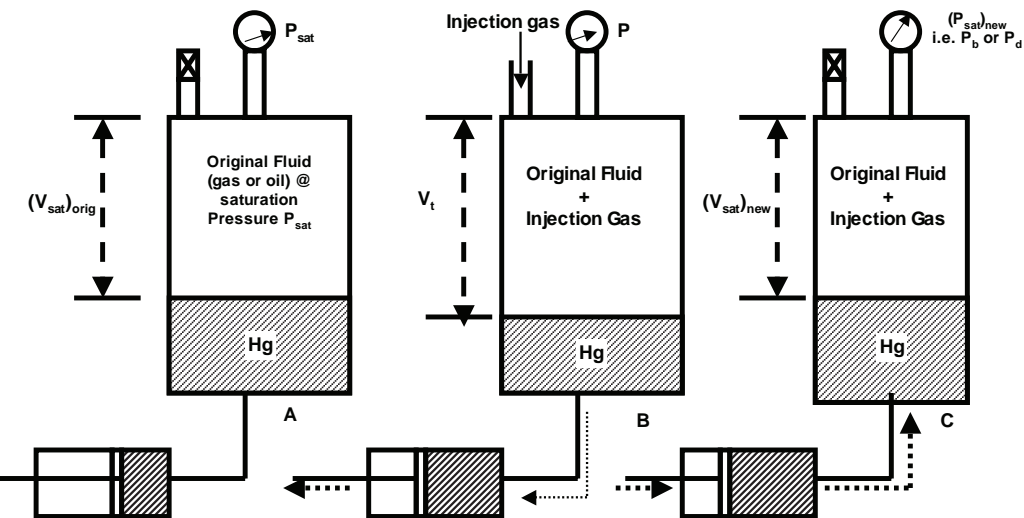


FIGURE 5–22 Schematic illustration of the swelling test.

The volume at the saturation pressure is recorded and designated $(V_{\text{sat}})_{\text{orig}}$. This step is illustrated schematically in Figure 5–22, section A.

Step 2 A predetermined volume of gas with a composition similar to the proposed injection gas is added to the hydrocarbon mixture. The cell is pressured up until only one phase is present, as shown in Figure 5–22, section B. The new saturation pressure and volume are recorded and designated p_s and V_{sat} , respectively. The original saturation volume is used as a reference value and the results are presented as relative total volumes:

$$V_{\text{rel}} = V_{\text{sat}} / (V_{\text{sat}})_{\text{orig}}$$

where V_{rel} = relative total volume and $(V_{\text{sat}})_{\text{orig}}$ = original saturation volume.

Step 3 Repeat step 2 until the mole percent of the injected gas in the fluid sample reaches a preset value (around 80%).

Typical laboratory results of a gas-condensate swelling test with lean gas of a composition given in Table 5–1 is shown numerically in Table 5–2 and graphically in Figures 5–23 and 5–24. The dew-point pressure behavior, as a function of the cumulative lean gas injected, is shown in Table 5–2. Note by examining Table 5–1 that the injection of lean gas into the reservoir fluid caused the dew-point pressure of the mixture to increase above the original dew point. Each addition of injection gas caused the dew-point pressure and the

TABLE 5–1 Composition of the Lean Gas

Component	y_i
CO ₂	0.0000
N ₂	0.0000
C ₁	0.9468
C ₂	0.0527
C ₃	0.0005

TABLE 5-2 Solubility and Swelling Test at 200°F

Cumulative Gas Injected, scf/STB	Swollen Volume, bbl/bbl	Dew-Point Pressure, psig
0	1.0000	3428
190	1.1224	3635
572	1.3542	4015
1523	1.9248	4610
2467	2.5043	4880

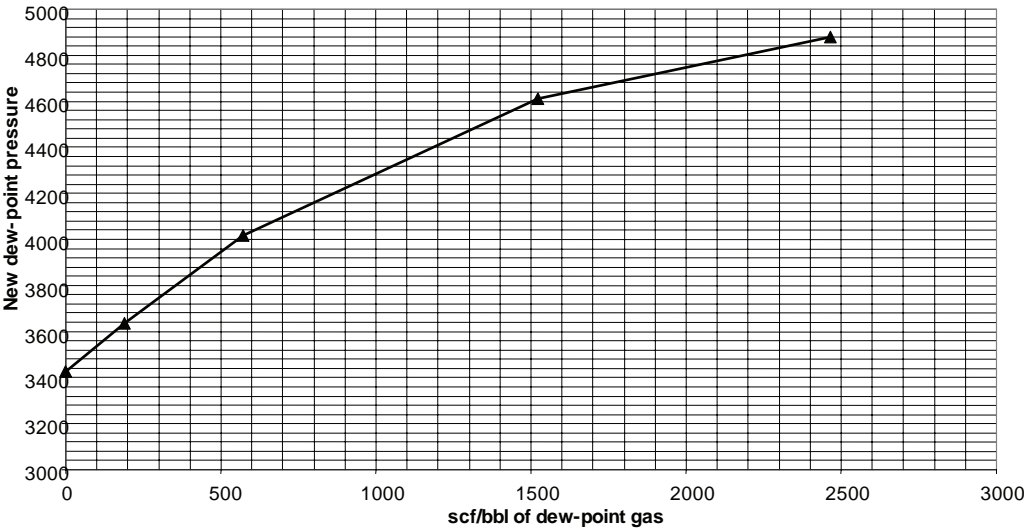


FIGURE 5-23 Dew-point pressure during swelling of reservoir gas with lean gas at 200°F.

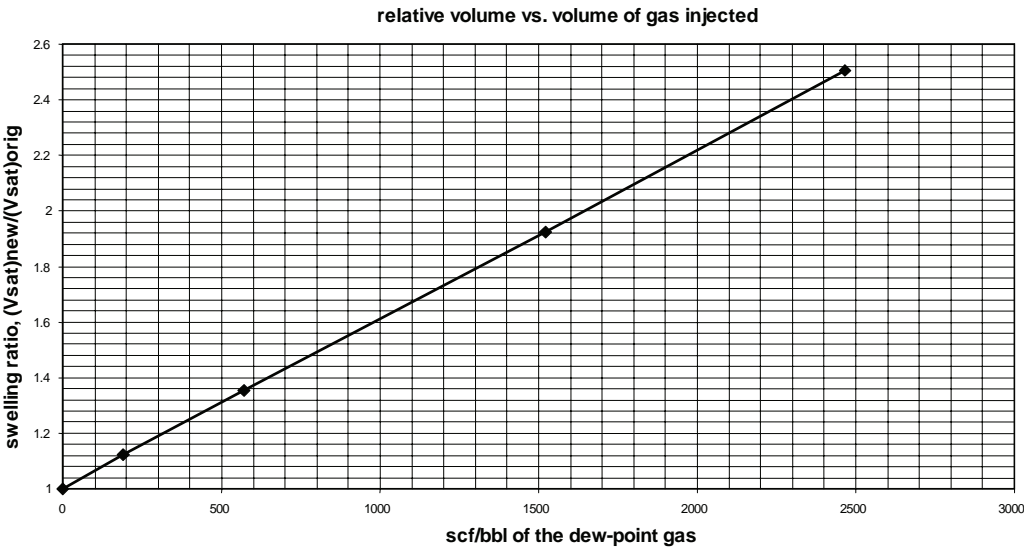


FIGURE 5-24 Reservoir gas swelling with lean gas at 200°F, expressed in terms of relative volume versus volume of gas injected.

relative volume (swollen volume) to increase. The dew point increased from 3428 to 4880 psig and relative total volume from 1 to 2.5043 after the final addition, as shown in Figures 5–23 and 5–24, respectively.

Simulation of the Swelling Test by EOS

The simulation procedure of the swelling test by the PR EOS is summarized in the following steps.

Step 1 Assume the hydrocarbon system occupies a total volume of 1 bbl at the saturation pressure, p_s , and reservoir temperature, T . Calculate the initial moles of the hydrocarbon system from the following expression:

$$n_i = \frac{5.615 p_{\text{sat}}}{ZRT}$$

where

n_i = initial moles of the hydrocarbon system

p_{sat} = saturation pressure, that is, p_b or p_d , depending on the type of the hydrocarbon system, psia

Z = gas or liquid compressibility factor

Step 2 Given the composition y_{inj} of the proposed injection gas, add a predetermined volume (as measured in scf) of the injection gas to the original hydrocarbon system and calculate the new overall composition by applying the molal and component balances, respectively:

$$n_t = n_i + n_{\text{inj}},$$

$$z_i = \frac{y_{\text{inj}} n_{\text{inj}} + (z_{\text{sat}})_i n_i}{n_t}$$

with

$$n_{\text{inj}} = \frac{V_{\text{inj}}}{379.4}$$

where

n_{inj} = total moles of the injection gas

V_{inj} = volume of the injection gas, scf

$(z_{\text{sat}})_i$ = mole fraction of component i in the saturated hydrocarbon system

Step 3 Using the new composition, z_i , calculate the new saturation pressure, p_b or p_d , using the Peng-Robinson EOS as outlined in this chapter.

Step 4 Calculate the relative total volume (swollen volume) by applying the relationship

$$V_{\text{rel}} = \frac{Z n_t RT}{5.615 p_{\text{sat}}}$$

where V_{rel} = swollen volume and p_{sat} = saturation pressure.

Step 5 Steps 2 through 4 are repeated until the last predetermined volume of the lean gas is combined with the original hydrocarbon system.

Compositional Gradients

Vertical compositional variation within a reservoir is expected during early reservoir life. One might expect the reservoir fluids to have attained equilibrium at maturity due to molecular diffusion and mixing over geological time. However, the diffusive mixing may require many tens of million years to eliminate compositional heterogeneities. When the reservoir is considered mature, it often is assumed that fluids are at equilibrium at uniform temperature and pressure and the thermal and gravitational equilibrium are established, which lead to the uniformity of each component fugacity throughout all the coexisting phases. For a single phase, the uniformity of fugacity is equivalent to the uniformity of concentration.

The pressure and temperature, however, are not uniform throughout a reservoir. The temperature increases with depth with a gradient of about 1°F/100 ft. The pressure also changes according to the hydrostatic head of fluid in the formation. Therefore, compositional variations within a reservoir, particularly those with a tall column of fluid, should be expected. Table 5–3 shows the fluid compositional variation of a North Sea reservoir at different depths.

TABLE 5–3 *Variations in Fluid Composition with Depth in a Reservoir*

Fluid	D, Well 1	C, Well 2	B, Well 2	A, Well 2
Depth (meters subsea)	3136	3156	3181	3217
Nitrogen	0.65	0.59	0.60	0.53
Carbon dioxide	2.56	2.48	2.46	2.44
Methane	72.30	64.18	59.12	54.92
Ethane	8.79	8.85	8.18	9.02
Propane	4.83	5.60	5.50	6.04
i-Butane	0.61	0.68	0.66	0.74
n-Butane	1.79	2.07	2.09	2.47
n-Pentane	0.75	0.94	1.09	1.33
Hexanes	0.86	1.24	1.49	1.71
Heptanes	1.13	2.14	3.18	3.15
Octanes	0.92	2.18	2.75	2.96
Nonanes	0.54	1.51	1.88	2.03
Decanes	0.28	0.91	1.08	1.22
Undecanes-plus	3.49	6.00	9.25	10.62
Molecular weight	33.1	43.6	55.4	61.0
Undecanes-plus characteristics				
Molecular weight	260	267	285	290
Specific gravity	0.8480	0.8625	0.8722	0.8768

Note that the methane concentration decreases from 72.30 mole% to 54.92 mole% over a depth interval of only 81 meters. Such a major change in composition cannot be ignored, as it strongly affects the estimation of reserves and production planning.

In general, the mixture is expected to get richer in heavier compounds, containing less of light components such as methane, with depth. The variations in the composition and

temperature of fluid with depth result in changes of saturation pressure with depth. The oil saturation pressure generally decreases with decreasing methane concentration, whereas the gas condensate dew point increases with increasing heavy fractions.

The compositional gradients, as shown in Table 5–3, can be used to locate the gas/oil contact (GOC). As shown in Figure 5–25, the GOC is defined as the depth at which the fluid system changes from a mixture with a dew point, that is, gas, to a mixture with a bubble point, oil. This may occur at a saturated condition, in which the GOC “gas” is in thermodynamic equilibrium with the GOC “oil” at the gas/oil contact reservoir pressure. By this definition, the following equality applies:

$$p_b = p_d = p_{\text{GOC}}$$

where

p_b = bubble-point pressure

p_d = dew-point pressure

p_{GOC} = reservoir pressure at GOC

Figure 5–26 shows an undersaturated GOC that describes the transition from dew-point gas to bubble-point oil through a “critical” or “new-critical” mixture with critical temperatures that equal the reservoir temperature. However, the critical pressure of this critical GOC mixture is lower than reservoir pressure. Hoier and Whitson (2001) termed the gas/oil contact *undersaturated GOC*.

Hoier and Whitson (2001) point out that composition variation with depth can result for several reasons, including:

1. Gravity segregates the heaviest components toward the bottom of the structure and lighter components toward the top of the structure. The lightest and heaviest com-

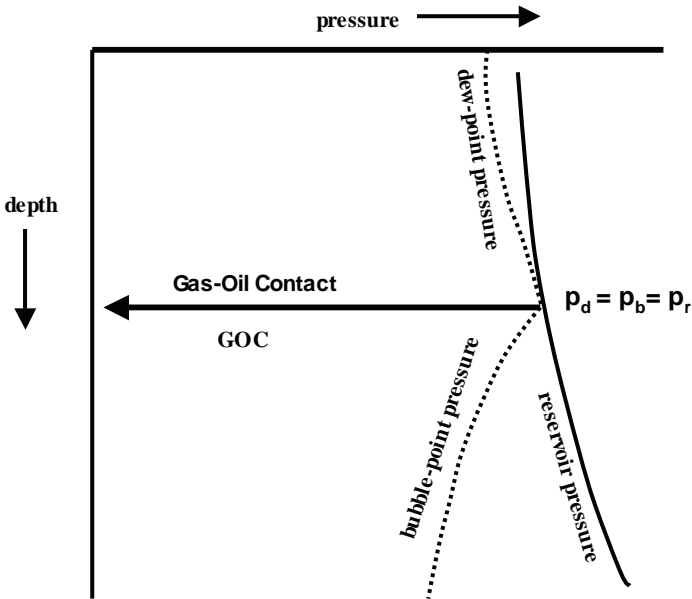


FIGURE 5–25 Determination of GOC from pressure gradients.

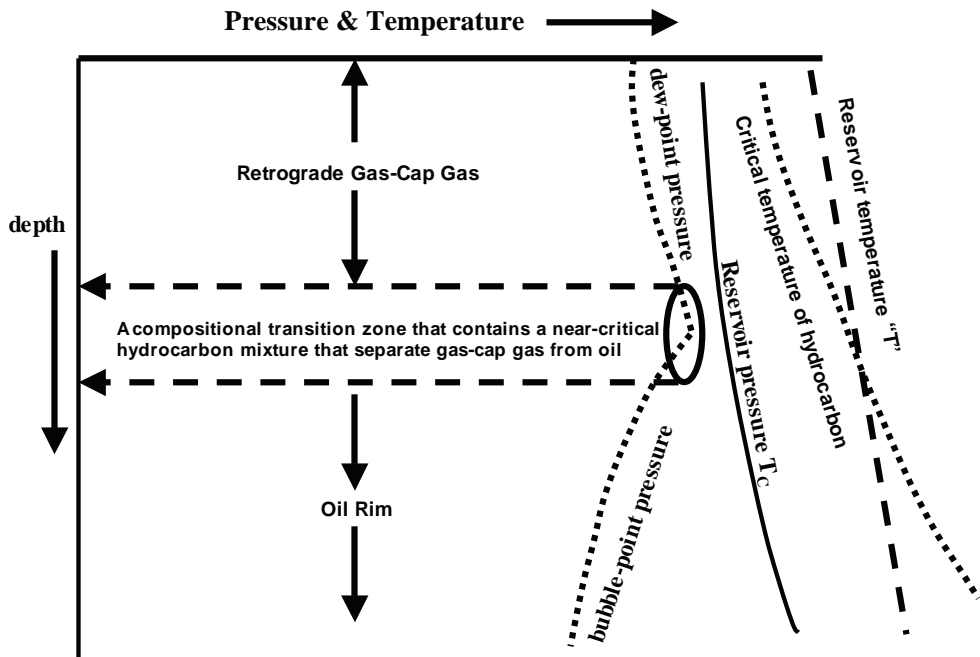


FIGURE 5-26 Undersaturated GOC.

ponents of a homogenous system tend to grade more significantly than intermediate ones.

2. Thermal diffusion generally segregates the lightest components toward the bottom of the structure, which is characterized by higher temperature, with the heavier components toward top, with a lower temperature.
3. As the thermal and gravitational effects generally oppose each other, it is conceivable that a fluid may maintain the same composition with depth.
4. Precipitation of asphaltene during its migration may lead to a distribution of varying oil types in the high- and low-permeability layers.
5. Biodegradation varying laterally and with depth may cause significant variation in, for example, H_2S content and API gravity.
6. Multiple source rocks migrate differentially into different layers and geological units.
7. As aromatic compounds are relatively denser than paraffins and naphthenes with similar molecular weights and volatility, these compounds tend to concentrate with depth and, therefore, increase the concentration of light components at the top.

Gradient calculations always require the following data at a specific reference condition: depth, fluid composition, pressure, and temperature.

Gibbs (1948) described the compositional variation under the force of gravity for an isothermal system by the following expression:

$$\mu_i(p_{ref}, z_{ref}, T) = \mu(p_i, z_i, T) + M_i g(h - h_{ref}) \quad (5-208)$$

with $i = 1, 2, \dots, N$,

where

μ_i = chemical potential of component i

h_{ref} = reference depth

p_{ref} = pressure at reference depth

M_i = molecular weight of component i

p = pressure at depth h

z_i = mole fraction of component i at depth h

N = total number of components

This condition represents N equations with the constraint that the sum of the mole fraction at depth h , $z_i(h)$, must equal 1:

$$\sum_{i=1}^N z_i(h) = 1.0 \quad (5-209)$$

The main objective is to determine the composition of fluid $z_i(h)$ and pressure $p(h)$ at a specified depth, h .

Whitson and Belery (1994) point out that combining the mechanical/equilibrium condition, that is,

$$\frac{dp}{dh} = -\rho g \quad (5-210)$$

with equation (5-208) guarantees automatic satisfaction of the condition

$$p(h) = p(h_{\text{ref}}) + \int_{h_{\text{ref}}}^h [\rho(h)g]dh \quad (5-211)$$

where $\rho(h)$ = fluid density at depth h and g = acceleration due to gravity.

The chemical potential essentially is a quantity that measures how much energy a component brings to a mixture. It can be expressed in terms of fugacity by the following expression:

$$\mu_i = RT \ln(f_i) + [\mu_i^o - RT \ln(f_i^o)] \quad (5-212)$$

where

R = constant

f_i = fugacity of component i at p , T

f_i^o = fugacity of component i at a reference state

μ_i^o = chemical potential of component i at a reference state

The term between the two brackets usually drops out in most of the calculations. Combining equation (5-208) with (5-212) gives

$$\ln[f_i(p_{\text{ref}}, z_{\text{ref}}, T)] = \ln[f_i(p, z, T)] + \frac{gM_i(b - h_{\text{ref}})}{1 - RT} \quad (5-213)$$

For convenience, defining

$$f_i(p_{\text{ref}}, z_{\text{ref}}, T) = f_i(h_{\text{ref}})$$

$$f_i(p, z, T) = f_i(h)$$

equation (5-213) can be written as

$$f_i(b) = f_i(b_{\text{ref}}) \exp \left[\frac{-M_i(b - b_{\text{ref}})}{144RT} \right] \quad (5-214)$$

where

R = gas constant, 10.73 psi-ft³/lb-mol °R

T = temperature, °R

M_i = molecular weight, lbm/lb-mol

It should be pointed out that, when calculating the fugacity using the SRK or PR EOS, the volume-translation method must be used in the fugacity expression; that is,

$$(f_i)_{\text{modified}} = (f_i)_{\text{original}} \exp \left(\frac{-c_i p}{RT} \right) \quad (5-215)$$

where c_i = component-dependent volume shift parameter.

Equation (5-215) suggests that compositional grading becomes more significant when the mixture is composed of molecules with widely different molecular weights. This is of particular significance in oil systems with large concentrations of heavy components such as asphaltenes. It should be pointed out that the heavy ends generally are reported as pseudo components or groups, each composed of several compounds characterized by an assigned fixed average molecular weight. When compositional grading occurs, the concentration of compounds within each pseudo component changes and the use of a fixed value of molecular weight reduces the reliability of the predicted results.

Whitson and Belery (1994) and Whitson and Brule (2000) presented an efficient algorithm for solving equation (5-214). The methodology is summarized in the following steps.

Step 1 Using the composition, $z_{i,\text{ref}}$ at the reference depth, b_{ref} , calculate the reference feed fugacity, $f_i(p_{\text{ref}}, T_{\text{ref}})$. Note that each fugacity value must be corrected using the volume shift parameter; that is,

$$f_i(p_{\text{ref}}, T_{\text{ref}}) \exp \left(\frac{-c_i p}{RT} \right)$$

Step 2 Calculate the gravity-corrected fugacity $\tilde{f}_i(p_{\text{ref}}, T_{\text{ref}})$ from

$$\tilde{f}_i(p_{\text{ref}}, T_{\text{ref}}) = f_i(p_{\text{ref}}, T_{\text{ref}}) \exp \left[\frac{-M_i(b - b_{\text{ref}})}{144RT} \right]$$

Whitson and his coauthors point out that $\tilde{f}_i(p_{\text{ref}}, T_{\text{ref}})$ needs to be made only once.

Step 3 Assume the composition and pressure at depth b , that is, $z_i(b)$ and $p(b)$. The initial estimates can be simply

$$z_i(b) = z_i(b_{\text{ref}})$$

and

$$p(b) = p(b_{\text{ref}})$$

Step 4 Calculate fugacities of the composition estimate, z_i , at the pressure estimate, p .

Step 5 Calculate the following two parameters as defined by Whitson and his coworkers:

$$Y_i = z_i \left[\frac{\tilde{f}_i(p_{\text{ref}}, z_{\text{ref}})}{f_i(p, z)} \right], \quad i = 1, \dots, N$$

$$Q(p, z) = 1 - \sum_{i=1}^N Y_i$$

where Y_i is termed the *mole number*.

Step 6 Calculate the fugacity ratio correction from

$$R_i = \left[\frac{\tilde{f}_i(p_{\text{ref}}, z_{\text{ref}})}{f_i(p, z)} \right] \frac{1}{\sum_{i=1}^N Y_i}$$

Step 7 Update mole numbers using the following expression:

$$Y_i^{n+1} = Y_i^n [R_i^n]^\lambda$$

Using the method of successive substitution with four iterations (initially $\lambda = 1$), followed by accelerated successive substitution with λ as given by

$$\lambda = \left| \frac{a}{a+b} \right|$$

with

$$a = \sum_{i=1}^N [\ln(R_i^n) \ln(R_i^{n-1})]$$

$$b = \sum_{i=1}^N [\ln(R_i^{n-1}) \ln(R_i^{n-1})]$$

where n is the iteration number, that is, $n = 4$.

Step 8 Calculate the composition at depth h , that is, $z^{(n+1)}$ from Y_i^{n+1} , using

$$z_i = \frac{Y_i}{\sum_{i=1}^n Y_i}$$

Step 9 Update the reservoir pressure estimated depth, h , using a Newton-Raphson estimate:

$$p^{n+1} = p^n - \frac{Q^n}{(\partial Q / \partial p)^n}$$

where

$$\frac{\partial Q}{\partial p} = \sum_{i=1}^N \left[Y_i R_i \frac{(\partial f_i / \partial p)}{f_i(p, z)} \right]$$

Step 10 Check for convergence using the criterion

$$\sum_{i=1}^N \left[\ln \left(\frac{Y_i}{z_i} \right) \right]^2 < 10^{-4}$$

Iterate until convergence is achieved.

Step 11 After finding the composition, $z(b)$, and pressure, $p(b)$, a phase-stability test as proposed by Michelsen (1984) must be made to establish that the solution is valid. A valid solution has a single phase that is thermodynamically stable. An unstable solution indicates that the calculated z and p will split into two or more phases, thereby making the solution invalid.

Whitson and Brule (2000) point out that, if the gradient solution is unstable, then the stability-test composition should be used to reinitialize the gradient calculation. The starting pressure for the new gradient calculation can be p_{ref} or, preferably, the converged pressure from the gradient calculation that led to the instable solution.

It should be noted that, when tuning an EOS to match a variety of experimental data on hydrocarbon samples taken from different depths and within a certain range of temperatures, the resulting tuned EOS generally is capable of predicting the PVT properties and the compositional gradient within that range of the temperatures; that is, it can interpolate and generate accurate PVT and compositional fluid data at temperatures within that range. However, the degree accuracy usually decreases when extrapolating outside the range of temperatures used in tuning the selected EOS. This attributed to the fact that equation-of-state's parameter, $a(T)$, is a highly dependent temperature parameter. This is evident when using the EOS to locate the gas/oil contact using different reference points, that is, $T_{\text{ref}}, p_{\text{ref}}, (z_i)_{\text{ref}}$, each will not predict the same GOC.

The ternary diagram (as defined in Chapter 1 and shown in Figure 1–32) with equilateral triangles defines the compositional boundaries that separate different types of hydrocarbon systems. This diagram can be conveniently used to approximate the location of the GOC from compositional gradients. Figure 5–27 shows the compositional gradient of five fields and illustrates the transition from gas to oil as the compositional gradients cross the boundary between the condensate gas cap and volatile oil. For example, Figure 5–27 shows the changes in the composition of the Orocual field hydrocarbon system as it approaches the boundary that separates the gas from oil. The composition at the boundary can be read as

$$C_1 + N_2 = 70.0 \text{ mol\%}$$

$$C_2-C_6, CO_2 = 17.5 \text{ mol\%}$$

$$C_{7+} = 12.5 \text{ mol\%}$$

Figures 5–28 through 5–30 show the compositional variations of $C_1 + N_2$, C_2-C_6 , CO_2 , and C_{7+} as function of depth, respectively, of the Orocual hydrocarbon system. Entering these graphs with composition of the transition mixtures gives an approximation of the GOC at 13,500 ft. Plotting the composition gradient as a function of depth is a linear form worth investigating.

Minimum Miscibility Pressure

Several schemes for predicting MMP based on the equation-of-state approach have been proposed. Benmekki and Mansoori (1988) applied the PR EOS with different mixing rules that were joined with a newly formulated expression for the unlike three-body interactions

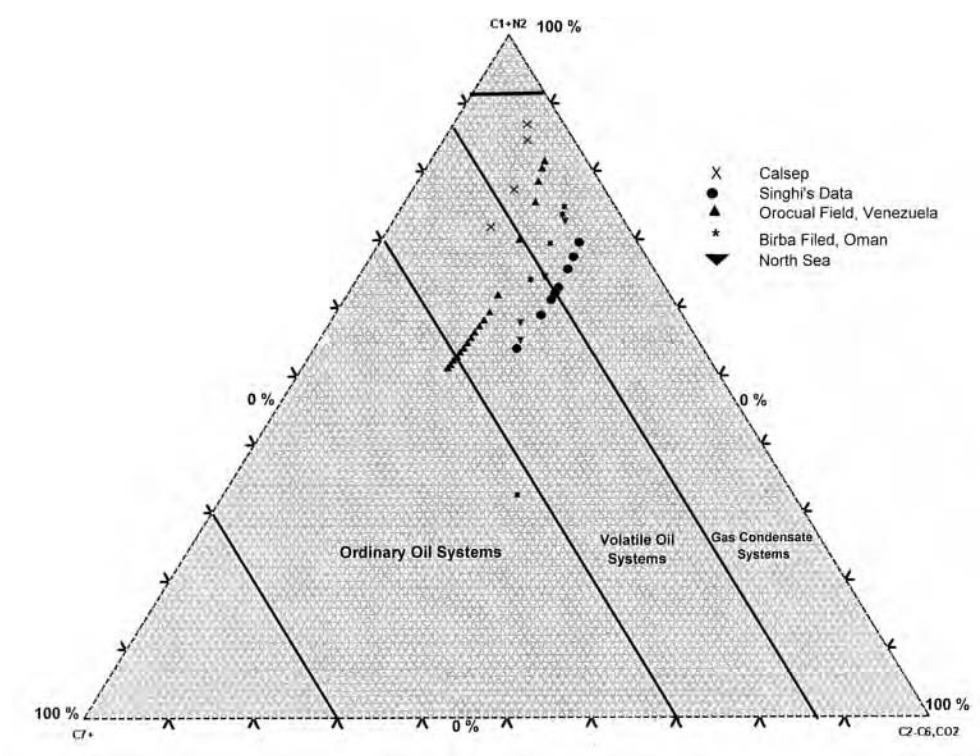


FIGURE 5-27 A simplistic approach for locating GOC.

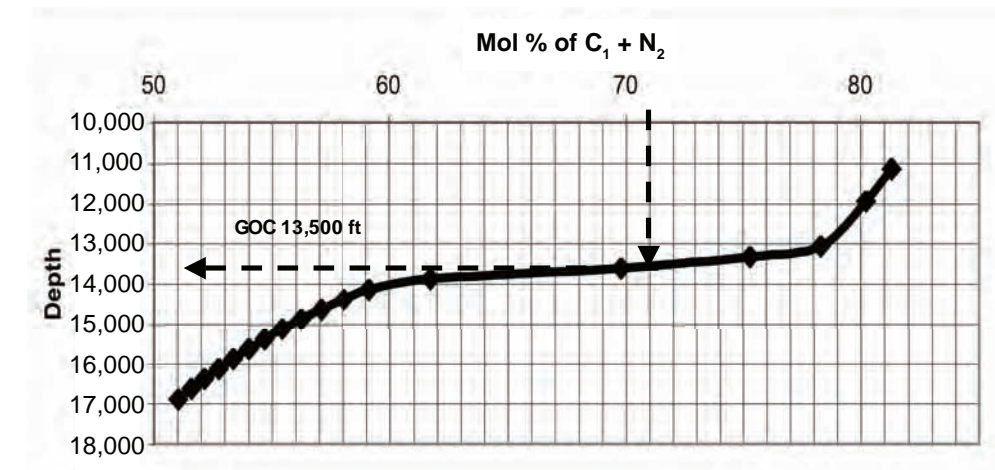


FIGURE 5-28 Mol% of $(C_1 + N_2)$ versus depth of the Orocual field.

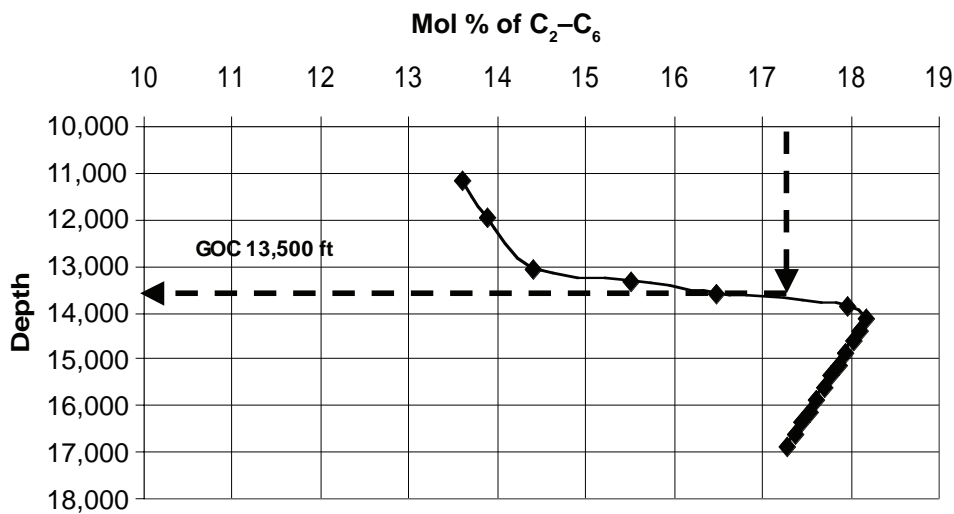


FIGURE 5-29 Mol% of C_2-C_6 versus depth of the Orocual field.

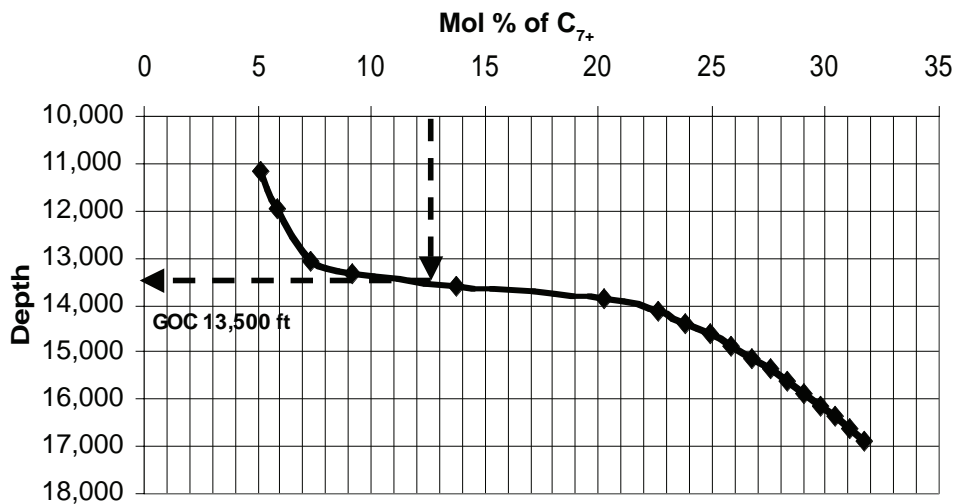


FIGURE 5-30 Mol% of C_{7+} versus depth of the Orocual field.

between the injection gas and the reservoir fluid. Several authors used upward pressure increments to locate the MMP, taking advantage through extrapolation of the fact the K -values approach unity as the limiting coincident tie-line is approached.

A simplified scheme proposed by Ahmed (1997) is based on the fact that the MMP for a solvent/oil mixture generally is considered to correspond to the critical point at which

the K -values for all components converge to unity. The following function, miscibility function, is found to provide accurate miscibility criteria as the solvent/hydrocarbon mixture approaches the critical point. This miscibility function, as defined next, approaches 0 or a very small value as the pressure reaches the MMP:

$$F_M = -\sum_{i=1}^n \left[z_i \left(1 - \frac{[\Phi(y_i)]_i^v}{[\Phi(z_i)]_i^L} \right) \right] \approx 0$$

where F_M = miscibility function and Φ = fugacity coefficient.

This expression shows that, as the overall composition, z_i , changes by gas injection and reaches the critical composition, the miscibility function is monotonically decreasing and approaching 0 or a negative value. The specific steps of applying the miscibility function follow.

Step 1 Select a convenient reference volume (e.g., one barrel) of the crude oil with a specified initial composition and temperature.

Step 2 Combine an incremental volume of the injection gas with the crude oil system and determine the overall composition, z_i .

Step 3 Calculate the bubble-point pressure, p_b , of the new composition by applying the PR EOS (as given by equation 5-145)

Step 4 Evaluate the miscibility function, F_M , at this pressure using the calculated values $\Phi(z_i)$, $\Phi(y_i)$, and the overall composition at the bubble-point pressure.

Step 5 If the value of the miscibility function is small, then the calculated p_b is approximately equal to the MMP. Otherwise, repeat steps 2 through 7.

Two example applications of the behavior of the miscibility function in determining the MMP are shown in Figures 5-31 and 5-32. The first case (Figure 5-31) is presented by Rathmell, Stalkup, and Hassinger (1971) for a pure CO_2 and the second example case (Figure 5-32) is presented by Glaso (1990) for a lean gas mixture that contains 82.17% C_1 .

Tuning EOS Parameters

Equations-of-state calculations are frequently burdened by the large number of fractions necessary to describe the hydrocarbon mixture for accurate phase behavior simulation. However, the cost and computer resources required for compositional reservoir simulation increase considerably with the number of components used in describing the reservoir fluid. For example, solving a two-phase compositional simulation problem of a reservoir system that is described by N_c components requires the simultaneous solution of $2N_c + 4$ equations for each grid block. Therefore, reducing the number of components through *lumping* has been a common industry practice in compositional simulation to significantly speed up the simulation process. As discussed previously in this chapter, calculating EOS parameters, that is, a_i , b_i , and α_i , requires component properties such as T_c , p_c , and ω . These properties generally are well-defined for pure components; however, determining these properties for the heavy fractions and lumped components rely on empirical

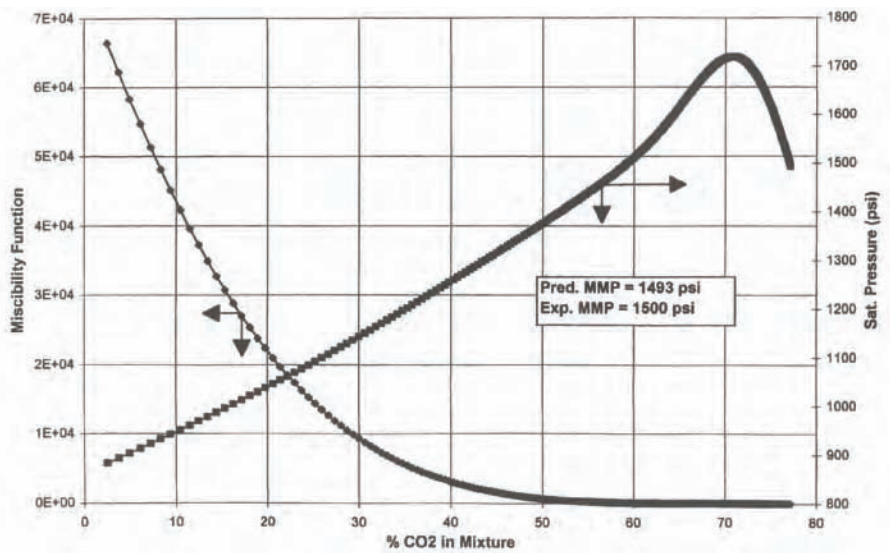


FIGURE 5-31 Oil at 109°F (pure CO₂ injection).

Source: J. Rathmell, F. Stalkup, and R. Hassinger, "A Laboratory Investigation of Miscible Displacement by Carbon Dioxide," paper SPE 3483 presented at the Fourth Annual Fall Meeting, New Orleans, October 3-6, 1971.

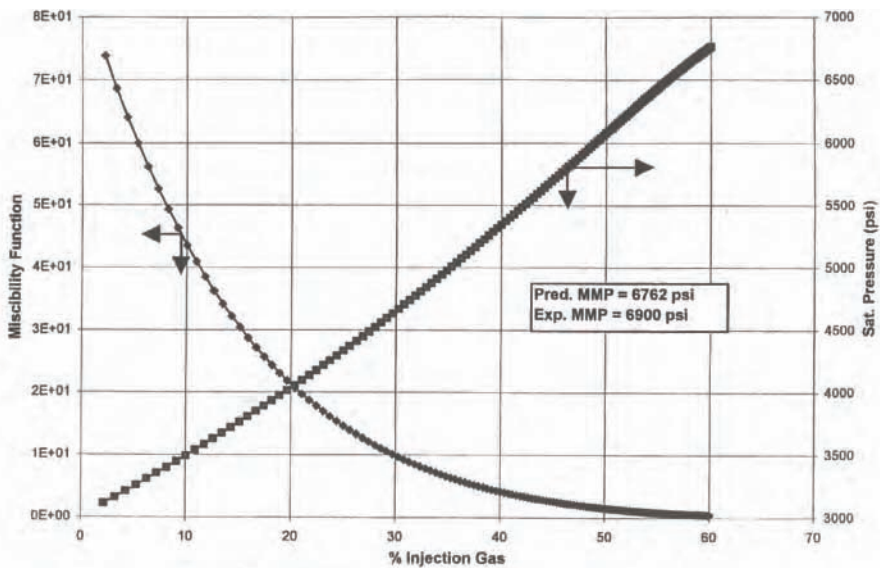


FIGURE 5-32 Injection gas 82.17% C₁ at 174°F.

Source: O. Glaso, "Miscible Displacement with Nitrogen," *SPE Reservoir Engineering* 5, no. 1 (February 1990).

correlations and the use of mixing rules. Inevitably, these empirical correlations and the selected mixing rules introduce uncertainties and errors in equation-of-state predictions.

Whenever a lumping scheme is used, tuning the selected equation of state is an important prerequisite to provide meaningful and reliable predictions. *Tuning an equation of state* refers to adjusting the parameters of the selected EOS to achieve a satisfactory

match between the laboratory fluid PVT data and EOS results. The experimental data used should be closely relevant to the reservoir fluid and other recovery processes implemented in the field. The most commonly available PVT experiments, as summarized by Wang and Pope (2001), include:

- Saturation pressure, p_{sat} , which refers to the dew-point pressure or bubble-point pressure.
- Density at the saturation pressure, ρ_{sat} .
- Constant-volume depletion (CVD), which is designed to simulate the process of retrograde condensation in gas reservoirs.
- Constant-composition expansion (CCE) based on a series of volume measurements performed on the reservoir fluid at different pressures starting at the saturation pressure.
- Differential-liberation expansion (DL), which essentially is designed to approximate the fluid-property changes with pressure for crude oil during natural depletion.
- Separator tests (SEP) based on a series of fluid flashes with the liquid from one flash becoming the feed for the next flash at different separation conditions.
- Swelling test (SW), which measures the change of the fluid properties with the amount of injection gas added to the original fluid.
- Multiple-contact test (MCT), forward and backward, to simulate the dynamic phase behavior during gas injection. The forward process simulates the mixing of the injected gas at the gas front with the original oil. The backward process represents the continuous contact of the injected gas with the oil left behind the gas front.
- The slim-tube test, which simulates the dynamic phase-behavior test, where the injection gas displaces oil from uniform sand or glass beads packed in a small-diameter tube. The minimum miscibility pressure is determined from the recovery/injection pressure curve.

Manual adjustments through trial and error or by an automatic nonlinear regression approach are used to adjust the EOS parameters to achieve a match between laboratory and EOS results. The regression variables essentially are a selected number of EOS parameters that may be adjusted or tuned to achieve a match between the two results, experimental and EOS. Coats and Smart (1986) recommend modifying the following regression variables, that is, EOS parameters:

- Properties of the undefined fractions that include T_c , p_c , and ω or alternatively through the adjustments of Ω_a and Ω_b of these fractions. The Ω modifications should be interpreted as modifications of the critical properties, since they are related by the expressions:

$$a = \Omega_a \frac{R^2 T_c^2}{p_c}$$

$$b = \Omega_b \frac{RT_c}{p_c}$$

However, the manual adjustment of ω is not recommended.

- Ω_a and Ω_b of methane.
- Binary interaction coefficient, k_{ij} , between the methane and C_{7+} fractions.
- When an injection gas contains significant amounts of nonhydrocarbon components, CO_2 and N_2 , the binary interaction, k_{ij} , between these fractions and methane also should be modified.

The regression is a nonlinear mathematical model that places global upper and lower limits on each regression variable, Ω_{aC_1} , Ω_{bC_1} , and so forth. The nonlinear mathematical model determines the optimum values of these regression variables that minimize the objective function, defined as

$$F = \sum_j^{N_{\text{exp}}} W_j \left| \frac{E_j^{\text{exp}} - E_j^{\text{cal}}}{E_j^{\text{exp}}} \right|$$

where

N_{exp} = total number of experimental data points

E_j^{exp} = experimental (laboratory) value of observation j , such as p_d , p_b , or ρ_{ob}

E_j^{cal} = EOC-calculated value of observation j , such as p_d , p_b , or ρ_{ob}

W_j = weight factor on observation j

The values of the weight factors in the objective function are internally set with default or user-override values. The default values are 1.0 with the exceptions of values of 40 and 20 for saturation pressure and density, respectively. Note that the calculated value of any observation, such as E_j^{cal} , is a function of the all-regression variables:

$$E_j^{\text{cal}} = f(\Omega_{aC_1}, \Omega_{bC_1}, \dots, \text{etc.})$$

Whitson and Brule (2000) and Coats and Smart (1986) suggested a stepwise and consistent procedure for tuning the parameters of the equation of state and the associated lumping technique. Whitson and Brule extended Coats and Smart's regression parameters to include the volume correction parameter, c_p , and the molecular weight, M . Liu points out that the fluid properties of an original hydrocarbon system, as predicted by a cubic equation of state, depend on the values of mixture parameters a and b and suggested that, if the *lumped* fluid system has the same values of a and b as those from original fluid system, the EOS will predict the same fluid properties. The observation, called *equal property constraints*, is mathematically expressed as

$$a_{\text{original}} = a_{\text{lumped}}$$

$$b_{\text{original}} = b_{\text{lumped}}$$

Assume that L components are lumped into one pseudo component; based on the equal property constraints, the properties of the pseudo component can be calculated from the following relationships (assuming PR EOS is the selected equation).

1. Pseudo-component composition, z_L :

$$z_L = \sum_{i \in L} z_i$$

2. EOS parameters Ω_a and Ω_b of the pseudo component (lumped fractions):

$$\Omega_{aL} = \left[\frac{1}{z_L} \sum_{i \in L} z_i \sqrt{\Omega_{ai}} \right]^2$$

$$\Omega_{bL} = \frac{1}{z_L} \sum_{i \in L} z_i \Omega_{bi}$$

3. Critical temperature, T_{cL} , and pressure, p_{cL} , of the pseudo component. Define the following coefficients for each individual component, component i in the lumped group, as

$$D_i = z_i T_{ci} \sqrt{\frac{\Omega_{ai}}{p_{ci}}}$$

$$m_i = 0.3796 + 1.54226\omega_i - 0.2699\omega_i^2$$

$$\alpha_i = \left[1 + m_i (1 - \sqrt{T_r}) \right]^2$$

Calculate the mixing parameters A , B , C , and D for the lumped fractions:

$$A = \left[z_m \left(\frac{\Omega_{aL}}{\Omega_{bL}} \right) \sum_{i \in L} z_i \Omega_{bi} \frac{T_{ci}}{p_{ci}} \right] - \sum_{j \in L} \sum_{i \in L} \left[\frac{m_i m_j D_i D_j (1 - k_{ij})}{\sqrt{T_{ci} T_{cj}}} \right]$$

$$B = \sum_{j \in L} \sum_{i \in L} D_i D_j (1 - k_{ij}) \left[\frac{(1 + m_j) m_i}{\sqrt{T_{ci}}} + \frac{(1 + m_i) m_j}{\sqrt{T_{cj}}} \right]$$

$$C = \sum_{j \in L} \sum_{i \in L} D_i D_j (1 - k_{ij}) (1 + m_i) (1 + m_j)$$

$$D = \frac{1}{z_L} \sum_{i \in L} z_i D_i$$

Solve the following quadratic equation for the critical temperature of the lumped group:

$$AT_{cL} + B\sqrt{T_{cL}} - C = 0$$

and the critical pressure by

$$p_{cL} = \frac{z_L \Omega_{bL} T_{cL}}{\sum_{i \in L} z_i \Omega_{bi} \left(\frac{T_{ci}}{p_{ci}} \right)}$$

4. Calculate the EOS parameters of the pseudo component. The lumped parameters a_L , b_L , m_L , and α_L of the PR EOS then can be determined by applying equations (5-111) and (5-112):

$$a_L = \Omega_{aL} \frac{R^2 T_{cL}^2}{p_{cL}}$$

$$b_L = \Omega_{bL} \frac{RT_{cL}}{p_{cL}}$$

$$m_L = \frac{\frac{1}{D} \sqrt{\sum_{i \in L} \sum_{j \in L} D_i D_j [\alpha_i \alpha_j]^{0.5} (1 - k_{ij})} - 1}{1 - \sqrt{T/T_{cL}}}$$

$$\alpha_L = \left[1 + m_L \left(1 - \sqrt{T/T_{cl}} \right) \right]^2$$

5. Calculate the volume correction parameter, c_L , shift parameter, S , and molecular weight of the lumped group:

$$c_L = \frac{1}{z_L} \sum_{i \in L} z_i c_i$$
$$S_L = \frac{1}{b_L z_L} \sum_{i \in L} z_i b_i S_i$$
$$M_L = \frac{1}{z_L} \sum_{i \in L} z_i M_i$$

The stepwise regression procedure in tuning EOS parameters is summarized next.

Step 1 Using the *original composition* of the hydrocarbon system, describe the plus fraction, such as C_{7+} , with at least three to five pseudo components. For clarity and brevity, assume that the C_{7+} is characterized by three fractions, F_1 , F_2 , and F_3 , to give the original composition shown in the table below.

Group	Original Component, Step 1	k_{ij}	Ω_a	Ω_b
1	N ₂			
2	CO ₂			
3	C ₁	X	X	X
4	C ₂			
5	C ₃			
6	i-C ₄			
7	n-C ₄			
8	i-C ₅			
9	n-C ₅			
10	C ₆			
11	F ₁	X	X	X
12	i ₂	X	X	X
13	F ₃	X	X	X

Using the original composition, perform a comprehensive match of the exiting laboratory PVT data by adjusting the regression variables Ω_a and Ω_b of C_1 , F_1 , F_2 , and F_3 , and the binary interaction coefficients between methane C_1 and the three C_{7+} fractions, F_1 , F_2 , and F_3 . All the subsequent grouping (lumping) should be compared and reasonably close with the prediction of the original composition.

Step 2 Create two new pseudo components from the existing set of original components by combing N₂ with C₁ and CO₂ with C₂. Using the appropriate mixing rules as discussed previously to determine the parameters of the two new pseudo components.

Step 3 Use regression to fine tune Ω_{aL} and Ω_{bL} of the lumped fractions as well as key binary interaction coefficients, such as those between the two lumped fractions and the heavy fractions, that is, binary interaction between N₂ + C₁ and C_{7+} fractions (F_1 , F_2 , and F_3) and between CO₂ + C₂ and C_{7+} fractions.

Step 4 Repeat these steps until the quality of the characterization deteriorates with the *continuous reduction* of the number of components by lumping. Whitson and Brule (2000) summarized the stepwise regression procedure in a tabulated form as shown in Table 5–4.

If the stepwise regression is not possible, the following standard procedure is recommended:

1. Using the original composition of the system, extend the C_{7+} fraction to C_{45+} using any of the distribution functions (see Chapter 2) that honor the measured molecular weight and specific gravity of C_{7+} .
2. Assign T_c , p_c , and ω to these split pseudo components by use of empirical correlations or from the tabulated values given in Table 2–1.
3. Lump these split pseudo components into four (or more) groups, for example, F_1 , F_2 , F_3 , and F_4 .
4. Match the exiting laboratory PVT data by adjusting the regression variables Ω_a and Ω_b of F_1 , F_2 , F_3 , and F_4 , and the binary interaction coefficients between methane C_1 and the C_{7+} fractions, as illustrated in Table 5–5.
5. Having achieved a satisfactory match with the experimental data and obtained the “optimum” values of Ω_a and Ω_b of F_1 , F_2 , F_3 , and F_4 , further reduce the number of fractions representing the system by forming the following groups:

TABLE 5–4 *Example of a Stepwise-Regression Procedure for Pseudoization to Fewer Components for a Gas-Condensate Fluid Undergoing Depletion*

Original Component Number	Original Component	Step 1	Step 2	Step 3	Step 4	Step 5
1	N ₂	N ₂ + C ₁ ^a	N ₂ + C ₁	N ₂ + C ₁	N ₂ + C ₁ + CO ₂ + C ₂ ^a	N ₂ + C ₁ + CO ₂ + C ₂
2	CO ₂	CO ₂ + C ₂ ^a	CO ₂ + C ₂	CO ₂ + C ₂	C ₃ + i-C ₄ + n-C ₄ + i-C ₅ + n-C ₅ + C ₆ ^a	C ₃ + i-C ₄ + n-C ₄ + i-C ₅ + n-C ₅ + C ₆
3	C ₁	C ₃	C ₃	C ₃ + i-C ₄ + n-C ₄ ^a	F ₁	F ₁
4	C ₂	i-C ₄	i-C ₄ + n-C ₄ ^a	i-C ₅ + n-C ₅ + C ₆ ^a	F ₂	F ₂ + F ₃ ^a
5	C ₃	n-C ₄	i-C ₅ + n-C ₅ ^a	F ₁	F ₃	
6	i-C ₄	i-C ₅	C ₆	F ₂		
7	n-C ₄	n-C ₅	F ₁	F ₃		
8	i-C ₅	C ₆	F ₂			
9	n-C ₅	F ₁	F ₃			
10	C ₆	F ₂				
11	F ₁	F ₃				
12	F ₂					
13	F ₃					
Regression Parameters						
k_{ij}		1, 9, 10, 11	1, 7, 8, 9	1, 5, 6, 7	1, 3, 4, 5	1, 3, 4
Ω_a		1	4	3	1	3
Ω_b		1	4	3	1	3
Ω_a^a		2	5	4	2	4
Ω_b^a		2	5	4	2	4

^aIndicates the grouped pseudo components being regressed in a particular step.
Source: Permission to publish by SPE. © SPE, 2000.

TABLE 5-5 *Original Composition*

Group	Original Component, Step 1	k_{ij}	Ω_a	Ω_b
1	N ₂			
2	CO ₂			
3	C ₁	X		
4	C ₂			
5	C ₃			
6	i-C ₄			
7	n-C ₄			
8	i-C ₅			
9	n-C ₅			
10	C ₆			
11	F ₁	X	X	X
12	F ₂	X	X	X
13	F ₃	X	X	X
14	F ₄	X	X	X

Group 1 = N₂ + C₁

Group 2 = CO₂ + C₂

Group 3 = C₃ + i-C₄ + n-C₄

Group 4 = i-C₅ + n-C₅ + C₆

Group 5 = F₁

Group 6 = F₂

Group 7 = F₃

Group 8 = F₄

6. Keep the “optimum” values of Ω_a and Ω_b of F₁, F₂, F₃, and F₄ from step 4, tune the eight pseudo-component hydrocarbon systems by adjusting the following regression variables:
- Ω_a and Ω_b of (C₃ + i-C₄ + n-C₄) and (i-C₅ + n-C₅ + C₆).
 - Binary interaction coefficient, k_{ij} , between (N₂ + C₁) and F₁, F₂, F₃, and F₄ plus (CO₂ + C₂) and F₁, F₂, F₃, and F₄.

A summary of this step is shown in the table below.

Group	Original Component, Step 1	k_{ij}	Ω_a	Ω_b
1	N ₂ + C ₁	X		
2	CO ₂ + C ₂	X		
3	C ₃ + i-C ₄ + n-C ₄		X	X
4	i-C ₅ + n-C ₅ + C ₆		X	X
5	F ₁	X		
6	F ₂	X		
7	F ₃	X		
8	F ₄	X		

As pointed out in Chapter 4, the Lohrenz, Bray, and Clark (LBC) viscosity correlation has become a standard in compositional reservoir simulation. When observed viscosity data are available, *values of the coefficients* a_1 – a_5 in equation (4–86) and the *critical volume* of C_{7+} are adjusted and used as tuning parameters until a match with the experimental data is achieved. These adjustments are performed independent of the process of tuning equation-of-state parameters to match other PVT data. The key relationships of the LBC viscosity model follow:

$$\mu_{\text{ob}} = \mu^o + \frac{[a_1 + a_2 \rho_r + a_3 \rho_r^2 + a_4 \rho_r^3 + a_5 \rho_r^4]^4 - 0.0001}{\xi_m}$$

$$\rho_r = \frac{\left(\sum_{\substack{i=1 \\ i \notin C_{7+}}}^n [(x_i M_i V_i)] + x_{C_{7+}} V_{C_{7+}} \right) \rho_o}{M_a}$$

where

$$\begin{aligned} a_1 &= 0.1023 \\ a_2 &= 0.023364 \\ a_3 &= 0.058533 \\ a_4 &= -0.040758 \\ a_5 &= 0.0093324 \end{aligned}$$

Original Fluid Composition from a Sample Contaminated with Oil-Based Mud

As pointed out by Gozalpour et al. (2002), hydrocarbon-based fluids (natural or synthetic oils) generally are used in oil-base mud (OBM). Because these fluids are soluble in the reservoir fluid, they can render the fluid analysis limited in value. Contamination with an oil-based mud filtrate could affect reservoir fluid properties such as

- Saturation pressure.
- Formation volume factor.
- Gas/liquid ratio.
- Stock-tank liquid density.

Determination of the original fluid composition from the analysis of a contaminated sample is feasible, but isolating the properties of the reservoir fluid free from contamination is not easily accomplished. Despite the recent improvements in sampling reservoir fluids, obtaining a contamination-free formation fluid is a major challenge, particularly in open-hole wells. Therefore, modeling techniques are required, along with the laboratory studies, to determine the composition and PVT properties of the uncontaminated fluid.

Because collecting a reservoir fluid sample is expensive and accurate reservoir fluid properties are needed in reservoir development, it is highly desirable to determine accurate composition and phase behavior for the reservoir fluid from contaminated samples.

It is well known that an exponential relationship exists between the concentration of components in the C_{8+} portion of real reservoir fluids and the corresponding molecular weights. For example, if the molar concentration of single carbon number groups is plotted against their molecular weights, it will give a straight line on a semi-logarithmic scale. Based on this feature of natural fluids, Gozalpour and his coauthors proposed two methods to retrieve the original composition of reservoir fluid from contaminated samples: the skimming method and the subtraction method.

The Skimming Method

The skimming method is based on plotting the composition of the C_{8+} portion of a contaminated sample against molecular weight on a semi-logarithmic scale. The plotted data show a departure from the line over the range affected by the contaminants, as shown in Figure 5–33. Gozalpour and his coauthors suggest that the concentrations of the contaminants are skimmed from the semi-log straight line, presumed to be valid for the uncontaminated reservoir fluid. The fitted line is used to determine the composition of the uncontaminated fluid.

Figure 5–33 shows a plot of the weight fraction of C_{10} – C_{30} of a contaminated condensate versus the molecular weight on a semi-logarithmic scale. It shows a departure from the linear trend over the range affected by the contaminants. Excluding the contaminant components from the contaminated composition, an exponential distribution function (linear on a semi-logarithmic scale) can be fitted to the rest of the components. MacMillan

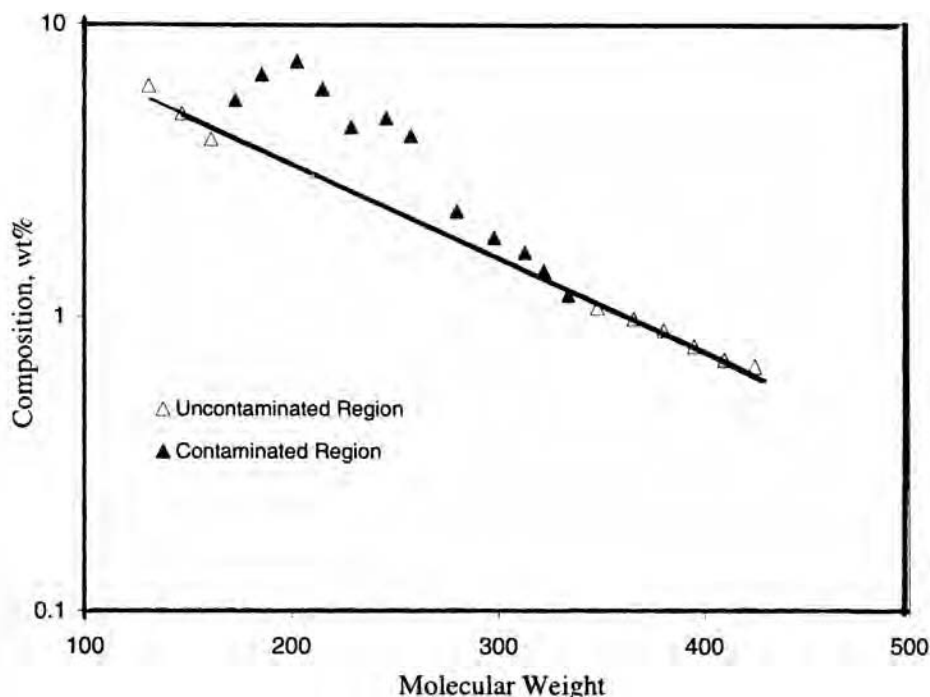


FIGURE 5–33 Contaminated condensate sample with OBM.

Source: After Gozalpour et al. (2002). Copyright SPE, 2002.

et al. (1997) developed a similar method. They fitted a gamma distribution function to the composition of the C_{7+} portion of contaminated oil samples, excluding the composition of contaminants from the data-fitting procedure.

The Subtraction Method

In the second method, the subtraction method, a known amount of drilling fluid with known composition is subtracted from that of the contaminated sample. The C_{8+} portion of the resultant composition is used to fit an exponential distribution function. The procedure is repeated for different levels of drilling fluid subtracted from the contaminated sample. The composition that gives the best fit to the exponential distribution function is treated as the retrieved original reservoir fluid composition. This approach can retrieve the original composition reliably, even when the mud filtrate is composed of a wide range of natural hydrocarbon components.

Problems

1. A hydrocarbon system has the following overall composition:

COMPONENT	z_i
C_1	0.30
C_2	0.10
C_3	0.05
i- C_4	0.03
n- C_4	0.03
i- C_5	0.02
n- C_5	0.02
C_6	0.05
C_{7+}	0.40

given:

System pressure = 2100 psia

System temperature = 150°F

Specific gravity of C_{7+} = 0.80

Molecular weight of C_{7+} = 140

Calculate the equilibrium ratios of this system assuming both an ideal solution and real solution behavior.

2. A well is producing oil and gas with the following compositions at a gas/oil ratio of 500 scf/STB:

COMPONENT	x_i	y_i
C_1	0.35	0.60
C_2	0.08	0.10
C_3	0.07	0.10
n- C_4	0.06	0.07

COMPONENT	x_i	y_i
n-C ₅	0.05	0.05
C ₆	0.05	0.05
C ₇₊	0.34	0.03

given:

Current reservoir pressure = 3000 psia

Bubble-point pressure = 2800 psia

Reservoir temperature = 120°F

Molecular weight of C₇₊ = 160

Specific gravity of C₇₊ = 0.823

Calculate the overall composition of the system, that is, z_i .

3. The hydrocarbon mixture with the following composition exists in a reservoir at 234°F and 3500 psig:

COMPONENT	z_i
C ₁	0.3805
C ₂	0.0933
C ₃	0.0885
C ₄	0.0600
C ₅	0.0378
C ₆	0.0356
C ₇₊	0.3043

The C₇₊ has a molecular weight of 200 and a specific gravity of 0.8366. Calculate

- The bubble-point pressure of the mixture.
 - The compositions of the two phases if the mixture is flashed at 500 psia and 150°F.
 - The density of the resulting liquid phase.
 - The density of the resulting gas phase.
 - The compositions of the two phases if the liquid from the first separator is further flashed at 14.7 psia and 60°F.
 - The oil formation volume factor at the bubble-point pressure.
 - The original gas solubility.
 - The oil viscosity at the bubble-point pressure.
4. A crude oil exists in a reservoir at its bubble-point pressure of 2520 psig and a temperature of 180°F. The oil has the following composition:

COMPONENT	x_i
CO ₂	0.0044
N ₂	0.0045
C ₁	0.3505
C ₂	0.0464
C ₃	0.0246

COMPONENT	x_i
i-C ₄	0.0683
n-C ₄	0.0083
i-C ₅	0.0080
n-C ₅	0.0080
C ₆	0.0546
C ₇₊	0.4224

The molecular weight and specific gravity of C₇₊ are 225 and 0.8364. The reservoir initially contains 122 MMbbl of oil. The surface facilities consist of two separation stages connected in series. The first separation stage operates at 500 psig and 100°F. The second stage operates under standard conditions.

- a. Characterize C₇₊ in terms of its critical properties, boiling point, and acentric factor.
 - b. Calculate the initial oil in place in STB.
 - c. Calculate the standard cubic feet of gas initially in solution.
 - d. Calculate the composition of the free gas and the composition of the remaining oil at 2495 psig, assuming the overall composition of the system remains constant.
5. A pure n-butane exists in the two-phase region at 120°F. Calculate the density of the coexisting phase using the following equations of state:
- a. van der Waals.
 - b. Redlich-Kwong.
 - c. Soave-Redlich-Kwong.
 - d. Peng-Robinson.
6. A crude oil system with the following composition exists at its bubble-point pressure of 3250 psia and 155°F.

COMPONENT	x_i
C ₁	0.42
C ₂	0.08
C ₃	0.06
C ₄	0.02
C ₅	0.01
C ₆	0.04
C ₇₊	0.37

If the molecular weight and specific gravity of the heptanes-plus fraction are 225 and 0.823, calculate the density of the crude using the

- a. Standing-Katz density correlation.
- b. Alani-Kennedy density correlation.
- c. van der Waals correlation.
- d. Redlich-Kwong EOS.
- e. Soave-Redlich-Kwong correlation.

- f. Soave-Redlich-Kwong correlation with the shift parameter.
 - g. Peneloux volume correction.
 - h. Peng-Robinson EOS.
7. The following reservoir oil composition is available:

COMPONENT	MOL% OIL
C ₁	40.0
C ₂	8.0
C ₃	5.0
i-C ₄	1.0
n-C ₄	3.0
i-C ₅	1.0
n-C ₅	1.5
C ₆	6.0
C ₇₊	34.5

- The system exists at 150°F. Estimate the MMP if the oil is to be displaced by
- a. Methane.
 - b. Nitrogen.
 - c. CO₂.
 - d. 90% CO₂ and 10% N₂.
 - e. 90% CO₂ and 10% C₁.
8. The compositional gradients of the Nameless field are as follows:

C ₁ + N ₂	C ₇₊	C ₂ –C ₆	TVD, ft
69.57	6.89	23.54	4500
67.44	8.58	23.98	4640
65.61	10.16	24.23	4700
63.04	12.54	24.42	4740
62.11	13.44	24.45	4750
61.23	14.32	24.45	4760
58.87	16.75	24.38	4800
54.08	22.02	23.9	5000

Estimate the location of the GOC.

References

Ahmed, T. “A Practical Equation of State” [translation]. *SPE Reservoir Engineering* 291 (February 1991).

Ahmed, T. “A Generalized Methodology for Minimum Miscibility Pressure.” Paper SPE 39034 presented at the Latin American Petroleum Conference, Rio de Janeiro, Brazil, August 30–September 3, 1997.

Amyx, J. M., D. M. Bass, and R. Whiting. *Petroleum Reservoir Engineering—Physical Properties*. New York: McGraw-Hill, 1960.

- Benmekki, E., and G. Mansoori. "Minimum Miscibility Pressure Prediction with EOS." *SPE Reservoir Engineering* (May 1988).
- Brinkman, F. H., and J. N. Sicking. "Equilibrium Ratios for Reservoir Studies." *Transactions of the AIME* 219 (1960): 313–319.
- Campbell, J. M. *Gas Conditioning and Processing. Campbell Petroleum Series*, vol. 1. Norman, OK: Campbell, 1976.
- Clark, N. *Elements of Petroleum Reservoirs*. Dallas: Society of Petroleum Engineers, 1960.
- Coats, K., and G. Smart. "Application of Regression-Based EOS PVT Program to Laboratory Data." *SPE Reservoir Engineering* (May 1986).
- Dake, L. P. *Fundamentals of Reservoir Engineering*. Amsterdam: Elsevier Scientific Publishing Company, 1978.
- Dodson, C., D. Goodwill, and E. Mayer. "Application of Laboratory PVT Data to Engineering Problems." *Journal of Petroleum Technology* (December 1953).
- Dykstra, H., and T. D. Mueller. "Calculation of Phase Composition and Properties for Lean-or Enriched-Gas Drive." *Society of Petroleum Engineers Journal* (September 1965): 239–246.
- Edmister, W., and B. Lee. *Applied Hydrocarbon Thermodynamics*, vol. 1, 2nd ed. Houston: Gulf Publishing Company, 1986, p. 52.
- Elliot, J., and T. Daubert. "Revised Procedure for Phase Equilibrium Calculations with Soave Equation of State." *Industrial Engineering and Chemical Process Design Development* 23 (1985): 743–748.
- Gibbs, J. *The Collected Works of J. Willard Gibbs*. New Haven, CT: Yale University Press, 1948.
- Glaso, O. "Miscible Displacement with Nitrogen." *SPE Reservoir Engineering* 5, no. 1 (February 1990).
- Gozalpour, F., et al. "Predicting Reservoir Fluid Phase and Volumetric Behavior from Samples Contaminated with Oil-Based Mud." *SPE Reservoir Evaluation and Engineering* (June 2002).
- Graboski, M. S., and T. E. Daubert. "A Modified Soave Equation of State for Phase Equilibrium Calculations, 1. Hydrocarbon System." *Industrial Engineering and Chemical Process Design Development* 17 (1978): 443–448.
- Hadden, J. T. "Convergence Pressure in Hydrocarbon Vapor-Liquid Equilibria." *Chemical Engineering Progress Symposium Series* 49, no. 7 (1953): 53.
- Hoffmann, A. E., J. S. Crump, and R. C. Hocott. "Equilibrium Constants for a Gas-Condensate System." *Transactions of the AIME* 198 (1953): 1–10.
- Hoier, L., and C. Whitson. "Compositional Gradient—Theory and Practice." *SPE Reservoir Evaluation and Engineering* (December 2001).
- Jhaveri, B. S., and G. K. Youngren. "Three-Parameter Modification of the Peng-Robinson Equation of State to Improve Volumetric Predictions." Paper SPE 13118, presented at the SPE Annual Technical Conference, Houston, September 16–19, 1984.
- Katz, D. L., and K. H. Hachmuth. "Vaporization Equilibrium Constants in a Crude Oil-Natural Gas System." *Industrial Engineering and Chemistry* 29 (1937): 1072.
- Katz, D., et al. *Handbook of Natural Gas Engineering*. New York: McGraw-Hill, 1959.
- Katz, D., et al. "Overview of Phase Behavior of Oil and Gas Production." *Journal of Petroleum Technology* (June 1983): 1205–1214.
- Kehn, D. M. "Rapid Analysis of Condensate Systems by Chromatography." *Journal of Petroleum Technology* (April 1964): 435–440.
- Lim, D., and T. Ahmed. "Calculation of Liquid Dropout for Systems Containing Water." Paper SPE 13094, presented at the 59th Annual Technical Conference of the SPE, Houston, September 16–19, 1984.
- Lohrenze, J., G. Clark, and R. Francis. "A Compositional Material Balance for Combination Drive Reservoirs." *Journal of Petroleum Technology* (November 1963).
- MacMillan, D., et al. *How to Obtain Reservoir Fluid Properties from an Oil Sample Contaminated with Synthetic Drilling Mud*. SPE paper 38852. Richardson, TX: Society of Petroleum Engineers, 1997.

- Michelson, M. "Collection of Critical Points and Phase Boundaries in the Critical Region." *Fluid Phase Equilibria* 16 (1984).
- NGPSA. *Engineering Data Book*. Tulsa, OK: National Gas Producers Suppliers Association, 1978.
- Nikos, V., et al. "Phase Behavior of Systems Comprising North Sea Reservoir Fluids and Injection Gases." *Journal of Petroleum Technology* (November 1986): 1221–1233.
- Pedersen, K., P. Thomassen, and A. Fredenslund. "Phase Equilibria and Separation Processes." Report SEP 8207, Institute for Kemiteknik, Denmark Tekniske Højskole, July 1982.
- Pedersen, K., P. Thomassen, and A. Fredenslund. "Characterization of Gas Condensate Mixtures." In *Advances in Thermodynamics*. New York: Taylor and Francis, 1989.
- Peneloux, A., E. Rauzy, and R. Freze. "A Consistent Correlation for Redlich-Kwong-Soave Volumes." *Fluid Phase Equilibria* 8 (1982): 7–23.
- Peng, D., and D. Robinson. "A New Two Constant Equation of State." *Industrial Engineering and Chemistry Fundamentals* 15, no. 1 (1976a): 59–64.
- Peng, D., and D. Robinson. "Two and Three Phase Equilibrium Calculations for Systems Containing Water." *Canadian Journal of Chemical Engineering* 54 (1976b): 595–598.
- Peng, D., and D. Robinson. *The Characterization of the Heptanes and Their Fractions*. Research Report 28. Tulsa, OK: Gas Producers Association, 1978.
- Peng, D., and D. Robinson. "Two and Three Phase Equilibrium Calculations for Coal Gasification and Related Processes." ACS Symposium Series no. 133, Thermodynamics of Aqueous Systems with Industrial Applications, 1980.
- Rathmell, J., F. Stalkup, and R. Hassinger. "A Laboratory Investigation of Miscible Displacement by Carbon Dioxide." Paper SPE 3483 presented at the Fourth Annual Fall Meeting, New Orleans, October 3–6, 1971.
- Redlich, O., and J. Kwong. "On the Thermodynamics of Solutions. An Equation of State. Fugacities of Gaseous Solutions." *Chemical Reviews* 44 (1949): 233–247.
- Reid, R., J. M. Prausnitz, and T. Sherwood. *The Properties of Gases and Liquids*, 4th ed. New York: McGraw-Hill, 1987.
- Rzasa, M. J., E. D. Glass, and J. B. Opfell "Prediction of Critical Properties and Equilibrium Vaporization Constants for Complex Hydrocarbon Systems." *Chemical Engineering Progress*, Symposium Series 48, no. 2 (1952): 28.
- Sim, W. J., and T. E. Daubert. "Prediction of Vapor-Liquid Equilibria of Undefined Mixtures." *Industrial Engineering and Chemical Process Design Development* 19, no. 3 (1980): 380–393.
- Slot-Petersen, C. "A Systematic and Consistent Approach to Determine Binary Interaction Coefficients for the Peng-Robinson Equation of State." Paper SPE 16941, presented at the 62nd Annual Technical Conference of the SPE, Dallas, September 27–30, 1987.
- Soave, G., "Equilibrium Constants from a Modified Redlich-Kwong Equation of State." *Chemical Engineering and Science* 27 (1972): 1197–1203.
- Standing, M. B. *Volumetric and Phase Behavior of Oil Field Hydrocarbon Systems*. Dallas: Society of Petroleum Engineers of AIME, 1977.
- Standing, M. B. "A Set of Equations for Computing Equilibrium Ratios of a Crude Oil/Natural Gas System at Pressures Below 1,000 psia." *Journal of Petroleum Technology* (September 1979): 1193–1195.
- Stryjek, R., and J. H. Vera. "PRSV: An Improvement Peng-Robinson Equation of State for Pure Compounds and Mixtures." *Canadian Journal of Chemical Engineering* 64 (April 1986): 323–333.
- Van der Waals, J. D. "On the Continuity of the Liquid and Gaseous State." Ph.D. dissertation, Sigthoff, Leiden, 1873.
- Vidal, J., and T. Daubert. "Equations of State—Reworking the Old Forms." *Chemical Engineering and Science* 33 (1978): 787–791.
- Whitson, C., and P. Belery. "Composition of Gradients in Petroleum Reservoirs." Paper SPE 28000 presented at the University of Tulsa/SPE Centennial Petroleum Engineering Symposium, Tulsa, OK, August 29–31, 1994.

- Whitson, C. H., and M. R. Brule. *Phase Behavior*. Richardson, TX: SPE, 2000.
- Whitson, C. H., and S. B. Torp. "Evaluating Constant Volume Depletion Data." Paper SPE 10067, presented at the SPE 56th Annual Fall Technical Conference, San Antonio, October 5–7, 1981.
- Wilson, G. "A Modified Redlich-Kwong EOS, Application to General Physcial Data Calculations." Paper 15C, presented at the Annual AIChE National Meeting, Cleveland, May 4–7, 1968.
- Winn, F. W. "Simplified Nomographic Presentation, Hydrocarbon Vapor-Liquid Equilibria." *Chemical Engineering Progress*, Symposium Series 33, no. 6 (1954): 131–135.

6

Flow Assurance

THE TERM *FLOW ASSURANCE* is used to evaluate the effects of fluid hydrocarbon solids (i.e., asphaltene, wax, and hydrate) and their potential to disrupt production due to deposition in the flow system. It should be pointed out that the deposition of inorganic solids arising from the aqueous phase (i.e., scale) also poses a serious threat to flow assurance. With the ongoing trend to deepwater developments, future oil and gas discoveries increasingly will be produced through multiphase flow lines from remote facilities in deepwater environments. These multiphase fluids are a combination of gas, oil, condensate, and water. Together with sand and scales, they have the potential to cause many problems, including

- Asphaltene deposition.
- Wax deposition.
- Formation of hydrates.
- Corrosion and erosion.
- Emulsions.
- Slugging.

Jamaluddin, Nighwander, and Joshi (2001b) presented an excellent review of various flow-assurance management strategies designed to identify the potential for hydrocarbon solid deposition in deepwater production systems. As a background, brief discussions of the individual phase behavior of the various hydrocarbon elements are discussed.

Asphaltenes are high molecular weight aromatic organic substances soluble in aromatic solvents (e.g., toluene, diesel) but precipitated by the addition of molecular-weight alkenes (e.g., n-heptane/n-pentane). The molecular weight of asphaltene ranges from 1000 to several hundreds of thousands with a microparticles density of approximately 1.2 gm/cc. Generally, asphaltenes tend to remain in solution or colloidal suspension under reservoir temperature and pressure conditions. They may start to precipitate once the stability of the colloidal suspension is destabilized, which is caused by the changes in temperature or

pressure during primary depletion. On the other hand, asphaltenes have been reported to become unstable as a result of fluid blending (comingling) of fluid streams as well as by gas injection during improved oil recovery (IOR) operations. It is important to note that the asphaltenes precipitated by pressure drop in a reservoir production system are different from the asphaltenes deposited by destabilizing the solution.

Asphaltene solubility is highly dependent on the composition of the crude, less dependent on the pressure, and hardly dependent on temperature. Asphaltene solubility is higher when the crude is heavier and more aromatic, that is, tends to remain in the crude oil system. A high asphaltene content of crude does not necessarily mean that flowing problems will occur during production; often the contrary is the case. For example, the Venezuelan Boscan crude, which is very heavy, containing 17% of asphaltenes, was produced nearly trouble free. On the other hand, the Algerian Hassi-Messaoud crude, which is very light, contains only 0.062% of asphaltenes, met with difficulties during production.

Waxes are also high molecular weight, highly saturated organic substances. The formation of wax crystals depends significantly on temperature change. Pressure and composition also affect their formation but not to a significant extent. In general, the wax fraction can be characterized by its melting point temperature, its molecular weight, or the corresponding chain length.

Gas hydrates are the “clathrate” inclusion compounds. They are formed by the contact of hydrate-forming gases (primarily methane, ethane, propane, carbon dioxide, and hydrogen sulfide) and liquid water at low temperature (0–40°C) and high-pressure conditions. Two types of gas hydrates are classified in the literature: Structure I and Structure II. Each hydrate building block has a central cavity to encapsulate molecules of hydrate forming gases.

As shown schematically in Figure 6-1 by Jamaluddin et al. (2001a), hydrocarbon solids have the potential to deposit anywhere from the near well bore and perforations to the surface facilities.

Jamaluddin et al. (2001a and 2001b), Ratulowski et al. (2004), and Willmon and Edwards (2005) point out that flow assurance is a critical issue that must be addressed early in the design process for offshore production systems. Jamaluddin and his coauthors noted that a systematic approach to defining the thermodynamic and hydrodynamic characteristics of a deepwater discovery is essential to assess the risk of hydrocarbon-solid formation and deposit. This approach generally consists of the following phases: fluid sampling and transport; characterization of fluid composition; preliminary screening for hydrocarbon solids; and experimental measurements on asphaltene, wax, and hydrates. These four steps are briefly discussed next.

Hydrocarbon Solids: Assessment of Risk

Phase 1. Fluid Sampling and Transport

Many authors agree that flow assurance measurements have led to a new awareness of the need to have representative samples. The goal of any sampling procedure is to bring a sample back to the lab that is identical in composition to the fluid in the reservoir. Unfortunately, many of the solids that cause flow assurance problems come out of solution during the sampling process just as they do in production systems. Changes in pressure and

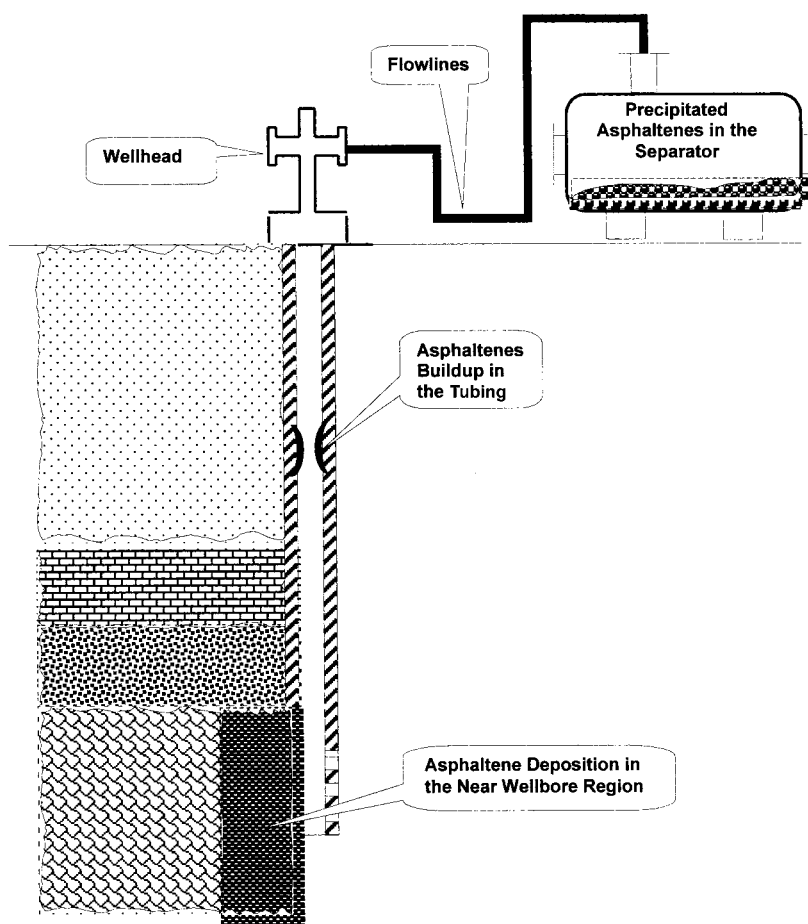


FIGURE 6-1 Possible locations for asphaltene deposit.

Source: After A. K. M. Jamaluddin et al., "Laboratory Techniques to Measure Thermodynamic Asphaltene Instability." Paper SPE 72154, SPE Asia Pacific Improved Oil Recovery Conference, Kuala Lumpur, Malaysia, October 2001.

temperature can cause phase changes that lead to sample alteration. Introduction of contaminants during the sample acquisition process can also alter the fluid composition. The most common source of contamination is from drilling fluids.

The perfect sample would be collected contamination free from the reservoir at constant temperature and pressure and transported intact to the laboratory maintaining both temperature and pressure. In this way alteration associated with phase changes, transfers, or contamination is eliminated. In practice, this is not possible today. A more realistic goal is to reduce the potential for phase changes through pressure and potentially temperature compensation.

During open-hole Modular Formation Dynamics Testing (MDTTM), a Single-Phase Multi-Chamber (SPMCTM) module normally is used in collecting single-phase reservoir fluid samples for asphaltene analysis. In the SPMC module, the fluid pressure is maintained above the reservoir pressure while the sample is retrieved to the surface by having a precharge nitrogen cushion in the sample chamber, thus, making the SPMC suitable for asphaltene precipitation testing. In the MDT module, other conventional chambers that

are not pressure compensated also are used to collect the reservoir fluid samples. In these conventional sample modules, fluid may undergo phase change phenomenon and, hence, render the sample invalid for asphaltene analysis.

Phase 2. Fluid Compositional Characterization

On arrival of fluid samples in the laboratory, the sample chambers are first validated by determining the opening pressure. Subsequently, a sample is chosen for study, and the sample is heated to the reservoir temperature using a custom-made heating jacket. The sample bottle then is placed into a rocking stand and agitated for a minimum of five days to ensure homogenization of the reservoir fluid. After stabilization, a small portion of the single-phase reservoir fluid is subjected to a single-stage flash experiment to determine:

- The gas/oil ratio (GOR).
- C_{31+} composition.
- Density at sample pressure and temperature.
- Stock oil density (API gravity).

A single-stage flash test usually is conducted from a pressure slightly above the bubble point at the reservoir temperature down to ambient conditions. The resulting mass and volumes of gas and liquid is recorded and the flashed fluids (gas and liquid) are analyzed using gas chromatography. The live oil composition then is calculated based on the measured gas and liquid compositions and GOR values. Finally, if the samples were obtained by open-hole sampling the level of oil-base mud (OBM) contamination in the stock tank, the oil needs to be determined. This is completed by a subtraction method taking into account the OBM filtrate composition of the contaminated stock-tank oil composition.

The most complex and least understood fraction of petroleum is residuum. The principal constituents are some of the very heavy oils, resins, asphaltenes, and high-molecular-weight waxes. Treatment of the residuum with liquid propane at temperatures not exceeding 70°F precipitates the resins and asphaltenes. This fraction, when treated with normal pentane, dissolves the resins and precipitates the asphaltenes as shown in Figure 6–2.

In going from oils to resins to asphaltenes, there are increases in molecular weight, aromaticity, and nitrogen, oxygen, and sulfur compounds. A simple, rapid way to compare the paraffinicity or aromaticity of any oil or its fraction, such as resins and asphaltenes, is by determining the ratio of hydrogen to carbon atoms, H/C. For example, the paraffin n-hexane C_6H_{14} has 14 hydrogen atoms to 6 carbon atoms with a ratio of H/C of 2.3, that is, $14/6 = 2.3$, whereas the aromatic benzene H_6C_6 has 6 to 6 with $H/C = 1.0$. As the hydrocarbon becomes more compact, with more-condensed aromatic rings having less hydrogen, the H/C ratio continues to drop. Resins have H/C ratios ranging from 1.3 to 1.6, where as most asphaltenes range from 1.0 to 1.3.

It should be pointed out that asphaltenes, together with resins, form the disperse phase of the crude oils, while maltenes form the continuous phase.

In addition to the grouped carbon number analysis just provided for, a portion of stock-tank liquid is prepared for saturate aromatic resin asphaltene (SARA) analysis. The objective of this analysis scheme is to divide oil into its saturate, aromatic, resin, and asphaltene (i.e.,

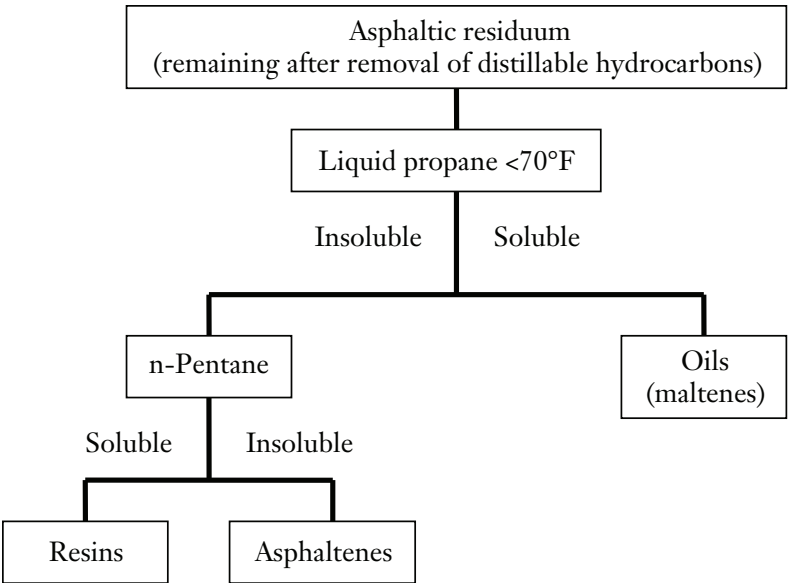


FIGURE 6-2 *Composition of asphaltene residuum.*

SARA) fractions. The saturate fraction consists of nonpolar material including linear, branched, and cyclic saturated hydrocarbons. Aromatics, which contain one or more aromatic rings, are more polarizable. The remaining two fractions, resins and asphaltenes, have polar substituents. The distinction between the two is that asphaltenes are insoluble in an excess of heptane (or pentane) whereas resins are miscible with heptane (or pentane). This classification system is useful because it identifies the fractions of the oil that pertain to asphaltene stability and so should be useful in identifying oils with the potential for asphaltene problems. The SARA, the separation scheme as just described, is summarized in Figure 6-3.

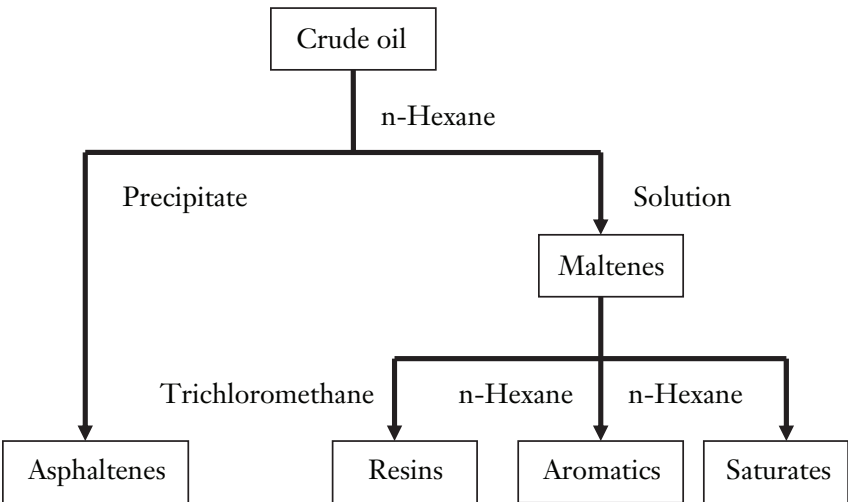


FIGURE 6-3 *SARA.*

It should be noted that the solubility of the heaviest oil fraction, the asphaltenes, depends on a delicate balance between this fraction and the lighter fractions of the crude oil. Any unfavorable disturbance in this balance may induce asphaltene aggregation. For instance, the addition of light, paraffin components to an asphaltene containing crude oil lowers the solubility power with respect to the asphaltenes. As already stated, resin molecules react to the addition of the light paraffin components by desorbing from the asphaltenes in an attempt to reestablish thermodynamic equilibrium, thus increasing the probability of asphaltene self-aggregation.

Asphaltenes are also known to aggregate by pressure depletion alone. By decreasing the pressure, the relative volume fraction of the light components within the crude oil increases. This causes an increase in the solubility parameter difference between the crude oil and the asphaltenes, reaching a maximum at the bubble-point pressure. Below the bubble point, asphaltenes are more soluble again due to evaporation of light crude oil components. The relative change in asphaltene solubility has been shown to be highest for light crude oils that are undersaturated with gas and usually contain only a small amount of asphaltenes. This means, somewhat surprisingly, that heavy crudes usually present fewer problems with asphaltene aggregation and precipitation, despite their higher asphaltene content. Of course, heavy crude oils generally possess higher resin amounts, which can explain some of this behavior.

Temperature has a less pronounced effect on aggregation than crude oil composition and pressure, but an increase in temperature generally affects the aggregation of asphaltenes by decreasing the solvating power of the crude oil. However, some controversy regarding the temperature effect exists in the literature. Some authors state that the asphaltene aggregate size decreases with increasing temperature, while others state that the precipitation of asphaltenes increases with temperature.

The reversibility of the asphaltene aggregation also is a subject of some controversy. Hirschberg et al. (1984) assumed that the aggregation was reversible but probably very slow. Joshi et al. (2001) found the precipitation from a live crude oil to be reversible in a matter of minutes, except for a subtle irreversibility observed for the first depressurization of the crude oil. They also discussed the different behavior of asphaltenes precipitated from crude oils with excess n-alkanes and that of asphaltenes contained in the original crude oil. Hammami et al. (1999) also found that the aggregation was generally reversible, but the kinetics of the redissolution varied significantly depending on the physical state of the system. Peramanu et al. (2001) reported differences in the reversibility of solvent- and temperature-induced aggregation.

Fan, Jianxin, and Buckley (2002) observed that the proportions of each of the SARA fractions in a crude oil are related to the stability of asphaltenes in that oil. Cabbognani, Rogel, and Espidel (1999) demonstrated that reservoirs with asphaltene problems were not primarily those with large amounts of asphaltenes in the oil but those with high saturate fractions. Leontaritis and Mansoori (1987) recommended using the ratio of resins to asphaltenes, R/S, as an indicator of asphaltene stability recommendation, based on the hypothesis that resins confer asphaltene stability by “coating” asphaltenes. Jamaluddin et al. (2001b) presented a complete laboratory fluid characterization data set as given in Tables 6–1 through 6–3.

TABLE 6-1 *Preliminary Fluid Properties*

Parameters	Units	Description
Reservoir pressure, p_i	psia	7393
Reservoir temperature	°F	152
Flash gas/oil ratio	scf/STB	1037
Bubble-point pressure p_b at T_{res}	psia	6267
Density of stock-tank oil (STO)	g/cc	0.898
Density of reservoir fluid at p_b	g/cc	0.801
Density of reservoir fluid at p_i	g/cc	0.819
OBM contamination in STO	% (w/w)	0.845
OBM contamination in reservoir fluid	% (w/w)	0.717

TABLE 6-2 *Reservoir Fluid Composition*

Components	Flashed Liquid	Flashed Gas, mol%	Reservoir Fluid
Nitrogen	0.00	0.10	0.07
Carbon dioxide	0.00	0.14	0.10
Hydrogen sulfide	0.00	0.00	0.00
Methane	0.00	84.92	60.99
Ethane	0.00	6.08	4.37
Propane	0.00	3.45	2.48
i-Butane	0.00	0.76	0.54
n-Butane	0.01	1.54	1.11
i-Pentane	0.04	0.96	0.70
n-Pentane	0.09	0.65	0.49
Pseudo C_8H_{14}	1.65	0.74	1.00
Pseudo C_{7+}	98.21	0.67	28.15
Total	100	100	100
MW	293.42	20.85	97.66
Mol%			
C_{7+}	98.21	0.67	28.15
C_{12+}	71.29	0.00	20.09
C_{20+}	35.80		10.09
Molar Mass			
C_{7+}	297.27	100.31	293.9
C_{12+}	362.94	165.43	362.94
C_{20+}	515.90		515.90
Density (g/cc)			
C_{7+}	0.899		
C_{12+}	0.920		0.920
C_{20+}	0.959		0.959
Fluid at 60°F	0.898		
Mole ratio	0.2818	0.7182	

TABLE 6-3 SARA Analysis of Stock-Tank Oil

Cylinder	Saturates, wt%	Aromatics, wt%	Resins, wt%	Asphaltenes, wt%	Wax, wt%
Sample 1	49.53	31.70	18.10	0.67	0.86

These laboratory data show that the fluid has a low GOR of 1037 scf/STB for a high bubble-point pressure of 6267 psia and relatively high stock-oil density of 0.8818 gm/cm³ (26°API). Also note from the SARA analysis that the asphaltene (0.67 wt %) and wax (0.86 wt %) contents of the crude oil are quite low.

Phase 3. Preliminary Screening for Hydrocarbon Solids

De Boer and Leeriooyer (1992) compared the properties of some crude oils in which asphaltene problems were encountered with those that operated trouble free. This comparison is shown in Table 6-4 for 10 oil systems.

Table 6-4 shows, in addition to observations by De Boer and Leeriooyer, several parameters can be used to identify crudes with the potential to cause flow assurance problems, these are

- Light crudes high in C₁–C₃ with relatively low C₇₊ content.
- High bubble-point pressure, *p_b*.

TABLE 6-4 Comparison of Properties of Crudes with Asphalt-Related Operating Problems and Crudes with No Asphalt-Related Operating Problems

	Crudes with No or Few Problems	Crudes with Severe Problems
Name	North Sea Oil D1 North Sea Oil D2 North Sea Oil D3 North Sea Oil D4 North Sea Oil A1	North Sea Oil F Kuwait Oil A2 Kuwait Oil B Kuwait Oil M1 Kuwait Oil M2
Crude composition		
C ₁ –C ₃	<27 mole%	>37 mole%
C ₇₊	>59 mole%	<46 mole%
Asphaltenes	>3 weight%	<0.5% weight
Tank oil composition		
Saturates	≤62 weight%	≥75 weight%
Aromatics	≥26 weight%	≤22 weight%
Heavy ends	>11 weight%	<4 weight%
Asphaltenes	>3 weight%	≤1 weight%
Properties		
Bubble point	<6.2 MPa	>10 MPa
Reservoir pressure	<95 MPa	>40 MPa
C _o (<i>p_b</i> , <i>T_r</i>)	<1.6 × 10 ⁻⁹ /Pa	>2.3 × 10 ⁻⁹ /Pa
C _o (<i>p_i</i> , <i>T_r</i>)	<1.0 × 10 ⁻⁹ /Pa	>1.2 × 10 ⁻⁹ /Pa

- Large difference between reservoir pressure, p_r , and bubble-point pressure; that is, undersaturation, $\Delta p = p_i - p_b$, is high.
- High oil-compressibility coefficient, c_o .

Additional literature review suggests:

- Maximum solids deposit occurs near or at the bubble-point pressure in the piping system.
- Precipitation occurs during gas lift if gas bubbles are formed.
- Asphaltene deposit can occur as a result of exposure of oil to a low-pH environment (typically, pH less than 4) during acid treatment of wells.
- Reservoir wettability reversal occurs after asphaltene deposit.
- The risk of asphaltene deposit due to gas injection.

De Boer and Leeriooyer proposed a plot that can be used as a first screening tool to identify the potential for the oil to exhibit solid formation problems. The plot, called a De Boer plot, was developed based on laboratory data and numerous field observations. The plot, as shown in Figure 6-4, defines the following three regions:

- Region with possible severe solid deposit problems.
- Region with mild problems.
- Region with no solid deposit problems.

Denoting p_i and p_b as the initial pressure and bubble-point pressure, respectively, the boundaries of the three regions are defined by the undersaturation pressure difference ($p_i - p_b$) on the y -axis and the oil density at the initial reservoir pressure on the x -axis.

EXAMPLE 6-1

Using the fluid data given in Table 6-1, determine if this fluid might develop an asphaltene deposition problems using the De Boer plot.

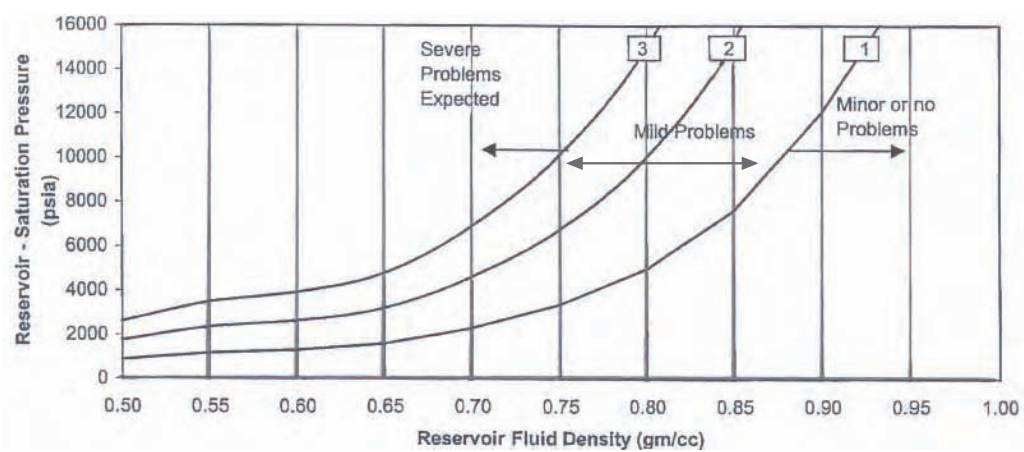


FIGURE 6-4 De Boer plot.

SOLUTION

Step 1 Calculate the undersaturation pressure difference:

$$\Delta p = p_i - p_b = 7393 - 6267 = 1126 \text{ psia}$$

Step 2 Enter the De Boer plot with 1126 psia and oil density of 0.819 gm/cm^3 , as shown in Figure 6–1, to conclude that this fluid will not exhibit any problems in the field.

Jamaluddin and coauthors proposed a second screening criterion, based on the asphaltene versus resin relationship as shown in Figure 6–5. The y -axis represents the asphaltene weight percent and x -axis represents the resins weight percent. The graph identifies two regions, an unstable region with asphaltene deposit problems and a stable region with no asphaltene problems.

EXAMPLE 6-2

Rework Example 6–1 using the asphaltene versus resin graph.

SOLUTION

Step 1 From Table 6–3, read the resin and asphaltene weight percent, to give:

Resins = 18%

Asphaltene = 0.67%

Step 2 Plot the coordinate of the sample, that is, sample 1, to conclude that the system is stable.

The colloidal instability index (CII) is another screening criteria, suggested by Yen, Yin, and Asomaning (2001), that can be used to identify crude oil systems with deposit problems. The colloidal instability index is expressed as the ratio of the sum of asphaltenes and saturates to the sum of aromatics and resins:

$$\text{CII} = \frac{\text{saturates} + \text{asphaltenes}}{\text{aromatics} + \text{resins}}$$

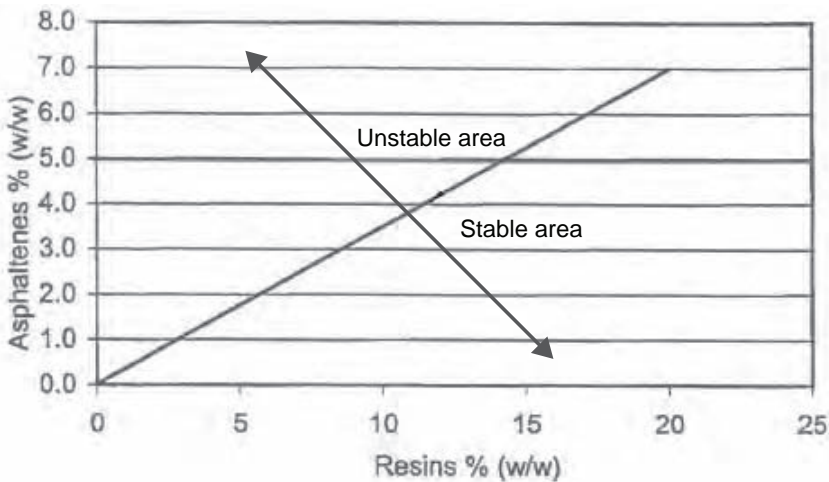


FIGURE 6-5 Asphaltene resin ratio approach.

Oils with a CII below 0.7 are considered stable while those of above 0.9 are considered very unstable. A graphical presentation of this screening approach is shown in Figure 6–6 as expressed in terms of (asphaltenes + saturates) content versus (aromatics + resins) content in the hydrocarbon system. This graphical relationship identifies three regions:

- Unstable.
- Mild problems.
- Stable.

EXAMPLE 6-3

Rework Example 6–1 by using the colloidal instability index criteria.

SOLUTION

Step 1 From Table 6–3 determine

Asphaltene + saturates = 0.67 + 49.53 = 50.20%

Aromatics + resins = 31.70 + 18.10 = 49.80%

Step 2 The coordinate of the SARA content, as shown in Figure 6–5, indicates that there is a potential for asphaltene formation in this crude.

Similarly, we can identify the stability of the oil from the expression

$$CII = \frac{\text{saturates} + \text{asphaltenes}}{\text{aromatics} + \text{resins}} = \frac{50.20}{49.80} = 1.00803$$

Based on the CII criteria, the system is highly unstable.

Finally, an asphaltene stability index developed by Oilphase-Schlumberger is shown in Figure 6–7. The illustration suggests that, if

$(\rho_{oi} - \rho_{ob}) > 0.025$, system is unstable

$(\rho_{oi} - \rho_{ob}) < 0.025$, system is stable

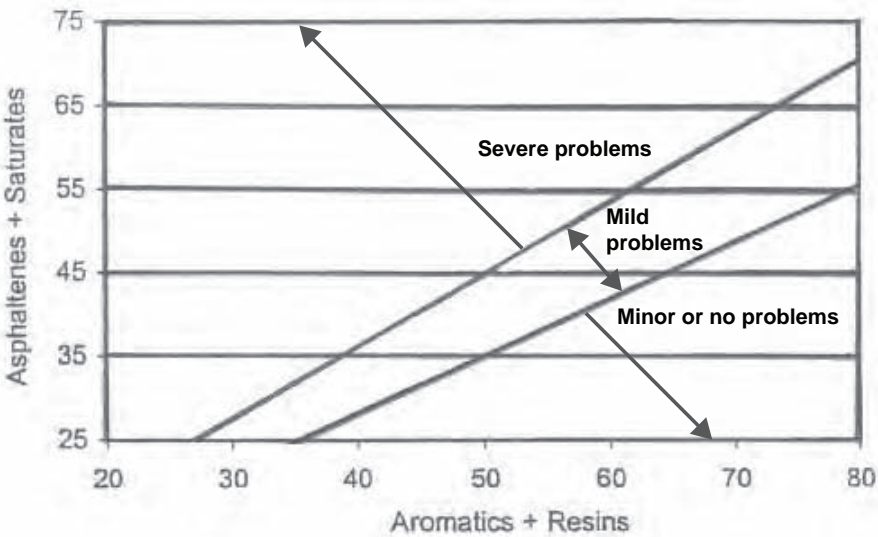


FIGURE 6-6 Colloidal instability index approach.

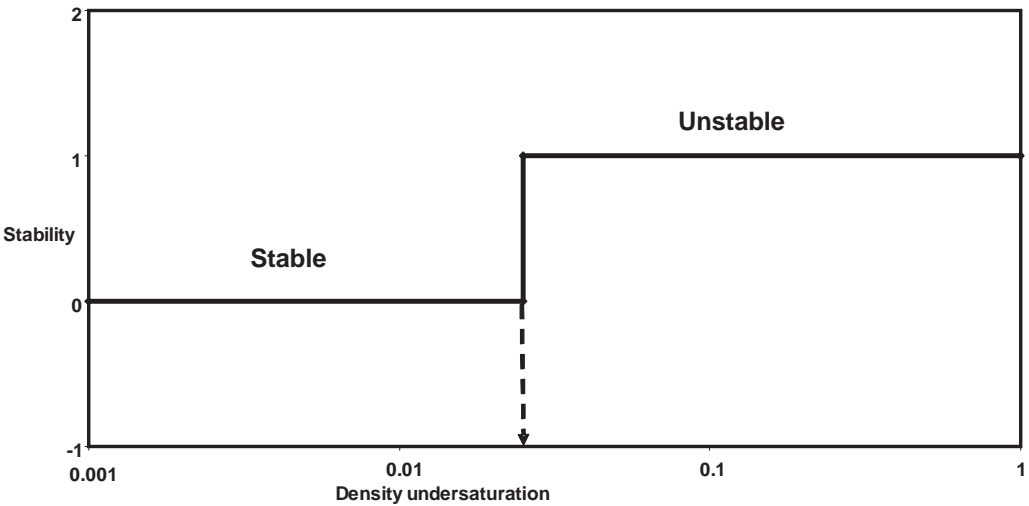


FIGURE 6-7 Asphaltene stability index.

where ρ_{oi} = oil density at initial reservoir pressure, gm/cm³ and ρ_{ob} = oil density at bubble-point pressure, gm/cm³.

For the crude oil of Example 6-1 and from Table 6-1:

$$\rho_{oi} - \rho_{ob} = 0.819 - 0.801 = 0.018 \text{ gm/cm}^3$$

The criteria indicate that the system is on the border between stable and unstable. Based on the conflicting results obtained by applying these four criteria, Jamaluddin and coauthors felt that there was a probability of asphaltene formation, justifying further laboratory testing to clarify this potential.

Preliminary screening for wax formation generally involves considerations of the stock-tank oil wax content (UOP procedure), wax appearance temperature, and preliminary thermodynamic modeling. If wax content is greater than 2 wt% and the measured or predicted stock-tank oil (STO) wax appearance temperature are in excess of 120°F, this may indicate a significant concern.

For hydrate screening, thermodynamic models and correlations (to be discussed later in the chapter) provide reasonable initial estimates of hydrate-forming conditions. If these techniques predict hydrate formation at a temperature above those anticipated during production, complete experiments to quantify the actual hydrate formation conditions might be necessary.

Phase 4. Experimental Measurements

Willmon and Edwards (2005) state that, once the initial assessment has been completed, a more-thorough, detailed, and expensive laboratory testing program, using the bulk of the qualified samples, can be performed. A variety of tests are available using pressurized, live-oil samples that can confirm the initial evaluations. This testing can be performed in conjunction with the standard pressure-volume-temperature (PVT) testing. The live-oil

testing is basically a manipulation of the samples' pressure and temperature while monitoring for solids deposit, a simulation of what the fluids will experience during production.

The flow assumption determines that the boundaries of solids formation for these samples are a combination of visual technologies and deposition measurements:

- *Asphaltene tests* Asphaltene deposit and precipitation is primarily pressure driven. Isothermal depressurization techniques (including near infrared [NIR] light-scattering techniques; high-pressure microscopy [HPM]; and high-temperature, high-pressure filtration) can be used to define the asphaltene precipitation boundaries.
- *Wax tests* Wax/paraffin deposit is primarily temperature driven. Again, isothermal depressurization techniques can be used to define the wax precipitation envelope.
- *Hydrate tests* Isobaric cooling using visual and mechanical observation can be used to determine the hydrate formation decomposition temperatures for the subject samples.

Figure 6–8 schematically shows the pressure/temperature phase boundaries for wax, asphaltene, and hydrate along with the phase envelope of the hydrocarbon.

Figure 6–8 shows the potential well-flow pressure/temperature path that obviously would be dependent on the specific hydrodynamic and heat transfer characteristics of a

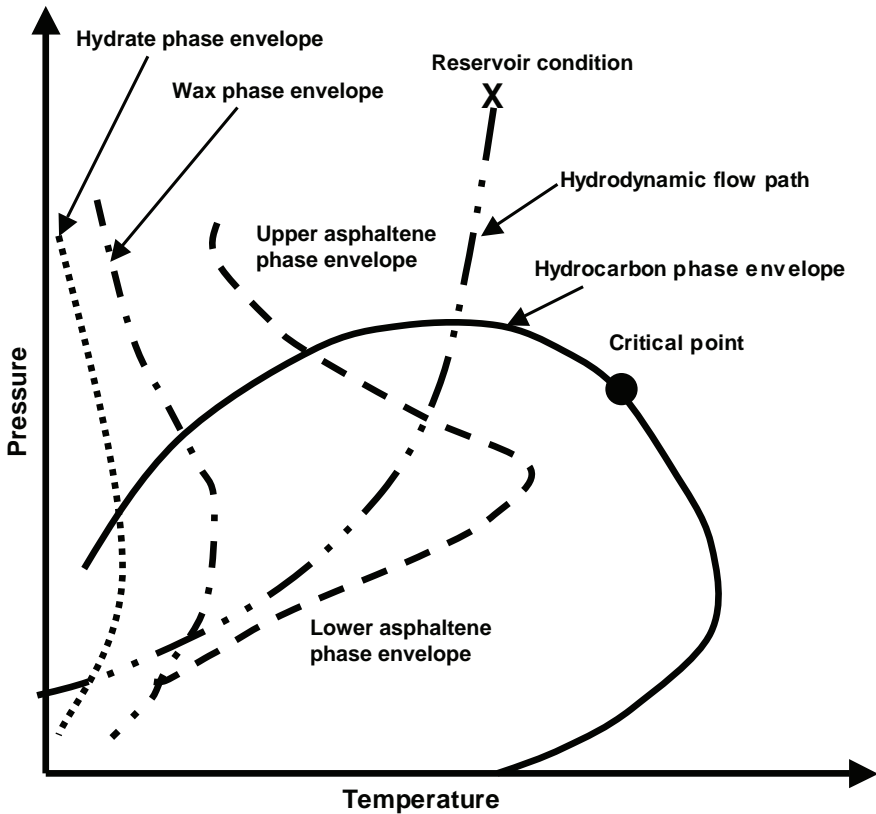


FIGURE 6–8 Schematic representation of the thermodynamic conditions of the flow-assurance elements.

given completion and facility systems. As can be seen, the pressure and temperature pathway can intersect one or all three elements of hydrocarbon solid formation and, consequently, result in potential flow-assurance problems whenever these boundaries are crossed. Jamaluddin and others point out that crossing the thermodynamic boundaries of hydrocarbon solid formation does not necessarily imply that a flow-assurance problem will occur. In other words, if hydrocarbon solids form but do not deposit, they are not a problem. A variety of flow-assurance management strategies may be tailored to address the specific problems expected in the system; they include:

- Thermal management, such as hot water circulation electrical heating.
- Pressure management, such as pumping, boosting, blowdown for hydrates.
- Chemical treatment.
- Routine or periodic remediation processes, such as pigging, jetting, cutting.

Phase Behavior of Asphaltenes

An understanding of asphaltene phase behavior is important in both the petroleum and processing industries because of the asphaltene potential to phase separate and aggregate with changes in crude oil temperature, pressure, and composition. As the oil industry moves toward deeper reservoirs and relies more on integrated production systems, the probability of encountering asphaltene precipitation problems and the costs associated with their remediation will only increase.

The currently accepted definition of asphaltenes, based on its solubility, states that “asphaltenes are insoluble by alkenes, e.g., n-pentane, n-heptane, however, they are soluble in aromatic solvents such as benzene and toluene.” The definition indicates that the asphaltenes can be precipitated with addition of alkenes to the crude oil. When compared with other crude oil components, asphaltenes are the heaviest fraction of a distribution in terms of molecular weight as well as aromaticity. Studies on asphaltene structure show that the basic asphaltene “molecule” (asphaltene sheet) has a molecular weight on the same order of magnitude as that of resins in the range of 500–1000. Asphaltenes, however, can form aggregates with molecular weight distribution of 1000–100,000. Asphaltenes carry an intrinsic charge that may be positive or negative, depending on the oil composition. If placed in an electrical field, they migrate to the oppositely charged electrode. Resins can be defined as the fraction of crude oil that is soluble in n-heptane, toluene, and benzene at room temperature. Resins have a strong tendency to associate with asphaltenes due to their opposite charge. They are adsorbed by asphaltenes and act as a protective layer. This reduces the aggregation of asphaltenes, which determines to a large extent their solubility in crude oil. It should be pointed out that *asphalt* is a term used to designate the combination of asphaltenes and resins.

The most common theory for describing the asphaltene/resin interaction is based on the assumption that asphaltene micelles (aggregates) exist in the oil as solid particles in colloidal suspension and stabilized by resins absorbed on their surface. It is also assumed that the short-range intermolecular repulsive forces between resin molecules absorbed on

different asphaltene particles keep them from flocculating. Because asphaltene particles are stabilized by this “protective shield” of resins, any action of a chemical, electrical, or mechanical nature that deprotects these particles or removes the resin protective layer might lead to flocculation and precipitation of asphaltenes. Other potential operating conditions that affect asphaltene stability include changes in temperature, pressure, and crude oil composition. A schematic illustration of the resin “protective shield” is shown in Figure 6–9. In more general terms, asphaltenes can be considered to be material in the oils that can aggregate in response to changes in these conditions.

Alkafeef et al. (2005) point out that the destabilization (i.e., flocculation) of colloidal asphaltenes in oil-production flowing systems depends principally on breaking up the balances of attraction forces between the absorbed resin molecules and asphaltene particles. Resins are highly polar and, hence, attracted by the asphaltene kernels (i.e., micelle centers). Resins and asphaltenes together are called *micelles*. These micelles have separate molecular entities of the crude oil and subject to all thermodynamic changes the rest of the components undergo.

It should be noted that the amount of asphaltene present in oil can be readily quantified by simple solvent precipitation tests (e.g., titration experiment), but whether that asphaltene causes problems depends on whether or not it reaches instability during its removal from the reservoir and subsequent transport to the refinery. Detecting the onset of asphaltene precipitation presents greater technical challenges than quantifying the amount initially presented in the oil.

It is appropriate at this time to define the following terms: *onset point*, *flocculation onset point*, *asphaltene onset pressure*, *stability of asphaltene*, *titration measurement*, and *refractive index*.

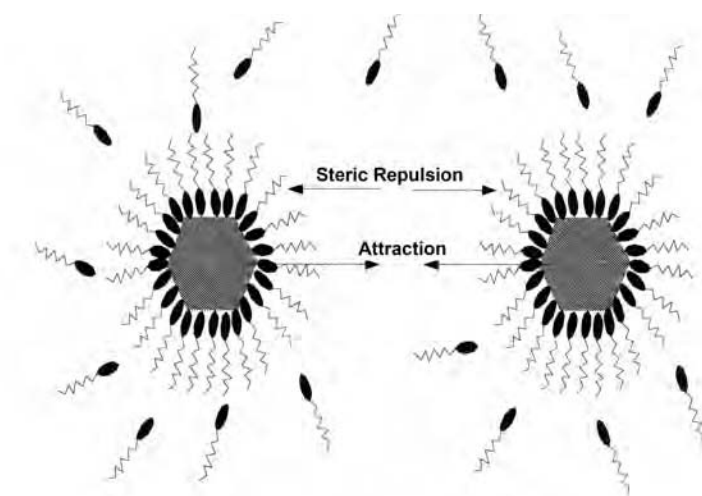


FIGURE 6–9 Force balance on asphaltene micelles showing the attraction and steric repulsion forces.

Source: After S. F. Alkafeef, paper 65018, SPE International Symposium on Oil Field Chemistry, Houston, February 13–16, 2001.

Onset Point

The *onset point* is defined as the mixture with the least amount of flocculent in which aggregated asphaltene particles appear.

Flocculation Onset Point

The *flocculation onset point* is defined as the ability of the colloidal particles to flocculate (aggregate) at any change in conditions, such as changes in temperature, pressure, or composition. Alkafeef, Gochin, and Smith (2001) point out that the mechanism of flocculation describes the growth of asphaltene particles to larger sizes while the precipitation mechanism represents the settling and deposit of the asphaltene particles.

Asphaltene Onset Pressure

The *asphaltene onset pressure*, p_{ao} , is defined as the pressure at which asphaltene flocculation begins. Flocculation is the first step toward asphaltene problems and, therefore, must be predicted accurately if asphaltene problems are to be anticipated and avoided.

Stability of Asphaltene

It is generally accepted that crude oil is considered to be a colloidal system comprising fractions of saturates, asphaltenes, resins, and aromatics. Asphaltene fractions are dispersed colloids in the oil phase, stabilized by the resin molecules that act as protective bodies for asphaltene particles. The precipitation of asphaltenes depends on the colloidal stability of these complex systems. Alkafeef, Fahad, and al-Shammari (2003) define the stability of a colloid dispersion as its resistance to flocculation, and the degree of “resistance” is used as a measure of the dispersion stability.

Titration and Other Asphaltene Content Measurements

It is well known that low-molecular-weight paraffin hydrocarbons, such as pentanes, precipitate asphaltenes, which are dispersed colloiddally in the crude oil. It should be pointed out that the amount of precipitation increases enormously by using lighter components than pentanes, as shown in Figure 6–10.

The test is designed to measure the amount of asphaltene that will precipitate when an oil sample is diluted with various ratios of n-alkene agent, n-pentane, and n-heptane. Essentially, the test is conducted by placing a known quantity of the reservoir oil in a special PVT cell and allowing it to reach reservoir temperature. The precipitating agent then is injected and the mixture is pressurized to the initial reservoir pressure. After agitation, the fluid remains undisturbed for 24 hours, allowing the asphaltenes to settle and adhere to the bottom of the vessel. Multiple tests should be performed to check the reproducibility of the collected data. The asphaltene sludge is recovered and rinsed with heptane to remove any resins or waxes. The amount of asphaltenes that precipitated is reported on the basis of weight percent of live oil. It should be pointed out that the flashed stock-tank oil is also tested for asphaltene content. Burke, Hobbs, and Kasbou (1990) reported precipitation tests on a mixture containing P20, 40, 60, and 80 mol% of solvent in the total mix as shown in Table 6–5.

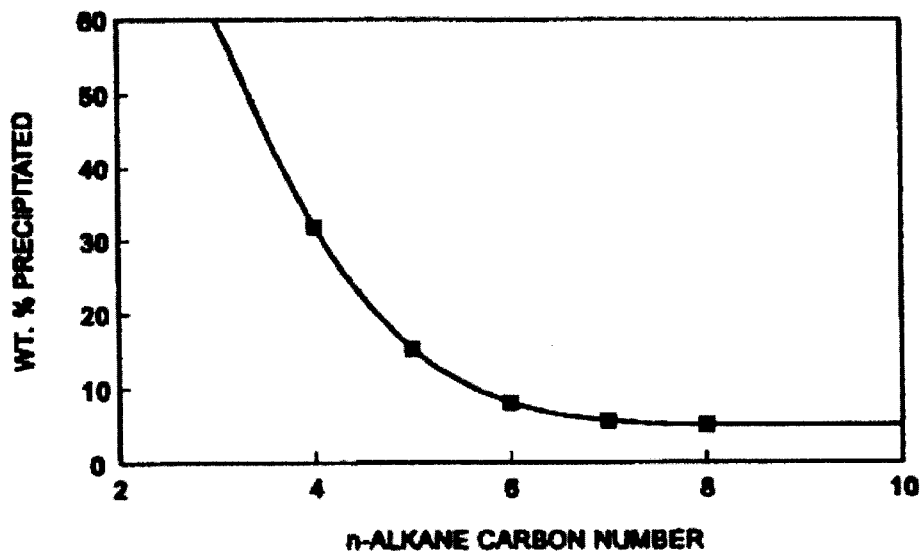


FIGURE 6-10 *Effect of solvent carbon number on insolubles.*

TABLE 6-5 *Static Precipitation Test Results for an Oil System at 212°F*

Solvent, mol%	Mixture Saturation Pressure, psia	Precipitates from Live Oil, wt%	Precipitates Remaining in Residual Stock-Tank Oil, wt%
0	2950	0.742	15.06
20	4128	0.699	15.71
40	5723	0.659	16.36
60	8175	0.797	15.61
80	12,585	0.807	15.69

Reported in the table are the amount of precipitates that formed and deposited from the live oil and the asphaltene content of the residual stock-tank oil after the static test was conducted. Numerous experimental tests suggest that the maximum amount of asphaltenes are precipitated at the bubble-point pressure. Hence, to quantify the maximum amount of asphaltenes that may precipitate during production, a filtration test (called *bulk deposition test*) is conducted at the bubble-point pressure in a high-pressure filtration apparatus. The apparatus consists of two cylinders, one of them connected to a pump. The sample is placed in this cylinder at constant pressure and temperature, representing reservoir conditions, and is equilibrated for 48 hours. The sample is then transferred into the second empty cylinder through a filter assembly with a 0.20 μm filter paper. To prevent flashing of the reservoir fluid as it passes through the filter, high-pressure helium is used to maintain a back pressure on the downstream side of the filter. As a result, the filtration process is very close to an isobaric transfer. The deposited asphaltenes are trapped on the filter assembly, which is removed at the end of the test and weighted. The amount of asphaltenes precipitates is calculated in ppm or as a percent of the total oil changed.

Jamaluddin et al. (2001a) present an excellent documentation of various laboratory techniques used to measure thermodynamic asphaltene instability. The light-scattering technique (LST) is one of these tests used to determine the onset of solid formation conditions. The LST apparatus is essentially a PVT cell equipped with fiber-optic light-transmittance probes to measure the thermodynamic conditions for the formation of hydrocarbon solids due to changes in the temperature, pressure, or composition. The fiber-optic probes are mounted across the windows of the visual cell. The principle behind the measurement is based on the transmittance of a near infrared light through the test fluid undergoing temperature, pressure, or the fluid composition changes. A computerized pump is used to either maintain the system pressure during temperature sweeps (to identify wax nucleation) or at a preset constant rate for isothermal pressure drop or injections of precipitating solvents (to study asphaltene precipitation). The process variables (i.e., temperature, pressure, solvent volume, time, and transmitted light power level) are recorded and displayed continuously during the course of the test. The fiber-optic light transmittance system is commonly referred to as the *light scattering system* (LSS).

Onset of asphaltene precipitation (OAP) measurements using the light-scattering system involves charging a known volume of the test fluid at reservoir (or specified) temperature and pressure to the PVT cell. The LSS components then are mounted across the windows of the PVT cell. The cell contents are homogenized at a maximum mixer speed of 1400 rpm for about 30 minutes. Subsequently, a light transmittance scan is conducted to establish a reference baseline. The depressurization experiment then is started, with simultaneous measurement of light transmittance power. The maximum depressurization rate used in this system is on the order of 40 psi/min.

The average transmitted light power and the corresponding pressure are recorded every minute, and the experiment is stopped after reaching a certain predefined lower pressure. During the depressurization run, any change in the light transmittance characteristics is a reflection of various fluid property and phase change phenomenon (i.e., appearance of solids or gas bubbles) that may occur. Visual observation of the cell contents are made and recorded during the course of the experiment. At the end of the experiment, the PVT cell is depleted and rinsed with toluene to measure the amount of any residual asphaltenes that may remain. The quantity obtained provides a qualitative indication of the percentage of total asphaltenes that may precipitate during production, whereas the rest tend to flow with the oil.

The recorded transmitted light power as a function of pressure is plotted in a Cartesian scale, as shown schematically in Figure 6–11, for a precipitating and nonprecipitating fluid. For the nonprecipitating fluid, the laser power increases monotonically (almost linearly) with a decrease in pressure, resulting from a decrease in fluid density. As the pressure approaches the bubble-point pressure, the evolved gas bubbles scatter light and transmittance drops sharply. However, for the precipitating fluid, the laser power drops before the bubble point. The point at which the curve deviates from the straight line break points is the onset of asphaltene pressure. This drop in the laser power is related to the flocculation of solids that scatter light and cause the power of the transmitted light to deviate from the expected linear relationship.

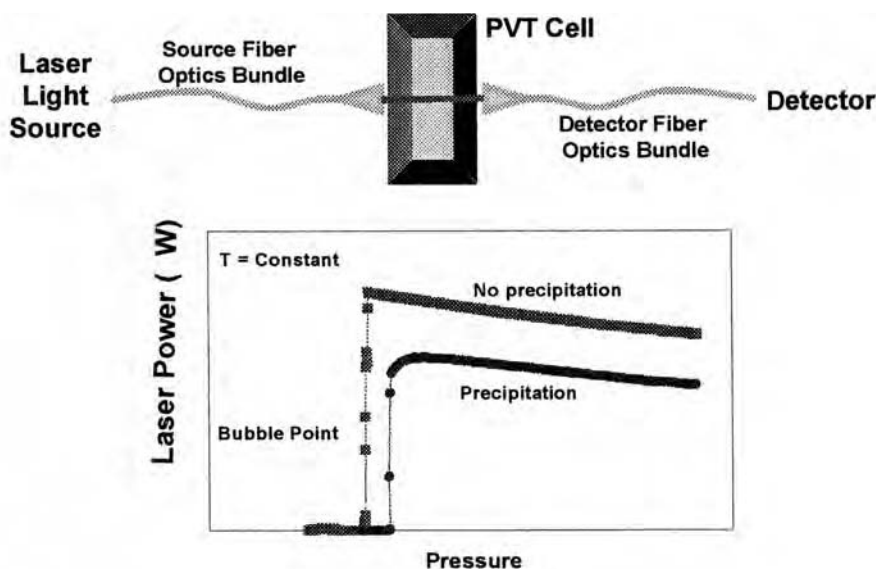


FIGURE 6-11 Schematic illustration of the principle behind the operation of the asphaltene precipitation cell.

Source: After Kokal et al., paper 81567, SPE Middle East Oil Show, Bahrain, June 9–12, 2003. Courtesy of SPE. © SPE 2003.

It should be pointed out that, in fluid operations, the phenomenon of asphaltene flocculation and deposit in well tubing appears to be influenced by the following two mechanisms: the fluid-phase (gas/liquid/solid) separation and the well flow regime.

Although a continuous source of flocculate asphaltenes exists, it is generally believed the deposit can occur between the asphaltene-onset pressure and the bubble-point pressure, as shown in Figure 6-12. One possible explanation is that turbulence through two-phase flow does not allow efficient deposition. Also, the solvency of the crude for asphaltene increases below the bubble-point pressure as a result of the loss of the lighter ends to the gas phase. Therefore, it is possible that flocculated asphaltenes may be redissolved before aggregation into larger particles. Thawer, David, and Dick (1990) point out that the redissolution of the asphaltene is possible only if a significant quantity of resins is still associated with the asphaltene particles.

A historical review of deposition depths in the west Kuwait Marrat Jurassic wells by Alkafeef et al. (2005) shows that the top of the asphaltenes deposits was found to be within the onset and bubble-point depth window. Figure 6-13 shows asphaltene-deposition depth in the Marrat well.

Alkafeef and coauthors estimated the deposit thickness of the asphaltenes in the West Kuwait Marrat wells by analyzing their flowing wellhead pressure (FWHP) data. The authors presented a case study where a Marrat well was shut in after cleaning the well of asphaltenes. As the subject well is opened to production, the FWHP dropped and stabilized at 1200 psig for approximately one month, as shown in Figure 6-14. After the stabilization period, the FWHP declined at a normal drawdown decline rate $(dp/dt)_{DD}$ of -2 psig/day for approximately 130 days. However, when the wellhead pressure reached 875

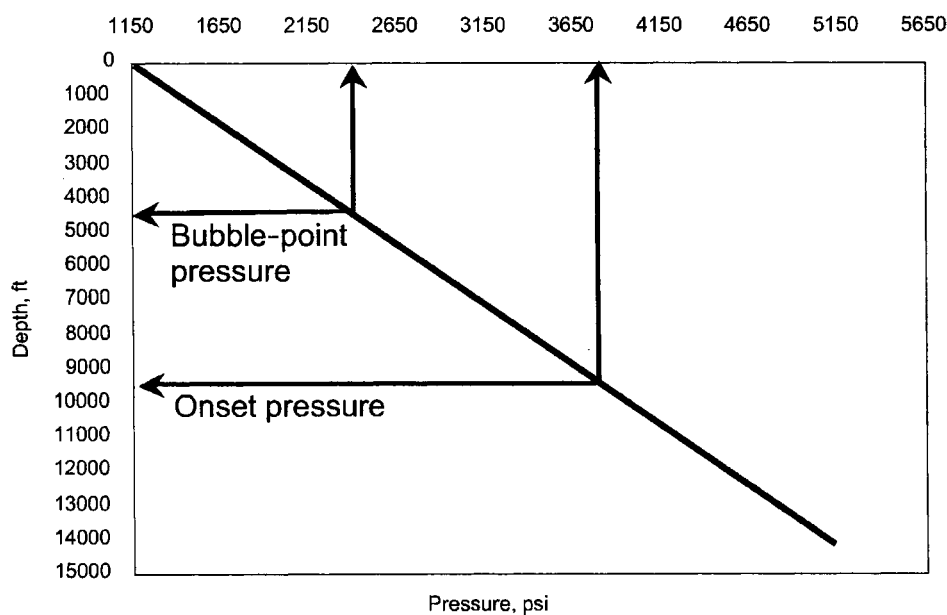


FIGURE 6-12 Typical pressure of a Marrat well versus depth.
Source: After S. F. Alkafeef et al., “A Simplified Method to Predict and Prevent Asphaltene Deposition in Oil Well Tubing, Field Case.” *SPE Production and Facilities* 20, no. 2 (May 2005). Courtesy of SPE. © SPE 2005.

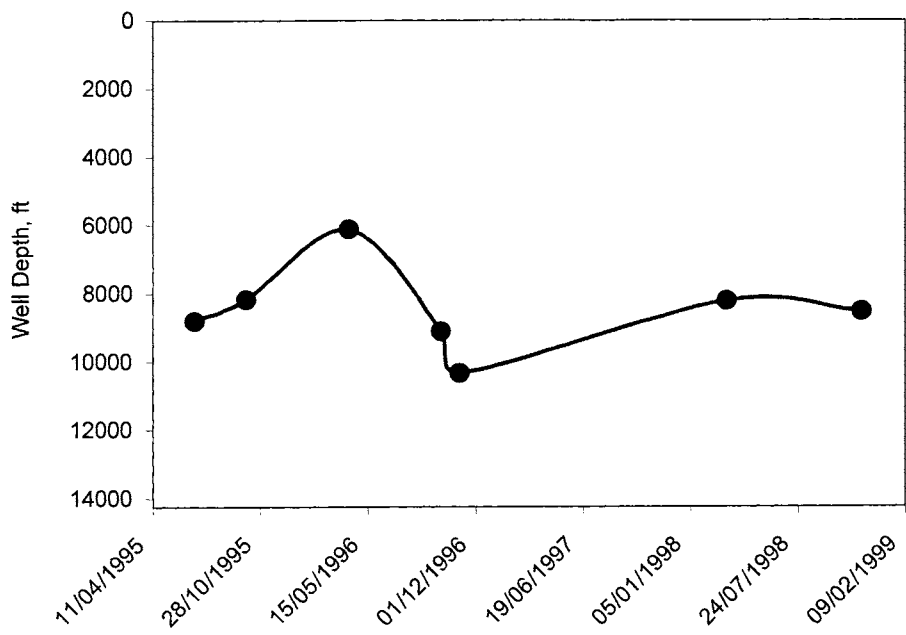


FIGURE 6-13 Asphaltene deposit depth in a Marrat well.
Source: After S. F. Alkafeef et al., “A Simplified Method to Predict and Prevent Asphaltene Deposition in Oil Well Tubing, Field Case.” *SPE Production and Facilities* 20, no. 2 (May 2005). Courtesy of SPE. © SPE 2005.

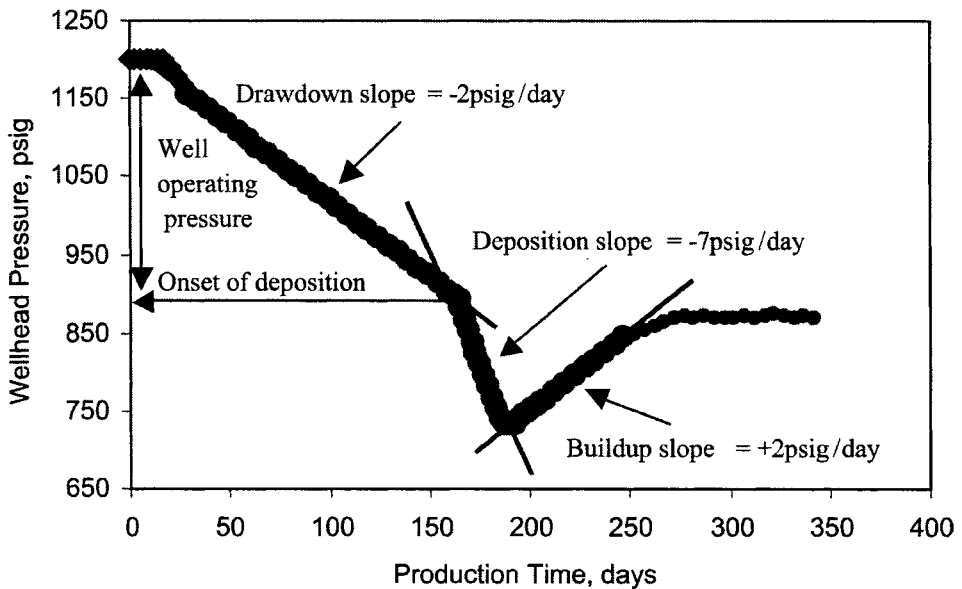


FIGURE 6-14 FWHP data versus time for a Marrat well.

Source: After S. F. Alkafeef et al., "A Simplified Method to Predict and Prevent Asphaltene Deposition in Oil Well Tubing, Field Case," *SPE Production and Facilities* 20, no. 2 (May 2005). Courtesy of SPE. © SPE 2005.

psig, a steeper decline of -7 psig/day was observed and continued for 25 days. At the end of this pressure decline period, an increase in the wellhead pressure of $+2$ psig/day that mirrored image of the initial decline behavior was recorded but with a positive slope.

To explain the previous behaviors indicated by FWHP data, it appears the well passes through deferent flow conditions. The first condition is a normal well stabilization after a shut-in period. The second condition is because of the lower drawdown pressure near the well bore, and it is a characteristic of both the reservoir formation and reservoir fluid. The third condition indicates the deposition of asphaltenes in the well tubing, as described by an asphaltene deposition decline rate $(dp/dt)_{AD}$ of -7 psig/day. This interpretation is supported by the buildup behavior in the FWHP, as attributed to the reduction in the well-tubing area caused by the deposit. The authors support their theory by observing that the slopes of the buildup and drawdown pressures are equal but in different directions. Behaviors of both drawdown and buildup pressures are caused by the characteristics of reservoir-formation and reservoir-fluid properties.

Alkafeef et al. used the normal pressure drawdown decline rate $(dp/dt)_{AD}$ to estimate the asphaltene deposition thickness, h_a , from

$$h_a = r \left\{ 1 - \left[\frac{(dp/dt)_{DD}}{(dp/dt)_{AD}} \right]^{0.25} \right\} \quad (6-1)$$

where

$(dp/dt)_{DD}$ = normal drawdown decline rate

$(dp/dt)_{AD}$ = asphaltene deposit decline rate

h_a = asphaltene-deposit thickness, in.

r = tubing radius, in.

EXAMPLE 6-4

Using the wellhead pressure data given in Figure 6-13 and an average tubing radius of 1.24 in., estimate the thickness of the asphaltene in the tubing.

SOLUTION

Step 1 Calculate $(dp/dt)_{DD}$ and $(dp/dt)_{AD}$ from the pressure data of Figure 6-13, to give

$$(dp/dt)_{DD} = -2 \text{ psig/day}$$

$$(dp/dt)_{AD} = -7 \text{ psig/day}$$

Step 2 Estimate the asphaltene thickness from equation (6-1):

$$h_a = r \left\{ 1 - \left[\frac{(dp/dt)_{DD}}{(dp/dt)_{AD}} \right]^{0.25} \right\}$$

$$h_a = 1.24 \left[1 - \left(\frac{-2}{-7} \right)^{1/4} \right] = 0.33 \text{ in.}$$

The authors indicated that estimated value of 0.33 in. is in excellent agreement with the value obtained from a caliper test.

Refractive Index

The refractive index (RI) is the degree to which light bends (refraction) when passing through a medium. It can also be defined as the sine of the angle of incidence divided by the sine of the angle of refraction, as light passes from air to the substance. The RI can be measured accurately by a refractometer. For example, RI for air is 1.00 and for water is 1.33. Studies at ambient conditions by Wand et al. (2000) have shown that the refractive index at the onset of precipitation is an important characteristic of oil/precipitant mixtures. The authors point out that the attraction interaction forces experienced by the colloidal-sized asphaltenes aggregates near the onset of precipitation is dominated by non-polar van der Waals forces. These attraction forces increase as the difference in refractive index between the colloidal asphaltenes and the rest of the oil phase (the maltenes) increases. Generally speaking, anything that decreases the maltene RI also decreases asphaltene stability. An exception is the effect of increasing temperature, which causes thermal disaggregation even though RI decreases.

Fan et al. (2002) defined PRI as the refractive index at the onset asphaltene precipitation and proposed that the difference between the refractive index of the oil $(RI)_{oil}$ and P_{RI} can be used as a measure of the asphaltene stability. Defining

$$\Delta(RI) = (RI)_{oil} \times P_{RI}$$

and based on six crude oil systems with experimental measured data for $(RI)_{oil}$ and P_{RI} , Fan and his coauthors proposed the following stability criteria:

- Crude oil with $\Delta(RI) > 0.060$ are more likely to have stable asphaltenes.

- Crude oil with $\Delta(\text{RI}) < 0.045$ are more likely to have asphaltene deposit problems.
- Crude oil with $0.045 < \Delta(\text{RI}) < 0.060$ are in the border region.

The data from the six crude oil systems is given in Table 6–6.

Applying the asphaltene stability criteria on the six crude oil systems, oils A-95 and C-LH-99 are likely to be stable, oil C-R-00 appears in the unstable region, and the remaining three are in the boundary line region.

Fan and his coworkers related the refractive index of oil, $(\text{RI})_{\text{oil}}$, to the SARA fraction by the following empirical equation:

$$(\text{RI})_{\text{oil}} \approx 0.001452S + 0.0014982A + 0.0016624 (R + As)$$

where

As = wt% of asphaltenes

S = wt% of saturates

A = wt% of aromatics

R = wt% of resins

This empirical expression is based on data for 67 crude oil systems.

To describe the phase behavior of solid precipitation (i.e., asphaltene, wax, and hydrate), it is beneficial to review and identify key properties of a pure component on the pressure/temperature diagram, as shown in Figure 6–15. This figure illustrates the concept of phase equilibrium and the critical point. The solid lines in the illustration clearly represent phase boundaries. The fusion or melting curve (line 2–3) normally has a steep positive slope, but for few substances (water is the best known), it has a negative slope. The melting curve is believed to continue upward indefinitely and essentially divides the solid-phase area from the liquid-phase area. The corresponding temperature at any point on the fusion curve is identified as the “fusion or melting-point temperature” of a specific pure component. The curves 1–2 and 2–C represent the vapor pressure of the solid and liquid, respectively. The terminal point, C, is the critical point that represents the highest pressure and highest temperature at which liquid and gas can coexist in equilibrium.

The intersection of the solid/liquid, liquid/vapor, and solid/vapor coexistence curves is called the *triple point*. Since the solid/liquid melting curve has a steep slope, the triple point temperature for most fluids is close to their normal melting temperature. The relationship

TABLE 6–6 Crude Oil Sample Properties

Oil	°API	Density at 20°C, g/cm ³	MW, g/mol	RI at 20°C	P_{RI}	Asphaltenes, %	$\Delta(\text{RI})$
A-95	25.2	0.8956	236	1.5128	1.4513	8.7	0.062
C-LH-99	22.6	0.9161	268	1.5137	1.4231	2.8	0.091
C-R-00	31.3	0.8673	235	1.4851	1.4444	1.9	0.041
S-Ven-39	28.8	0.8795	240	1.4976	1.4465	5.8	0.051
SQ-95	37.2	0.8409	213	1.4769	1.4223	1.3	0.055
Tensleep-99	31.1	0.8685	270	1.4906	-1.44	4.1	0.051

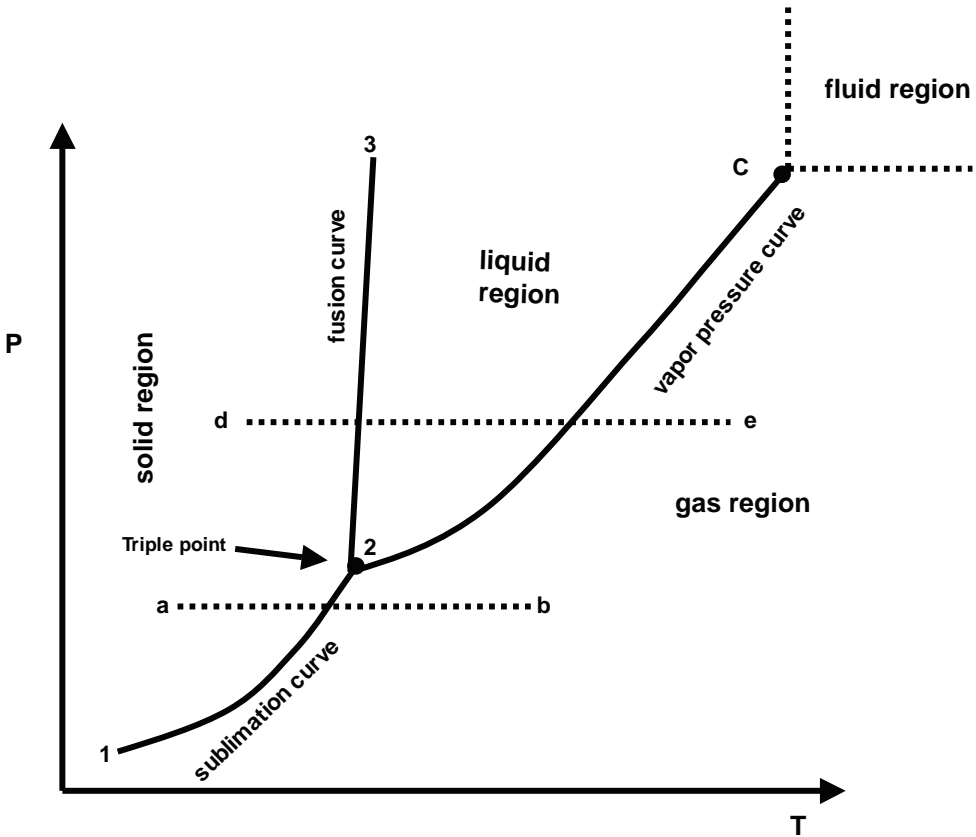


FIGURE 6-15 Pressure/temperature diagram for a pure component.

of specific or molar volume to temperature and pressure for a pure component in equilibrium states can be represented by a surface in three dimensions, as shown in Figure 6-16. The surfaces marked *S*, *L*, and *G* represent the solid, liquid, and gas regions respectively.

Asphaltene Deposit Envelope

Asphaltene precipitation from reservoir fluids during oil production is a serious problem because it can plug the formation, well bore, and production facilities. This precipitation can occur during primary depletion of highly undersaturated reservoirs or gas injection for improved oil recovery. Asphaltene flocculation depends on the composition of the hydrocarbon system, temperature, and pressure. In terms of composition, the peptizing power of the oil and its ability to keep asphaltenes in stable suspension depends on its relative amounts of paraffins, aromatics, and resins. Leontaritis et al. (1994) point out the fact that asphaltenes are deposited *only* after flocculation. During flocculation, the asphaltene micelles (aggregates) form larger-size asphaltene particles, causing formation damage by plugging the pore throats and reducing the effective hydrocarbon permeability. When asphaltene flocculation occurs in the rock matrix, some asphaltenes may drop out in the

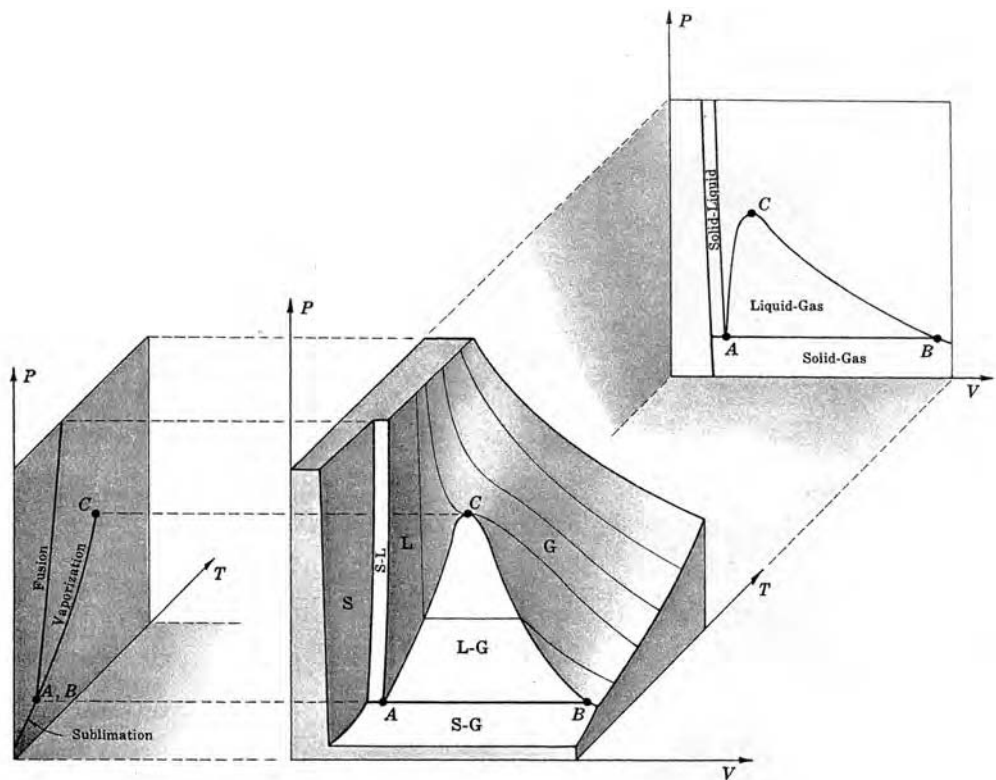


FIGURE 6-16 Schematic illustration of the relationship of volume to pressure and temperature for a pure substance.

pores because of their large size; others may be carried by the flowing fluid until they arrive simultaneously at the pore throats to bridge and reduce effective permeability.

Leontaritis and his coauthors pointed out that the region where asphaltene precipitation occurs is bounded by an asphaltene deposit envelope (ADE), as shown in Figure 6-17. The illustration also shows the saturation curve (pressure/temperature diagram) of the crude oil with the asphaltene deposit problem. The asphaltene onset pressures, p_{ao} , refer to corresponding points on the upper curve of the ADE. The precipitation typically occurs above the saturation pressure, that is, upper ADE pressure, and continues to increase until it reaches a maximum value around saturation pressure. The asphaltene precipitation process decreases as pressure drops further and ceases as pressure drops below the lower ADE pressure. Note that, when the reservoir pressure is above the saturation pressure, the precipitation is due solely to pressure, while below the saturation pressure both pressure and composition affect the precipitation behavior.

The asphaltene deposit envelope of oil is a very useful tool for evaluating the potential and severity of asphaltene problems. The ADE shows the thermodynamic path that must be followed during reservoir oil-recovery processes to avoid or minimize asphaltene problems. If possible, the oil should be maintained outside or as far away from the center of the ADE as possible.

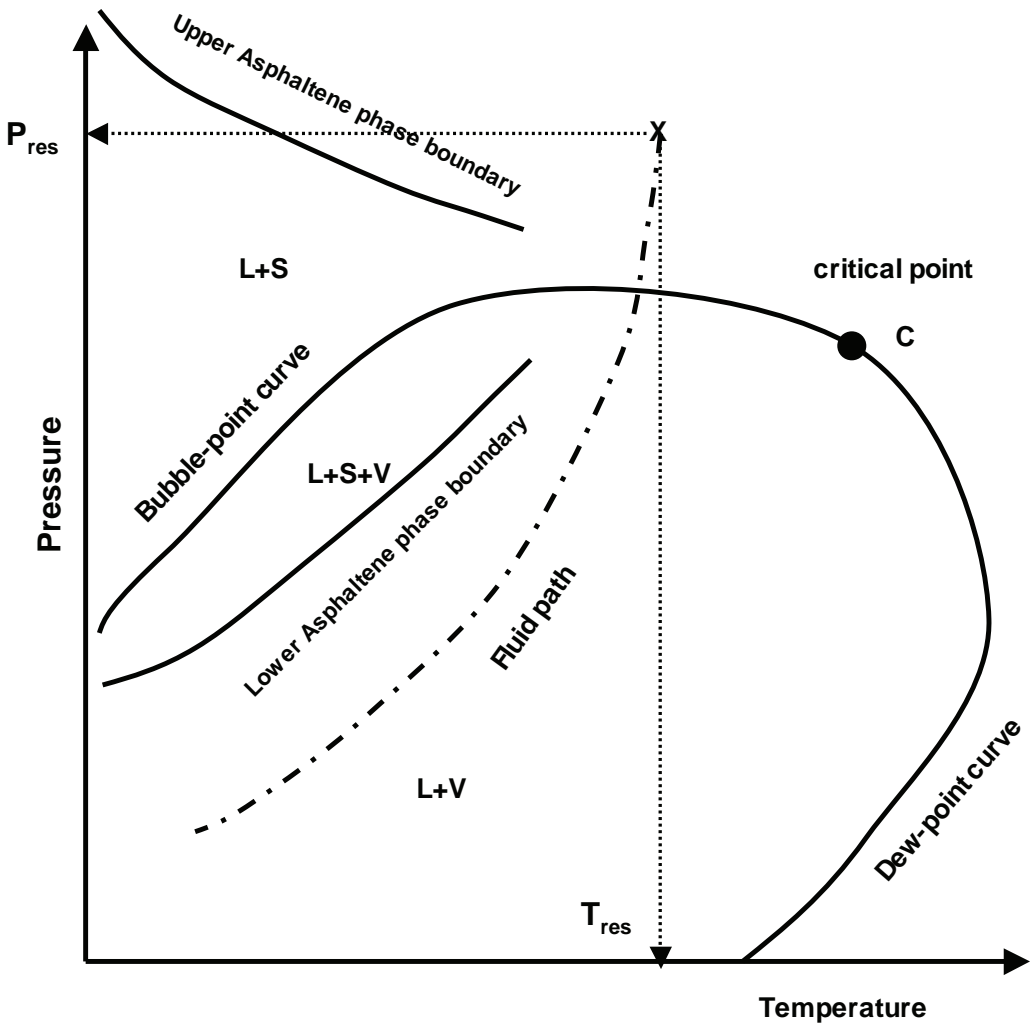


FIGURE 6-17 Pressure/temperature diagram of asphaltene deposit envelope.

Modeling the Asphaltene Deposit

Numerous laboratory investigations have indicated that precipitation occurs above the saturation pressure, reaches a maximum value around the saturation pressure, and decreases as the pressure drops further. This precipitation can cause serious problems because it can plug the formation and well bores.

Two approaches are used for modeling asphaltene precipitation:

- The first approach considers the asphaltene precipitation process to be thermodynamically reversible. The complete dissolution of asphaltenes in some organic solvents, such as toluene and benzene, supports this assumption.
- The second approach is based on the assumption that asphaltenes are solid particles colloiddally suspended in crude oil, which are stabilized by adsorbed resin molecules. When the adsorbed resin molecules are dissolved into solution, asphaltene particles

may aggregate mechanically or by electrostatic attraction. This concept is based mainly on titration experiments, which demonstrate that, once the adsorption equilibrium of resins between solid (asphaltene) and liquid phases is disturbed by adding paraffinic solvents, the asphaltene particles flocculate irreversibly.

Although research on the state of asphaltenes in crude oils is ongoing, a widely held view is that asphaltenes exist as colloidal particles held in suspension with associated resin molecules, which act as surfactants to stabilize the colloidal suspension. These colloidal particles may exist as a separate phase dispersed in the crude oil, or they may be dissolved in the oil, forming a true single-phase solution. In either case, the suspension is stable over geologic time.

When pressure in the reservoir is reduced or light hydrocarbons or other gaseous injectants introduced, the colloidal suspension may become destabilized, resulting in asphaltene and resin molecules precipitating out of the oil. Recent research has shown that this precipitation process, whether it is due to pressure depletion or gas injection, is largely reversible. However, there can be significant hysteresis in the redissolution process, which is the time required for asphaltenes to go back into solution, and may be considerably longer than the time required for the original precipitate to form. The highest pressure at which asphaltenes are first for a given oil or oil/solvent mixture is referred to as the *upper onset pressure*. As pressure is reduced below the onset pressure, further precipitation of asphaltenes occurs, and asphaltene particles flocculate into larger aggregates. Maximum precipitation occurs around the vapor/liquid saturation pressure for a fluid; further decrease in the pressure and the accompanying liberation of gas from the oil phase results in an increase in the solvating power of the oil and precipitated asphaltenes go back into solution.

Once asphaltenes have been precipitated from the oil, they may continue to flow as suspended particles, or they may deposit onto the rock surface, causing plugging and altered wettability. Deposition begins with adsorption of flocculated asphaltene particles onto active sites on the rock surface, particularly onto high specific area clayey minerals such as kaolinite. This is followed by a hydrodynamic retention or trapping of particles at the pore throats. Deposition of solid asphaltenes causes a reduction of the pore space available for fluids. Other formation damage mechanisms may include permeability reduction and alteration of rock wettability from water wet to oil wet. Deposited asphaltene particles also may be reentrained in the flowing oil stream due to a mechanical erosion or ablation effect if the interstitial velocity of the fluids becomes high enough. This effect has also been observed in studies of wax deposit in pipelines.

Nghiem et al. (1993 and 1997) proposed a thermodynamic model that is capable of describing the asphaltene precipitation behavior over a wide range of pressure, temperature, and composition conditions. The model is based on treating the asphaltene as a pure solid phase while the gas and oil are modeled with a cubic equation of state. The solid phase referred to as the asphalt phase and can either be a liquid or solid. The crucial step in modeling asphaltene precipitation is the characterization of the asphaltene.

Nghiem et al. (1993) point out that the assumption of asphaltene as the heaviest component in the hydrocarbon system is flawed because it contradicts observations reported in the literature of other heavy components (e.g., resins and paraffins) that may not precipi-

tate. The authors suggest that the asphaltene can be assumed to exist within the C_{31+} fractions group of the crude oil system. Nghiem and coauthors proposed that the C_{31+} group should be split into the following two fractions:

- A nonprecipitating asphaltene component, A , designated C_{31A+} .
- A precipitating asphaltene component, B , designated C_{31B+} .

The two components must have identical critical properties and be acentric, with a default set of physical property values as given by

$$\begin{aligned}T_c^A &= 1398.5^\circ\text{F} \\p_c^A &= 216.83 \text{ psia} \\\omega_c^A &= 1.274\end{aligned}$$

where

$$\begin{aligned}T_c^A &= \text{critical temperature of the asphaltene fraction} \\p_c^A &= \text{critical pressure of the asphaltene fraction} \\\omega_c^A &= \text{acentric factor of the asphaltene fraction}\end{aligned}$$

However, the binary interaction coefficients between the precipitated and nonprecipitated asphaltene and the light components are different. The precipitating component has larger binary interaction coefficients with the light components, which correspond to greater “incompatibility” between components and favor the formation of the asphalt phase. The binary interaction coefficient, k_{ij} , traditionally is calculated from the following expression:

$$k_{ij} = 1 - \left[\frac{2(V_{ci})^{1/6} (V_{cj})^{1/6}}{(V_{ci})^{1/3} + (V_{cj})^{1/3}} \right]^\theta$$

where k_{ij} = binary interaction coefficient between components i and j and V_{ci} = critical volume of component i .

The exponent θ is a regression parameter or an adjustable parameter that can be applied to different groups of components. Assuming that the last heavy fraction (e.g., C_{31+}) is split to C_{31A+} and C_{31B+} , Kohse et al. (2000) suggest that, to adjust the interaction parameters for the asphaltene component independently, the following three groups are identified for the exponent θ :

1. *Exponent θ_1* Applies to interactions between C_{31B+} and the components C_1 – N_2 through C_5 . This value ranges between 0.20 to 0.24.
2. *Exponent θ_2* Applies to binary interaction coefficients between C_{31B+} and components C_6 through C_{31A+} . The corresponding values are in the range of 1.8 to 2.5.
3. *Exponent θ* Applies to all other pairs of hydrocarbon components with an average value of 1.2.

Note that the two components also may have different volume shift parameters. The precipitating asphaltene component B (e.g., C_{31B+}) *can exit only in the liquid phase or as a pure solid*. The proposed methodology of splitting the asphaltene fraction into two components requires data from asphaltene precipitation experiments that can be used to determine the mole fraction of the precipitated component by applying the following relationship:

$$z_{C_{31B+}} = \frac{W_{C_{31B+}} M_{oil}}{M_{C_{31B+}}}$$

(6-2)

where

- $z_{C_{31B+}}$ = mole fraction of the precipitating fraction
- M_{oil} = molecular weight of the oil
- $M_{C_{31+}}$ = molecular weight of heavy fraction
- $W_{C_{31B+}}$ = total weight percent of the precipitate

EXAMPLE 6-5

The following oil and solvent composition and asphaltene precipitation (Table 6-7) data are given by Burke et al. (1990) with the asphaltene fractions group identified as C_{30+} . Split the C_{30+} into two components, a nonprecipitating component, $C_{30.4++}$, and a precipitating component, C_{30B++} :

COMPONENT	OIL, MOL%	SOLVENT, MOL%
CO ₂	1.42	17.76
N ₂ + C ₁	6.55	33.50
C ₂₊	7.00	26.92
C ₃	6.86	13.09
C _{4G+}	0.00	8.73
C ₄ -C ₉	24.66	
C ₁₀ -C ₁₆	22.41	
C ₁₇ -C ₃₀	19.62	
C ₃₀₊	11.48	

with

- Molecular weight of oil = 202.4
- Molecular weight of C_{30+} = 617.6

TABLE 6-7 Asphaltene Precipitation Data

Solvent, mol%	Mixture Sat. Pressure, psia	Test Pressure, psia	Precipitates from Live Oil, wt%	Precipitates in Residual STO, wt%	Total Precipitates
0	600	3014.7	0.14	8.83	8.97
20	1050	3014.7	0.27	7.56	7.83
50	2310	3014.7	1.46	5.50	6.96
78	4510	5014.7	3.21	4.63	7.84
85	5000	5014.7	1.29	6.73	8.02
90	4250	5014.7	1.10	6.07	7.17
90	4250	5014.7	1.10	6.07	7.17
					Avg = 7.8%

SOLUTION

Step 1 Calculate the average of the total weight percent of the precipitate, to give:

$$\text{Avg. wt \% of precipitate} = 7.8\%$$

Step 2 Calculate the mole fraction of the precipitating component, C_{31B+} , by applying equation (6-2):

$$\begin{aligned} z_{C_{30B+}} &= \frac{W_{C_{30B+}} M_{\text{oil}}}{M_{C_{30B+}}} \\ z_{C_{30B+}} &= \frac{(0.078)(202.4)}{617.6} = 0.0256 \\ z_{C_{30A+}} &= 0.1148 - 0.0256 = 0.0892 \end{aligned}$$

The precipitating component, C_{30B+} , may be considered to include asphaltene and resin molecules.

It should be pointed out that, when performing flash calculations, the precipitating component, such as C_{31A+} or C_{31B+} , under certain stability conditions, can exit in the liquid phase and as a pure solid, as described later in this chapter.

The fluid phases, liquid and gas, can be described within the framework of the equation of state, while the precipitated pure solid phase is described by an additional equation derived from the Flory-Huggins solubility model. Let s represent the solid phase in equilibrium with the two fluid hydrocarbon phases: liquid, L , and vapor, v . The thermodynamic basis for phase equilibrium conditions states that the fugacity, f_i , for each component i in the entire system is the same in all phases. In a mixture of n components, let the asphaltene component be the n th component. When the vapor, liquid, and solid phases coexist at equilibrium, the following thermodynamic equilibrium conditions must be satisfied:

$$f_i^V = f_i^L \quad (6-3)$$

$$f_n^V = f_n^L = f_n^s \quad (6-4)$$

Equation (6-3) expresses the equality of fugacity of component i in the vapor phase and liquid phase. Equation (6-4) expresses the equality of fugacity of the precipitating solid component in vapor, liquid, and solid phases. The vapor and liquid phases are described by an EOS, such as the Peng-Robinson EOS, with the *Peneloux volume shift parameter* (see Chapter 5, equation 5-132). The Peneloux volume shift parameter is designed to improve liquid density predictions and has been shown to model the effect of pressure on asphaltene precipitation as well as compensate for the error in the solid volume, V_s . The modified fugacity of component i in the vapor phase, f_i^V , and liquid phase, f_i^L , is given by

$$f_i^V = [f_i^V]^{\text{EOS}} \exp \left[\frac{C_i p}{RT} \right] \quad (6-5)$$

$$f_i^L = [f_i^L]^{\text{EOS}} \exp \left[\frac{C_i p}{RT} \right] \quad (6-6)$$

with the parameter C_i defined by equation (5-132) as

$$C_i = S_i b_i$$

where

S_i = Peneloux volume shift parameter

b_i = EOS b parameter for component i

f_i = fugacity with the volume shift parameter

$[f_i]^{\text{EOS}}$ = fugacity without the shift parameter, as given by equation (5-117) for the liquid phase and vapor phase, that is

$$\ln \left[\frac{[f_i^L]^{\text{EOS}}}{x_i p} \right] = \ln(\Phi_i^L) = \frac{b_i(Z^L - 1)}{b_m} - \ln(Z - B) \\ - \frac{A}{2\sqrt{2}B} \left[\frac{2\Psi_i}{(a\alpha)_m} - \frac{b_i}{b_m} \right] \ln \left[\frac{Z^L + (1 + \sqrt{2})B}{Z^L - (1 - \sqrt{2})B} \right]$$

$$\ln \left[\frac{[f_i^V]^{\text{EOS}}}{y_i p} \right] = \ln(\Phi_i^V) = \frac{b_i(Z^V - 1)}{b_m} - \ln(Z - B) \\ - \frac{A}{2\sqrt{2}B} \left[\frac{2\Psi_i}{(a\alpha)_m} - \frac{b_i}{b_m} \right] \ln \left[\frac{Z^V + (1 + \sqrt{2})B}{Z^V - (1 - \sqrt{2})B} \right]$$

where

$$\Phi_i^L = \text{fugacity coefficient of component } i \text{ in the liquid phase, } \frac{[f_i^L]^{\text{EOS}}}{x_i p}$$

$$\Phi_i^V = \text{fugacity coefficient of component } i \text{ in the vapor phase, } \frac{[f_i^V]^{\text{EOS}}}{y_i p}$$

As pointed out in Chapter 5, the volume shift parameter does not change the fugacity ratio, as shown by dividing equation (6-6) by (6-5) to give:

$$\frac{f_i^L}{f_i^V} = \frac{[f_i^L]^{\text{EOS}}}{[f_i^V]^{\text{EOS}}}$$

The fugacity of the precipitated asphaltene fraction, that is, n_{B+} , can be calculated by applying the solubility equation that relates the solid fugacity to the liquid fugacity as given by

$$\ln(f_s) = \ln(f_s^*) + \frac{V_s}{R} \left[\frac{p - p_{\text{tp}}}{T} - \frac{p^* - p_{\text{tp}}}{T^*} \right] - \frac{\Delta H_{\text{tp}}}{R} \left[\frac{1}{T} - \frac{1}{T^*} \right] \\ - \frac{\Delta C_p}{R} \left[\ln \left(\frac{T^*}{T} \right) - T_{\text{tp}} \left(\frac{1}{T} - \frac{1}{T^*} \right) \right]$$

where

p^* = reference pressure

p = system pressure

p_{tp} = triple-point pressure

ΔH_{tp} = triple-point enthalpy of fusion

ΔC_p = heat capacity difference between liquid and solid

T_{tp} = triple-point temperature

T = system temperature

R = gas constant

f_S = solid fugacity at p and T

f_S^* = solid fugacity at p^* and T

V_S = solid molar volume

To use this fugacity relationship, the triple-point temperature and pressure, enthalpy of fusion at the triple point, and the liquid/solid heat capacity difference must be known. The triple point is shown in Figure 6-15, where solid, vapor, and liquid coexist in equilibrium. For the asphaltene, the triple-point pressure, p_{tp} , is very low and can be set equal to zero. The triple-point temperature is close to the melting-point temperature, as the solid/liquid meeting (fusion) curve has a very steep slope (see Figure 6-15). The preceding equation can then be rewritten as

$$\ln(f_S) = \ln(f_S^*) + \frac{V_S}{R} \left[\frac{p}{T} - \frac{p^*}{T^*} \right] - \frac{\Delta H_f}{R} \left[\frac{1}{T} - \frac{1}{T^*} \right] - \frac{\Delta C_p}{R} \left[\ln \left(\frac{T^*}{T} \right) - T_f \left(\frac{1}{T} - \frac{1}{T^*} \right) \right] \quad (6-7)$$

where

p^* = reference pressure

p = system pressure

ΔC_p = heat capacity of fusion

T_f = melting-point temperature

ΔH_f = melting-point enthalpy of fusion

The experimental onset pressures at either two or three temperatures may be used to tune the parameters in the solid model. There are three unknowns in the model: reference fugacity, f_S^* , heat of fusion, ΔH_f , and heat capacity difference, ΔC_p .

For the defined components up to C_6 , the melting-point (fusion) temperature and enthalpy of fusion can be found in tabulated forms in many textbooks. For the wax forming components, the following expressions as proposed by Won (1986a and 1986b) and Pedersen (1995) can be used:

$$T_i^f = 374.5 + 0.02617 M_i - \frac{20,172}{M_i} \quad (6-8)$$

$$\Delta H_i^f = 0.1426 M_i T_i^f \quad (6-9)$$

$$\Delta C_{\text{pi}} = 0.3033 M_i - 0.0004635 M_i T \quad (6-10)$$

where

ΔC_{pi} = heat capacity of fusion of component i , cal/K-mol

T_i^f = melting-point temperature of component i , K

ΔH_i^f = melting-point enthalpy of fusion, cal/mol

If only two experimental data points are used, one of the unknowns must be estimated. Usually, the heat capacity difference is set equal to zero, a common practice for

solids modeling. Fugacities of the asphaltene component in the liquid phase are determined using an equation of state at two different experimental onset pressures. One of the fugacities then is assigned to the reference fugacity f_s^* , while the other is used to calculate the value of heat of fusion or the heat capacity difference.

Equation (6–7) is in a generalized form of the asphaltene fugacity that can be used to study the effect of pressure and temperature on asphaltene precipitation. However, for isothermal prediction, the preceding expression can be reduced to the following simplified form:

$$f_s = f_s^* \exp \left[\frac{V_s(p - p^*)}{RT} \right] \quad (6-11)$$

where

p^* = reference pressure, psia

p = system pressure, psi

T = system temperature, °R

R = gas constant, 10.73 psi – ft³/mol – °R

f_s = solid fugacity at p and T , psia

f_s^* = solid fugacity at p^* and T , psia

V_s = solid molar volume, ft³/mol

Equivalently, equation (6–11) can be expressed in terms of molecular weight, M_s , and density, ρ_s , of the solid by defining the solid molar volume as

$$V_s = \frac{M_s}{\rho_s}$$

Combining with equation (6–11) gives:

$$f_s = f_s^* \exp \left[\frac{M_s(p - p^*)}{RT\rho_s} \right]$$

where M_s = molecular weight of a pure solid and ρ_s = density of a pure solid, lb/ft³.

The fugacity coefficient of the pure solid fraction, Φ_s , then can be calculated by applying its definition, as illustrated in Chapter 5 by equation (5–91), to give

$$\Phi_s = \frac{f_s}{Sp}$$

Since the solid phase is considered pure and contains only n_{B+} , the asphaltene mole fraction, S , in the solid phase is then equal to 1; that is,

$$\Phi_s = \frac{f_s}{p}$$

The use of equation (6–11) requires the knowledge of f_s^* and V_s at p^* and T . These parameters can be estimated based on the methodology developed by Nghiem et al. (1993). The authors propose that the crucial step in the modeling of asphaltene is the split of the n th component in the oil, C_{n+} , such as C_{31+} , into a nonprecipitating component, C_{nA+} (e.g., C_{31A+}) and a precipitating component, C_{nB+} (e.g., C_{31B+}). Based on this assumption, the parameters of equation (6–7) can be defined and determined as follows:

- *Reference pressure, p^** The reference pressure is selected as the asphaltene onset pressure as determined in the lab and defined as the highest pressure at which the first asphaltene particles appear.
- *Reference fugacity, f_S^** The fugacity of the precipitated asphaltene fraction, C_{nB+} , in the oil phase is calculated by an equation of state at the reference pressure, p^* , and system temperature, T , and then equated to the reference solid fugacity, f_S^* .
- *Asphaltene molar volume, V_S* The solid molar volume is calculated from an EOS at system pressure and temperature. The molar volume affects the amount of asphaltene precipitation within the asphaltene deposit envelope. Increasing the solid molar volume results in a greater amount of solid precipitated. If experimental deposition data are available, the value of V_S can be adjusted until a match between the predicted and experimental values is achieved.

The equilibrium ratio, K_p , can be introduced for the three-phase system as illustrated conceptually in Figure 6–18. The illustration indicates that the gas phase does not contain the precipitated fraction, C_{nB+} , of the asphaltene; on the other hand, it can exist only in the liquid or solid phase.

Because the main assumption of the model is that the precipitating asphaltene component can exist only in the liquid phase or as a pure solid, the mole fraction of C_{nB+} must be set equal to 1. Therefore, there are two sets of equilibrium ratios:

- A set of equilibrium ratios between the liquid and vapor phase, K_i .
- A set between the liquid phase and solid phase, K_i^s .

For the vapor/liquid equilibrium ratio, K_i , the traditional approach of calculating the equilibrium ratio, K_p , using an equation of state is given by

$$K_i = \frac{\Phi_i^L}{\Phi_i^V} = \frac{f_i^L / (x_i p)}{f_i^V / (y_i p)} = \frac{y_i}{x_i} \quad (6-12)$$

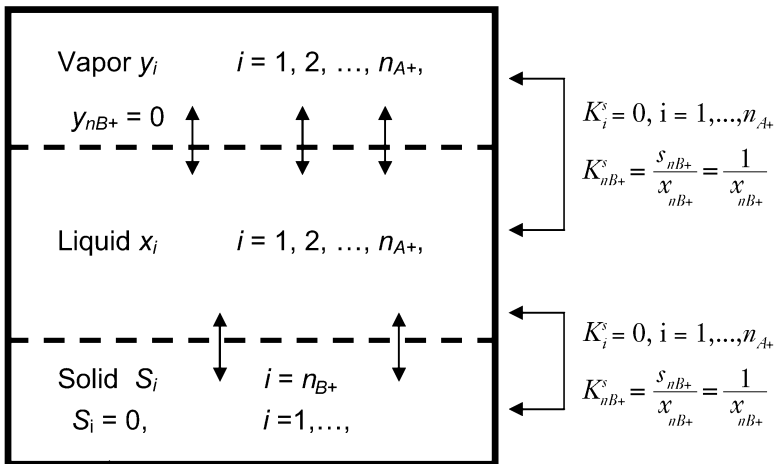


FIGURE 6–18 Three-phase system.

Similarly, for *the liquid-solid equilibrium ratio*, K_i^s . The main assumption, that solid phase contains no fraction except the precipitating part of the asphaltene component, can be expressed mathematically by

$$K_i^s = 0, \quad i = 1, \dots, n_{A+}$$

$$K_{nB+}^s = \frac{\Phi_{nB+}}{\Phi_s} = \frac{S_{nB+}}{x_{nB+}} = \frac{1}{x_{nB+}} \quad (6-13)$$

Three-Phase Flash Calculations

The component and phase material balance constraints state that 1 mole of feed with composition z_i can be distributed into three phases:

- Vapor phase with composition y_i and n_V moles.
- Liquid phase with composition x_i and n_L moles.
- Solid phase with composition S_i and n_S moles.

The material balance can then be written as:

$$n_i + n_V = n_S = 1.0 \quad (6-14)$$

$$n_i x_i + n_V y_i + n_S S_i = z_i \quad (6-15)$$

$$\sum x_i = \sum y_i = \sum S_i = \sum z_i = 1.0 \quad (6-16)$$

Combining equations (6-12) through (6-16) gives the following nonlinear equations:

$$f(n_v, n_s) = \sum_{i=1}^n \left[\frac{z_i (K_i - 1)}{n_v (K_i - 1) + (K_i^s - 1) + 1} \right] = 0 \quad (6-17)$$

$$g(n_v, n_s) = \sum_{i=1}^n \left[\frac{z_i (K_i^s - 1)}{n_v (K_i - 1) + n_s (K_i^s - 1)} \right] = 0 \quad (6-18)$$

In solving these two expressions for n_v and n_s , it should be noticed that:

$$K_i^s = 0, \quad i \neq n_{B+}$$

These two relationships can be solved tentatively for the number of moles of the vapor phase n_v and solid phase n_s . The phase composition can then be determined from:

$$x_i = \frac{z_i}{1 + n_v (K_i - 1) + n_s (K_i^s - 1)} \quad (6-19)$$

$$y_i = x_i K_i \quad (6-20)$$

$$S_{nB+} = x_{nB+} K_{nB+}^s = 1.0 \quad (6-21)$$

The Stability Test

The preceding calculations are complicated because the number of phases in equilibrium at a specified pressure and temperature are not known in advance. Nghiem et al. (1993) point out that the traditional Gibbs free surface energy can be used for testing the existence of the solid phase. The testing methodology is based on the following criteria:

- The solid phase exists if $\ln(f_{nB+}^L) \geq \ln(f_S)$.

- The solid phase does not exist if $\ln(f_{nB+}^L) < \ln(f_S)$.

Nghiem and Coombe (1997) conducted several simulation runs based on the asphaltene deposit model, described previously, to study the effect of changing the volume shift parameter and binary interaction coefficients of the asphaltene component, C_{nB+} , on the asphaltene precipitation. The authors concluded the following:

- The volume shift parameter of the asphaltene component in a solution is an important parameter for modeling the pressure effect. It affects the precipitation both above and below the saturation pressure. Large volume shift parameters yield more precipitation.
- The interaction coefficients between the asphaltene component and light components are essential in modeling the compositional effect. These have a strong influence on the prediction of the lower asphaltene deposition envelope. Essentially, the change in interaction coefficients can significantly affect the results below the saturation pressure and only to a small extent the results above the saturation pressure.

In reservoirs containing heavier crude oils, compositional variation as a function of depth may influence field development. An example is a North African field in which strong grading in stock-tank oil gravity and a related variation in reservoir-oil viscosity have been documented. In this particular field, the presence of highly viscous oil near the oil/water contact forced production from updip and would be a serious problem for down dip water injection.

As pointed out by Hirschberg (1988), an extreme manifestation of compositional variation is the presence of a tar mat at the bottom of the reservoir, which can significantly influence water drive performance.

In a reservoir at thermodynamic equilibrium, a segregation profile is established under the influence of gravitational forces. The time necessary to achieve compositional equilibrium is comparable to the geologic life time of a typical reservoir. Complete thermodynamic equilibrium might never be achieved because a uniform temperature, which does not occur in reality, would be required. As proposed by Schulte (1980) and Hirschberg (1988), the gradient dx_i/dh of the mole fraction x_i of component i is related to the chemical potential μ_i by

$$\sum_i \left[\left(\frac{d\mu_i}{dx_i} \right)_{P,T} \frac{dx_i}{dh} \right] = (\rho V_i - M_i)g$$

where

h = elevation

M_i = molecular weight

ρ = density

V_i = molar volume

x_i = mole fraction

μ_i = chemical potential

g = acceleration due to gravity

imposing the following mechanical and thermal equilibrium conditions:

$$\frac{dp}{dh} = -\rho g$$

and

$$\frac{dT}{dh} = 0$$

Assuming an ideal solution behavior, the solution to the compositional gradient solution is given by the following simplified form:

$$x_i(h) = x_i(h_{\text{ref}}) \exp \left[\frac{-(h - h_{\text{ref}})}{h_g} \right]$$

with

$$h_g = 1543.875 \left[\frac{T}{\left(\frac{\rho_o}{\rho_i} - 1 \right) M_i} \right]$$

where

- $x_i(h_{\text{ref}})$ = mole fraction of component i at reference level h_{ref}
- h_{ref} = reference level in feet, usually $h_{\text{ref}} = 0$ at GOC
- $x_i(h)$ = mole fraction of component i at level h
- h = depth level below the reference level, ft
- ρ_o = fluid density a lb/ft³
- ρ_{oi} = density of component i , lb/ft³
- M_i = molecular weight
- T = temperature, °R
- h_g = gradient height, ft

The following example illustrates the dependence of the gradient height h_g on the molecular weight and the chemical type of component i .

EXAMPLE 6-6

A heavy crude oil with a density of 50 lb/ft³ at 80.3°F has the following PNA analysis for the plus fractions:

COMPONENT TYPE	P	N	A
ρ_{oi} , lb/ft ³	8736	68.64	56.16

Show the effects of the following four molecular weights on the gradient height h_g : molecular weight = 10², 10³, 10⁴, and 10⁵.

SOLUTION

Step 1 Simplify the gradient height by substituting for T and ρ_o :

$$b_g = 1543.875 \left[\frac{T}{\left(\frac{\rho_o}{\rho_i} - 1 \right) M_i} \right]$$
$$b_g = \frac{1543.875(80.3 + 460)}{\left(\frac{50}{\rho_{oi}} - 1 \right) M_i}$$
$$b_g = \frac{834,155.66}{\left(\frac{50}{\rho_{oi}} - 1 \right) M_i}$$

Step 2 Tabulate results of b_g in terms of ρ_i and m_i as shown in the table below.

Component Type	P	N	A
ρ_{oi} , lb/ft ³	87.36	68.64	56.16
M_i			
10 ²	-19,500	-30,700	-76,000
10 ³	-19,500	-3,070	-7,600
10 ⁴	-19,500	-307	-760
10 ⁵	-19,500	-30	-76

Step 3 Assuming the GOC is the reference level, $b_{ref} = 0$, the gradient equation is reduced to

$$x_i(b) = x_i(b_{ref} = 0) \exp \left[\frac{b}{b_g} \right]$$

The tabulated values of b_g suggest that alkanes, A , with a molecular weight on the order of 100 to 1000 show no significant gravity segregation over a vertical of approximately 330 ft; for example,

$$\text{For } M = 10^2: \exp \left[\frac{330}{-76,000} \right] \approx 0.995$$
$$\text{For } M = 10^2: \exp \left[\frac{330}{-7600} \right] \approx 0.957$$

The heaviest paraffinic fractions (asphaltenes) with molecular weight between -1000 and -10,000 show significant sedimentation over a vertical distance of a few hundred feet. This indicates that asphaltenes play a key role in gravity-induced compositional grading.

Hirschberg et al. (1984) used a simplified molecular theory of asphalt phase behavior to predict the influence of temperature, pressure, and gas dissolution on asphaltene flocculation. They applied the theory to estimate the effect of departing from ideal solution behavior on asphalt segregation. The authors suggest that strong asphalt segregation is expected when there is a large difference in chemical type between asphalt and oil and when the asphaltene content of the oil is high. Under such conditions, significant departure from ideal solution behavior can be expected.

Tar Mat Formation

In extreme cases of asphalt segregation, a highly viscous, tarlike material is present at the bottom of the reservoir. By using the theory described, we can obtain some insight into the parameters controlling the formation of such tar mats in (relatively) light oil reservoirs.

Theory indicates that two types of tar mats may be formed, depending on oil and asphalt properties. The first type experiences a gradual transition from oil to tar. This corresponds to a situation in which the asphalt and oil are miscible in all proportions. If the asphalt is only partially soluble in the oil, the maximum amount of asphalt that is soluble is reached as the depth increases, and a phase transition is observed within the reservoir hydrocarbon column. The position of the transition appears to depend strongly on the assumed molecular weight of asphalt. It is also extremely sensitive to rather small changes in the reservoir oil properties.

Another interesting aspect is that pressure variation can cause a significant change in asphaltene solubility. The strong influence of pressure on solubility implies that, next to the addition of gas, a pressure change caused by uplift should be considered as a possible cause of tar-mat formation. Similarly, the pressure decline imposed by bringing a core sample to the surface may induce asphalt precipitation, resulting in precipitated asphalt particles that were not present originally and (possibly) a change in wettability.

Phase Behavior of Waxes

Waxes are not a single component, as treated in the asphaltene description by C_{nB+} but a multitude of higher-molecular-weight paraffinic components. These components are minutely soluble in the liquid phase of crude oils and condensate systems. The solubility of paraffin waxes is very sensitive to temperature changes. The factors that reduce crude oil temperature contribute to the wax crystallization process. Paraffin waxes remain soluble constituents of crude oil under most reservoir conditions in a state of thermodynamic equilibrium. As in asphaltene precipitation, when this thermodynamic equilibrium is disturbed by such factors as change in temperature or pressure, paraffin may crystallize or precipitate. Paraffin also may precipitate as a result of the loss of volatile light ends, which act as naturally-occurring solvents. As the fluid cools, each wax component becomes less soluble until the higher-molecular-weight components solidify. The *onset of wax crystallization* at this specific temperature is known as the *cloud point* or *wax appearance temperature* (WAT). As the fluid continues to cool, lower-molecular-weight fractions also solidify, adding to the solid fraction. Figure 6–19 illustrates a correlation of the solidification temperature for various high-molecular-weight n-alkane paraffin hydrocarbons. When a reservoir fluid cools to temperature T , a paraffin hydrocarbon having a solidification temperature greater than T tends to precipitate from the solution.

Note that the locus of all thermodynamic points in a pressure/temperature phase diagram at which wax crystallization occurs is called the *wax deposit envelope* (WDE). As with asphaltene, wax deposit can occur only at thermodynamic conditions within the WDE, hence the word *deposit* in the name. A schematic illustration of the WDE is shown in Figure 6–20.

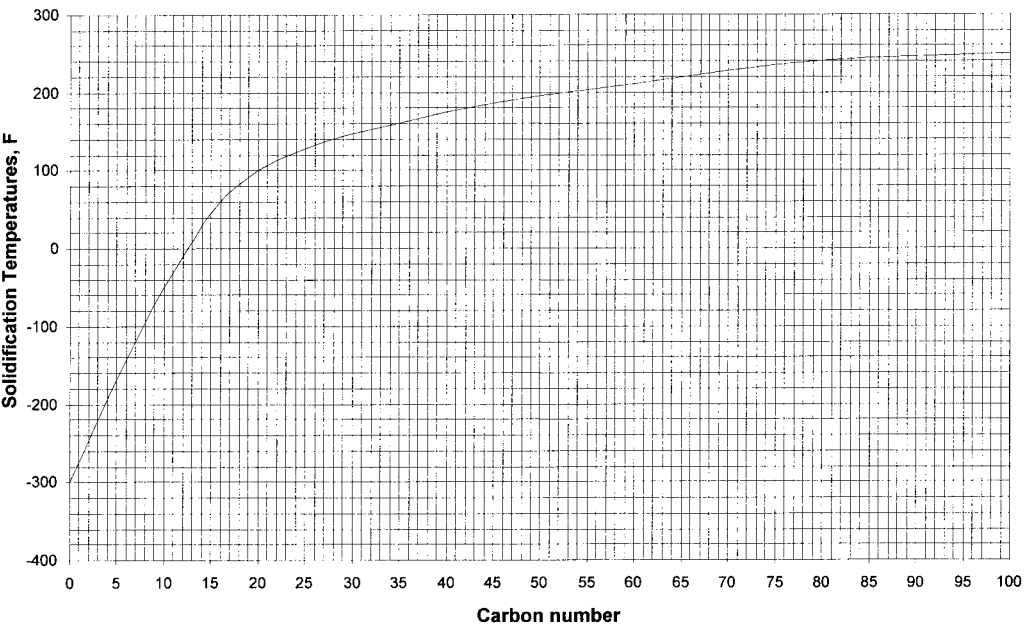


FIGURE 6-19 Solidification temperatures versus carbon number for normal paraffin hydrocarbons.

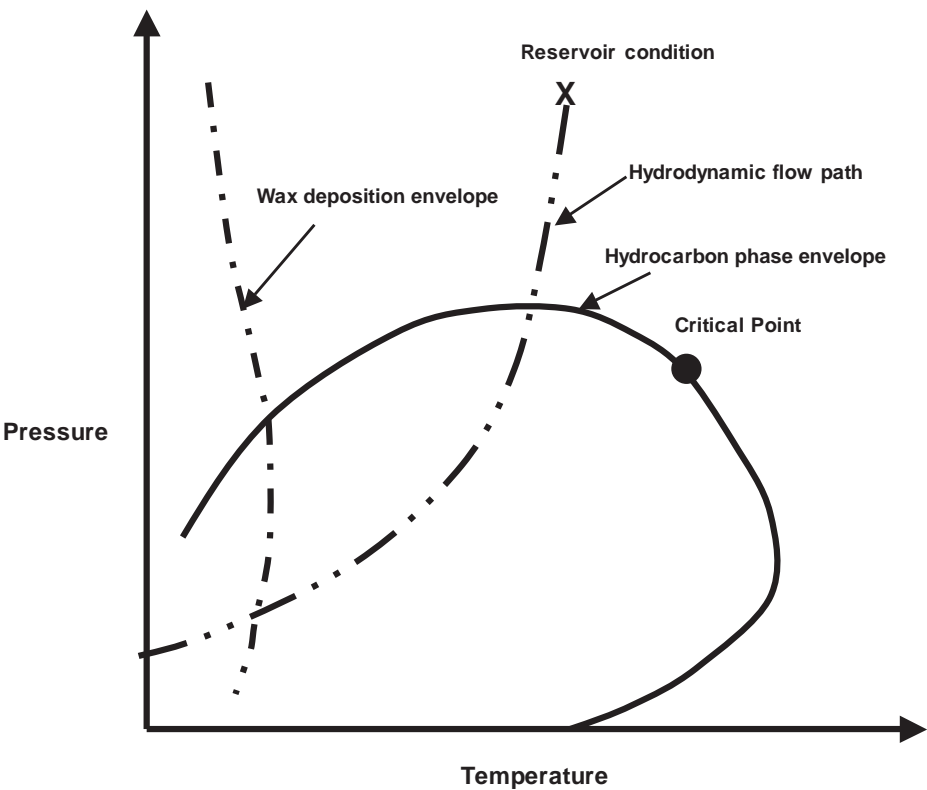


FIGURE 6-20 Schematic illustration of the wax deposit envelope.

Leontaritis et al. presented an excellent review of wax deposit measurement techniques. The authors point out that wax deposit is a serious field problem, encountered during crude oil production, that causes plugging of pipelines, well tubing, and surface and process equipment. Wax crystals change the flow behavior of crude oil from Newtonian to non-Newtonian. The wax crystals lead to higher viscosity, with increased energy consumption for pumping and decreased pumping capacity. Wax deposit increases the pipeline roughness, which increases pressure drop. The other effect is to reduce the effective cross-sectional area of the pipe. The deposits also cause subsurface and surface equipment plugging and malfunction, especially when oil mixtures are transported across Arctic regions or cold oceans. Wax deposit leads to more frequent pigging requirements. If the deposits get too thick, they reduce the capacity of the pipeline and cause the pigs to get stuck. Wax deposition in well tubing and process equipment may lead to more frequent shutdowns and operational problems. Also, some investigators report that wax deposit can result in severe formation damage. If the temperature of the fluid in the formation falls below the cloud point, wax precipitates and may deposit in the formation pores, partially blocking or plugging the fluid-flow channels and thus restricting the flow.

The two major parameters that affect the solubility of wax are the temperature and composition. The pressure has a lesser effect. Wax precipitation sometimes is irreversible, in that the wax, once it is removed from solution, is very difficult to redissolve, even after the original formation temperatures are restored.

Kunal et al. (2000) suggest that flow assurance studies for such waxy systems often require measurements of at least three crude oil properties:

- The *wax appearance temperature*.
- The *pour point temperature* (PP).
- The *gel strength*.

Using the WAT and PP, the rheological and problematic behavior of waxy crude can be mapped into three regions on a temperature scale:

- A region defined by the temperatures above the WAT, where the fluid acts as a Newtonian fluid and there is no risk of wax deposition.
- A region defined by temperatures below the PP, where the fluid exhibits highly non-Newtonian behavior and oil may gel under quiescent conditions.
- A region of mildly non-Newtonian behavior defined by the temperature between the WAT and PP.

Generally, the WAT and PP measurements are performed on stock-tank oil samples and used as conservative estimates for making flow-assurance-related decisions. An operational decision with respect to wax deposit and the ability of the pipeline to restart is easy when temperatures encountered are above the measured dead-oil WAT and PP. However, for offshore fields and subsea transportation, the sea temperature generally is lower than the dead oil WAT and PP. Kunal and coauthors presented a comprehensive treatment of the laboratory measurements of the WAT, PP, and gel strength. These three important properties are described next.

Wax Appearance Temperature

WAT is the most difficult point on the precipitation curve to measure, as is theoretically defined as the temperature at which the first infinitesimally small amount of wax is formed. In practice, it is possible to detect only a finite amount of wax, and different experimental methods usually generate different results. If waxy crude is cooled at the WAT, the wax begins to separate out as solid crystals when the solubility limit is exceeded. A distinction must be made between the thermodynamic WAT and the experimental WAT. The thermodynamic WAT defines the true solid/liquid phase boundary temperature, that is, the maximum temperature at which the solid and liquid phases exist in equilibrium at a fixed pressure (designated $(WAT)_{\text{true}}$), while the experimental wax appearance temperature, $(WAT)_{\text{exp}}$, represents the temperature at which the first crystals are detected. The value of $(WAT)_{\text{exp}}$ depends on the sensitivity of the measurement technique. A recent industry survey revealed that the uncertainties in WAT using modern measurements may be $\pm 5^\circ\text{F}$. Normally, the experimental $(WAT)_{\text{exp}}$ would be well within the thermodynamic solid/liquid phase envelope, that is, at a fixed pressure, $(WAT)_{\text{exp}} < (WAT)_{\text{true}}$. All procedures for measuring wax appearance temperatures in crude oils yield a point inside of the true thermodynamic envelope.

Pour Point

When a waxy crude is allowed to cool quiescently below the WAT, precipitation of waxes continues, resulting in an increase in the number and size of wax crystals. These crystals, if undisturbed, tend to cohere together to form a netlike structure trapping oil within. As a result, the oil attains gel-like characteristics and the oil viscosity increases. At a certain temperature, depending on the amount of wax precipitated and the strength of the network, the oil may cease to flow; this temperature is called the *pour point* of the crude oil. The PP is a rheological property of a waxy crude and a qualitative test used for determining “waxiness” of a crude oil.

Gel Strength

When a crude oil continues to be cooled below its PP or is maintained at a temperature below the PP under quiescent conditions, the network of crystals continues to develop the strength of the interlocking structure. Such conditions may exist when pipelines undergo a planned or unplanned shutdown and the ambient temperature is less than the PP. Under such conditions the oil in the pipeline cools quiescently to temperatures close to ambient. Depending on the shutdown time and ambient temperature, among other variables, the waxy crude may gel and become solid. To restart such a gelled pipeline, to make the oil flow, high pressure must be applied so that the shear stress at the wall exceeds a certain minimum value. This minimum value is called the *gel strength* or the *yield stress*. Another definition of yield stress is the minimum stress required to produce a shear flow.

Note that it has been established experimentally that, in precipitated wax, only hydrocarbons heavier than C_{14} , that is, C_{15+} fractions, are present. However, the amount of wax content of an oil has little relevance to waxing characteristics or to operations. The thermodynamic phase behavior of waxes is very useful in assessing the potential for problems but is only a part of the process for modeling the deposit rate. Unfortunately, the wax phase behavior modeling cannot predict how much of the solidifying wax condenses and adheres

to the surface or how this affects viscosity. The majority of waxes crystallize in the bulk fluid and are transported through the system without ever depositing or adhering to the walls.

Mechanism of Wax Deposit

Misra et al. (1995) presented an outstanding review of paraffin problems in crude oil production and transportation. The authors stated that the mechanism of wax deposition is governed by the molecular diffusion of wax molecules and the shear dispersion of wax crystallites. Gravity setting of wax crystals in flow-line conditions is negligible because it is dominated by shear dispersion. However, gravity settling may contribute more in static conditions, such as storage tanks.

Factors Affecting Wax Deposit

The mechanism and extent of wax deposition in a flowing system have been studied by many workers. Different methods have been adopted to study the phenomenon of wax deposition (discussed later). Three factors contribute to the extent of wax deposit in a flowing system; as best illustrated by Bott and Gudmundsson (1977a), these factors are the flow rate, temperature differential and cooling rate, and surface properties.

Flow Rate

In laminar flow, wax deposit increases with the flow rate. This can be explained by the availability of more particles for deposit at the surface. As the flow rate increases to turbulent regimes, wax deposit decreases because of shear dispersion. Thus, wax deposition gradually decreases with increases in turbulence and flow rate. Shear dispersion is predominant in turbulent flow in all stages. The flow behavior in a flowing stream is described by the Reynolds number.

The wax that deposits at a higher flow rate is harder and more compact. In other words, only those wax crystals and crystal clusters capable of firm attachment to the surface, with good cohesion among themselves, will not be removed from the deposit.

Wax deposit is found to be problematic in low-flow-rate wells. Low flow rates affect wax deposit mainly because of the longer residence time of the oil in the tubing. This increased residence time permits more heat loss and leads to a lower oil temperature, which in turn leads to wax precipitation and deposition. The minimum flow rate to avoid deposition has been proposed to be 0.56 ft/sec.

Temperature Differential and Cooling Rate

In addition to the cooling rate, the temperature differential between the bulk of solution and a cold surface is another factor for wax deposit. Wax deposit increases with an increase in temperature difference. Cole and Jessen (1960) opined that the temperature differential between the solution cloud point and a cold surface is more important than that between the bulk and a cold surface. Wax deposit would occur only when the surface temperature is below both the solution temperature and the solution cloud point.

Initially, the rate of wax deposit is higher but it slows down as more wax is deposited on the pipe surface. The thickness of the wax layer increases, and this layer acts as insulation

and reduces the effective temperature differential. This lowers the availability of the wax crystals for further deposit.

The size and number of crystals formed are also important for wax deposit. At a higher rate of cooling, the wax precipitates out in smaller crystals and a large number of crystals are formed because of the large number of crystallization sites available. At a lower rate of cooling, the crystallization process is more uniform. Thus, more uniformly packed crystals are formed, which possess a relatively small surface area and free energy.

Temperature differential also affects the composition of deposited wax. If it is high, cooling is rapid and both lower and higher melting waxes crystallize simultaneously, forming a weak porous structure (owing to malcrystallization) with cavities full of oil.

Surface Properties

It is evident that, during deposit, wax crystals adhere to the pipe surface. So wax deposit also can be a function of surface properties. Parks (1960) demonstrated that the presence of certain adsorbed films on a metal surface reduces the adherence of paraffin to that surface. Zisman (1963) showed that the nature of the compounds adsorbed on a surface determine its wettability characteristics. Cole and Jessen (1960) studied the effect of wettability on paraffin deposit and found that the amount of wax deposited for a given temperature difference decreases with decreasing free surface energy. It was found that the temperature difference and free surface energy acted independently in determining the amount of wax deposition. As the paraffin wax is deposited on a surface, it is held in place by adsorption forces. These adsorption forces depend on the free surface energy of both the paraffin and surface. Hunt (1962) studied the effect of roughness on paraffin deposition and concluded that the deposits do not adhere to the metals themselves but are held in place by surface roughness. Jorda (1966) observed that paraffin deposit increases with an increase in surface roughness. Patton and Casad (1970) observed that there is no direct correlation between wax deposit and surface roughness. However, they argued that the adhesion bond at a surface should be proportional to the total contact area and therefore related to surface roughness. Jessen and Howell (1958) studied wax deposit in pipes of different types of material and concluded that the amount of wax deposited on a smooth surface is less than that deposited on steel.

Wax Control

Forsdyke (1997) presented a detailed overview of current and future deepwater production challenges and flow assurance in a multiphase environment. The author discussed and summarized the current wax control techniques. Forsdyke points out that the onset temperatures for wax formation are usually somewhat higher than for hydrates and cannot easily be avoided in the field. We therefore require tools to control the problem. Currently, no magic bullets eliminate wax over the wide range of conditions experienced in multiphase systems. Intervention to clean a subsea multiphase line is technically difficult and likely to be very costly. We currently rely on a combination of inhibiting strategies to minimize the frequency of intervention, while using the most-effective cleaning technologies available. However, this requires the potential deposition rates to be quantified to

ensure that the strategy is both feasible and cost effective. Not only are the current predictive tools inadequate, but our understanding of our mitigation technologies, specifically their efficiency, also is poor. Ideally, the cleaning frequency should be determined by the impact of wax on flow-line performance. In reality, it often is determined by the limitations of the cleaning technology.

Forsdyke discussed the following three techniques for removing or controlling the wax: thermal, mechanical, and chemical.

Thermal Techniques

Thermal techniques are widely applied to avoid waxing by keeping the flowing fluids above the appearance temperature. As in the case of hydrates, this is limited by distance. Even the use of super-insulation systems, such as pipe in pipe, cannot realistically prevent fluids from cooling below the onset temperature much beyond 20 km. However, once below the appearance temperature, insulation still offers significant benefits. Wax deposit buildup rates are directly proportional to the rate of heat loss from the pipeline. Insulation therefore can reduce the buildup rates significantly but, unfortunately, can seldom totally prevent it. During a long shutdown, the fluids cool to ambient temperature, but improved insulation can reduce the rate of cooling and extend the period before any anticipated restart issues associated with gelled or very viscous fluids occur. The addition of heat, using induction heating or hot fluid circulation, prevents and removes waxes, but as already described, there are cost and reliability issues to be addressed.

Thermal methods also are utilized to remediate paraffin wax deposit. Providing the line or well is not totally blocked, the use of hot fluids to melt the deposit are widely used. The common fluids used are water, and solvents such as diesel, xylene, or the actual production fluid. The hot flushing of subsea flow lines can be feasible, providing sufficient insulation and heat are available to maintain the required flushing temperature over the desired length. Twin flow lines would be required and care must be taken when flushing so as not to push the waxy material down the tubing and into the reservoir. Several subsea systems are being designed to hot flush flow lines of use to 10 km.

Mechanical Systems

Mechanical systems are essentially used to scrape the wax out of the well bore or flow line. Typical systems include wire-line scrapers and flow-line pigging. These are very effective providing the wax layers are not too thick. However, depending on the magnitude of the problem, the frequency of intervention may be uneconomical. This is especially true for subsea completions, where access into the system is very limited. If regular intervention is required, then roundtrip pigging and TFL are available, but these systems require twin flow lines and complex completions.

Many of these systems require production to be stopped during cleaning, resulting in significant costs associated with lost or deferred production. As a result, operators often choose not to run the tools on a regular basis. When a tool finally is run, it may not be able to dislodge the wax, or a long wax plug forms ahead of it and the tool becomes stuck. Significant

time and effort are required to recover the tool or, if this proves impossible, replace the line. Regular cleaning would avoid such problems, but the cost of delivering a tool on a regular basis is prohibitively expensive at present. Attempts to overcome these difficulties include the delivery of foam pigs along utility lines.

Chemical Inhibitors

Chemical inhibitors are available that can modify the wax deposit rate and fluid rheological properties (viscosity and restart pressures). Most of these are crystal modifiers, which are thought to either cocrystallize with the wax crystals or adsorb onto their surface, altering the wax crystal morphology. Because of the complexity of waxes and their behavior, these types of additives tend to be very crude dependent.

When used to modify the viscosity or restart characteristics, these additives are known as *pour-point depressants* (PPDs). Most laboratory studies are generally adequate for determining inhibitor requirements and screening candidates. However, it is not sufficient to rely on just the pour point. An additive that apparently lowers the pour point, in reality, may have little effect on viscosities at low temperatures and flow rates.

If wax inhibitors are to be the primary wax control strategy, which is a preferred option for many subsea systems, they must be able to totally prevent wax deposit over a mid-range of conditions.

Modeling Wax Deposit

Several authors have shown that the wax-forming components consist primarily of n-paraffins. However, iso-paraffins and naphthenes can also be found in the precipitated wax. The aromatics do not precipitate as wax. It also has been established experimentally that the precipitate wax contains only hydrocarbon components heavier than C_{14} , such as C_{15} , C_{16} , and so forth. Based on results from a thermodynamic model, Pan and Firoozabadi (1996) suggest that

- The precipitated wax does not contain aromatics.
- The n-paraffins with the same carbon number as naphthenes precipitate first.
- At higher temperatures, n-paraffins essentially constitute the wax phase, however, at lower temperatures, naphthenes contribution becomes more important.
- The lightest component that can be found in the wax phase is n-paraffin C_{15} , which precipitates around 237 K.

A definition suggesting that the n-paraffins are the only wax-forming components that would be difficult to model for practical reasons. The compositional analyses available usually are expressed and presented in terms of carbon number fractions; that is, they do not consider the structural difference between components of the same molecular weight.

Pedersen (1995) point out that, to be able to take into account the possible formation of a wax phase, it is essential to divide the C_{7+} pseudo components into a potentially wax-

forming part and a part that cannot form wax. The author proposed the following relationship for expressing the mole fraction z_i^s of pseudo component i having a total mole fraction of z_i^{tot} :

$$z_i^s = z_i^{\text{tot}} \left[1 - (0.8824 + 0.0005353M_i) \left(\frac{\rho_i - \rho_i^p}{\rho_i^p} \right) \right] \quad (6-22)$$

with

$$\rho_i^p = 0.3915 + 0.0675 \ln(M_i) \quad (6-23)$$

where

M_i = molecular weight of component i

ρ_i^p = density of normal paraffin with the same molecular weight as pseudo component i , gm/cm³

ρ_i = density of pseudo component i

The non-wax-forming part of the pseudo component will have a mole fraction of

$$z_i^{\text{non}} = z_i^{\text{tot}} - z_i^s$$

EXAMPLE 6-7

Given the composition in the following table and assuming the wax fractions group identified as C₇ through C₁₀₊, divide these fractions into a wax-forming part and a part that cannot form wax using Pedersen's approach.

Component	z_i , %	M_i	ρ_i , gm/cm ³
C ₁	0		
C ₂	0.087		
C ₃	0.536		
C ₄	1.541		
C ₅	2.738		
C ₆	3.701		
C ₇	8.213	91.94	0.7368
C ₈	10.623	105.45	0.7543
C ₉	6.672	120.23	0.7640
C ₁₀₊	65.888	282.15	0.8621

SOLUTION

Step 1 Calculate the density of the normal paraffin for each of the wax fractions group using equation (6-23):

$$\rho_i^p = 0.3915 + 0.0675 \ln(M_i)$$

and tabulate the results as shown in column 5 of the following table.

Step 2 Calculate the potentially wax-forming part using equation (6-22):

$$z_i^s = z_i^{\text{tot}} \left[1 - (0.8824 + 0.0005353M_i) \left(\frac{\rho_i - \rho_i^p}{\rho_i^p} \right) \right]$$

and tabulate the results as shown in column 6 of the following table.

Step 3 Calculate the non-wax-forming part of the pseudo component group using

$$z_i^{\text{non}} = z_i^{\text{tot}} - z_i^s$$

The results are shown in column 7 of the following table.

(1) Comp.	(2) z_i , %	(3) M_i	(4) ρ_i , gm/cm ³	(5) ρ_i^p , gm/cm ³	(6) z_i^s , %	(7) z_i^{non} , %
C ₁	0					
C ₂	0.087					
C ₃	0.536					
C ₄	1.541					
C ₅	2.738					
C ₆	3.701					
C ₇	8.213	91.94	0.7368	0.6967	2.6932	5.5198
C ₈	10.623	105.45	0.7543	0.7059	3.2836	7.3394
C ₉	6.672	120.23	0.7640	0.7148	2.0209	4.6511
C ₁₀₊	65.888	282.15	0.8621	0.7724	12.660	53.228

Brown, Niesen, and Erickson (1993) developed an expression for calculating the solid/liquid equilibrium ratio that takes the form

$$K_i^S = \frac{\Phi_i^L}{\Phi_i^o} \exp\left(\frac{p\Delta V_i}{RT}\right) \exp\left[\frac{\Delta H_i^f}{RT}\left(1 - \frac{T}{T_i^f}\right)\right] \tag{6-24}$$

where

ΔV_i = difference between the liquid and solid molar volume, cm³/mol

Φ_i^o = fugacity coefficient of pure liquid component i

Φ_i^L = fugacity coefficient of component i in the liquid mixture

with the fraction properties T_i^f and ΔH_i^f as defined by equations (6–8) and (6–9); that is,

$$T_i^f = 374.5 + 0.02617M_i - \frac{20,172}{M_i}$$

$$\Delta H_i^f = 0.1426M_i T_i^f$$

Brown and his coauthors point out that it is reasonable to expect that the liquid and solid molar volumes of n-paraffins to be a linear function of the molecular weight, particularly for carbon numbers greater than 10. The authors then proposed the following expression for calculating ΔV_i :

$$\Delta V_i = 0.17M_i$$

Assuming we employ the PR EOS, the fugacity coefficient of the pure liquid component, Φ_i^o , and fugacity coefficient of component in the liquid mixture, Φ_i^L , are defined by equations (5–116) and (5–117), as

$$\ln(\Phi_i^o) = (Z - 1) - \ln(Z - B) - \frac{A}{2\sqrt{2}B} \ln\left[\frac{Z^L + (1 + \sqrt{2})B}{Z^L - (1 - \sqrt{2})B}\right]$$
$$\ln(\Phi_i^L) = \frac{b_i(Z^L - 1)}{b_m} - \ln(Z - B) - \frac{A}{2\sqrt{2}B} \left[\frac{2\Psi_i}{(a\alpha)_m} - \frac{b_i}{b_m}\right] \ln\left[\frac{Z^L + (1 + \sqrt{2})B}{Z^L - (1 - \sqrt{2})B}\right]$$

The division of each C_{7+} component into a wax-forming part and a part that cannot form, as illustrated in Example 6-7, implies that the number of C_{7+} components is twice the number of that in the vapor/liquid equilibrium calculations. The EOS parameters of the wax-forming and non-wax-forming parts of the pseudo component are equal, but the wax model parameters differ. In addition to the EOS parameters, Φ_i^o and Φ_i^L , the wax K -values equation (equation 6-24) contains other parameters that must be determined from equations (6-8) and (6-9). Pedersen (1995) points out that, to avoid the presence of non-wax-forming components in the wax phase, assign these components very large values for the fugacity coefficients in the wax phase, such as $\ln(\Phi_i^L) \approx 50$.

Prediction of Wax Appearance Temperature

Generally, the WAT measurements are performed on stock-tank oil samples (dead oil) and used as conservative estimates for making flow-assurance-related decisions. The WAT is theoretically defined as the temperature at which the first, infinitesimally small amount of wax is formed, that is, with the number of moles of the solid $n_s \approx 0$. The calculation of the WAT using the wax formulation as described is analogous to the bubble-point calculation of oil mixtures. Assume that we desire to determine the WAT for a stock-tank (dead) crude oil system; that is, no vapor phase will evolve. Defining:

z_i = mole fraction of component i in the entire hydrocarbon mixture

n = total number of moles of the hydrocarbon mixture, lb-mole

n_L = total number of moles in the liquid phase

n_s = total number of moles in the solid phase

By definition,

$$n = n_L + n_s \quad (6-25)$$

Equation (6-25) indicates that the total number of moles in the system is equal to the total number of moles in the liquid phase plus the total number of moles in the solid phase. A material balance on the i th component results in

$$z_i n = x_i n_L + s_i n_s \quad (6-26)$$

where

$z_i n$ = total number of moles of component i in the system

$x_i n_L$ = total number of moles of component i in the liquid phase

$s_i n_s$ = total number of moles of component i in the solid phase

Also by the definition of the total mole fraction in a hydrocarbon system, we may write

$$\sum_i z_i = 1 \quad (6-27)$$

$$\sum_i x_i = 1 \quad (6-28)$$

$$\sum_i s_i = 1 \quad (6-29)$$

It is convenient to perform all the phase-equilibria calculations on the basis of 1 mole of the hydrocarbon mixture, that is, $n = 1$. That assumption reduces equations (6–25) and (6–26) to

$$n_L = n_S = 1 \quad (6-30)$$

$$x_i n_L + s_i n_S = z_i \quad (6-31)$$

Introducing the wax K -value in equation (6–31) to eliminate S_i , gives

$$x_i n_L + (x_i K_i^S) n_S = z_i$$

Solving for x_i yields

$$x_i = \frac{z_i}{n_L + n_S K_i^S} \quad (6-32)$$

Equation (6–32) can also be solved for S_i as

$$S_i = x_i K_i^S = \frac{z_i K_i^S}{n_L + n_S K_i^S} \quad (6-33)$$

Taking the summation of equation (6–32) with (6–33) gives

$$\sum_i x_i = \sum_i \frac{z_i}{n_L + n_S K_i^S} = 1 \quad (6-34)$$

$$\sum_i s_i = \sum_i \frac{z_i K_i^S}{n_L + n_S K_i^S} = 1 \quad (6-35)$$

At the wax appearance temperature, equation (6–35) can be reduced to

$$\sum z_i K_i^S = 1 \quad (6-36)$$

Equations (6–17) and (6–18) can be used to perform three-phase flash calculations for the wax, liquid, and vapor. The calculation procedure is similar to that of the asphaltene deposition prediction.

Gas Hydrates

Gas hydrates are solid crystalline compounds formed by the physical combination of gases (primarily methane, ethane, propane, CO_2 , and H_2S) and water under pressure and temperatures considerably above the freezing point of water. In the presence of free water, hydrate forms when the temperature is below a certain degree; this temperature is called the *hydrate temperature*, T_b . Gas hydrate crystals resemble ice or wet snow in appearance but do not have the solid structure of ice. The main framework of the hydrate crystal is formed with water molecules. The gas molecules occupy void spaces (cages) in the water-crystal lattice; however, enough cages must be filled with hydrocarbon molecules to stabilize the crystal lattice. When the hydrate “snow” is tossed on the ground, it causes a distinct cracking sound resulting from the escaping gas molecules, as they rupture the crystal lattice of the hydrate molecules.

Two types of hydrate crystal lattices are known, each containing void spaces of different sizes:

- Structure I lattice has voids of a size to accept small molecules such as methane and ethane. These “guest” gas molecules are called *hydrate formers*. In general, light components such as C_1 , C_2 and CO_2 form structure I hydrates.
- Structure II lattice has larger voids, “cages” or “cavities,” that allow the entrapment of the heavier alkanes with medium-sized molecules, such as C_3 , $i-C_4$, and $n-C_4$, in addition to methane and ethane to form structure II hydrates. Several studies have shown that the stable hydrate structure is hydrate structure II. However, the gases are very lean; structure I is expected to be the hydrate stable structure.

All components heavier than C_4 , that is, C_{5+} , do not contribute to the formation of hydrates and therefore are identified as “nonhydrate components.”

Gas hydrates generate considerable operational and safety concerns in subsea pipelines and process equipment. The current practice in the petroleum industry for avoiding gas hydrates is to operate outside the hydrate stability zone. During the flow of natural gas, it becomes necessary to define, and thereby avoid, conditions that promote the formation of hydrates. This is essential, since hydrates can cause numerous problems such as

- Choke the flow string, surface lines, and other equipment.
- Completely block flow lines and surface equipment.
- Through formation in the flow string, result in a lower value of measured wellhead pressures.

Sloan (1991) lists several conditions that tend to promote the formation of gas hydrates:

- The presence of free water and gas molecules that range in size from methane to butane.
- The presence of H_2S or CO_2 as a substantial factor contributing to the formation of hydrate since these acid gases are more soluble in water than hydrocarbons.
- Temperatures below the “hydrate formation temperature” for the pressure and gas composition considered.
- High operating pressures that increase the “hydrate formation temperature.”
- High velocity or agitation through piping or equipment.
- Presence of small “seed” crystals of hydrate.
- Natural gas at or below its water dew point with liquid water present.

These conditions necessary for hydrate formation lead to the following four classic thermodynamic prevention methods:

1. Water removal provides the best protection.
2. Maintain a high temperature throughout the flow system: insulation, pipe bundling, and electrical heating.

3. Hydrate prevention is achieved most frequently by injecting an inhibitor, such as methanol or monoethylene glycol, which acts as an antifreeze.
4. Kinetic inhibitors are low-molecular-weight polymers dissolved in a carrier solvent and injected into the water phase in the pipeline. These inhibitors bond to the hydrate surface and prevent significant crystal growth for a period longer than the free-water residence time in a pipeline.

Phase Diagrams for Hydrates

The temperature and pressure conditions for hydrate formation in surface gas-processing facilities generally are much lower than those considered in production and reservoir engineering. The conditions of initial hydrate formation often are given by simple pressure/temperature phase diagrams for water/hydrocarbon systems. A schematic illustration of the phase diagram for a typical mixture of water and light hydrocarbon is shown in Figure 6-21. A lower quadruple point, Q_1 , and upper quadruple point, Q_2 , have been defined. The quadruple point defines the condition at which four phases are in equilibrium.

Each quadruple point is at the intersection of four three-phase lines. The lower quadruple point, Q_1 , represents the point at which ice, hydrate, water, and hydrocarbon gas exist in equilibrium. At temperatures below the temperature that corresponds to point Q_1 , hydrates form from vapor and ice. The upper quadruple point, Q_2 , represents the point at which water, liquid hydrocarbon, hydrocarbon gas, and hydrate exist in equilibrium and marks the upper temperature limit for hydrate formation for that particular gas/water system. Some of the lighter natural-gas components, such as methane and nitrogen, have no upper quadruple point, so no upper temperature limit exists for hydrate formation. This is the reason that hydrates can still form at high temperatures (up to 120°F) in the surface facilities of high-pressure wells.

The line Q_1 – Q_2 separates the area in which water and gas combine to form hydrates. The vertical line extending from point Q_2 separates the area of water and hydrocarbon liquid from the area of hydrate and water.

It is convenient to divide hydrate formation into the following two categories:

1. Hydrate formation due to a decrease in temperature with no sudden pressure drop, such as in the flow string or surface line.
2. Hydrate formation where sudden expansion occurs, such as in orifices, back-pressure regulators, or chokes.

Figure 6-21 presents a graphical method for approximating hydrate formation conditions and estimating the permissible expansion condition of natural gases without the formation of hydrates. Figure 6-22 shows the hydrate-forming conditions as described by a family of “hydrate formation lines” representing natural gases with various specific gravities. Hydrates form whenever the coordinate of the point representing the pressure and temperature is located to the *left of the hydrate formation line for the gas in question*. This graphical correlation can be used to approximate the hydrate-forming temperature as the temperature decreases along flow string and flow lines, that is, category 1.

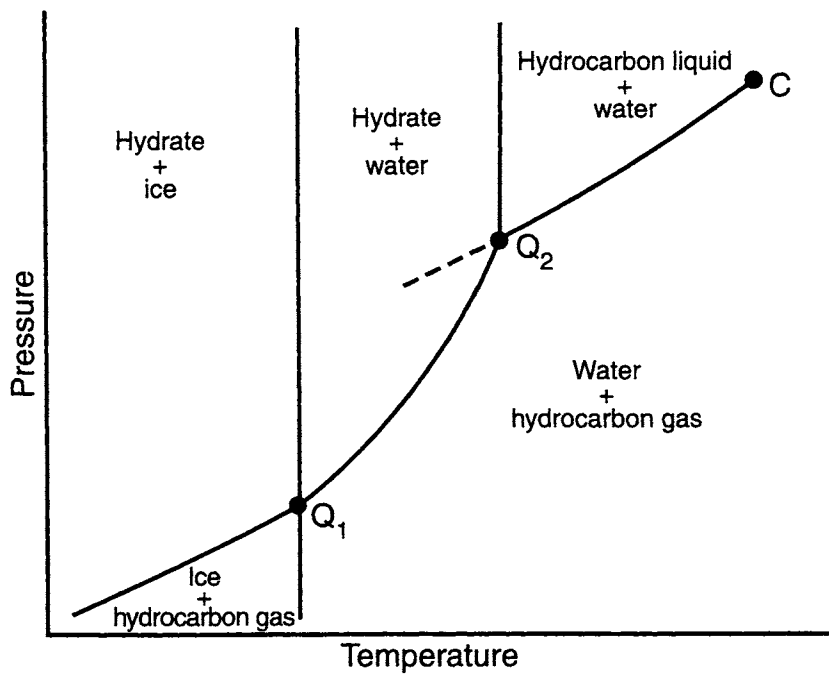


FIGURE 6-21 Permissible expansion of a 0.6 gravity natural gas without hydrate formation.
Source: Courtesy of the Gas Processors Suppliers Association.

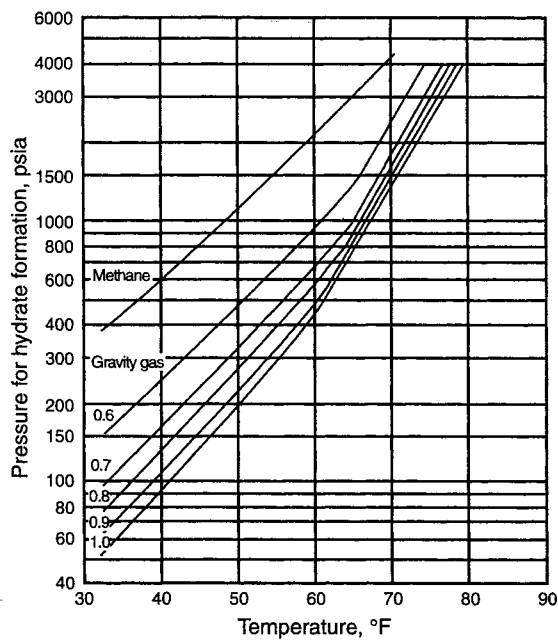


FIGURE 6-22 Pressure/temperature curves for predicting hydrate formation.
Source: Courtesy of the Gas Processors Suppliers Association.

EXAMPLE 6-8

A 0.8 specific gravity gas is at 1000 psia. To what extent can the temperature be lowered without hydrate formation in the presence of free water?

SOLUTION

From Figure 6-22, at a specific gravity of 0.8 and a pressure of 1000 psia, the hydrate temperature is 66°F. Thus, hydrates may form at or below 66°F.

EXAMPLE 6-9

A gas has a specific gravity of 0.7 and exists at 60°F. What would be the pressure above which hydrates could be expected to form?

SOLUTION

From Figure 6-22, hydrates will form above 680°psia.

It should be pointed out that the graphical correlation presented in Figure 6-22 was developed for pure water/gas systems, however, the presence of dissolved solids in the water reduces the temperatures at which natural gases form hydrates.

When a water/wet gas expands rapidly through a valve, orifice, or other restriction, hydrates may form because of rapid gas cooling caused by Joule-Thomson expansion:

$$\frac{\partial T}{\partial p} = \frac{RT^2}{pC_p} \left(\frac{\partial Z}{\partial T} \right)_p$$

where

T = temperature

p = pressure

Z = gas compressibility factor

C_p = specific heat at constant pressure

This reduction in temperature due to the sudden reduction in pressure, that is, $\partial T/\partial p$, could cause the condensation of water vapor from the gas and bring the mixture to the conditions necessary for hydrate formation. Figures 6-23 through 6-27 can be used to estimate the maximum reduction in pressure without causing the formation of hydrates.

The chart is entered at the intersection of the initial pressure and initial temperature isotherm; and the lowest pressure to which the gas can be expanded without forming hydrate is read directly from the x -axis below the intersection.

EXAMPLE 6-10

How far can a 0.7 gravity gas at 1500 psia and 120°F be expanded without hydrate formation?

SOLUTION

From Figure 6-23, enter the graph on the y -axis with the initial pressure of 1500 psia and move horizontally to right to intersect with the 120°F temperature isotherm. Read the “final” pressure on the x -axis, to give 300 psia. Hence, this gas may be expanded to a final pressure of 300 psia without the possibility of hydrate formation.

Ostergaard et al. (1998) proposed a new correlation to predict the hydrate-free zone of reservoir fluids that range in composition from black oil to lean natural gas systems.

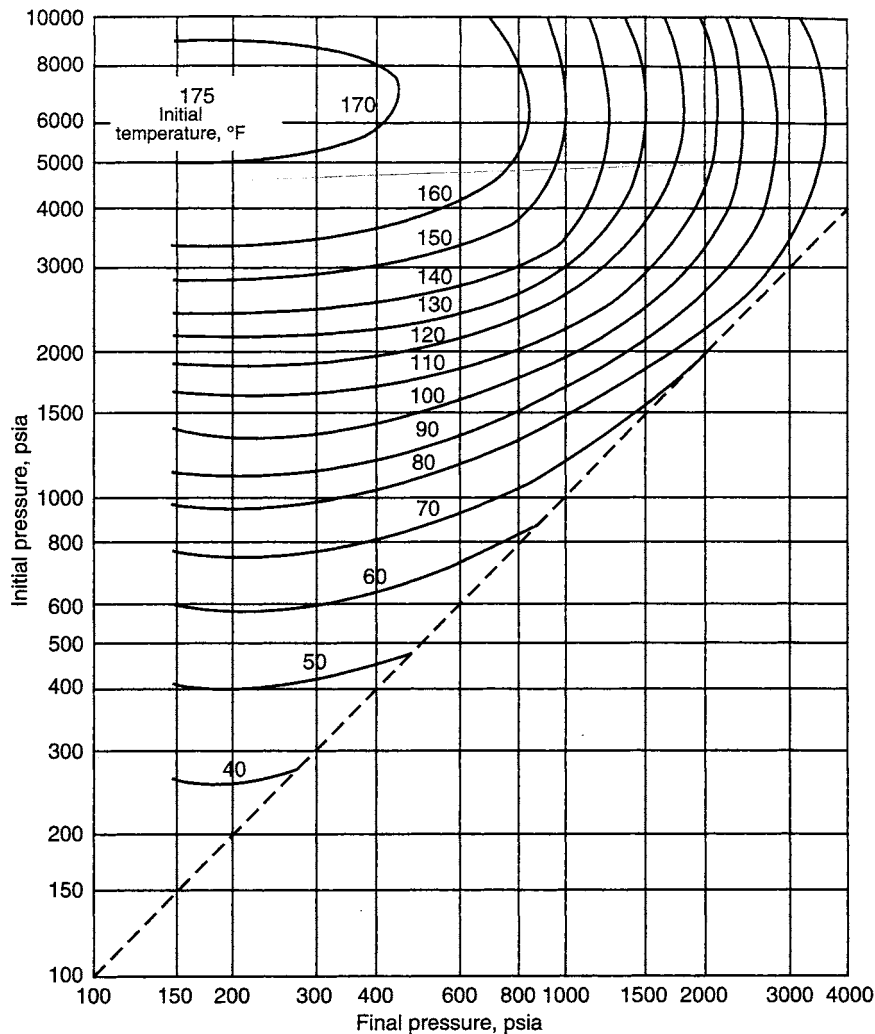


FIGURE 6-23 Permissible expansion of 0.6 gravity natural gas without hydrate formation.
Source: Courtesy of the Gas Processors Suppliers Association.

The authors separated the components of the hydrocarbon system into the following two groups:

- Hydrate-forming hydrocarbons, *b*, that include methane, ethane, propane, and butanes.
- Non-hydrate-forming hydrocarbons, *nh*, that include pentanes and heavier components.

We define the following correlating parameters:

$$f_b = y_{C_1} + y_{C_2} + y_{C_3} + y_{i-C_4} + y_{n-C_4} \tag{6-37}$$

$$f_{nh} = y_{C_{5+}} \tag{6-38}$$

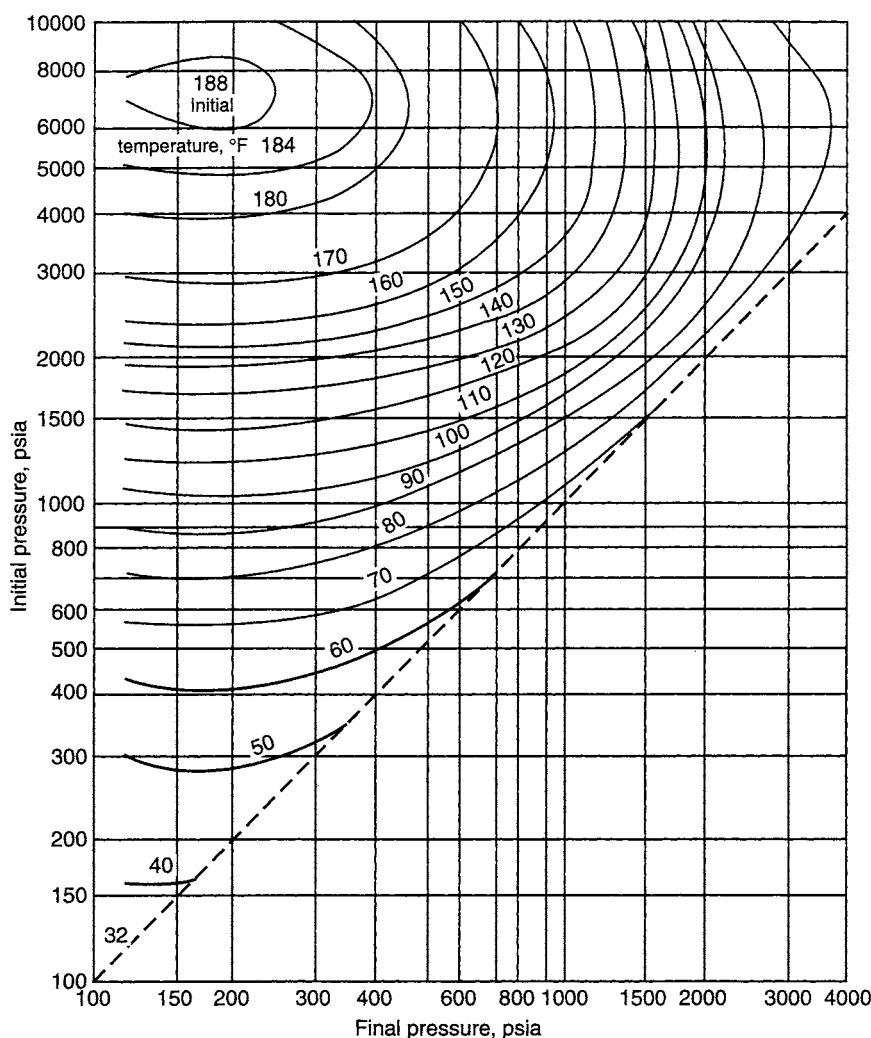


FIGURE 6-24 Permissible expansion of 0.7 gravity gas with hydrate formation.
Source: Courtesy of the Gas Processors Suppliers Association.

$$F_m = \frac{f_{nh}}{f_b} \tag{6-39}$$

$$\gamma_b = \frac{M_b}{28.96} = \frac{\sum_{i=C_1}^{n-C_4} y_i M_i}{28.96} \tag{6-40}$$

where

- b = hydrate-forming components, C_1 through C_4
- nh = non-hydrate-forming components, C_5 and heavier
- F_m = molar ratio between the non-hydrate-forming and hydrate-forming components
- γ_h = specific gravity of hydrate-forming components
- M_b = molecular weight of hydrate-forming components

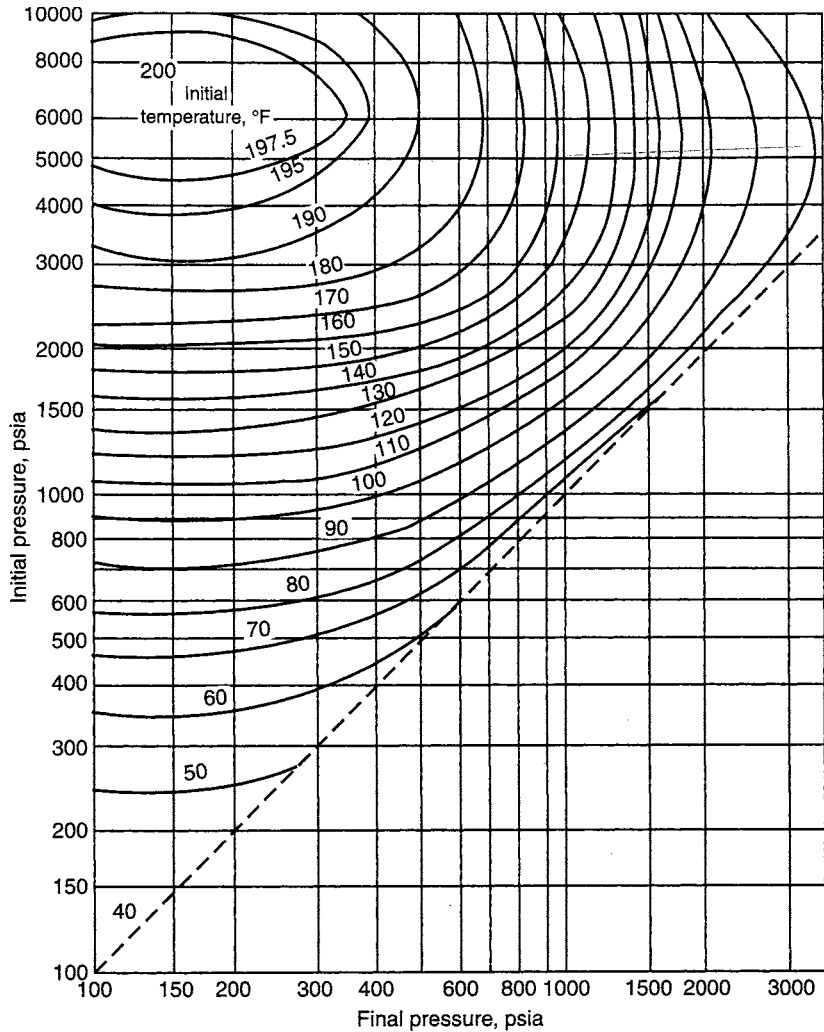


FIGURE 6-25 Permissible expansion of 0.8 gravity gas with hydrate formation.

Source: Courtesy of the Gas Processors Suppliers Association.

The authors correlated the hydrate dissociation pressure, p_b , of fluids containing only hydrocarbons as a function of these defined parameters by the following expression:

$$p_b = 0.1450377 \exp \left\{ \left[\frac{a_1}{(\gamma_b + a_2)^3} + a_3 F_m + a_4 F_m^2 + a_5 \right] T + \frac{a_6}{(\gamma_b + a_7)^3} + a_8 F_m + a_9 F_m^2 + a_{10} \right\} \quad (6-41)$$

where

p_b = hydrate dissociation pressure, psi
 T = temperature, °R

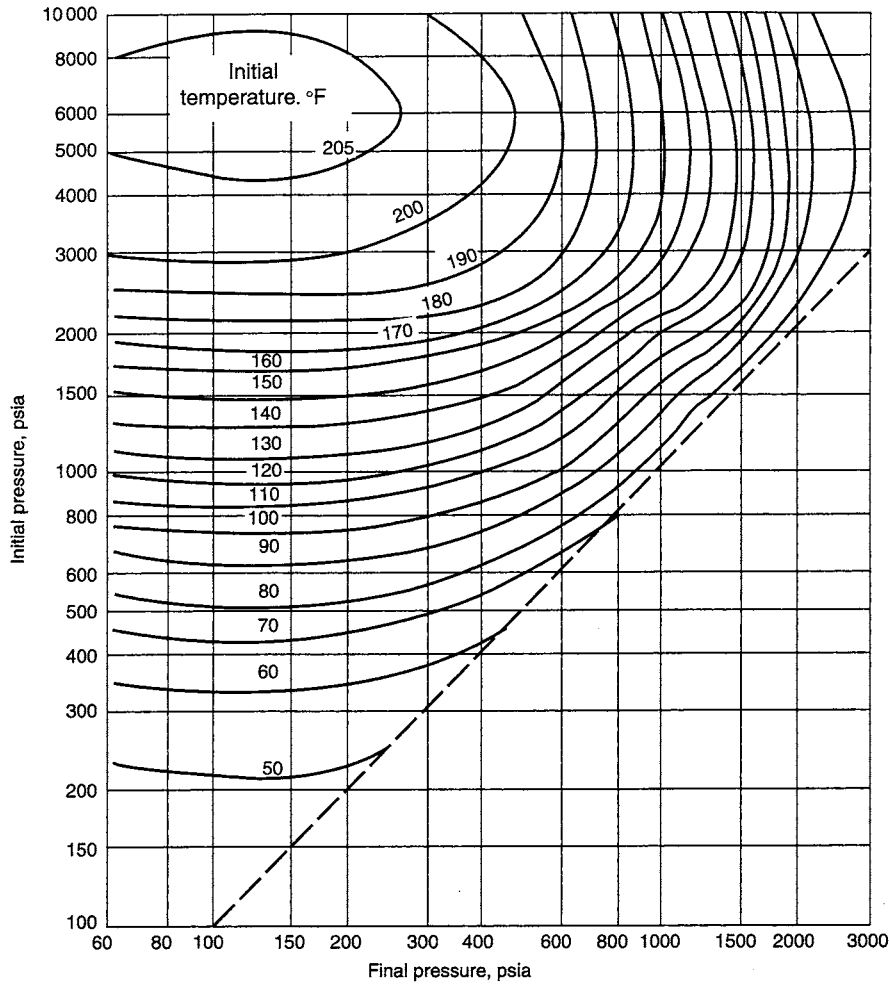


FIGURE 6-26 Permissible expansion of 0.9 gravity gas with hydrate formation.
Source: Courtesy of the Gas Processors Suppliers Association.

a_i = constants as follows:

$$a_1 = 2.5074400 \times 10^{-3}$$

$$a_2 = 0.4685200$$

$$a_3 = 1.2146440 \times 10^{-2}$$

$$a_4 = -4.6761110 \times 10^{-4}$$

$$a_5 = 0.0720122$$

$$a_6 = 3.6625000 \times 10^{-4}$$

$$a_7 = -0.4850540$$

$$a_8 = -5.4437600$$

$$a_9 = 3.8900000 \times 10^{-3}$$

$$a_{10} = -29.9351000$$

Equation (6-41) was developed using data on black oil, volatile oil, gas condensate, and natural gas systems in the range of 32°F to 68°F, which covers the practical range of hydrate formation for reservoir fluids transportation.

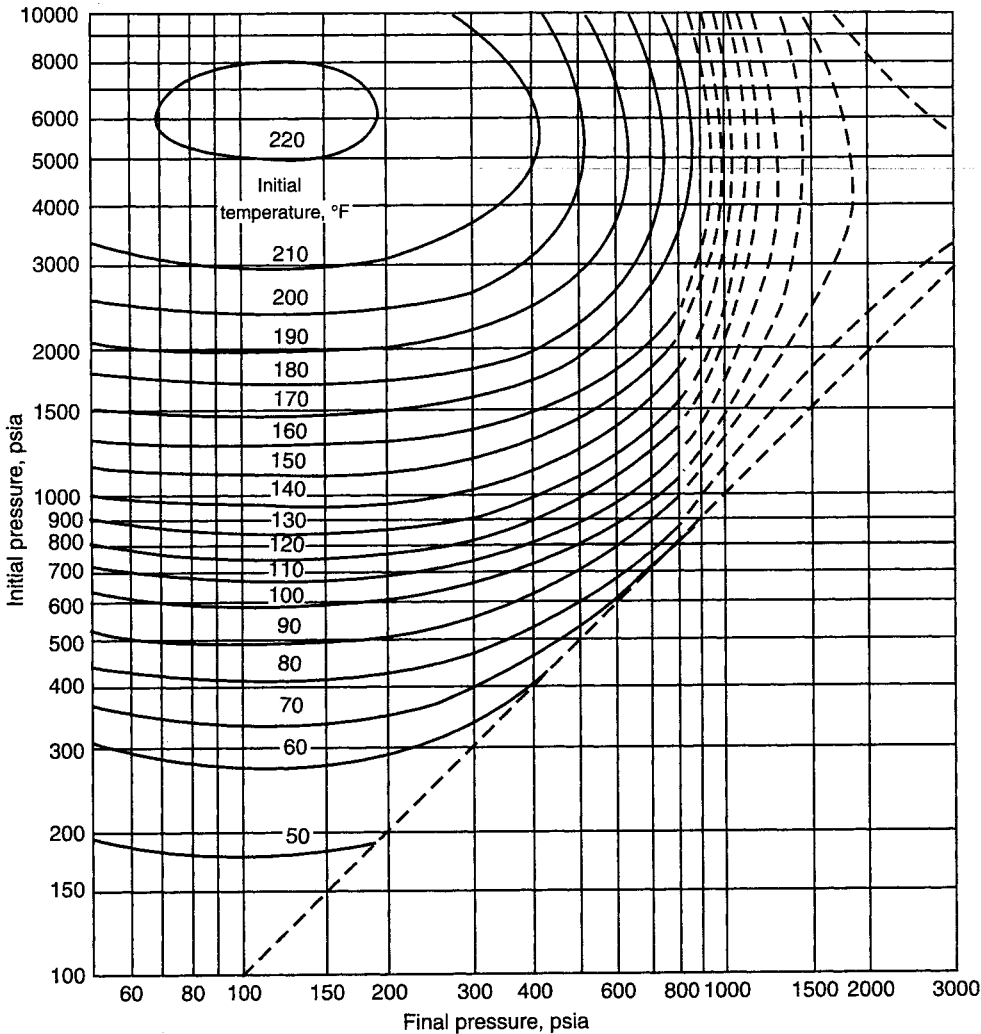


FIGURE 6-27 Permissible expansion of 1.0 gravity gas with hydrate formation.
Source: Courtesy of the Gas Processors Suppliers Association.

Equation (6-41) can also be arranged and solved for the temperature:

$$T = \frac{\ln(6.89476 p_b) - \frac{a_6}{(\gamma_b + a_7)^3} + a_8 F_m + a_9 F_m^2 + a_{10}}{\left[\frac{a_1}{(\gamma_b + a_2)^3} + a_3 F_m + a_4 F_m^2 + a_5 \right]}$$

The authors point out that nitrogen and carbon dioxide do not obey the general trend given for hydrocarbons in equation (6-41). Therefore, to account for the pressure of N₂ and CO₂ in the hydrocarbon system, they treated each of these two nonhydrocarbon fractions separately and developed the following correction factors:

$$E_{\text{CO}_2} = 1.0 + \left[(b_1 F_m + b_2) \frac{y_{\text{CO}_2}}{1 - y_{\text{N}_2}} \right] \tag{6-42}$$

$$E_{N_2} = 1.0 + \left[(b_3 F_m + b_4) \frac{y_{N_2}}{1 - \gamma_{CO_2}} \right] \quad (6-43)$$

with

$$b_1 = -2.0943 \times 10^{-4} \left(\frac{T}{1.8} - 273.15 \right)^3 + 3.809 \times 10^{-3} \left(\frac{T}{1.8} - 273.15 \right)^2 - 2.42 \times 10^{-2} \left(\frac{T}{1.8} - 273.15 \right) + 0.423 \quad (6-44)$$

$$b_2 = 2.3498 \times 10^{-4} \left(\frac{T}{1.8} - 273.15 \right)^2 - 2.086 \times 10^{-3} \left(\frac{T}{1.8} - 273.15 \right) + 1.63 \times 10^{-2} \left(\frac{T}{1.8} - 273.15 \right) + 0.650 \quad (6-45)$$

$$b_3 = 1.1374 \times 10^{-4} \left(\frac{T}{1.8} - 273.15 \right)^3 + 2.61 \times 10^{-4} \left(\frac{T}{1.8} - 273.15 \right)^2 + 1.26 \times 10^{-2} \left(\frac{T}{1.8} - 273.15 \right) + 1.123 \quad (6-46)$$

$$b_4 = 4.335 \times 10^{-5} \left(\frac{T}{1.8} - 273.15 \right)^3 - 7.7 \times 10^{-5} \left(\frac{T}{1.8} - 273.15 \right)^2 + 4.0 \times 10^{-3} \left(\frac{T}{1.8} - 273.15 \right) + 1.048 \quad (6-47)$$

where

y_{N_2} = mole fraction of N_2

y_{CO_2} = mole fraction of CO_2

T = temperature, °R

F_m = molar ratio as defined by equation (6-39)

The total, that is, *corrected*, hydrate dissociation pressure, p_{corr} , is given by

$$p_{\text{corr}} = p_b E_{N_2} E_{CO_2} \quad (6-48)$$

To demonstrate these correlations, Ostergaard and coworkers presented the following example.

EXAMPLE 6-11

A gas condensate system has the following composition:

COMPONENT	y_i	M_i
CO_2	2.38%	44.01
N_2	0.58%	28.01
C_1	73.95%	16.04
C_2	7.51%	30.07
C_3	4.08%	44.10
i- C_4	0.61%	58.12
n- C_4	1.58%	58.12

COMPONENT	y_i	M_i
i-C ₅	0.50%	72.15
n-C ₅	0.74%	72.15
C ₆	0.89%	84.00
C ₇₊	7.18	

Calculate the hydrate dissociation pressure at 45°F, that is, 505°R.

SOLUTION

Step 1 Calculate f_b and f_{nh} from equations (6–37) and (6–38):

$$\begin{aligned}
 f_b &= y_{C_1} + y_{C_2} + y_{C_3} + y_{i-C_4} + y_{n-C_4}, \\
 f_b &= 73.95 + 7.51 + 4.08 + 0.61 + 1.58 = 87.73\% \\
 f_{nh} &= y_{C_{5+}} = y_{i-C_5} + y_{n-C_5} + y_{C_6} + y_{C_{7+}}, \\
 f_{nh} &= 0.5 + 0.74 + 0.89 + 7.18 = 9.31\%
 \end{aligned}$$

Step 2 Calculate F_m by applying equation (6–39):

$$F_m = \frac{f_{nh}}{f_b} = \frac{9.31}{87.73} = 0.1061$$

Step 3 Determine the specific gravity of the hydrate-forming components by normalizing their mole fractions as shown in the table below and

$$\gamma_b = \frac{19.598}{28.96} = 0.6766$$

Component	y_i	Normalized y_i^*	M_i	$M_i y_i^*$
C ₁	0.7395	0.8429	16.04	13.520
C ₂	0.0751	0.0856	30.07	2.574
C ₃	0.0408	0.0465	44.10	2.051
i-C ₄	0.0061	0.0070	58.12	0.407
n-C ₄	0.0158	0.0180	58.12	1.046
	$\Sigma = 0.8773$	$\Sigma = 1.0000$		$\Sigma = 19.5980$

Step 4 Using the temperature, T , and the calculated values of F_m and γ_b in equation (6–41) gives

$$p_b = 236.4 \text{ psia}$$

Step 5 Calculate the constants b_1 and b_2 for CO₂ by applying equations (6–44) and (6–45), to give

$$\begin{aligned}
 b_1 &= -2.0943 \times 10^{-4} \left(\frac{505}{1.8} - 273.15 \right)^3 + 3.809 \times 10^{-3} \left(\frac{505}{1.8} - 273.15 \right)^2 \\
 &\quad - 2.42 \times 10^{-2} \left(\frac{505}{1.8} - 273.15 \right) + 0.423 = 0.368 \\
 b_2 &= 2.3498 \times 10^{-4} \left(\frac{505}{1.8} - 273.15 \right)^2 - 2.086 \times 10^{-3} \left(\frac{505}{1.8} - 273.15 \right) \\
 &\quad + 1.63 \times 10^{-2} \left(\frac{505}{1.8} - 273.15 \right) + 0.650 = 0.752
 \end{aligned}$$

Step 6 Calculate the CO₂ correction factor E_{CO_2} using equation (6-42):

$$E_{\text{CO}_2} = 1.0 + \left[(b_1 F_m + b_2) \frac{y_{\text{CO}_2}}{1 - y_{\text{N}_2}} \right]$$

$$E_{\text{CO}_2} = 1.0 + \left[(0.368 \times 0.1061 + 0.752) \frac{0.0238}{1 - 0.0058} \right] = 1.019$$

Step 7 Correct for the presence of N₂:

$$b_3 = 1.1374 \times 10^{-4} \left(\frac{505}{1.8} - 273.15 \right)^3 + 2.61 \times 10^{-4} \left(\frac{505}{1.8} - 273.15 \right)^2$$

$$+ 1.26 \times 10^{-2} \left(\frac{505}{1.8} - 273.15 \right) + 1.123 = 1.277$$

$$b_4 = 4.335 \times 10^{-5} \left(\frac{505}{1.8} - 273.15 \right)^3 - 7.7 \times 10^{-5} \left(\frac{505}{1.8} - 273.15 \right)^2$$

$$+ 4.0 \times 10^{-3} \left(\frac{505}{1.8} - 273.15 \right) + 1.048 = 1.091$$

$$E_{\text{N}_2} = 1.0 + \left[(b_3 F_m + b_4) \frac{y_{\text{N}_2}}{1 - y_{\text{CO}_2}} \right]$$

$$E_{\text{N}_2} = 1.0 + \left[(1.277 \times 0.1061 + 1.091) \frac{0.0058}{1 - 0.00238} \right] = 1.007$$

Step 8 Estimate the total (corrected) hydrate dissociation pressure using equation (6-48):

$$p_{\text{corr}} = p_b E_{\text{N}_2} E_{\text{CO}_2}$$

$$p_{\text{corr}} = (236.4)(1.019)(1.007) = 243 \text{ psia}$$

Makogon (1981) developed an analytical relationship between hydrates and conditions in terms of pressure and temperature as a function of specific gravity of the gas. The expression is given by

$$\log(p) = b + 0.0497(T + kT^2) \quad (6-49)$$

where T = temperature, °C, and p = pressure, atm.

The coefficients b and k are expressed graphically as a function of the gas specific gravity in Figure 6-28.

EXAMPLE 6-12

Find the pressure at which hydrate forms at $T = 40^\circ\text{F}$ for a natural gas with a specific gravity of 0.631 using equation (6-49).

SOLUTION

Step 1 Convert the given temperature from °F to °C:

$$T = (40 - 32)/1.8 = 4.4^\circ\text{C}$$

Step 2 Determine values of the coefficients b and k from Figure 6-28, to give

$$b = 0.91$$

$$k = 0.006$$

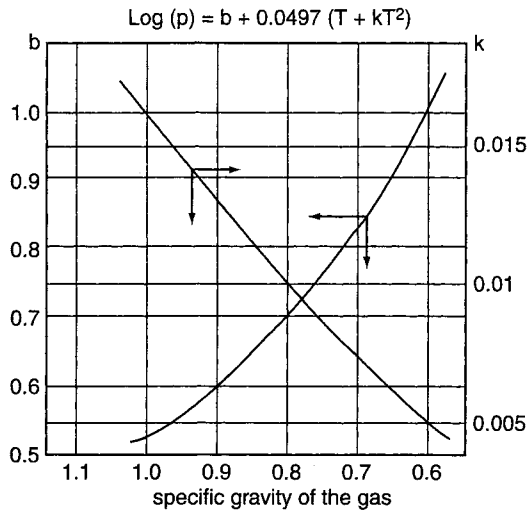


FIGURE 6-28 Coefficients of b and k in equation (6-49).

Step 3 Solve for p by applying equation (6-49):

$$\begin{aligned}\log(p) &= b + 0.0497(T + kT^2) \\ \log(p) &= 0.91 + 0.0497[4.4 + 0.006(4.4)^2] = 1.1368 \\ p &= 10^{1.1368} = 13.70 \text{ atm} = 201 \text{ psia}\end{aligned}$$

Figure 6-22 gives a value of 224 psia as compared with this value of 201.

Carson and Katz (1942) adopted the concept of the equilibrium ratios, that is, K -values, for estimating hydrate-forming conditions. They proposed that hydrates are the equivalent of solid solutions and not mixed crystals and, therefore, postulated that hydrate-forming conditions could be estimated from empirically determined vapor/solid equilibrium ratios, as defined by

$$K_{i(v-S)} = \frac{y_i}{x_{i(S)}} \tag{6-50}$$

where

- $K_{i(v-S)}$ = equilibrium ratio of component i between vapor and solid
- y_i = mole fraction of component i in the vapor (gas) phase
- $x_{i(S)}$ = mole fraction of component i in the solid phase on a water-free basis

The calculation of the hydrate-forming conditions in terms of pressure or temperature is analogous to the dew-point calculation of gas mixtures. In general, a gas in the presence of free-water phase forms a hydrate when

$$\sum_{i=1}^n \frac{y_i}{K_{i(v-S)}} = 1 \tag{6-51}$$

Whitson and Brule (2000) point out that the vapor/solid equilibrium ratio cannot be used to perform flash calculations and determine hydrate-phase splits or equilibrium-

phase compositions, since $K_{i(S)}$ is based on the mole fraction of a “guest” component in the solid-phase hydrate mixture on a water-free basis.

Carson and Katz developed K -value charts for the hydrate-forming molecules that include methane through butanes, CO_2 , and H_2S , as shown in Figures 6–29 through 6–35. It should be noted that $K_{i(S)}$ for non-hydrate-formers are assumed to be infinity, that is, $K_{i(S)} = \infty$.

The solution of equation (6–51) for the hydrate-forming pressure or temperature is an iterative process. The process involves assuming several values of p or T and calculating the equilibrium ratios at each assumed value until the constraint represented by equation (6–51) is met, that is, summation is equal to 1.

EXAMPLE 6–13

Using the equilibrium ratio approach, calculate the hydrate-formation pressure, p_b , at 50°F for the following gas mixture:

COMPONENT	y_i
CO_2	0.002
N_2	0.094
C_1	0.784
C_2	0.060
C_3	0.036
i- C_4	0.005
n- C_4	0.019

The experimentally observed hydrate-formation pressure is 325 psia at 50°F.

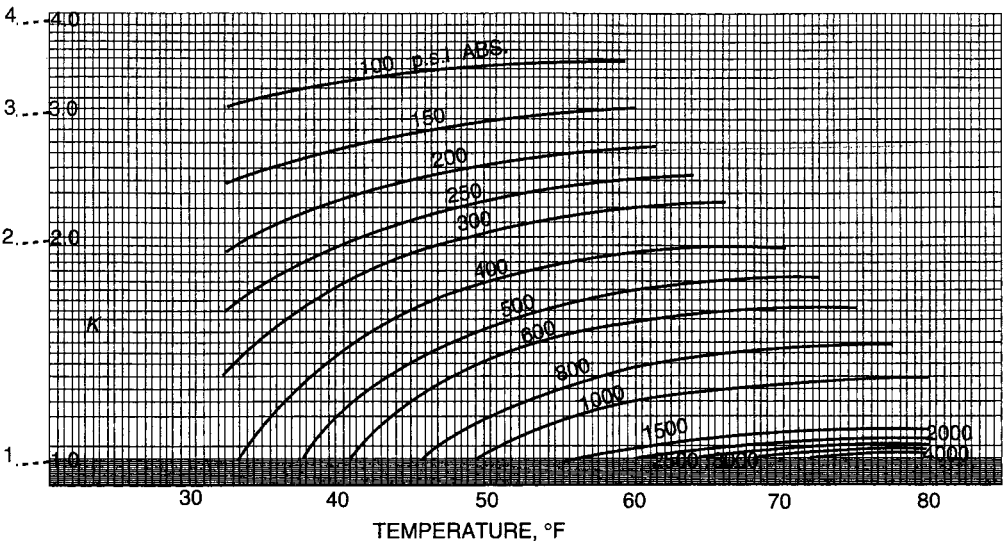


FIGURE 6–29 Vapor/solid equilibrium constant for methane.
Source: D. Carson and D. Katz, “Natural Gas Hydrates,” *Transactions of the AIIME* 146 (1942): 150. Courtesy of the Society of Petroleum Engineers of the AIIME.

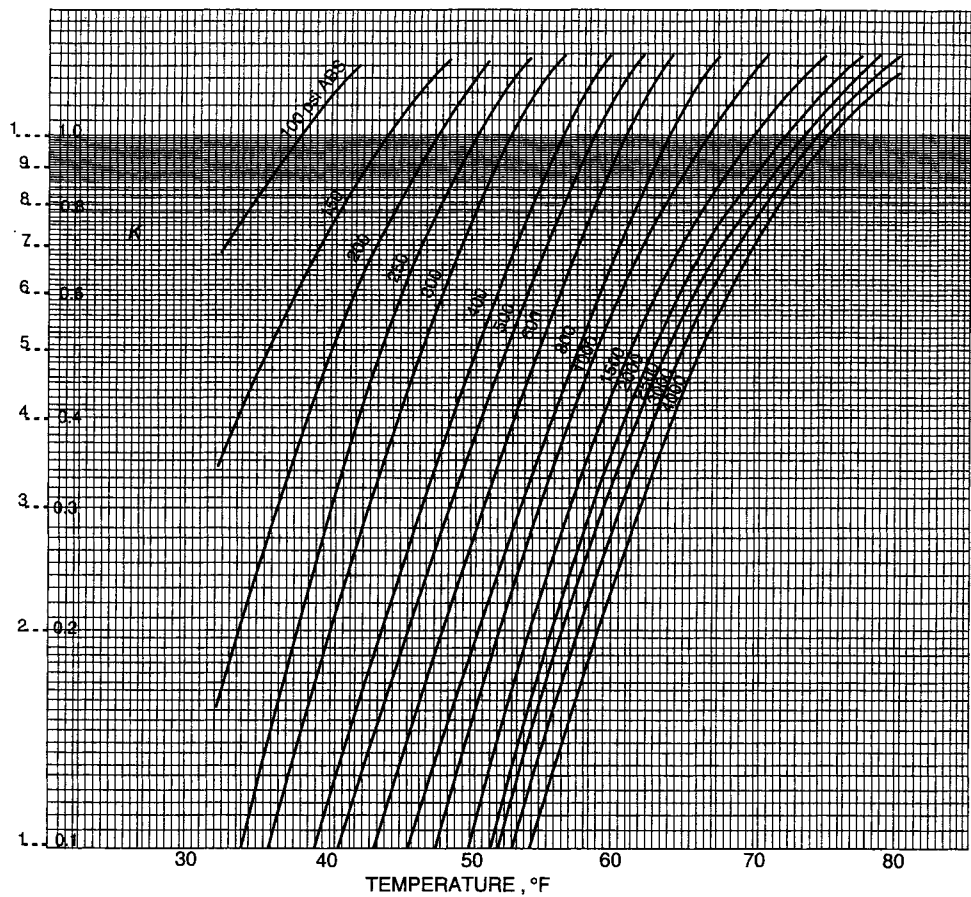


FIGURE 6-30 Vapor/solid equilibrium constant for ethane.
Source: D. Carson and D. Katz, "Natural Gas Hydrates," *Transactions of the AIME* 146 (1942): 150. Courtesy of the Society of Petroleum Engineers of the AIME.

SOLUTION

Step 1 For simplicity, assume two different pressures, 300 psia and 350 psia, and calculate the equilibrium ratios at these pressures, to give the results in the table below.

Component	y_i	At 300 psia		At 350 psia	
		$K_{i(v-S)}$	$y_i/K_{i(v-S)}$	$K_{i(v-S)}$	$y_i/K_{i(v-S)}$
CO ₂	0.002	3.0	0.0007	2.300	0.0008
N ₂	0.094	∞	0	∞	0
C ₁	0.784	2.04	0.3841	1.900	0.4126
C ₂	0.060	0.79	0.0759	0.630	0.0952
C ₃	0.036	0.113	0.3185	0.086	0.4186
i-C ₄	0.005	0.0725	0.0689	0.058	0.0862
n-C ₄	0.019	0.21	0.0900	0.210	0.0900
Σ	1.000		0.9381		1.1034

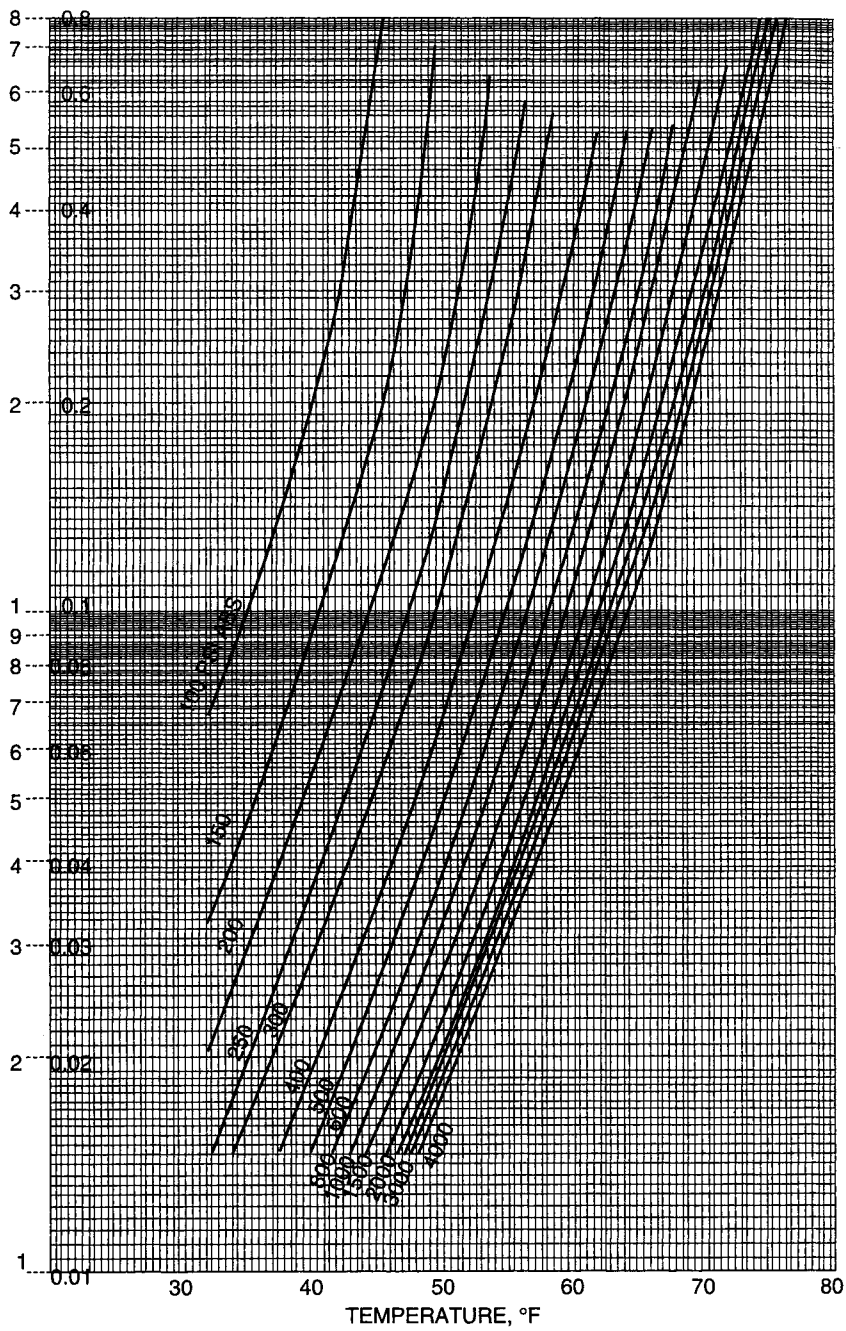


FIGURE 6-31 Vapor/solid equilibrium constant for propane.
Source: D. Carson and D. Katz, "Natural Gas Hydrates," *Transactions of the AIIME* 146 (1942): 150. Courtesy of the Society of Petroleum Engineers of the AIIME.

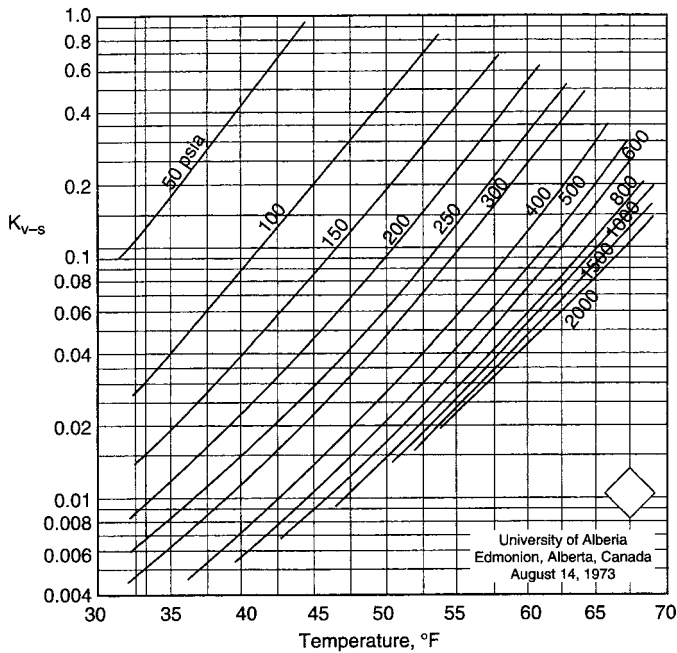


FIGURE 6–32 Vapor/solid equilibrium constant for *i*-butane.
Source: D. Carson and D. Katz, “Natural Gas Hydrates,” *Transactions of the AIME* 146 (1942): 150. Courtesy of the Society of Petroleum Engineers of the AIME.

Step 2 Interpolating linearly at $\sum y_i/K_{i(v-s)} = 1$ gives

$$\frac{350 - 300}{1.1035 - 0.9381} = \frac{p_b - 300}{1.0 - 0.9381}$$

Hydrate-forming pressure $p_b = 319$ psia, which compares favorably with the observed value of 325 psia.

EXAMPLE 6–14

Calculate the temperature for hydrate formation at 435 psi for a 0.728 specific gravity gas with the following composition:

COMPONENT	y_i
CO ₂	0.04
N ₂	0.06
C ₁	0.78
C ₂	0.06
C ₃	0.03
i-C ₄	0.01
C ₅₊	0.02

SOLUTION

The iterative procedure for estimating the hydrate-forming temperature is given in the following table. The temperature at which hydrates form is approximately 54°F.

Component	y_i	$T = 59^{\circ}\text{F}$		$T = 50^{\circ}\text{F}$		$T = 54^{\circ}\text{F}$	
		$K_{i(v-s)}$	$y_i / K_{i(v-s)}$	$K_{i(v-s)}$	$y_i / K_{i(v-s)}$	$K_{i(v-s)}$	$y_i / K_{i(v-s)}$
CO ₂	0.04	5.00	0.0008	1.700	0.0200	3.000	0.011
N ₂	0.06	∞	0	∞	0	∞	0
C ₁	0.78	1.80	0.4330	1.650	0.4730	1.740	0.448
C ₂	0.06	1.30	0.0460	0.475	0.1260	0.740	0.081
C ₃	0.03	0.27	0.1100	0.066	0.4540	0.120	0.250
i-C ₄	0.01	0.08	0.1250	0.026	0.3840	0.047	0.213
C ₅₊	0.02	∞	0	∞	0	∞	0
Total	1.00				1.457		1.003

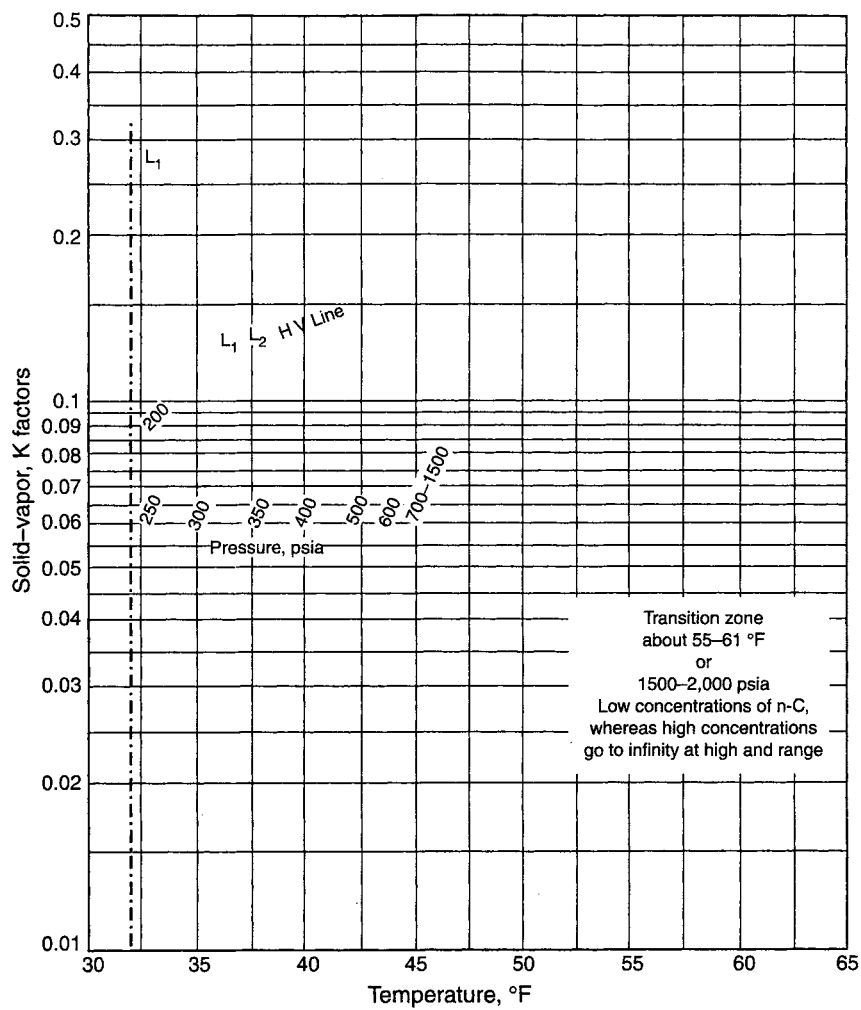


FIGURE 6-33 Vapor/solid equilibrium constant for *n*-butane.

Source: D. Carson and D. Katz, "Natural Gas Hydrates," *Transactions of the AIME* 146 (1942): 150. Courtesy of the Society of Petroleum Engineers of the AIME.

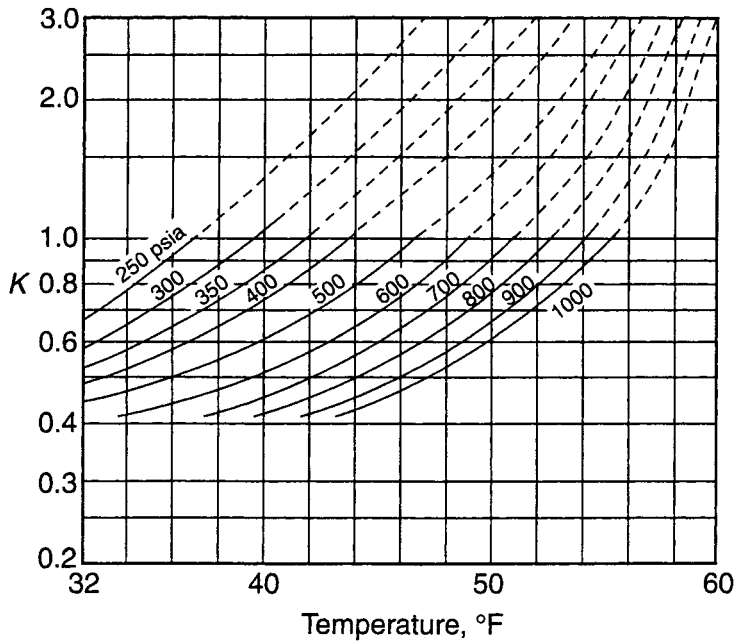


FIGURE 6-34 Vapor/solid equilibrium constant for CO_2 .
Source: D. Carson and D. Katz, "Natural Gas Hydrates," *Transactions of the AIME* 146 (1942): 150. Courtesy of the Society of Petroleum Engineers of the AIME.

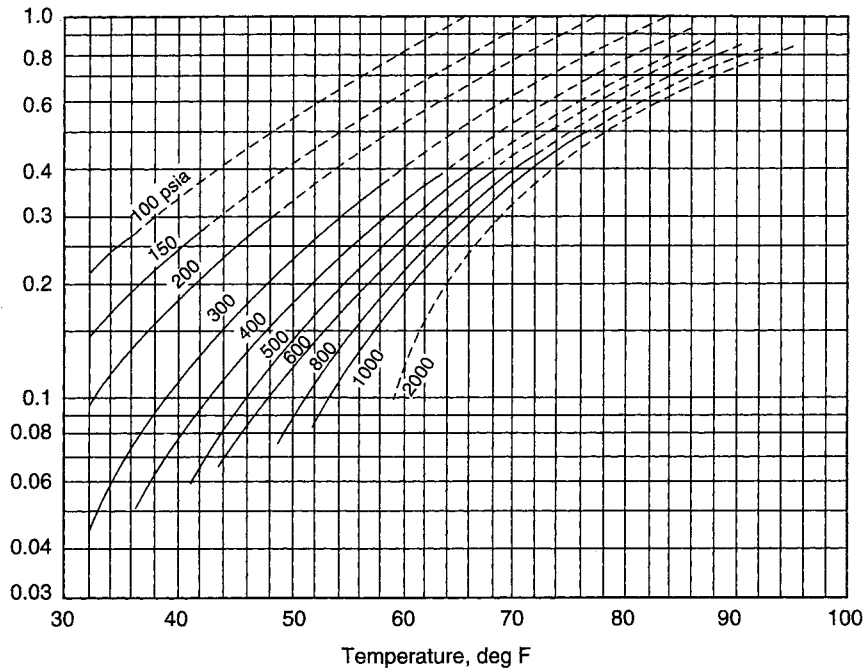


FIGURE 6-35 Vapor/solid equilibrium constant for H_2S .
Source: D. Carson and D. Katz, "Natural Gas Hydrates," *Transactions of the AIME* 146 (1942): 150. Courtesy of the Society of Petroleum Engineers of the AIME.

Sloan (1984) curve-fitted the Katz-Carson charts by the following expression:

$$\ln(K_{i(v-S)}) = A_0 + A_1T + A_2p + \frac{A_3}{T} + \frac{A_4}{p} + A_5pT + A_6T^2 + A_7p^2 + A_8\left(\frac{p}{T}\right) + A_9\ln\left(\frac{p}{T}\right) + \frac{A_{10}}{p^2} + A_{11}\left(\frac{T}{p}\right) + A_{12}\left(\frac{T^2}{p}\right) + A_{13}\left(\frac{p}{T^2}\right) + A_{14}\left(\frac{T}{p^3}\right) + A_{15}T^3 + A_{16}\left(\frac{p^3}{T^2}\right) + A_{17}T^4$$

where T = temperature, °F, and p = pressure, psia. The coefficients A_0 through A_{17} are given in Table 6–8.

EXAMPLE 6–15

Resolve Example 6–14 using equation (6–49).

SOLUTION

Step 1 Convert the given pressure from psia to atm, to give

$$p = 435/14.7 = 29.6$$

Step 2 Determine the coefficients b and k from Figure 6–27 at the specific gravity of the gas, 0.728, to give

$$b = 0.8$$
$$k = 0.0077$$

TABLE 6–8 Visual Coefficients A_0 through A_{17} in Sloan’s Equation

	CH ₄	C ₂ H ₆	C ₃ H ₈	i-C ₄ H ₁₀	n-C ₄ H ₁₀	N ₂	CO ₂	H ₂ S
A_0	1.63636	6.41934	−7.8499	−2.17137	−37.211	1.78857	9.0242	−4.7071
A_1	0.0	0.0	0.0	0.0	0.86564	0.0	0.0	0.06192
A_2	0.0	0.0	0.0	0.0	0.0	−0.001356	0.0	0.0
A_3	31.6621	−290.283	47.056	0.0	732.20	−6.187	−207.033	82.627
A_4	−49.3534	2629.10	0.0	0.0	0.0	0.0	0.0	0.0
A_5	5.31×10^{-6}	0.0	$−1.17 \times 10^{-6}$	0.0	0.0	0.0	4.66×10^{-5}	$−7.39 \times 10^{-6}$
A_6	0.0	0.0	7.145×10^{-4}	1.251×10^{-3}	0.0	0.0	$−6.992 \times 10^{-3}$	0.0
A_7	0.0	9.0×10^{-8}	0.0	1.0×10^{-8}	9.37×10^{-6}	2.5×10^{-7}	2.89×10^{-6}	0.0
A_8	0.128525	0.129759	0.0	0.166097	−1.07657	0.0	$−6.223 \times 10^{-3}$	0.240869
A_9	−0.78338	−1.19703	0.12348	−2.75945	0.0	0.0	0.0	−0.64405
A_{10}	0.0	$−8.46 \times 10^4$	1.669×10^4	0.0	0.0	0.0	0.0	0.0
A_{11}	0.0	−71.0352	0.0	0.0	−66.221	0.0	0.0	0.0
A_{12}	0.0	0.596404	0.23319	0.0	0.0	0.0	0.27098	0.0
A_{13}	−5.3569	−4.7437	0.0	0.0	0.0	0.0	0.0	−12.704
A_{14}	0.0	7.82×10^4	$−4.48 \times 10^4$	$−8.84 \times 10^2$	9.17×10^5	5.87×10^5	0.0	0.0
A_{15}	$−2.3 \times 10^{-7}$	0.0	5.5×10^{-6}	0.0	0.0	0.0	8.82×10^{-5}	$−1.3 \times 10^{-6}$
A_{16}	$−2.0 \times 10^{-8}$	0.0	0.0	$−5.7 \times 10^{-7}$	4.98×10^{-6}	1.0×10^{-8}	2.25×10^{-6}	0.0
A_{17}	0.0	0.0	0.0	$−1.0 \times 10^{-8}$	$−1.26 \times 10^{-6}$	1.1×10^{-7}	0.0	0.0

Step 3 Apply equation (6-49), to give

$$\begin{aligned}\log(p) &= b + 0.0497(T + kT^2) \\ \log(29.6) &= 0.8 + 0.0497(T + 0.0077T^2) \\ 0.000383T^2 + 0.0497T - 0.6713 &= 0\end{aligned}$$

Using the quadratic formula gives

$$T = \frac{-0.497 + \sqrt{(0.0497)^2 - (4)(0.000383)(-0.6713)}}{(2)(0.000383)} = 12.33^\circ\text{C}$$

or

$$T = (1.8)(12.33) + 32 = 54.2^\circ\text{F}$$

Hydrates in Subsurface

One explanation for hydrate formation is that the entrance of the gaseous molecules into vacant lattice cavities in the liquid water structure causes the water to solidify at temperatures above the freezing point of water. In general, ethane, propane, and butane raise the hydrate-formation temperature for methane. For example, 1% propane raises the hydrate-forming temperature from 41 to 49°F at 600 psia. Hydrogen sulfide and carbon dioxide also are relatively significant contributors in causing hydrates, whereas N_2 and C_{5+} have no noticeable effect. These solid icelike mixtures of natural gas and water have been found in formations under deep water along the continental margins of America and beneath the permafrost (i.e., permanently frozen ground) in Arctic basins. The permafrost occurs where the mean atmospheric temperature is just under 32°F.

Muller (1947) suggests that the lowering of the earth's temperature took place in early Pleistocene times, "perhaps a million years ago." If the formation natural gases were cooled under pressure in the presence of free water, hydrates would form in the cooling process before ice temperatures were reached. If further lowering of temperature brought the layer into a permafrost condition, then the hydrates would remain as such. In colder climates (such as Alaska, northern Canada, and Siberia) and beneath the oceans, conditions are appropriate for gas-hydrate formation.

The essential condition for gas-hydrate stability at a given depth is that the actual earth temperature at that depth is lower than the hydrate-forming temperature, corresponding to the pressure and gas composition conditions. The thickness of a potential hydrate zone can be an important variable in drilling operations, where drilling through hydrates require special precautions. It also can be of significance in determining regions where hydrate occurrences might be sufficiently thick to justify gas recovery. The existence of a gas-hydrate stability condition, however, *does not ensure that hydrates exist in that region* but only that they can exist. In addition, if gas and water coexist within the hydrate-stability zone, then they must exist in gas-hydrate form.

Consider the earth temperature curve for the Cape Simpson area of Alaska, as shown in Figure 6-36. Pressure data from the drill stem test and repeat formation tester indicate a pressure gradient of 0.435 psi/ft. Assuming a 0.6 gas gravity with its hydrate-forming pressure and temperature as given in Figure 6-23. This hydrate pressure/temperature curve can be converted into a depth versus temperature plot by dividing the pressures by 0.435; as shown by Katz (1971) in Figure 6-37. These two curves intersect at 2100 ft in

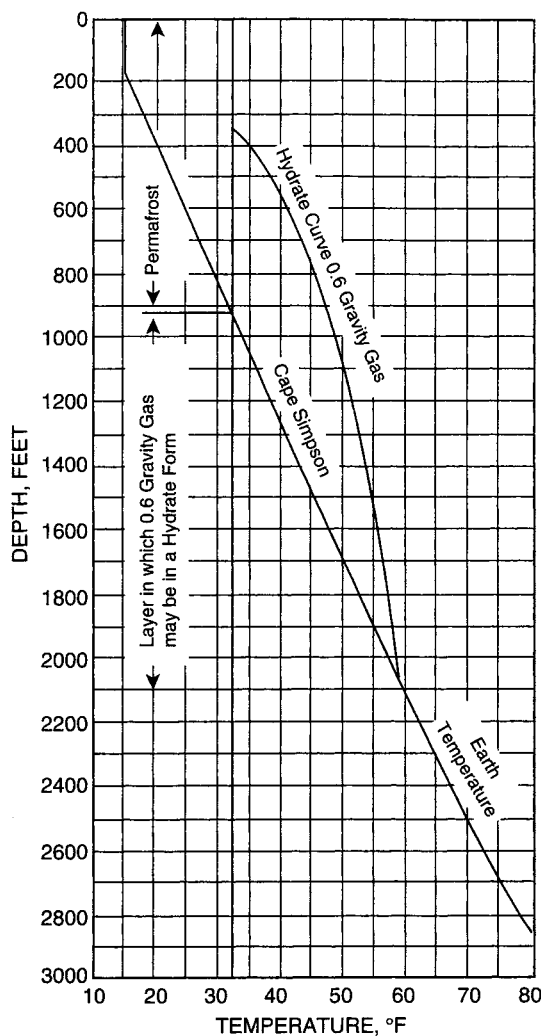


FIGURE 6-36 Method for locating thickness of hydrate layer.
Source: D. Katz, “Depths to which Frozen Gas Fields May Be Expected.” *Journal of Petroleum Technology* (April 1971).
Courtesy of the Society of Petroleum Engineers of the AIME. © Society of Petroleum Engineers, 1971.

depth. Katz points out that, at Cape Simpson, we would expect to find water in the form of ice down to 900 ft and hydrates between 900 and 2100 ft of 0.6 gas gravity.

Using the temperature profile as a function of depth for the Prudhoe Bay Field as shown in Figure 6-37, Katz (1971) estimated that the hydrate zone thickness at Prudhoe Bay for a 0.6 gravity gas might occur between 2000 and 4000 ft. Godbole et al. (1988) point out that the first confirmed evidence of the presence of gas hydrates in Alaska was obtained on March 15, 1972, when Arco and Exxon recovered gas-hydrate core samples in pressurized core barrels at several depths between 1893 and 2546 ft from the Northwest Eileen well no. 2 in the Prudhoe Bay Field.

Studies by Holder et al. (1987) and Godbole et al. (1988) on the occurrence of in-situ natural gas hydrates in the Arctic North Slope of Alaska and beneath the ocean floor sug-

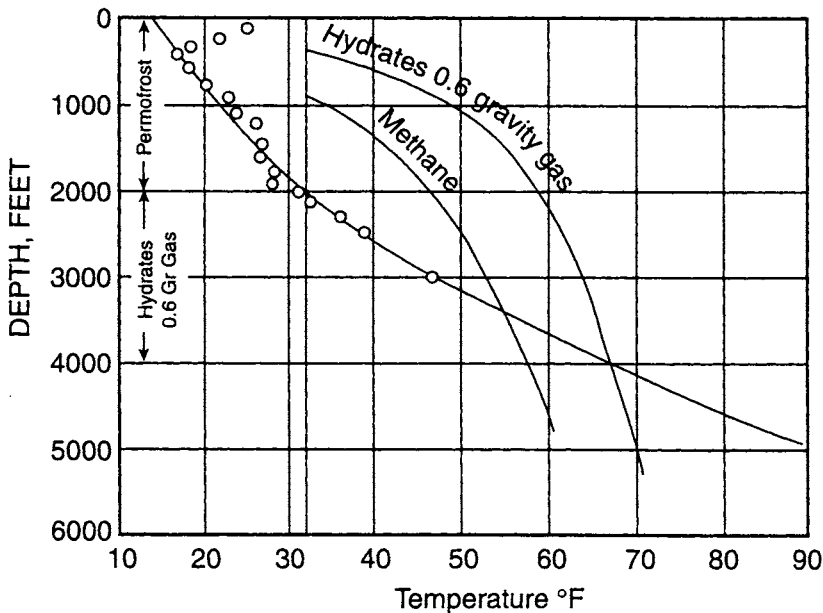


FIGURE 6-37 Hydrate zone thickness for temperature gradients at Prudhoe Bay.

Source: D. Katz, "Depths to Which Frozen Gas Fields May Be Expected," *Journal of Petroleum Technology* (April 1971). Courtesy of the Society of Petroleum Engineers of the AIME. © Society of Petroleum Engineers, 1971.

gest that the factors controlling the depth and thickness of natural gas–hydrate zones in these regions and affecting their stabilities include

- Geothermal gradient.
- Pressure gradient.
- Gas composition.
- Permafrost thickness.
- Ocean-bottom temperature.
- Mean average annual surface temperature.
- Water salinity.

Various methods have been proposed for harvesting the gas in hydrate form that essentially require heat to melt the hydrate or lowering the pressure on the hydrate to release the gas: specifically, injection of steam, hot brine, or chemicals; fire-flood; and depressurizing.

Holder and Angert (1982) suggest that, in the depressurizing scheme, pressure reduction causes destabilization of hydrates. As hydrates dissociate, they absorb heat from the surrounding formation. The hydrates continue to dissociate until they generate enough gas to raise the reservoir pressure to the equilibrium pressure of hydrates at a new temperature, which is lower than the original value. A temperature gradient is thus generated between hydrates (sink) and surrounding media (source), and heat flows to hydrates. The rate of dissociation of hydrates, however, is controlled by the rate of heat influx from the surrounding media or by the thermal conductivity of the surrounding rock matrix.

Many questions need to be answered if gas is to be produced from hydrates; for example:

- In what form do hydrates exist in a reservoir? Hydrates may exist in different types (all hydrates, excess water, and excess ice, in conjunction with free gas or oil) and in different forms (massive, laminated, dispersed, or nodular). Each case has a different effect on the method of production and economics.
- What is the saturation of hydrates in the reservoir?
- What problems are associated with gas production? Examples include pore blockage by ice and blockage of the well bore resulting from reformation of hydrates during the flow of gas through the production well.
- What are the economics of the project? This perhaps is the most important impact for the success of gas recovery from subsurface-hydrate accumulations.

Despite these above concerns, subsurface hydrates exhibit several characteristics, especially as compared with other unconventional gas resources, that increase their importance as potential energy resources and make their future recovery likely. These include higher concentration of gas in hydrated form, enormously large deposits of hydrates, and their widespread existence in the world.

Problems

1. Given the following experimental data, determine if this fluid might develop an asphaltene deposition problem using the De Boer plot:
 Reservoir pressure, p_i , = 8000 psia
 Reservoir temperature = 220°F
 Flash gas/oil ratio = 1000 scf/STB
 Bubble-point pressure, p_b , at T_{res} = 4300 psia
 Density of stock-tank oil = 0.873 g/cc
 Density of reservoir fluid at pb = 0.821 g/cc
2. Given the following SARA analysis of stock-tank oil, determine the stability of the oil using the following methods: colloidal instability index criteria and the asphaltene versus resin graphical solution:
 Saturates = 50.0 wt%
 Aromatics = 31.50 wt%
 Resins = 17.0 wt%
 Asphaltenes = 0.5 wt%
 Wax = 1.0 wt%
3. A 0.7 specific gravity gas is at 800 psia. To what extent can the temperature be lowered without hydrate formation in the presence of free water?
4. A gas has a specific gravity of 0.75 and exists at 70°F. What would be the pressure above which hydrates could be expected to form?
5. How far can a 0.76 gravity gas at 1400 psia and 110°F be expanded without hydrate formation?

References

- Alkafeef, S. F., A. Fahad, and A. al-Shammari. "Asphaltene Remedial Technology Using Advanced Deasphalted Oil." SPE paper 81750. Middle East Oil Show, Bahrain, June 9–12, 2003.
- Alkafeef, S. F., R. J. Gochin, and A. L. Smith. "The Effect of Double Layer Overlap on Measured Streaming Currents for Toluene Flowing through Sandstone Rock Cores." *Colloid and Surfaces, A, Physicochemical and Engineering Aspects* 195 (2001): 77–80.
- Alkafeef, S. F., et al. "A Simplified Method to Predict and Prevent Asphaltene Deposition in Oil Well Tubing, Field Case." *SPE Production and Facilities* 20, no. 2 (May 2005).
- Bott, T. R., and J. S. Gudmundsson. "Deposition of Paraffin Wax from Flowing Systems." Technical paper IP-77-007. *Institute of Petroleum*, 1977a.
- Bott, T. R., and J. S. Gudmundsson. "Deposition of Paraffin Wax from Kerosene in Cooled Heat Exchangers." *Canadian Journal of Chemical Engineering* 55 (August 1977b): 381.
- Brown, T. S., V. G. Niesen, and D. D. Erickson. "Measurement and Prediction of the Kinetics of Paraffin Deposition." SPE 26548. SPE meeting, Houston, October 3–6, 1993.
- Burke, N. E., R. E. Hobbs, and S. F. Kasbou. "Measurement and Modeling of Asphaltene Precipitation." *Journal of Petroleum Technology* (November 1990): 1440.
- Carbognani, L. D. Rogel, and L. Espidel. "Asphaltene Stability in Crude Oils." SPE paper 53998, Latin American Petroleum Engineering Conference, April 21–23, 1999.
- Carbognani, L., E. Contreras, R. Guimerans, O. Leon, E. Flores, and S. Moya. "Physicochemical Characterization of Crudes and Solid Deposits as a Guideline to Optimize Oil Production." SPE 64993, SPE International Symposium on Oilfield Chemistry, Houston, February 1995.
- Carson, D., and D. Katz. "Natural Gas Hydrates." *Transactions of the AIME* 146 (1942): 150.
- Cole, R. J., and F. W. Jessen. "Paraffin Deposition." *Oil and Gas Journal* 58 (September 1960): 87.
- De Boer, R. B., and K. Leeriooyer. "Screening of Crude Oils for Asphalt Precipitation." SPE 24987, SPE European Petroleum Conference, Cannes, France, November 1992.
- Fan, T., W. Jianxin, and Buckley. "Evaluating Crude Oils by SARA Analysis." SPE 7522, SPE/DOE Improved Oil Recovery Symposium, Tulsa, OK, April 12–17, 2002.
- Forsdyke, I. N. "Flow Assurance in Multiphase Environments." SPE 37237, unpublished ms, 1997.
- Godbole, S., V. Kamath, and C. Economides. "Natural Gas Hydrates in the Alaskan Arctic." *SPE Formation Evaluation* (March 1988).
- Hammami, A., C. H. Phelps, T. Monger-McClure, and T. M. Little. "Asphaltene Precipitation from Live Oils: An Experimental Investigation of the Onset Conditions and Reversibility." AICHE 1999 Spring National Meeting, Houston, March 1999.
- Hirschberg, A. "Role of Asphaltenes in Composition and Grading of a Reservoir Fluid Column." *Journal of Petroleum Technology* (January 1988).
- Hirschberg, A., et al. "Influence of Temperature and Pressure on Asphaltene Flocculation." *SPE Journal* 283 (June 1984).
- Holder, G., and P. Angert. "Simulation of Gas Production from a Reservoir Containing Gas Hydrates." SPE paper 11105, SPE annual conference, New Orleans, September 26–29, 1982.
- Holder, G., et al. "Effects of Gas Composition and Geothermal on the Thickness and Depth of Gas Hydrate Zones." *Journal of Petroleum Technology* (September 1987).
- Hunt, E. B., Jr. "Laboratory Study of Paraffin Deposition." *Journal of Petroleum Technology* (November 1962): 1259.
- Jamaluddin, A. K. M., J. Creek, C. S. Kabir, J. D., McFadden, D. D'Cruz, J. Manakalathil, N. Joshi, and B. Ross. "Laboratory Techniques to Measure Thermodynamic Asphaltene Instability." SPE 72154, SPE Asia Pacific Improved Oil Recovery Conference, Kuala Lumpur, Malaysia, October 2001a.
- Jamaluddin, A. K. M., J. Nighswander, and N. Joshi. "A Systematic Approach in Deepwater Flow Assurance Fluid Characterization." SPE 71546, 2001 SPE Annual Technical Conference and Exhibition, New Orleans, October 2001b.

- Jessen, F. W., and J. N. Howell. "Effect of Flow Rate on Paraffin Accumulation in Plastic, Steel and Coated Pipes." *Transactions of the AIME* 213 (1958): 80.
- Jorda, R. M. "Paraffin Deposition and Prevention in Oil Wells." *Journal of Petroleum Technology* (December 1966): 1605.
- Joshi, S., O. Mullins, A. Jamaluddin, J. Creek, and J. McFadden. "Asphaltene Precipitation from Live Crude Oil." *Energy and Fuels* 15, no. 4 (2001): 979–986.
- Katz, D. "Depths to Which Frozen Gas Fields May Be Expected." *Journal of Petroleum Technology* (April 1971).
- Kohse, B., et al. "Modeling Phase Behavior Including the Effect of Pressure and Temperature on Asphaltene Precipitation." SPE paper 64465, SPE Asia Pacific Oil and Gas Conference, Brisbane, Australia, October 16–18, 2000.
- Kunal, K., et al. "Measurement of Waxy Crude Properties Using Novel Laboratory Techniques." SPE 62945, unpublished ms., 2000.
- Leontaritis, K. J., J. O. Amaefule, and R. E. Charles. "A Systematic Approach for the Prevention and Treatment of Formation Damage Caused by Asphaltene Deposition." *SPE Production and Facilities* 157 (August 1994).
- Leontaritis, K. J., and G. A. Mansoori. "Asphaltene Flocculation during Oil Production and Processing: A Thermodynamic-Colloidal Model." SPE 16258, SPE International Symposium on Oil Field Chemistry, San Antonio, January 1987.
- Makogon, Y. *Hydrates of Natural Gas*. Tulsa, OK: Penn Well Books, 1981.
- Misra, S., et al. "Paraffin Problems in Crude Oil Production and Transportation: A Review." *SPE Production and Facilities* (February 1995).
- Muller, H. "On the Structure of Gas Hydrates." *Journal of Physical Chemistry* 19 (1947): 1319.
- Nghiem, L. X., and D. A. Coombe. "Modeling of Asphaltene Precipitation during Primary Depletion." *SPE Journal* 170 (June 1997).
- Nghiem, L. X., M. S. Hassam, R. Nutakki, and A. E. D. George. "Efficient Modeling of Asphaltene Precipitation." SPE 26642, SPE 68th Annual Technical Conference and Exhibition, Houston, October 1993.
- Ostergaard, K., et al. "Effect of Reservoir Fluid Production on Gas Hydrates Phase Boundaries." SPE paper 50689, European Petroleum Conference, the Hague, the Netherlands, October 20–22, 1998.
- Pan, H., and A. Firoozabad. "Pressure and Composition Effect on Wax Precipitation: Experimental Data and Model Results." SPE 36740. SPE annual meeting, San Antonio, September 26, 1996.
- Parks, C. F. "Chemical Inhibitors Combat Paraffin Deposition." *Oil and Gas Journal* 58 (April 1960): 97.
- Patton, C. C., and B. M. Casad. "Paraffin Deposition from Refined Wax-Solvent System." *SPE Journal* 17 (March 1970).
- Pedersen, K. "Prediction of Cloud Point Temperatures and Amount of Wax Precipitation." *SPE Production and Facilities* (February 1995).
- Peramanu, S., C. Singh, M. Agrawala, and H. W. Yarranton. "Investigation on the Reversibility of Asphaltene Precipitation." *Energy and Fuels* 15, no. 4 (2001): 910–917.
- Ratulowsti, J., et al. "Flow Assurance and Sub-Sea Productivity: Closing the Loop with Connectivity and Measurements." SPE 90244. SPE annual meeting, Houston, April 12–17, 2004.
- Schulte, A. "Compositional Variations within a Hydrocarbon Column Due to Gravity." SPE paper 9735, SPE annual conference, Dallas, September 21–24, 1980.
- Sloan, E. "Phase Equilibria of Natural Gas Hydrates." Paper presented at the Gas Producers Association Annual Conference, New Orleans, March 19–21, 1984.
- Sloan, E. "Natural Gas Hydrates." *Journal of Petroleum Technology* (December 1991).
- Thawer, R., C. A. David, and G. Dick. "Asphaltene Deposition in Production Facilities." *SPE Production Engineering* (November 1990): 277–287.
- Wand, J. et al. "Experimental and Theoretical Assessment of the Naphthalene Precipitation Characteristics." SPE paper 87292, Abu Dhabi International Petroleum Conference, Abu Dhabi, United Arab Emirates, October 13–15, 2000.

- Whitson, C. H., and M. R. Brule. *Phase Behavior*. Richardson, TX: SPE, 2000.
- Willmon, J., and M. Edwards. "Recommissioning to Startup: Getting Chemical Injection Right." SPE paper 96144, SPE Annual Conference, Dallas, October 9–12, 2005.
- Won, K. W. "Thermodynamics for Solid-Liquid Equilibria: Wax Formation from Heavy Hydrocarbon Mixtures." *Fluid Phase Equilibria* 30 (1986a): 265–279.
- Won, K. W. "Thermodynamics for Solid Solution-Liquid-Vapor Equilibria: Wax Phase Formation from Heavy Hydrocarbon Mixtures." *Fluid Phase Equilibria* 30 (1986b): 265–279.
- Yen, A., Y. R. Yin, and S. Asomaning. "Evaluating Asphaltene Inhibitors: Laboratory Tests and Field Studies." SPE 65376, 2001 SPE International Symposium on Oilfield Chemistry, Houston, February 2001.
- Zisman, W. A. "Influence of Constitution on Adhesion." *Industrial Engineering and Chemistry* 55, no. 10 (1963): 18.

APPENDIX

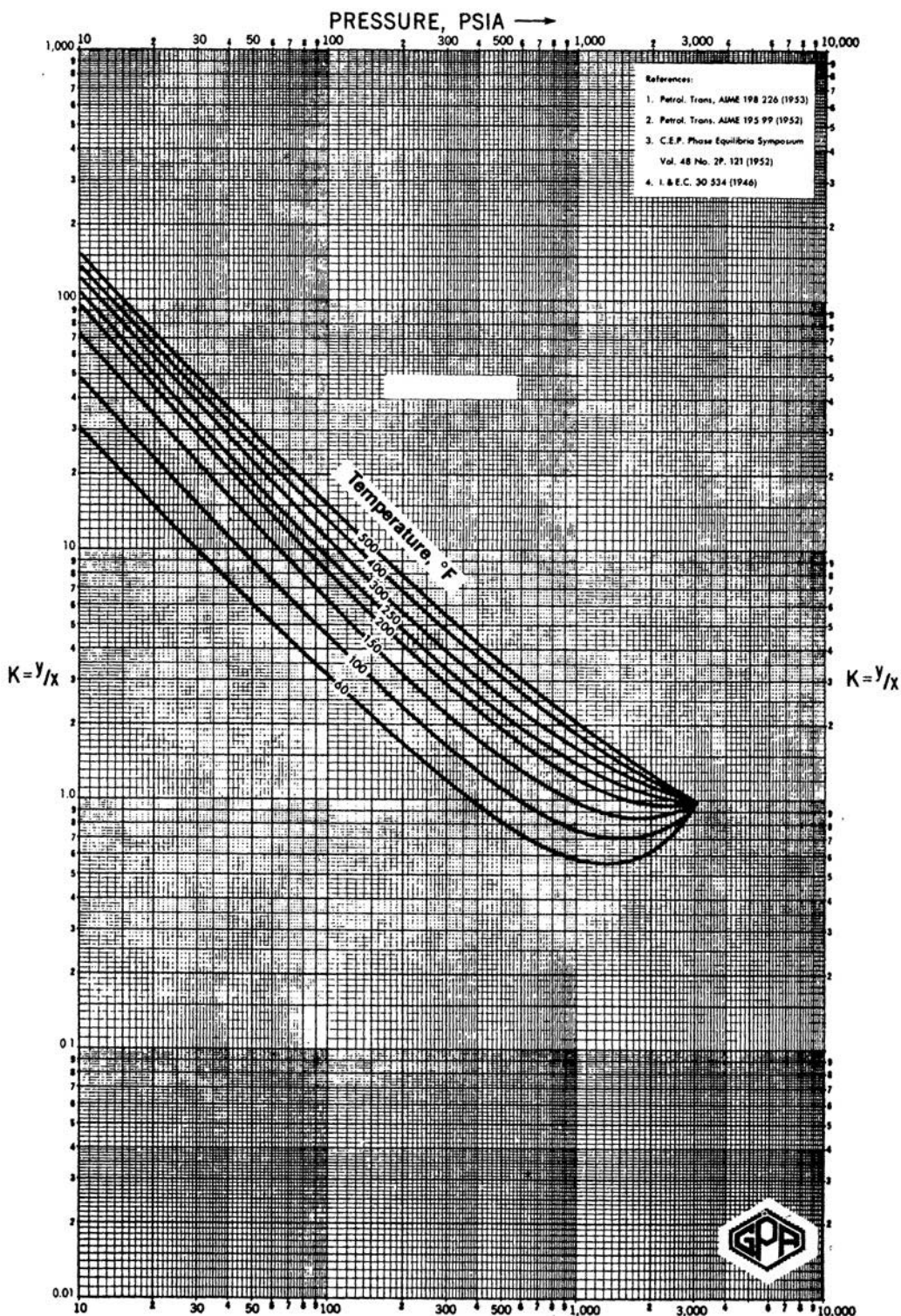


FIGURE A-1 Hydrogen sulfide conversion pressure, 3000 psia.
Courtesy of the Gas Processors Suppliers Association. Published in the *GPSA Engineering Data Book*, 10th edition, 1987.

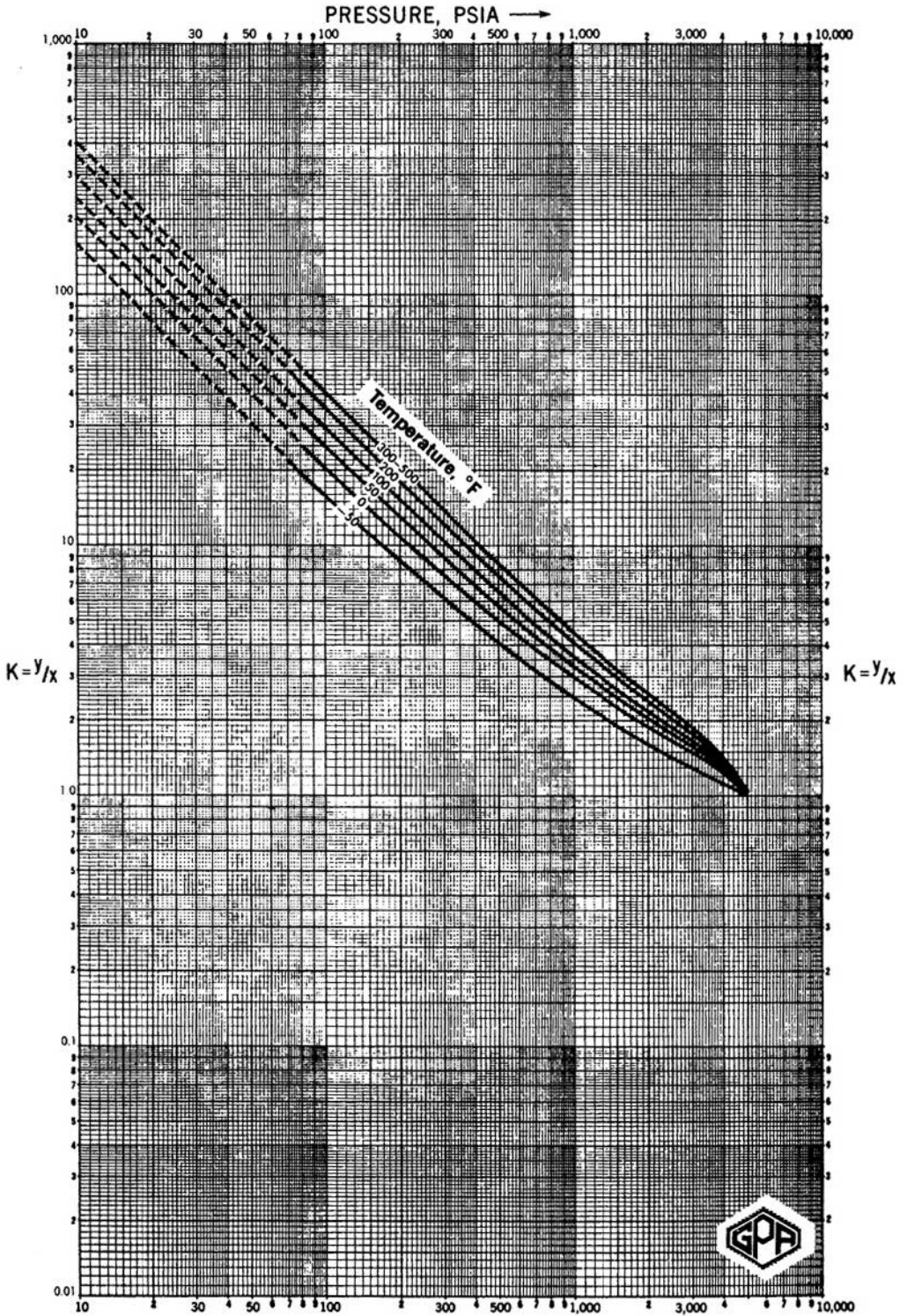


FIGURE A-2 Methane conversion pressure, 5000 psia.

Courtesy of the Gas Processors Suppliers Association. Published in the *GPSA Engineering Data Book*, 10th edition, 1987.

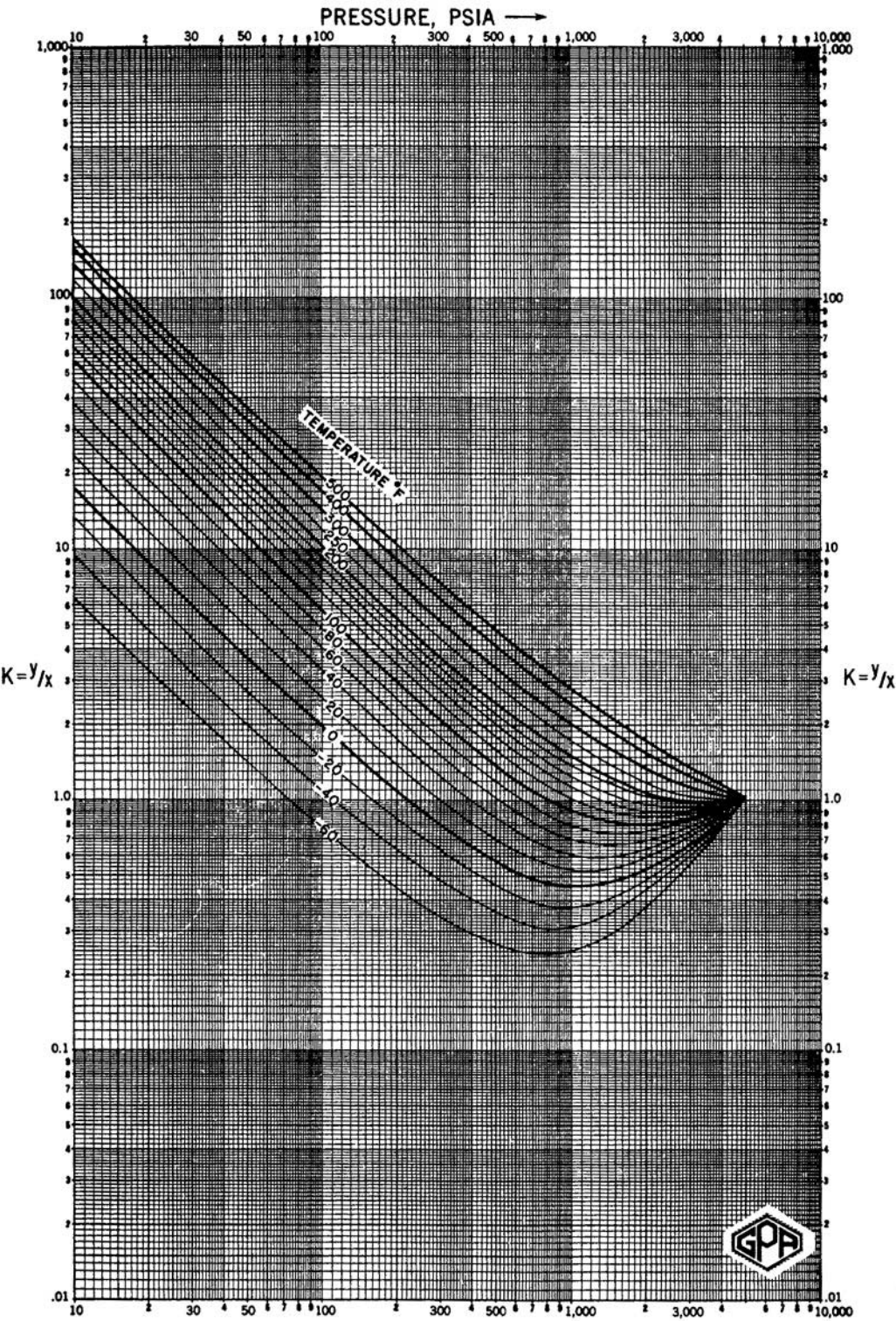


FIGURE A-3 Ethane conversion pressure, 5000 psia.
Courtesy of the Gas Processors Suppliers Association. Published in the *GPSA Engineering Data Book*, 10th edition, 1987.

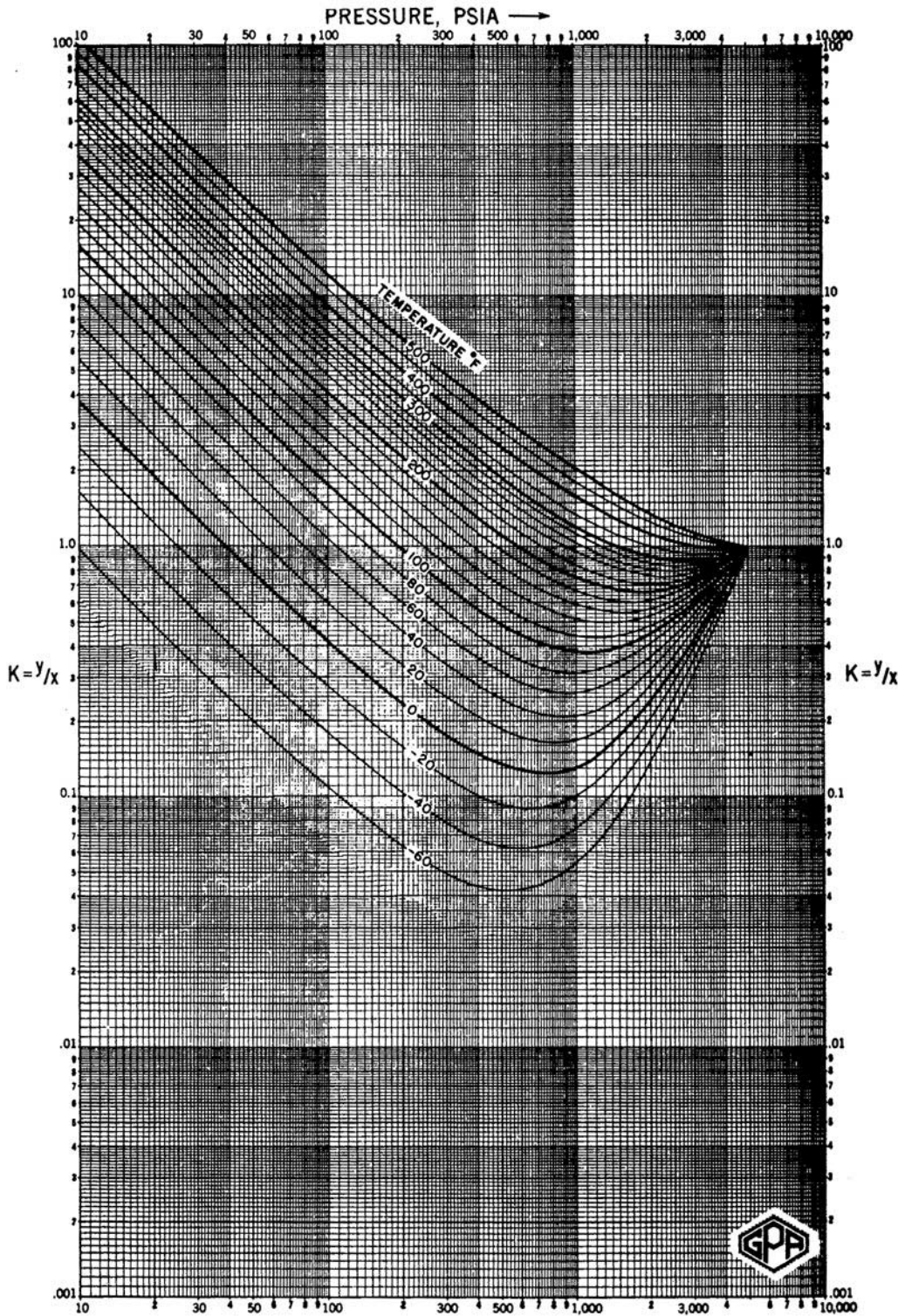


FIGURE A-4 Propane conversion pressure, 5000 psia.
Courtesy of the Gas Processors Suppliers Association. Published in the *GPSA Engineering Data Book*, 10th edition, 1987.

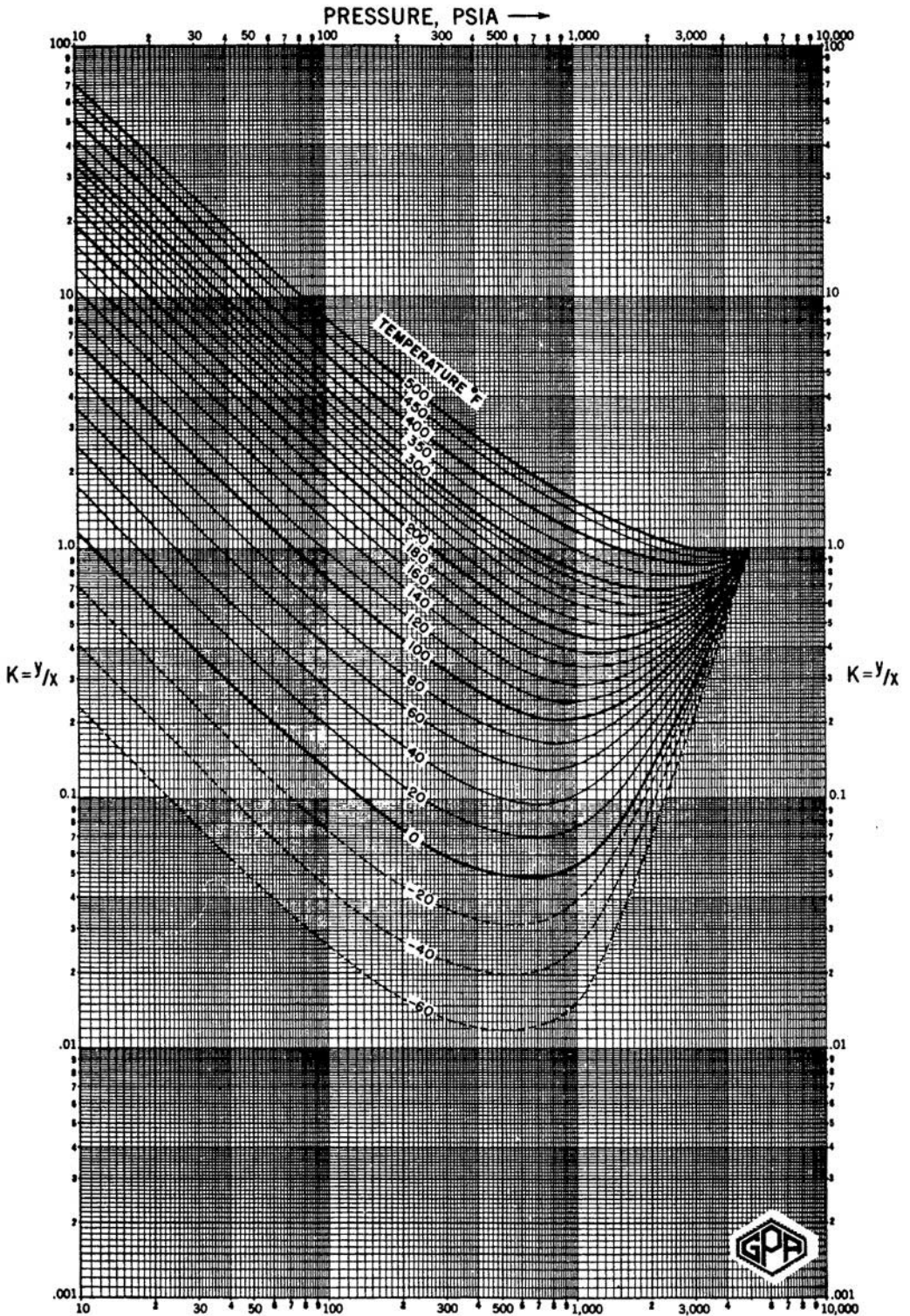


FIGURE A-5 *i*-Butane conversion pressure, 5000 psia.

Courtesy of the Gas Processors Suppliers Association. Published in the *GPSA Engineering Data Book*, 10th edition, 1987.

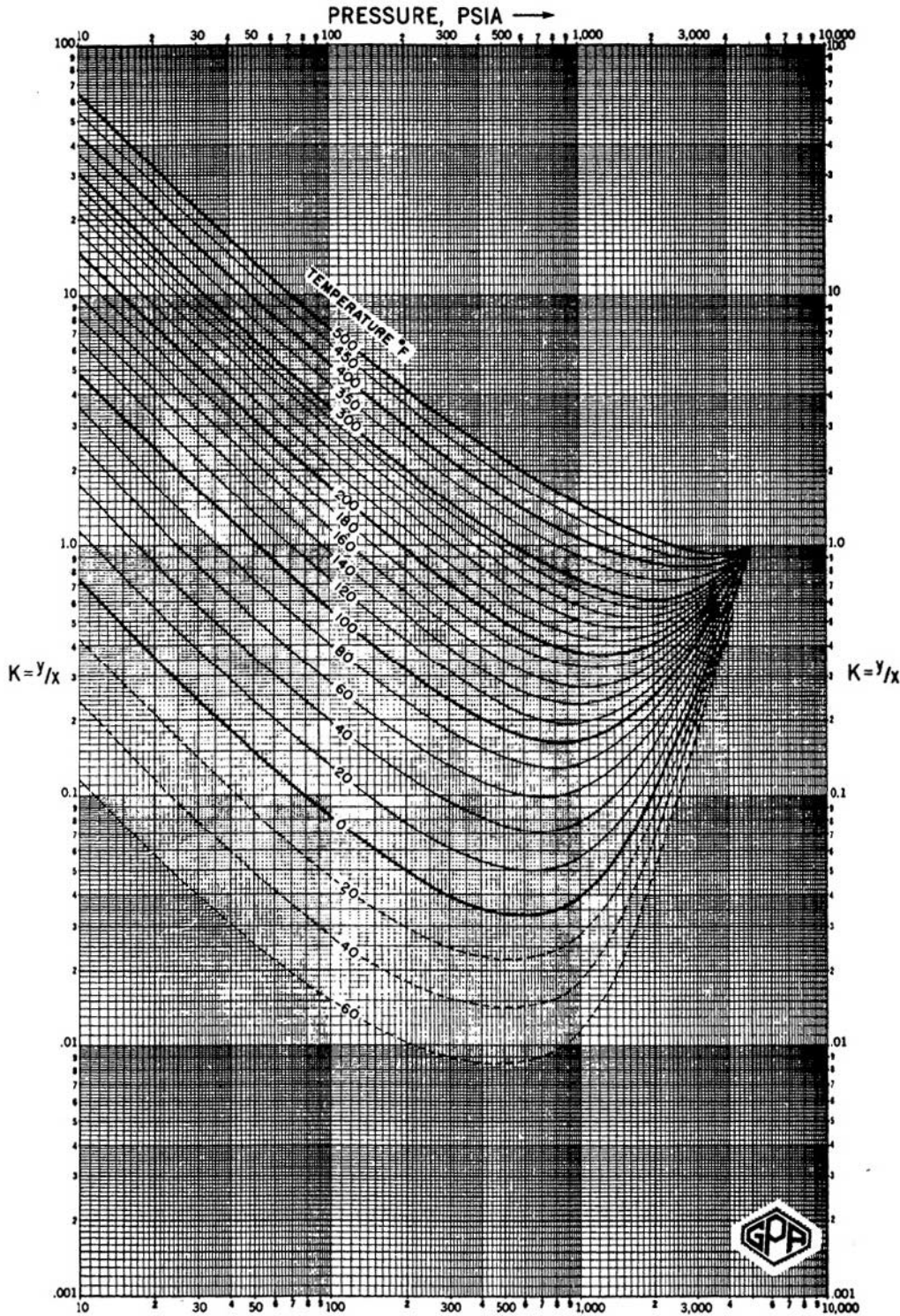


FIGURE A-6 *n*-Butane conversion pressure, 5000 psia.
Courtesy of the Gas Processors Suppliers Association. Published in the *GPSA Engineering Data Book*, 10th edition, 1987.

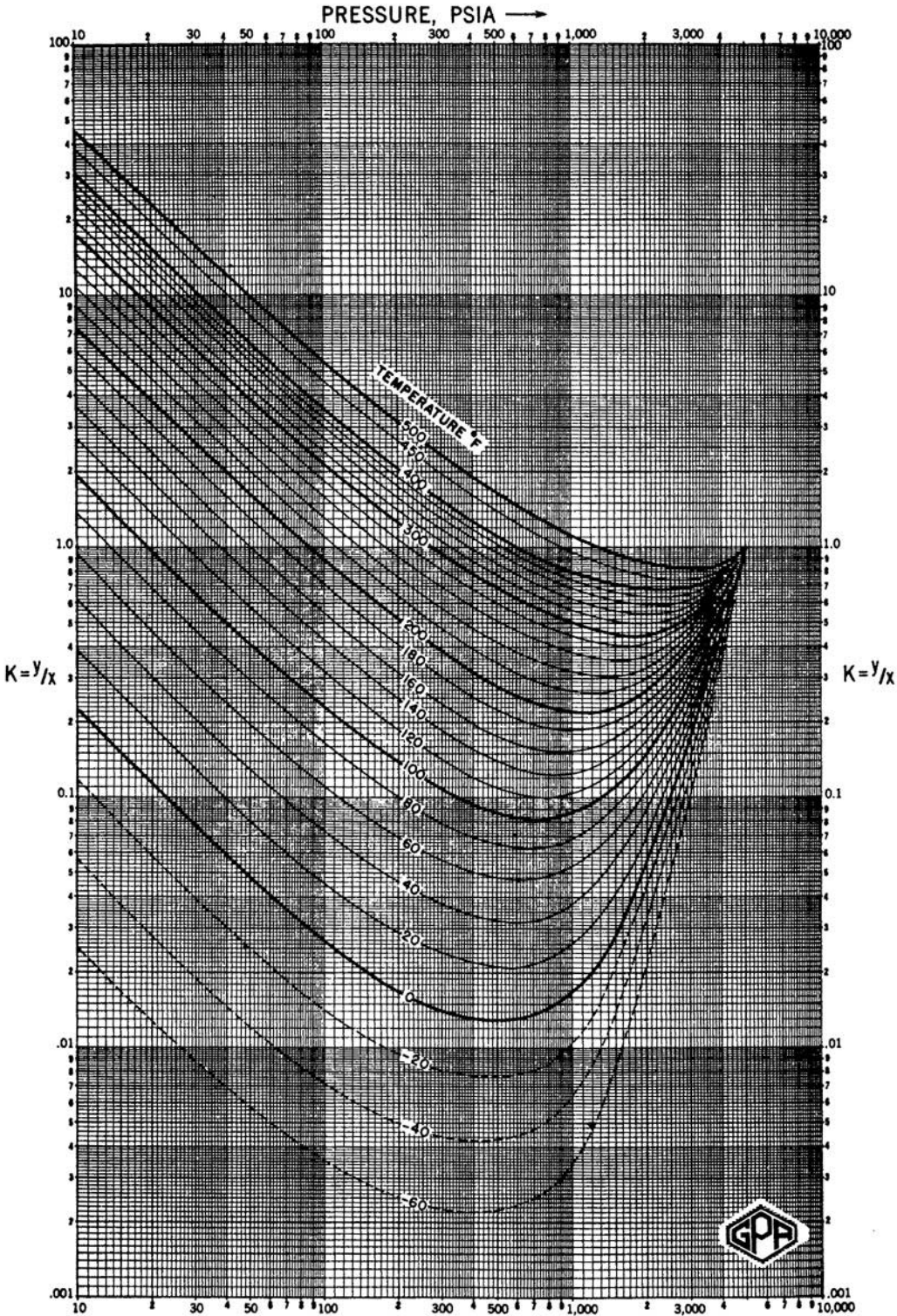


FIGURE A-7 *i*-Pentane conversion pressure, 5000 psia.
Courtesy of the Gas Processors Suppliers Association. Published in the *GPSA Engineering Data Book*, 10th edition, 1987.

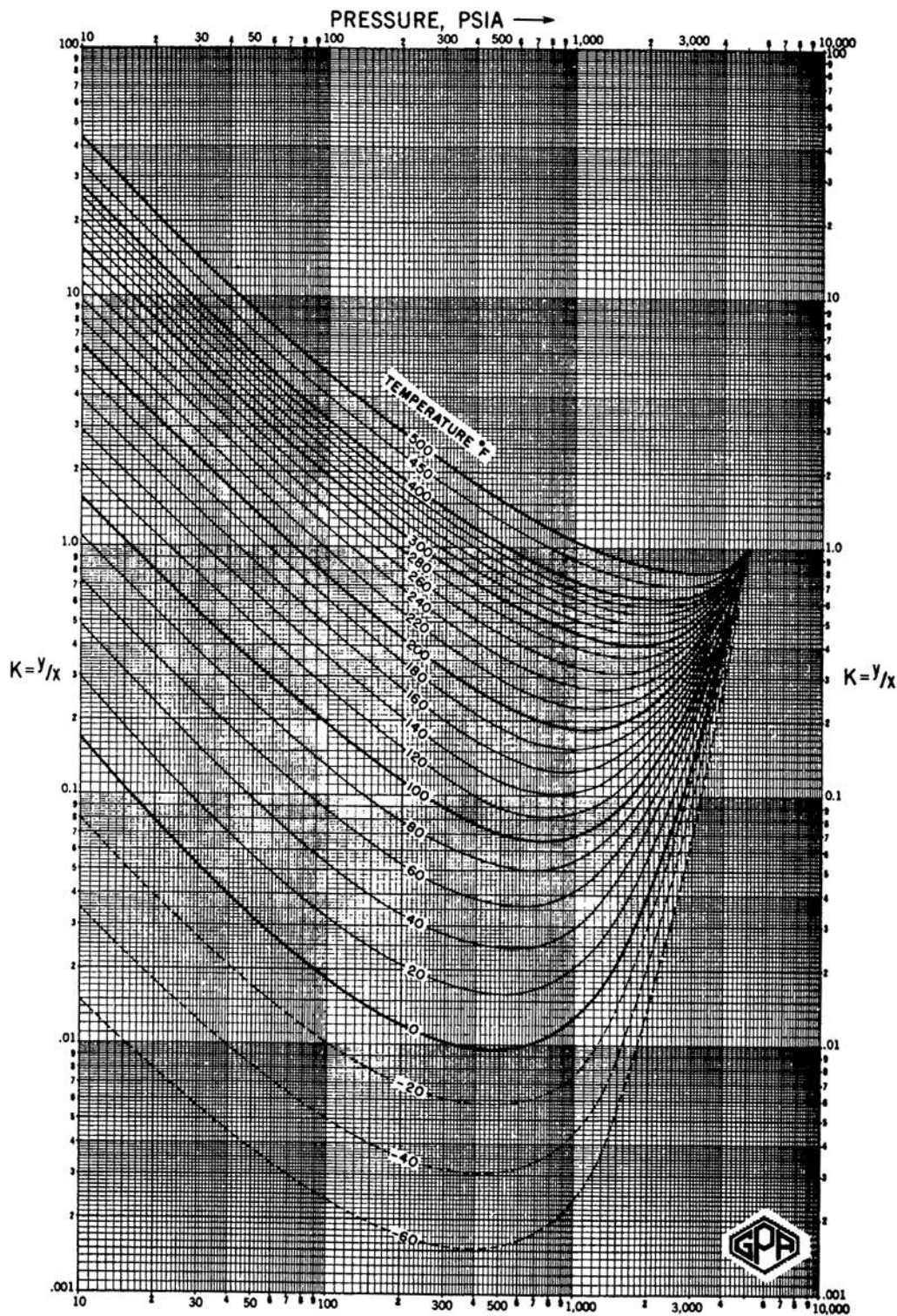


FIGURE A-8 *n*-Pentane conversion pressure, 5000 psia.

Courtesy of the Gas Processors Suppliers Association. Published in the *GPSA Engineering Data Book*, 10th edition, 1987.

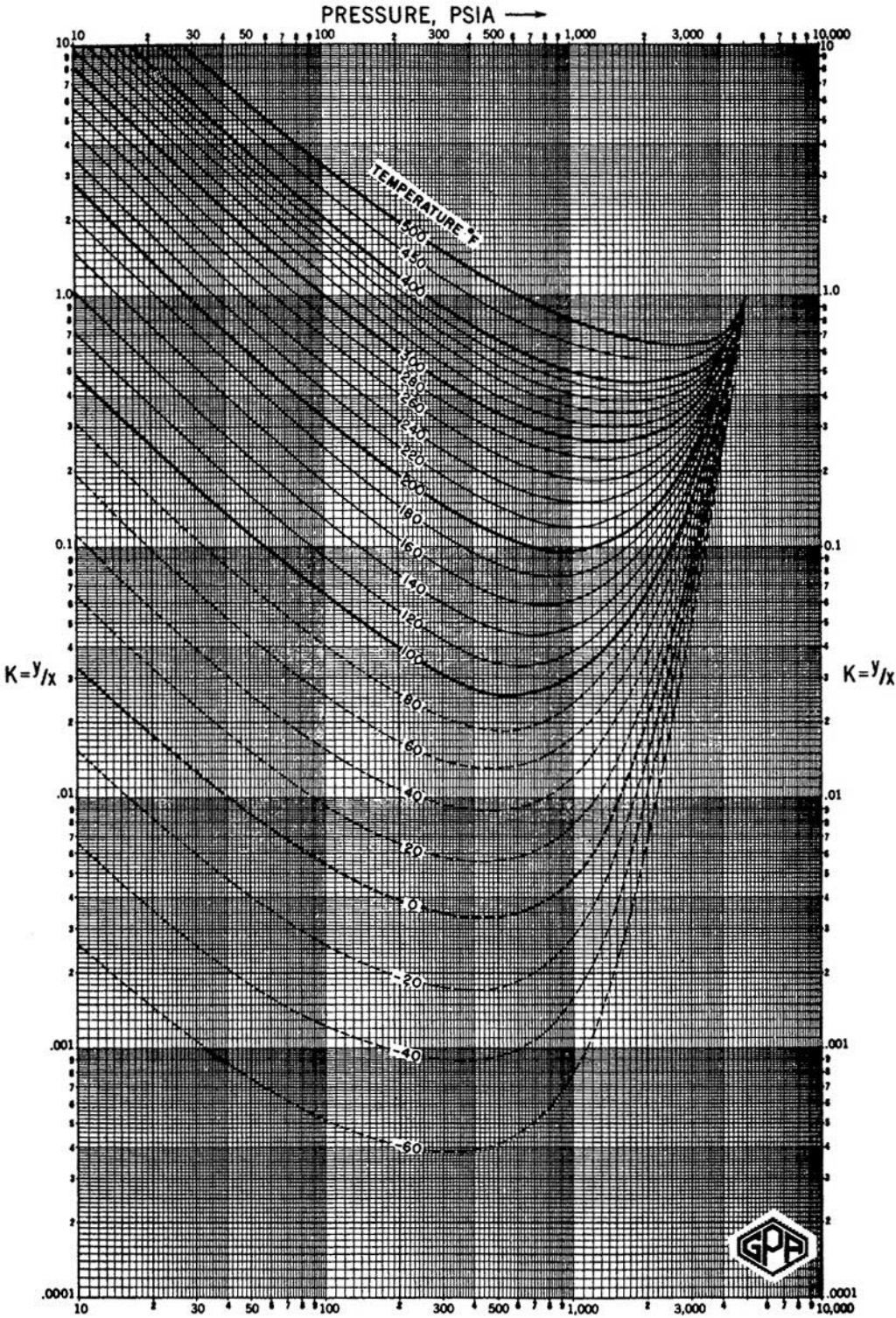


FIGURE A-9 Hexane conversion pressure, 5000 psia.
Courtesy of the Gas Processors Suppliers Association. Published in the *GPSA Engineering Data Book*, 10th edition, 1987.

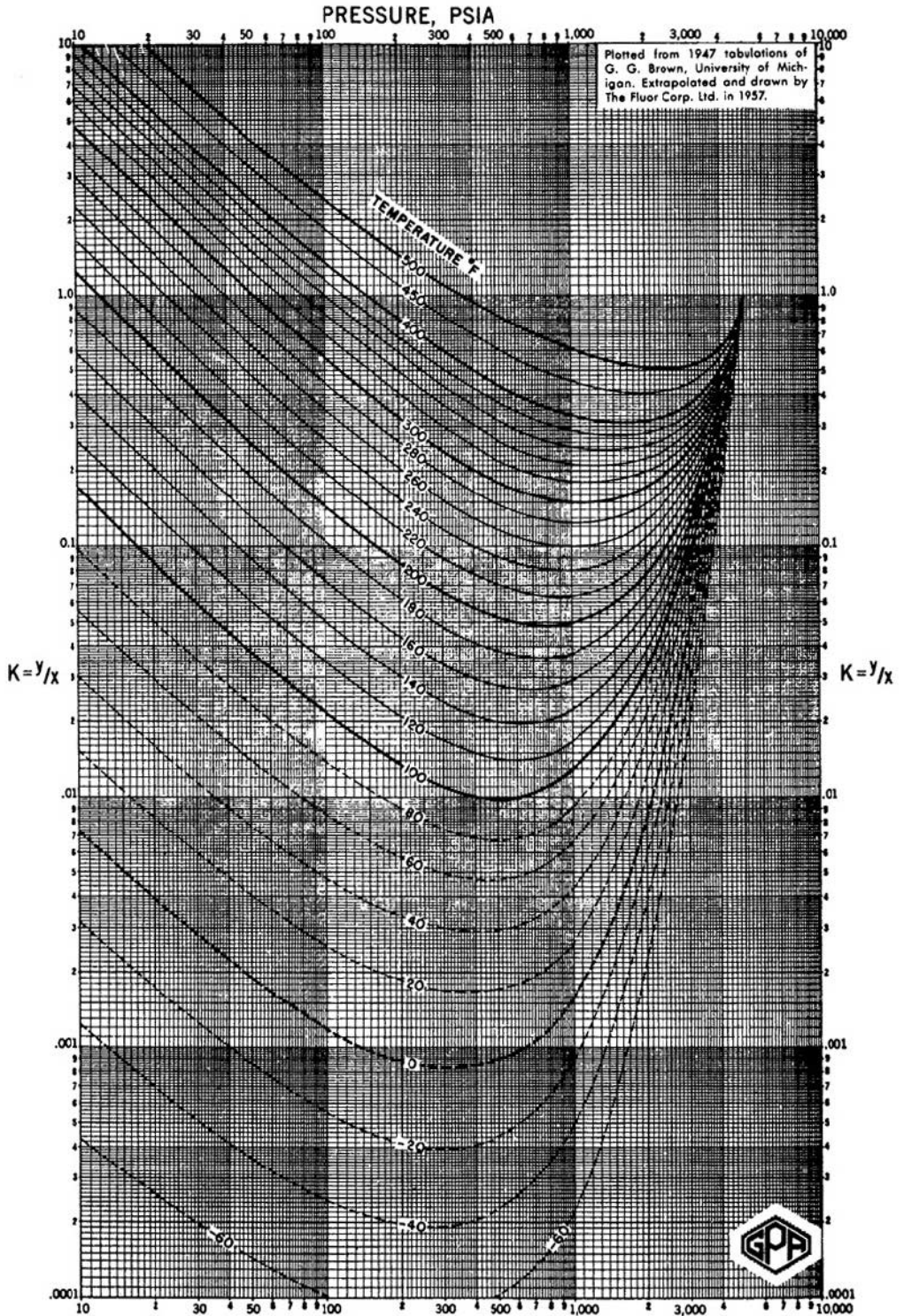


FIGURE A-10 *Heptane conversion pressure, 5000 psia.*

Courtesy of the Gas Processors Suppliers Association. Published in the *GPSA Engineering Data Book*, 10th edition, 1987.

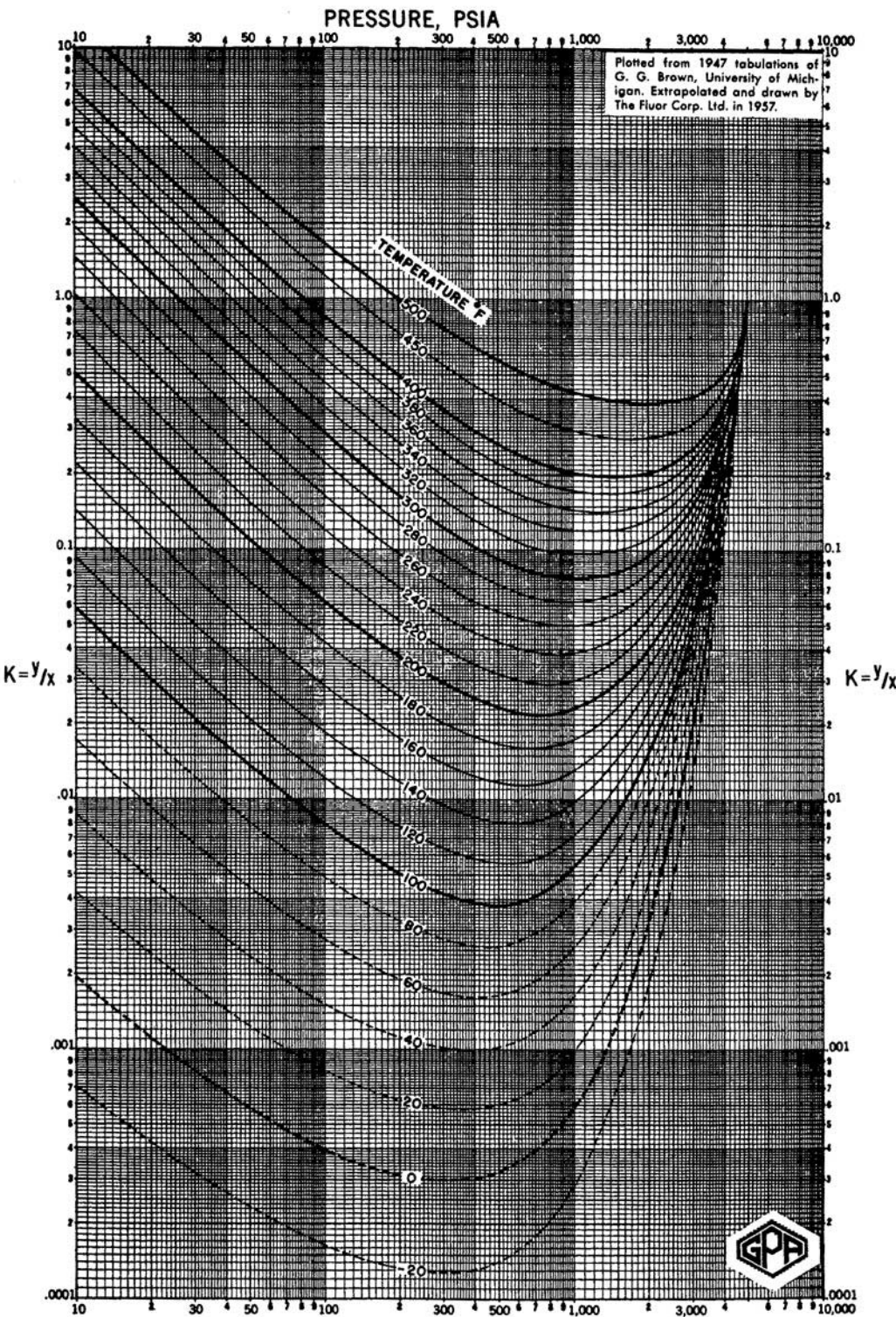


FIGURE A-11 Octane conversion pressure, 5000 psia.
Courtesy of the Gas Processors Suppliers Association. Published in the *GPSA Engineering Data Book*, 10th edition, 1987.

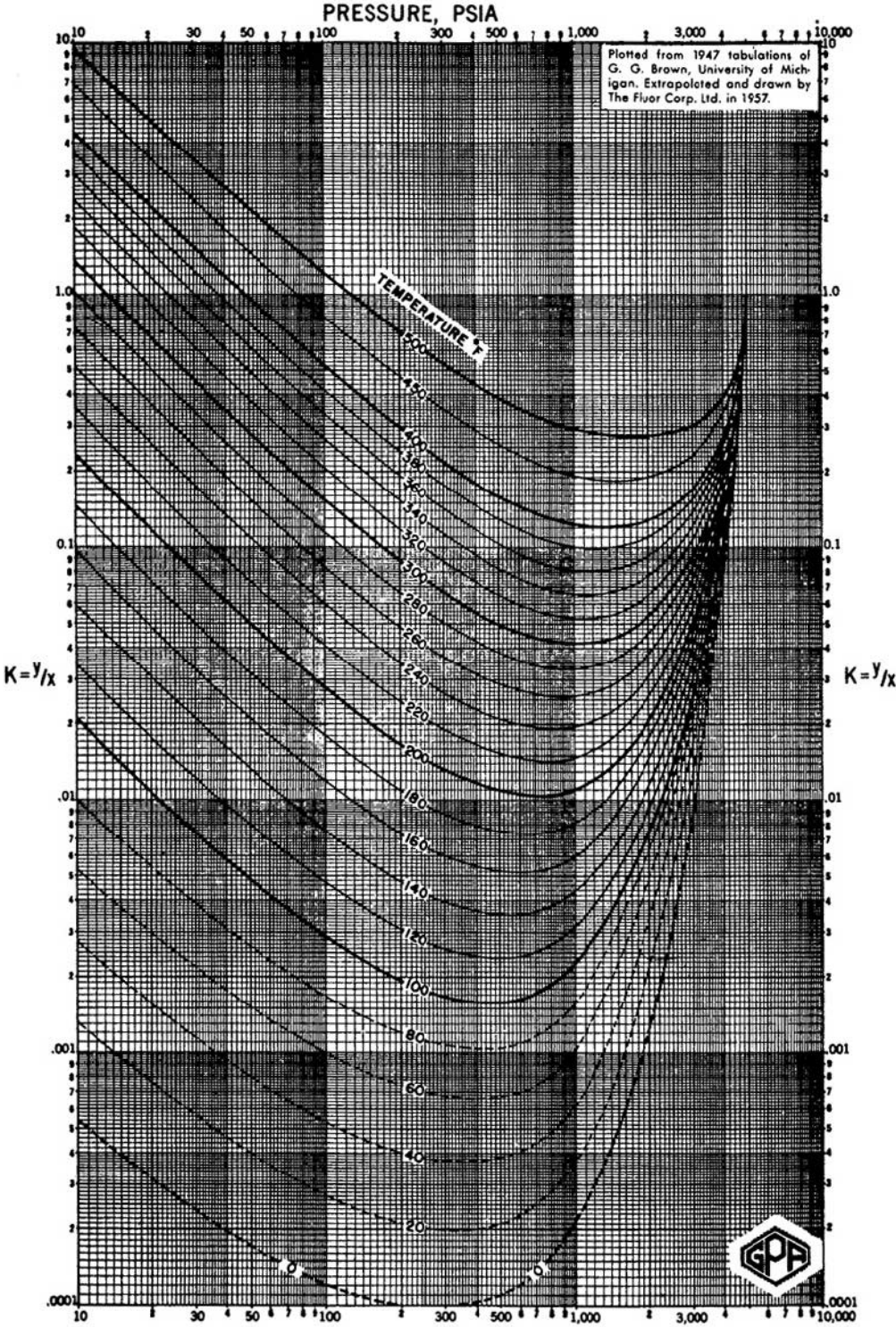


FIGURE A-12 Nonane conversion pressure, 5000 psia.
Courtesy of the Gas Processors Suppliers Association. Published in the *GPSA Engineering Data Book*, 10th edition, 1987.

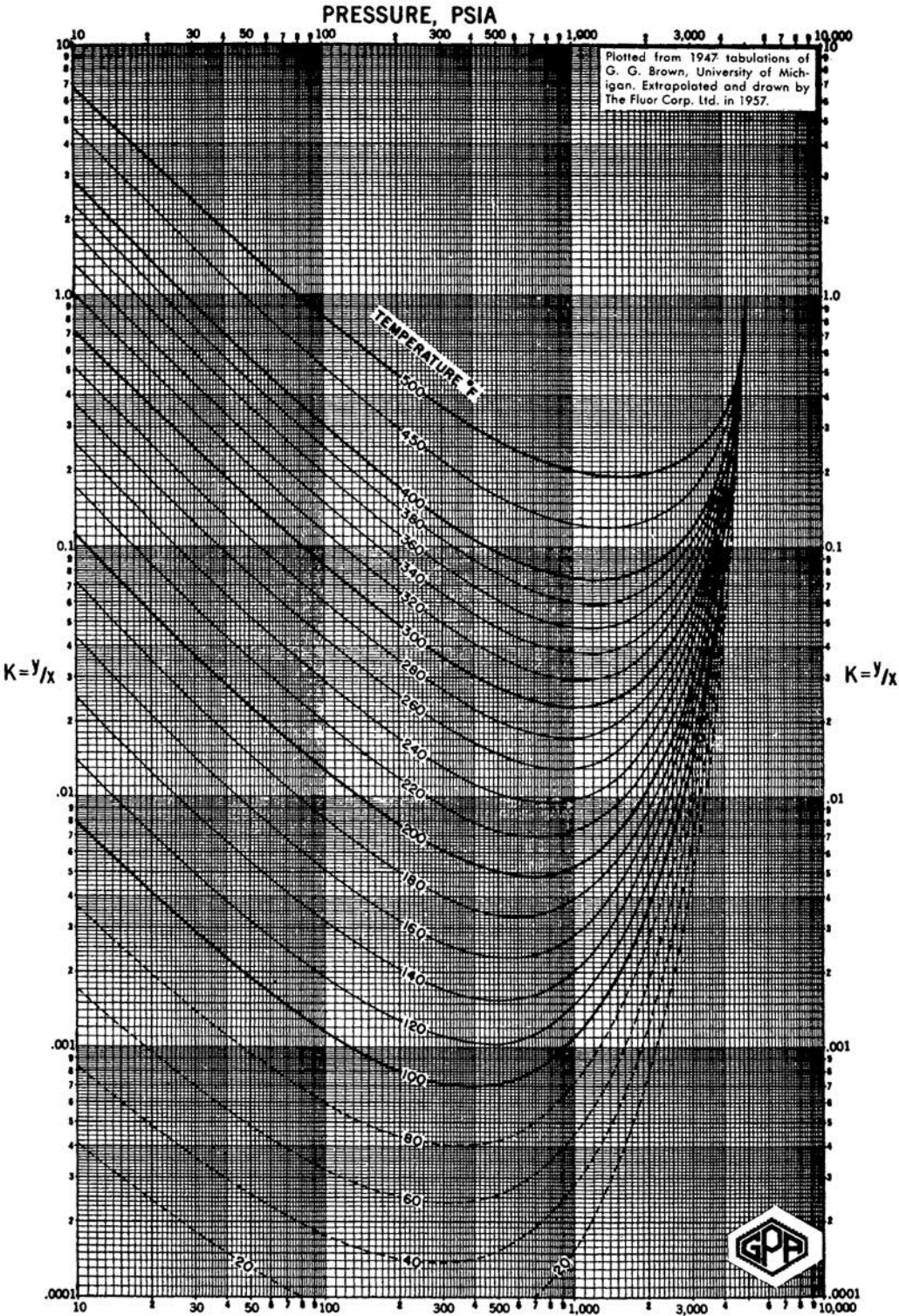


FIGURE A-13 Decane conversion pressure, 5000 psia.
Courtesy of the Gas Processors Suppliers Association. Published in the *GPSA Engineering Data Book*, 10th edition, 1987.

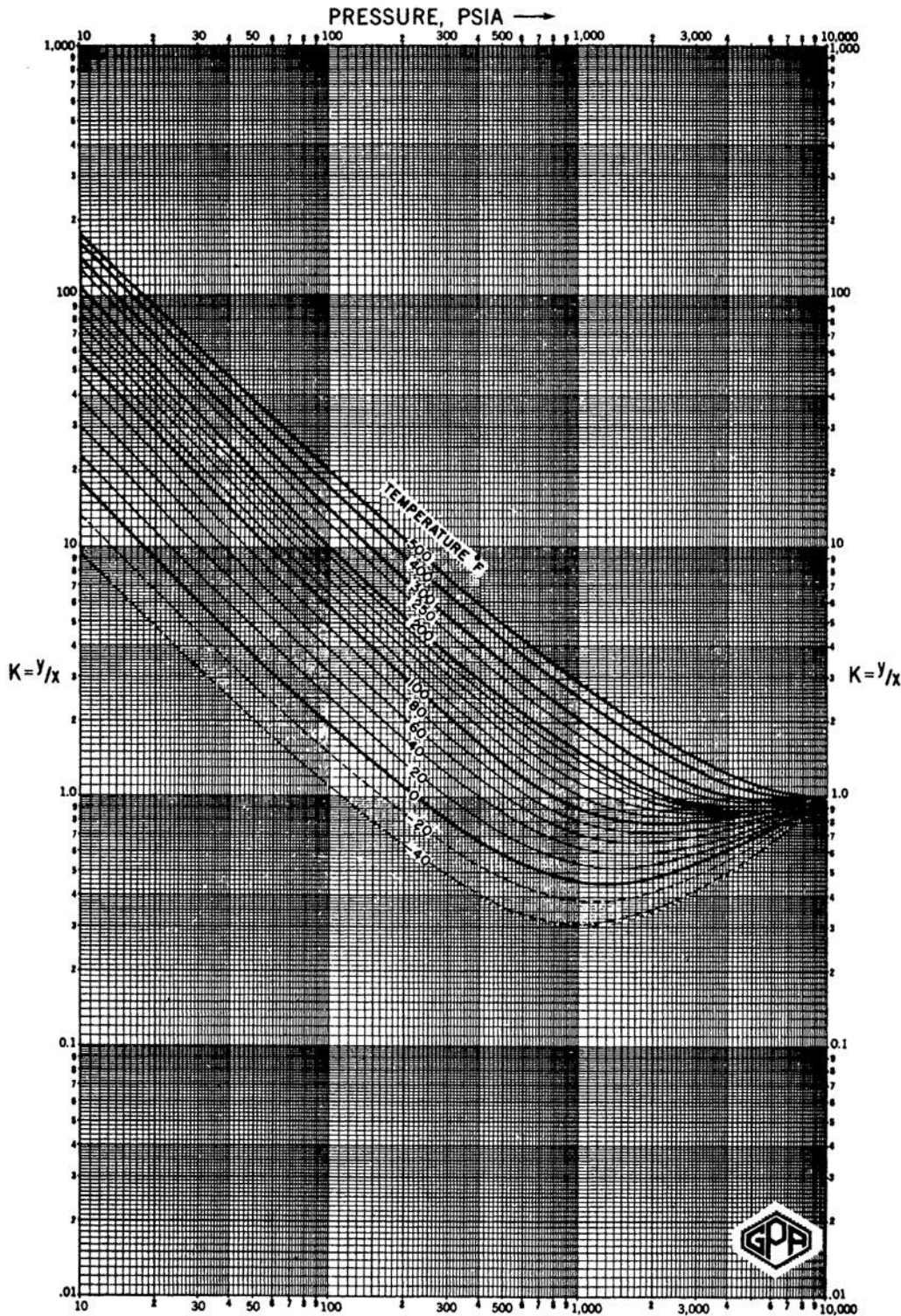


FIGURE A-14 *Ethane conversion pressure, 10,000 psia.*

Courtesy of the Gas Processors Suppliers Association. Published in the *GPSA Engineering Data Book*, 10th edition, 1987.

Index Terms

Links

A

Acentric factor	4	10
API gravity	182	
Apparent molecular weight	137	
Asphaltene		
onset pressure	472	
phase behavior	470	
phase envelope	482	
Average boiling point	85	

B

Bubble-point pressure	2	19	207	354	402
Bubble-point pressure correlations	207				

C

CCE	260	
Characterization of multiple samples	126	
Characterizing plus-fraction	59	
Chemical potential	384	
Classification of reservoirs and fluids	32	
Colloidal instability index	466	
Compositional gradient	431	
Compressibility factor	141	155
Constant composition expansion	260	415
Constant volume depletion	289	409
Contaminated oil sample	448	
Convergence pressure	344	
Correlations	346	
Bergman	90	
Cavett	66	

Index Terms

Links

Correlations (<i>Cont.</i>)			
Edmister	69		
Hall-Yarborough	72		
Kesler-Lee	67		
Magoulas-Tessios	72		
Riazi-Daubert	65		
Standing	71		
TWU	72		
Watansiri	69		
Willman-Teja	71		
Winn-Sim	68		
Cox chart	10		
Cricondenbar	30		
Cricondentherm	30		
Critical			
compressibility	4		
density	12		
mixture	433		
point	2	13	30
pressure	3	98	
temperature	3	95	
volume	3	14	72
Crude oils			
high-shrinkage	33	35	
low-shrinkage	33		
near critical	33	37	
ordinary	33		
volatile oil	35		
Cubic EOS	331		
Curve boiling-point	4	92	
bubble-point	3	32	
dew-point	3	32	
fusion	4	5	
melting point	4	5	
sublimation pressure	4	5	
vapor pressure	4		

<u>Index Terms</u>	<u>Links</u>		
CVD	289		
D			
DE	269	417	
De Boer plot	465		
Dew-point pressure	2	19	400
Differential expansion	269	417	
E			
Effect of nonhydrocarbon components on the Z-factor	147		
EOS	331		
Equations of state	331		
Peng-Robinson	388		
Redlich-Kwong	371		
Soave-Redlich-Kwong	376		
van der Waals	365		
Equilibrium ratios	332	339	
correlations	339		
Equivalent gas volume	173		
F			
Flash calculations	335		
Flow assurance	457		
Fugacity	382		
Fugacity coefficient	382		
Fusion temperature	5		
G			
Gibbs free energy	384		
Gas density	139		
Gas deviation factor	141	155	
Gas expansion factor	164		
Gas formation volume factor	163		
Gas gravity	139		

<u>Index Terms</u>	<u>Links</u>		
Gas isothermal compressibility	159		
Gas properties	135		
Gas reservoirs			
dry	38	43	
near critical	38	41	
retrograde	38	39	
wet	38	41	
Gas solubility	200		
correlations	201		
Gas density	139	144	
Gas hydrates	509		
Gas specific gravity	139		
Gas viscosity	166		
Gas/oil contact	46	53	432
Gibbs energy	384		
GOC	46	53	432

H

Hall-Yarborough correlation	72
High molecular weight gases	151
Hydrates	509

I

Ideal gases	136
Interfacial tension	246
Inverse lever rule	27
Isothermal compressibility coefficient of crude oil	218

K

K-value	332
---------	-----

L

Laboratory analysis of reservoir fluids	256
Liquid blockage	304

<u>Index Terms</u>	<u>Links</u>	
Liquid dropout	40	290
Lumping schemes	112	
M		
Melting-point temperature	5	
Minimum miscibility pressure	309	
MMP correlations	312	
Multicomponent systems	29	
N		
Near-critical gas-condensate reservoirs	41	
Nonhydrocarbon components	147	
O		
Oil-based mud	448	
Oil compressibility	218	
Oil density	184	
correlations	195	
Oil-formation volume factor	213	
correlations	214	
Oil API gravity	182	
Oil properties	181	
undersaturated	228	
Oil reservoirs		
gas-cap	33	
saturated	32	
undersaturated	32	
Oil viscosity	237	
P		
P-X diagram	23	
P-T diagram	30	
PNA	62	82
Phase rule	54	
Plait point	30	

<u>Index Terms</u>	<u>Links</u>				
Pour point	498				
Pressure					
bubble-point	2	19	207	354	402
dew-point	2	20			
vapor	10				
Pressure-composition diagram	23				
Properties of gases	135				
Pseudo-critical					
pressure	146				
temperature	146				
PVT properties of crude oils	181				
Q					
Quality lines	32				
R					
Racket's compressibility factor	17				
Real gases	141				
Refractive index	478				
Resins	461				
Riazi-Daubert correlation	65				
Routine laboratory PVT tests	260				
S					
SARA analysis	460				
Separator					
calculations	356	422			
tests	271	422			
Shift parameter	394				
Simulation of laboratory data by EOS	409				
Single-component systems	1				
Slim-tube test	308				
Solution gas specific gravity	183				

<u>Index Terms</u>	<u>Links</u>	
Specific gravity		
of oil	182	
of solution gas	183	
of wet gases	171	
Specific volume	139	
Spencer-Danner	17	
Splitting	99	
Splitting and lumping	99	
Surface tension	246	
Swelling test	307	427
T		
TBP	61	
Ternary diagram	29	
Three-component systems	28	
Three-phase flash calculations	403	491
Tie line	29	
Total formation volume factor	231	
True boiling point	61	
Two-component systems	19	
Two-phase formation volume factor	231	
Tuning EOS parameters	440	
Types of crude oil	33	
U		
Undefined heavy fraction	59	
Undersaturated oil properties	228	
Universal oil products	62	
UOP	62	
V		
Vapor pressure	10	407
Viscosity		
gas	166	
oil	237	

<u>Index Terms</u>	<u>Links</u>	
Volume shift parameter	394	
W		
WAT	495	498
Water properties	253	
Water-oil contact	52	53
Watson characterization factor	62	
Wax appearance temperature	495	498
Wax phase envelope	495	
WOC	52	53
Y		
Y-function	264	
Z		
Z-factor	141	155
Z-factor direct calculations	155	